AD-A101 684 SCIENTIFIC AND ENGINEERING STUDIES COMPILED 1979 1/8
COHERENCE ESTIMATION(U) NAVAL UNDERWATER SYSTEMS CENTER
NEWPORT RI G C CARTER ET AL. 1979

UNCLASSIFIED F/G 9/1 NL

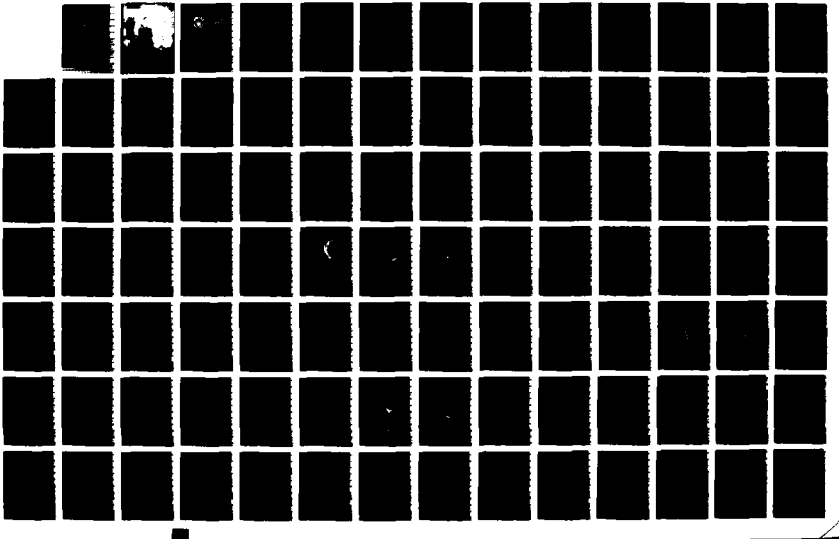

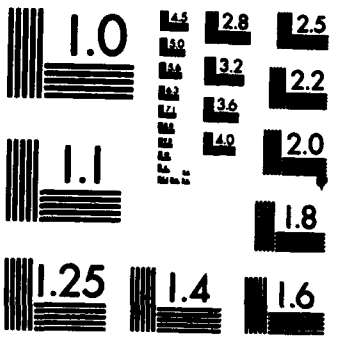

MICROCOPY RESOLUTION TEST CHART
NATIONAL BUREAU OF STANDARDS-1963-A

Scientific and Engineering Studies

Compiled 1979

Coherence Estimation

G. C. Carter
A. H. Nuttall

Scientific and Engineering Studies

Compiled 1979

Coherence Estimation

G. C. Carter
A. H. Nuttall

PUBLISHED BY

NAVAL UNDERWATER SYSTEMS CENTER

NEWPORT LABORATORY, NEWPORT, RHODE ISLAND

NEW LONDON LABORATORY, NEW LONDON, CONNECTICUT

Foreword

This collection of technical reports, documents, and memoranda deals with estimation of the coherence function between two wide-sense stationary random processes. Topics covered include accuracy and stability of the estimate, including the effects of weighting; approximations for the statistics of the estimate; the use of coherence in time-delay estimation; interpretation of the Fourier transform of the coherence; generation of processes with specified coherence; and alternative methods of estimating coherence. Applications of coherence estimation are given; they include systems identification, measurement of signal-to-noise ratio, and determination of relative time delay. This book furnishes a handy reference for anyone interested in obtaining high resolution and stable coherence estimates from limited data records.

In addition to the results presented here, other work done by the authors is available in the open literature, as listed below.

1. G. C. Carter and A. H. Nuttall, "Statistics of the Estimate of Coherence," *IEEE Proceedings*, vol 60, no. 4, 1972, pp. 465-466.

2. G. C. Carter, C. H. Knapp, and A. H. Nuttall, "Estimation of the Magnitude-Squared Coherence Function Via Overlapped Fast Fourier Transform Processing." *IEEE Transactions on Audio and Electroacoustics*, vol AU-21, no. 4, 1973, pp. 337-344.

3. G. C. Carter, C. H. Knapp, and A. H. Nuttall, "Statistics of the Estimate of the Magnitude-Coherence Function," *IEEE Transactions on Audio and Electroacoustics*, vol AU-21, no. 4, 1973, pp. 388-389.

4. G. C. Carter, A. H. Nuttall, and P. G. Cable, "The Smoothed Coherence Transform," *IEEE Proceedings*, vol 61, no. 10, 1973, pp. 1497-1498.

5. G. C. Carter and C. H. Knapp, 'Coherence and Its Estimation Via the Partitioned Chirp-Z Transform, *IEEE Transactions on Acoustics, Speech, and Signal Processing*, vol 23, no. 3, 1975, pp. 257-264.

6. C. H. Knapp and G. C. Carter, "The Generalized Correlation Method for Estimation of Time Delay," *IEEE Transactions on Acoustics, Speech, and Signal Processing*, vol 24, no. 4, 1976, pp. 320-327.

7. *Aspects of Signal Processing Part I*, D. Reidel Publishing Co., Boston, MA, 1977, pp. 251-256.

8. *Programs for Digital Signal Processing*, IEEE Press, NY, to appear 1979.

9. A. H. Nuttall and G. C. Carter, "Bias of the Estimate of Magnitude-Squared Coherence," *IEEE Transactions on Acoustics, Speech, and Signal Processing*, vol 24, no. 6, 1976, pp. 582-583.

10. G. C. Carter, "Receiver Operating Characteristics for a Linearly Thresholded Coherence Estimation Detector," *IEEE Transactions on Acoustics, Speech, and Signal Processing*, vol 25, no. 1, 1977, pp. 90-92.

11. E. H. Scannell, Jr., and G. C. Carter, "Confidence Bounds for Magnitude-Squared Coherence Estimates," *IEEE Transactions on Acoustics, Speech, and Signal Processing*, vol 26, no. 5, 1978, pp. 475-477.

12. *Aspects of Signal Processing Part I*, D. Reidel Publishing Co., Boston, MA, 1977, pp. 251-256.

Dr. William A. Von Winkle
Associate Technical Director
for Technology
NAVAL UNDERWATER SYSTEMS CENTER

Compiled 1979

Table of Contents

Copies of the studies included in this volume may be purchased from the National Technical Information Service, U. S. Department of Commerce, Springfield, Va. 22161.

NUSC Technical Memorandum TC-187-71
22 September 1971

On Generating Processes With Specified Coherence

A. H. Nuttall
G. C. Carter

ABSTRACT

For purposes of investigating the bias of different estimators of coherence, it is necessary to generate processes with accurately specified known values of coherence. A method of minimizing the effects of unknown power levels on the coherence of the generated processes is presented, such that desired values of coherence can be very accurately realized. Comparison with the standard approach reveals a much smaller error for the new method.

TABLE OF CONTENTS

INTRODUCTION

For purposes of investigating the bias of different estimators of coherence, it is necessary to generate processes with accurately specified known values of coherence. This is commonly done by adding together different fractions of two uncorrelated processes. However, if the two uncorrelated processes do not have the anticipated spectral levels in the frequency regions of interest, the resultant values of coherence will not be the design values. This occurs, for example, when two different physical noise sources are filtered by two different filters, and the gains or levels of the two channels are not identical. This situation can apparently be eliminated by using only one physical noise source and one filter, and taking two sufficiently disjoint time sections of the output to represent the two desired uncorrelated processes. However, if there are line voltage fluctuations or gain changes during the time taken to generate the two time sections, the same problem arises. In this memorandum, a method of minimizing the effects of unknown power levels on the coherence of the generated processes is presented, such that desired values of coherence can be very accurately realized.

PROBLEM SOLUTION

The problem is as follows: two* stationary uncorrelated processes $x(t)$ and $y(t)$ are available, with power density spectra $G_x(f)$ and $G_y(f)$, respectively. The ratio $R(f)$, defined by

$$R(f) = \frac{G_y(f)}{G_x(f)}, \tag{1}$$

is hopefully unity, but its exact value is not known. Two new processes

---

* $y(t)$ may be a sufficiently delayed version of $x(t)$, as discussed in the Introduction; in fact, this is recommended because of limitations in the state of the art in selecting two different filters having the same characteristics.

$$u(t) = x(t) + \int dt_1\, a(t_1) y(t-t_1),$$
$$v(t) = y(t) + \int dt_2\, b(t_2) x(t-t_2), \tag{2}$$

are constructed, where filters $a(t)$ and $b(t)$ are to be chosen so that the coherence of $u(t)$ and $v(t)$ is a specified function of frequency. The following analysis will allow for complex processes $x(t)$ and $y(t)$, and complex filters $a(t)$ and $b(t)$. Specialization to real processes and filters is immediate. Equation (2) constitutes linear operations only; non linear operations on $x(t)$ and $y(t)$ are disallowed because knowledge of the statistics of a higher order than the power spectra would be required.

The correlation of $u(t)$ and $v(t)$ is defined as

$$R_{uv}(\tau) = \overline{u(t)\, v^*(t-\tau)}, \tag{3}$$

and the cross-power spectrum is defined as

$$G_{uv}(f) = \int d\tau\, \exp(-i2\pi f\tau)\, R_{uv}(\tau). \tag{4}$$

Using (2) - (4), we find that the auto- and cross-power spectra of the processes in (2) are

$$G_{uv}(f) = B^*(f) G_x(f) + A(f) G_y(f),$$
$$G_u(f) = G_x(f) + |A(f)|^2 G_y(f), \tag{5}$$
$$G_v(f) = G_y(f) + |B(f)|^2 G_x(f),$$

where

$$A(f) = \int dt\, \exp(-i2\pi f t)\, a(t),$$
$$B(f) = \int dt\, \exp(-i2\pi f t)\, b(t), \tag{6}$$

are the transfer functions of the linear filters.

The complex coherence between $u(t)$ and $v(t)$ is then

$$\gamma(f) \equiv \frac{G_{uv}(f)}{[G_u(f)G_v(f)]^{1/2}} = \frac{B^*(f) + A(f)R(f)}{[1+|A(f)|^2R(f)]^{1/2}[R(f)+|B(f)|^2]^{1/2}}, \tag{7}$$

using (5) and (1). For notational simplicity, we will suppress the f-dependence in (7) and write

$$\gamma = \frac{B^* + AR}{[1+|A|^2R]^{1/2}[R+|B|^2]^{1/2}}. \tag{8}$$

In order to make the complex coherence γ insensitive to the exact value of R in the neighborhood of $R=1$, we will force the partial derivatives with respect to R, of both the real and imaginary parts of γ, equal to zero at $R=1$. This can be accomplished by setting $\partial\gamma/\partial R = 0$ at $R=1$. We find from (8),

$$\frac{\partial\gamma}{\partial R} = \frac{A\left[\frac{1}{2}R(1+|A|^2|B|^2)+|B|^2\right] - B^*\left[\frac{1}{2}(1+|A|^2|B|^2)+|A|^2R\right]}{[1+|A|^2R]^{3/2}[R+|B|^2]^{3/2}}. \tag{9}$$

At $R=1$, (9) becomes

$$\left.\frac{\partial\gamma}{\partial R}\right|_{R=1} = \frac{A\left[\frac{1}{2}(1+|A|^2|B|^2)+|B|^2\right] - B^*\left[\frac{1}{2}(1+|A|^2|B|^2)+|A|^2\right]}{[1+|A|^2]^{3/2}[1+|B|^2]^{3/2}}. \tag{10}$$

For (10) to equal zero, it is necessary (but not sufficient) that

$$\arg(B) = -\arg(A). \tag{11}$$

Under this choice, (10) becomes

$$\left.\frac{\partial\gamma}{\partial R}\right|_{R=1} = \exp\left[i\arg(A)\right] \frac{\frac{1}{2}(|A|-|B|)(1-|A||B|)^2}{\left[1+|A|^2\right]^{3/2}\left[1+|B|^2\right]^{3/2}}. \tag{12}$$

Equation (12) equals zero only if

$$|B| = |A| \quad \text{or} \quad |B| = 1/|A|. \tag{13}$$

Combining (13) and (11), we find that the two possible solutions are

$$B = A^* \quad \text{or} \quad B = 1/A. \tag{14}$$

However, the solution $B = 1/A$ substituted in (8) yields $\gamma = \exp[i\arg(A)]$, which is unacceptable, since it always has magnitude unity. The other solution

$$B = A^* \tag{15}$$

yields, upon substitution in (8),

$$\gamma = \exp\left[i\arg(A)\right] \frac{|A|\,(1+R)}{\left[1+|A|^2R\right]^{1/2}\left[R+|A|^2\right]^{1/2}}. \tag{16}$$

This is acceptable, since values of $|\gamma|$ between 0 and 1 are attainable through choice of $|A|$. For example, $|A| = 0$ yields $|\gamma| = 0$, while $|A| = 1$ yields $|\gamma| = 1$. Thus only filter gains $|A|$ between zero and unity are necessary to realize prescribed $|\gamma|$. The filter phase $\arg(A)$ is chosen to realize

specified arg (γ) . The relationship (15) between filters forces the impulse responses to satisfy

$$b(t) = a^*(-t). \tag{17}$$

Thus one filter must have a time-reversed impulse response of the other filter. Physical realization of these filters and processes will require recording and delaying various processes.

We notice from (16) that R has no effect upon the phase of the complex coherence. The phase of the complex coherence depends solely upon the phase of the filter A, and is independent of relative spectral levels.

For $R = 1$, (16) yields

$$\gamma\Big|_{R=1} \equiv \gamma_1 = \exp\left[i \arg(A)\right] \frac{2|A|}{1+|A|^2}. \tag{18}$$

The value γ_1 is the design (or desired) value of coherence. The required filter gain and phase are given in terms of γ_1 by

$$|A| = \frac{1-\sqrt{1-|\gamma_1|^2}}{|\gamma_1|}, \quad 0 < |\gamma_1| \le 1,$$
$$\arg(A) = \arg(\gamma_1). \tag{19}$$

(For $|\gamma_1| = 0$, $|A| = 0$).

We notice that since

$$\frac{\partial}{\partial R}|\gamma|^2 = \frac{\partial}{\partial R}\left(\gamma_r^2 + \gamma_i^2\right) = 2\gamma_r \frac{\partial \gamma_r}{\partial R} + 2\gamma_i \frac{\partial \gamma_i}{\partial R}, \tag{20}$$

it follows that

$$\frac{\partial}{\partial R}|\gamma|^2\Big|_{R=1} = 0, \tag{21}$$

because the requirement $\partial\gamma/\partial R = 0$ at $R=1$ causes the real and imaginary parts of γ to have zero slope at $R = 1$. Thus the magnitude-squared coherence $|\gamma|^2$ is also insensitive to values of R near $R = 1$. The magnitude-coherence $|\gamma|$ is similarly insensitive.

It should be noted that even if all the processes and filters in (2) are real, complex values of coherence are still attainable, because A can be complex, even when $q(t)$ is real. For example, an odd impulse response $q(t)$ results in an imaginary coherence.

SENSITIVITY ANALYSIS

For a design value γ_1 of coherence, the required filter characteristics are given by (19). When these filter characteristics are substituted in (16), we find the attained coherence γ for arbitrary R. For convenience, we first define the error in R as Δ:

$$R = 1 + \Delta. \tag{22}$$

Then there follows

$$\gamma = \gamma_1 \frac{1 + \frac{1}{2}\Delta}{\left[1 + \Delta + \frac{1}{4}|\gamma_1|^2\Delta^2\right]^{1/2}}. \tag{23}$$

For $\Delta = 0$, $\gamma = \gamma_1$ as desired. For $\Delta \neq 0$, we will investigate the dependence of the magnitude-squared coherence $|\gamma|^2$ on Δ.

We define the error

$$E = |\gamma|^2 - |\gamma_1|^2 = |\gamma_1|^2\left(1 - |\gamma_1|^2\right)\frac{\frac{1}{4}\Delta^2}{1 + \Delta + \frac{1}{4}|\gamma_1|^2\Delta^2}, \tag{24}$$

upon usage of (23). The error is zero for magnitude-squared coherences of zero and unity. To third-order in Δ,

$$E \cong |\gamma_1|^2 (1-|\gamma_1|^2) \frac{1}{4} \Delta^2 (1-\Delta). \tag{25}$$

This quantity is maximum for $|\gamma_1|^2 = \frac{1}{2}$, yielding

$$E_{max} \cong \left(\frac{1}{4}\Delta\right)^2 (1-\Delta). \tag{26}$$

Thus the error depends on R mainly through the quadratic behavior $(R-1)^2$ for R near 1.

In Table 1 are presented attained values of $|\gamma|^2$ for several desired values $|\gamma_1|^2$, as a function of R. Thus a 1% error in R causes an error of 6.3×10^{-6} in the magnitude-squared coherence at the value 0.5. And a 5% error causes an error of 1.6×10^{-4}.

Table 1. Attained Magnitude-Squared Coherence

R	$\|\gamma\|^2$				
	$\|\gamma_1\|^2 = .3$	$\|\gamma_1\|^2 = .4$	$\|\gamma_1\|^2 = .5$	$\|\gamma_1\|^2 = .6$	$\|\gamma_1\|^2 = .7$
0.95	.3001381	.4001579	.5001644	.6001578	.7001381
0.99	.3000053	.4000061	.5000063	.6000061	.7000053
1.00	.3000000	.4000000	.5000000	.6000000	.7000000
1.01	.3000052	.4000059	.5000062	.6000059	.7000052
1.05	.3001250	.4001428	.5001488	.6001428	.7001249

For comparison purposes, suppose filter B were not used at all in the construction of processes $u(t)$ and $v(t)$ in (2). By a procedure analogous to that developed above, it may be shown that the error in magnitude-squared coherence is

$$E = |\gamma_1|^2 (1-|\gamma_1|^2) \frac{\Delta}{1+|\gamma_1|^2 \Delta}, \tag{27}$$

which is linear in Δ, for small Δ. To first-order in Δ, the maximum error is

$$E_{max} \cong \frac{1}{4} \Delta. \tag{28}$$

Comparison of (26) and (28) indicates that careful choice of two filters yields an error that behaves as the square of the error for one filter. For a 4% error in relative power levels R, this is two orders of magnitude improvement.

SPECIAL CASE

In order to accurately investigate the bias of coherence estimators, it is often convenient to generate two processes with constant magnitude-squared coherence for all frequencies. This is most easily accomplished by choosing

$$a(t) = b(t) = G\,\delta(t), \; G \text{ real}, \tag{29}$$

in (2). The processes are then

$$\begin{aligned} u(t) &= x(t) + G\,y(t), \\ v(t) &= y(t) + G\,x(t). \end{aligned} \tag{30}$$

The transfer function of this filter is $A(f) = G$, all f; the gain G is available from (19) as

$$G = \frac{1-\sqrt{1-|\gamma_1|^2}}{|\gamma_1|}, \quad 0 < |\gamma_1| \leq 1, \tag{31}$$

where $|\gamma_1|$ is the desired magnitude-coherence. For $|\gamma_1| = 0$, $G = 0$.

SUMMARY

A method of minimizing the effects of unknown power levels on the coherence of generated processes has been presented. For example, a 1% variation in power levels (.04 dB fluctuation) will affect the desired value of magnitude-squared coherence by only six parts in the sixth place. Hence, state of the art power supply fluctuations can now be tolerated in the generation of processes with accurately specified known values of coherence.

NUSC Technical Memorandum TC1-193-71
28 September 1971

Evaluation of the Statistics Of the Estimate of Magnitude-Squared Coherence

G. C. Carter
A. H. Nuttall

ABSTRACT

Closed form expressions for the statistics of the estimate of magnitude-squared coherence are presented. These statistics include the probability density function, the cumulative distribution function, the bias, and the variance. The expressions presented are in convenient and accurate forms for digital computer evaluation; examples of their computation are included. Simple approximations are also given for the bias and variance.

INTRODUCTION

Consider two wide-sense stationary random processes $x(t)$ and $y(t)$ with auto-power spectra $G_x(f)$ and $G_y(f)$, respectively, and cross-power spectrum $G_{xy}(f)$. The magnitude-squared coherence between the two processes is defined as

$$C(f) = \frac{|G_{xy}(f)|^2}{G_x(f)\,G_y(f)}.$$

Estimates of $C(f)$ from n independent segments (or pieces) of data are frequently made according to

$$\hat{C}(f) = \frac{\left|\sum_{i=1}^{n} X_i(f)\,Y_i^*(f)\right|^2}{\sum_{i=1}^{n}|X_i(f)|^2 \sum_{i=1}^{n}|Y_i(f)|^2}, \tag{1}$$

where $X_i(f)$ and $Y_i(f)$ are the Fourier coefficients at frequency f, obtained from the i-th weighted segments. The problem we address here is the statistics of the random variable $\hat{C}(f)$.

STATISTICS OF THE ESTIMATOR

There has been much related past work on statistics of the form of (1) (Refs. 1-7). For $x(t)$ and $y(t)$ Gaussian zero-mean processes, the probability density function (PDF) of* $\hat{C}$ (Refs. 2 and 5) can be manipulated into the form

$$p(\hat{C}) = (n-1)\frac{(1-C)^2}{(1-C\hat{C})^3}\left[\frac{(1-C)(1-\hat{C})}{(1-C\hat{C})^2}\right]^{n-2} {}_2F_1\left(1-n, 1-n; 1; C\hat{C}\right), C<1. \tag{2}$$

This is a convenient form, since the hypergeometric function is a $(n-1)$-st order polynomial, all the terms of which are positive. (For $C=1$, $p(\hat{C}) = \delta(\hat{C}-1)$.) The density function can also be written as

$$p(\hat{C}) = (n-1)\left(\frac{1-C}{1-C\hat{C}}\right)^2\left[\frac{(1-C)(1-\hat{C})}{1-C\hat{C}}\right]^{n-2} P_{n-1}\left(\frac{1+C\hat{C}}{1-C\hat{C}}\right), \quad C<1,$$

*The f-dependence is suppressed for notational simplicity.

where $P_{n-1}(\cdot)$ is a Legendre polynomial.

The cumulative distribution function (CDF) of $\hat{C}$ can also be written in closed form, through proper identification of variables in the work of Fisher (Ref. 1):

$$P(\hat{C}) = \hat{C}\left[\frac{1-C}{1-C\hat{C}}\right]^n \sum_{k=0}^{n-2}\left[\frac{1-\hat{C}}{1-C\hat{C}}\right]^k {}_2F_1\left(-k, 1-n; 1; C\hat{C}\right), \quad C<1.$$

The k-th hypergeometric function is a k-th order polynomial, all the terms of which are positive. The probability density function and cumulative distribution function are plotted for $n = 32$ in Figures 1a-1d, and for $n=64$ in Figures 1e-1h. The method for determining confidence intervals from the cumulative distribution function is given in the appendix.

In order to obtain the moments of $\hat{C}$, we rewrite (2) as (Ref. 8, eq. 9. 131 1)

$$p(\hat{C}) = (n-1)(1-C)^n(1-\hat{C})^{n-2}\,{}_2F_1\left(n, n; 1; C\hat{C}\right), \quad C<1. \tag{3}$$

The m-th moment of $\hat{C}$ is immediately available (Ref. 8, eq. 7.512 12):

$$E\{\hat{C}^m\} = \frac{\Gamma(n)\Gamma(m+1)}{\Gamma(m+n)}(1-C)^n\,{}_2F_2\left(m+1, n, n; m+n, 1; C\right), \quad C<1. \tag{4}$$

By proper identification of variables, this result can be shown equal to that of Anderson (Ref. 3). The series (4) is easily evaluated with computer aid.

The first moment is available from (4) by setting $m=1$. It can be manipulated into the simpler (and rapidly convergent) form

$$E\{\hat{C}\} = \frac{1}{n} + \frac{n-1}{n+1}C\;{}_2F_1\left(1, 1; n+2; C\right), \quad C<1.$$

By expanding ${}_2F_1$ in a power series in C, a simple approximation for the bias is made available:

$$\text{Bias} = E\{\hat{C}\} - C \tag{5a}$$

$$\cong \frac{1}{n} - \frac{2}{n+1}C + \frac{n-1}{(n+1)(n+2)}C^2 + 2\,\frac{n-1}{(n+1)(n+2)(n+3)}C^3 . \tag{5b}$$

(Where (5b) goes negative, replace it by zero). As an example, for n=8, the bias lies in the range (0,.125), and the maximum error in (5b) is .0027 at C=.86. Expression (5b) is a generalization of an empirical result of Benignus (Ref. 7). The bias (5a) is plotted in Figure 2; no approximations are involved here.

The variance of the estimator $\hat{C}$ is available from (4) by expanding ${}_3F_2$ in a power series in C:

$$\text{Var}\{\hat{C}\} = E\{\hat{C}^2\} - E^2\{\hat{C}\} \tag{6a}$$

$$\cong \frac{n-1}{n(n+1)}\left[\frac{1}{n} + 2\,\frac{n-2}{n+2}C - 2\,\frac{2n^3-n^2-2n+3}{(n+1)(n+2)(n+3)}C^2\right. \tag{6b}$$

$$\left. + 2\,\frac{n^4-6n^3-n^2+10n-8}{(n+1)(n+2)(n+3)(n+4)}C^3 + \frac{13n^5-15n^4-113n^3+27n^2+136n-120}{(n+1)(n+2)^2(n+3)(n+4)(n+5)}C^4\right].$$

(Where (6b) goes negative, replace it by zero). For n=8, the variance lies in the range (0,.031), and the maximum error is .0067 at C=.83. This result is a generalization of Jenkins (Ref. 6). The variance (6a) is plotted in Figure 3, again without any approximations.

ACKNOWLEDGEMENT

The authors wish to acknowledge the direction of Prof. Charles H. Knapp, University of Connecticut.

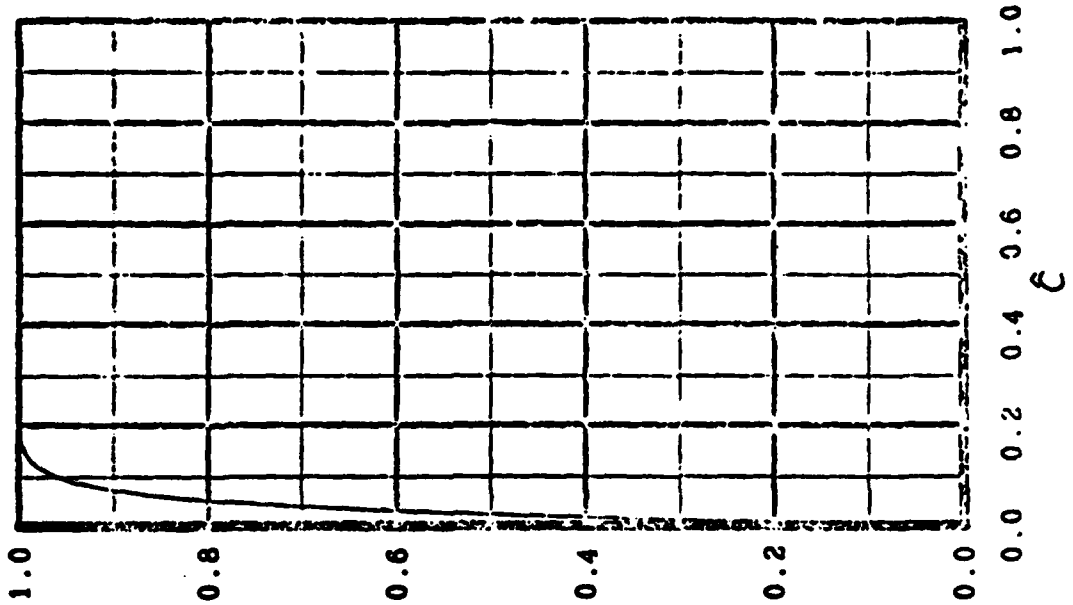

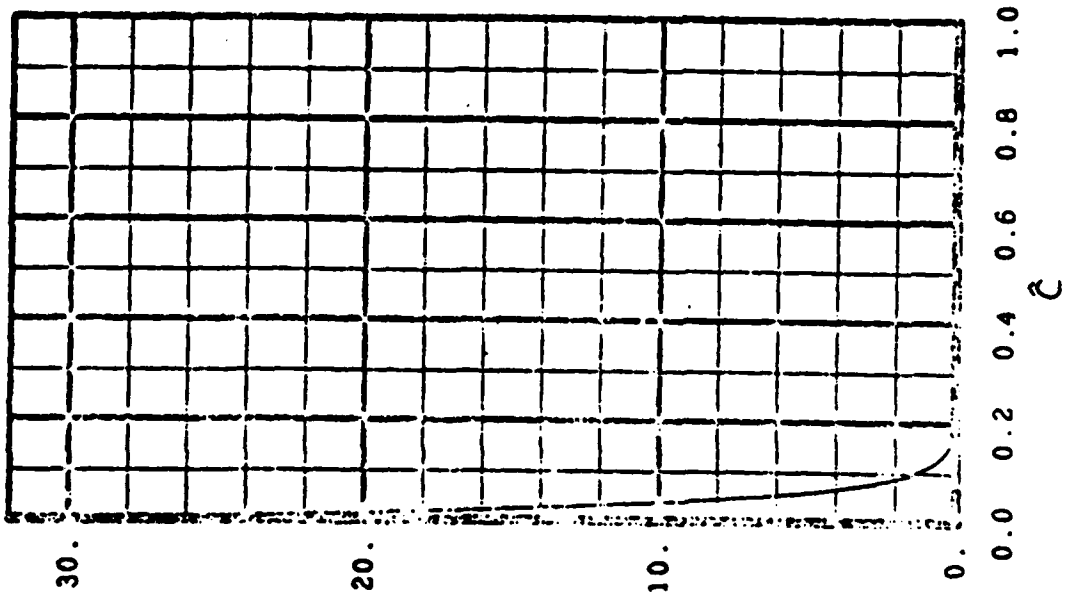

Figure 1a. PDF and CDF for n=32, C=0.0

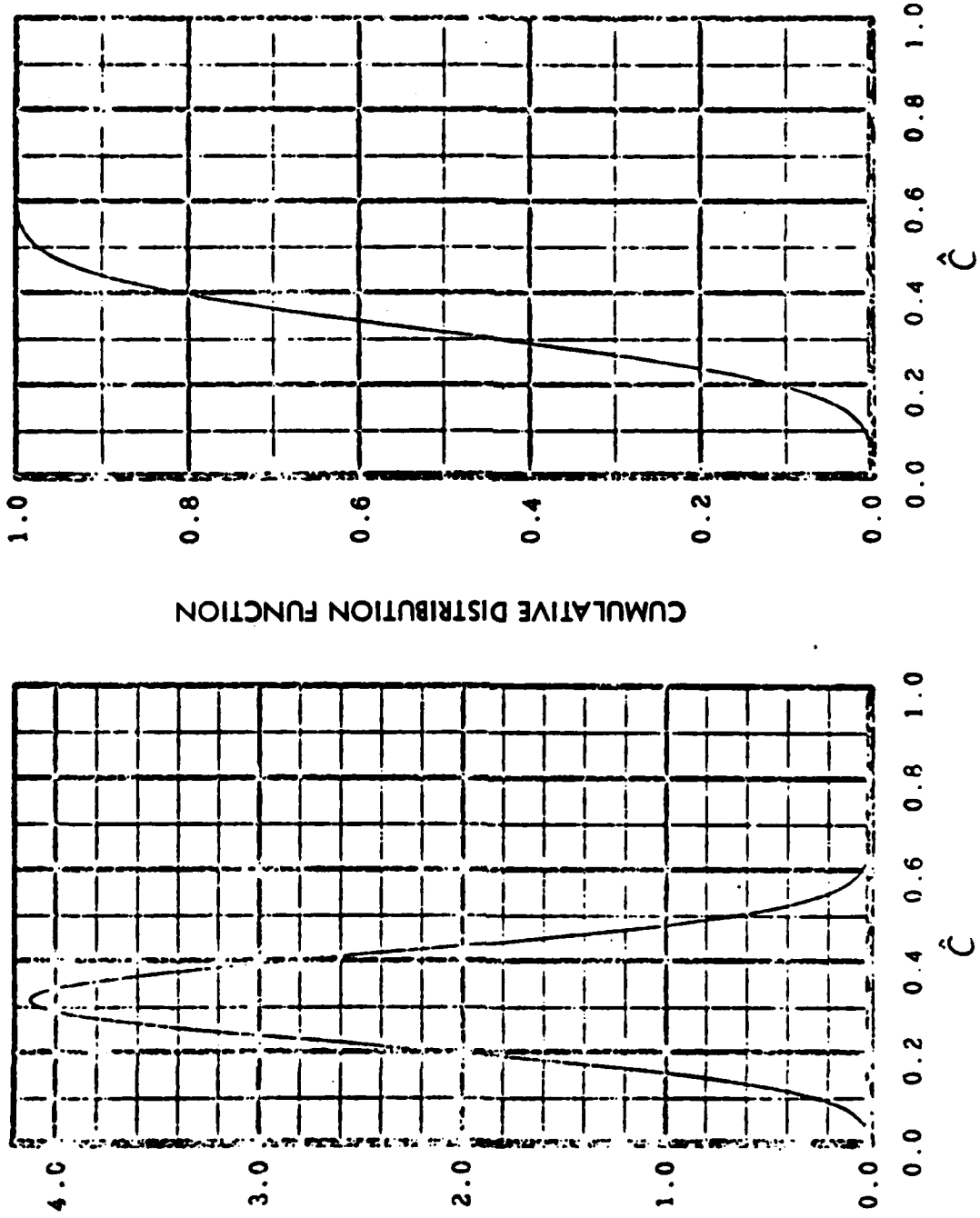

Figure 1b. PDF and CDF for n=32, C=0.3

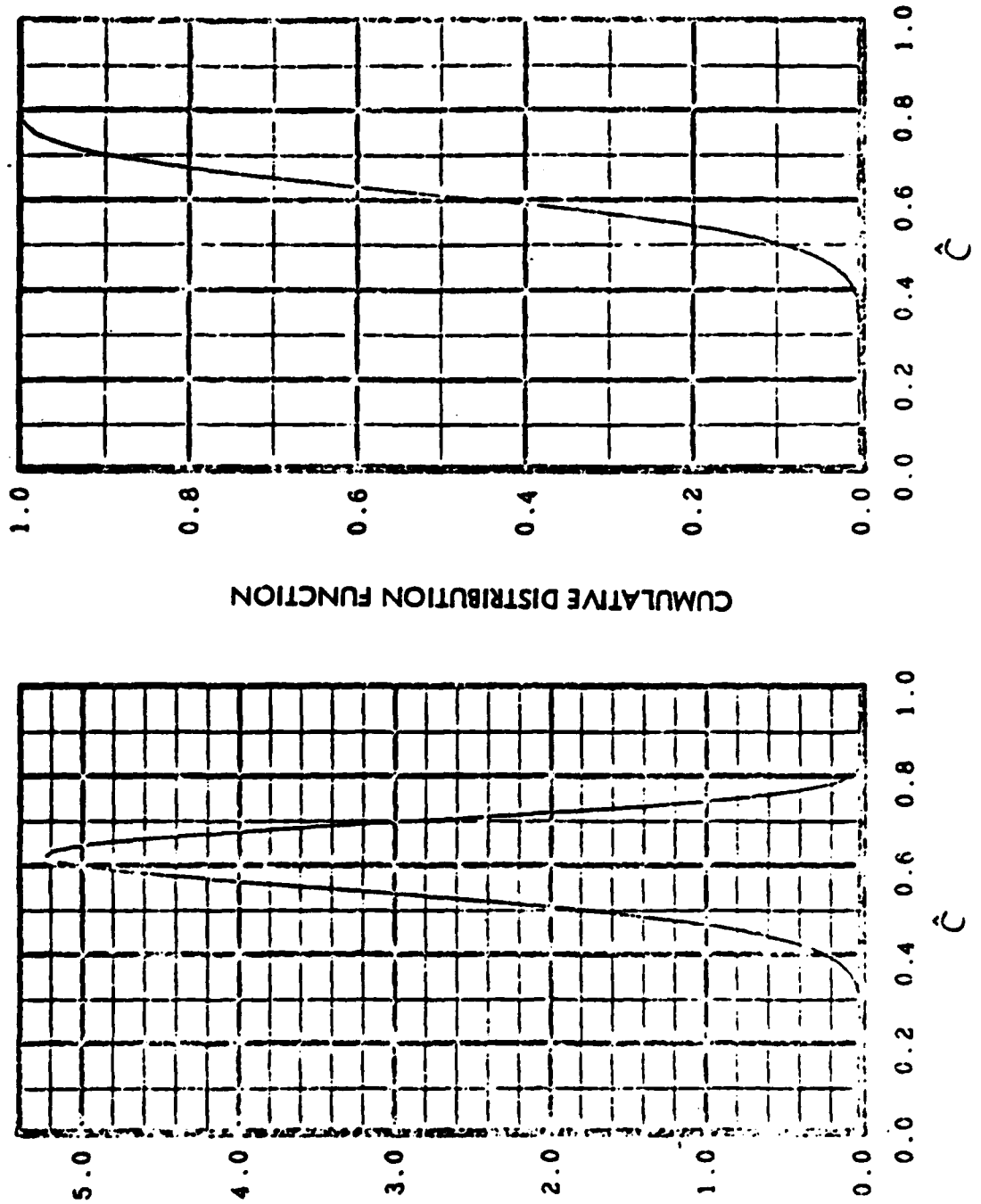

Figure 1c. PDF and CDF for n=32, C=0.6

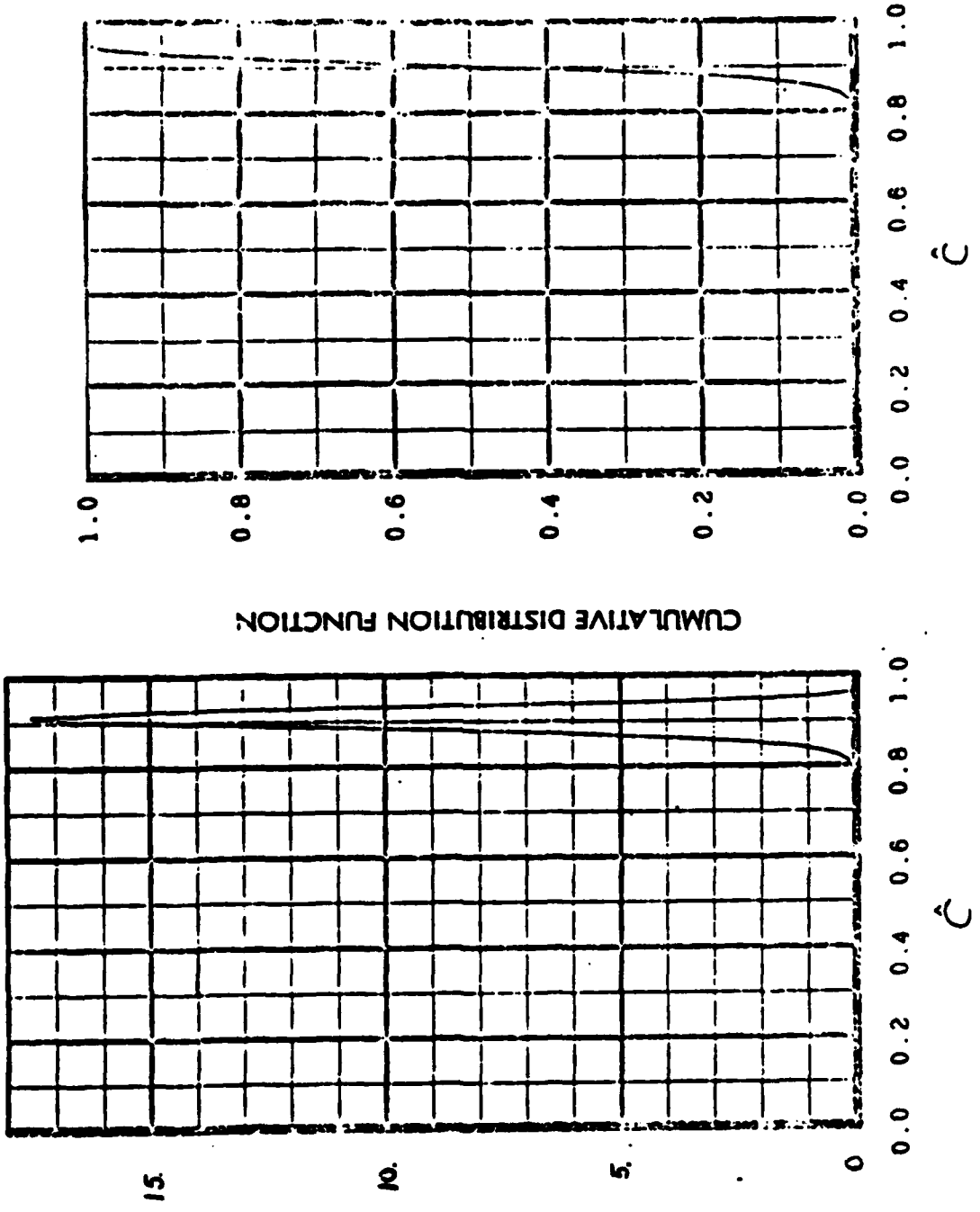

Figure 1d. PDF and CDF for n=32, C=0.9

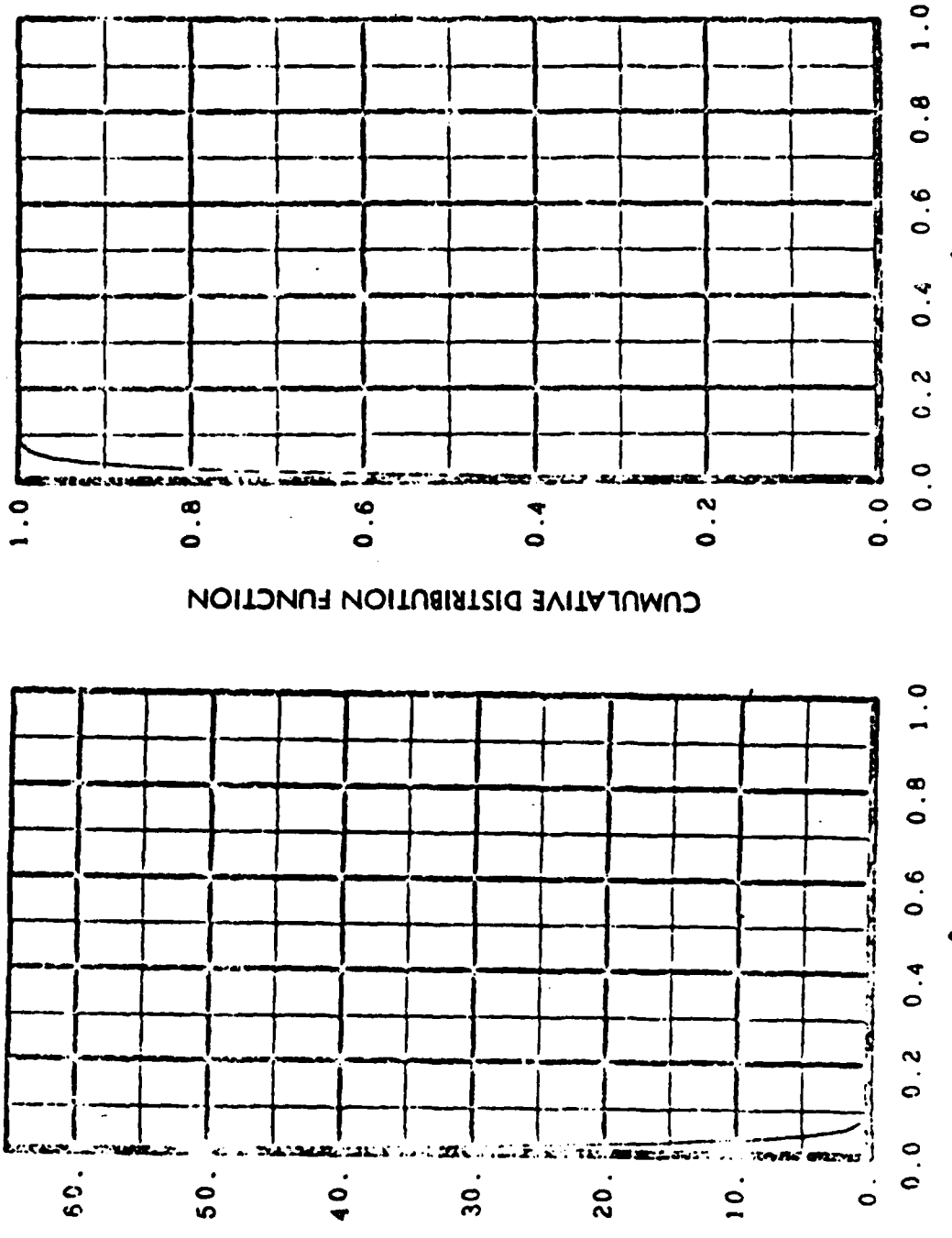

Figure 1e. PDF and CDF for n=64, C=0.0

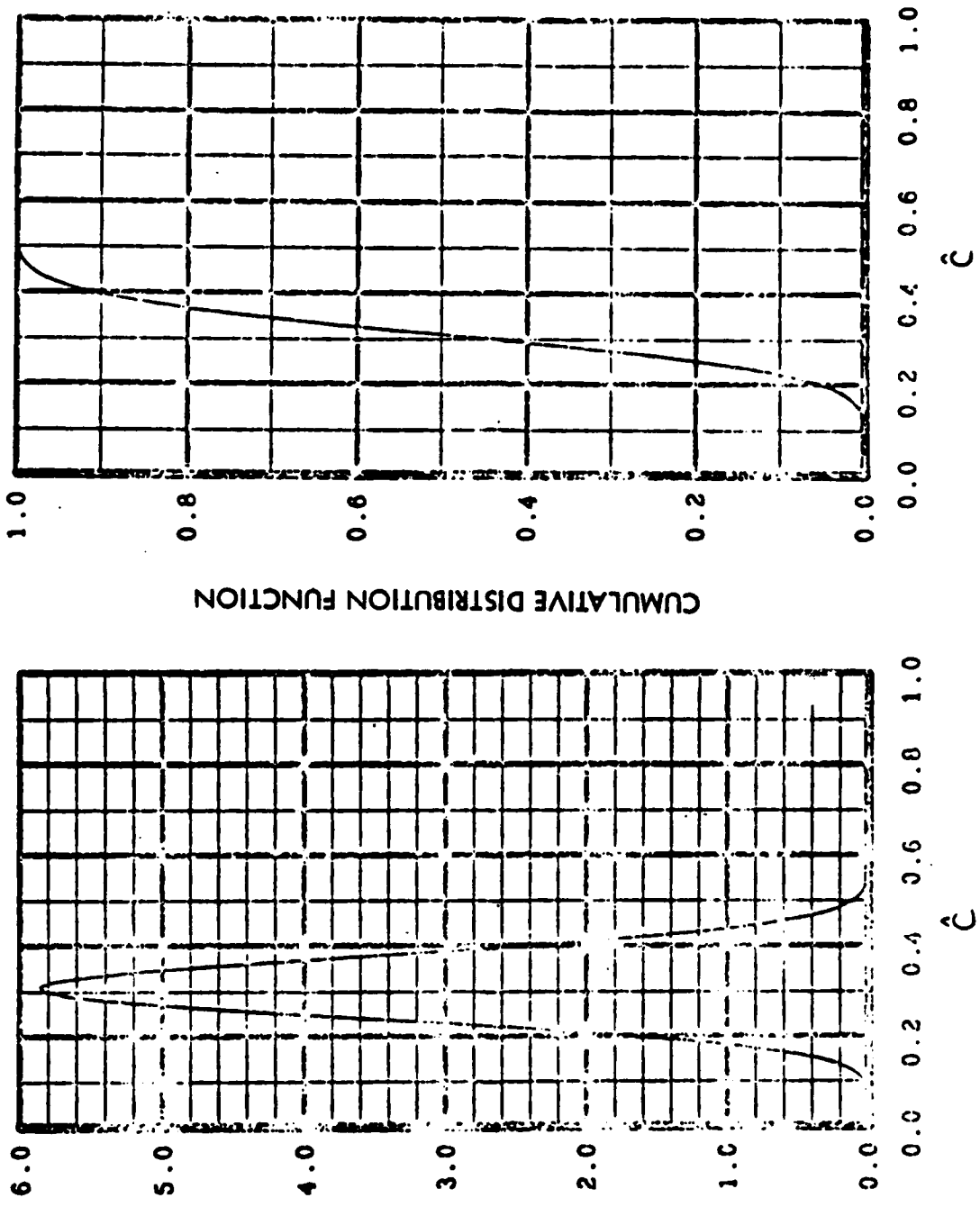

Figure 1f. PDF and CDF for n=64, C=0.3

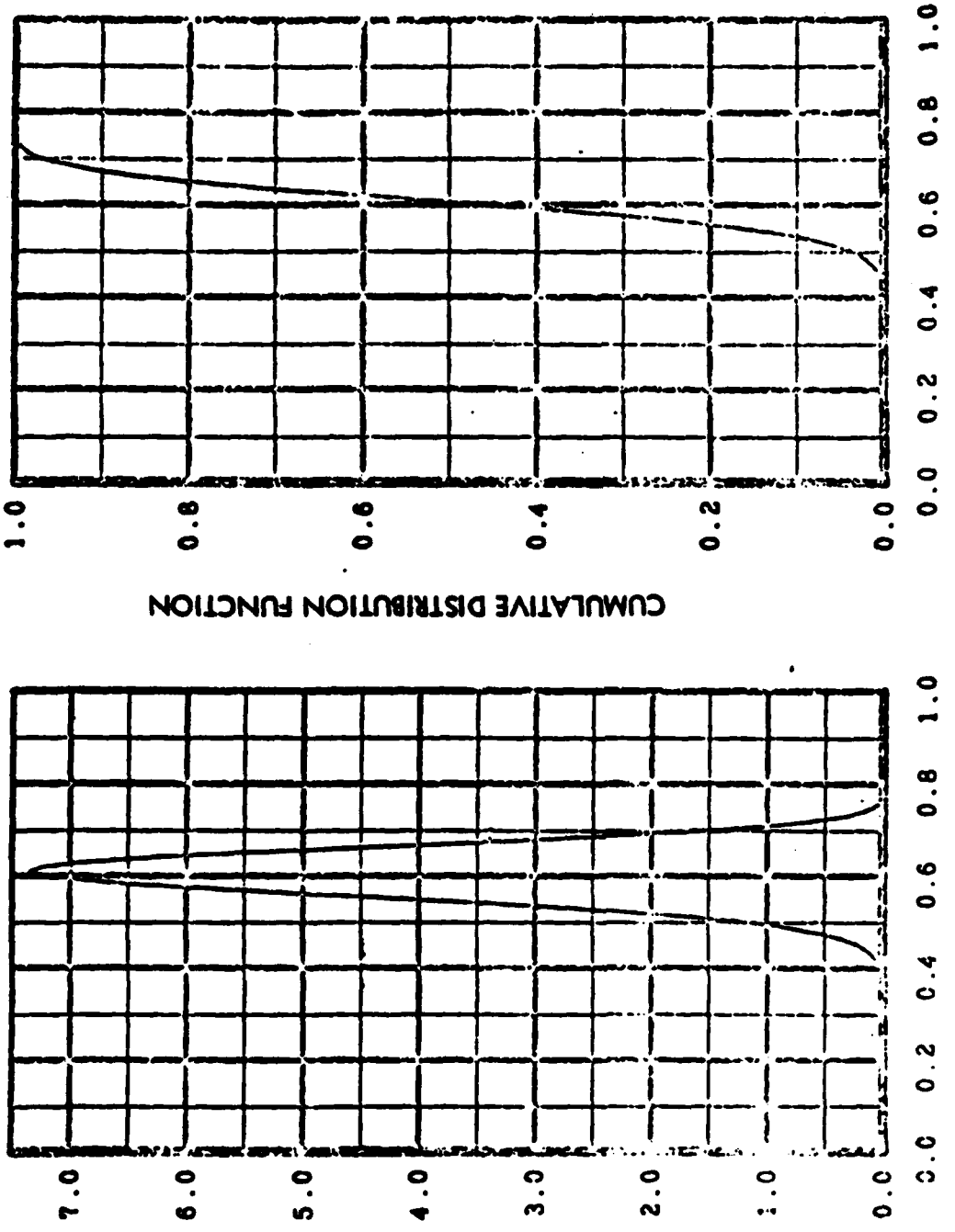

Figure 1g. PDF and CDF for n=64, C=0.6

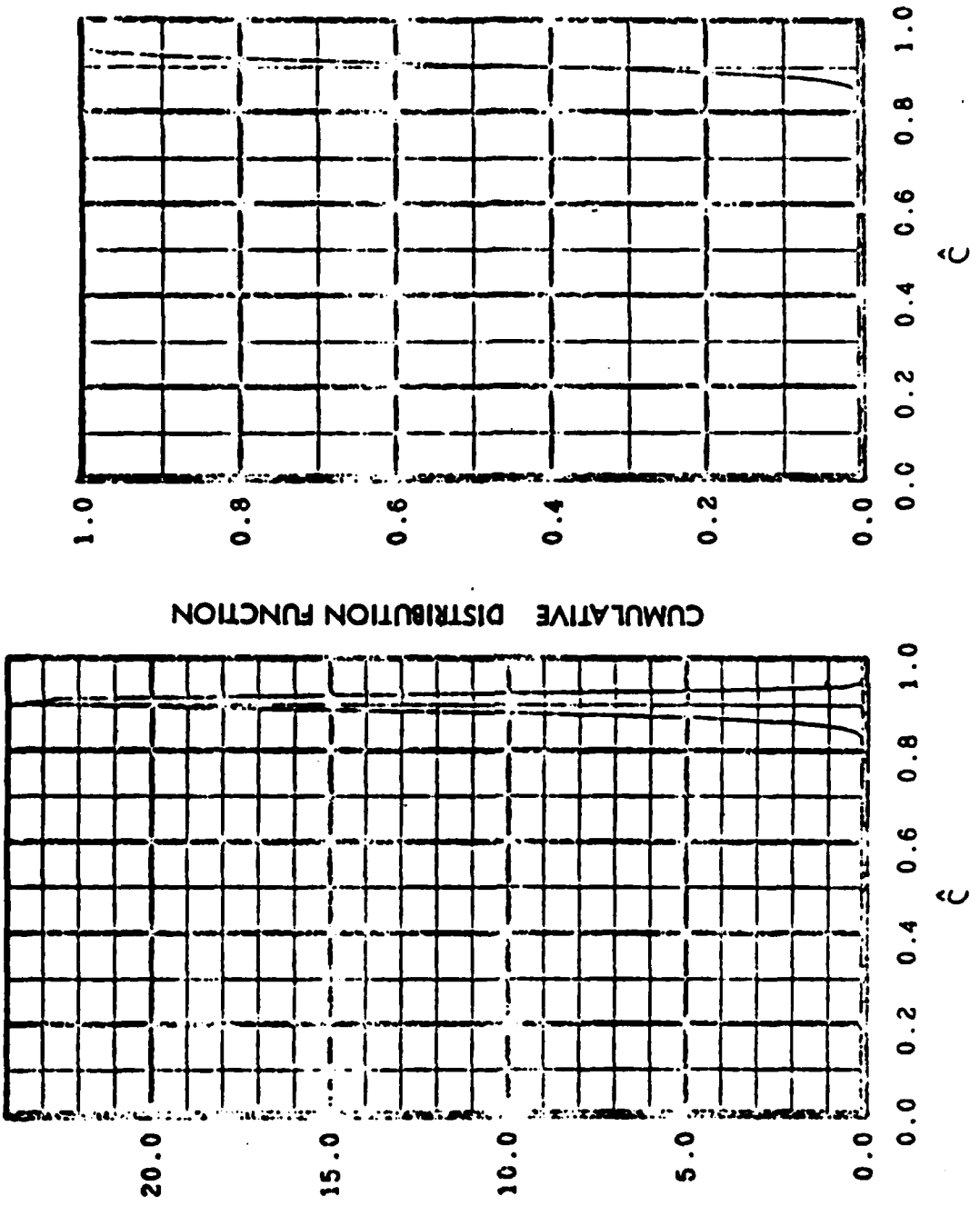

Figure 1h. PDF and CDF for n=64, C=0.9

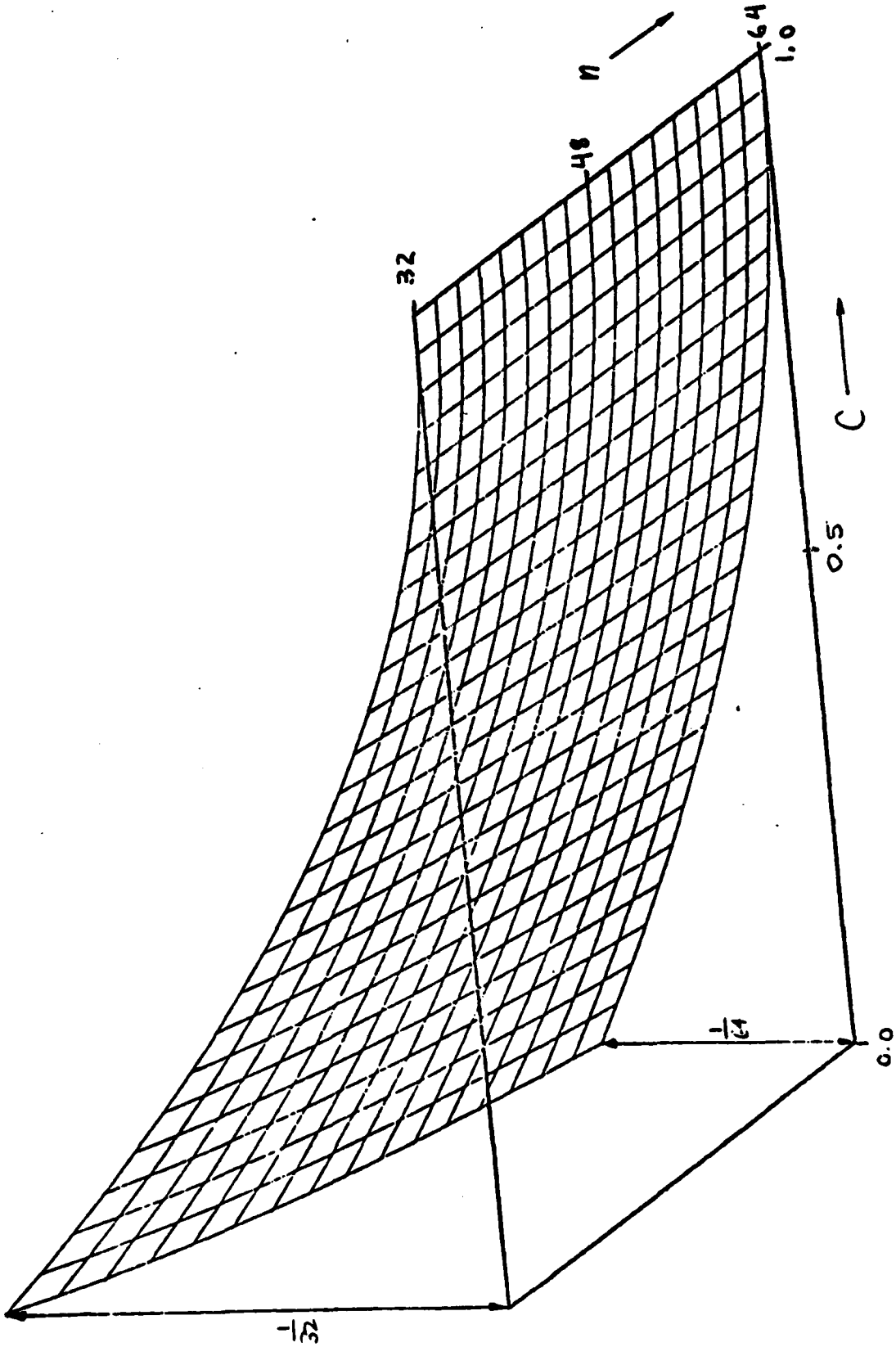

Figure 2. Bias of $\hat{C}$ versus n and C

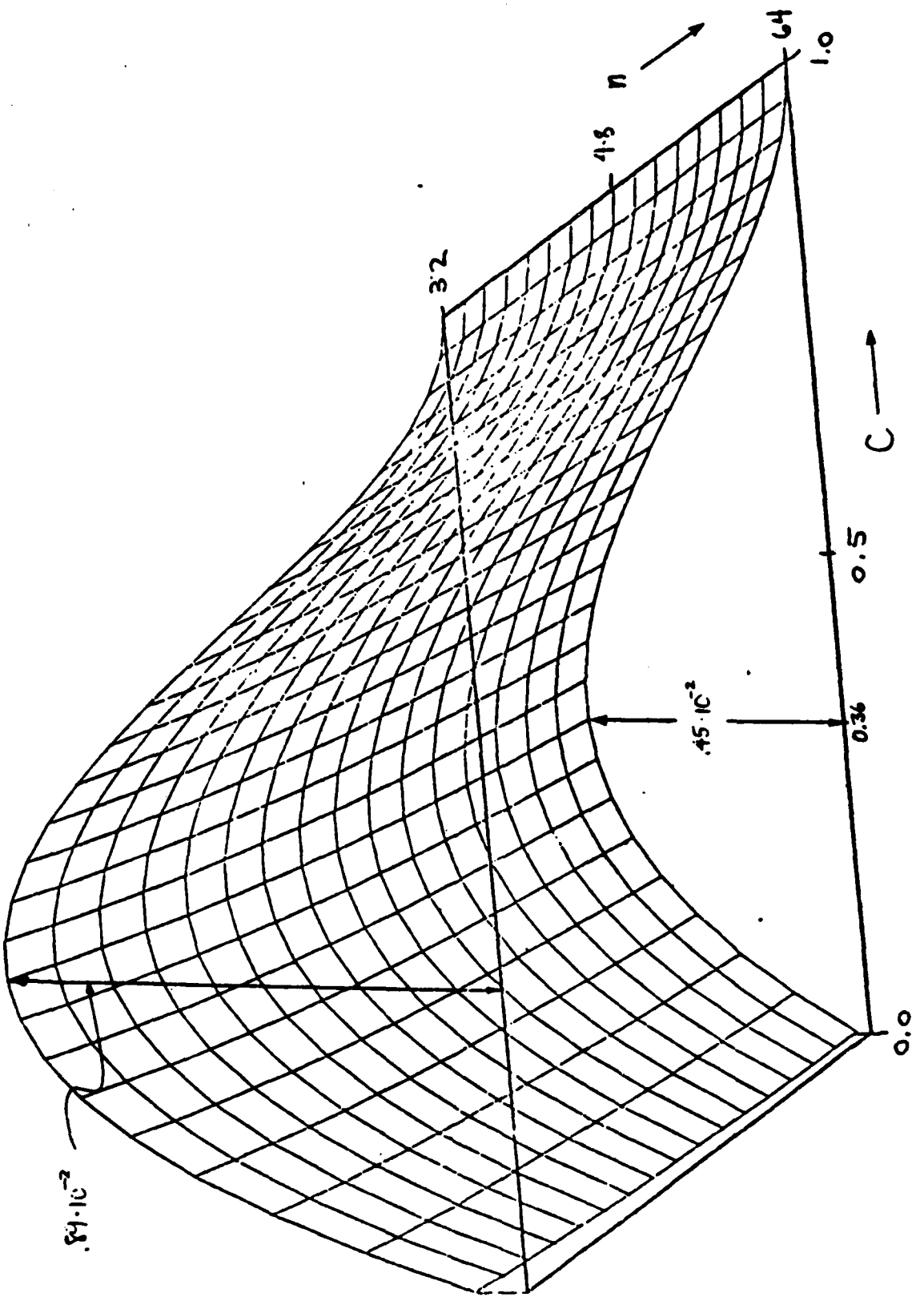

Figure 3. Variance of $\hat{C}$ versus n and C

REVERSE BLANK

APPENDIX

DETERMINATION OF CONFIDENCE INTERVALS FROM THE CUMULATIVE DISTRIBUTION FUNCTION

Let γ be the true value of an unknown parameter, and let $\hat{\gamma}$ be its estimate. $\hat{\gamma}$ is a random variable (RV) with a known probability density function (PDF) $p(\hat{\gamma};\gamma)$. (The conditioning on γ indicates that the shape of the PDF of $\hat{\gamma}$ depends on the exact (unknown) value of γ.)

Suppose we choose $A_L(\gamma)$ and $A_U(\gamma)$ such that

$$\text{Prob}\left(A_L(\gamma) < \hat{\gamma};\gamma\right) = \int_{A_L(\gamma)}^{\infty} d\hat{\gamma}\, p(\hat{\gamma};\gamma) = .95 \text{ (say)},$$

$$\text{Prob}\left(\hat{\gamma} < A_U(\gamma);\gamma\right) = \int_{-\infty}^{A_U(\gamma)} d\hat{\gamma}\, p(\hat{\gamma};\gamma) = .95 \text{ (say)}.$$

Then the probability that RV $\hat{\gamma}$ lies in the range $(A_L(\gamma), A_U(\gamma))$ is

$$\text{Prob}\left(A_L(\gamma) < \hat{\gamma} < A_U(\gamma);\gamma\right) = .9 .$$

Now assume that $A_L(\gamma)$ and $A_U(\gamma)$ are monotonically increasing with γ, and continuous. Then there follows

$$\text{Prob}\left(A_U^{-1}(\hat{\gamma}) < \gamma < A_L^{-1}(\hat{\gamma});\gamma\right) = .9 .$$

Therefore the confidence interval for γ is*

$$\left(A_U^{-1}(\hat{\gamma}), A_L^{-1}(\hat{\gamma})\right), \qquad \text{with confidence coefficient } .9.$$

Given a measurement $\hat{\gamma}$, this interval can be computed once the functions $A_U^{-1}(\cdot)$ and $A_L^{-1}(\cdot)$ are known.

*An excellent discussion of confidence intervals is given in Ref. 9, Chapter 34.

In order to evaluate these functions, consider the plot of the cumulative distribution function $P(A;\gamma)$,

$$P(A;\gamma) = \int_{-\infty}^{A} d\hat{\gamma}\, p(\hat{\gamma};\gamma),$$

versus A, for a particular value of γ, as indicated in Fig. 1. The

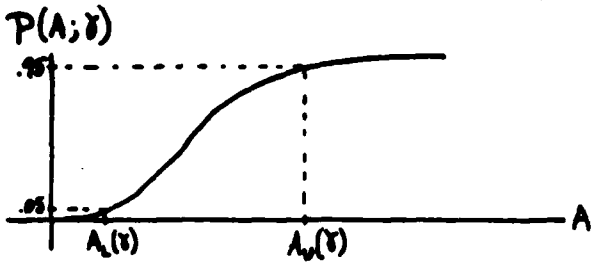

Fig. 1. Cumulative Distribution Function

points indicated on the abscissa enable determination of $A_L(\gamma)$ and $A_U(\gamma)$ for this value of γ. Now suppose $A_L(\gamma)$ and $A_U(\gamma)$ are plotted versus γ as indicated in Fig. 2. (This requires many plots like Fig. 1 for different values of γ.)

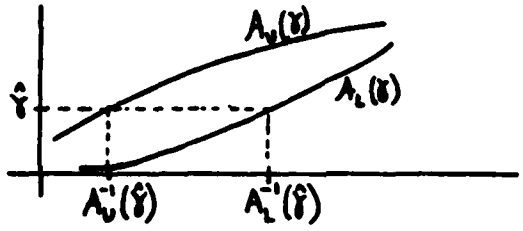

Fig. 2. Determination of Confidence Interval, for .9 Confidence Coefficient

Then given a value on the ordinate such as $\hat{\gamma}$, the points indicated on the abscissa of Fig. 2 are the confidence interval limits for .9 confidence coefficient.

The general results of this appendix apply immediately to coherence estimation when we identify γ as C, and $\hat{\gamma}$ as $\hat{C}$.

REFERENCES

1. Fisher, R. A. Contributions to Mathematical Statistics, Wiley, New York, 1950. (Chapter 14 originally published as "The General Sampling Distribution of the Multiple Correlation Coefficient," Proceedings of the Royal Society, Series A, Vol. 121, pp. 654-673, 1928)

2. Goodman, N. R., "On the Joint Estimation of the Spectra, CoSpectrum and Quadrature Spectrum of a Two Dimensional Stationary Process," Scientific Paper 10, NYU, New York, 1957 (AD 134 919).

3. Anderson, T. W., An Introduction to Multivariate Statistical Analysis, Wiley, New York, 1958.

4. Haubrich, Richard A., "Earth Noise 5 to 500 Millicycles per Second," Vol. 70, No. 6, Journal of Geophysical Research, March 1965, pp. 1415-1427.

5. Enochson, L. D. and Goodman, N. R., "Gaussian Approximations to the Distribution of Sample Coherence," Air Force Flight Dynamics Lab., Research and Tech. Div., AF Systems Command, Wright-Patterson AFB, Ohio, Bull. AFFDL-TR-65-67, June 1965 (AD620987).

6. Jenkins, Gwilym M. and Watts, Donald G., Spectral Analysis and Its Applications, Holden Day, San Francisco, California, 1968.

7. Benignus, Vernon A., "Estimation of Coherence Spectrum and Its Confidence Interval Using the Fast Fourier Transform," Vol. AU-17, No. 2, IEEE Transactions on Audio and Electroacoustics, June 1969.

8. Gradshteyn, I. S. and Ryzhik, I. M., Table of Integrals, Series, and Products, Academic Press, N.Y., 1965.

9. Cramér, Harald, Mathematical Methods of Statistics, Princeton University Press, Princeton, 1946.

NUSC Technical Memorandum TD113-19-71
22 November 1971

Some Practical Considerations of Coherence Estimation

G. C. Carter
C. R. Arnold

ABSTRACT

Given two processes, the complex coherence spectrum is the complex cross spectral density function divided by the square root of the product of the two auto spectral density functions.

Estimation of coherence in light of the fast Fourier transform (FFT) is investigated for synthetic data. The procedure used is to segment the given finite time histories to NSEG segments of size NNN. Each segment is multiplied by a weighting function (in this case a cosine bell) prior to computation of the FFT. Cross and auto spectra are then averaged over the NSEG segments prior to forming the coherence ratio.

Practical conclusions drawn are that for non-flat auto spectrum, multiplication by a weighting function is necessary, that NSEG must be on the order of 64, that NNN must be large enough to insure sufficient spectral resolution.

TABLE OF CONTENTS

INTRODUCTION

The coherence function is in some sense a normalized complex cross spectral density function. Specifically, given two processes, the coherence function is the complex cross spectral density function divided by the square root of the product of the auto spectral density functions of the two processes.

The coherence function can be used to determine a measure of statistical independence between two processes. When two processes are independent, their correlation function is zero. Hence the cross spectral density function (numerator of the coherence) is zero and so is the coherence.

The coherence can also be used to determine a measure of a linear relationship between two processes. If the two processes happen to be the input and the output from a general system, the magnitude squared coherence is a measure of the linearity of the system. Thus if a good estimate of coherence could be obtained, it would be a useful statistic in measuring the linearity of a system.

The estimation procedure, like most spectral analysis computations, is rather straightforward in implementing, but often subtle, and indeed difficult, in proper interpretation. A minimum requirement for its interpretation is an appreciation for spectral analysis techniques.

To illustrate some of the problems and pitfalls in coherency estimation, the authors have simulated various synthetic signals and input/outputs. The results are most illuminating, and add insight to coherence estimation procedures.

II. THE COHERENCE FUNCTION

II.A. Definition

The coherence function is in some sense a normalized complex cross spectral density function. Given two processes $x(t)$ and $y(t)$ with auto power spectral density functions $\mathbf{S}_x(f)$ and $\mathbf{S}_y(f)$, respectively, and complex cross spectral

density function $\Phi_{xy}(f)$, then the complex coherence function is defined as in reference (a) by:

$$\gamma(f) = \frac{\Phi_{xy}(f)}{\sqrt{\Phi_x(f)\,\Phi_y(f)}} \qquad \text{Eq. (1)}$$

and the magnitude squared coherence function as

$$|\gamma(f)|^2 = \frac{|\Phi_{xy}(f)|^2}{\Phi_x(f)\,\Phi_y(f)} \qquad \text{Eq. (2)}$$

II.B. Squared Coherence as a Measure of System Linearity

If we consider the linear system with input, x(t), impulse response h(t), and output y(t), as follows:

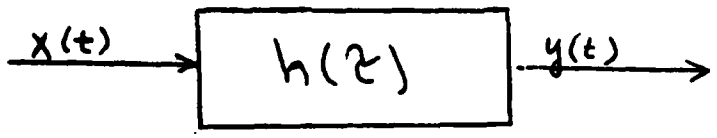

Fig. (1)

then the output, y(t), is obtained by the convolution integral

$$y(t) = \int_{-\infty}^{\infty} h(\tau)\, x(t-\tau)\, d\tau$$

The frequency domain equivalent is a multiplication, namely,

$$Y(f) = H(f)X(f)$$

where the transformation from the time domain to frequency domain is via the Fourier integral:

$$Z(f) = \int_{-\infty}^{\infty} z(t)\, e^{-j2\pi ft}\, dt$$

From reference (a) we know that

$$H(f) = \frac{\Phi_{xy}(f)}{\Phi_x(f)}, \quad \Phi_x(f) \neq 0 \qquad \text{Eq. (3)}$$

and also that

$$\Phi_y(f) = |H(f)|^2 \Phi_x(f),$$

that is,

$$\Phi_y(f) = H(f)H^*(f)\Phi_x(f),$$

where * indicates complex conjugation. Substituting for H(f), we see that

$$\Phi_y(f) = \frac{\Phi_{xy}(f)}{\Phi_x(f)} H^*(f) \Phi_x(f),$$

that is,

$$\Phi_y(f) = \Phi_{xy}(f) H^*(f),$$

or conjugating both sides, we see that

$$\Phi_y^*(f) = \Phi_{xy}^*(f) H(f),$$

but $\Phi_y(f)$ is real so that

$$\frac{1}{H(f)} = \frac{\Phi_{xy}^*(f)}{\Phi_y(f)}. \qquad \text{Eq. (4)}$$

Now equation (2) can be rewritten as

$$|\gamma(f)|^2 = \frac{\Phi_{xy}(f)\,\Phi_{xy}^*(f)}{\Phi_x(f)\Phi_y(f)} \qquad \text{Eq. (5)}$$

Substituting from equations 3 and 4, we see

$$|\gamma(f)|^2 = H(f)\frac{1}{H(f)} = 1. \qquad \text{Eq. (6)}$$

Thus for the assumptions made, namely that the system is linear, we have $|\gamma(f)|^2 = 1$. If $|\gamma(f)|^2$ is not equal to 1, then either the observations of x(t) and y(t) have been corrupted in some manner by noise or our assumption was in error and the system is nonlinear.

This could be expressed as a theorem: If a system is linear, then the coherence between the input and output is equal to unity.

III. THE COHERENCE ESTIMATOR

III.A. Definition

While several references (e.g., (a), (b), (c), (d), and (e)) introduce the coherence function, only a few (references (b), (c), (d), (e)) address its estimation.

The method implemented for obtaining good coherence estimation is explained below. Briefly it consists of obtaining two finite time series from the random processes being investigated and segmenting these time series into NSEG segments.

The NSEG pieces may be either "overlapped" or "disjoint" from other segments. Each piece is comprised of NNN data points. A weighting or windowing function is then applied to each piece and the fast Fourier transform (FFT) of the weighted NNN point sequence is performed. The Fourier coefficients for the p-th weighted piece are then used to compute the two auto and the co- and quad-spectral estimates which are then averaged over all NSEG pieces. The coherence function is then finally computed from a ratio of the average spectral estimates. (Note for real data NSEG number of FFT's must be computed each of complex size NNN.)

Specifically, let $\hat{\Phi}_{xy}(f_k)$ denote the estimate of the power spectral density (PSD) function at the k-th frequency, f_k, obtained from the p-th weighted segment of size NNN of

the stationary random process x(t). Similarly, let $\hat{\Phi}_{yy}(f_k)$ be the estimate of the PSD function of the stationary random process y(t). Also, let $\hat{C}_p(f_k)$ and $\hat{Q}_p(f_k)$ denote respectively the real (co-) and imaginary (quad-) part of the estimate of the complex cross-spectral density function of the two processes. The estimate of the magnitude squared coherence function implemented by the authors is given by:

$$|\hat{\gamma}(f_k)|^2 = \frac{\left[\sum_{p=1}^{NSEG} \hat{C}_p(f_k)\right]^2 + \left[\sum_{p=1}^{NSEG} \hat{Q}_p(f_k)\right]^2}{\left[\sum_{p=1}^{NSEG} \hat{\Phi}_{x_p}(f_k)\right]\left[\sum_{p=1}^{NSEG} \hat{\Phi}_{y_p}(f_k)\right]} \qquad \text{Eq. (7)}$$

where the circumflex denotes estimate and NSEG is the number of weighted segments (overlapped or disjoint) over which the estimates are averaged.

Because the squared coherence estimator is the ratio of random variables, it is imperative that good spectral estimates of C(f), Q(f), $\Phi_x(f)$ and $\Phi_y(f)$ be obtained. Random fluctuations and bias of any of the four spectral estimators become significant in the ratio used to estimate the coherence function.

III.B. The Computer Implementation

NUSC FORTRAN program designated S1741 implements eq. (7). A capsulized flowchart of the program's basic version is presented in Figure 2. Specific input parameters include: DT, the basic increment in time between samples; NSEG, the number of segments of data; and NNN, the FFT size. Programmable options include DC removal, linear trend removal, different

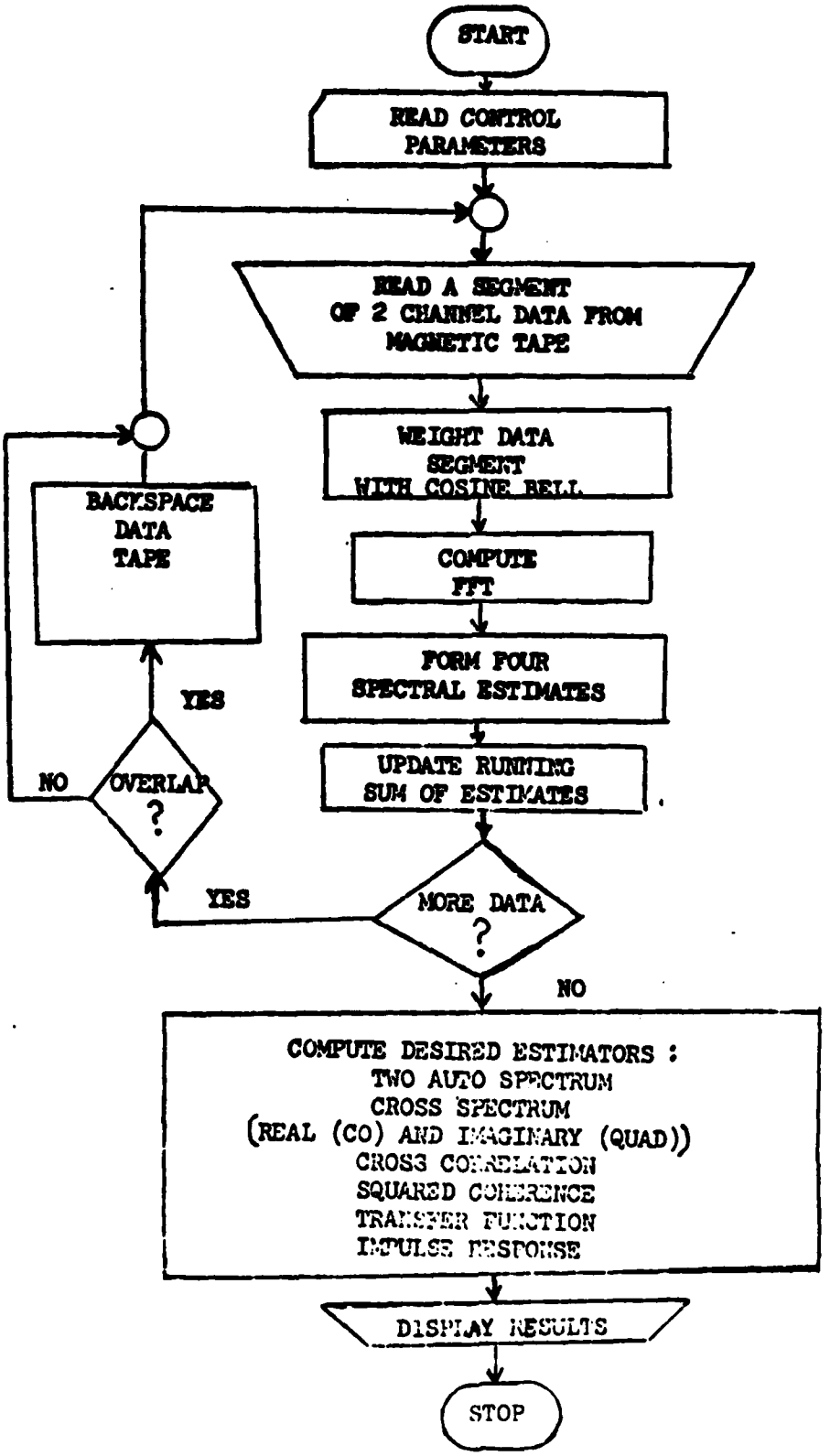

Figure 2. Summary Flow Chart for Basic Version of NUSC S-1741. FFT Spectrum Analysis Program

weighting functions, overlapped processing, IGS plots, and printer displays.

The program's modularized nature, together with its all-FORTRAN implementation, has made updates and modifications straightforward to fill many Center requirements. The fast Fourier transform (FFT) was coded by R. S. Singleton (reference (i)). The cosine weighting function was coded by A. H. Nuttall of NUSC.

III.C. Choice of Program Parameters and Options

III.C.1. Windowing the Data Segments

The first program option is the application of a window or weighting function. The ideal FFT resolution, Δf, specified by 1/(DT*NNN) cannot be achieved without a phenomenon known as leakage taking place (reference (f)). This is due to the non-ideal bandpass characteristics of the FFT's when considered as a bank of filters. When an NNN point sequence is multiplied by a rectangular window (no weighting), the transfer function for each FFT filter is sin(x)/x. Therefore, each FFT filter centered at a specific frequency sees energy not only from the band about that frequency but also from frequency bands not desired.

This leakage results in biased estimators $\hat{\Phi}_{xx}(f_k)$, $\hat{\Phi}_{yy}(f_k)$, $\hat{C}_{xy}(f_k)$, and $\hat{Q}_{xy}(f_k)$. This bias becomes a critical factor in coherence estimation because it is then a ratio of biased estimators. This is well illustrated in the example cases in the next section.

A technique to reduce leakage, and hence the bias, is to window each segment of time history by multiplying it by a data window. The authors have implemented a cosine bell window which is equivalent to convolving the complex discrete Fourier coefficients with the weights (-1/4, 1/2, -1/4). (Different windows are also available, such as cubic and quartic.) Discussion of the merits of various windows to be selected is beyond the scope of this paper, but the important fact is that some windowing is required to reduce leakage.

Windowing, however, results in poorer frequency resolution; that is, of the effective frequency resolution, Δf_{eff}

becomes greater by a multiplicative factor K, dependent on the window. That is,

$$\Delta f_{eff} = K \cdot \Delta f$$

and K is approximately 1.44 for the cosine bell window when measured at the half power point.

III.C.2. Averaging the Spectral Estimators

The second choice of program parameters involves selection of NSEG, the number of segments of data and NNN, the FFT size. Given time series data limited in time and representative of two random processes, let each time series consist of NTS samples. Then, for non-overlapped segments, the total number of samples, NTS, can only be partitioned as:

$$NTS = NNN * NSEG \qquad \text{Eq. (8)}$$

It is easy to see but important to note that, for a fixed value of NTS, NNN can only be increased at the expense of decreasing NSEG, and vice versa.

Recall that the frequency resolution must be made fine enough to encompass all the detail of the data's true spectrum. Note that if fine resolution is required, then the FFT size, NNN, must be made large, and for a fixed total number of samples, NTS, the number of disjoint segment NSEG becomes small.

A small value for NSEG leads to two serious problems: low stability and biased cross power spectrum. For a fixed value of NTS, NSEG can be increased at the expense of decreasing NNN. This results in better stability and low bias in the cross spectrum but poorer resolution. Small NSEG implies less averaging of the numerator and denominator of the coherence ratio. This is most important in terms of serious positive bias problems. The bias problem is easy to see when x(t) and y(t) are uncorrelated. Recall that if x(t) and y(t) are uncorrelated, the cross correlation function is zero for all lags and its Fourier transform yields the complex cross spectral density which is zero for all frequencies. Hence the true coherence is zero for all frequencies. However, when no averaging is done (i.e., NSEG = 1), then the estimate of coherence (eq. (7)) can be shown to be unity. This serious positive bias can be shown to decrease as the amount of averaging increases.

Clearly there is a trade-off between the selection of NNN and NSEG. For a fixed value of NTS, NNN can not be increased without decreasing NSEG, and NSEG can not be increased without decreasing NNN. The important point, though, is that parameter selection for high resolution and stable estimates is at cross purposes.

IV. THE EXAMPLE CASES

Six examples are enclosed to illustrate coherence estimation. The first example illustrates estimating coherence for two independent noise sources. The remaining five examples illustrate estimating coherence for system input/output relations. The plot labels of the spectral estimates for the system input is "A/PHIX," for the output is "A/PHIY," for the transfer gain characterisitics is "MODH2," and for the phase characteristics is "PHASE".

IV.A. Independent Noise Case

The coherence between two independent noise sources is estimated by averaging more and more disjoint segments. The following set of figures illustrates the resulting coherence estimates for NSEG = 2, 4, 8, 16, 32, 64, 128, and 256. The results are most useful and concur with work by Haubrich, reference (d); Benignus, reference (e); and Carter and Nuttall, reference (j). Recall that independent noise sources are uncorrelated, and therefore the inverse Fourier transform of the cross correlation function is zero for all frequencies. The positive bias associated with estimating the numerator of the coherence ratio is illustrated. Note that as the averaging increases, this type bias decreases and the estimate of coherence approaches the true value. By averaging over 64 segments, the authors achieve what can be considered an acceptable "estimate" of squared coherence when the true coherence is zero.

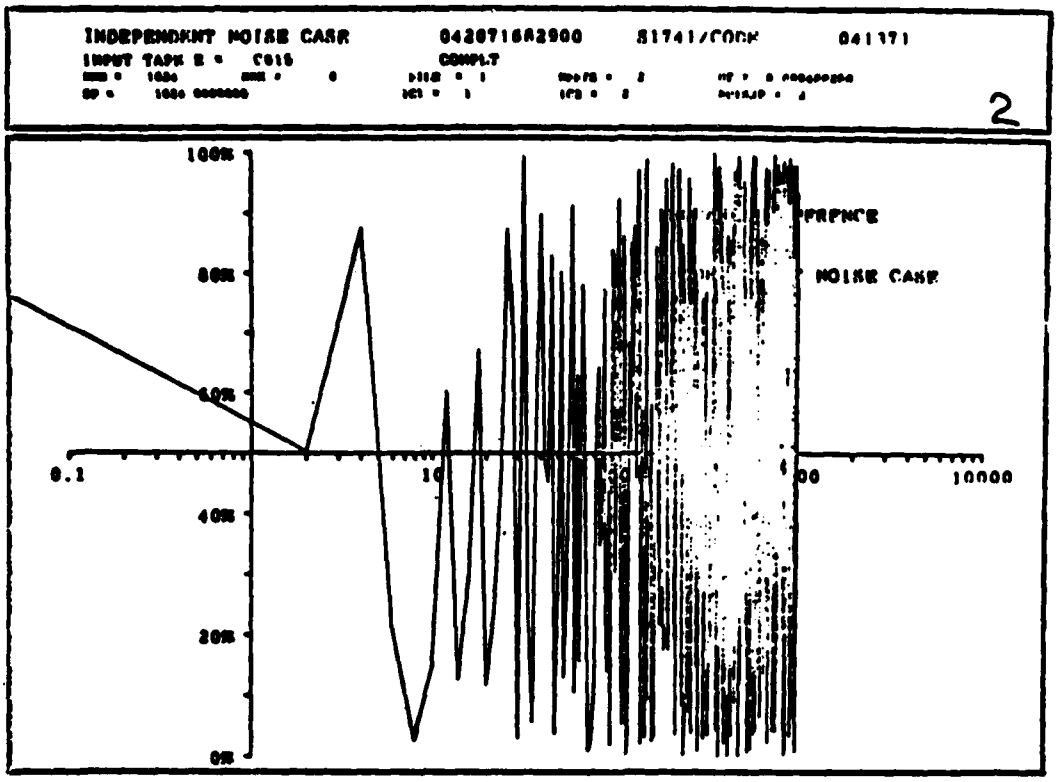
INDEPENDENT NOISE CASE
042071682900
S1741/CODR
041371
INPUT TAPE 8 = C015
COMPLT
2
100%
80%
60%
40%
20%
0%
0.1
10
100
1000
10000
FRENCE
NOISE CASE

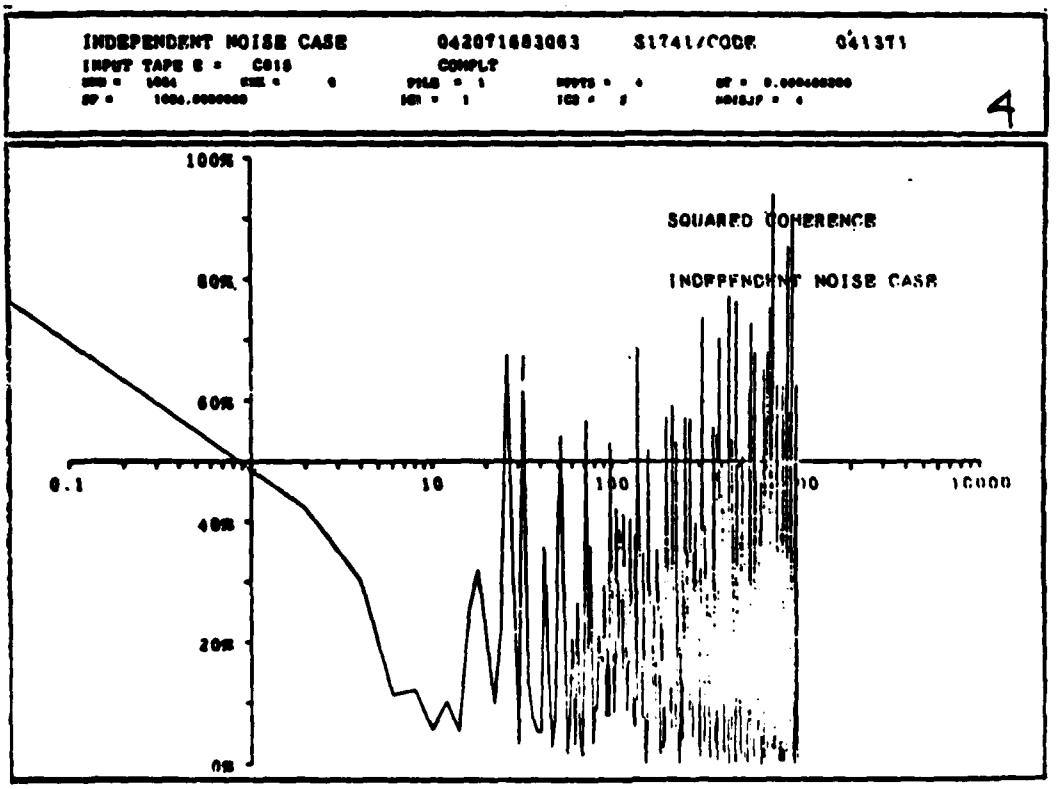
INDEPENDENT NOISE CASE
042071683063
S1741/CODR
041371
INPUT TAPE 8 = C015
COMPLT
4
100%
80%
60%
40%
20%
0%
0.1
10
100
1000
10000
SQUARED COHERENCE
INDEPENDENT NOISE CASE

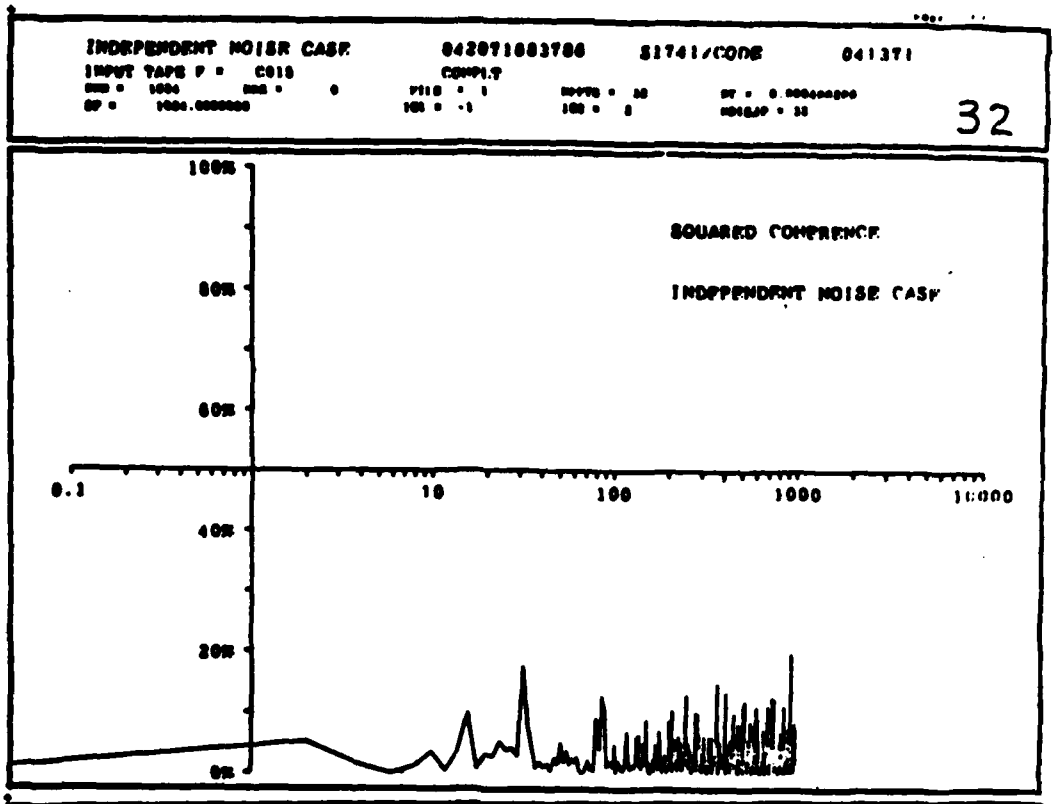
INDEPENDENT NOISE CASE
042071883786
S1741/CODE
041371
INPUT TAPE F = C015
COMPLT
32
100%
80%
60%
40%
20%
0%
0.1
10
100
1000
10000
SQUARED COHERENCE
INDEPENDENT NOISE CASE

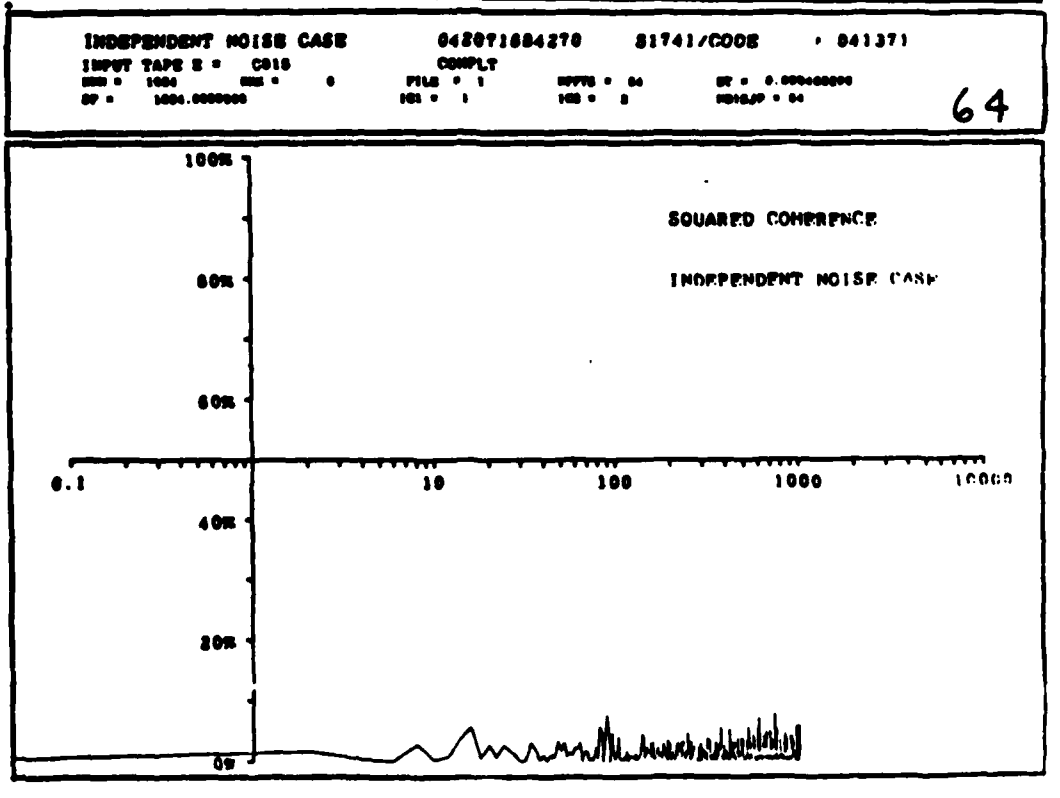
INDEPENDENT NOISE CASE
042071884270
S1741/CODE
041371
INPUT TAPE E = C015
COMPLT
64
100%
80%
60%
40%
20%
0%
0.1
10
100
1000
SQUARED COHERENCE
INDEPENDENT NOISE CASE

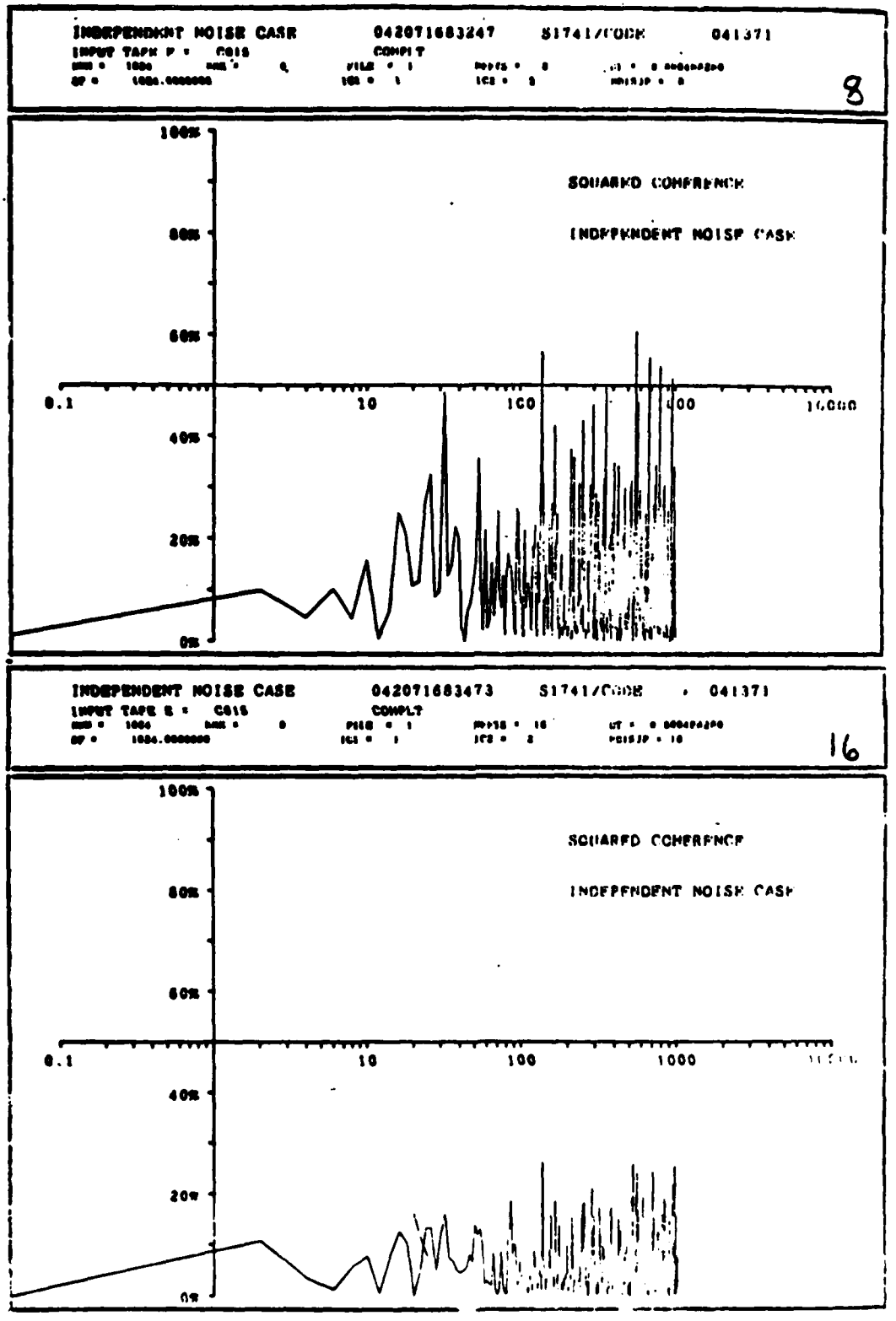
INDEPENDENT NOISE CASE
042071683247
S1741/CODE
041371
COMPLT
8
SQUARED COHERENCE
INDEPENDENT NOISE CASE
100%
80%
60%
40%
20%
0%
0.1
10
100
1000
INDEPENDENT NOISE CASE
042071683473
S1741/CODE
041371
COMPLT
16
SQUARED COHERENCE
INDEPENDENT NOISE CASE
100%
80%
60%
40%
20%
0%
0.1
10
100
1000

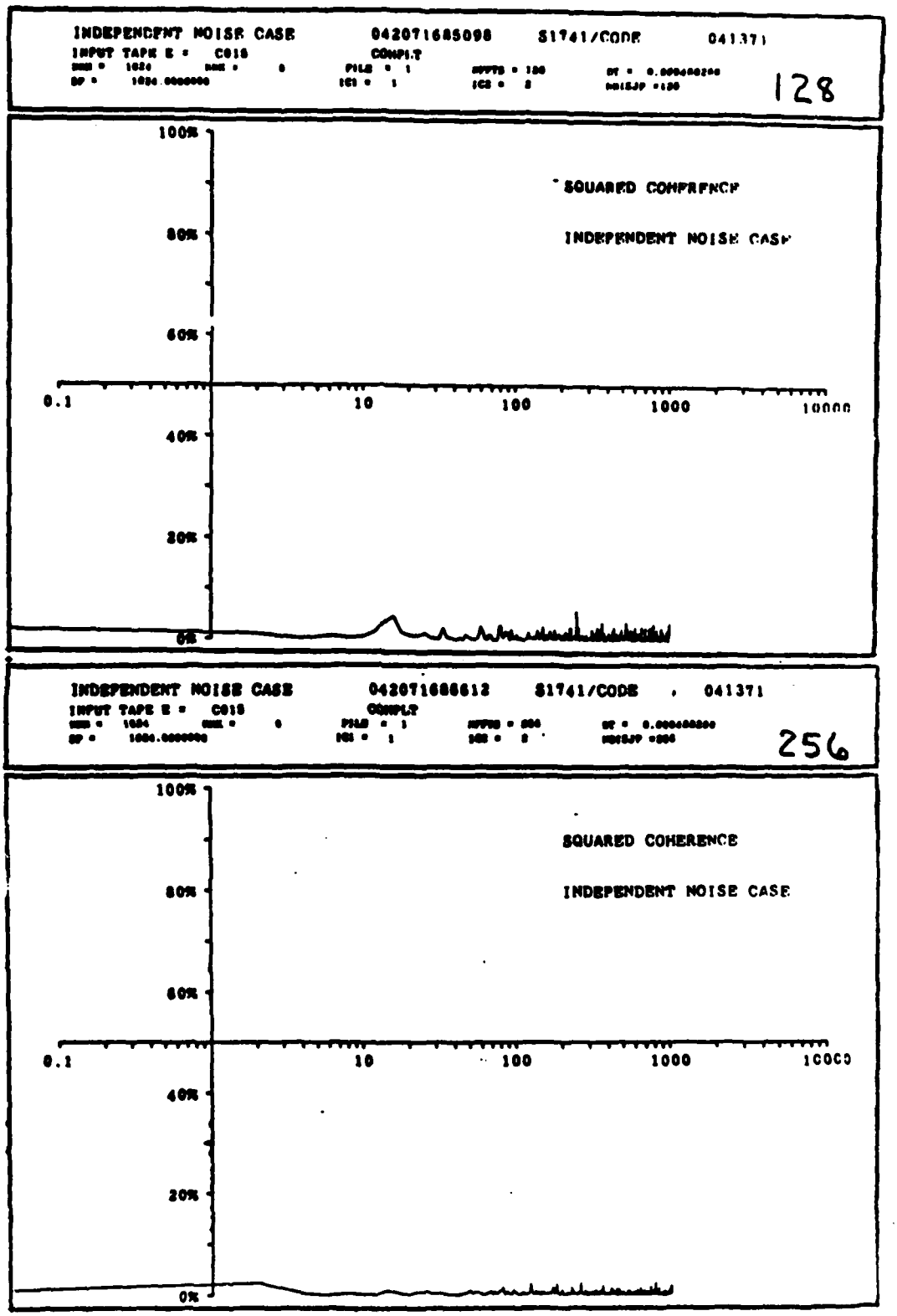
INDEPENDENT NOISE CASE
042071685098
S1741/CODE
041371
INPUT TAPE E = C015
COMPLT
128
100%
80%
60%
40%
20%
0%
0.1
10
100
1000
10000
SQUARED COHERENCE
INDEPENDENT NOISE CASE
INDEPENDENT NOISE CASE
042071686612
S1741/CODE
041371
INPUT TAPE E = C015
COMPLT
256
100%
80%
60%
40%
20%
0%
0.1
10
100
1000
SQUARED COHERENCE
INDEPENDENT NOISE CASE

IV.B. Smooth Filter Case

White Gaussian noise (flat spectrum) is filtered by the first order, low pass, digital filter specified by the recursion equation

$$Y_n = 7/8\ Y_{n-1} + 1/8\ X_n$$

The enclosed plots show the auto spectra of X and Y and the modulus (gain) and phase characteristics of the filter. The coherence estimate of the filter is 100% for all frequencies.

Note that the estimator is unbiased (since the true coherence is 100%) and has zero variance. This behavior of the coherence estimator was predicted by Benignus (ref. (e)), Carter and Nuttall (ref. (k)), and Carter (ref. (l)).

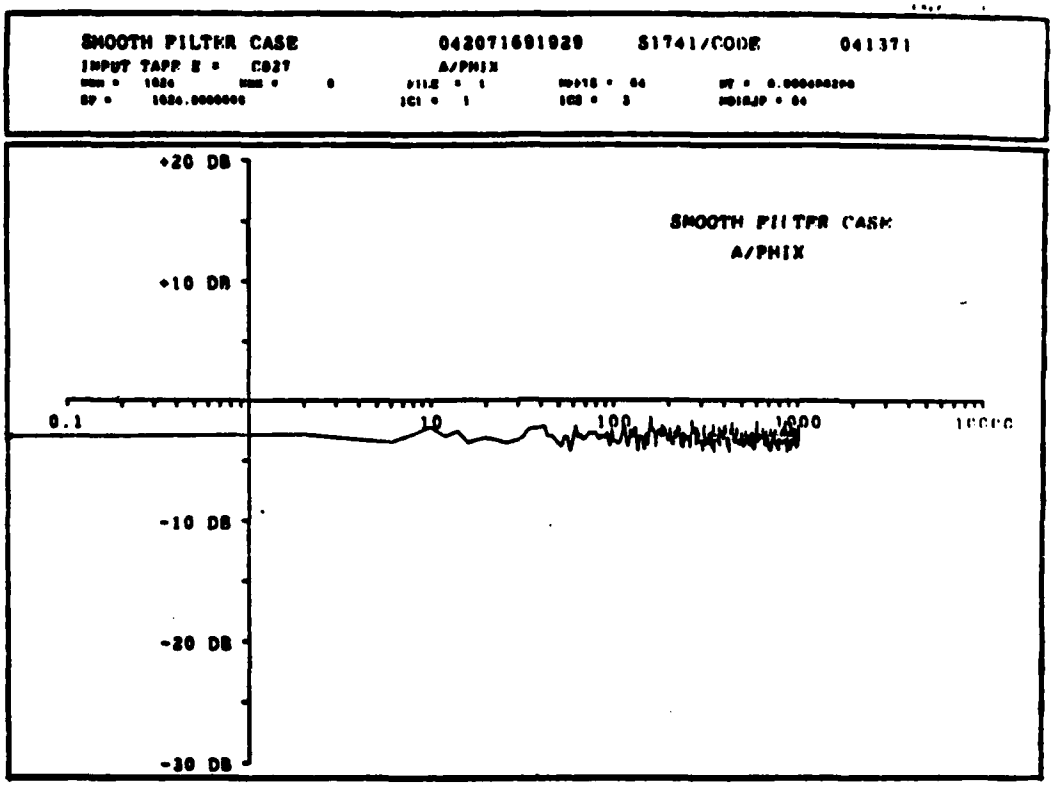
SMOOTH FILTER CASE 042071691929 S1741/CODE 041371
INPUT TAPE 8 = C027 A/PHIX
+20 DB
+10 DB
-10 DB
-20 DB
-30 DB
0.1
10
100
1000
SMOOTH FILTER CASE
A/PHIX

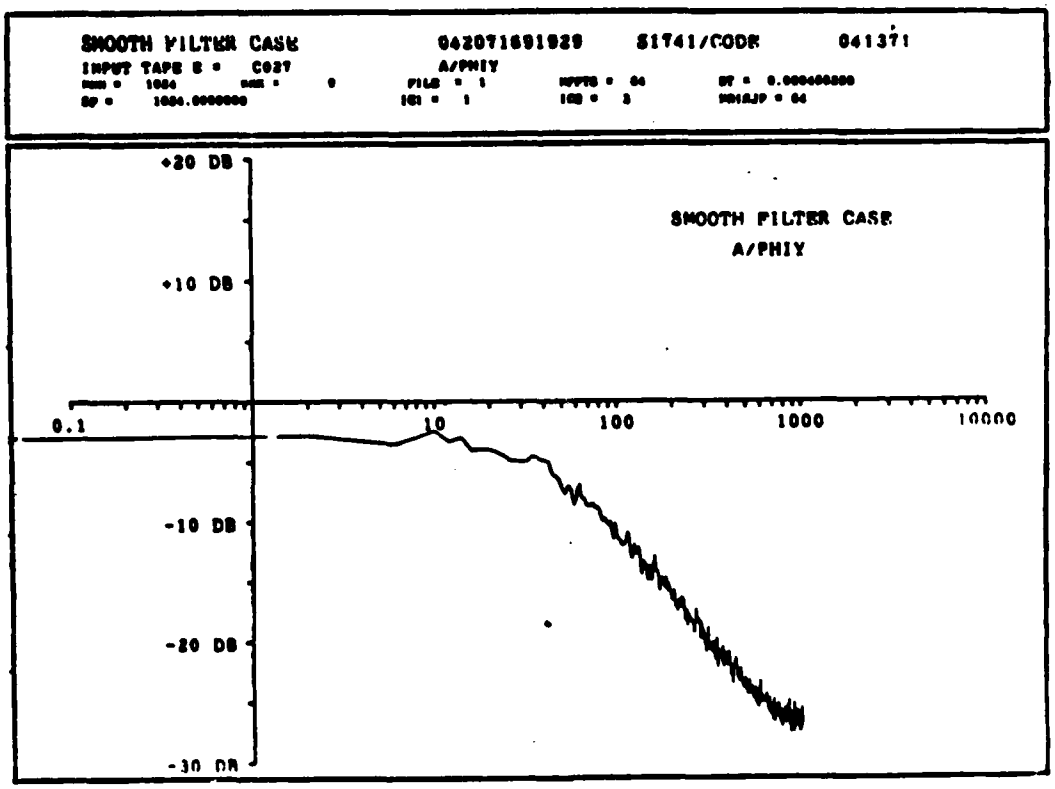
SMOOTH FILTER CASE 042071691929 S1741/CODE 041371
INPUT TAPE 8 = C027 A/PHIY
+20 DB
+10 DB
-10 DB
-20 DB
-30 DB
0.1
10
100
1000
10000
SMOOTH FILTER CASE
A/PHIY

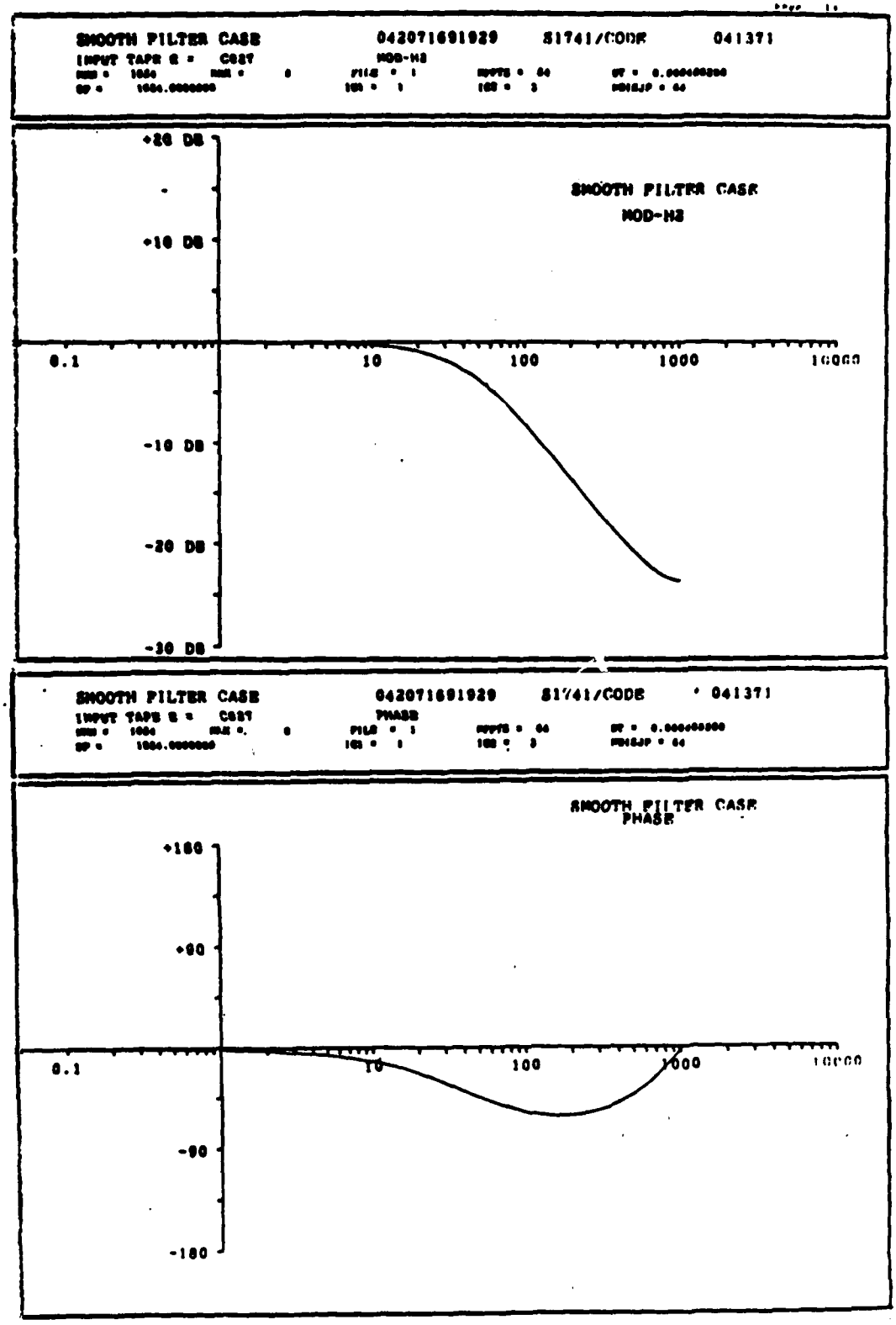
SMOOTH FILTER CASE 042071691929 S1741/CODE 041371
INPUT TAPE 2 = CSST MOD-H3
+20 DB
+10 DB
-10 DB
-20 DB
-30 DB
SMOOTH FILTER CASE
MOD-H3
0.1
10
100
1000
SMOOTH FILTER CASE 042071691929 S1741/CODE 041371
INPUT TAPE 2 = CSST PHASE
SMOOTH FILTER CASE
PHASE
+180
+90
-90
-180
0.1
10
100
1000

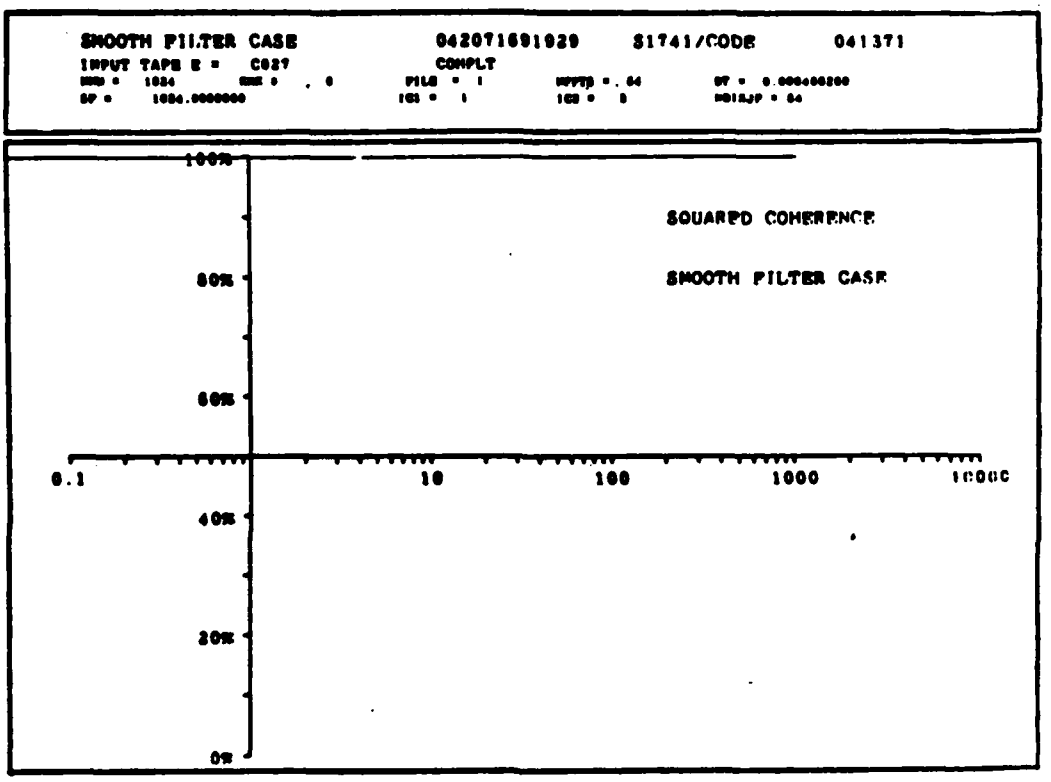
SMOOTH FILTER CASE
042071691929
S1741/CODE
041371
INPUT TAPE E = C027
COMPLT
100%
80%
60%
40%
20%
0%
0.1
10
100
1000
10000
SQUARED COHERENCE
SMOOTH FILTER CASE

The symmetry of the coherence function is also illustrated by designating y as the filter input and x as the filter output.

SMOOTH FILTER CASE		042371331133	S1741/CODP	041371
INPUT TAPE F = C027		COVER		
[illegible] = 1024	[illegible] = 5	[illegible] = 1	[illegible] = 64	[illegible] = [illegible]
SP = 1024.0000000		IC1 = 3	IC2 = 1	[illegible] = 64

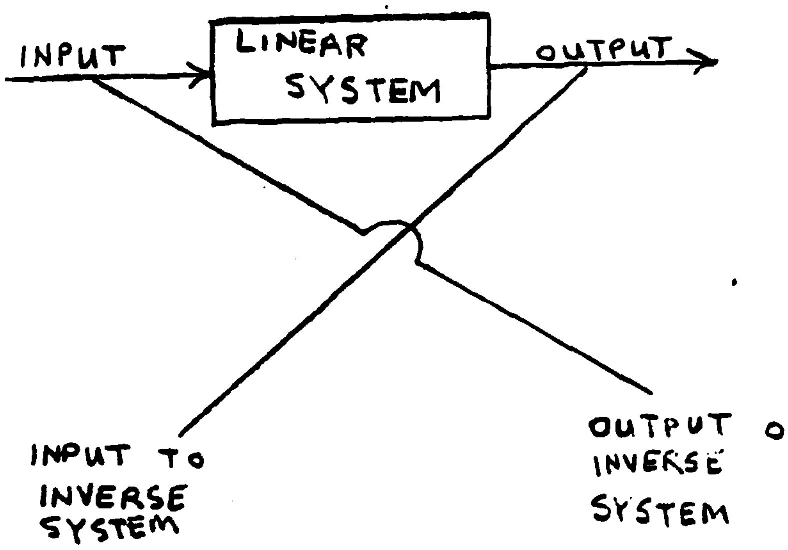

Quite naturally the estimates of the filter characteristics change. Note, though, that the coherence, being symmetric, does not change.

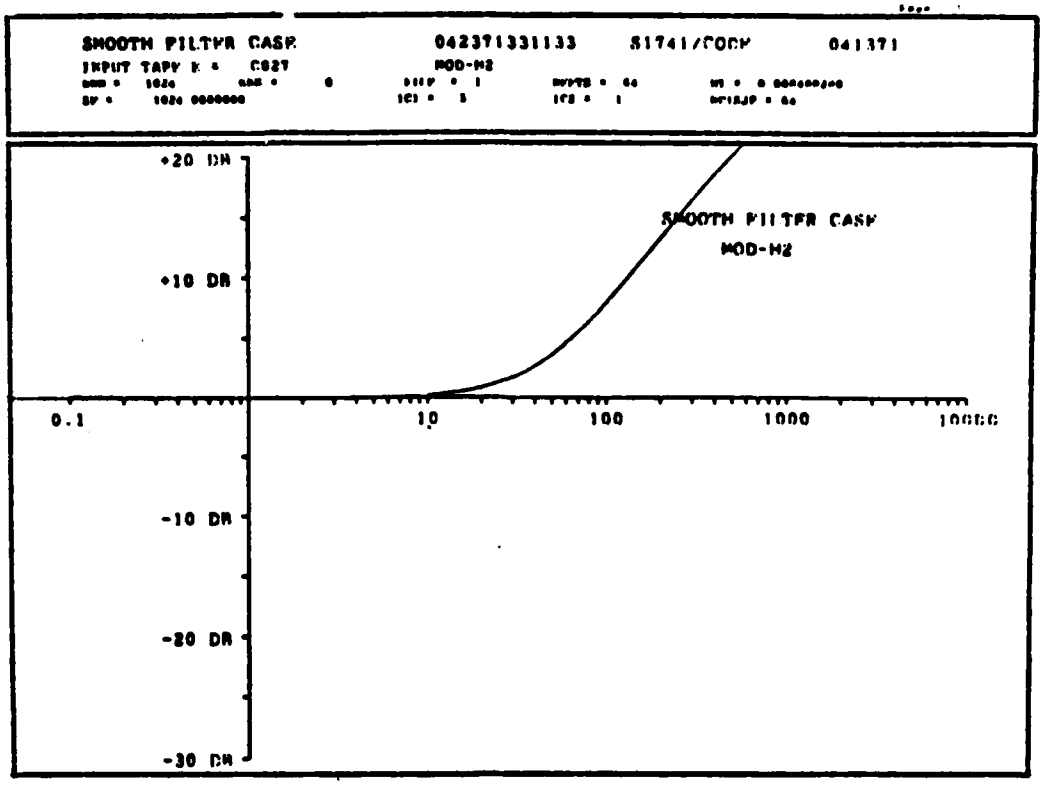
SMOOTH FILTER CASE
042371331133
MOD-M2
+20 DB
+10 DB
-10 DB
-20 DB
-30 DB
0.1
10
100
1000
10000
SMOOTH FILTER CASE
MOD-M2

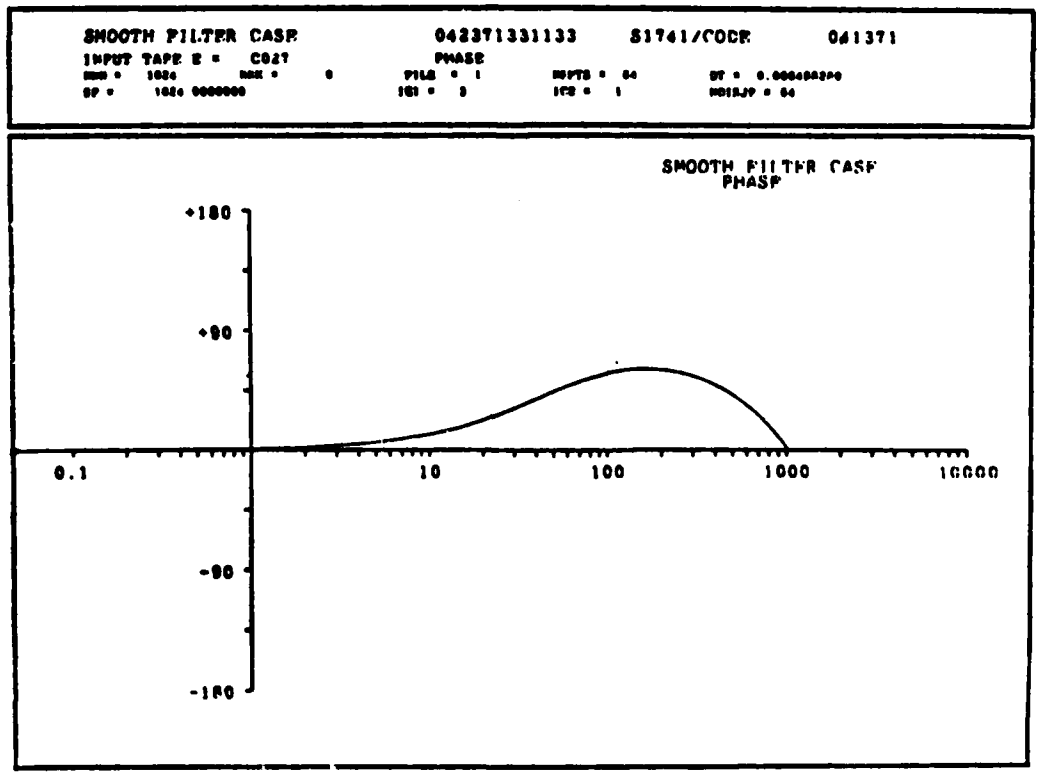
SMOOTH FILTER CASE
042371331133
PHASE
+180
+90
-90
-180
0.1
10
100
1000
10000
SMOOTH FILTER CASE
PHASE

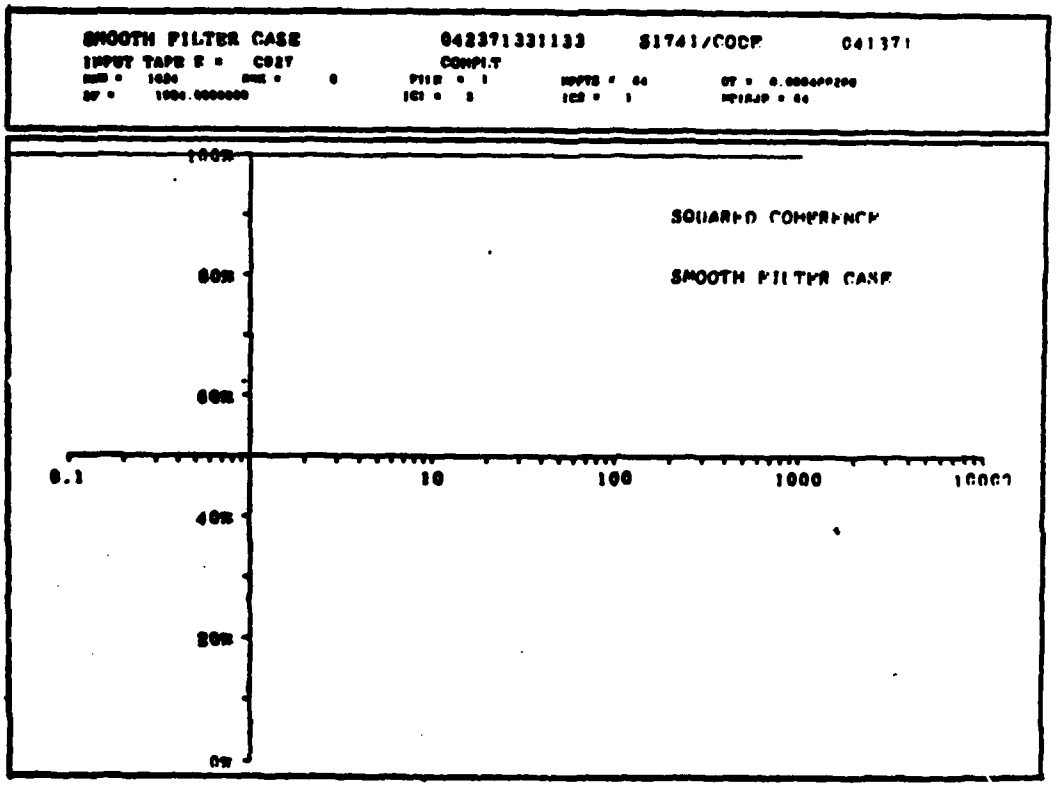
SMOOTH FILTER CASE
042371331133
S1741/COCP
041371
INPUT TAPE 2 = C027
COMPLT
SQUARED COHERENCY
SMOOTH FILTER CASE
100%
80%
60%
40%
20%
0%
0.1
10
100
1000

IV.C. Sharp Filter Case

IV.C.1. With Weighting Function

White Gaussian noise (flat spectrum) is filtered by the second order low pass digital filter specified by the recursion equation:

$$Y_n = AY_{n-1} + BY_{n-2} + CX_n$$

where

A = 1.97330
B = -0.98202
C = 0.00872

The plot labeled "A/PHIY" shows the spectrum of the filter output. The modulus and phase of the filter are displayed (Note: the band of sharp resonance and rapidly phase change at 30 Hz). The true coherence is 100%. The estimate of squared coherence is given and fails in the band of poor resolving power (relative to true spectrum). This is a different type of bias than previously discussed. It can be most severe when estimating coherence. This behavior of the coherence estimator was predicted by Jenkins and Watts (ref. (c)).

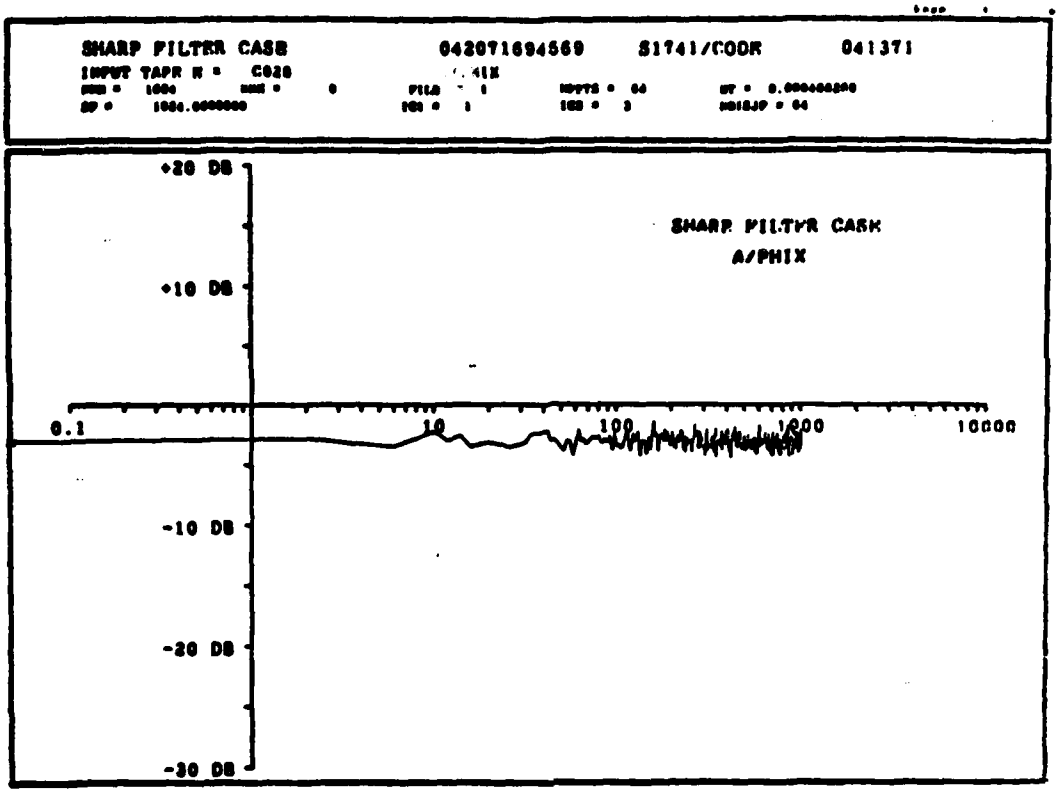
SHARP FILTER CASE
042071694569
S1741/CODR
041371
INPUT TAPE N = C028
A/PHIX
+20 DB
+10 DB
-10 DB
-20 DB
-30 DB
0.1
10
100
1000
10000
SHARP FILTER CASE
A/PHIX

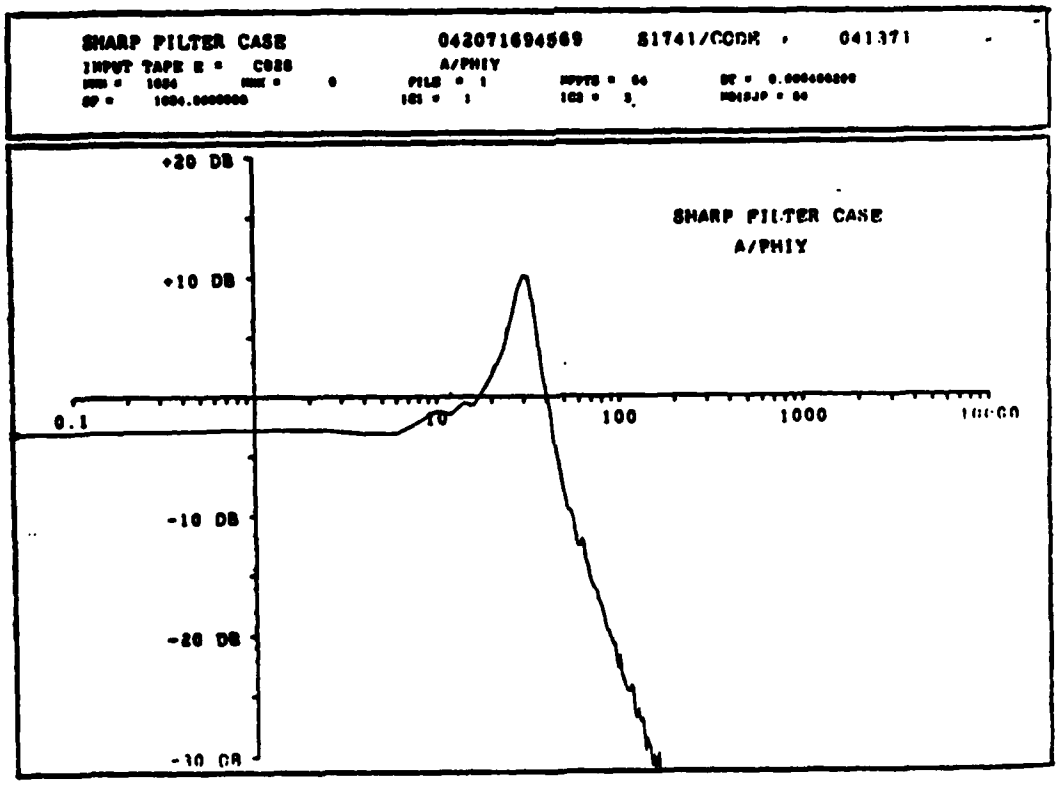
SHARP FILTER CASE
042071694569
S1741/CODR
041371
INPUT TAPE N = C028
A/PHIY
+20 DB
+10 DB
-10 DB
-20 DB
0.1
10
100
1000
SHARP FILTER CASE
A/PHIY

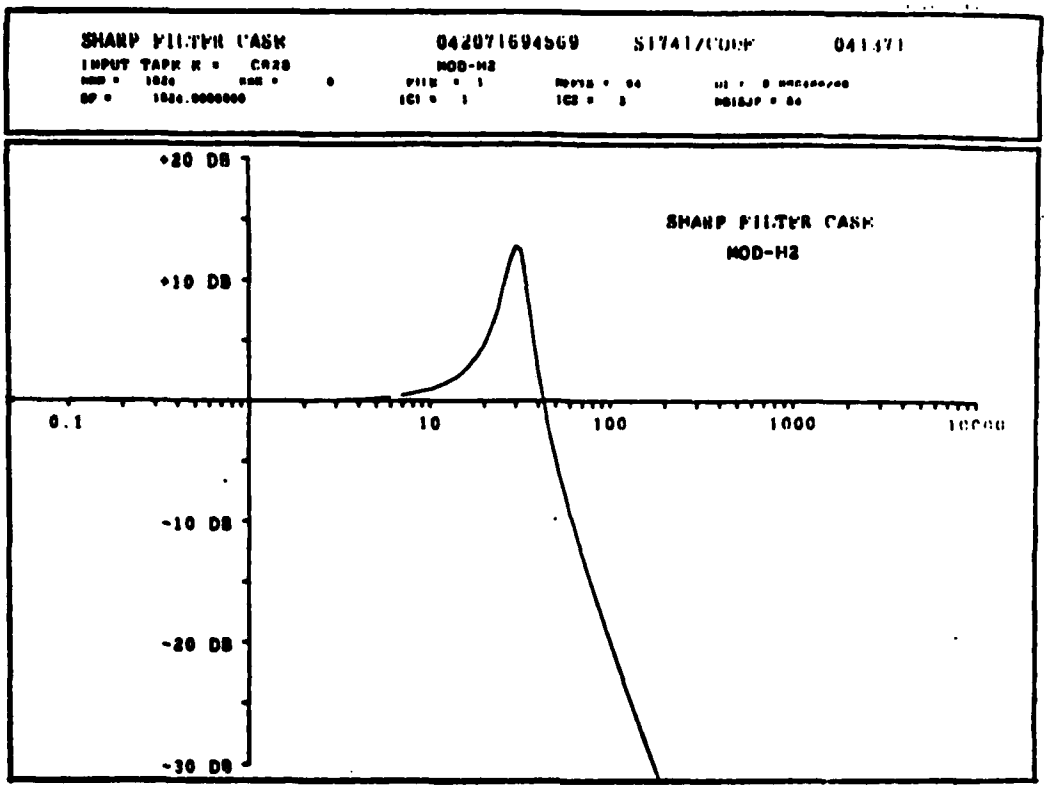
SHARP FILTER CASE
042071694569
S1741/CODE
041371
INPUT TAPE # = C828
MOD-H2
+20 DB
+10 DB
-10 DB
-20 DB
-30 DB
SHARP FILTER CASE
MOD-H2
0.1
10
100
1000

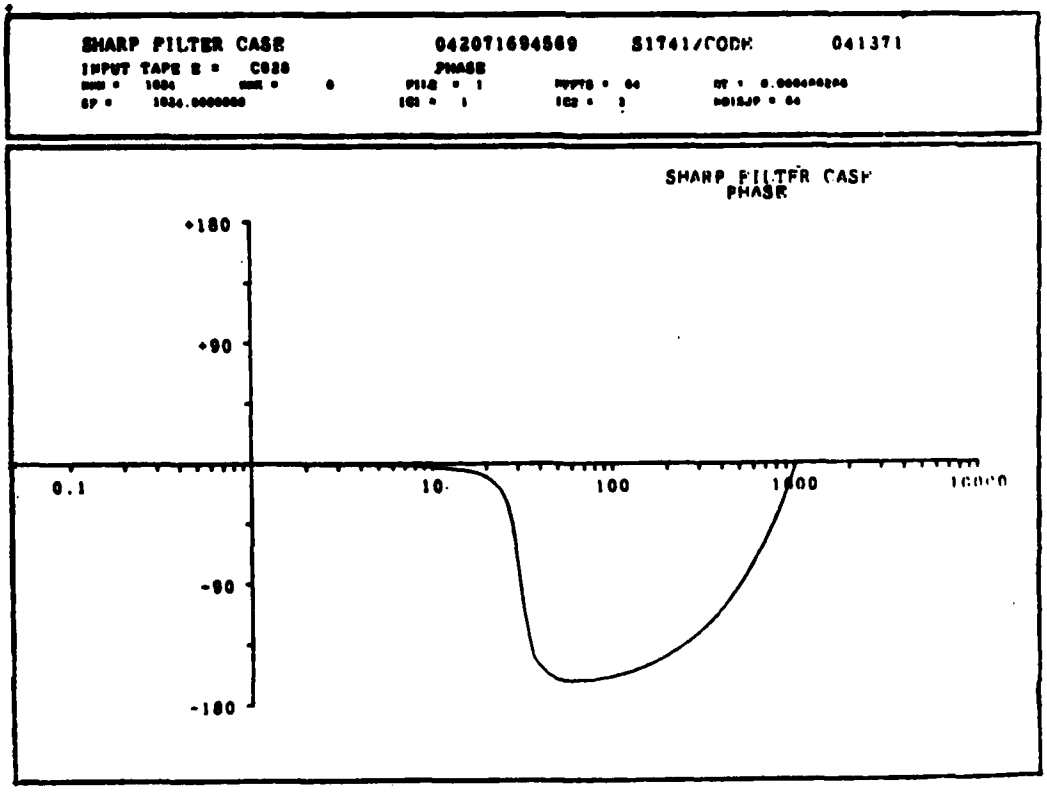
SHARP FILTER CASE
042071694569
S1741/CODE
041371
INPUT TAPE # = C828
PHASE
SHARP FILTER CASE
PHASE
+180
+90
-90
-180
0.1
10
100

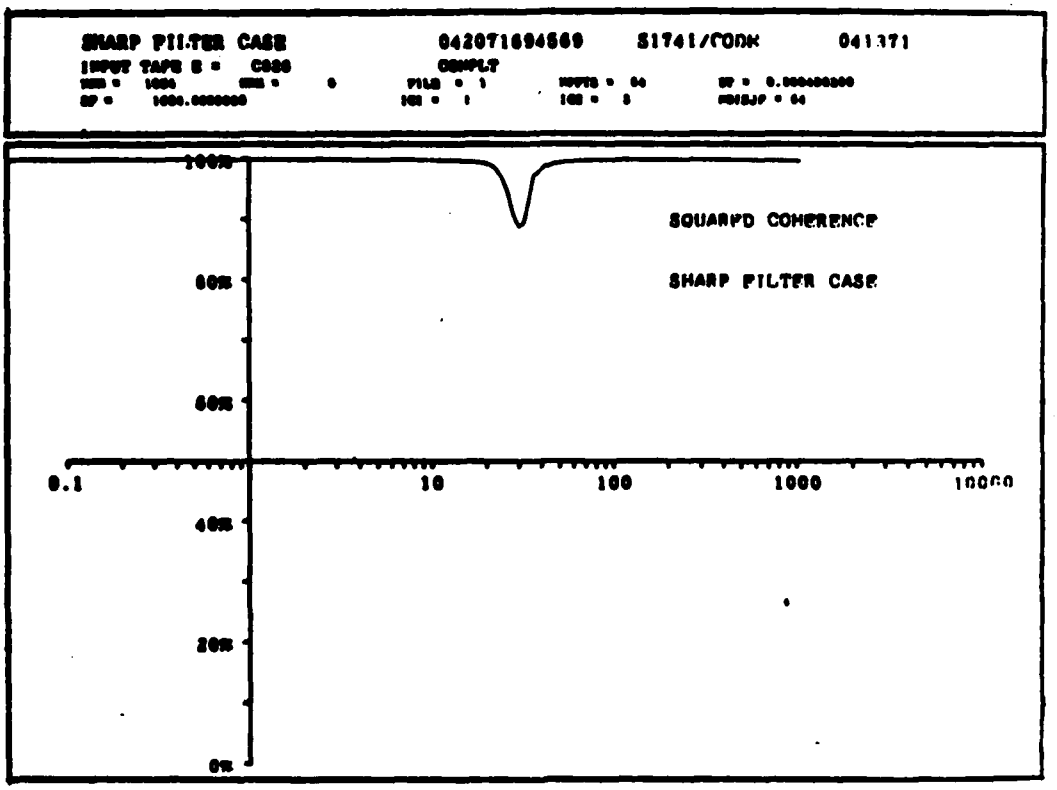
SHARP FILTER CASE
042071694569
S1741/CODK
041371
INPUT TAPE 8 = CODE
COMPLT
SQUARED COHERENCE
SHARP FILTER CASE
100%
80%
60%
40%
20%
0%
0.1
10
100
1000
10000

Increasing the resolving power can improve the coherence estimator though for a finite time history, increasing resolving power means decreasing the amount of averaging possible.

The same data from the Sharp Filter Case was reprocessed with 16 disjoint pieces of size 4096 (vice 64 of 1024).

Note the improvement of the estimator at 30 Hz due to higher resolving power.

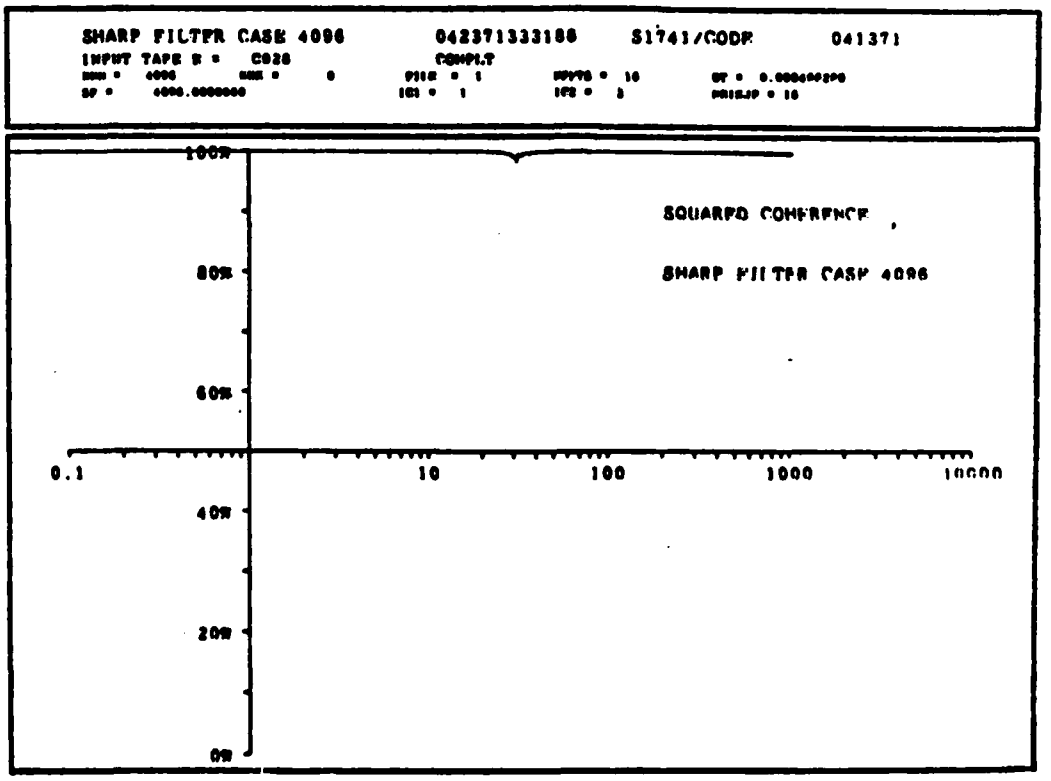

The same data from the Sharp Filter Case was again reprocessed, this time with 256 disjoint pieces of size 1024.

Note that the bias due to poor resolution <u>can not</u> be corrected by increased averaging.

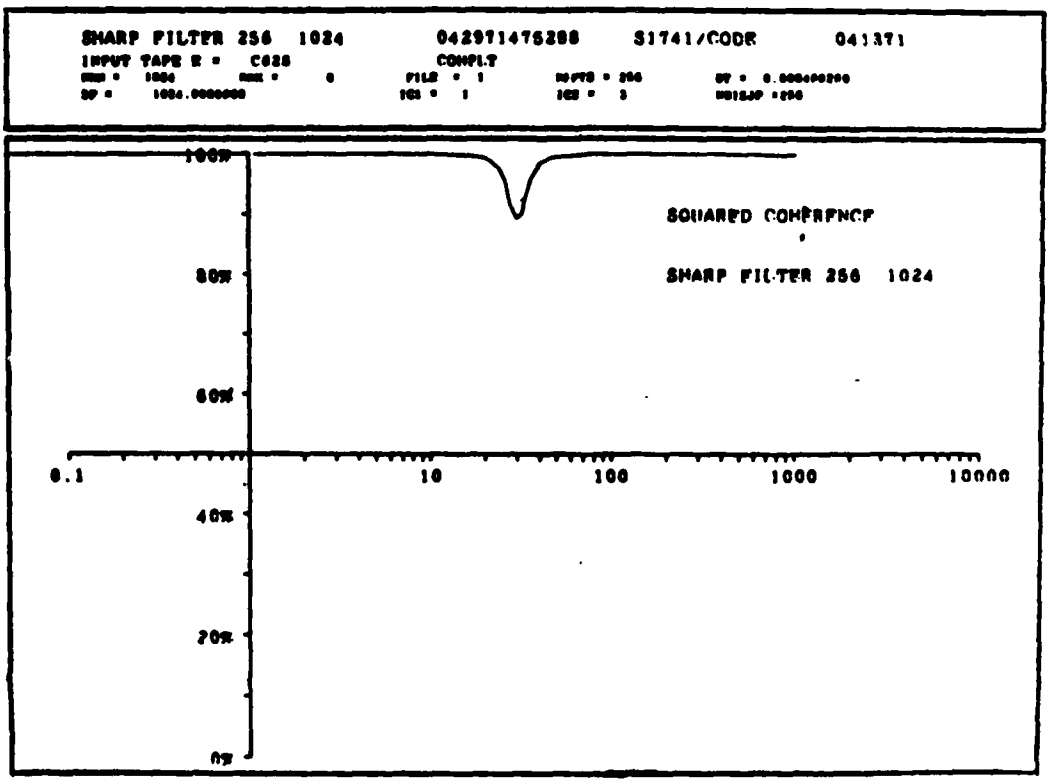

IV.C. Sharp Filter Case

IV.C.2. With No Weighting Function

The "sharp filter case" data was used again to estimate squared coherence. This time the data segments were not multiplied by a weighting function. The FFT side lobe "leakage" problem, reference (f), corrupts the estimator. Note that even though the true value of coherence is 100%, the estimator fails to attain the true value. Also the estimates of filter gain and phase are not as good as with the use of a weighting function.

The result dramatically portrays the need to apply a weighting function.

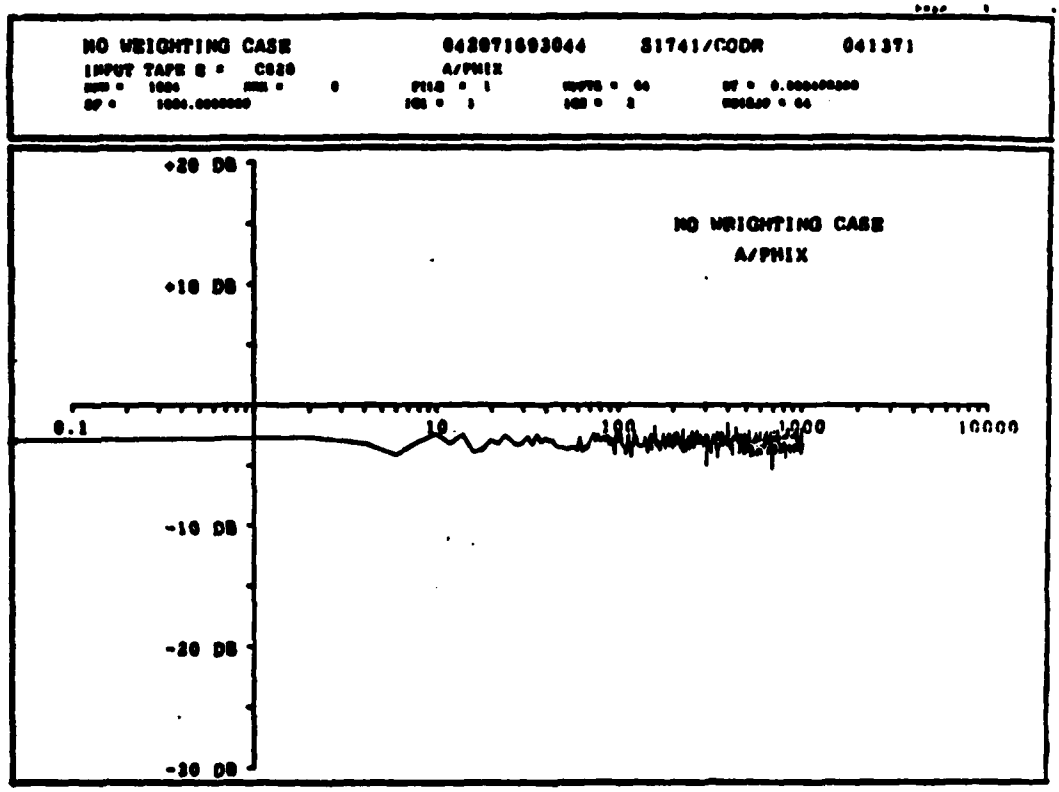
NO WEIGHTING CASE
042071693044
S1741/CODR
041371
INPUT TAPE # = C020
A/PHIX
+20 DB
+10 DB
-10 DB
-20 DB
-30 DB
0.1
10
100
1000
10000
NO WEIGHTING CASE
A/PHIX

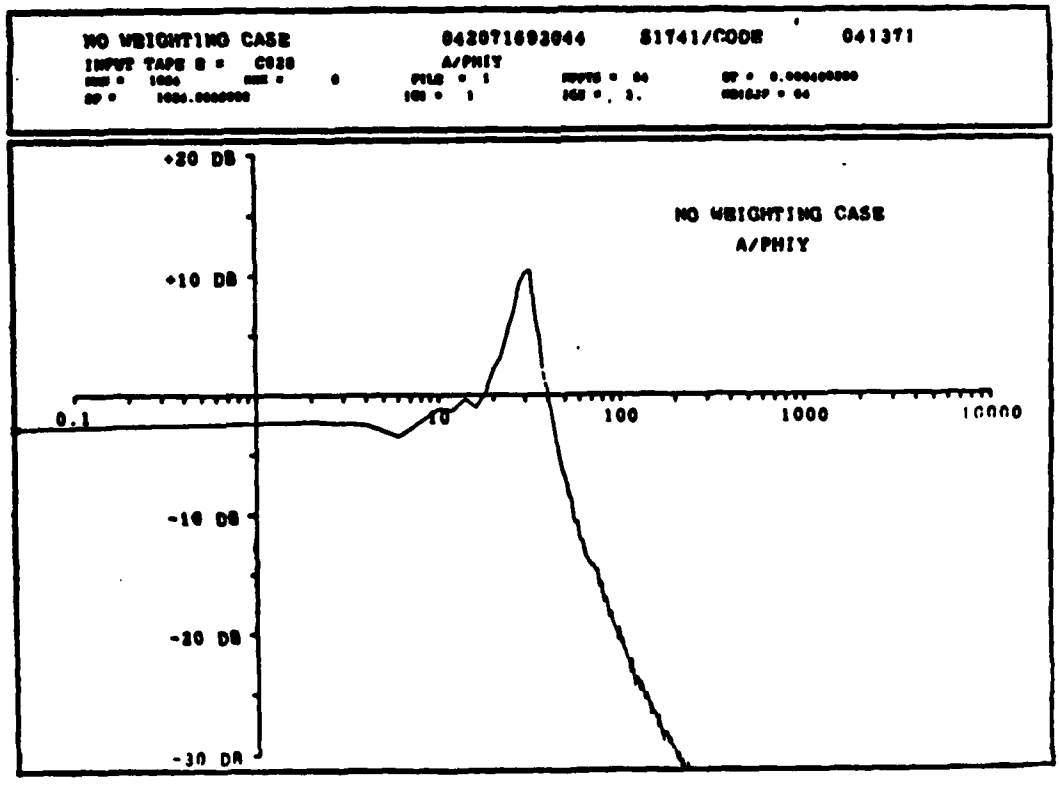
NO WEIGHTING CASE
042071693044
S1741/CODR
041371
INPUT TAPE # = C020
A/PHIY
+20 DB
+10 DB
-10 DB
-20 DB
-30 DB
0.1
10
100
1000
10000
NO WEIGHTING CASE
A/PHIY

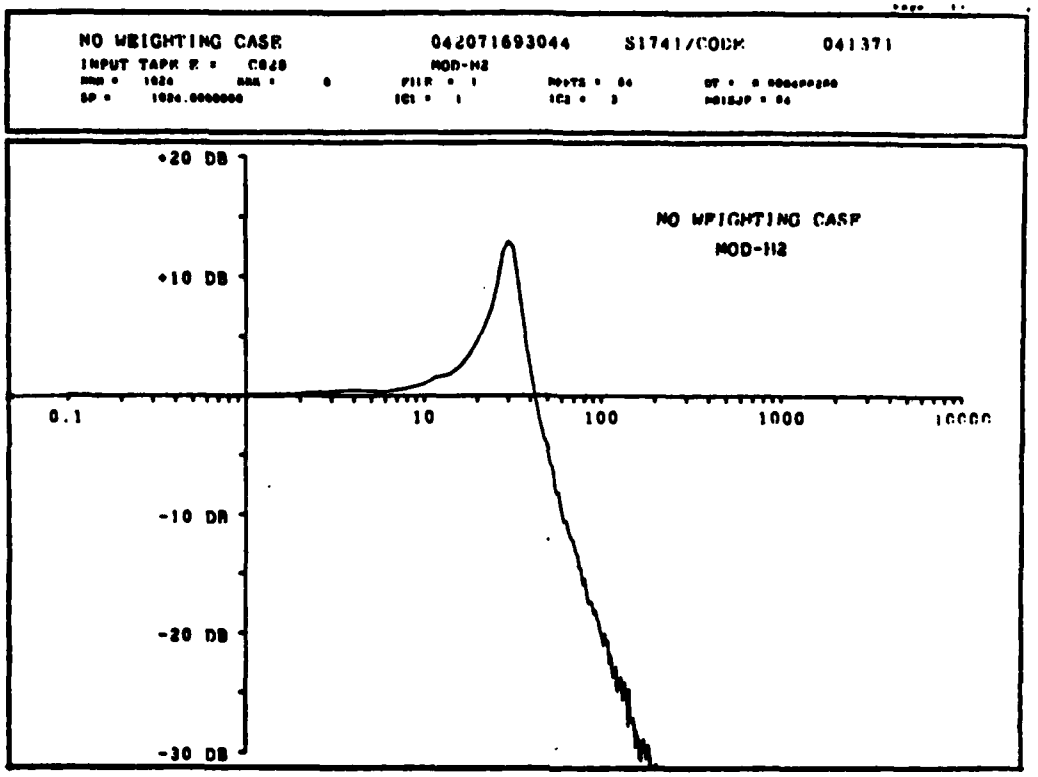
NO WEIGHTING CASE
042071693044
S1741/CODE
041371
INPUT TAPE E = C828
MOD-H2
+20 DB
+10 DB
-10 DB
-20 DB
-30 DB
NO WEIGHTING CASE
MOD-H2
0.1
10
100
1000

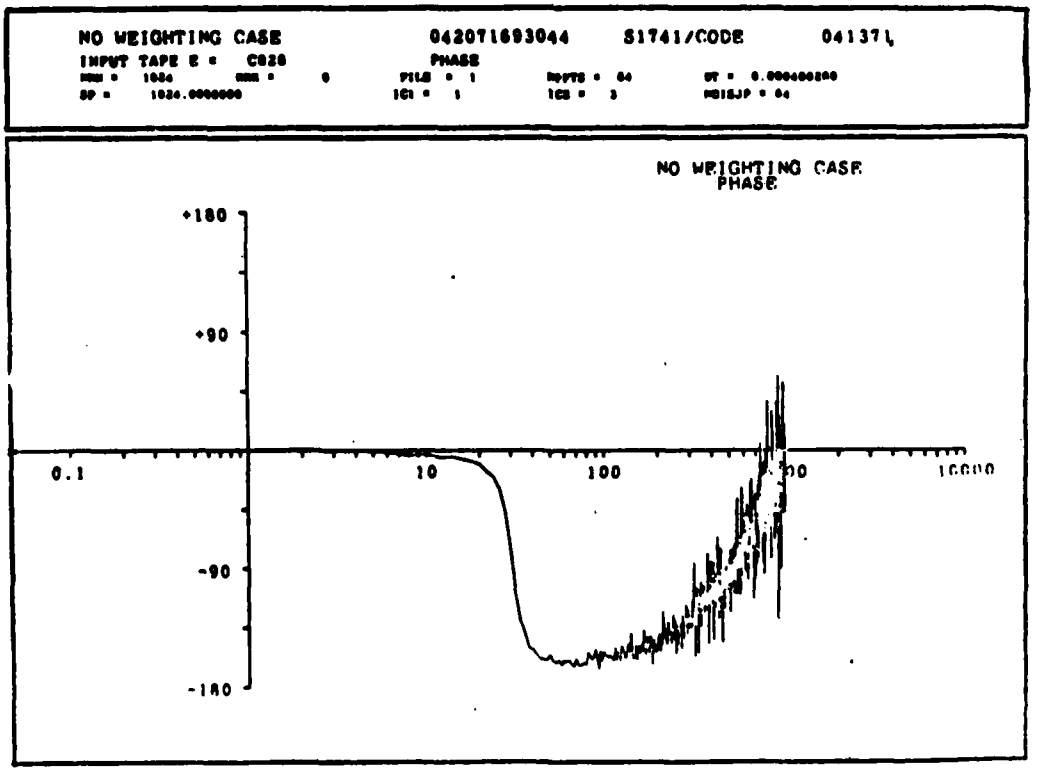
NO WEIGHTING CASE
042071693044
S1741/CODE
041371
INPUT TAPE E = C828
PHASE
NO WEIGHTING CASE
PHASE
+180
+90
-90
-180
0.1
10
100

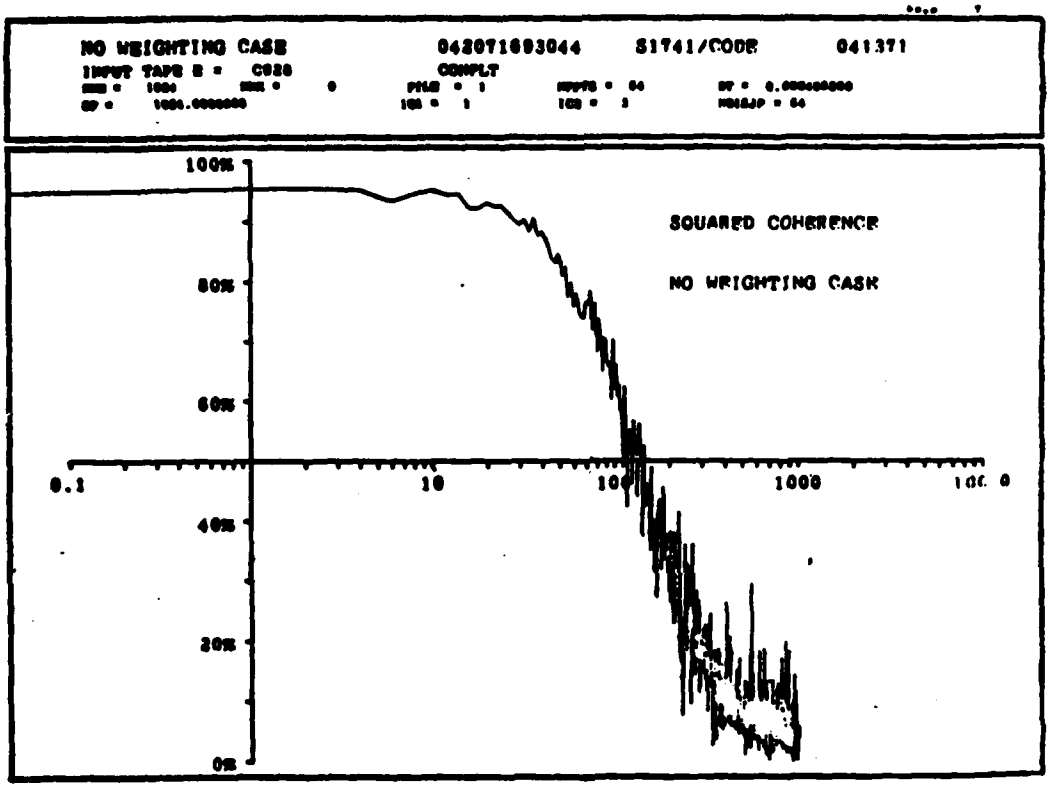
NO WEIGHTING CASE
042071693044
S1741/CODE
041371
INPUT TAPE 8 = C026
COMPLT
100%
80%
60%
40%
20%
0%
0.1
10
1000
SQUARED COHERENCE
NO WRIGHTING CASK

The data from the Sharp Filter Case were reprocessed with NO weighting function applied to the time series but with higher resolving power.

Here 16 disjoint pieces of size 4096 (vice 64 of 1024) are processed.

Note that higher resolving power without weighting function still yields poor results.

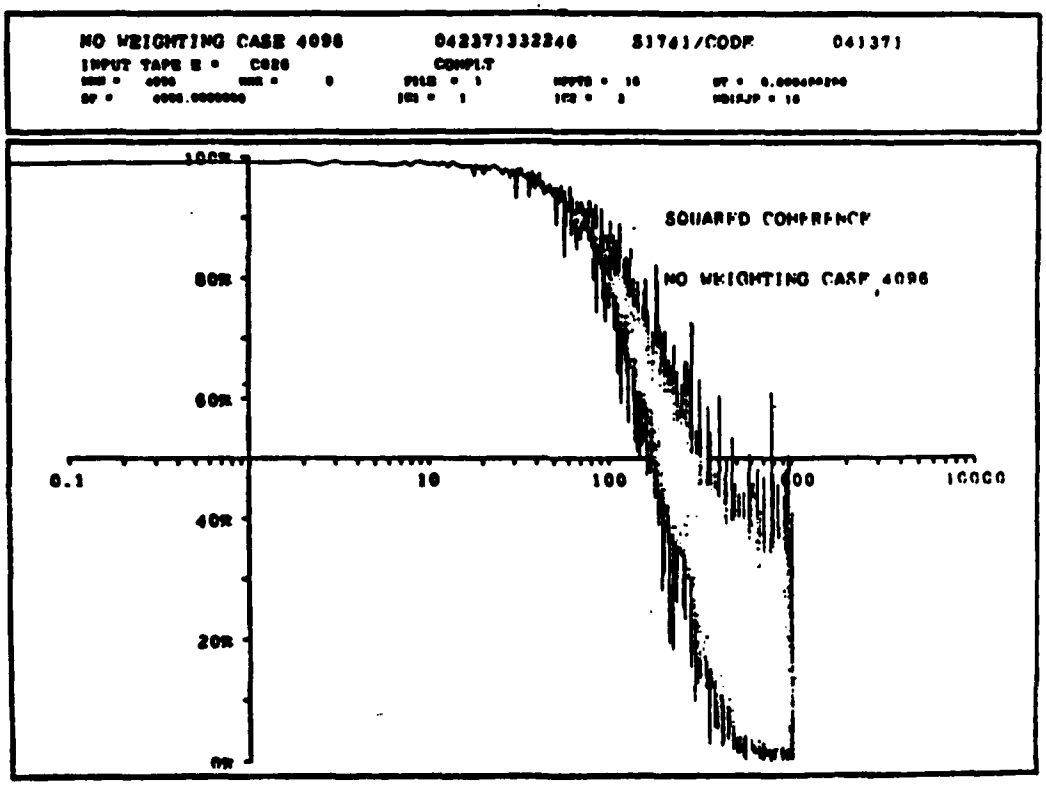

The data from the Sharp Filter Case were reprocessed with NO weighting function applied to the time series but with higher resolving power and more averaging.

Here 64 disjoint pieces of size 4096 are processed.

Note that the estimator is stabilizing but not about the correct answer.

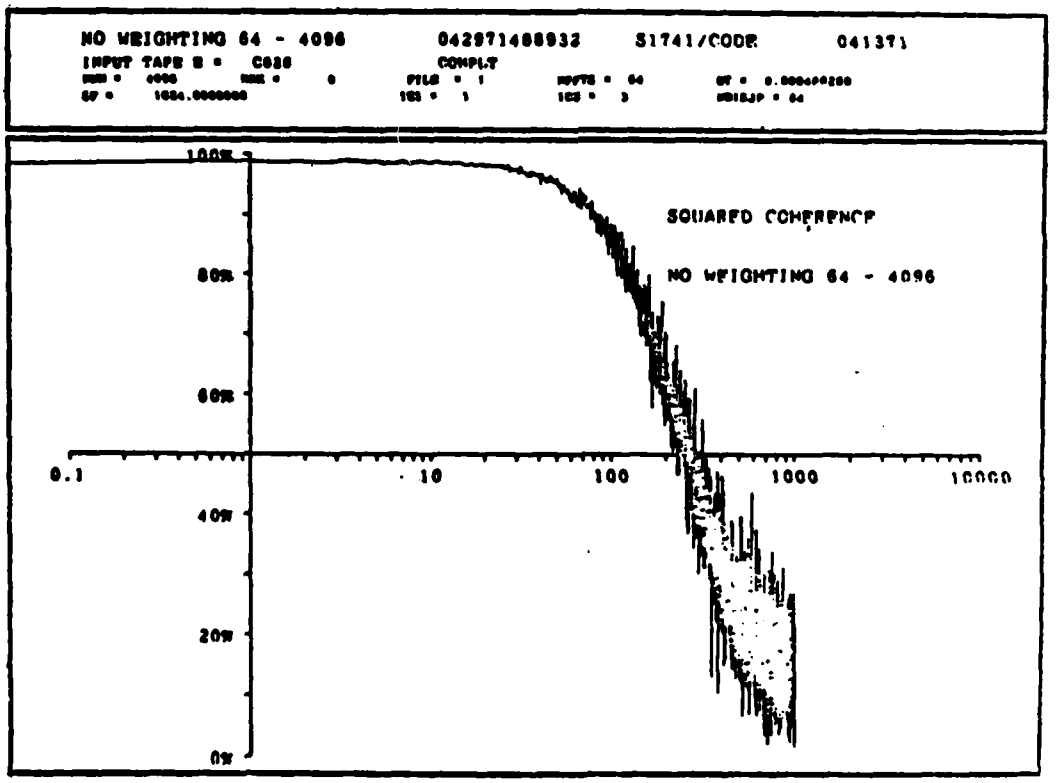

IV.D. Tones Thru Filter Case

The question of resolving power leads to the investigation of tones through a filter. That is, if there are fine lines in the input spectrum, plot "A/PHIX," the coherence can be estimated for a smooth filter. The smooth filter is again specified by the recursion equation:

$$Y_n = 7/8\ Y_{n-1} + 1/8\ X_n$$

The input sequence is generated by summing noise and two sine waves (one centered in an FFT frequency bin, one out). The results show our ability to estimate coherence in this environment.

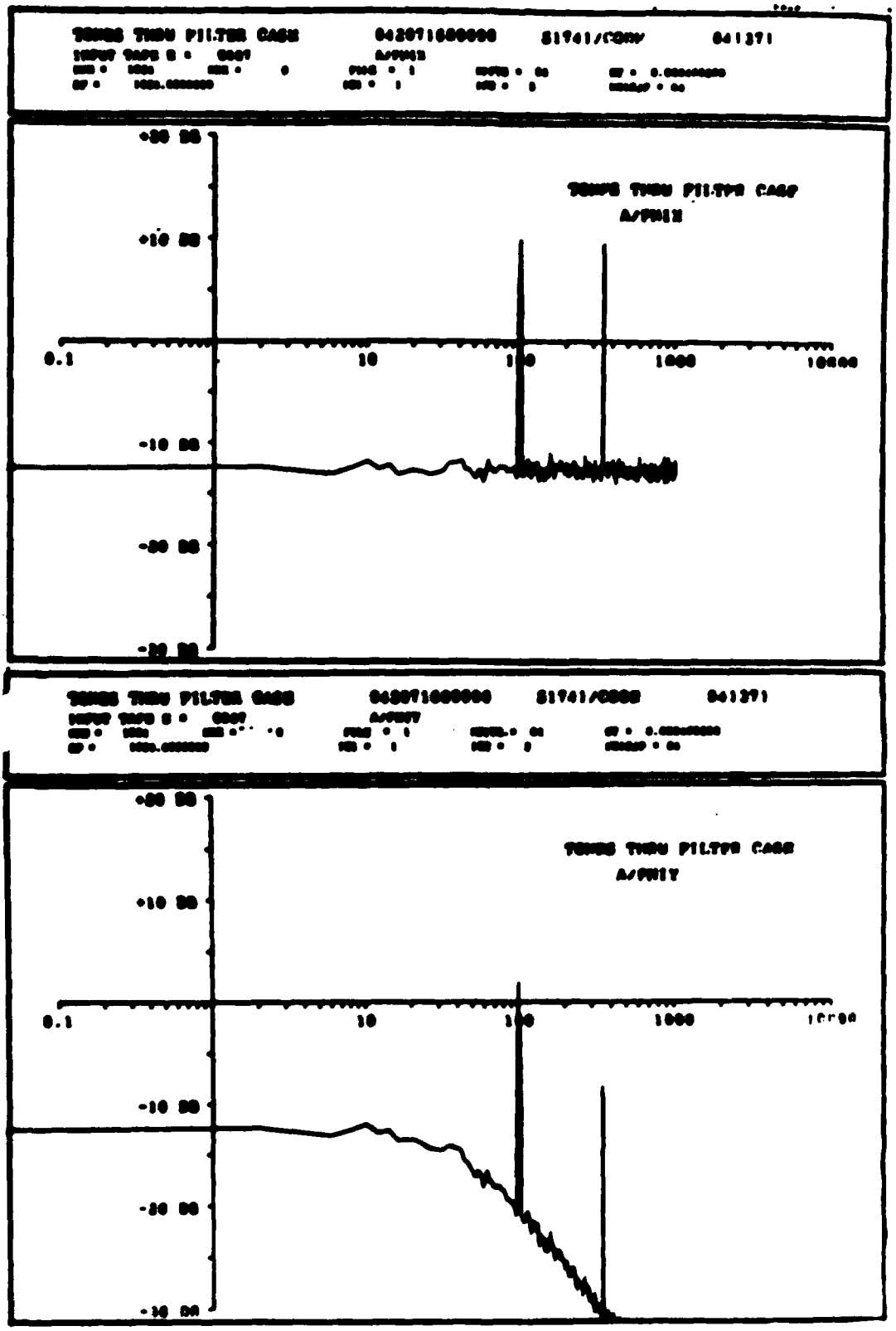
+20 DB
+10 DB
0.1
10
1000
-10 DB
-20 DB
+20 DB
+10 DB
0.1
10
1000
-10 DB
-20 DB

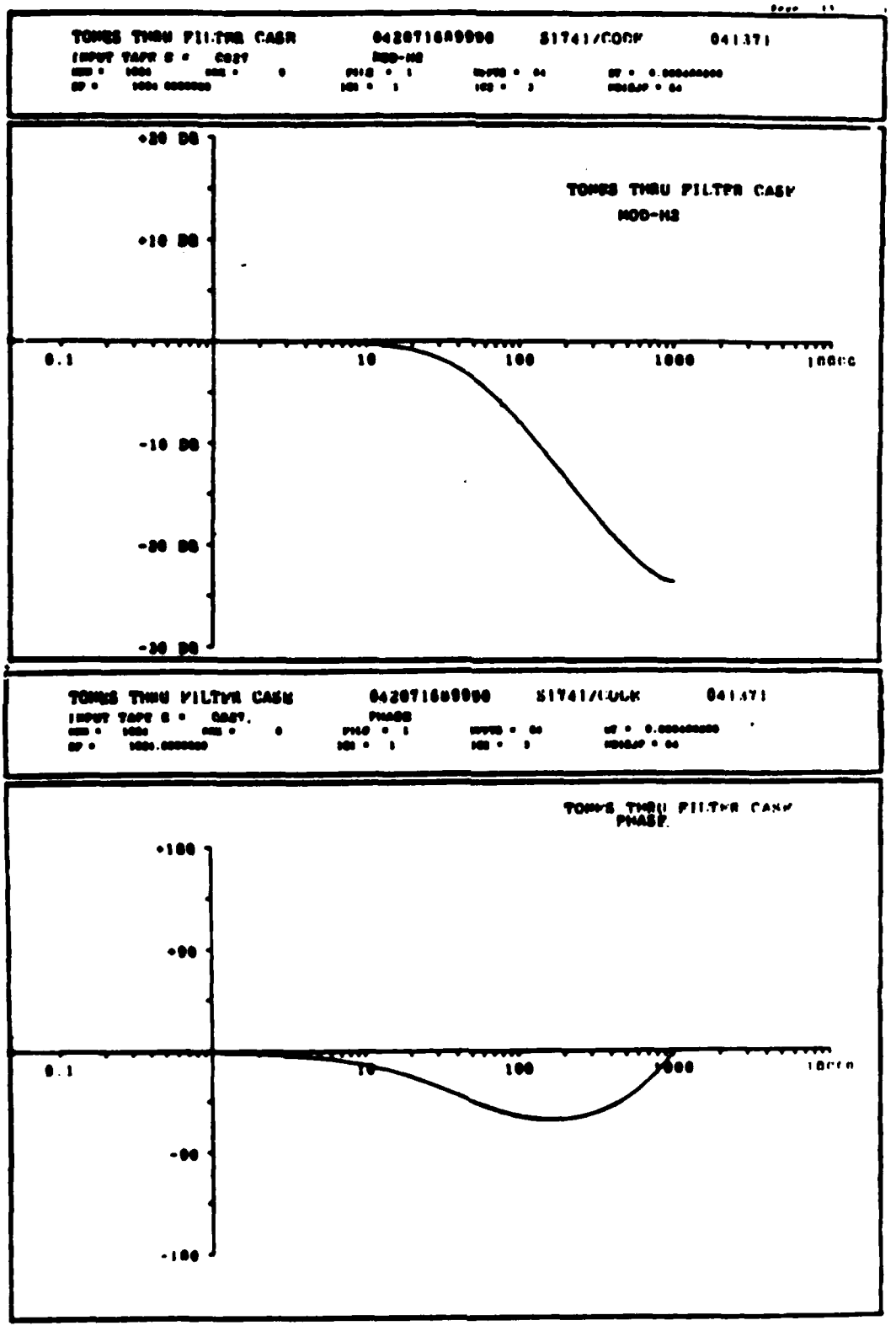
TONES THRU FILTER CASE
MOD-M2
+20 DB
+10 DB
-10 DB
-20 DB
0.1
10
100
1000
TONES THRU FILTER CASE
PHASE
+180
+90
-90
-180
0.1
100

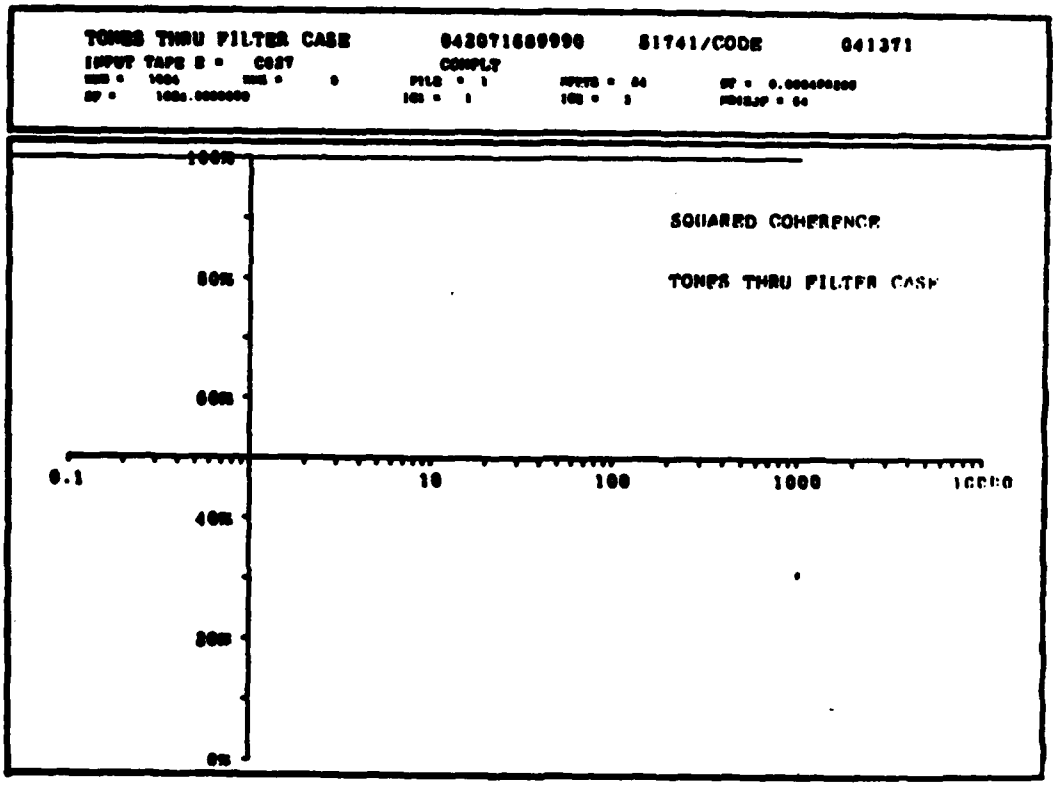
TONES THRU FILTER CASE
041371
SQUARED COHERENCE
TONES THRU FILTER CASE
80%
60%
40%
20%
0%
0.1
10
100
1000

IV.E. Variable Coherent Case

White Gaussian noise source 1 (flat spectrum) is filter through the first order low pass digital filter specified by the recursion equation:

$$Z_n = 31/32\ Z_{n-1} + 1/32\ X_n$$

The output Z_n is corrupted (intentionally) with additive Gaussian noise source 2 (flat spectrum) independent of noise source 1. The observed output Y_n is specified by the equation

$$Y_n = Z_n + 1/4\ r_n$$

where: r_n is noise source 2

The output Y_n becomes dominated by additive noise as the frequency increases, hence the squared coherence decreases with increasing frequency. Estimating the "transfer function" between X_n and Y_n is shown.

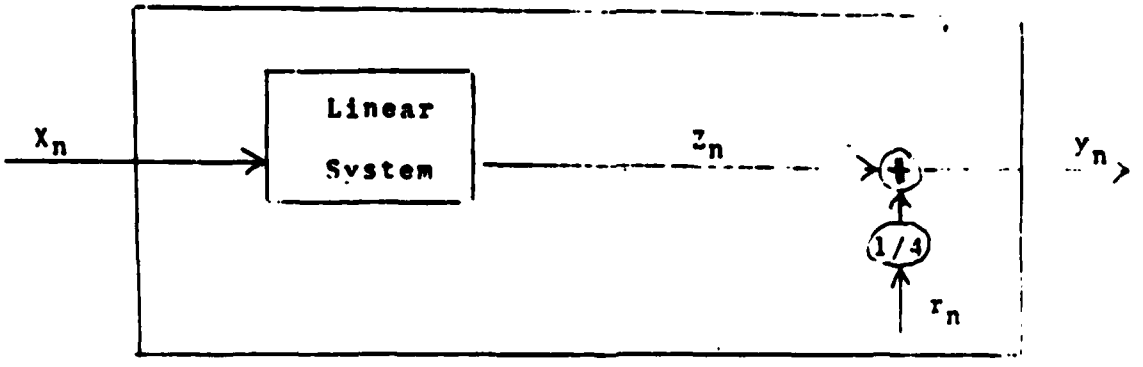

This behavior of the true coherence was predicted by Roth (ref. (i)) and Carter (ref. (l)). The tendency for the variability of the estimator to be greater at true coherence about 0.3 was predicted by Jenkins and Watts (ref. (c)), Carter and Nuttall (ref. (k)), and Carter (ref. (l)).

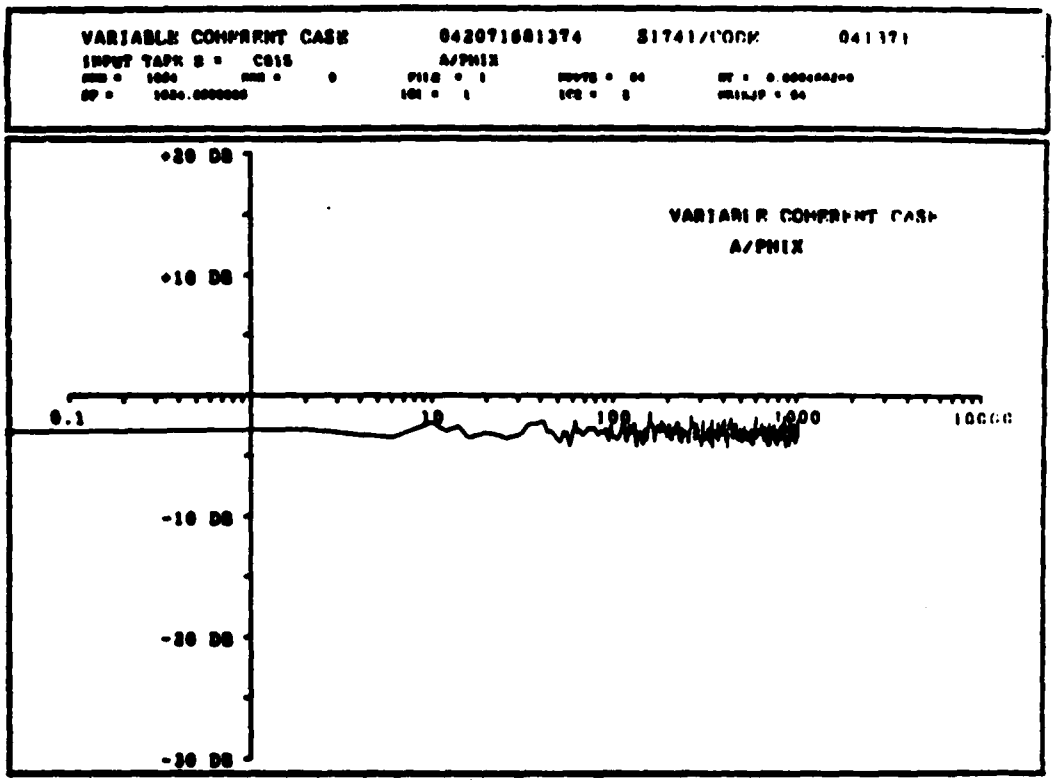
VARIABLE COHERENT CASE
042071681374
S1741/COOK
041171
INPUT TAPE 8 = C015
A/PNIX
+20 DB
+10 DB
-10 DB
-20 DB
-30 DB
0.1
10
100
1000
10000
VARIABLE COHERENT CASE
A/PNIX

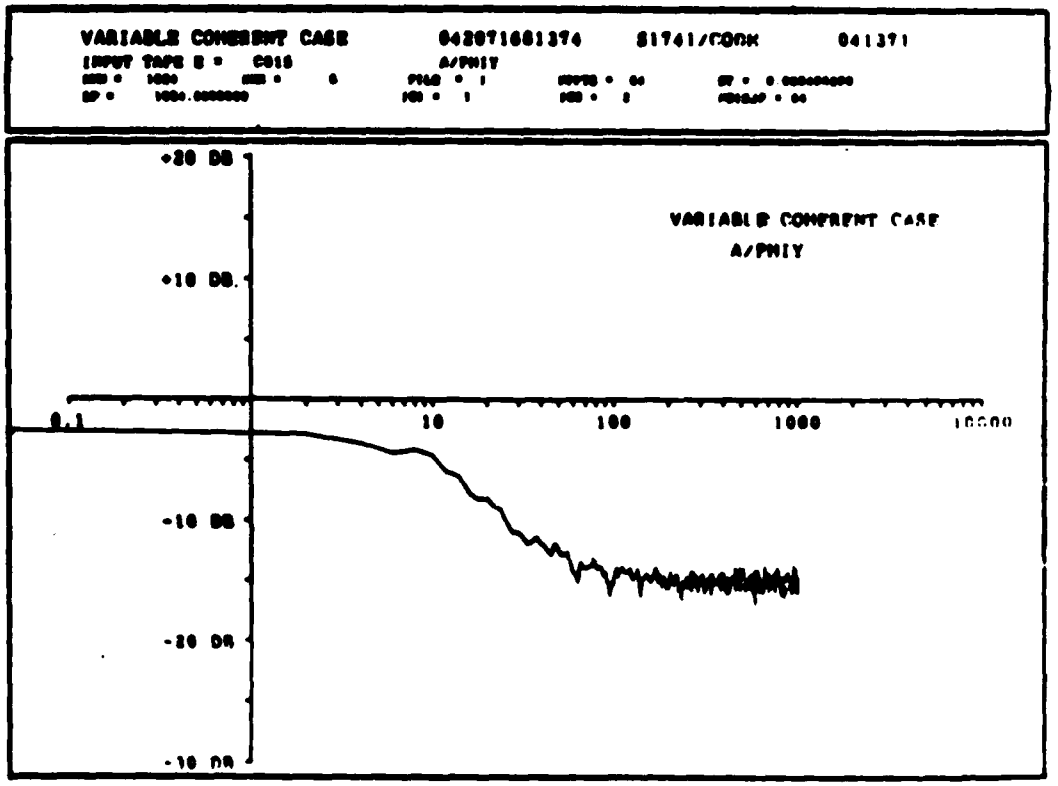
VARIABLE COHERENT CASE
042071681374
S1741/COOK
041171
INPUT TAPE 8 = C015
A/PNIY
+20 DB
+10 DB
-10 DB
-20 DB
0.1
10
100
1000
10000
VARIABLE COHERENT CASE
A/PNIY

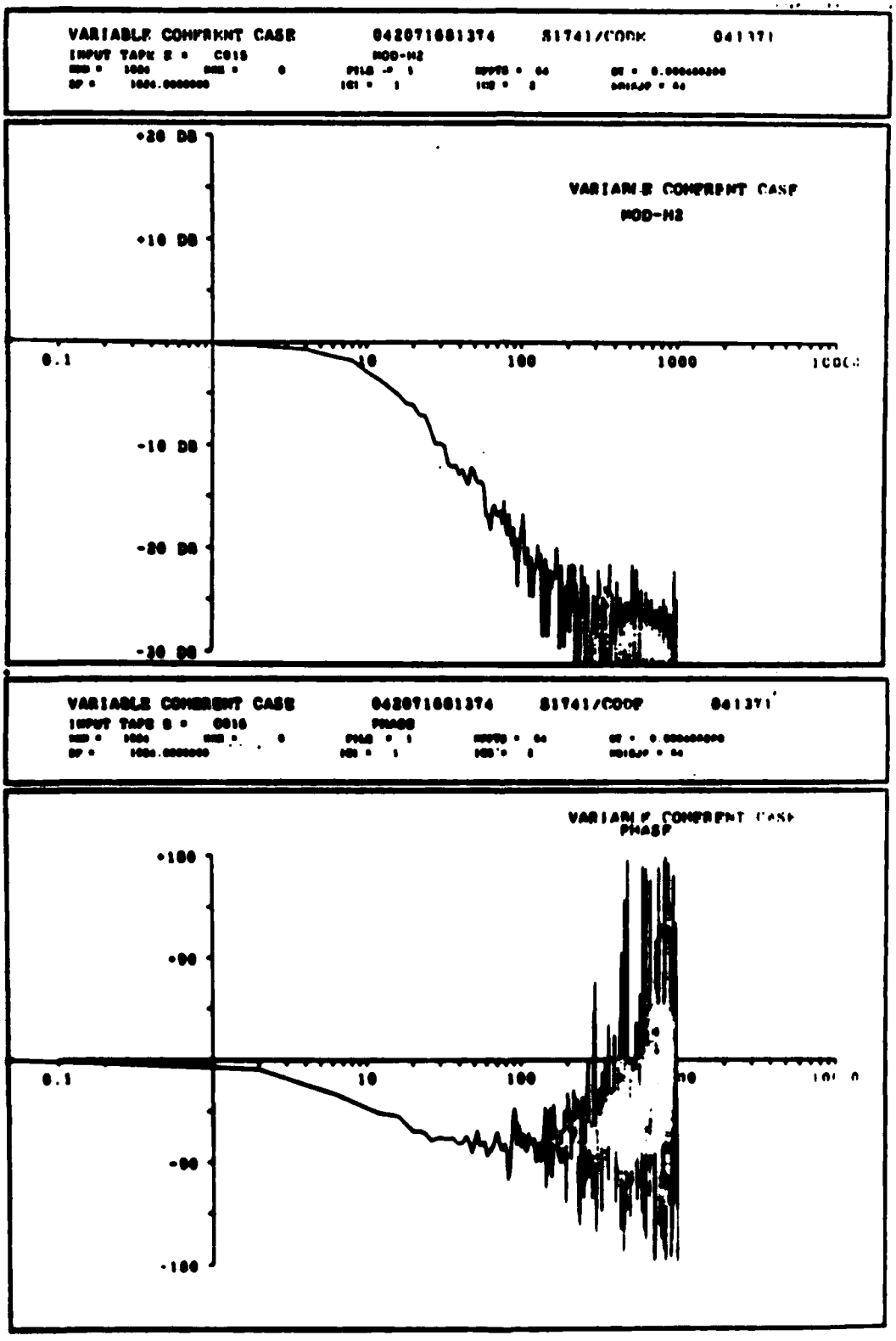
VARIABLE COHERENT CASE
MOD-M2
+20 DB
+10 DB
-10 DB
-20 DB
-30 DB
0.1
10
100
1000
VARIABLE COHERENT CASE
PHASE
+180
+90
-90
-180
0.1
10
100

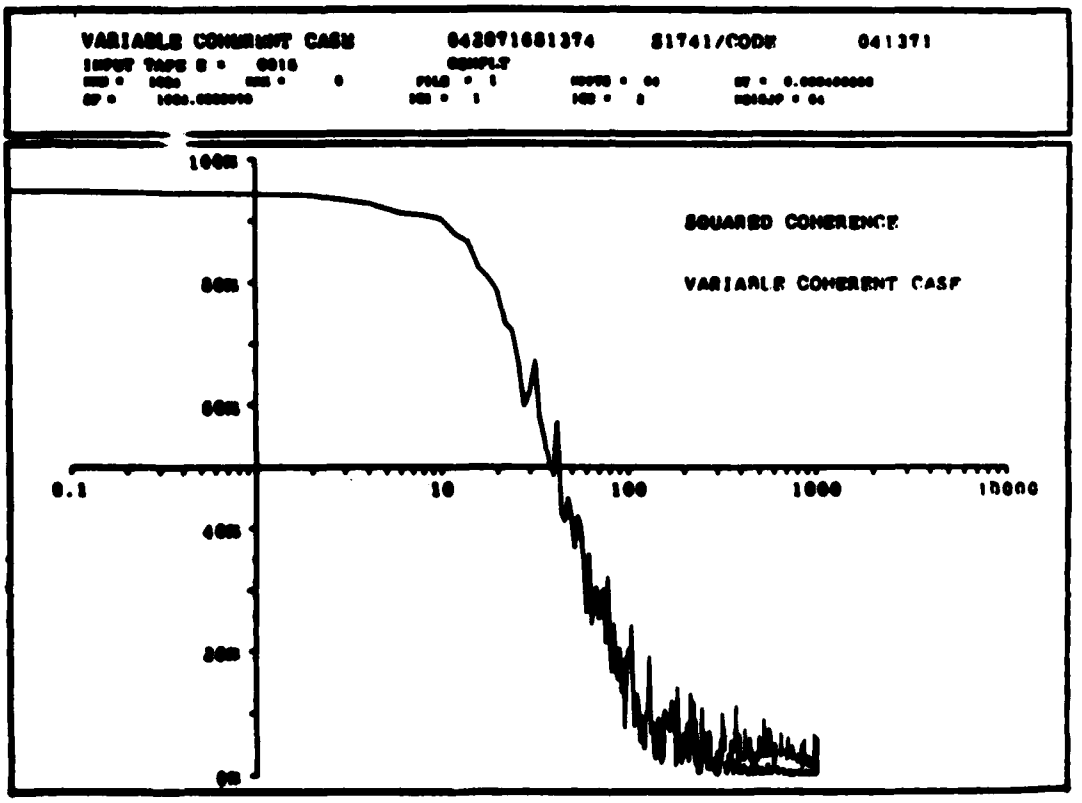
VARIABLE COHERENT CASE
SQUARED COHERENCE
VARIABLE COHERENT CASE
0.1
10
100
1000
10000

IV.F. True Coherence Equal 0.3 Case

Two processes with true coherence equal to 0.3 for all frequencies were generated (Nuttall and Carter ref. (m) and Carter ref. (l)). The following set of figures illustrates the resulting coherence estimates for NSEG = 8, 16, 32, 64, 128, and 256. The variance of the estimator agrees with theoretical predictions (Carter and Nuttall ref. (k) and Carter ref. (l)).

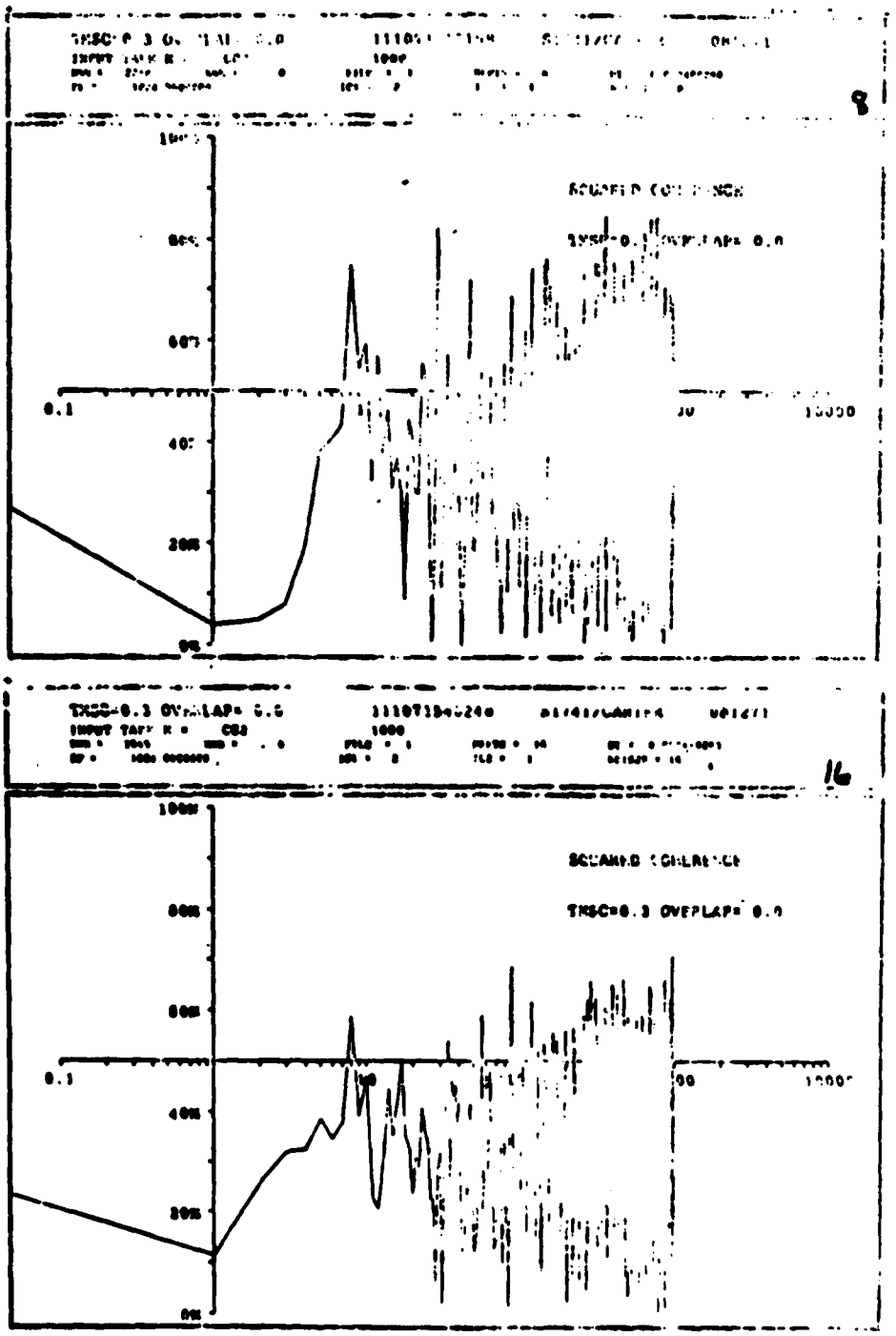
8
0.1
16
0.1

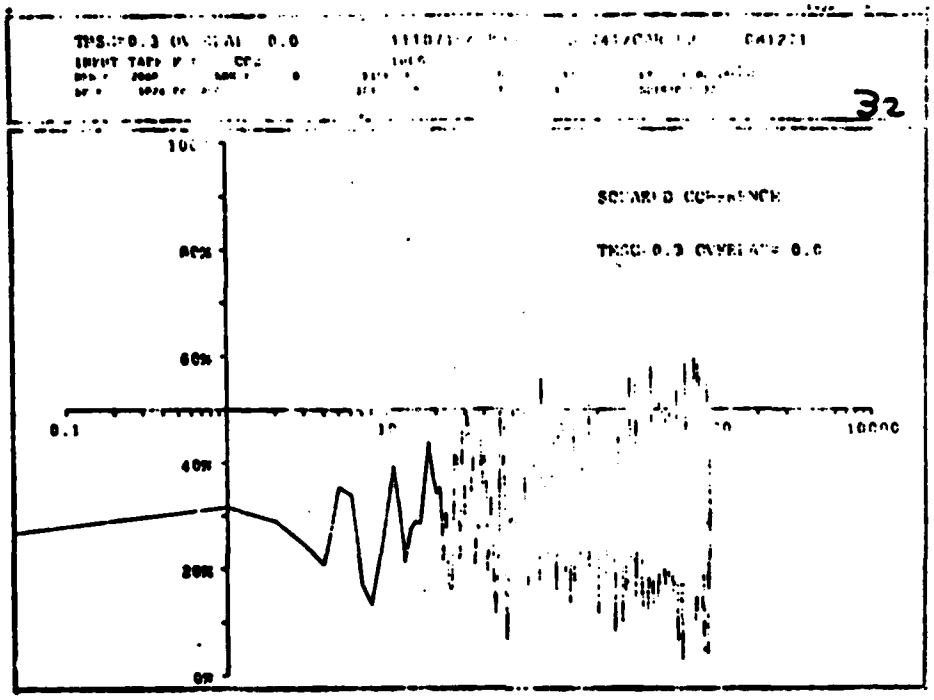
32
SQUARED COHERENCE
100%
80%
60%
40%
20%
0%
0.1
10
100
1000

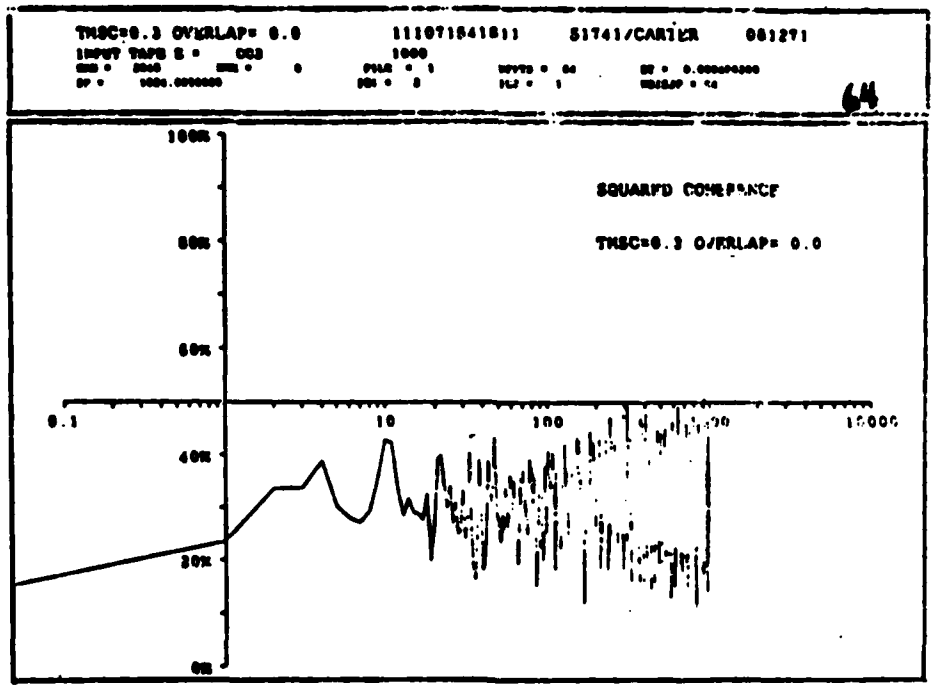
TNSC=0.3 OVERLAP= 0.0
111071841811
51741/CARTER
081291
64
SQUARED COHERENCE
TNSC=0.3 OVERLAP= 0.0
100%
80%
60%
40%
20%
0%
0.1
10
100
1000

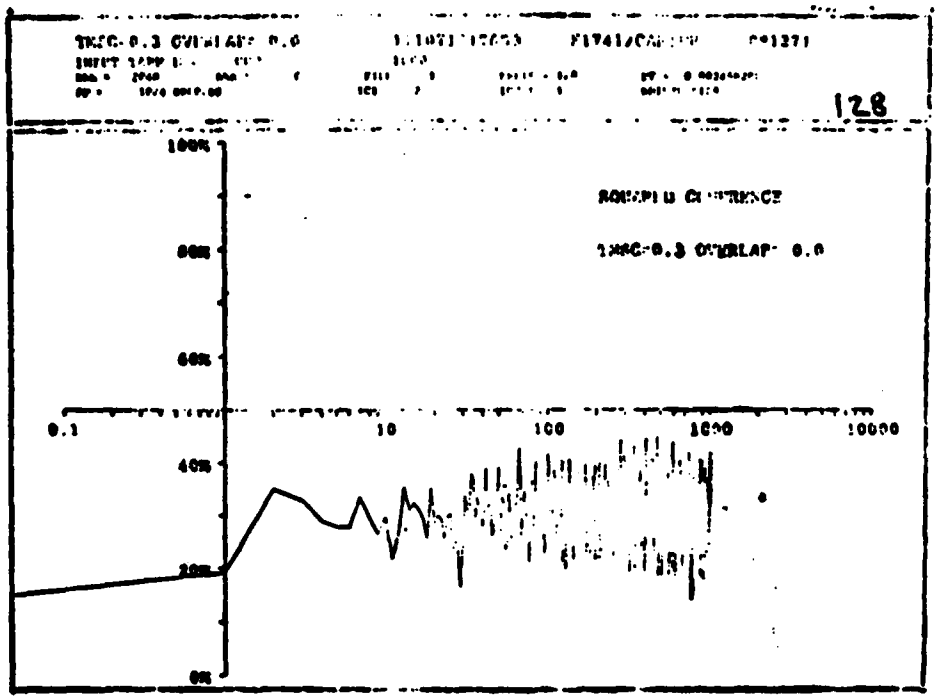
128
100%
80%
60%
40%
20%
0%
0.1
10
100
1000
10000

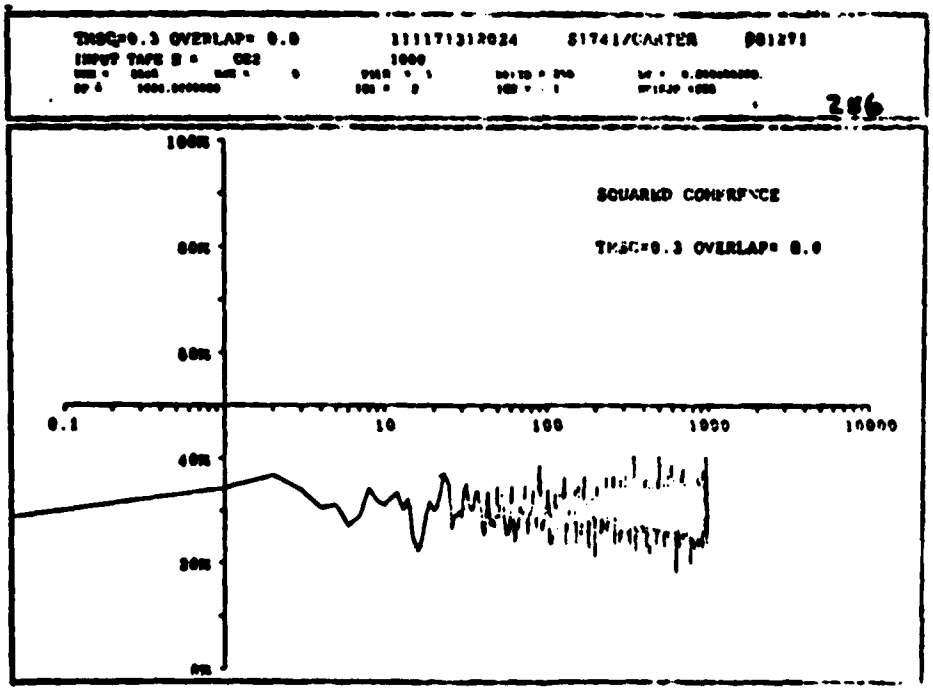
286
100%
80%
60%
40%
20%
0%
0.1
10
100
1000
10000

V. CONCLUSIONS

Some of the practical aspects of estimating the coherence function have been presented. The problems of analyzing the results are harsh. The two most significant points are weighting functions and stability. First, a weighting function must be applied to the data to estimate the coherence spectrum. Second, averaging is required, dictating time series of long duration which are stationary over the period of observation.

Extracting from Tick reference (b), "I wonder how many conclusions have been drawn over the years because of poor estimation procedures."

This field of spectral estimation is open to further in-depth research and the authors will not be surprised to see significant contributions over the next several years.

REFERENCES

(a) Bendat, Julius, S. and Piersol, Allan G., Measurement and Analysis of Random Data, Wiley, New York, 1966.

(b) Tick, Leo J., "Estimation of Coherency," ed. Bernard Harris, Spectral Analysis of Time Series, Wiley, 1967.

(c) Jenkins, Gwilym M. and Watts, Donald G., Spectral Analysis and Its Applications, Holden Day, San Francisco, California, 1968.

(d) Haubrich, Richard A., "Earth Noise 5 to 500 Millicycles per Second," Journal of Geophysical Research, Vol. 70, No. 6, March 1965, pp 1415-1427.

(e) Benignus, Vernon A., "Estimation of Coherence Spectrum and Its Confidence Interval Using the Fast Fourier Transform," IEEE Transactions on Audio and Electroacoustics, Vol. AU-17, No. 2, June 1969, pp 145-150.

(f) Bingham, Christopher, Godfrey, Michael D., and Tukey, John W., "Modern Techniques of Power Spectrum Estimation," IEEE Trans. on Audio and Electroacoustics, Vol. AU-15, No. 2, June 1967, pp 56-66.

(g) Welch, Peter D., "The Use of Fast Fourier Transform for the Estimation of Power Spectra; A Method Based on Time Averaging Over Short Modified Periodograms," IEEE Trans. on Audio and Electroacoustics, Vol. AU-15, No. 2, June 1967, pp 70-73.

(h) Roth, Peter R., "Effective Measurements Using Digital Signal Analysis," IEEE Spectrum, April 1971, pp 62-70.

(i) Singleton, Richard C., "An Algorithm for Computing the Mixed Radix Fast Fourier Transform," IEEE Trans. on Audio and Electroacoustics, Vol. AU-17, No. 2, June 1969, pp 93-103.

(j) Nuttall, Albert H., "Spectral Estimation by Means of Overlapped FFT Processing of Windowed Data," NUSC Report No. 4169, 13 October 1971.

(k) Carter, G. C., and Nuttall, Albert H., "Evaluation of the Statistics of the Estimate of Magnitude-Squared Coherence," NUSC Tech. Memo. TC-193-71, 28 September 1971.

(l) Carter, G. C., "Estimation of the Magnitude Squared Coherence Function (Spectrum)," University of Connecticut Master's Thesis (to be published).

(m) Nuttall, A. H., and Carter, G. C., "On Generating Processes with Specified Coherence," NUSC Tech. Memo. TC-187071, 22 September 1971.

NUSC Technical Report 4343
19 May 1972

Estimation of the Magnitude-Squared Coherence Function (Spectrum)

G. C. Carter

ABSTRACT

A method of estimating the magnitude-squared coherence function (spectrum) for zero-mean processes that are wide-sense stationary and random is presented. The estimation technique utilizes the weighted overlapped segmentation fast Fourier transform (FFT) approach. Analytical and empirical results for statistics of the estimator are presented for the processes. Analytical expressions are derived in the non-overlapped case. Empirical results show a decrease in bias and variance of the estimator with increasing overlap and suggest that a 50-percent overlap is highly desirable when cosine (Hanning) weighting is used.

TABLE OF CONTENTS

TABLE OF CONTENTS (Cont'd)

LIST OF ILLUSTRATIONS

LIST OF ILLUSTRATIONS (Cont'd)

LIST OF TABLES

REVERSE BLANK

GLOSSARY

$C_{xy}(f)$	Real part of $\Phi_{xy}(f)$
$\hat{C}_{xy_s}(f_k)$	Real part of $\hat{\Phi}_{xy_s}(f_k)$
$E[\ ]$	Expectation
$\mathbf{M}_{xy}(f)$	Power spectral density matrix
$Q_{xy}(f)$	Imaginary part of $\Phi_{xy}(f)$
$\hat{Q}_{xy_s}(f_k)$	Imaginary part of $\hat{\Phi}_{xy_s}(f_k)$
$R_{xx}(\tau)$	Autocorrelation function of x(t) process
$R_{xy}(\tau)$	Cross-correlation function of x(t) and y(t)
$\mathbf{R}_{xy}(\tau)$	Cross-correlation matrix
$R_{yy}(\tau)$	Autocorrelation function of y(t) process
$X_s(f_k)$	kth discrete Fourier coefficient obtained from sth weighted segment of x(t) data
$Y_s(f_k)$	kth discrete Fourier coefficient obtained from sth weighted segment of y(t) data
$\Gamma(\ )$	Gamma function
$\lvert\gamma_{xy}(f)\rvert^2$	Magnitude-squared coherence (MSC) function (spectrum)
$\lvert\hat{\gamma}_{xy}(f_k)\rvert^2$	Estimate of MSC at kth frequency

$|\gamma_{xy}(f)|$ Magnitude coherence (MC) function (spectrum)

$|\hat{\gamma}_{xy}(f_k)|$ Estimate of MC at kth frequency

$\Phi_{xx}(f)$ Auto power spectral density function of x(t) process

$\hat{\Phi}_{xx_s}(f_k)$ Estimate of $\Phi_{xx}(f)$ at kth frequency obtained from sth weighted segment of data

$\Phi_{xy}(f)$ Cross-power spectral density function of x(t) and y(t)

$\hat{\Phi}_{xy_s}(f_k)$ Estimate of $\Phi_{xy}(f)$ at kth frequency obtained from sth weighted segment of data

$\Phi_{yy}(f)$ Auto-power spectral density function of y(t) process

$\hat{\Phi}_{yy_s}(f_k)$ Estimate of $\Phi_{yy}(f)$ at kth frequency obtained from sth weighted segment of data

$*$ Complex conjugation

$\forall$ For all

ESTIMATION OF THE MAGNITUDE-SQUARED COHERENCE FUNCTION (SPECTRUM)

I. INTRODUCTION

The complete probability structure of the zero-mean processes x(t) and y(t), which are wide-sense stationary and jointly Gaussian, is specified by the spectral density matrix,

$$\mathbf{M}_{xy}(f) = \begin{bmatrix} \Phi_{xx}(f) & \Phi_{xy}(f) \\ \Phi_{yx}(f) & \Phi_{yy}(f) \end{bmatrix} , \tag{1.1}$$

where

$\Phi_{xx}(f)$ is the (real) auto power spectral density function of x(t),

$\Phi_{yy}(f)$ is the (real) auto power spectral density function of y(t), and

$\Phi_{xy}(f)$ is the (complex) cross power spectral density function of x(t) and y(t) and consists of a real or coincidental (CO) spectrum and an imaginary or quadrature (quad) spectrum.[1]

A simplifying ratio is the complex coherence function (spectrum),

$$\gamma_{xy}(f) = \frac{\Phi_{xy}(f)}{\sqrt{\Phi_{xx}(f)\,\Phi_{yy}(f)}} , \tag{1.2}$$

or, more commonly, the magnitude-squared coherence function,

$$\left|\gamma_{xy}(f)\right|^2 = \frac{\left|\Phi_{xy}(f)\right|^2}{\Phi_{xx}(f)\,\Phi_{yy}(f)} \qquad (1.3)$$

The term "coherence" can imply Eqs. (1.2), (1.3), or the positive square root of Eq. (1.3).

Equation (1.3) possesses a number of useful attributes: First, it always falls between zero and one. Second, it is zero if the processes x(t) and y(t) are uncorrelated. Third, it is equal to unity if and only if there exists a linear relation between x(t) and y(t).[2]

These attributes are of particular significance in sonar systems where a waveform received at two spatially separated elements of a hydrophone array may be corrupted by additive noise uncorrelated from the first to the second element.

Unfortunately, the difficulty in estimating the true coherence has plagued modern statisticians.[3] An analytical expression was derived by Goodman[1] for the probability density function of the estimate of magnitude coherence $|\hat{\gamma}|$ when several independent observations (or segments) of the processes are available. A closed-form solution for the cumulative distribution function, as a finite sum of hypergeometric functions, can be found by proper identification of variables in the work of Fisher.[4] The application of Fisher's work to this problem is believed original in this thesis. Earlier, statistics for coherence estimation were found in tables, and graphs,[5-7] and transformations to be performed on the coherence estimator were suggested so as to "normalize" (make Gaussian) the density function.[8, 9]

Certain empirical studies have also been conducted. Haubrich suggested that the total time series under investigation be segmented into a number of shorter segments overlapping one another by 50 percent and that a triangular weighting function be applied to each segment.[7] Tick showed empirical examples of the types of estimates to anticipate when the true coherence is 0.2 and mean lagged product techniques are used.[3] Benignus empirically showed the bias and confidence intervals to expect when n independent segments are processed using a rectangular weighting function.[10]

Current techniques for coherence estimation involve applying the fast Fourier transform (FFT).[11] Some of the latest published results on coherence estimation are limited in scope to processes that have relatively flat spectra.[10] The problems associated with nonflat spectra can be avoided through judicious choice of a time-weighting (or windowing) function.[12-14] The use of a weighting function is necessary for data not spectrally flat and should be prudently selected for unknown data. In coherence estimation, the application of a weighting function results in wasted data (loss of stability and increase of bias) unless overlapped processing[14] is employed. In underwater acoustic environments, which require weighting functions and good spectral resolution, but which remain stationary only for limited amounts of time, such wastage can not be permitted.

This thesis empirically determines the effect of overlap processing on the estimated magnitude-squared coherence function when cosine (or Hanning, after Julius von Hann) weighting has been applied.

The empirical method for determining the effect of overlap has been limited in scope to a cosine weighting function, a finite time history, and a desired

frequency resolution (half-power) bandwidth. Under these conditions, estimates of bias and variance of the estimate of magnitude-squared coherence have been made for two values of coherence. The behavior of these statistics as a function of increasing overlap is presented and is believed original.

II. COHERENCE FUNCTION (SPECTRUM) AND ITS USES

This chapter defines the coherence function (spectrum). Additionally, it reviews those terms necessary for its definition or helpful in its estimation. Finally, this chapter presents some examples of the uses of coherence to lay a background for why this particular function is meaningful.

II.A. COHERENCE FUNCTION

The essense of the coherence function is a collapsed power spectral density matrix. To fully appreciate the intricacies of its definition, it is first necessary to review some basic concepts. They include the correlation matrix, wide-sense stationarity, ergodicity, Gaussian assumption, and power spectral density matrix.

II.A.1. Correlation Matrix and Wide-Sense Stationarity

The general correlation function between zero-mean processes x(t) and y(t), which are real and nonstationary, is defined by Davenport and Root,[15] as follows:

$$R_{xy}(t_1, t_2) \triangleq E\left[x(t_1)\, y(t_2)\right] , \qquad (2\ 1)$$

AD-A101 684 SCIENTIFIC AND ENGINEERING STUDIES COMPILED 1979 2/2
COHERENCE ESTIMATION(U) NAVAL UNDERWATER SYSTEMS CENTER
NEWPORT RI G C CARTER ET AL. 1979

UNCLASSIFIED F/G 9/1 NL

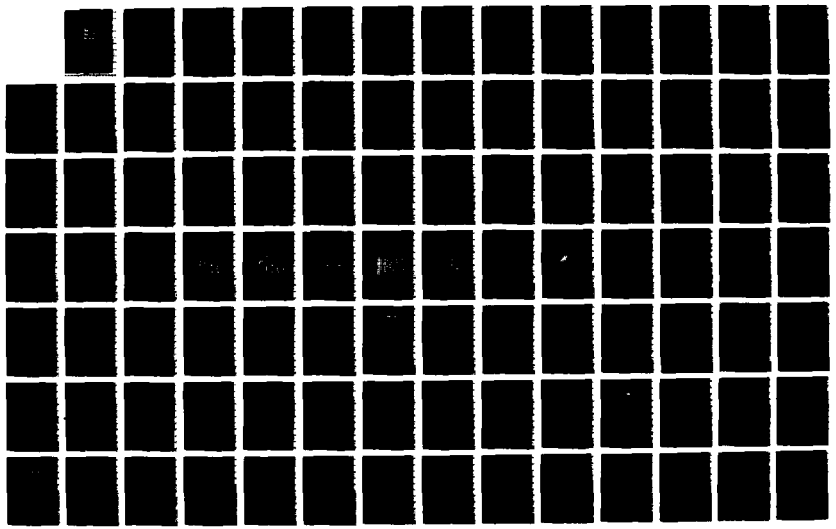

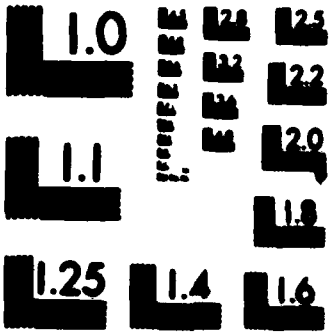

which depends on the absolute time instants t_1 and t_2. If the cross-correlation function depends only on the time difference $\tau = t_2 - t_1$ and does not depend on the time origin, that is, if

$$R_{xy}(t_1, t_1 + \tau) = R_{xy}(\tau) \triangleq E\left[x(t) y(t + \tau)\right], \tag{2.2}$$

then the processes are called wide-sense stationary. It is not necessary for $R_{xy}(\tau)$ to be an even or an odd function.

Similarly, the autocorrelation function in the wide-sense stationary case becomes

$$R_{xx}(\tau) \triangleq E\left[x(t) x(t + \tau)\right], \tag{2.3}$$

which is an even function. The autocorrelation function of the process $y(t)$ is similarly defined.

The correlation matrix for the wide-sense stationary processes $x(t)$ and $y(t)$ may now be defined by

$$[R_{xy}(\tau)] \triangleq \begin{bmatrix} R_{xx}(\tau) & R_{xy}(\tau) \\ R_{yx}(\tau) & R_{yy}(\tau) \end{bmatrix} \tag{2.4}$$

When two zero-mean random processes have a correlation matrix that depends only on the time difference, it is meaningful to talk about the Fourier transformation of the correlation matrix.[16]

II.A.2. Ergodicity

Random processes can be characterized by an infinite number of waveforms. Each of these waveforms is referred to as a sample or member function of the random process and is itself infinite in duration.[17] Statistics of an order higher than the correlation function can be computed by averaging over the ensemble of all sample functions. These statistics can also be computed from any one of the sample functions.

If all the higher order statistics, when computed from any one of the sample functions, are the same as the ensemble average over all the sample functions, then the processes are called ergodic. In particular, the correlation matrix computed over any one sample function is the same as the correlation matrix computed over an ensemble of sample functions. It should be noted that it is possible for the correlation matrix to be the same when computed over different sample functions and yet for some higher order statistics to differ when computed over different sample functions.

It is important for the results presented in this thesis that the correlation matrix be the same when computed over different sample functions. This, in essence, allows the correlation matrix (or its linear transformations) to be specified with probability one from one sample function. If the correlation matrix does not differ when computed over different sample functions, the processes are still called ergodic, but now some qualifying adjective must be applied to denote the strength of the ergodicity.[18] This author chooses to use the adjective "wide-sense" to specify the strength of the ergodicity. Processes that are wide-sense ergodic are also wide-sense stationary.

II.A.3. Gaussian Assumption

If two zero-mean processes are jointly Gaussian and wide-sense stationary, then their correlation matrix defines all higher order statistics.[16]

II.A.4. Power Spectral Density Matrix

Several important concepts have preceded this section: First, in order to mathematically determine the power spectral density matrix, the processes must be stationary (in the wide sense). In practical estimation situations ergodicity is presumed, and only one time-limited sample function is collected for each process under investigation. It is desirable, but not necessary, that the two processes be jointly Gaussian. When the two processes are both stationary and jointly Gaussian, then knowledge of their correlation matrix completely specifies the statistics of the processes.

Given the zero-mean processes $x(t)$ and $y(t)$, which are real, stationary, and jointly Gaussian, a complete characterization for the probability structure of the processes is specified in terms of the power spectral density matrix $\mathbf{\Phi}_{xy}(f)$:[1]

$$\mathbf{\Phi}_{xy}(f) \triangleq \begin{bmatrix} \Phi_{xx}(f) & \Phi_{xy}(f) \\ \Phi_{yx}(f) & \Phi_{yy}(f) \end{bmatrix} . \tag{2.5}$$

The power spectral density functions composing the elements of the power spectral density matrix are the Fourier transforms of the associated correlation functions. The cross power spectral density function is

$$\Phi_{xy}(f) \triangleq \int_{-\infty}^{\infty} R_{xy}(\tau)\, e^{-j2\pi f\tau}\, d\tau \quad . \tag{2.6}$$

In general, this function is complex since $R_{xy}(\tau)$ is not necessarily odd or even. Similarly,

$$\Phi_{xx}(f) \triangleq \int_{-\infty}^{\infty} R_{xx}(\tau)\, e^{-j2\pi f\tau}\, d\tau \quad , \tag{2.7}$$

which is purely real since $R_{xx}(\tau)$ is even.

II.A.5. Definition

The complex coherence function for two wide-sense stationary processes is a normalized complex cross power spectral density function given by

$$\gamma_{xy}(f) \triangleq \frac{\Phi_{xy}(f)}{\sqrt{\Phi_{xx}(f)\ \Phi_{yy}(f)}} \quad . \tag{2.8}$$

Since $\Phi_{xy}(f)$ is complex,

$$\Phi_{xy}(f) = C_{xy}(f) + j\, Q_{xy}(f) \quad . \tag{2.9}$$

Further, $\Phi_{xx}(f)$ and $\Phi_{yy}(f)$ are nonnegative, real functions of f,

$$\Phi_{xx}(f) \geq 0 \tag{2.10}$$

and

$$\Phi_{yy}(f) \geq 0 \quad . \tag{2.11}$$

The magnitude of the complex coherence function (or, simply, the magnitude coherence) is

$$\left| \gamma_{xy}(f) \right| = \frac{\left| \Phi_{xy}(f) \right|}{\sqrt{\Phi_{xx}(f)\, \Phi_{yy}(f)}} \quad . \tag{2.12}$$

It follows directly that the square of the magnitude of the complex coherence function (or, simply, the magnitude-squared coherence) is

$$\left| \gamma_{xy}(f) \right|^2 = \frac{\left| \Phi_{xy}(f) \right|^2}{\Phi_{xx}(f)\, \Phi_{yy}(f)} \quad , \tag{2.13a}$$

$$= \frac{C_{xy}^2(f) + Q_{xy}^2(f)}{\Phi_{xx}(f)\, \Phi_{yy}(f)} \quad . \tag{2.13b}$$

Although the term "coherence" can imply Eqs. (2.8), (2.12), or (2.13), it usually refers to Eq. (2.13).

For ease of notation, the dependence on f is often not specified; for example,

$$\left| \gamma_{xy} \right|^2 = \frac{C_{xy}^2 + Q_{xy}^2}{\Phi_{xx}\, \Phi_{yy}} \quad . \tag{2.14}$$

II. B. USES OF COHERENCE FUNCTION

The magnitude-squared coherence function for the zero-mean, wide-sense stationary processes x(t) and y(t) is useful in several ways, which will be proved in the following sections. First, for two processes that are linearly related, the magnitude-squared coherence function is unity. Second, for two independent processes, the magnitude-squared coherence function is zero. Third, under the assumptions to be presented, the magnitude-squared coherence function serves as a signal-to-noise measure.

II. B. 1. A Measure of System Linearity

The magnitude-squared coherence function can be used to measure system linearity.[12] In Fig. 1 consider the linear system with input x(t), impulse response $h(\tau)$, and output y(t). The output y(t) is expressed by the convolution integral

$$y(t) = \int_{-\infty}^{\infty} h(\tau)\, x(t-\tau)\, d\tau \quad . \tag{2.15}$$

Fig. 1. Linear System with Impulse Response $h(\tau)$

The frequency-domain equivalent is a multiplication obtained via the Fourier transformation:

$$Y(f) = H(f)\, X(f) \tag{2.16}$$

If x(t) is a sample function of a stationary random process,[2] then

$$\Phi_{xy}(f) = H(f)\, \Phi_{xx}(f) \tag{2.17}$$

and

$$\Phi_{yy}(f) = H(f)\, H^{*}(f)\, \Phi_{xx}(f) = H(f)\, \Phi^{*}_{xy}(f) \ . \tag{2.18}$$

Since the magnitude-squared coherence defined by Eq. (2.13) can be written as

$$\left| \gamma_{xy}(f) \right|^2 = \frac{\Phi_{xy}(f)\, \Phi^{*}_{xy}(f)}{\Phi_{xx}(f)\, \Phi_{yy}(f)} \ , \tag{2.19}$$

application of Eqs. (2.17) and (2.18) yields

$$\left| \gamma_{xy}(f) \right|^2 = H(f)\, \frac{1}{H(f)} = 1 \ , \ \forall\ f \ . \tag{2.20}$$

Consequently, the magnitude-squared coherence between the input and output of a linear system is unity.

II. B. 2. A Measure of Correlation

If the zero-mean processes x(t) and y(t) are independent, they are also uncorrelated and orthogonal; that is

$$R_{xy}(\tau) = E\left[x(t)y(t+\tau)\right] = E\left[x(t)\right] E\left[y(t+\tau)\right] = 0 \ , \tag{2.21}$$

$$\Phi_{xy}(f) = \int_{-\infty}^{\infty} R_{xy}(\tau)\, e^{-j2\pi f\tau}\, d\tau \ = 0 \ , \tag{2.22}$$

and

$$\left|\gamma_{xy}(f)\right|^2 = 0 \ , \quad \forall\ f \ . \tag{2.23}$$

Hence, if the two processes are independent or uncorrelated with zero mean, the magnitude-squared coherence between them is zero.

II. B. 3. A Measure of Signal-to-Noise Ratio

Consider a signal, s(t), passed through two linear filters and received at two sensors where it is corrupted by uncorrelated additive noises. The received waveform at each sensor is then passed through two linear filters, as shown in Fig. 2.

Assume that s(t), $n_1(t)$, and $n_2(t)$ are uncorrelated; that is,

$$E\left[n_1(t)\, n_2(t+\tau)\right] = 0 \ , \tag{2.24}$$

$$E\left[n_1(t)\ s(t+\tau)\right] = 0 \ , \tag{2.25}$$

and

$$E\left[n_2(t)\, s(t+\tau)\right] = 0 \quad . \tag{2.26}$$

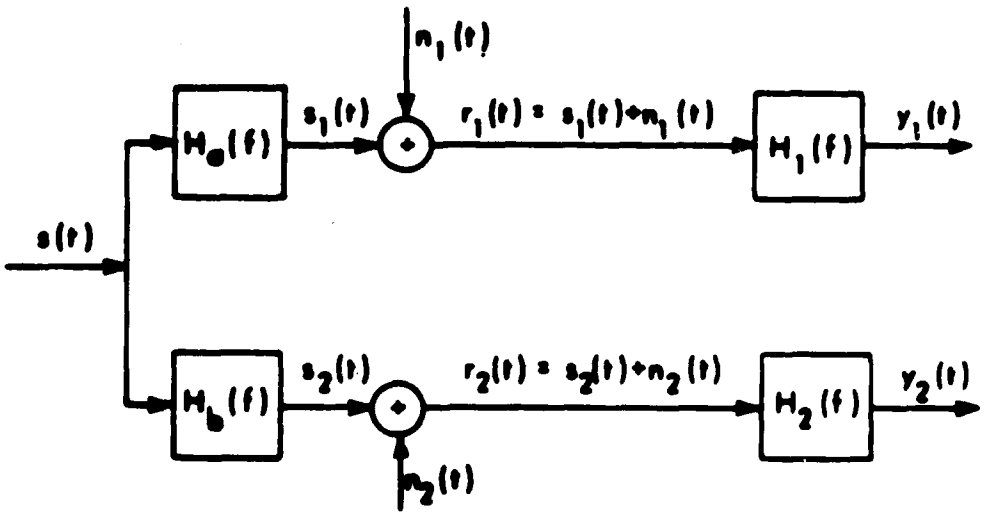

Fig. 2. Signal s(t) as Received at Two Sensors

Then,

$$\Phi_{y_1y_1}(f) = \Phi_{r_1r_1}(f)\left|H_1(f)\right|^2 \quad , \tag{2.27a}$$

$$= \left[\Phi_{s_1s_1}(f) + \Phi_{n_1n_1}(f)\right]\left|H_1(f)\right|^2 \quad , \tag{2.27b}$$

and

$$= \left[\Phi_{ss}(f)\left|H_a(f)\right|^2 + \Phi_{n_1n_1}(f)\right]\left|H_1(f)\right|^2 \quad ; \tag{2.27c}$$

$$\Phi_{y_2y_2}(f) = \Phi_{r_2r_2}(f)\left|H_2(f)\right|^2 \quad , \tag{2.28a}$$

$$= \left[\Phi_{s_2s_2}(f) + \Phi_{n_2n_2}(f)\right]\left|H_2(f)\right|^2 \quad , \tag{2.28b}$$

and

$$= \left[\Phi_{ss}(f)\left|H_b(f)\right|^2 + \Phi_{n_2n_2}(f)\right]\left|H_2(f)\right|^2 ; \qquad (2.28c)$$

$$\Phi_{y_1y_2}(f) = H_1(f)\,H_2^*(f)\,\Phi_{r_1r_2}(f) , \qquad (2.29a)$$

$$= H_1(f)\,H_2^*(f)\,\Phi_{s_1s_2}(f) , \qquad (2.29b)$$

and

$$= H_1(f)\,H_2^*(f)\,H_a(f)\,H_b^*(f)\,\Phi_{ss}(f) ; \qquad (2.29c)$$

$$\left|\gamma_{y_1y_2}(f)\right|^2 = \frac{\Phi_{ss}^2(f)\left|H_a(f)\,H_b^*(f)\right|^2}{\left[\Phi_{ss}(f)\left|H_a(f)\right|^2 + \Phi_{n_1n_1}(f)\right]\left[\Phi_{ss}(f)\left|H_b(f)\right|^2 + \Phi_{n_2n_2}(f)\right]} . \qquad (2.30a)$$

and

$$= \left|\gamma_{r_1r_2}(f)\right|^2 \qquad (2.30b)$$

Equation (2.30b) is independent of both $H_1(f)$ and $H_2(f)$; that is, the coherence between the two received waveforms is not changed by linear filtering.

There are two special cases of Eq. (2.30a) that are of interest: First, when

$$\Phi_{n_1n_1}(f) = \Phi_{n_2n_2}(f) = \Phi_{nn}(f) \qquad (2.31)$$

and

$$\left|H_a(f)\right|^2 = \left|H_b(f)\right|^2 = 1 \qquad (2.32)$$

(as, for example, if

$$H_a(f) = e^{-j2\pi f \tau_a} \tag{2.33}$$

and

$$H_b(f) = e^{-j2\pi f \tau_b} \tag{2.34}$$

corresponding to time delays τ_a and τ_b or a directional signal), then

$$\left|\gamma_{y_1 y_2}(f)\right|^2 = \frac{\Phi_{ss}^2(f)}{\left[\Phi_{ss}(f) + \Phi_{nn}(f)\right]^2} \tag{2.35}$$

and

$$\frac{\Phi_{ss}(f)}{\Phi_{nn}(f)} = \frac{\left|\gamma_{y_1 y_2}(f)\right|}{1 - \left|\gamma_{y_1 y_2}(f)\right|} . \tag{2.36}$$

Second, when

$$n_1(t) = 0 , \tag{2.37}$$

$$\Phi_{n_2 n_2}(f) = \Phi_{nn}(f) , \tag{2.38}$$

and

$$\left|H_a(f)\right|^2 = \left|H_b(f)\right|^2 = 1 , \tag{2.39}$$

then

$$\left|\gamma_{y_1 y_2}(f)\right|^2 = \frac{\Phi_{ss}^2(f)}{\left[\Phi_{ss}(f) + \Phi_{nn}(f)\right]\Phi_{ss}(f)} \tag{2.40}$$

and

$$\frac{\Phi_{ss}(f)}{\Phi_{nn}(f)} = \frac{\left| \gamma_{y_1 y_2}(f) \right|^2}{1 - \left| \gamma_{y_1 y_2}(f) \right|^2} \qquad (2.41)$$

This is a generalization of work done by Roth,[19] Carter and Arnold,[12] and Knapp.[20]

III. COHERENCE-ESTIMATION PROCEDURE

The procedure for estimating the coherence or magnitude-squared coherence functions for wide-sense ergodic (and, hence, wide-sense stationary), zero-mean random processes x(t) and y(t) is discussed in this chapter. (References within this chapter to x(t) and y(t) apply to those specific processes with the noted characteristics, that is, zero-mean, wide-sense ergodic.) The basic objective is to obtain estimates of the elements of the spectral density matrix,

$$\mathbf{M}_{xy}(f) = \begin{bmatrix} \Phi_{xx}(f) & \Phi_{xy}(f) \\ \Phi_{yx}(f) & \Phi_{yy}(f) \end{bmatrix} , \qquad (3.1)$$

in order to form the magnitude-squared coherence estimator.

The estimation procedure described is the direct method, which is discussed in part by Welch,[21] Knapp,[22] Bingham,[13] Benignus,[10] Nuttall,[14] and Carter and Arnold.[12] It includes cosine weighting and overlapped processing and is used because of the computational advantage of the FFT.[11]

Briefly, the method implemented consists of obtaining two finite-time series from the random processes being investigated. The time series are segmented into n segments, each having P-data points. For example, from each process there may be 32 segments, each segment having 4096 points. The segments may be overlapped or disjoint. Each segment is multiplied by a weighting function,

and the FFT of the weighted P-point sequence is performed. The Fourier coefficients for each weighted segment are then used to estimate the elements of the power spectral density matrix. The power spectral estimates thus obtained from each set of weighted sequences are then averaged over all the a segments. Next, the resultant estimates are used to form the magnitude-squared coherence.[12]

III.A. QUANTIZED SEQUENCE OBTAINED FROM WEIGHTED SEGMENT OF DATA

Consider the time-limited sample functions of processes x(t) and y(t) (specified in Chapter III.). Let the sample functions be further constrained so that they have the same bandwidth. This may come about as a result of (1) the physics of the experiment, (2) the bandpass characteristics of some recording device, or (3) the intentional introduction of bandpass or low-pass filters to prevent aliasing. Analog to digital (A/D) conversion of the signals is now accomplished by sampling the two analog signals at a frequency, f_s Hz, greater than twice the bandwidth of the signals. This technique yields two quantized sequences of numbers or time series. The quantization error decreases as the number of bits in the quantizer increases. (Errors as a result of quantization are beyond the scope of this work.)

Let these two time series from processes x(t) and y(t), which are drawn continuously for convenience, be depicted as in Fig. 3.

The method of overlapped weighted segmentation requires that before estimating the coherence between x(t) and y(t) both x(t) and y(t) be

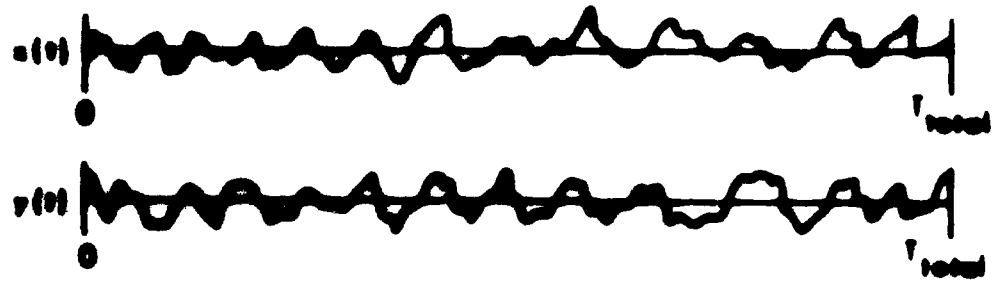

Fig. 3. Two Time Series from Processes x(t) and y(t) multiplied by a series of real weighting functions, $w_s(t)$, or sampled and quantized versions thereof, as in Fig. 4.

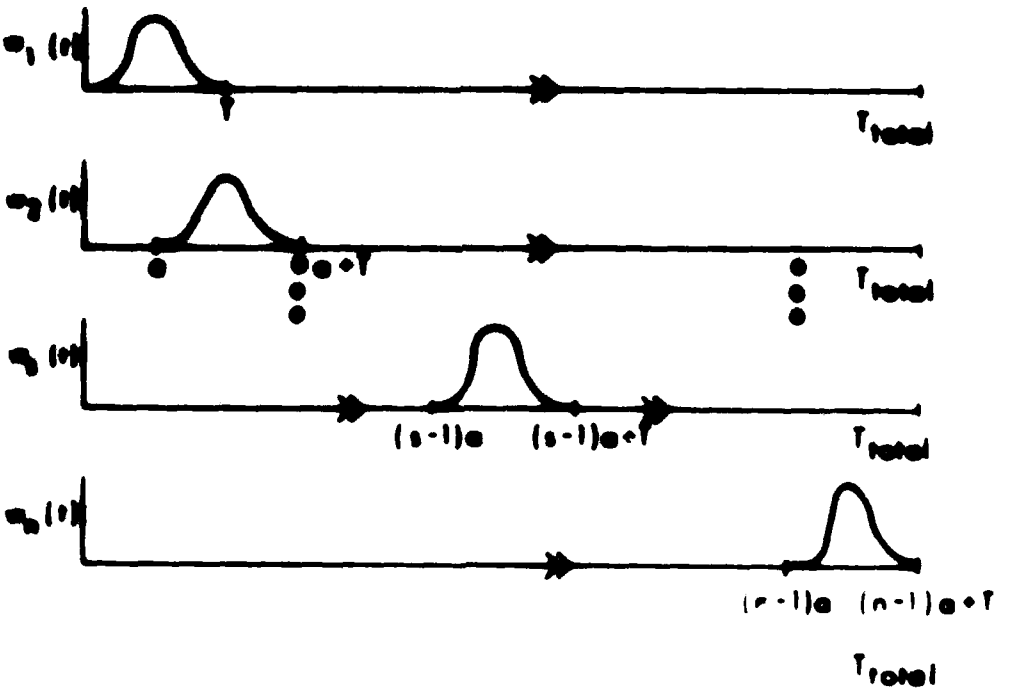

Fig. 4. Overlapped Weighting Functions (Modified from Knapp[22])

The method implemented computes a P-point discrete Fourier transform (DFT) for each of the weighted segments. The frequency-domain equivalent of multiplying each segment by a weighting function is a convolution of the true

spectrum with the Fourier transform of the weighting function. Hence, the weighting function should be judiciously selected in order that the true spectrum be least distorted.

The factors affecting the selection of the segment length and window shape are

1. $w_s(t)$ should be relatively easy to compute.

2. T_{total}/T should be large in order that the amount of averaging be sufficient to reduce the bias and variance of the spectral estimates.

3. $\frac{d^n}{dt^n} w_s(t)$ should be continuous for $n = 0, 1, 2, \ldots,$ up to some reasonable limit, since this ensures that the sidelobes of the Fourier transform of $w_s(t)$ die off rapidly.

4. The Fourier transform of $w_s(t)$ should also be narrow in the main lobe (narrower than the finest detail of the true spectral density matrix of processes x(t) and y(t)). Generally, this lobe is narrowed by increasing T.

The specific selection of a weighting function involves a number of tradeoffs. A commonly used weighting (or windowing) function is the cosine (Hamming) function defined[13] by

$$w_s(t) = \begin{cases} \frac{1}{2}\left(1 - \cos\left\{2\pi\left[\frac{t-(s-1)a}{T}\right]\right\}\right), & (s-1)a \le t \le T + (s-1)a, \\ 0, & \text{elsewhere.} \end{cases} \tag{3.2}$$

The percentage overlap from Fig. 4 is, simply,

$$p_o = \begin{cases} \left(\frac{T-a}{T}\right) 100, & a \le T, \\ 0, & a > T. \end{cases} \tag{3.3}$$

Therefore, for example, if $T = 1$ and $a = \frac{1}{2}$, then $p_o = 50$ percent. Whereas if $T = 1$ and $a = 3/4$, then $p_o = 25$ percent.

Note that if $a \geq T$ there would be no overlap, and each segment would be virtually independent of the previous one (except for correlated edge effects). All theoretical results here are concerned with the case of independent segments, that is, no overlap. A detailed analysis of the effect of overlapped weighted segmentation for estimating auto power spectral density functions is given by Nuttall.[14]

III. B. COHERENCE ESTIMATOR

Let x_{sp}, where $p = 0, 1, 2, \ldots, P-1$ denote the P-point sequence obtained from the sth weighted segment of process $x(t)$. In estimating the coherence function, it is necessary to evaluate a transformation of this weighted sequence. The *FFT* is a fast algorithm for evaluating a special case of the Z-transform of a finite sequence of numbers. The two sided Z-transform of an infinite sequence is defined by

$$X_s(z) = \sum_{p=-\infty}^{\infty} x_{sp} z^{-p} \quad , \tag{3.4}$$

where z equals any complex variable.[23]

Evaluation of the Z-transform at P equally spaced points around the unit circle for a P-point sequence yields the P-point DFT:[23]

$$X_s(f_k) = \sum_{p=0}^{P-1} x_{sp} e^{-j2\pi f_k p/P} \quad , \tag{3.5}$$

where x_{sp} is the finite weighted sequence, $p = 0, 1, \ldots, P-1$, and $s = 1, 2, \ldots, n$. Equation (3.5) can be evaluated for $k = 0, 1, \ldots, P-1$, with a fast algorithm requiring on the order of $P \log_2 P$ complex multiplications and additions.[11]

Similarly, a vector, $Y_s(f_k)$, is formed for each segment (that is, $s = 1, 2, \ldots, n$).

The estimate of the auto power spectral density function of $x(t)$ at the kth frequency, obtained from the sth weighted segment, is given by

$$\hat{\Phi}_{xx_s}(f_k) = \frac{\Delta t}{P}\left[X_s(f_k)\, X_s^*(f_k)\right], \text{ where } \Delta t = 1/f_s . \quad (3.6)$$

Similarly,

$$\hat{\Phi}_{yy_s}(f_k) = \frac{\Delta t}{P}\left[Y_s(f_k)\, Y_s^*(f_k)\right], \quad (3.7)$$

and the estimate of the cross power spectral density function is

$$\hat{\Phi}_{xy_s}(f_k) = \frac{\Delta t}{P}\left[X_s(f_k)\, Y_s^*(f_k)\right] . \quad (3.8)$$

Equation (3.8) can be rewritten in terms of the real and imaginary parts,

$$\hat{C}_{xy_s}(f_k) = \frac{\Delta t}{P}\,\mathrm{Re}\left[X_s(f_k)\, Y_s^*(f_k)\right] \quad (3.9)$$

and

$$\hat{Q}_{xy_s}(f_k) = \frac{\Delta t}{P}\,\mathrm{Im}\left[X_s(f_k)\, Y_s^*(f_k)\right] . \quad (3.10)$$

Next, the estimates of the elements of the power spectral density matrix are obtained by averaging over the number of segments, n. The estimate of the magnitude-squared coherence follows directly:

$$\left|\hat{\gamma}(f_k)\right|^2 \triangleq \frac{\left[\frac{1}{n}\sum_{s=1}^{n}\hat{C}_{xy_s}(f_k)\right]^2 + \left[\frac{1}{n}\sum_{s=1}^{n}\hat{Q}_{xy_s}(f_k)\right]^2}{\left[\frac{1}{n}\sum_{s=1}^{n}\hat{\Phi}_{xx_s}(f_k)\right]\left[\frac{1}{n}\sum_{s=1}^{n}\hat{\Phi}_{yy_s}(f_k)\right]} , \tag{3.11}$$

where k indexes the discrete frequency of interest and n is the number of overlapped segments.

The estimate of magnitude coherence is

$$\left|\hat{\gamma}(f_k)\right| = +\sqrt{\left|\hat{\gamma}(f_k)\right|^2} . \tag{3.12}$$

It is of practical interest to note (as pointed out by Jenkins and Watts[8]) that an alternate and seemingly reasonable form of the estimate yields

$$\left|\hat{\gamma}_w(f_k)\right|^2 = \frac{1}{n}\sum_{s=1}^{n}\frac{\left|X_s(f_k)\,Y_s^*(f_k)\right|^2}{X_s(f_k)\,X_s^*(f_k)\,Y_s(f_k)\,Y_s^*(f_k)} \tag{3.13a}$$

and

$$= \frac{1}{n}\sum_{s=1}^{n}\frac{X_s(f_k)\,Y_s^*(f_k)\,X_s^*(f_k)\,Y_s(f_k)}{X_s(f_k)\,X_s^*(f_k)\,Y_s(f_k)\,Y_s^*(f_k)} = 1 . \tag{3.13b}$$

This fact is so basic that it is often not discussed. However, it points out that regardless of the value of the true magnitude-squared coherence, $\left|\hat{\gamma}\right|^2 = 1.0$

when $n = 1$. Consequently, the estimate is, in general, biased; the actual bias depends on $|\gamma|^2$ and n. In practice, n should be large, as will be shown.

IV. STATISTICS OF ESTIMATE OF COHERENCE

Goodman, in his Eqs. (4.51) and 4.60),[1] derived an analytical expression for the probability density function of the magnitude-coherence estimate, $|\hat{\gamma}|$, based on Eqs. (3.11) and (3.12). His results were based on two zero-mean processes that were stationary, Gaussian, and random and had been segmented into n independent observations (that is, nonoverlapped segments). Each segment was assumed large enough to ensure adequate spectral resolution. Further, each segment was assumed perfectly weighted (windowed), in the sense that the Fourier coefficient at some kth frequency was to have "leaked" no power from other bins. However, Hannan[24] points out that the statistics do not hold at the zeroth or folding frequencies.

The material in this chapter relating to magnitude-squared coherence is believed to be new (Carter and Nuttall[25]) and is a direct extension of Goodman's work.[1] All of Goodman's original assumptions hold. Statistics of the magnitude-coherence estimator are given in Appendix A.

IV.A. PROBABILITY DENSITY AND CUMULATIVE DISTRIBUTION FUNCTIONS

The first-order probability density and cumulative distribution functions for the estimate of magnitude-squared coherence, given the true value of magnitude-squared coherence and the number, n, of independent segments processed,

are presented in closed-form. The expressions are evaluated and plotted.

IV. A. 1. Probability Density Function

The conditional probability density function for the estimate of magnitude-squared coherence, $|\hat{\gamma}|^2$, between two processes, given $|\gamma|^2$ and n, is[9]

$$p\left(|\hat{\gamma}|^2 \,\middle|\, n, |\gamma|^2\right) = (n-1)\left(1-|\gamma|^2\right)^n \left(1-|\hat{\gamma}|^2\right)^{n-2}$$

$$\cdot\, {}_2F_1\left(n, n; 1; |\gamma|^2 |\hat{\gamma}|^2\right), \quad 0 \le |\gamma|^2 |\hat{\gamma}|^2 < 1 \tag{4.1}$$

It then follows, knowing $|\hat{\gamma}| = \left[|\hat{\gamma}|^2\right]^{\frac{1}{2}}$, that

$$p\left(|\hat{\gamma}| \,\middle|\, n, |\gamma|\right) = p\left(|\hat{\gamma}|^2 \,\middle|\, n, |\gamma|^2\right) 2|\hat{\gamma}| \,. \tag{4.2}$$

Equation (4.2) can be shown (Appendix A) to be Goodman's result.[1] The density function, Eq. (4.1), can be rewritten using Eq. (15.35) of Abramowitz[26] in the following alternate forms:

$$p\left(|\hat{\gamma}|^2 \,\middle|\, n, |\gamma|^2\right) = (n-1)\left(1-|\gamma|^2\right)^n \left(1-|\hat{\gamma}|^2\right)^{n-2}$$

$$\cdot \left(1-|\gamma|^2|\hat{\gamma}|^2\right)^{1-2n} {}_2F_1\left(1-n, 1-n; 1; |\gamma|^2|\hat{\gamma}|^2\right) \tag{4.3}$$

and

$$p\left(|\hat{\gamma}|^2 \,\middle|\, n, |\gamma|^2\right) = (n-1)\left[\frac{\left(1-|\gamma|^2\right)\left(1-|\hat{\gamma}|^2\right)}{\left(1-|\gamma|^2|\hat{\gamma}|^2\right)^2}\right]^n$$

$$\frac{\left(1-|\gamma|^2|\hat{\gamma}|^2\right)}{\left(1-|\hat{\gamma}|^2\right)^2}\ {}_2F_1\left(1-n,\ 1-n;\ 1;\ |\gamma|^2|\hat{\gamma}|^2\right). \quad (4.4)$$

Equations (4.3) and (4.4) are desirable because ${}_2F_1\left(1-n,\ 1-n;\ 1;\ |\gamma|^2|\hat{\gamma}|^2\right)$ can be expressed as an $(n-1)$st order polynomial (Abramowitz, Eq. (15.4.1)[26])

A special case of the density function occurs when $|\gamma|^2 = 0.0$. In that event,

$$p\left(|\hat{\gamma}|^2 \,\middle|\, n, |\gamma|^2 = 0.0\right) = (n-1)\left(1-|\hat{\gamma}|^2\right)^{n-2}. \quad (4.5)$$

IV.A.2. Cumulative Distribution Function

Fisher,[4] working on statistics of the estimate of the squared correlation coefficient, derived the probability density for that random variable. He integrated the result and achieved a closed-form solution for the cumulative distribution function; specifically the solution was a finite sum of ${}_2F_1$ functions, each one a finite-order polynomial. Although these statistics are for a different problem, proper identification of variables yields exactly the integration formula needed to find the cumulative distribution of the estimate of magnitude-squared coherence, namely,

$$p\left(|\hat{\gamma}|^2 \,\middle|\, n, |\gamma|^2\right) = |\hat{\gamma}|^2 \left[\left(\frac{1-|\gamma|^2}{1-|\gamma|^2|\hat{\gamma}|^2}\right)^n \sum_{k=0}^{n-2}\left(\frac{1-|\hat{\gamma}|^2}{1-|\gamma|^2|\hat{\gamma}|^2}\right)^k\right]$$

$$\cdot\, {}_2F_1\left(-k, 1-n; 1; |\gamma|^2|\hat{\gamma}|^2\right). \qquad (4.6)$$

In the special case when $|\gamma|^2 = 0$, the cumulative distribution function becomes

$$p\left(|\hat{\gamma}|^2 \,\middle|\, n, |\gamma|^2 = 0.0\right) = |\hat{\gamma}|^2 \sum_{k=0}^{n-2}\left(1-|\hat{\gamma}|^2\right)^k, \qquad (4.7)$$

which can be simplified to give

$$p\left(|\hat{\gamma}|^2 \,\middle|\, n, |\gamma|^2 = 0.0\right) = 1-\left(1-|\hat{\gamma}|^2\right)^{n-1}. \qquad (4.8)$$

Equation (4.8), when differentiated, yields the probability density function, Eq. (4.5).

IV.A.3. Computer Evaluation

The probability density function, Eq. (4.4), can be evaluated readily on a large digital computer in floating-point arithmetic. Evaluation for 100 values of $|\hat{\gamma}|^2$ between 0.0 and 0.99 requires computing 100 (n - 1)st order polynomials for each value of $|\gamma|^2$ and n. The

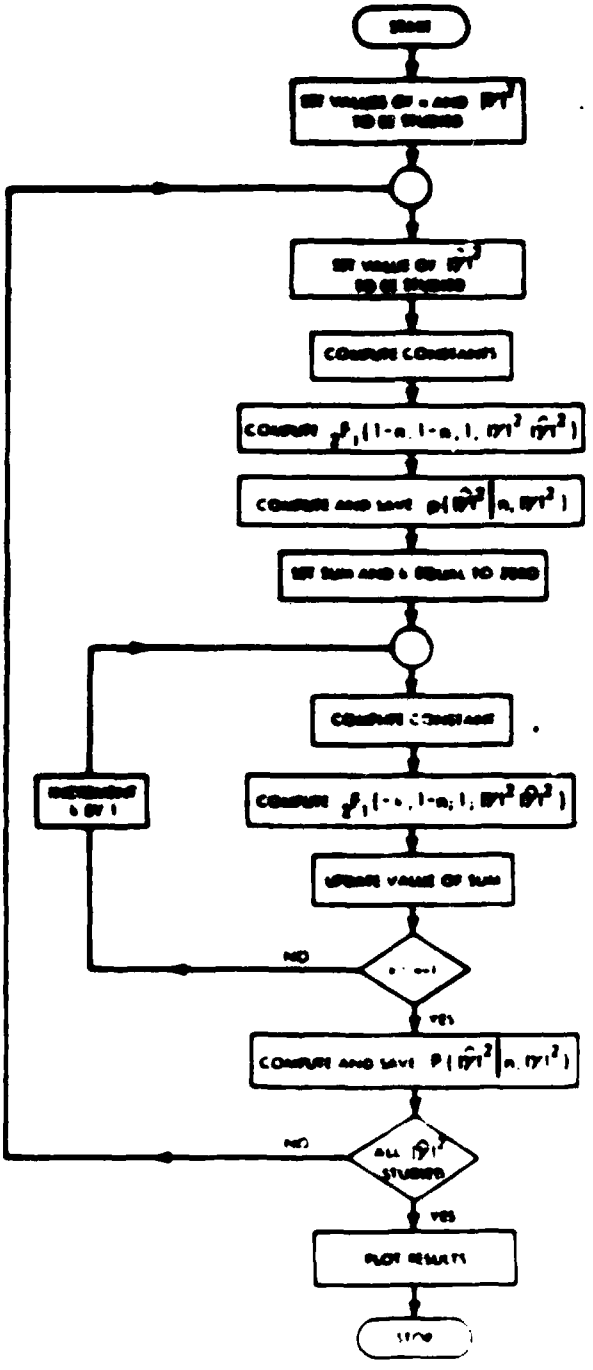

Fig. 5. Summary Flow Chart for Density and Cumulative Distribution

cumulative distribution, Eq. (4.6), can be similarly evaluated. The density function and the cumulative-distribution function were computed as illustrated in Fig. 5 for ten values of $|\gamma|^2$ and for $n = 32$, 40, 48, 56, and 64. (The computations and 100 plots were done on the UNIVAC 1108 in less than 5 minutes.) Example plots are included in Figs. 6 through 13.

One example of how these plots can be used is as follows: Magnitude-squared coherence, $|\hat{\gamma}|^2$, is estimated by averaging over 32 disjoint segments of data (that is, $n = 32$). Suppose the estimated value is approximately 0.3, then from Fig. 7

$$\text{Prob}\left(L < |\hat{\gamma}|^2 \,\middle|\, n = 32, |\gamma|^2 = 0.3\right) = \int_L^{\infty} p\left(|\hat{\gamma}|^2 \,\middle|\, n = 32, |\gamma|^2 = 0.3\right) d|\hat{\gamma}|^2 \qquad (4.9a)$$

and

$$= 1 - \int_{-\infty}^{L} p\left(|\hat{\gamma}|^2 \,\middle|\, n = 32, |\gamma|^2 = 0.3\right) d|\hat{\gamma}|^2 , \qquad (4.9b)$$

Equation (4.9b) could be set equal to, for example, 0.9, and the value of L, from Fig. 6, is 0.2.

The upper limit is found from

$$\text{Prob}\left(|\hat{\gamma}|^2 < U \,\middle|\, n = 32, |\gamma|^2 = 0.3\right) = \int_{-\infty}^{U} p\left(|\hat{\gamma}|^2 \,\middle|\, n = 32, |\gamma|^2 = 0.3\right) d|\hat{\gamma}|^2 , \qquad (4.10)$$

which could be set equal to, for example, 0.9, and the value of A, from Fig. 7, is 0.43. Hence,

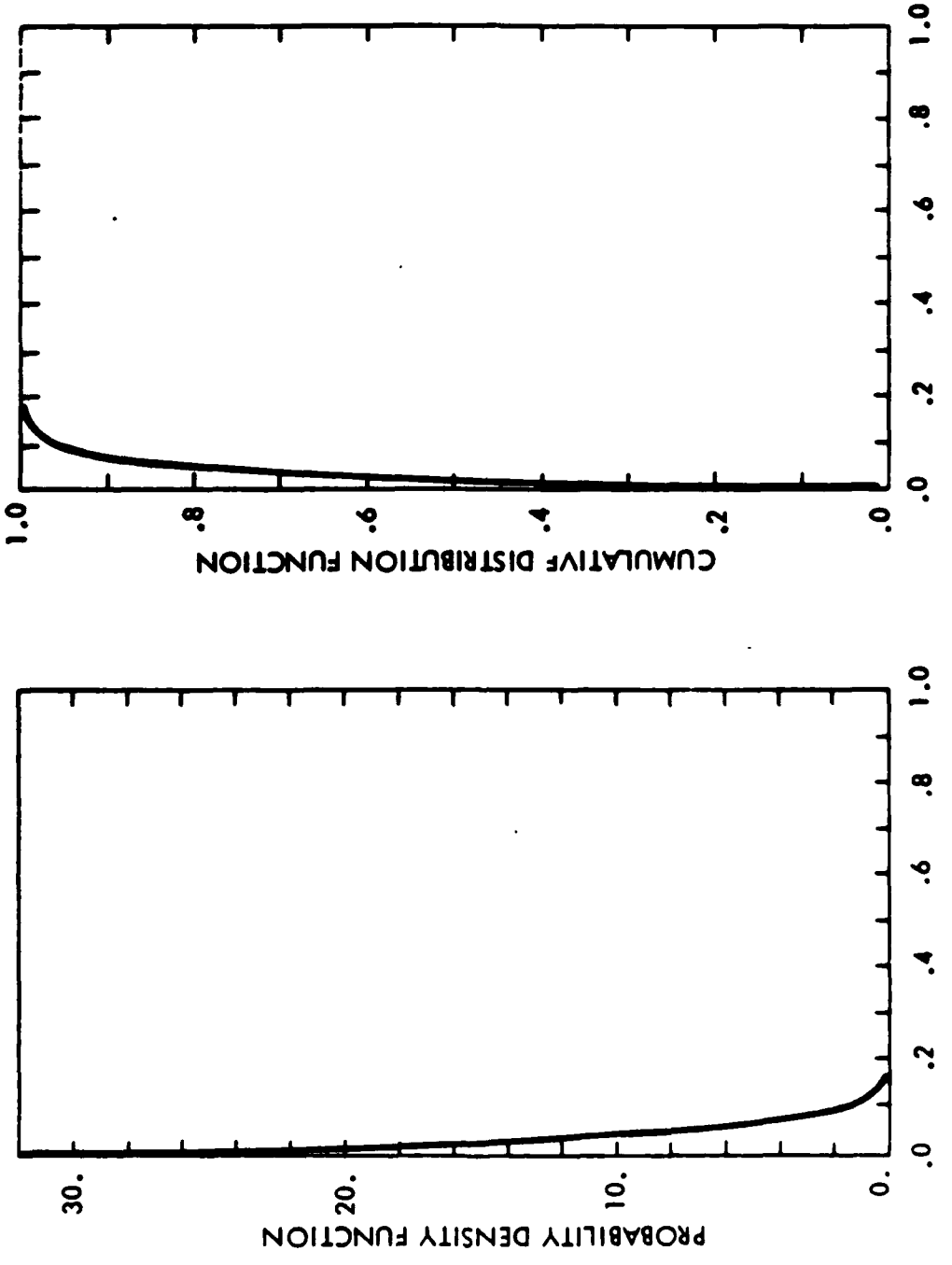

Fig. 6. Probability Density and Cumulative Distribution Functions for $|\hat{\gamma}|^2$ Given n = 32 and $|\gamma|^2 = 0.0$

Fig. 7. Probability Density and Cumulative Distribution Functions for $|\Phi|^2$ Given $\alpha = .22$ and $|\Gamma_1|^2 = 0.3$

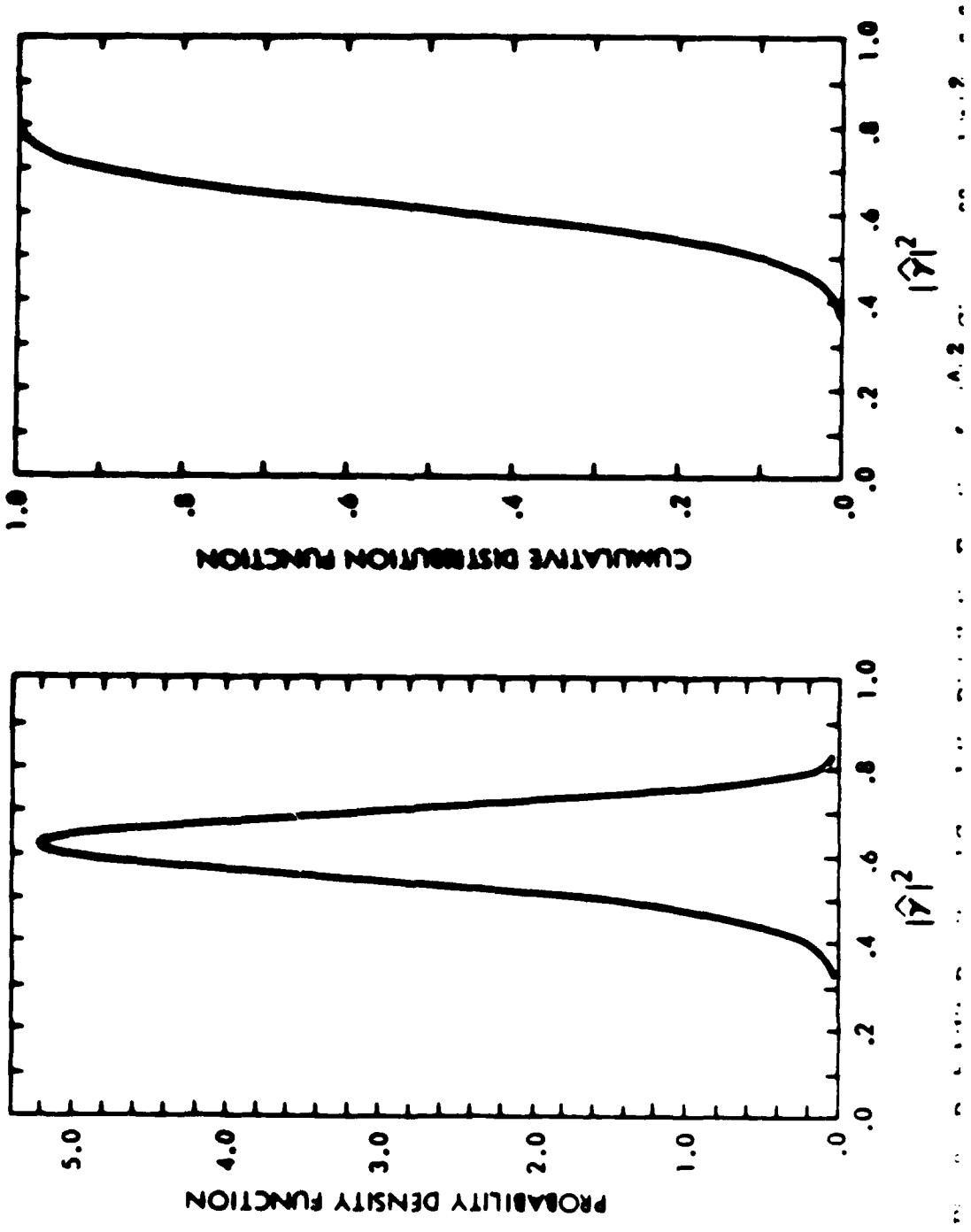
CUMULATIVE DISTRIBUTION FUNCTION
1.0
.8
.6
.4
.2
.0
$|\hat{r}|^2$
PROBABILITY DENSITY FUNCTION
5.0
4.0
3.0
2.0
1.0
.0
$|\hat{r}|^2$

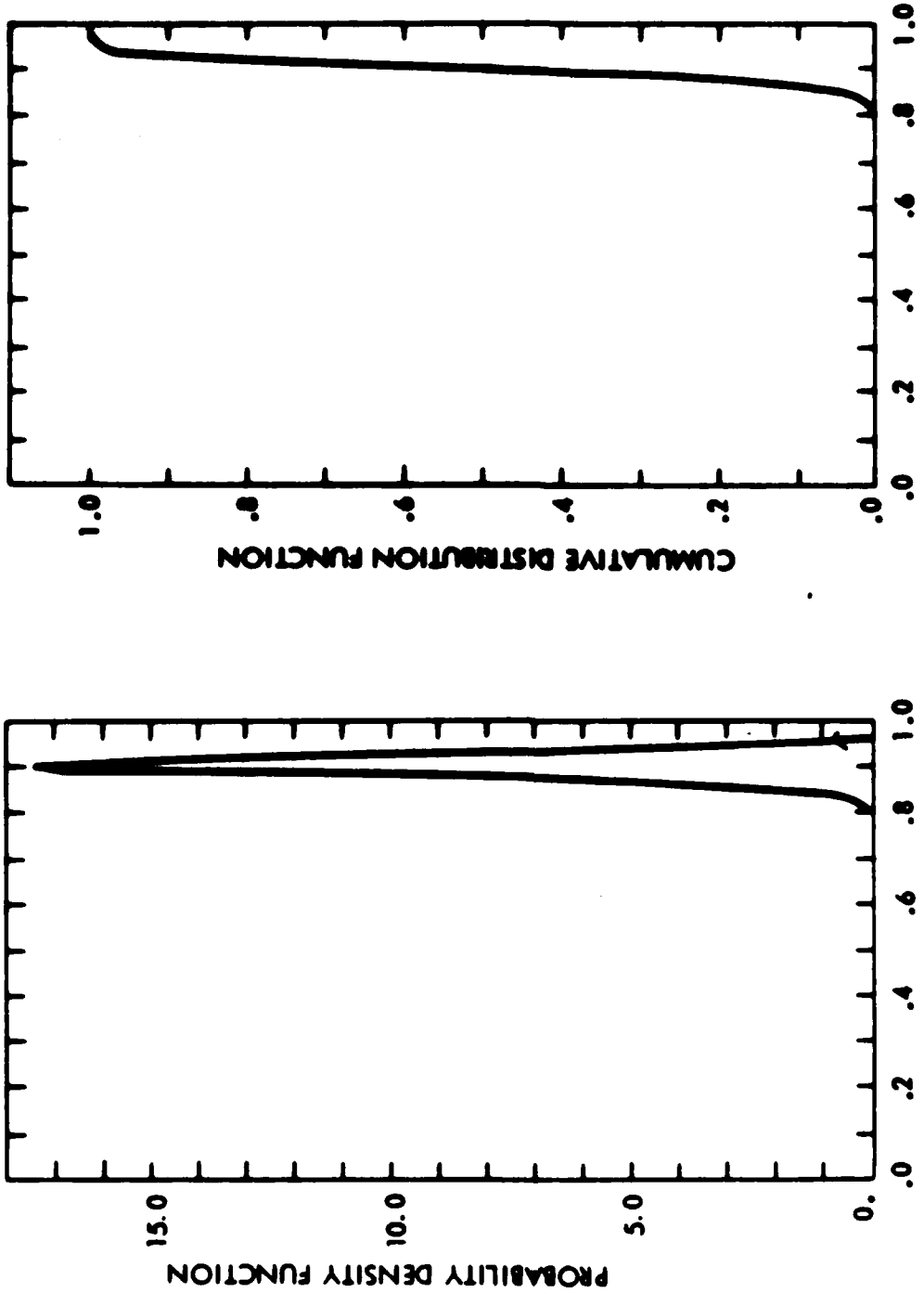

Fig. 9. Probability Density and Cumulative Distribution Functions for $|\hat{\gamma}|^2$ Given n = 32 and $|\gamma|^2 = 0.9$

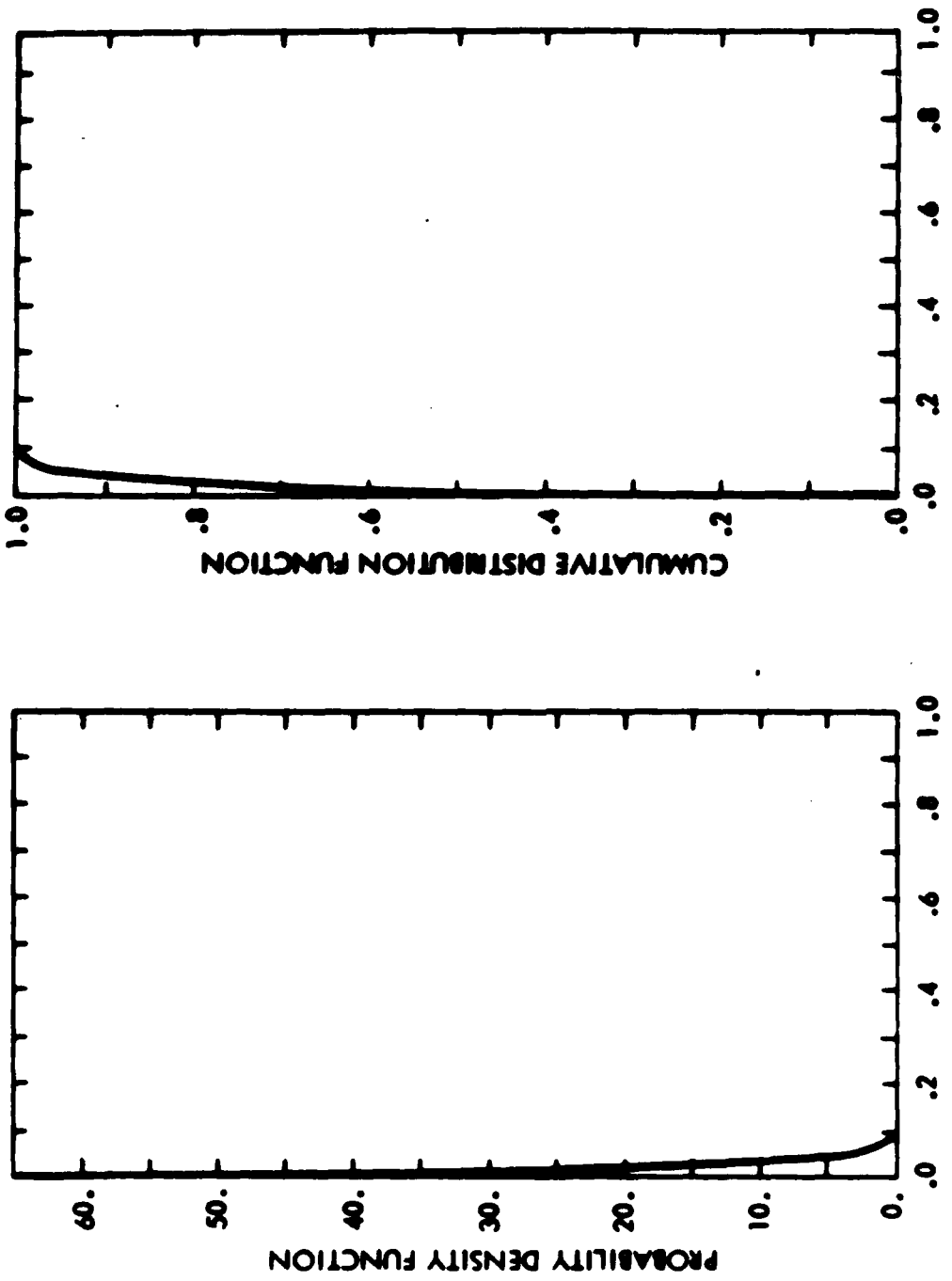

Fig. 10. Probability Density and Cumulative Distribution Functions for $|\hat{\gamma}|^2$ Given n = 64 and $|\gamma|^2 = 0.0$

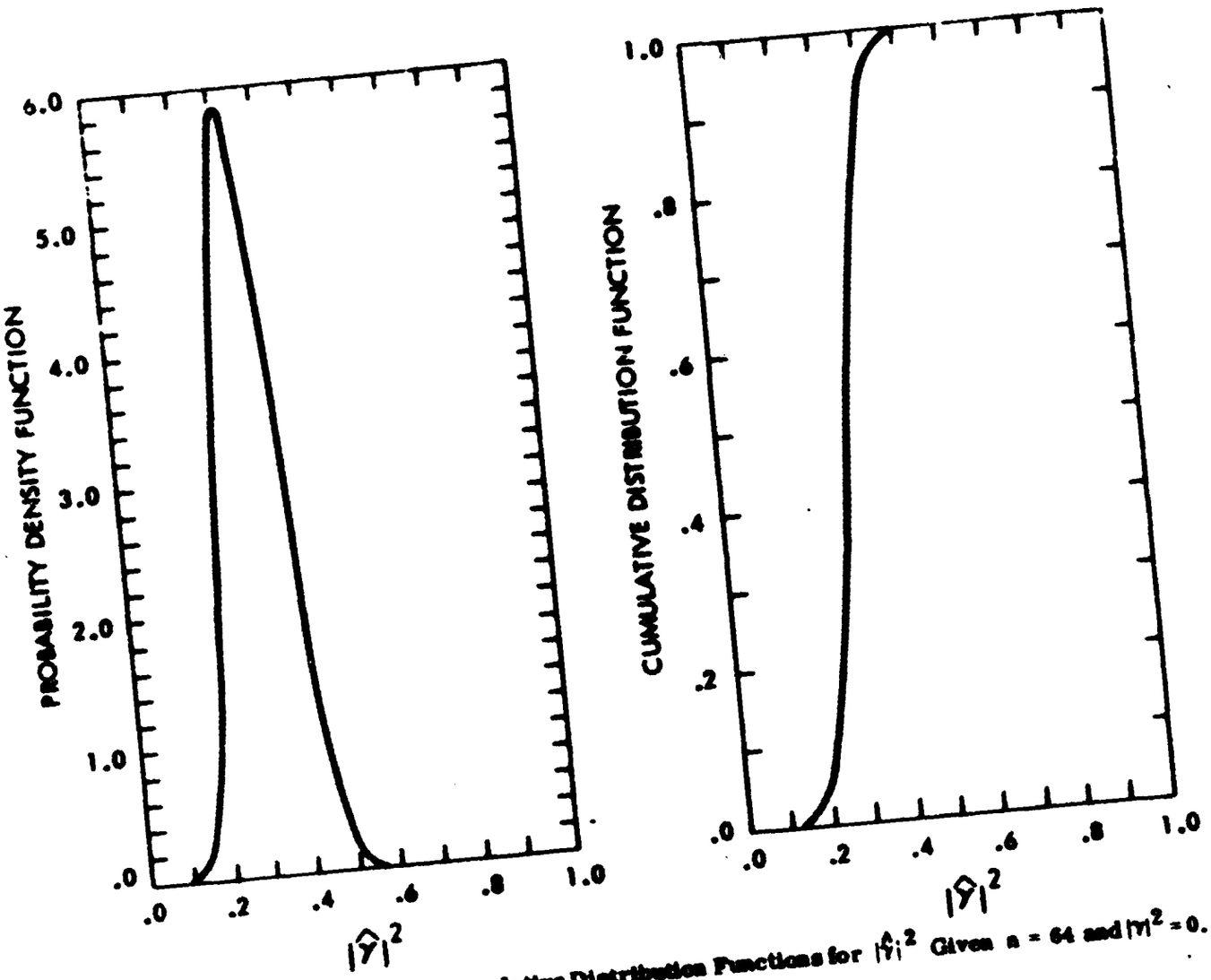

Fig. 11. Probability Density and Cumulative Distribution Functions for $|\hat{\gamma}_i|^2$ Given n = 64 and $|\gamma|^2 = 0.3$

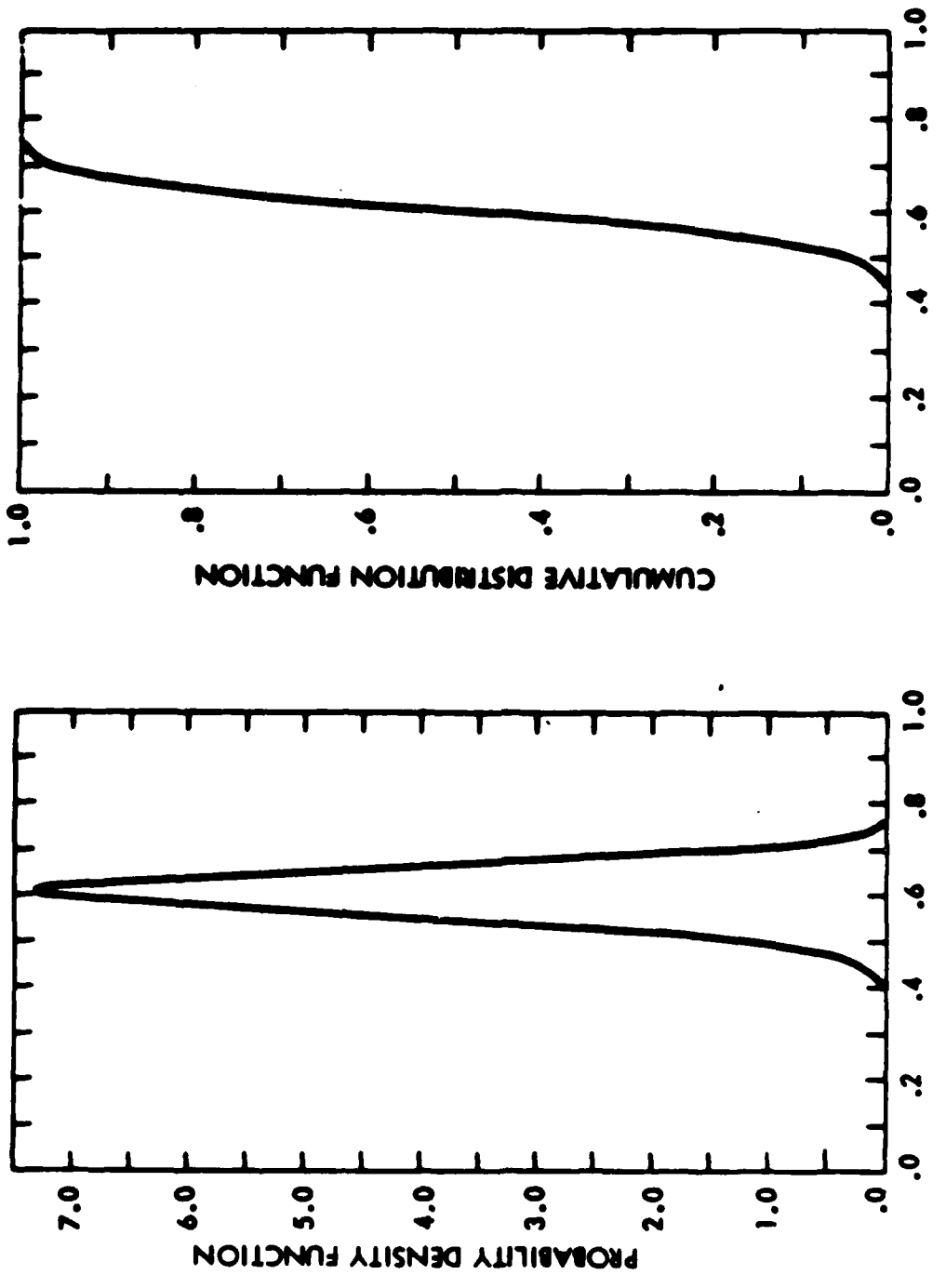

Fig. 12. Probability Density and Cumulative Distribution Functions for $|\hat{\gamma}|^2$ Given n = 64 and $|\gamma|^2 = 0.5$

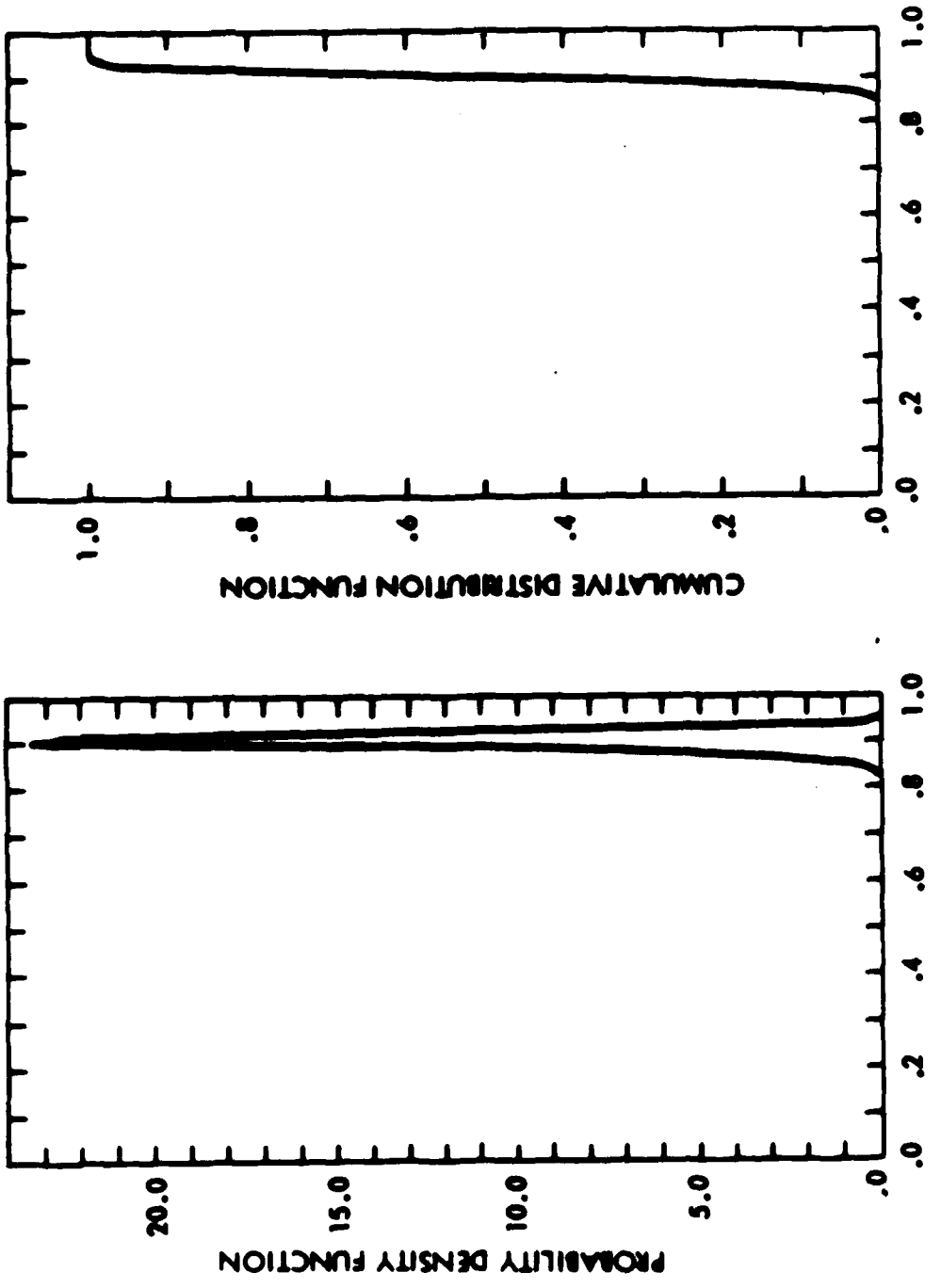

Fig. 13. Probability Density and Cumulative Distribution Functions for $|\hat{\gamma}|^2$ Given n = 64 and $|\gamma|^2 = 0.9$

$$\int_{0.2}^{0.43} p\left(|\hat{\gamma}|^2 \,\middle|\, n = 32, |\gamma|^2 = 0.3\right) d|\hat{\gamma}|^2 = 0.8 \quad . \tag{4.11}$$

On the basis of Eq. (4.11), the probability that the estimator falls in the range (0.2, 0.43) is 0.8, given that the exact value of the unknown parameter was 0.3 and that 32 disjoint segments were used.

Proper use of the cumulative distribution function yields confidence intervals for the estimate of magnitude-squared coherence or any "one for one" transformation of it, such as the positive square root or $10 \log_{10} \left(\frac{|\hat{\gamma}|^2}{1 - |\hat{\gamma}|^2} \right)$. (See, for example, Cramer[27] or Carter and Nuttall.[25])

IV. B. mth MOMENT OF DENSITY FUNCTION

The mth moment of the magnitude-squared coherence is given by

$$E\left[\left(|\hat{\gamma}|^2\right)^m \,\middle|\, n, |\gamma|^2\right] = \int_{-\infty}^{+\infty} p\left(|\hat{\gamma}|^2 \,\middle|\, n, |\gamma|^2\right) \left(|\hat{\gamma}|^2\right)^m d|\hat{\gamma}|^2 =$$

$$(n-1)\left(1 - |\gamma|^2\right)^n \int_0^1 \left(1 - |\hat{\gamma}|^2\right)^{n-2} {}_2F_1\left(n, n; 1; |\gamma|^2 |\hat{\gamma}|^2\right)$$

$$|\hat{\gamma}|^{2m} d|\hat{\gamma}|^2 \quad , \tag{4.12}$$

where use has been made of the density function, Eq. (4.1).

Application of Eq. 7.512(12) by Gradshteyn[28] yields

$$E\left[\left(|\hat{\gamma}|^2\right)^m \middle| n, |\gamma|^2\right] = \left(1 - |\gamma|^2\right)^n \frac{\Gamma(n)\ \Gamma(m+1)}{\Gamma(n+m)}$$

$$\cdot\, {}_3F_2\left(m+1, n, n;\ m+n, 1;\ |\gamma|^2\right). \quad (4.13)$$

The three-two hypergeometric functions denoting three numerator terms and two denominator terms are given by

$${}_3F_2(a, b, c;\ d, e; z) = \sum_{k=0}^{\infty} \frac{(a)_k (b)_k (c)_k}{(d)_k (e)_k} \frac{z^k}{k!}, \quad (4.14)$$

where the $(a)_k$ notation is Pochhammer's symbol[26] defined by

$$(a)_k \triangleq \frac{\Gamma(a+k)}{\Gamma(a)}. \quad (4.15)$$

The mth moment for the estimate of magnitude-coherence is given in Appendix A.

These results can be verified through proper identification of variables in the work of Anderson,[29] who extended Fisher's original work[4] on the squared correlation coefficient.

IV. C. BIAS AND VARIANCE

This section deals with the bias and variance of the estimator $|\hat{\gamma}|^2$. Exact and approximate expressions are presented. In addition, computer evaluation of the exact expressions is presented to lend meaning to these results.

IV.C.1. Bias

Consider now the first moment of the probability density function for the estimate of magnitude-squared coherence. This moment can be written

$$E\left[\left|\hat{\gamma}\right|^2 \middle| n, |\gamma|^2\right] = \frac{\left(1-|\gamma|^2\right)^n}{n} \; {}_3F_2\left(2, n, n;\; n+1, 1; |\gamma|^2\right) . \quad (4.16)$$

If $|\gamma|^2 = 1.0$, ${}_3F_2 = \infty$; therefore, the evaluation of Eq. (4.16) is not meaningful. When $|\gamma|^2 = 0.0$, ${}_3F_2 = 1.0$, which yields

$$E\left(\left|\hat{\gamma}\right|^2 \middle| n, |\gamma|^2 = 0.0\right) = \frac{1}{n} . \quad (4.17)$$

Tedious manipulation of Eq. (4.16) (Appendix B) yields the simpler result:

$$E\left(\left|\hat{\gamma}\right|^2 \middle| n, |\gamma|^2\right) = \frac{1}{n} + \frac{n-1}{n+1} |\gamma|^2 \; {}_2F_1\left(1, 1; n+2; |\gamma|^2\right) . \quad (4.18)$$

An extremely useful approximation can be made by expanding Eq. (4.18) to obtain

$$E\left(\left|\hat{\gamma}\right|^2 \middle| n, |\gamma|^2\right) \approx \frac{1}{n} + \frac{n-1}{n+1} |\gamma|^2 + \frac{(n-1)\,1!}{(n+1)(n+2)} \left(|\gamma|^2\right)^2 + \frac{(n-1)\,2!}{(n+1)(n+2)(n+3)} \left(|\gamma|^2\right)^3 . \quad (4.19)$$

Computation of higher order approximating polynomials is also easily performed and is based on an analytical expression for $E\left(\left|\hat{\gamma}\right|^2 \middle| n, |\gamma|^2\right)$.

The bias or expected estimation error is defined as

$$\text{Bias} \triangleq E\left(\left|\hat{\gamma}\right|^2 \middle| n, \left|\gamma\right|^2\right) - \left|\gamma\right|^2 \quad . \tag{4.20}$$

From Eq. (4.18), an exact expression for the bias is

$$\text{Bias} = \frac{1}{n} + \frac{n-1}{n+1}\left|\gamma\right|^2 \, {}_2F_1\left(1, 1; n+2; \left|\gamma\right|^2\right) - \left|\gamma\right|^2 \quad . \tag{4.21}$$

Expanding Eq. (4.21) gives the approximation

$$B_o \cong \frac{1}{n} - \frac{2}{n+1}\left|\gamma\right|^2 + \frac{1 \cdot (n-1)}{(n+1)(n+2)}\left(\left|\gamma\right|^2\right)^2 + \frac{(n-1)\,2\,!}{(n+1)(n+2)(n+3)}\left(\left|\gamma\right|^2\right)^3 . \tag{4.22a}$$

$$\text{Bias} \cong \begin{cases} B_o & , \quad B_o \geq 0 \\ 0 & , \quad B_o < 0 \end{cases} \tag{4.22b}$$

As an example of using this approximation for $n = 8$, the exact bias lies in the range (0.0, 0.125), depending on $\left|\gamma\right|^2$; and the maximum difference between Eqs. (4.21) and 4.22) is 0.0027 at $\left|\gamma\right|^2 = 0.86$. For large n, Eq. (4.22a and b) reduces to

$$\text{Bias} \cong \frac{1}{n}\left(1 - \left|\gamma\right|^2\right)^2 . \tag{4.22c}$$

It should be noted (see, for example, Eqs. (4.22a) and (4.22b)) that

$$\lim_{n \to \infty} (\text{Bias}) = 0 \; ; \tag{4.23}$$

therefore, the estimator may be referred to as asymptotically unbiased.

An empirically determined bias was found by Benignus[10] to be

$$\text{Bias} = \frac{1}{n}\left(1 - |\gamma|^2\right) \quad . \tag{4.24}$$

which fits the true curve for $|\gamma|^2 = 0.0$ and $|\gamma|^2 = 1.0$.

It is suggested that the higher order polynomial expression for bias, Eq. (4.22c), analytically derived, be used (as opposed to Benignus' result,[10] Eq. (4.24)), especially for small n. However, it can be shown that Benignus' result is an upper bound on the bias for any n.

A formula for the bias of $|\hat{\gamma}|^2$ owing to insufficient spectral resolving power (for example, FFT too small) is given by Jenkins and Watts,[8] but is beyond the scope of this thesis. The formula for bias derived above assumes sufficient resolving power.

IV.C.2. Variance

The variance of the estimator, namely, the second moment about the mean, is given by

$$\text{Variance} = V = E\left[\left(|\hat{\gamma}|^2\right)^2\right] - \left[E\left(|\hat{\gamma}|^2\right)\right]^2 \quad . \tag{4.25}$$

The second moment of the density function is, as a consequence of Eq. (4.16),

$$E\left[\left(|\hat{\gamma}|^2\right)^2 \mid n, |\gamma|^2\right] = \frac{2\left(1 - |\gamma|^2\right)^n}{n(n+1)}\, {}_2F_2\left(\cdot, n, n, n+2, \cdot, |\gamma|^2\right) \tag{4.26}$$

When $|\gamma|^2 = 0.0$, Eq. (4.26) yields the result

$$E\left[\left(|\hat{\gamma}|^2\right)^2 \mid n, |\gamma|^2 = 0.0\right] = \frac{2}{n(n+1)} \quad . \tag{4.27}$$

An exact expression for the variance of $|\hat{\gamma}|^2$ is obtained from Eqs. (4.16), (4.25), and (4.26). The result is

$$V = \frac{2\left(1-|\gamma|^2\right)^n}{n(n+1)}\ {}_3F_2\left(3, n, n; n+2, 1; |\gamma|^2\right) - \left[\frac{\left(1-|\gamma|^2\right)^n}{n}\ {}_3F_2\left(2, n, n; n+1, 1; |\gamma|^2\right)\right]^2 . \tag{4.28}$$

For the special case of $|\gamma|^2 = 0.0$,

$$V = \frac{2}{n(n+1)} - \left(\frac{1}{n}\right)^2 = \frac{n-1}{n^2(n+1)} \quad , \ |\gamma|^2 = 0.0 \tag{4.29a}$$

and

$$\cong \frac{1}{n^2} \quad , \text{ for large } n \text{ and } |\gamma|^2 = 0.0 \ . \tag{4.29b}$$

In order to avoid tedious and error-prone hand manipulation, computer-aided formula manipulation[30] of Eq. (4.26) was used to yield an approximation for the variance of $|\hat{\gamma}|^2$. The result is

$$V_o \cong \frac{(n-1)}{n(n+1)}\left[\frac{1}{n} + 2\frac{n-2}{n+2}|\gamma|^2 - 2\frac{2n^3 - n^2 - 2n + 3}{(n+1)(n+2)(n+3)}\left(|\gamma|^2\right)^2\right.$$

$$+ 2\frac{n^4 - 6n^3 - n^2 + 10n - 8}{(n+1)(n+2)\ (n+3)(n+4)}\left(|\gamma|^2\right)^3$$

$$\left. + \frac{13n^5 - 15n^4 - 113n^3 + 27n^2 + 136n - 120}{(n+1)(n+2)^2(n+3)(n+4)(n+5)}\left(|\gamma|^2\right)^4\right] \quad (4.30a)$$

or

$$V \cong \begin{cases} V_o\,, & V_o \geq 0 \\ 0\,, & V_o < 0 \end{cases} \quad . \quad (4.30b)$$

As an example of using the approximation given by Eq. (4.30) for $n = 8$, the exact variance lies in the range $(0.0, 0.031)$, and the maximum error due to the approximation in Eq. (4.30) is 0.0067 at $|\gamma|^2 = 0.83$. This result is a generalization of the third-order approximation by Jenkins and Watts,[8] which has no zeroth order term; that is, it assumes no variance of $|\hat{\gamma}|^2$ when $|\gamma|^2 = 0.0$.

In particular, for large n and $|\gamma|^2 \neq 0$, Eq. (4.30) reduces to

$$V \cong \frac{2}{n}|\gamma|^2\left(1 - |\gamma|^2\right)^2 \quad , \quad (4.31)$$

which has a maximum value of $8/27n$ at $|\gamma|^2 = 1/3$.

Hence, the variance of the estimator in the case where $|\gamma|^2$ is unknown (but nonzero) decreases inversely proportional to n.

IV.C.3. Digital Computer Evaluation Of Bias and Variance

Practical experience in estimating the magnitude-squared coherence function leads one to anticipate certain bias and variance problems. For a given number of segments, n, when $|\gamma|^2 = 1.0$, neither a bias nor a variance problem exists; however, when $|\gamma|^2 = 0.0$, the average value estimator always appears greater than 0.0. Further, when $|\gamma|^2$ is about 0.3 to 0.4, the variance of the estimator appears much greater than when $|\gamma|^2 = 0.0$. Primarily because this and the behavior of the estimator with increasing n can not be readily sensed from Eqs. (4.21) and (4.28), a computer program has been written to evaluate and plot these functions (see Fig. 14). The results, Tables 1 through 5 and Figs. 15 through 26, dramatically portray the behavior of these complicated (but readily evaluated) functions. Tables and graphs of this type have been prepared in the past by Amos and Koopmans.[5]

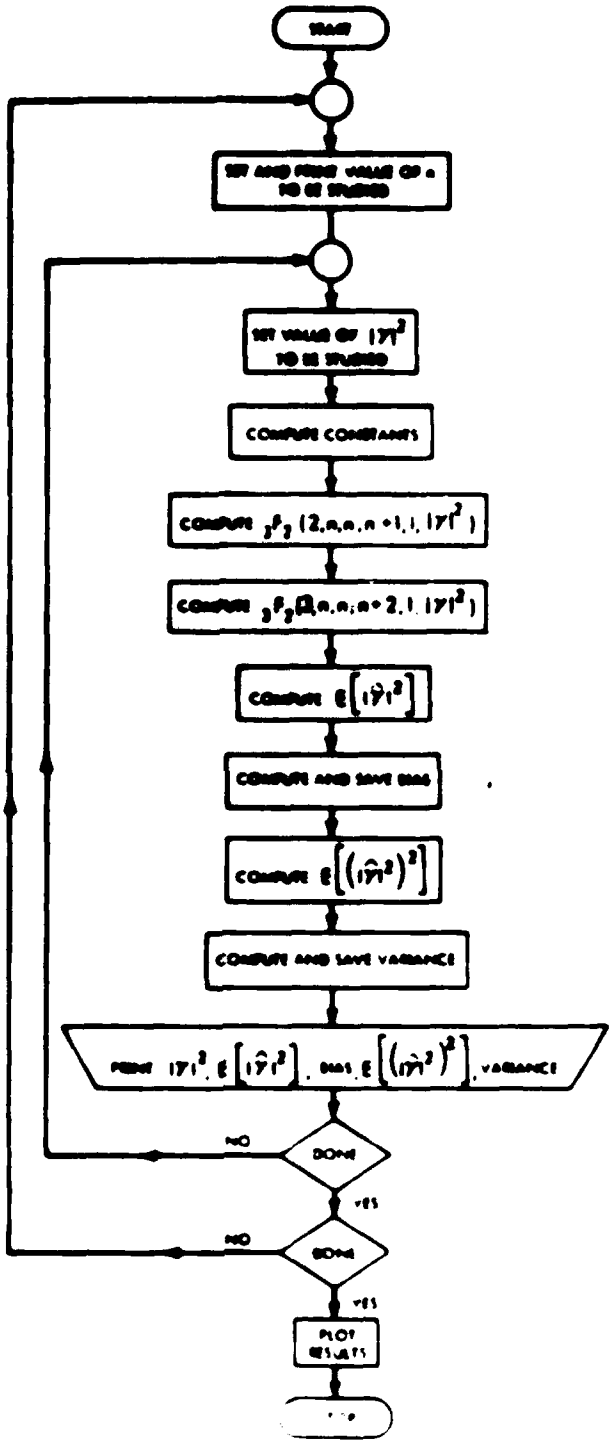

Fig. 14. Summary Flow Chart for Bias and Variance Computations

TABLE 1

BIAS AND VARIANCE OF $|\hat{\gamma}|^2$ FOR n = 32

$\lvert\gamma\rvert^2$	$E(\lvert\hat{\gamma}\rvert^2)$	Bias	$E\left[(\lvert\hat{\gamma}\rvert^2)\right]^2$	Variance
.00000	.31250-01	.31250-01	.18939-02	.91738-03
.40000-01	.68870-01	.28870-01	.75808-02	.28377-02
.80000-01	.10658+00	.26579-01	.15823-01	.44634-02
.12000+00	.14438+00	.24378-01	.26654-01	.58089-02
.16000+00	.18227+00	.22267-01	.40110-01	.68888-02
.20000+00	.22025+00	.20247-01	.56227-01	.77162-02
.24000+00	.25832+00	.18318-01	.75041-01	.83127-02
.28000+00	.29648+00	.16482-01	.96590-01	.86886-02
.32000+00	.33474+00	.14738-01	.12091+00	.88624-02
.36000+00	.37309+00	.13088-01	.14805+00	.88513-02
.40000+00	.41153+00	.11533-01	.17803+00	.86732-02
.44000+00	.45007+00	.10072-01	.21091+00	.83462-02
.48000+00	.48871+00	.87068-02	.24672+00	.78895-02
.52000+00	.52744+00	.74379-02	.28551+00	.73225-02
.56000+00	.56627+00	.62661-02	.32732+00	.66654-02
.60000+00	.60519+00	.51920-02	.37220+00	.59391-02
.64000+00	.64422+00	.42165-02	.42018+00	.51651-02
.68000+00	.68334+00	.33402-02	.47132+00	.43659-02
.72000+00	.72256+00	.25640-02	.52566+00	.35644-02
.76000+00	.76189+00	.18886-02	.58326+00	.27845-02
.80000+00	.80131+00	.13147-02	.64416+00	.20509-02
.84000+00	.84084+00	.84326-03	.70841+00	.13891-02
.88000+00	.88047+00	.47491-03	.77606+00	.82562-03
.92000+00	.92021+00	.21019-03	.84717+00	.38801-03
.96000+00	.96005+00	.48847-04	.92180+00	.10573-03
.10000+01	.10000+01	.00000	.10000+01	.00000

TABLE 2

BIAS AND VARIANCE OF $|\hat{\gamma}|^2$ FOR $n = 40$

$\lvert\gamma\rvert^2$	$E(\lvert\hat{\gamma}\rvert^2)$	Bias	$E\left[(\lvert\hat{\gamma}\rvert^2)\right]^2$	Variance
.00000	.25000-01	.25000-01	.12195-02	.59451-03
.40000-01	.63085-01	.23085-01	.61677-02	.21880-02
.80000-01	.10124+00	.21243-01	.13784-01	.35342-02
.12000+00	.13947+00	.19474-01	.24099-01	.46458-02
.16000+00	.17778+00	.17779-01	.37141-01	.55357-02
.20000+00	.21616+00	.16158-01	.52942-01	.62174-02
.24000+00	.25461+00	.14612-01	.71532-01	.67043-02
.28000+00	.29314+00	.13141-01	.92942-01	.70106-02
.32000+00	.33174+00	.11745-01	.11721+00	.71507-02
.36000+00	.37042+00	.10425-01	.14435+00	.71391-02
.40000+00	.40918+00	.91808-02	.17442+00	.69912-02
.44000+00	.44801+00	.80137-02	.20744+00	.67223-02
.48000+00	.48692+00	.69239-02	.24344+00	.63484-02
.52000+00	.52591+00	.59117-02	.28247+00	.58859-02
.56000+00	.56498+00	.49776-02	.32455+00	.53515-02
.60000+00	.60412+00	.41222-02	.36973+00	.47625-02
.64000+00	.64335+00	.33459-02	.41803+00	.41364-02
.68000+00	.68265+00	.26490-02	.46950+00	.34916-02
.72000+00	.72203+00	.20322-02	.52418+00	.28465-02
.76000+00	.76150+00	.14960-02	.58210+00	.22204-02
.80000+00	.80104+00	.10408-02	.64330+00	.16329-02
.84000+00	.84067+00	.66704-03	.70783+00	.11044-02
.88000+00	.88038+00	.37527-03	.77572+00	.65547-03
.92000+00	.92017+00	.16960-03	.84701+00	.30789-03
.96000+00	.96004+00	.37304-04	.92176+00	.84845-04
.10000+01	.10000+01	.00000	.10000+01	.00000

TABLE 3

BIAS AND VARIANCE OF $|\hat{\gamma}|^2$ FOR n = 48

$\lvert\gamma\rvert^2$	$E(\lvert\hat{\gamma}\rvert^2)$	Bias	$E[(\lvert\hat{\gamma}\rvert^2)]^2$	Variance
.00000	.20833-01	.20833-01	.85034-03	.41631-03
.40000-01	.59231-01	.19231-01	.52853-02	.17764-02
.80000-01	.97691-01	.17691-01	.12466-01	.29247-02
.12000+00	.13621+00	.16213-01	.22425-01	.38710-02
.16000+00	.17480+00	.14797-01	.35181-01	.46273-02
.20000+00	.21344+00	.13443-01	.50764-01	.52054-02
.24000+00	.25215+00	.12153-01	.69199-01	.56175-02
.28000+00	.29093+00	.10926-01	.90513-01	.58758-02
.32000+00	.32976+00	.97616-02	.11474+00	.59929-02
.36000+00	.36866+00	.86615-02	.14189+00	.59816-02
.40000+00	.40763+00	.76254-02	.17201+00	.58552-02
.44000+00	.44665+00	.66538-02	.20513+00	.56269-02
.48000+00	.48575+00	.57469-02	.24126+00	.53106-02
.52000+00	.52491+00	.49051-02	.28045+00	.49201-02
.56000+00	.56413+00	.41286-02	.32271+00	.44700-02
.60000+00	.60342+00	.34179-02	.36809+00	.39746-02
.64000+00	.64277+00	.27732-02	.41661+00	.34491-02
.68000+00	.68219+00	.21948-02	.46830+00	.29088-02
.72000+00	.72168+00	.16832-02	.52320+00	.23691-02
.76000+00	.76124+00	.12386-02	.58133+00	.18462-02
.80000+00	.80086+00	.86127-03	.64274+00	.13565-02
.84000+00	.84055+00	.55169-03	.70744+00	.91652-03
.88000+00	.88031+00	.31001-03	.77549+00	.54359-03
.92000+00	.92014+00	.13837-03	.84691+00	.25541-03
.96000+00	.96003+00	.29739-04	.92173+00	.71213-04
.10000+01	.10000+01	.00000	.10000+01	.00000

TABLE 4

BIAS AND VARIANCE OF $|\hat{\gamma}|^2$ FOR n = 56

$\lvert\gamma\rvert^2$	$E(\lvert\hat{\gamma}\rvert^2)$	Bias	$E[(\lvert\hat{\gamma}\rvert^2)]^2$	Variance
.00000	.17857-01	.17857-01	.62657-03	.30769-03
.40000-01	.58480-01	.18480-01	.46844-02	.14944-02
.80000-01	.95157-01	.15157-01	.11549-01	.24943-02
.12000+00	.13369+00	.13687-01	.21244-01	.33178-02
.16000+00	.17267+00	.12671-01	.33791-01	.39751-02
.20000+00	.21151+00	.11510-01	.49213-01	.44769-02
.24000+00	.25040+00	.10402-01	.67535-01	.48339-02
.28000+00	.28935+00	.93494-02	.88780-01	.50571-02
.32000+00	.32835+00	.83514-02	.11297+00	.51577-02
.36000+00	.36741+00	.74084-02	.14014+00	.51470-02
.40000+00	.40652+00	.65206-02	.17030+00	.50366-02
.44000+00	.44569+00	.56884-02	.20348+00	.48383-02
.48000+00	.48491+00	.49119-02	.23970+00	.45642-02
.52000+00	.52419+00	.41913-02	.27900+00	.42264-02
.56000+00	.56353+00	.35270-02	.32140+00	.38376-02
.60000+00	.60292+00	.29190-02	.36692+00	.34103-02
.64000+00	.64237+00	.23678-02	.41559+00	.29575-02
.68000+00	.68187+00	.18735-02	.46744+00	.24926-02
.72000+00	.72144+00	.14364-02	.52250+00	.20288-02
.76000+00	.76106+00	.10566-02	.58079+00	.15800-02
.80000+00	.80073+00	.73449-03	.64234+00	.11601-02
.84000+00	.84047+00	.47025-03	.70717+00	.78333-03
.88000+00	.88026+00	.26403-03	.77533+00	.46438-03
.92000+00	.92012+00	.11579-03	.84683+00	.21832-03
.96000+00	.96002+00	.24268-04	.92171+00	.61738-04
.10000+01	.10000+01	.00000	.10000+01	.00000

TABLE 5

BIAS AND VARIANCE OF $|\hat{\gamma}|^2$ FOR n = 64

$\lvert\gamma\rvert^2$	$E(\lvert\hat{\gamma}\rvert^2)$	Bias	$E[(\lvert\hat{\gamma}\rvert^2)]^2$	Variance
.00000	.15625-01	.15625-01	.48877-03	.23663-03
.40000-01	.5[illegible]-01	.14418-01	.42499-02	.12886-02
.80000-01	.9[illegible]-01	.13258-01	.10871-01	.21743-02
.12000+00	.1[illegible]+00	.12145-01	.20365-01	.29030-02
.16000+00	.1[illegible]+00	.11080-01	.32752-01	.34842-02
.20000+00	.2[illegible]+00	.10062-01	.48053-01	.39273-02
.24000+00	.2[illegible]+00	.90924-02	.66289-01	.42422-02
.28000+00	.2[illegible]+00	.81707-02	.87481-01	.44386-02
.32000+00	.3[illegible]+00	.72971-02	.11165+00	.45267-02
.36000+00	.3[illegible]+00	.64720-02	.13882+00	.45166-02
.40000+00	.4[illegible]+00	.56955-02	.16901+00	.44187-02
.44000+00	.4[illegible]+00	.49676-02	.20224+00	.42434-02
.48000+00	.4[illegible]+00	.42887-02	.23854+00	.40016-02
.52000+00	.5[illegible]+00	.36589-02	.27792+00	.37041-02
.56000+00	.5[illegible]+00	.30783-02	.32042+00	.33619-02
.60000+00	.6[illegible]+00	.25473-02	.36605+00	.29862-02
.64000+00	.6[illegible]+00	.20658-02	.41484+00	.25886-02
.68000+00	.6[illegible]+00	.16342-02	.46681+00	.21806-02
.72000+00	.7[illegible]+00	.12527-02	.52198+00	.17740-02
.76000+00	.7[illegible]+00	.92125-03	.58038+00	.13809-02
.80000+00	.8[illegible]+00	.64025-03	.64204+00	.10133-02
.84000+00	.8[illegible]+00	.40970-03	.70697+00	.68399-03
.88000+00	.8[illegible]+00	.22980-03	.77521+00	.40543-03
.92000+00	.9[illegible]+00	.10040-03	.84678+00	.19082-03
.96000+00	.9[illegible]+00	.20237-04	.92169+00	.54669-04
.10000+01	.1[illegible]+01	.00000	.10000+01	.00000

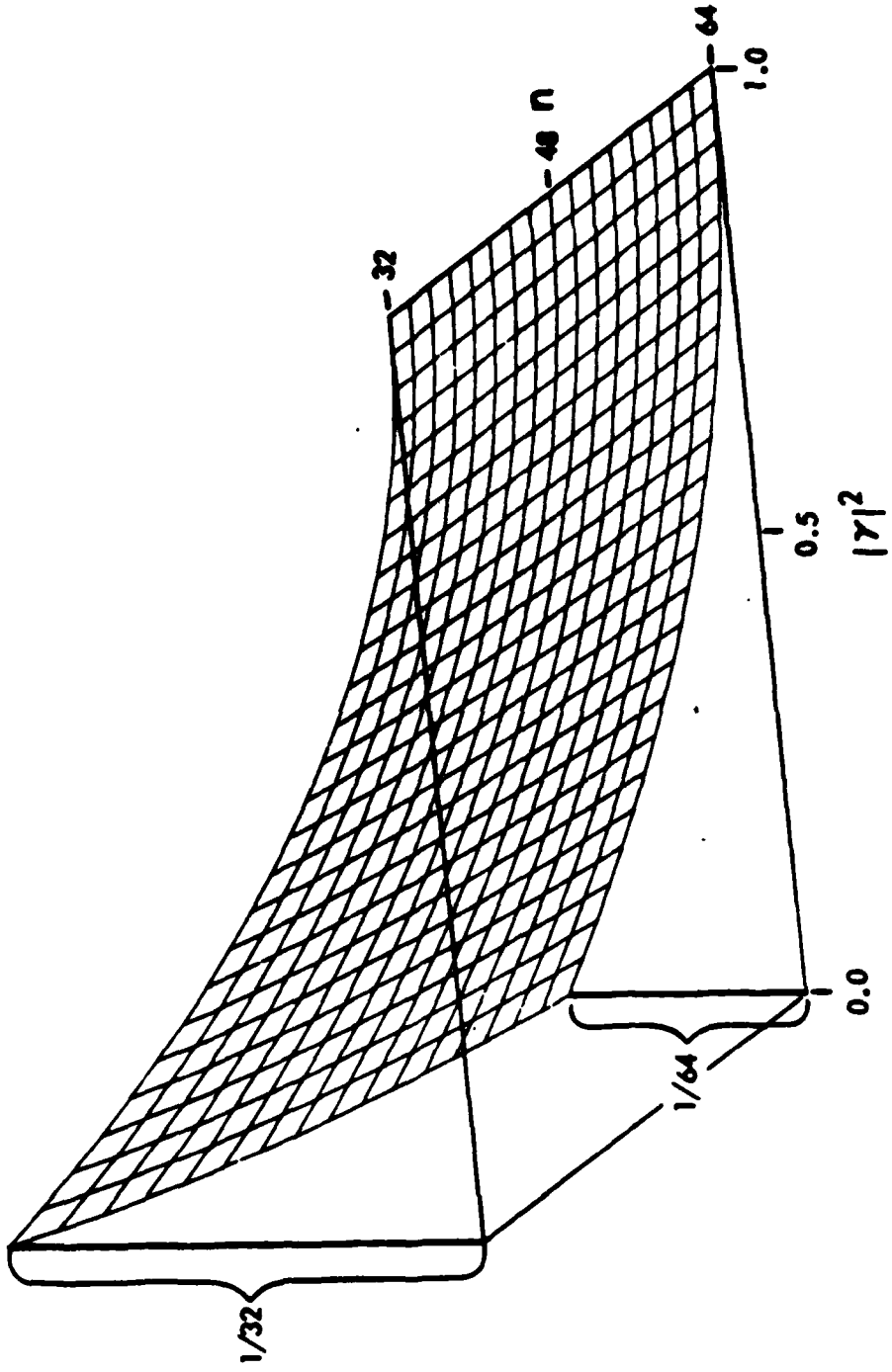

Fig. 15. Bias of $|\hat{\gamma}|^2$ versus $|\gamma|^2$ and n

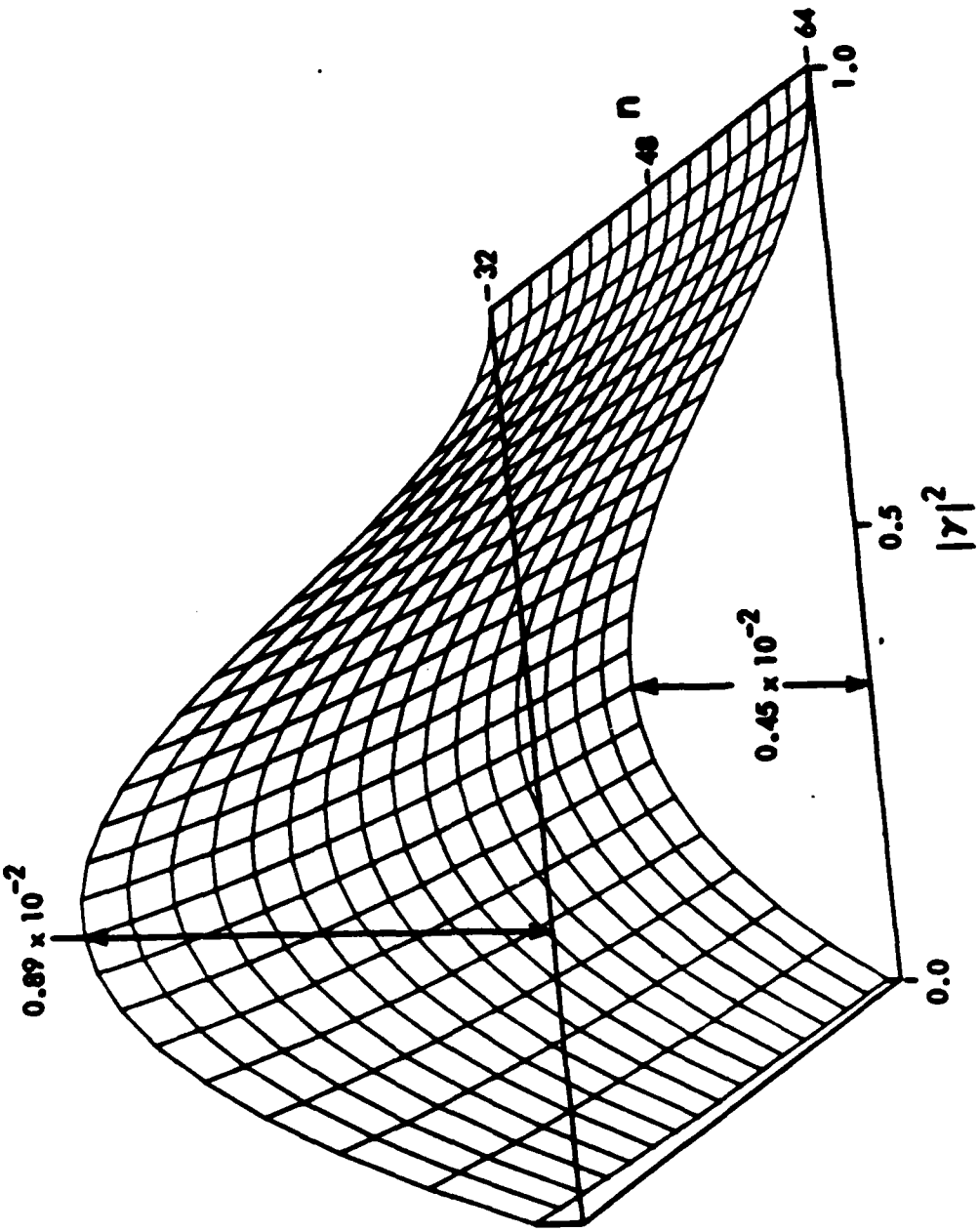

Fig. 16. Variance of $|\hat{\gamma}|^2$ versus $|\gamma|^2$ and n

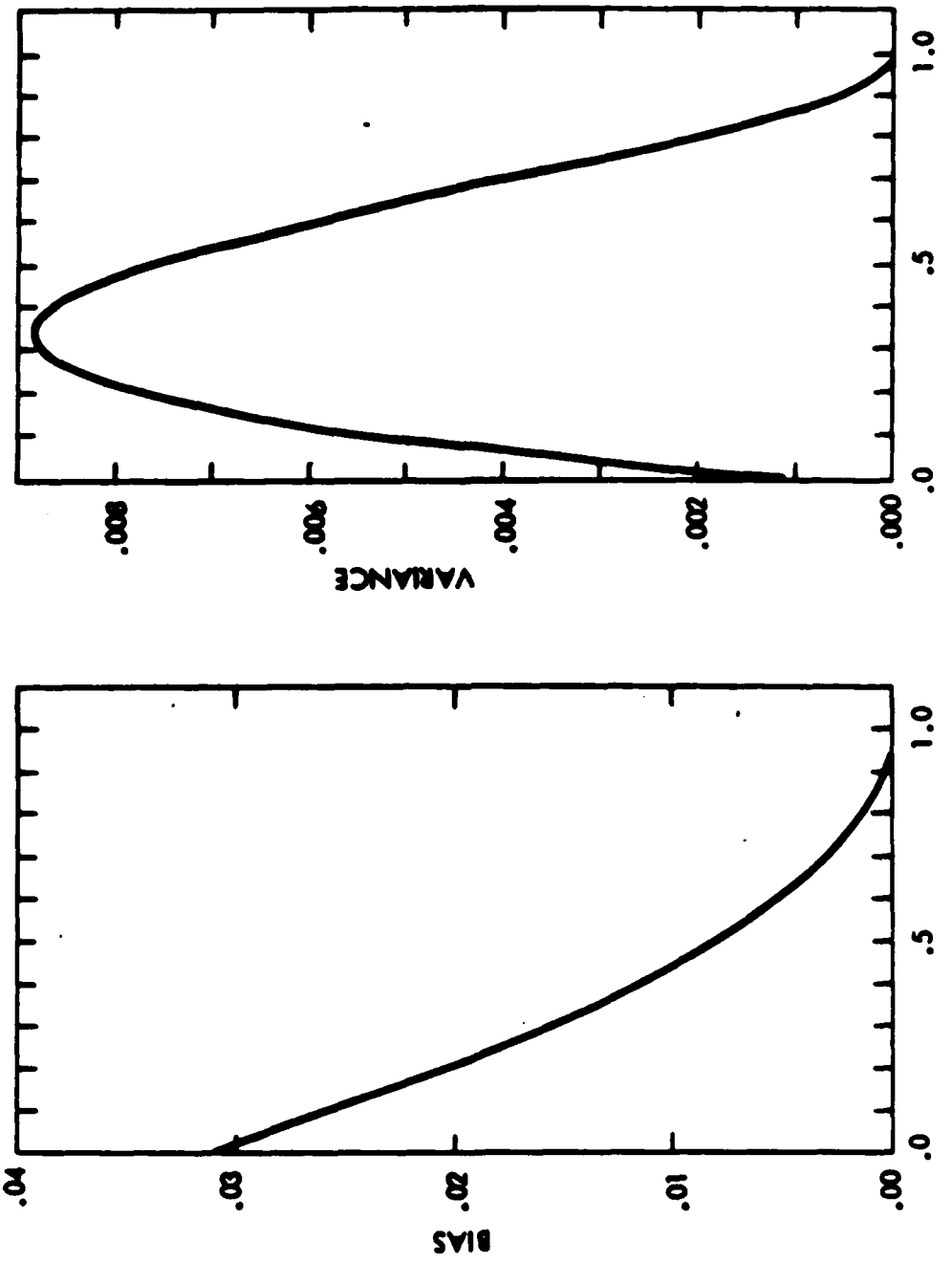

Fig. 17. Bias and Variance versus $|\gamma|^2$ for n = 32

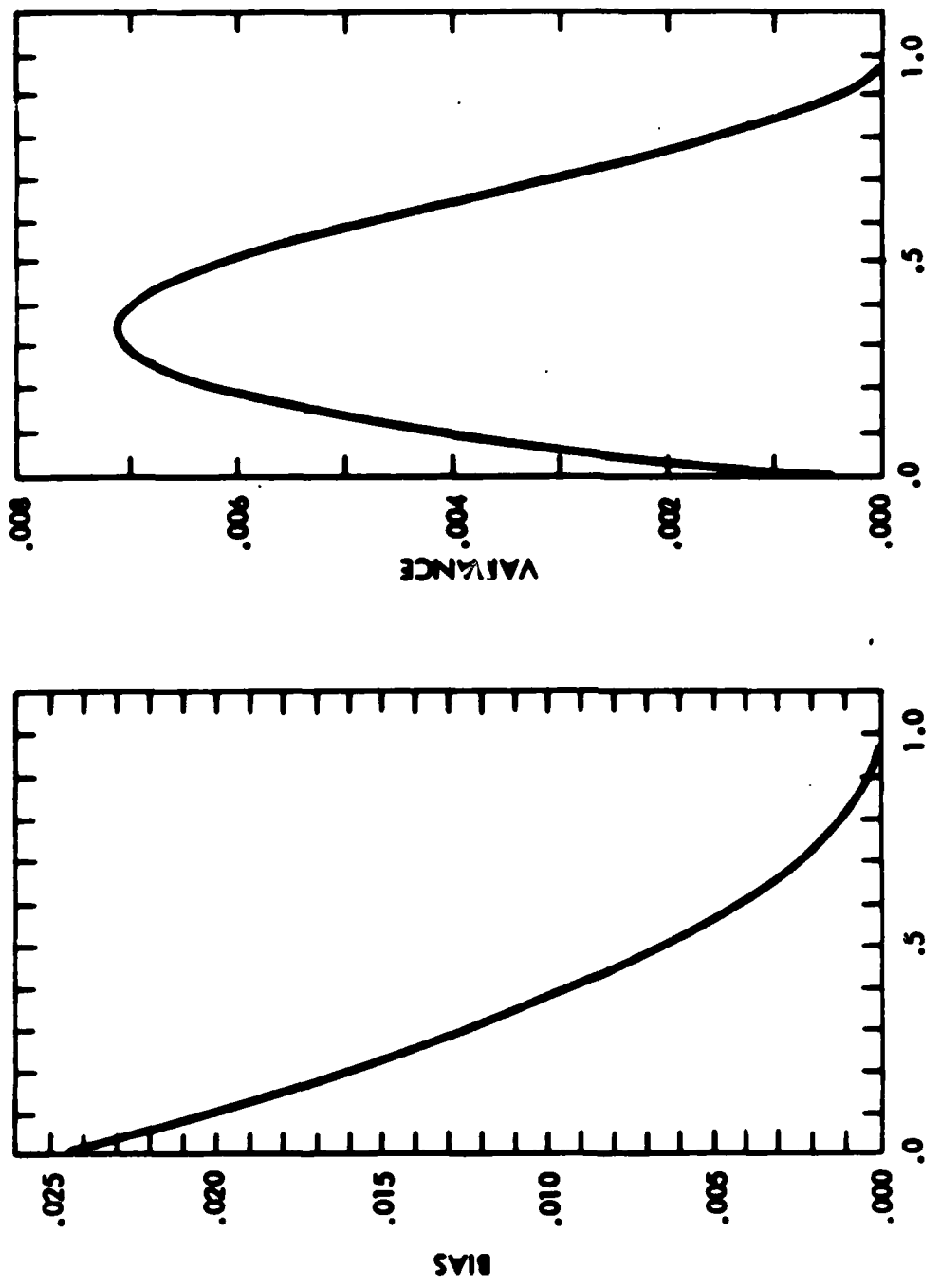

Fig. 18. Bias and Variance versus $|\gamma|^2$ for n = 40

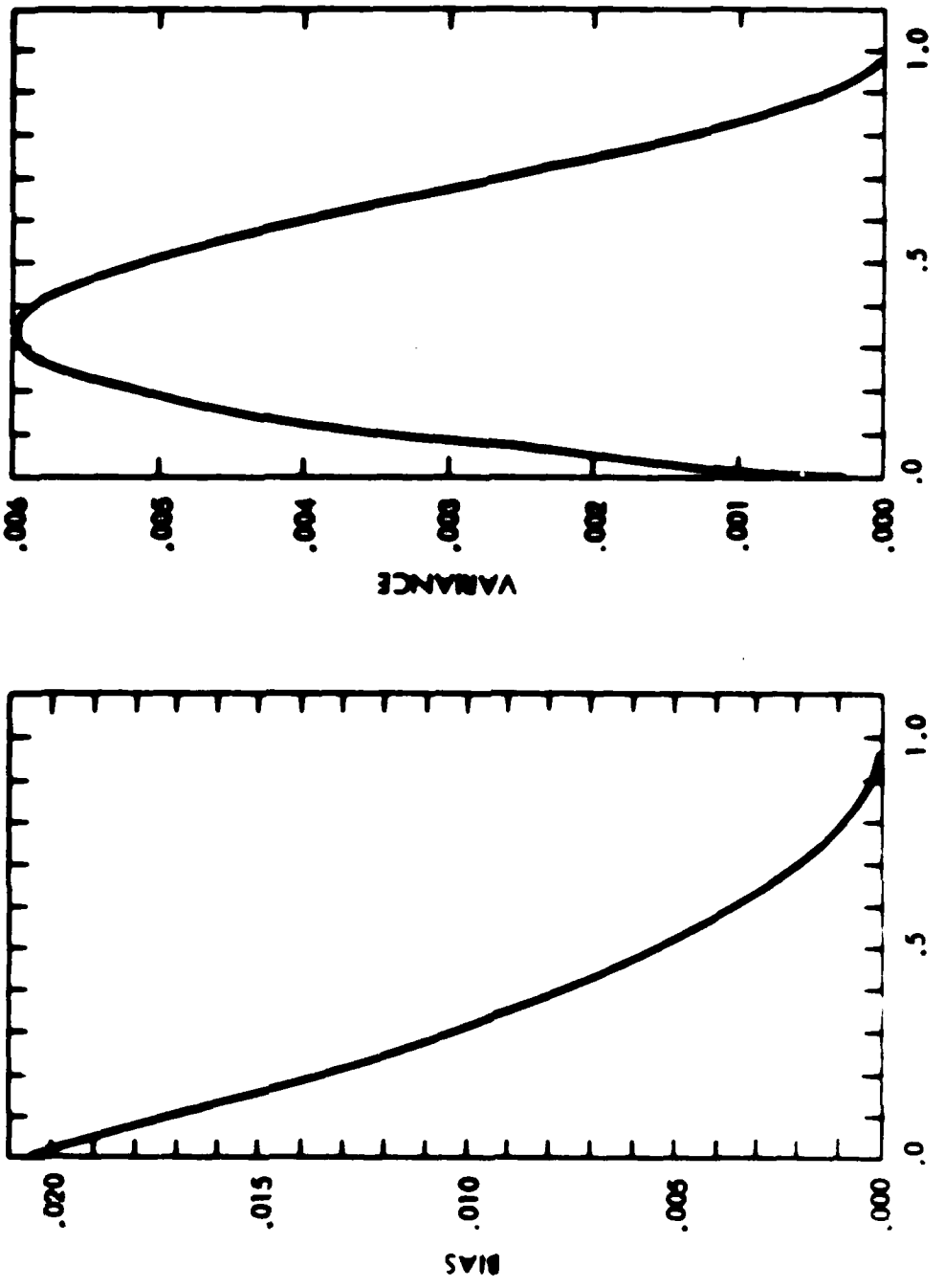

Fig. 19. Bias and Variance versus $|\gamma|^2$ for n = 48

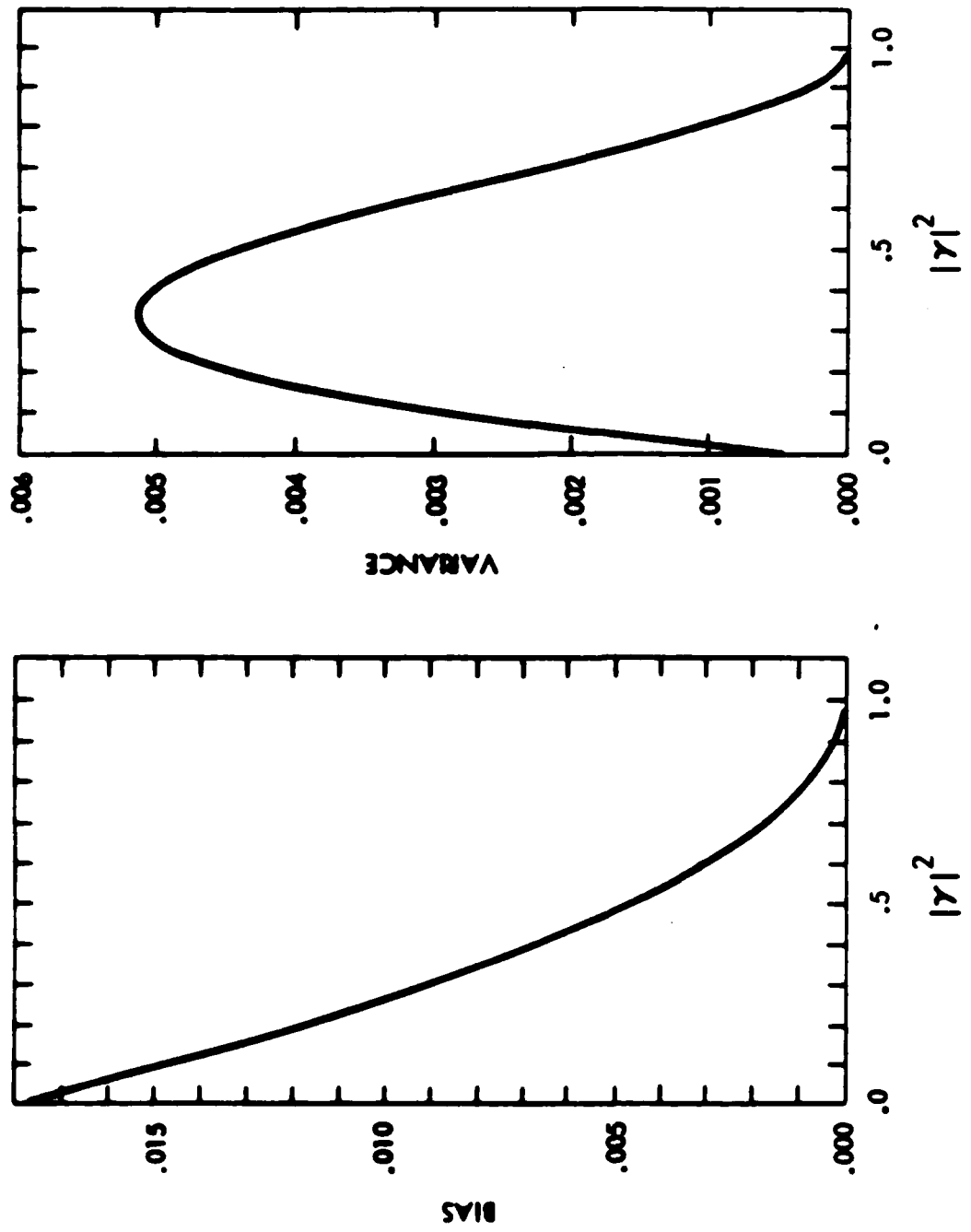

Fig. 20. Bias and Variance versus $|\gamma|^2$ for n = 56

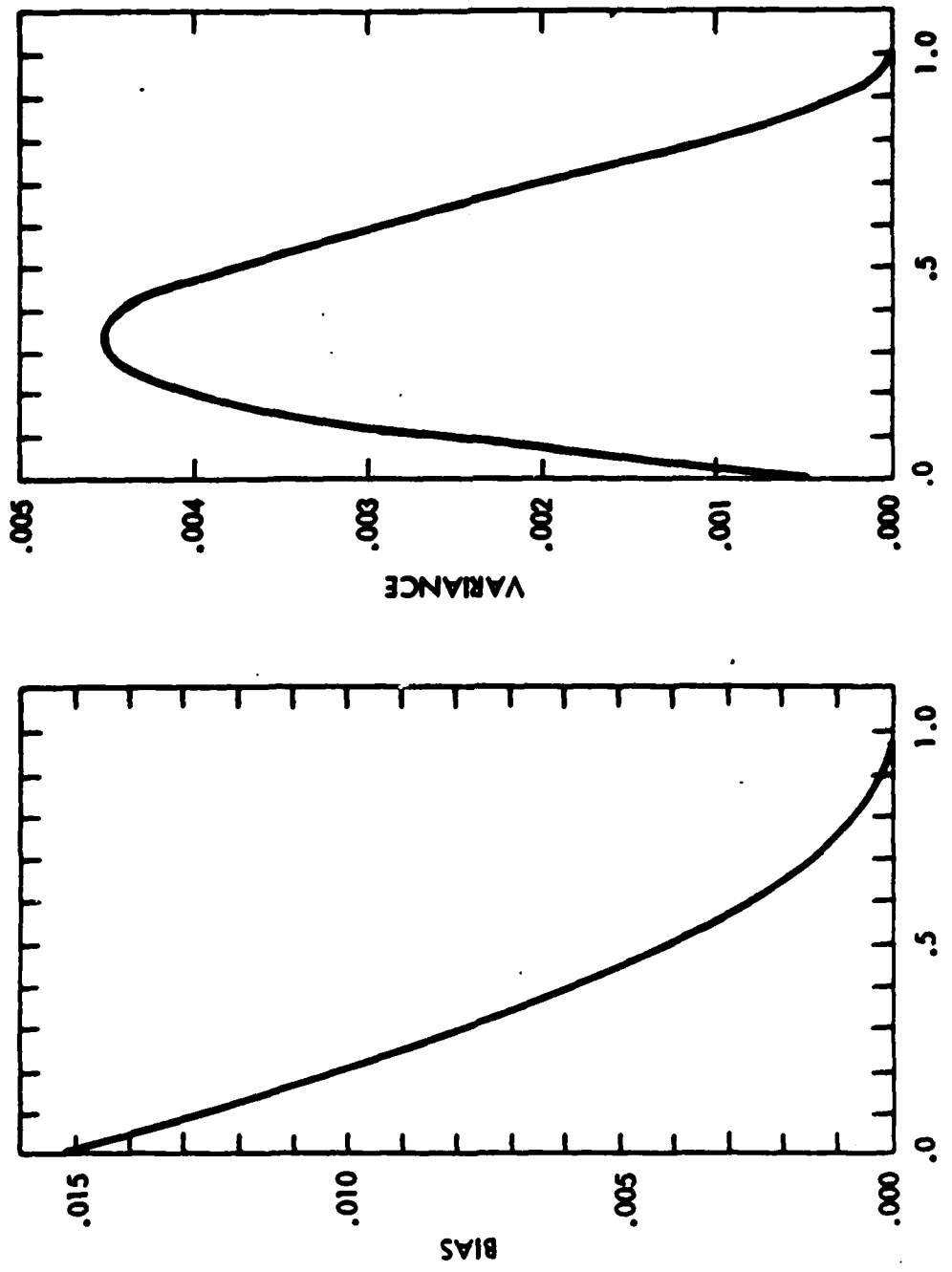

Fig. 21. Bias and Variance versus $|\gamma|^2$ for n = 64

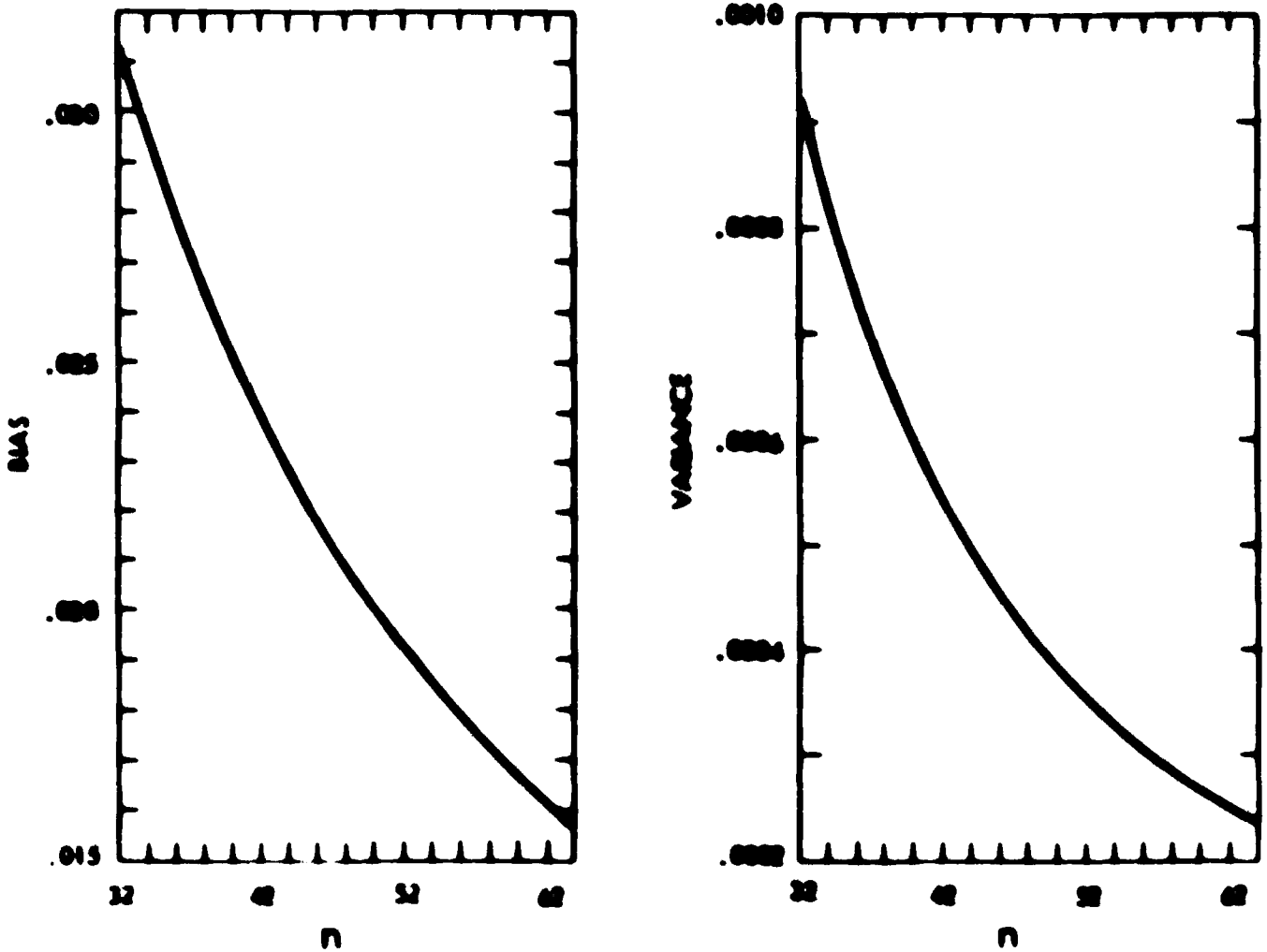

Fig. 22. Bias and Variance versus n for $|\gamma_1|^2 = 0.8$

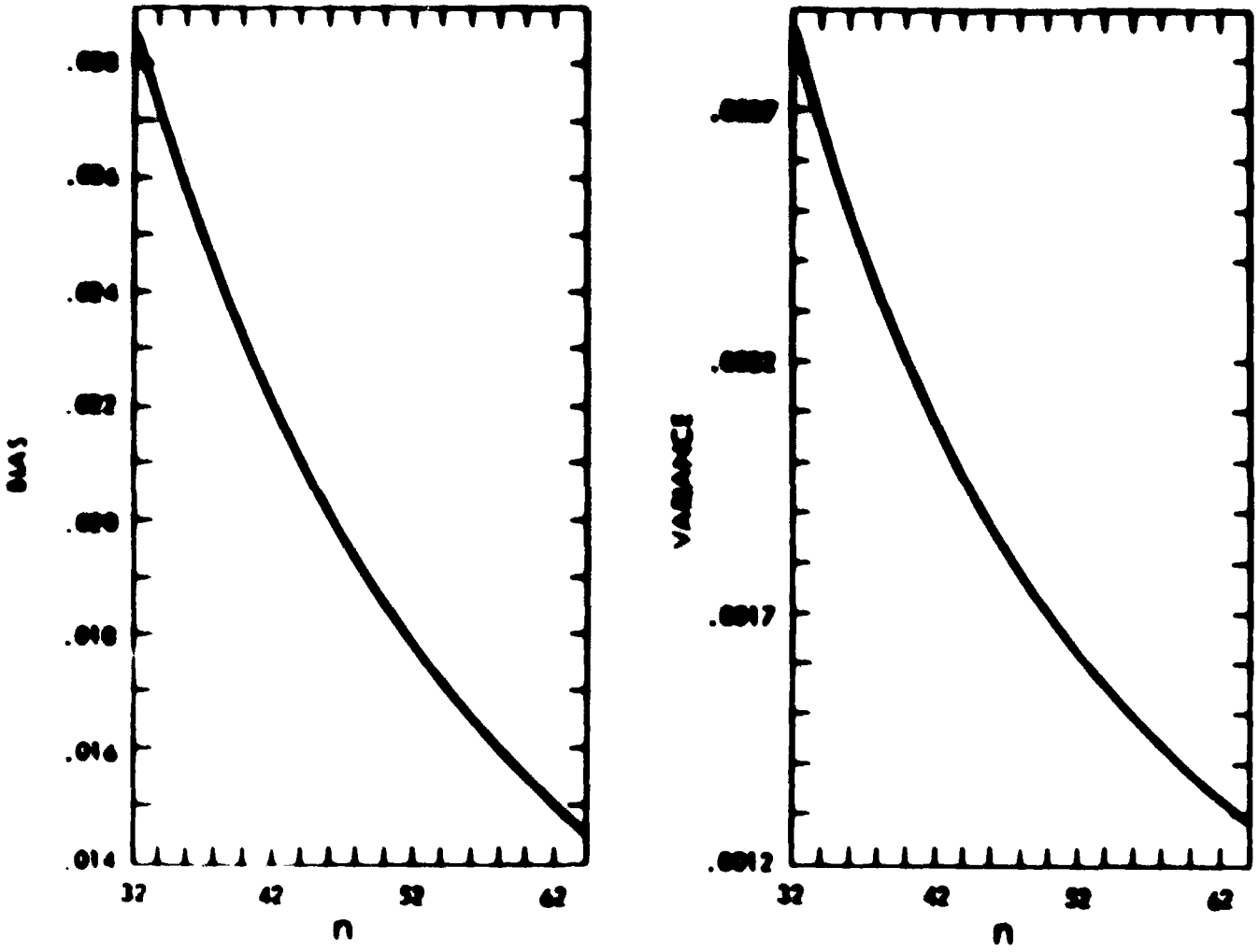

Fig. 23. Bias and Variance versus n for $|r|^2 = 0.64$

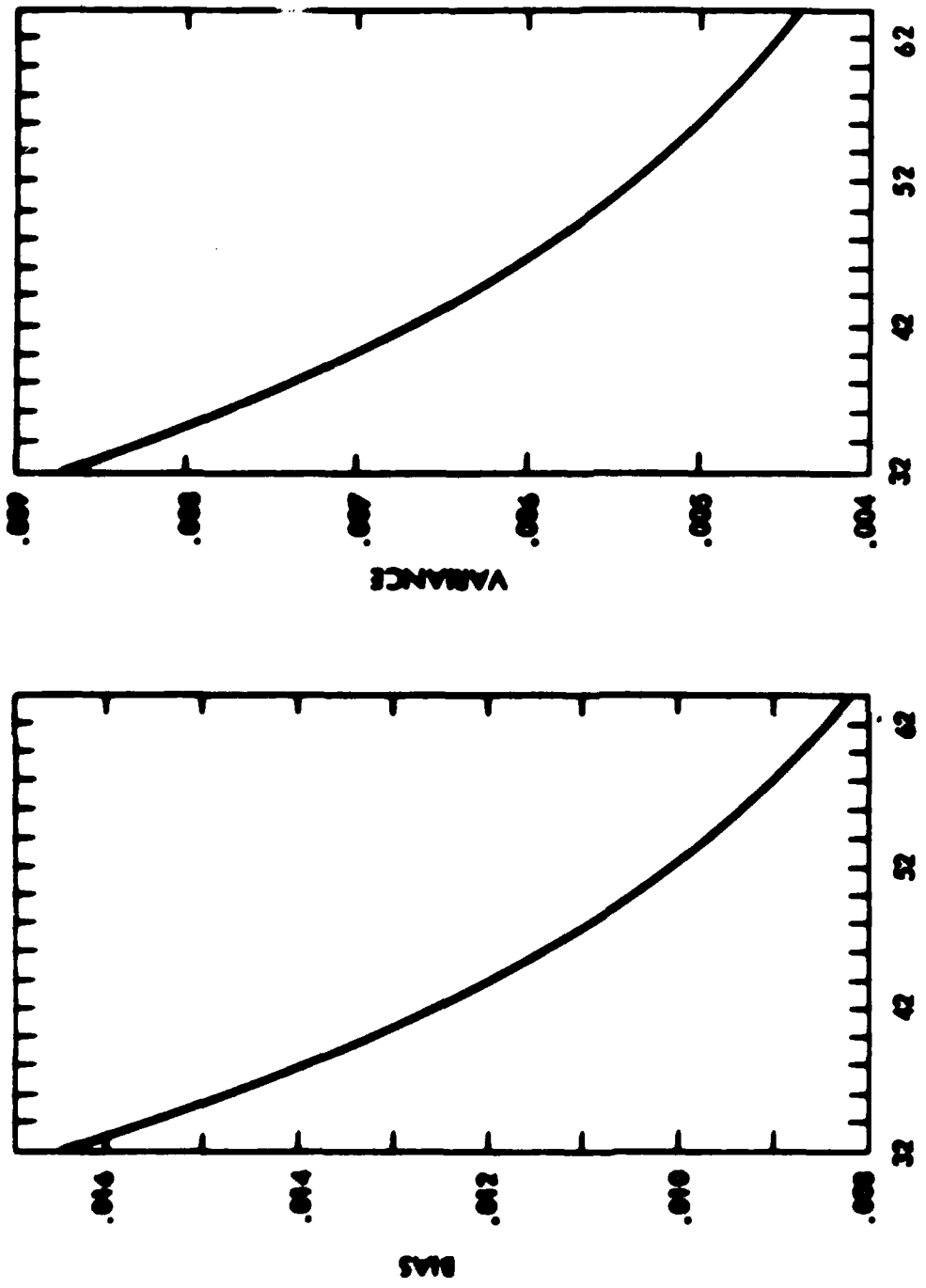

Fig. 34. Bias and Variance versus n for $|\gamma|^2 = 0.25$

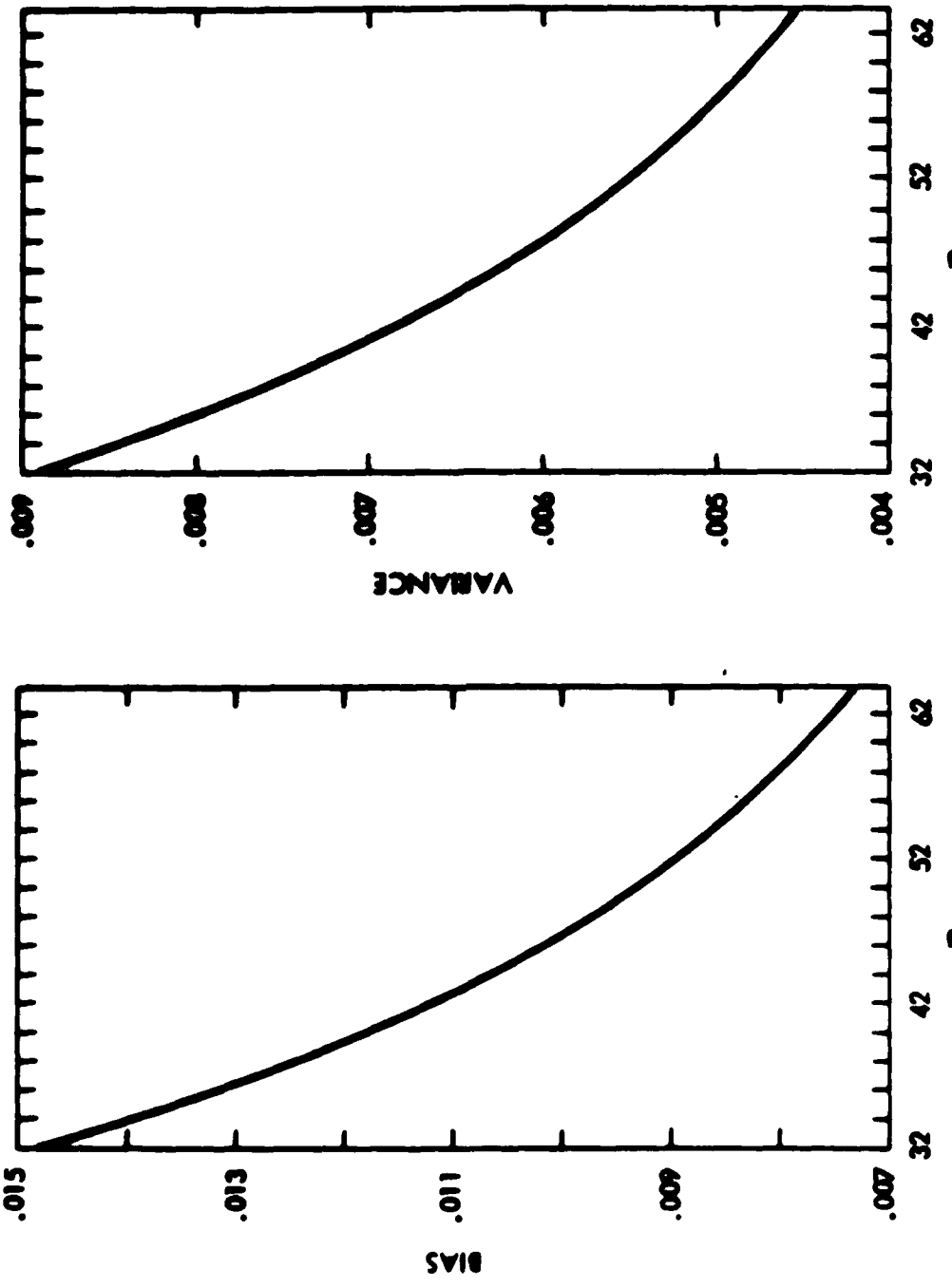

Fig. 25. Bias and Variance versus n for $|\gamma|^2 = 0.32$

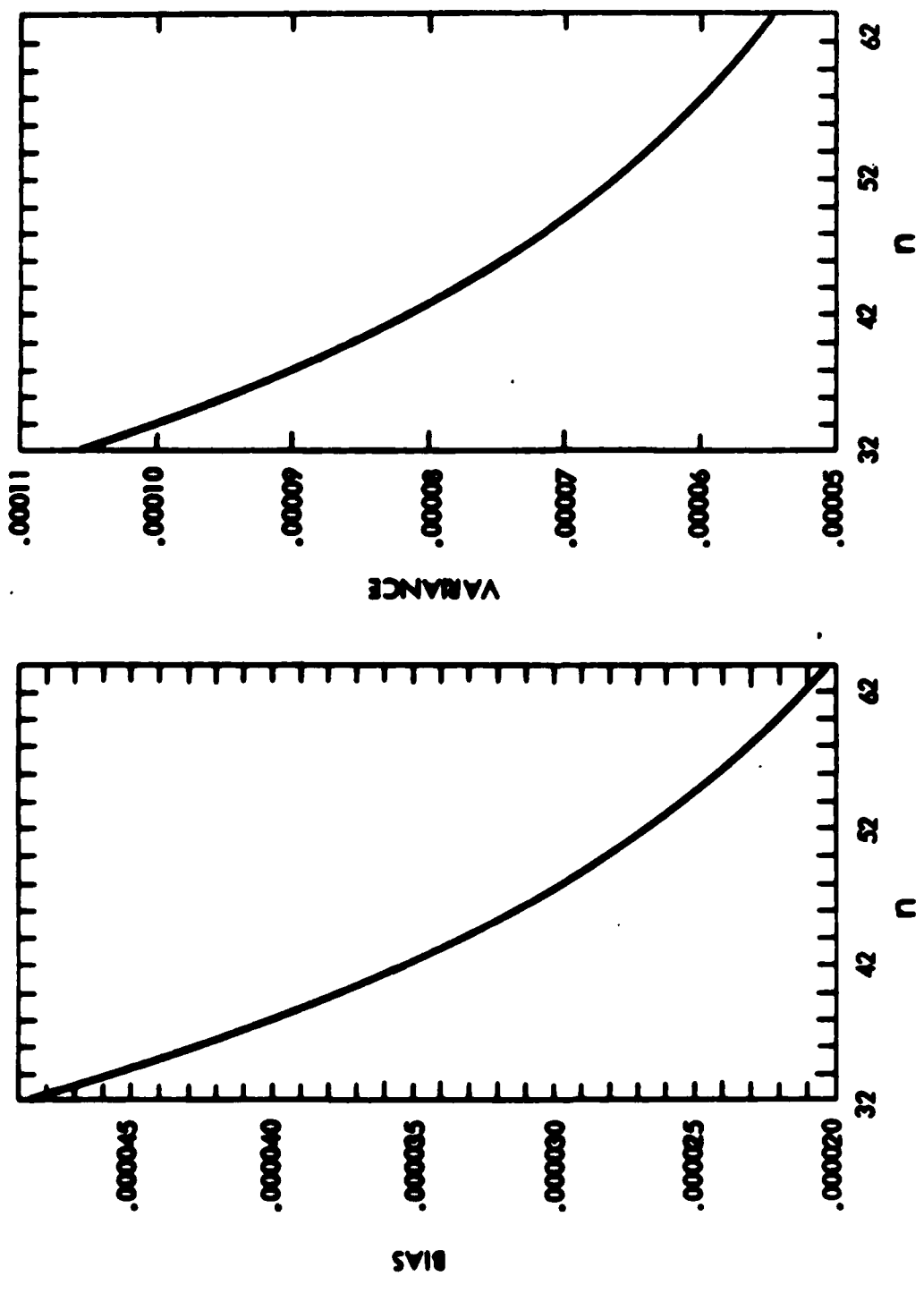

Fig. 26. Bias and Variance versus n for $|\gamma| = 0.96$

V. EXPERIMENTAL INVESTIGATION OF OVERLAP EFFECTS

An experiment has been conducted to study the effect of overlap of data on the estimate $\left|\hat{\gamma}\right|^2$. The analytical results presented earlier relate only to the case of independent segments (that is, the case of zero percent overlap). This experiment examines the effect of different amounts of overlap on bias and variance of $\left|\hat{\gamma}\right|^2$.

Intuitively, it seems that the application of nonoverlapping weighting function does not make the best use of the data when forming the estimator $\left|\hat{\gamma}\,(f_k)\right|^2$. This inefficiency is similar to the wastage in forming auto power spectral density functions shown by Nuttall.[14] When $\left|\hat{\gamma}\,(f_k)\right|^2$ is formed without overlap, larger bias and larger variance result than when $\left|\hat{\gamma}\,(f_k)\right|^2$ is formed from the same data with overlap. Because this inefficiency can not be permitted in many practical situations of interest (for example, underwater acoustic environments), it is desirable to know how much the bias and variance can be reduced and at what expense this reduction can be achieved.

V.A. METHOD

The method of achieving the desired objective is straightforward in concept Data are generated with an accurately prespecified value of magnitude-squared coherence, $\left|\gamma_g\right|^2$, which is independent of frequency, f. Since the data

have been generated so that the magnitude-squared coherence is independent of frequency, the sample mean and variance of $|\hat{\gamma}|^2$ can be empirically determined for the given overlap by averaging over frequency. These data can then be reprocessed at several different overlaps to form estimates of bias and variance.

V.A.1. Data Generation

Consider the zero-mean, wide-sense stationary, Gaussian waveforms $n_1(t)$ and $n_2(t)$ that are statistically independent and have power spectral density functions $\Phi_{n_1 n_1}(f)$ and $\Phi_{n_2 n_2}(f)$, respectively. Statistical independence dictates that they be uncorrelated; that is,

$$R_{n_1 n_2}(\tau) = E\left[n_1(t)\, n_2(t+\tau)\right] = 0 \quad . \tag{5.1}$$

In order to generate two processes with magnitude-squared coherence independent of frequency, let (Nuttall and Carter[31])

$$x(t) = n_1(t) + G n_2(t) \tag{5.2}$$

and

$$y(t) = n_2(t) + G n_1(t) \quad . \tag{5.3}$$

The cross-correlation of $x(t)$ and $y(t)$ is

$$R_{xy}(\tau) = E\left\{\left[(n_1(t) + G n_2(t)\right]\left[(n_2(t+\tau) + G n_1(t+\tau)\right]\right\} \quad . \tag{5.4}$$

Expanding, dropping terms that go to zero, and taking the Fourier transform of Eq. (5.4) yields

$$\Phi_{xy}(f) = G\Phi_{n_1n_1}(f) + G\Phi_{n_2n_2}(f) \quad . \tag{5.5}$$

The autocorrelation of x(t) is

$$R_{xx}(\tau) = E\left\{\left[n_1(t) + Gn_2(t)\right]\left[n_1(t+\tau) + Gn_2(t+\tau)\right]\right\} \quad . \tag{5.6}$$

Expanding, dropping terms that go to zero, and taking the Fourier transform of Eq. (5.6) yields

$$\Phi_{xx}(f) = \Phi_{n_1n_1}(f) + G^2\Phi_{n_2n_2}(f) \quad . \tag{5.7}$$

Similarly,

$$\Phi_{yy}(f) = \Phi_{n_2n_2}(f) + G^2\Phi_{n_1n_1}(f) \quad . \tag{5.8}$$

Thus, the magnitude-squared coherence between x(t) and y(t) is

$$\left|\gamma_{xy}(f)\right|^2 = \frac{\left|G\Phi_{n_1n_1}(f) + G\Phi_{n_2n_2}(f)\right|^2}{\left[\Phi_{n_1n_1}(f) + G^2\Phi_{n_2n_2}(f)\right]\left[\Phi_{n_2n_2}(f) + G^2\Phi_{n_1n_1}(f)\right]} \quad . \tag{5.9}$$

Now introducing the assumption that $\Phi_{n_1n_1}(f) = \Phi_{n_2n_2}(f) = \Phi_{nn}(f)$.

$$\left|\gamma_{xy}(f)\right|^2 = \frac{4G^2\,\Phi_{nn}^2(f)}{\left(1+G^2\right)^2\,\Phi_{nn}^2(f)} = \frac{4G^2}{\left(1+G^2\right)^2} \quad , \tag{5.10}$$

which is independent of frequency.

In order to prespecify a desired magnitude-squared coherence, $\left|\gamma_d\right|^2$, between x(t) and y(t), the gain G of Eqs. (5.2) and (5.3) must be selected by solving Eq. (5.10):

$$G = \begin{cases} \dfrac{1-\sqrt{1-\left|\gamma_d\right|^2}}{\left|\gamma_d\right|} & , \quad 0 < \left|\gamma_d\right| \le 1 \\ 0 & , \quad \left|\gamma_d\right|^2 = 0.0 \end{cases} \quad . \tag{5.11}$$

Under the assumptions made, a prespecified desired value for magnitude-squared coherence can be generated. Because the generated processes will later be used to empirically determine a very small quantity (bias), it is important that the generated value of coherence is indeed the desired value. In the actual generation of two processes, the assumption $\Phi_{n_1n_1}(f) = \Phi_{n_2n_2}(f)$ may be violated; therefore it becomes important to determine how sensitive Eq. (5.10) is to this assumption. Consider then

$$\frac{\Phi_{n_2n_2}(f)}{\Phi_{n_1n_1}(f)} = 1 + \Delta(f) \cong 1 \quad . \tag{5.12}$$

It is easily shown[31] by substituting Eq.(5.12) into Eq. (5.9) that the value of magnitude-squared coherence generated, $|\gamma_g|^2$, is

$$|\gamma_g|^2 = |\gamma_d|^2 \frac{1 + \Delta + \frac{1}{2}\Delta^2}{1 + \Delta + \frac{1}{2}\Delta^2 |\gamma_d|^2} \quad , \tag{5.13}$$

where $|\gamma_d|^2$ = desired value of $|\gamma|^2$, and the dependence of f is dropped for convenience.

The error in the generated value is

$$|\gamma_g|^2 - |\gamma_d|^2 = |\gamma_d|^2 \left(1 - |\gamma_d|^2\right) \frac{\frac{1}{2}\Delta^2}{1 + \Delta + \frac{1}{2}|\gamma_d|^2 \Delta^2} \quad . \tag{5.14}$$

Evaluation of Eq. (5.14) to third order in Δ yields

$$|\gamma_g|^2 - |\gamma_d|^2 \cong |\gamma_d|^2 \left(1 - |\gamma_d|^2\right) \tfrac{1}{2} \Delta^2 (1 - \Delta) \quad . \tag{5.15}$$

This quantity is maximum at $|\gamma_d|^2 = \frac{1}{2}$ and, hence, the maximum error is approximately

$$\text{Max error} \cong \left(\tfrac{1}{4} \Delta\right)^2 (1 - \Delta) \quad . \tag{5.16}$$

Therefore, for example, when $\Delta = 0.01$, the maximum error is approximately 6×10^{-6}; for $\Delta = 0.05$, the maximum error is approximately 1.5×10^{-4}. (A table of errors versus $|\gamma_d|^2$ and Δ,[31] as computed from Eq. (5.14), yields results similar to the given approximations.)

The processes generated according to Eqs. (5.2) and (5.3) have been shown to be relatively insensitive to minor differences in the power spectral density functions of the original uncorrelated waveforms $n_1(t)$ and $n_2(t)$.

The procedure for generating variable-coherence time series can briefly be summarized as follows: One Gaussian noise source uncorrelated from point to point was used to generate a time-limited sample function of $n_1(t)$ and, later, of $n_2(t)$. (This method eliminates the need for two identical filters.) The waveforms were band-limited using a low-pass filter and digitized. The digital data were then stored on magnetic tape in a format compatible with overlapped processing. Digital versions of $x(t) = n_1(t) + Gn_2(t)$ and $y(t) = n_2(t) + Gn_1(t)$ were generated from digital versions of $n_1(t)$ and $n_2(t)$ for two values of $|\gamma_{xy}|^2$. (Investigation for other values of true magnitude-squared coherence appeared to be unnecessary.)

A Hewlett Packard Noise Generator, Model No. HP3722A, was used for data generation with the following settings:

Sequence Length:	Infinite
Bandwidth:	5 kHz
Gaussian rms:	0.6 x 3.16 volts (open circuit)

The output power density function is flat to within $\pm$ 0.3 dB, provided the input power voltage fluctuates no more than $\pm$ 10 percent. This corresponds to a Δ, in Eq. (5.12), of 7.182×10^{-2} and a maximum error in the generated magnitude-squared coherence, from Eq. (5.16), of 3×10^{-4}. For example, if $|\gamma_d|^2 = 0.5000$ one could expect $0.5004 > |\gamma_g|^2 > 0.4996$, making it

impossible to measure extremely small bias.

The data were low-pass filtered through a two-section Krohn-hite filter, which was 6 dB down at 1200 Hz and rolling off at 96 dB per octave. These band-limited data were A/D converted with a Control Data Corporation (CDC) 16-bit converter. Sampling was done at $f_s = 4000$ Hz.

V.A.3. Analysis Program

The FORTRAN program (coded by G. C. Carter, C. R. Arnold, and J. F. Ferrie, of NUSC)(1) implements Eq. (3.11); (2) generates data with known coherence from two incoherent sources according to Section V. A 1, and (3) computes the sample mean, bias, and variance of the estimator, as described below. A summary flowchart of the program is presented in Fig. 27 The cosine weighting function was coded by A. H. Nuttall, of NUSC. Singleton[32] coded the mixed radix FFT. The FFT size used was 4096 data points (1 sec), which yields 2048 positive frequencies and direct current. Frequencies beyond 1000 Hz were discounted in making estimates of bias and variance to protect against (1) unknown noise in the digitizing system and (2) difference in the two auto power spectral density functions

Estimates of the bias are performed according to

$$\hat{\text{Bias}} = \left[\frac{1}{1000}\sum_{k=1}^{1000} |\hat{\gamma}(f_k)|^2\right] - |\gamma|^2 \qquad (5.17)$$

and estimates of the sample variance according to

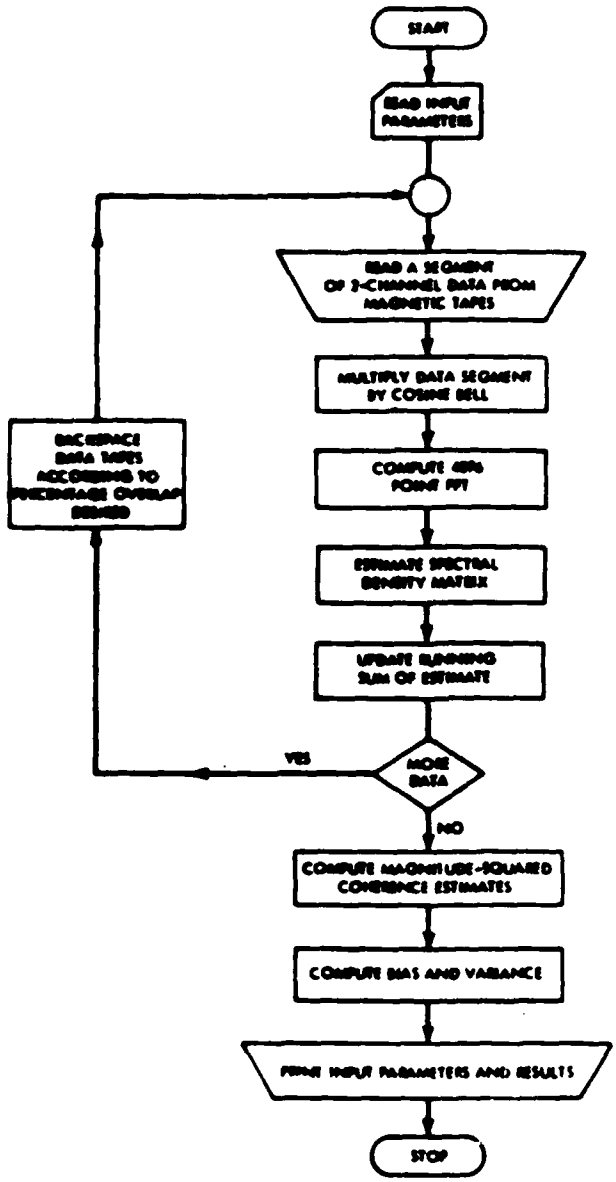

Fig. 37. Summary Flow Chart for Thesis Version of FFT Spectral Density Estimation Program

$$\widehat{\text{Var}} = \frac{1}{999} \sum_{k=1}^{1000} \left[\left| \hat{\gamma}(f_k) \right|^2 - \widehat{\text{Bias}} \right]^2 \quad . \tag{5.18}$$

Results of the experiment are described in the next section.

V. B. RESULTS

Results of the experiment for a joint set of data, each (32 x 4096) samples long, are included in tabular and graphic form. Confidence bands for the estimates of bias can be determined from the estimates of variance. However, it must be realized that 1000 samples (frequencies) were used to determine the average, and that each sample is correlated to the extent of approximately 0.5 with neighboring estimates (empirical results). This agrees with analytical results provided for auto spectral estimates.[14]

It is apparent from the results (Tables 6 and 7 and Figs. 28 through 31) that the bias and variance of $\left|\hat{\gamma}\right|^2$ can be reduced through the use of overlapped processing. For example, when $\left|\gamma\right|^2 = 0.0$, the variance of the estimator with 50-percent overlap equals 31 percent of the variance of the estimator with 0-percent overlap. With 50-percent overlap, the bias is 55 percent as large as with 0-percent overlap. Similarly, when $\left|\gamma\right|^2 = 0.3$, the variance is 55 percent of the 0-percent overlap estimator, and the bias is 50 percent as large. It also can be seen from the results that 62.5-percent overlap is similar to having processed twice as much data with 0-percent overlap. There is one possible exception: The bias for $\left|\gamma\right|^2 = 0.3$ is 36 percent as large as the 0-percent overlap estimator. This is better than 50 percent,

TABLE 6

EMPIRICAL RESULTS FOR $|v|^2 = 0.0$ AND $n = 32$

Percent Overlap	No. FFTs	Bias	Variance
0.0	32	$.3126 \times 10^{-1}$	$.0028 \times 10^{-3}$
12.5	36	$.2994 \times 10^{-1}$	$.7130 \times 10^{-3}$
25.0	42	$.2970 \times 10^{-1}$	$.5197 \times 10^{-3}$
37.5	50	$.2948 \times 10^{-1}$	$.4000 \times 10^{-3}$
50.0	63	$.1749 \times 10^{-1}$	$.3929 \times 10^{-3}$
62.5	83	$.1502 \times 10^{-1}$	$.3600 \times 10^{-3}$
75.0	125	$.1871 \times 10^{-1}$	$.3028 \times 10^{-3}$

TABLE 7

EMPIRICAL RESULTS FOR $|v|^2 = 0.3$ AND $n = 32$

Percent Overlap	No. FFTs	Bias	Variance
0.0	32	1.442×10^{-2}	$.8087 \times 10^{-2}$
12.5	36	1.093×10^{-2}	$.7770 \times 10^{-2}$
25.0	42	$.960 \times 10^{-2}$	$.5966 \times 10^{-2}$
37.5	50	$.717 \times 10^{-2}$	$.5067 \times 10^{-2}$
50.0	63	$.597 \times 10^{-2}$	$.4441 \times 10^{-2}$
62.5	83	$.515 \times 10^{-2}$	$.4063 \times 10^{-2}$
75.0	125	$.494 \times 10^{-2}$	$.4020 \times 10^{-2}$

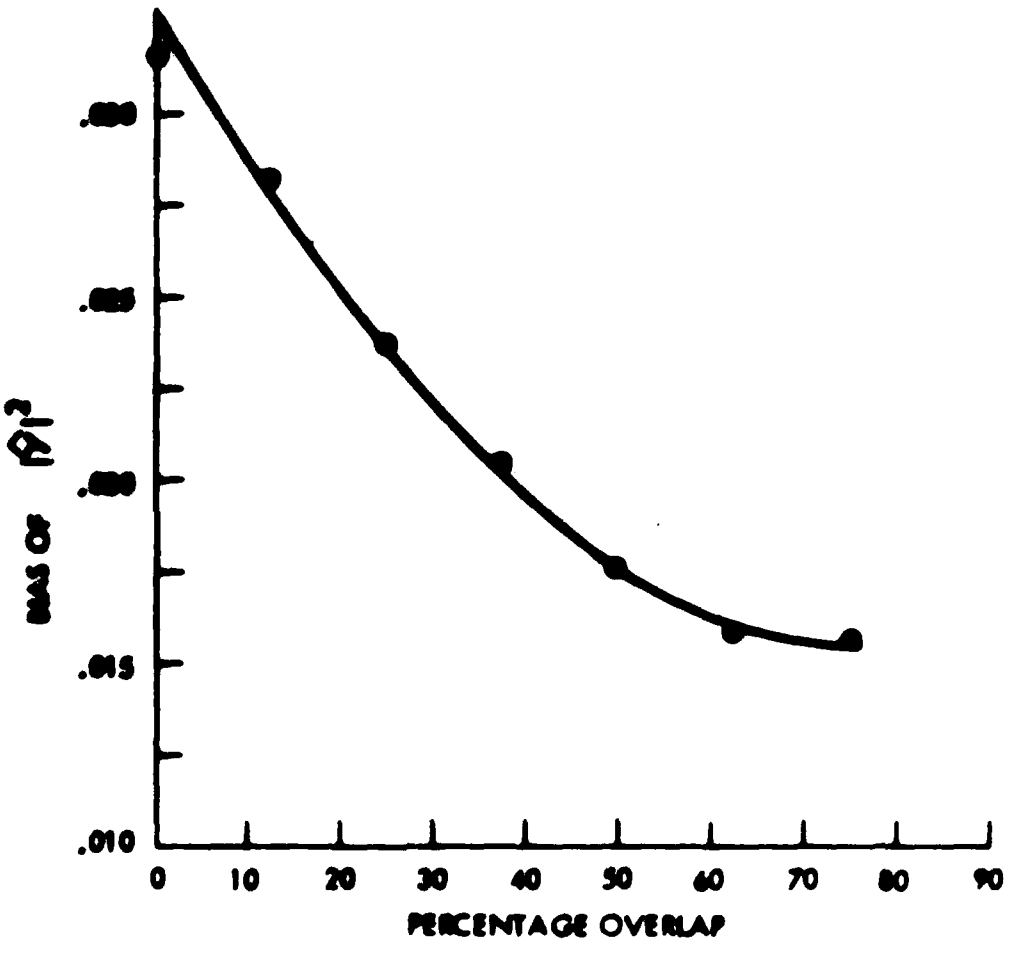

Fig. 38. Bias of $|\hat{\gamma}|^2$ When $|\gamma|^2 = 0.0$ and $n = 32$

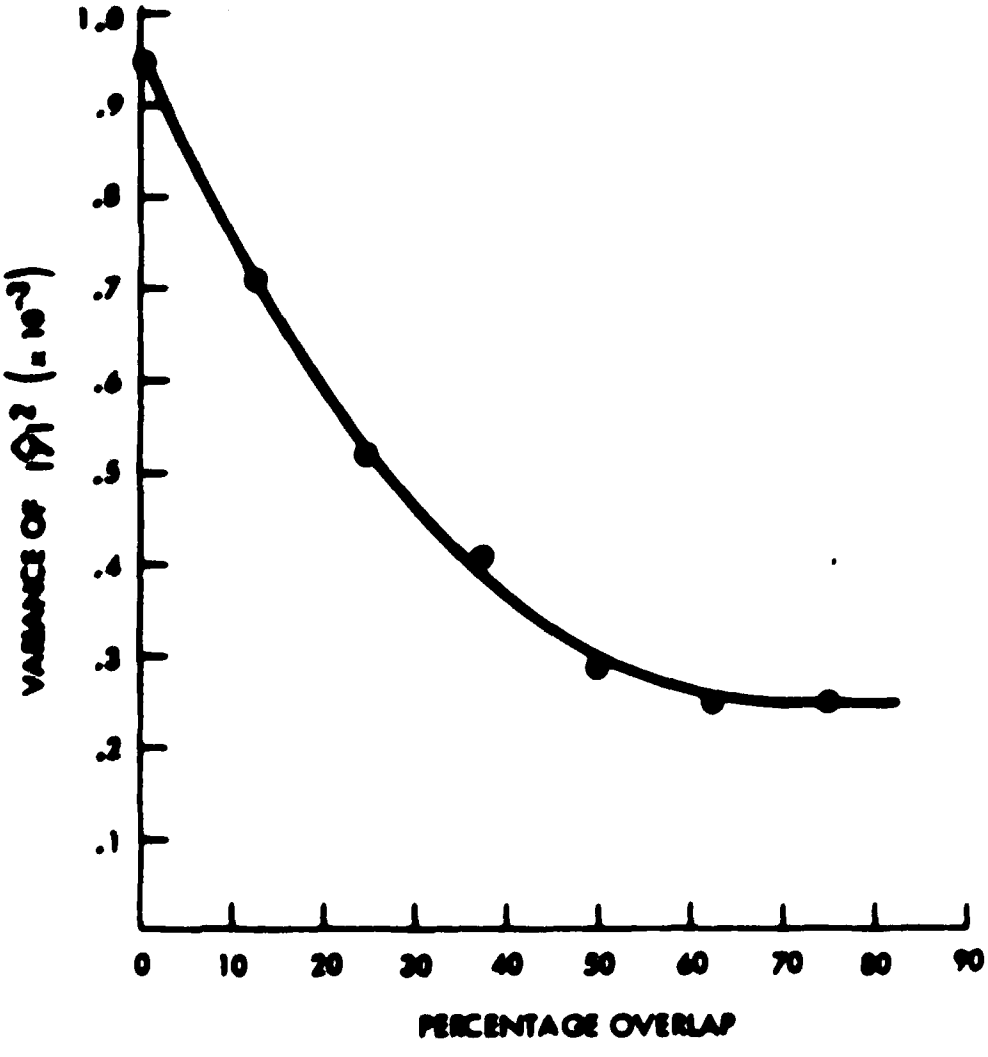

Fig. 20. Variance of $|\hat{\gamma}|^2$ When $|\gamma|^2 = 0.0$ and $n = 32$

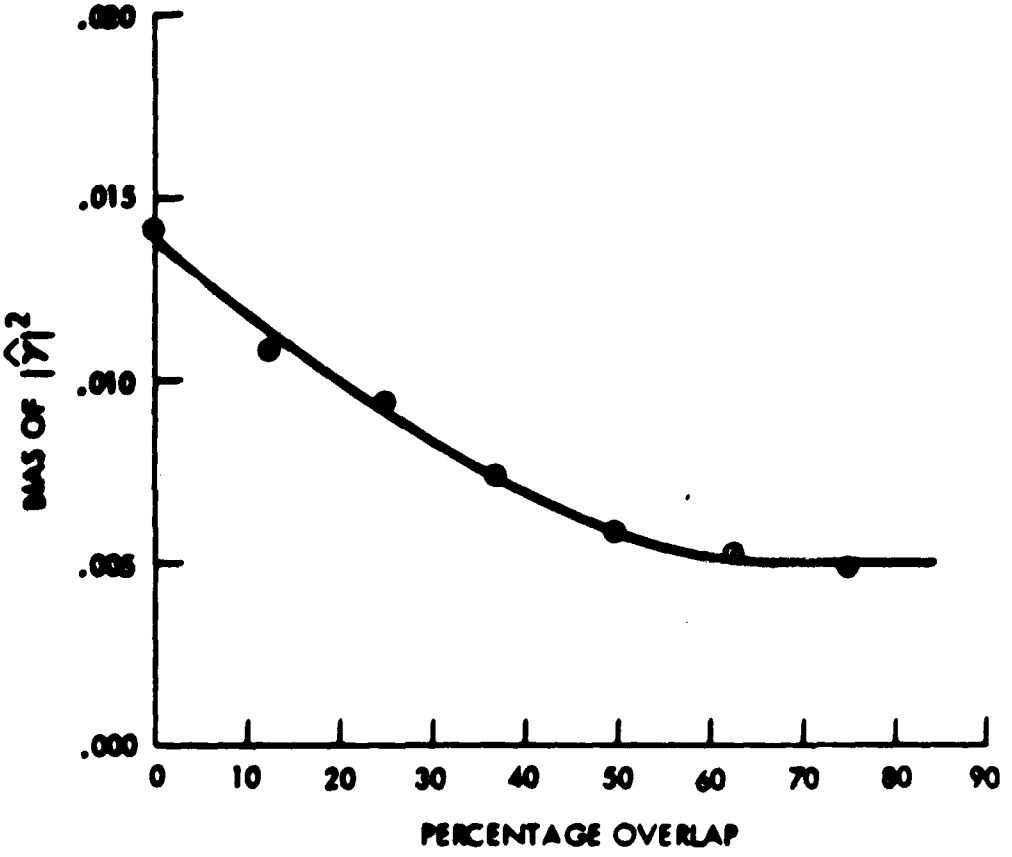

Fig. 30. Bias of $|\hat{\gamma}|^2$ When $|\gamma|^2 = 0.3$ and $n = 32$

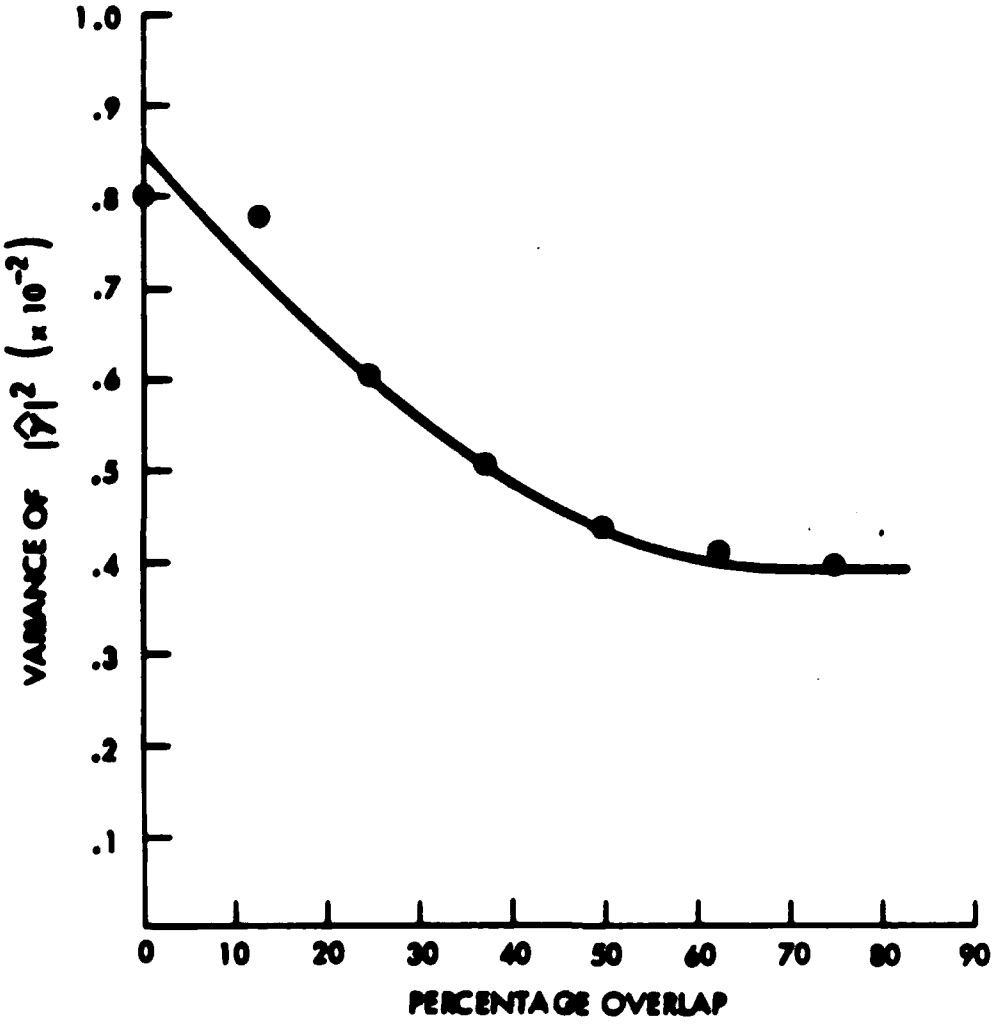

Fig. 31. Variance of $|\hat{\gamma}|^2$ When $|\gamma|^2 = 0.3$ and $n = 32$

which would be expected from twice as much data.

Quite naturally, there is an increase in computational cost associated with overlapped processing. Specifically, the number of FFTs to be performed (a measure of the computational cost) increases with the percent overlap specified (Fig. 32). The number of FFTs required for 50-percent overlap is approximately twice the number for 0-percent overlap.

Increasing the overlap from 50 percent to 62.5 percent, requires 32-percent more FFTs, but the variance of the estimator becomes only 80-95 percent of its value at 50-percent overlap. In most cases, the improvement to be derived from using 62.5-percent overlap, as opposed to 50-percent overlap, will not warrant the increased computational costs, and should be used only when stringent variance and bias reduction requirements are demanded.

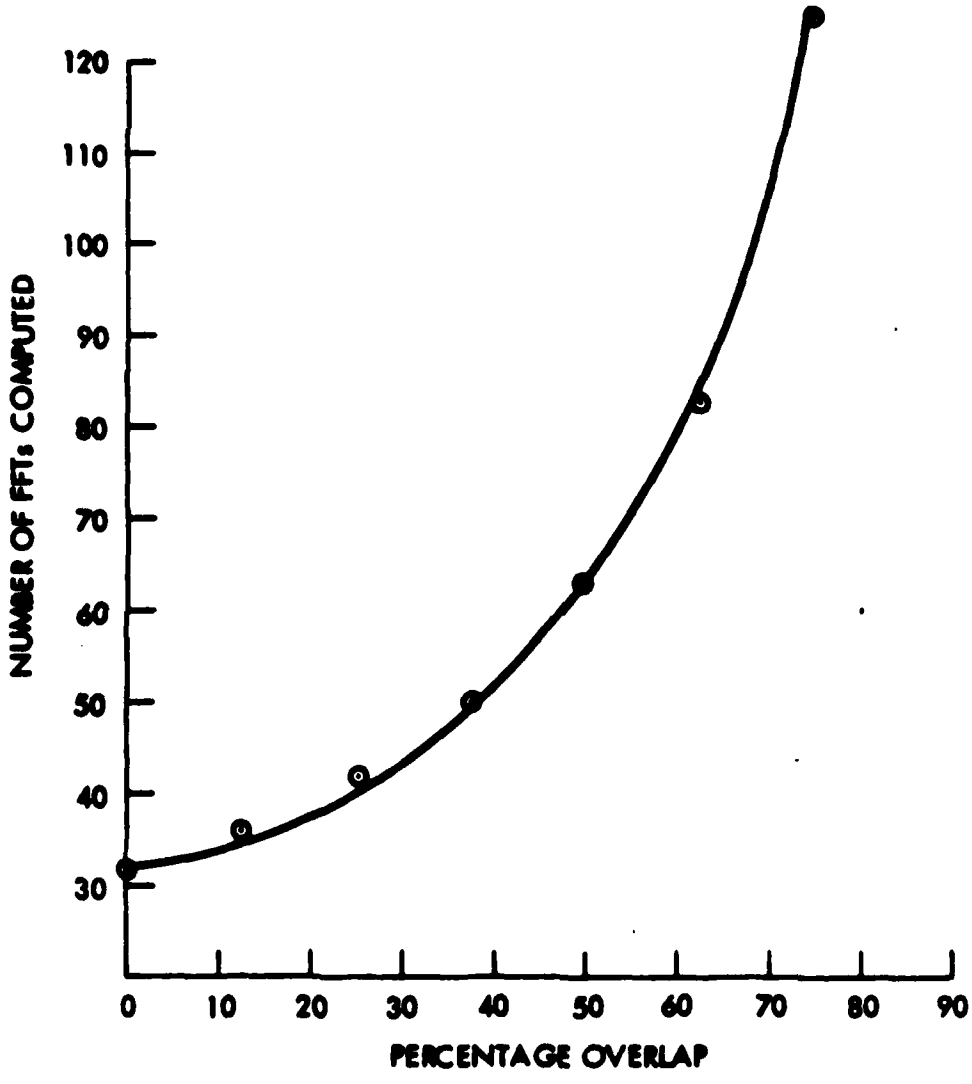

Fig. 32. Number of FFTs Required for Overlapped Processing

VI. CONCLUSIONS

A detailed analytical analysis of the statistics for estimating the magnitude-squared coherence function (spectrum) has been made. When such estimates are made, time-limited sample functions of long duration, which are stationary (in the wide sense) over the period of observation, must be available. Expressions for the probability density, the cumulative distribution, and the bias and variance of $\left|\hat{\gamma}\right|^2$ have been presented for the case where no overlap processing is used. Evaluation of these expressions, which are dependent on both the true value of coherence and the number of observed segments, n, dramatically portrays the requirement that n be large.

The application of a cosine-weighting function in order to reduce errors due to sidelobe leakage wastes the available data. As shown empirically, proper use of the data in terms of reduced bias and variance of the estimator can be achieved through overlapped processing. It appears that a 62.5-percent overlap is roughly equivalent to having twice as much data available. The reduced bias and variance of the estimator achieved through 62.5-percent overlapped processing can be realized almost entirely through a 50-percent overlap. The computational cost associated with 50-percent overlap is not unreasonable. With 50-percent overlap, variance and bias reductions are achieved that are similar to reductions resulting from processing twice as much data with 0-percent overlap. This significant gain to be obtained from 50-percent overlap processing

should not be overlooked in estimating the magnitude-squared coherence function (spectrum) when cosine (Hanning) weighting is used and data are limited.

APPENDIX A

STATISTICS OF MAGNITUDE-COHERENCE ESTIMATOR

Goodman, in his Eqs. (4.51) and (4.60), derived an analytical expression for the probability density function of the coherence estimate, $|\hat{\gamma}|$. His results are based on two zero-mean processes that are stationary, Gaussian, and random and are segmented into n independent observations (that is, n nonoverlapped segments). Each segment is assumed perfectly windowed, as defined in Chapter IV. The probability that the estimate of coherence would take on some value, $|\hat{\gamma}|$, conditioned on the true coherence being equal to $|\gamma|$ and upon n independent observations, was given by Goodman as

$$p\left(|\hat{\gamma}| \,\middle|\, |\gamma|, n\right) = \frac{2|\hat{\gamma}|\left(1-|\gamma|^2\right)^n}{\Gamma(n)\,\Gamma(n-1)}\left(1-|\hat{\gamma}|^2\right)^{n-2} \cdot \sum_{k=0}^{\infty} \frac{\Gamma^2(n+k)}{\Gamma^2(k+1)}\left(|\gamma|^2|\hat{\gamma}|^2\right)^k . \qquad \text{(A.1)}$$

where $\Gamma(n)$ is the Gamma function, namely,

$$\Gamma(m) = \int_0^\infty e^{-x} x^{m-1}\, dx \quad \text{and} \quad \Gamma(m) = (m-1)\,\Gamma(m-1)$$

This probability density function is also given by Shannon.[34] However, this form of the density function is rather cumbersome. A work by Esterbon and Goodman[9] suggests that it may be written in terms of the hypergeometric function. It is first necessary to observe, from Abramowitz and Stegun[36] that

$${}_2F_1\left(n, n-1; |\gamma|^2|\hat{\gamma}|^2\right) = \frac{1}{\Gamma^2(m)} \sum_{k=0}^{\infty} \frac{\Gamma^2(m+k)}{\Gamma(k+1)} \frac{\left(|\gamma|^2|\hat{\gamma}|^2\right)^k}{k!} \qquad (A.2)$$

Further, when k is an integer,

$$k! = \Gamma(k+1) \qquad (A.3)$$

(See, for example, Abramowitz and Stegun.[36]) Thus, Eq. (A.1) is

$$p\left(|\hat{\gamma}_1| \,|n, n\right) = 2|\hat{\gamma}|\left(1-|\gamma|^2\right)^n \left(1-|\hat{\gamma}|^2\right)^{n-2} \frac{(n-1)}{\Gamma(n)\,\Gamma(n)}$$

$$\cdot \sum_{k=0}^{\infty} \frac{\Gamma^2(n+k)}{\Gamma(k+1)} \frac{\left(|\gamma|^2|\hat{\gamma}|^2\right)^k}{k!} \qquad (A.4)$$

or, more simply, substituting Eq. (A.2) into (A.4),

$$p\left(|\hat{\gamma}| \,|\gamma|, n\right) = 2|\hat{\gamma}|\left(1-|\gamma|^2\right)^n \left(1-|\hat{\gamma}|^2\right)^{n-2} (n-1)$$

$$\cdot {}_2F_1\left(n, n-1; |\gamma|^2|\hat{\gamma}|^2\right) \qquad (A.5)$$

This form of the density function, Eq. (A.5), is more favorable than the form in Eq. (A.1) because the hypergeometric function is well documented.

The mth moment of magnitude coherence can be shown, as in Eq. (4.13) to be

$$E\left(|\hat{\gamma}|^m \mid n, |\gamma|\right) = \left(1 - |\gamma|^2\right)^n \frac{\Gamma(m+1)\,\Gamma\left(\frac{m}{2}+1\right)}{\Gamma\left(n+\frac{m}{2}\right)} \cdot {}_2F_1\left(\frac{m}{2}+1, n; n+\frac{m}{2}; |\gamma|^2\right) \qquad \text{(A.6)}$$

Exact expressions for the bias and variance follow directly in a manner parallel to that in part IV.C.

It is instructive to show the relation between the biases of estimates of the magnitude coherence and the magnitude-squared coherence. Define the biases as follows:

$$B_1 \triangleq E\left(|\hat{\gamma}|\right) - |\gamma| \qquad \text{(A.7)}$$

and

$$B_2 \triangleq E\left(|\hat{\gamma}|^2\right) - |\gamma|^2 \qquad \text{(A.8)}$$

Because the variance of $|\hat{\gamma}|$ must be nonnegative,

$$E\left(|\hat{\gamma}|^2\right) \geq \left[E\left(|\hat{\gamma}|\right)\right]^2 \qquad \text{(A.9)}$$

Using Eqs. (A.7) and (A.8) yields

$$B_2 + |\gamma|^2 \geq \left(B_1 + |\gamma|\right)^2 = B_1^2 + 2B_1|\gamma| + |\gamma|^2 \quad . \tag{A.10}$$

Thus,

$$B_2 \geq 2B_1|\gamma| + B_1^2 \quad . \tag{A.11}$$

For example, consider the case $|\gamma| = 1.0$. Now $B_1 = 0.0$, $B_2 = 0.0$, and Eq. (A.11) hold with equality. Consider also $|\gamma| = 0.0$. Then

$$E\left(|\hat{\gamma}| \,\middle|\, n, |\gamma| = 0.0\right) = \frac{\Gamma(n)\,\Gamma(3/2)}{\Gamma(n + 1/2)} \quad . \tag{A.12}$$

Using Eq. (6.1.47) of Abramowitz and Stegun,[26] Eq. (A.12) yields for large n

$$E\left(|\hat{\gamma}| \,\middle|\, n, |\gamma| = 0.0\right) \simeq \frac{\Gamma(3/2)}{\sqrt{n}} = \tfrac{1}{2}\sqrt{\pi/n} \quad . \tag{A.13}$$

For $|\gamma|^2 = 0$, Eq. (4.21) gives

$$B_2 = \frac{1}{n} \quad , \quad |\gamma|^2 = 0.0 \quad . \tag{A.14}$$

Thus, the inequality holds and Eq. (A.11) becomes

$$\frac{1}{n} \geq \frac{\pi}{4}\left(\frac{1}{n}\right) \quad , \quad |\gamma| = 0.0 \quad . \tag{A.15}$$

APPENDIX B

DERIVATION OF A SIMPLIFIED EXPRESSION FOR THE EXPECTATION OF THE ESTIMATE OF MAGNITUDE-SQUARED COHERENCE

The major steps in deriving a simplified expression for $E\left(|\hat{\gamma}|^2 \,|\, n, |\gamma|^2\right)$ are presented here.

According to Eq. (4.26),

$$E\left(|\hat{\gamma}|^2 \,|\, n, |\gamma|^2\right) = \frac{\left(1 - |\gamma|^2\right)^n}{n} \, {}_3F_2\left(2, n, n; n+1, 1; |\gamma|^2\right), \tag{B.1}$$

which can be manipulated into the form

$$E\left(|\hat{\gamma}|^2 \,|\, n, |\gamma|^2\right) = \left(1 - |\gamma|^2\right)^n \sum_{k=0}^{\infty} \frac{(n)_k \, (k+1)}{(n+k)} \, \frac{|\gamma|^{2k}}{k!} \,. \tag{B.2}$$

Adding and subtracting n from the numerator term in Eq. (B.2) yields

$$E\left(|\hat{\gamma}|^2 \,|\, n, |\gamma|^2\right) = \left(1 - |\gamma|^2\right)^n \left[\sum_{k=0}^{\infty} \frac{(n)_k}{k!} |\gamma|^{2k} + \sum_{k=0}^{\infty} \frac{(1-n)(n)_k}{(k+n)\, k!} |\gamma|^{2k}\right] \tag{B.3}$$

Recognizing that

$$\frac{1}{k+n} = \frac{(n)_k}{n(n+1)_k} \,, \tag{B.4}$$

it follows that

$$E\left(|\hat{\gamma}|^2 \,\middle|\, n, |\gamma|^2\right) = \left(1 - |\gamma|^2\right)^n \left[\sum_{k=0}^{\infty} \frac{(n)_k (b)_k}{(b)_k} \frac{|\gamma|^2}{k!} + \frac{(1-n)}{n} \right.$$

$$\left. \cdot \sum_{k=0}^{\infty} \frac{(n)_k (n)_k}{(n+1)_k} \frac{|\gamma|^{2k}}{k!} \right] . \qquad \text{(B.5)}$$

In terms of ${}_2F_1$ functions, Eq. (B.5) becomes

$$E\left(|\hat{\gamma}|^2 \,\middle|\, n, |\gamma|^2\right) = \left(1 - |\gamma|^2\right)^n \left[{}_2F_1\left(n, b; b; |\gamma|^2\right) \right.$$

$$\left. + \frac{(1-n)}{n} \, {}_2F_1\left(n, n; n+1; |\gamma|^2\right) \right] . \qquad \text{(B.6)}$$

By using Eq. (15.1.8) of Abramowitz and Stegun,[26] Eq. (B.6) reduces to

$$E\left(|\hat{\gamma}|^2 \,\middle|\, n, |\gamma|^2\right) = \left(1 - |\gamma|^2\right)^n \left[\left(1 - |\gamma|^2\right)^{-n} \right.$$

$$\left. + \frac{1-n}{n} \, {}_2F_1\left(n, n; n+1; |\gamma|^2\right) \right] . \qquad \text{(B.7)}$$

Simplifying and applying Eq. (15.3.3) of Abramowitz and Stegun,[26] Eq. (B.7) can be further reduced to

$$E\left(|\hat{\gamma}|^2 \,\middle|\, n, |\gamma|^2\right) = 1 + \frac{(1-n)}{n} \left(1 - |\gamma|^2\right) {}_2F_1\left(1, 1; n+1; |\gamma|^2\right) .$$

(B.8)

Finally, by applying Eq. (15.2.6) of Abramowitz and Stegun,[26] with $a = 1$, $b = 1$, and $c = n + 1$, Eq. (B.8) can be manipulated into the form

$$E\left(|\hat{\gamma}|^2 \,\middle|\, n, |\gamma|^2\right) = \frac{1}{n} + \frac{n-1}{n+1} |\gamma|^2 \, {}_2F_1\left(1, 1; n+2; |\gamma|^2\right). \quad \text{(B.9)}$$

LIST OF REFERENCES

[1]N. R. Goodman, "On the Joint Estimation of the Spectra, Cospectrum, and Quadrature Spectrum of a Two-Dimensional Stationary Gaussian Process," Scientific Paper 10, NYU, New York (March 1957).

[2]J. S. Bendat and A. G. Piersol, Measurement and Analysis of Random Data (New York: John Wiley & Sons, Inc., 1966).

[3]L. J. Tick, Spectral Analysis of Time Series, ed. by B. Harris (New York: John Wiley & Sons, Inc., 1967), 133-152.

[4]R. A. Fisher, Contributions to Mathematical Statistics (New York: John Wiley & Sons, Inc., 1950) (Chapter 14 originally published as "The General Sampling Distribution of the Multiple Correlation Coefficient," Proceedings of the Royal Society, Series A, Vol. 121 (1928), 654-673).

[5]D. E. Amos and L. H. Koopmans, "Tables of the Distribution of the Coefficient of Coherence for Stationary Bivariate Gaussian Processes," Sandia Corp. Monograph SCR-483 (1963).

[6]M. J. Alexander and C. A. Vok, "Tables of the Cumulative Distribution of Sample Multiple Coherence," Rocketdyne Division, North American Aviation, Inc., Research Report 63-67 (November, 1963).

[7]R. A. Haubrich, "Earth Noise, 5 to 500 Millicycles per Second, 1. Spectral Stationarity, Normality, and Nonlinearity, "Journal of Geophysical Research, Vol. 70, No. 6 (March, 1965), 1415-1427.

[8]G. M. Jenkins and D. G. Watts, Spectral Analysis and Its Applications (San Francisco: Holden-Day, Inc., 1968).

[9]L. D. Enochson and N. R. Goodman, "Gaussian Approximations to the Distribution of Sample Coherence," Air Force Flight Dynamics Lab., Research and Tech. Div., AF Systems Command, Wright-Patterson AFB, Ohio, Bull. AFFDL-TR-65-67 (June, 1965).

[10]V. A. Benignus, "Estimation of Coherence Spectrum and Its Confidence Interval Using the Fast Fourier Transform," IEEE Transactions of Audio and Electroacoustics, Vol. AU-17, No. 2, (June, 1969), 145-150.

[11]J. W. Cooley and J. W. Tukey, "An Algorithm for the Machine Calculation of Complex Fourier Series," Mathematics of Computation, Vol. 19 (April, 1965), 297-301.

[12]G. C. Carter and C. R. Arnold, "Some Practical Considerations of Coherence Estimation," NUSC Tech Memo TD 113-19-71, New London, Ct. (November, 1971)

[13]C. Bingham, M. D. Godfrey, and J. W. Tukey, "Modern Techniques of Power Spectrum Estimation," IEEE Transactions on Audio and Electroacoustics Vol. AU-15, No. 2 (June, 1967), 56-66.

[14]A. H. Nuttall, "Spectral Estimation by Means of Overlapped FFT Processing of Windowed Data," NUSC Report No. 4169, New London, Ct. (October, 1971).

[15]W. B. Davenport and W. L. Root, An Introduction to the Theory of Random Signals and Noise (New York: McGraw-Hill Book Co., Inc., 1958).

[16]J. M. Wozencraft and I. M. Jacobs, Principles of Communication Engineering (New York: John Wiley & Sons, Inc., 1967).

[17]H. L. Van Trees, Detection, Estimation, and Modulation Theory, Part I (New York: John Wiley & Sons, Inc., 1968).

[18]R. C. Dubes, The Theory of Applied Probability (Englewood Cliffs, N.J.: Prentice-Hall, Inc., 1968).

[19]P. R. Roth, "Effective Measurements Using Digital Signal Analysis," IEEE Spectrum, Vol. 8, No. 4 (April, 1971), 62-70.

[20]C. H. Knapp, personal communication.

[21]P. D. Welch, "The Use of Fast Fourier Transform for the Estimation of Power Spectra: A Method Based on Time Averaging Over Short, Modified Periodograms," IEEE Transactions on Audio and Electroacoustics, Vol. AU-15, No. 2 (June, 1967), 70-73.

[22]C. H. Knapp, "An Algorithm for Estimation of the Inverse Spectral Matrix," General Dynamics Electric Boat Research Project (April, 1969).

[23]B. Gold and C. M. Rader, Digital Processing of Signals (New York: McGraw-Hill Book Co., Inc., 1969).

[24]E. S. Hannan, Multiple Time Series (New York: John Wiley & Sons, Inc., 1970).

[25]G. C. Carter and A. H. Nuttall, "Evaluation of the Statistics of the Estimate of Magnitude-Squared Coherence," NUSC Tech Memo TC-193-71, New London, Ct. (28 September 1971).

[26]M. Arbramowitz and I. A. Stegun (Editors), Handbook of Mathematical Functions With Formulas, Graphs, and Mathematical Tables, U. S. Government Printing Office, Washington, D. C. (1964).

[27]H. Cramer, Mathematical Methods of Statistics (Princeton, N. J: Princeton University Press, 1946).

[28]I. S. Gradshteyn and I. M. Ryzhik, Table of Integrals, Series, and Products (New York: Academic Press, 1965).

[29]T. W. Anderson, An Introduction to Multivariate Statistical Analysis (New York: John Wiley & Sons, Inc., 1958).

[30]A. H. Nuttall and D. H. Wood, personal communication.

[31]A. H. Nuttall and G. C. Carter, "On Generating Processes with Specified Coherence," NUSC Tech Memo TC-187-71, New London, Ct. (22 September 1971

[32]R. C. Singleton, "An Algorithm for Computing the Mixed Radix Fast Fourier Transform," IEEE Transactions on Audio and Electroacoustics, Vol. AU-17, No. 2, (June, 1969), 93-102.

NUSC Technical Memorandum TD113-48-72
22 May 1972

Statistics of the Estimate of Magnitude Coherence

G. C. Carter

ABSTRACT

Expressions for the statistics of the estimate of magnitude coherence are presented. These statistics include the probability density function, the cumulative distribution function, the bias, and the variance. The expressions presented are in convenient and accurate forms for digital computer evaluation. Tabular and graphical examples of computing bias and variance are included. Simple approximations are also given for the maximum bias, variance, and mean square error.

TABLE OF CONTENTS

REVERSE BLANK

INTRODUCTION

Consider two wide-sense stationary random processes x(t) and y(t) with auto power spectral density functions $G_x(f)$ and $G_y(f)$, respectively, and cross power spectrum $G_{xy}(f)$. The magnitude-coherence between these two processes is defined as

$$|\gamma(f)| = \frac{|G_{xy}(f)|}{\sqrt{G_x(f)\, G_y(f)}} . \qquad (1)$$

Estimates of $|\gamma(f)|$ from n segments (or pieces) of data are frequently made according to

$$|\hat{\gamma}(f)| = \frac{\left|\sum_{i=1}^{n} X_i(f)\, Y_i^*(f)\right|}{\sqrt{\sum_{i=1}^{n} |X_i(f)|^2 \sum_{i=1}^{n} |Y_i(f)|^2}} , \qquad (2)$$

where $X_i(f)$ and $Y_i(f)$ are the Fourier coefficients obtained by performing a fast Fourier transform (FFT) of the ith weighted segment. The problem addressed here is the behavior of the bias and variance of the random variable $|\hat{\gamma}(f)|$.

STATISTICS OF THE ESTIMATOR

There has been much related past work on statistics of the form of (2) for n independent segments and x(t) and y(t) Gaussian zero-mean processes[1-12]. In particular, the probability density function (PDF) of* $|\hat{\gamma}|$ can be found in references 2, 5, and 10-12.

$$p(|\hat{\gamma}| \,||\gamma|, n) = 2|\hat{\gamma}|(1-|\gamma|^2)^n \left(1-|\hat{\gamma}|^2\right)^{n-2} (n-1) \cdot {}_2F_1\left(n, n; 1; |\gamma|^2 |\hat{\gamma}|^2\right). \qquad (3)$$

---

*The f dependency is dropped for notational simplicity.

The cumulative distribution is given by [12]:

$$P\left(|\hat{\gamma}| \,\middle|\, n, |\gamma|\right) = |\hat{\gamma}|^2 \left(\frac{1-|\gamma|^2}{1-|\gamma|^2|\hat{\gamma}|^2}\right)^n \cdot \sum_{K=0}^{n-2} \left(\frac{1-|\hat{\gamma}|^2}{1-|\gamma|^2|\hat{\gamma}|^2}\right)^K {}_2F_1\left(-K, 1-n; 1; |\gamma|^2|\hat{\gamma}|^2\right). \quad (4)$$

For the special case of $|\gamma| = 0$,

$$P\left(|\hat{\gamma}| \,\middle|\, n, |\gamma|=0\right) = 1 - \left(1-|\hat{\gamma}|^2\right)^{n-1}. \quad (5)$$

Differentiation yields the result

$$p\left(|\hat{\gamma}| \,\middle|\, n, |\gamma|=0\right) = 2|\hat{\gamma}|(n-1)\left(1-|\hat{\gamma}|^2\right)^{n-2}. \quad (6)$$

In general, for arbitrary $|\gamma|$, the mth moment (Ref. 12) is given by

$$E\left(|\hat{\gamma}|^m \,\middle|\, n, |\gamma|\right) = \left(1-|\gamma|^2\right)^n \frac{\Gamma(n)\Gamma\left(\frac{m}{2}+1\right)}{\Gamma\left(n+\frac{m}{2}\right)} \cdot {}_3F_2\left(\frac{m}{2}+1, n, n; \frac{m}{2}+n, 1; |\gamma|^2\right). \quad (7)$$

An exact expression for the

$$\text{bias} \triangleq E\left(|\hat{\gamma}| \,\middle|\, n, |\gamma|\right) - |\gamma| \quad (8)$$

is

$$\text{bias} = \left(1-|\gamma|^2\right)^n \frac{\Gamma(n)\Gamma(3/2)}{\Gamma(n+1/2)} {}_3F_2\left(\tfrac{3}{2}, n, n; n+\tfrac{1}{2}, 1; |\gamma|^2\right) - |\gamma| \quad (9)$$

An exact expression for the

$$\text{variance} \triangleq E\left(|\hat{\gamma}|^2\right) - E^2\left(|\hat{\gamma}|\right) \tag{10}$$

is

$$\text{variance} = \frac{\left(1-|\gamma|^2\right)^n}{n} {}_3F_2\left(2,n,n;n+1,1;|\gamma|^2\right)$$
$$-\left[\left(1-|\gamma|^2\right)^n \frac{\Gamma(n)\Gamma(3/2)}{\Gamma(n+1/2)} {}_3F_2\left(\tfrac{3}{2},n,n;n+\tfrac{1}{2},1;|\gamma|^2\right)\right]^2. \tag{11}$$

An approximation for the variance is given by [6]

$$\text{variance} \cong \frac{1}{2n}\left(1-|\gamma|^2\right)^2, \tag{12}$$

which has a peak value at $|\gamma| = 0$ such that

$$\text{maximum variance} \cong \frac{1}{2n}. \tag{13}$$

The mean square error of the magnitude-coherence estimator, $|\hat{\gamma}|$, from the true value is

$$\text{mean square error} = \text{variance} + [\text{bias}]^2 \tag{14}$$

$$= E\left(|\hat{\gamma}|^2\right) - E^2\left(|\hat{\gamma}|\right) + \left[E\left(|\hat{\gamma}|\right) - |\gamma|\right]^2 \tag{15}$$

$$= E\left(|\hat{\gamma}|^2\right) + |\gamma|^2 - 2E\left(|\hat{\gamma}|\right)|\gamma|. \tag{16}$$

Since the mean square error is always greater than the variance, it follows that equation (16) is an upper bound on the variance, though not a least upper bound.

COMPUTER EVALUATION

The FORTRAN computer program for the P_{32} function coded by A. H. Nuttall is included in Appendix A. The FORTRAN computer program for evaluating the bias, variance, variance approximation, mean square error, and 3σ points is included in Appendix B. Tabular results are given in Appendix C.

RESULTS

The tabular results, Appendix C, of the computer evaluation are given for 7 values of n and several values of $|\gamma|$. In particular, n = 4, 8, 16, 32, 64, 128, 256. For each value of n, $|\gamma|$ ranged from 0.0, in steps of 0.02, until the variance was .01 of its (approximate) peak value.

As shown in the tables, the bias (Eq. (9)) has a maximum value at $|\gamma| = 0$, namely (see ref. [12]),

$$\text{maximum bias} \cong \frac{1}{2}\sqrt{\pi/n} \qquad (17)$$

for large n.

Now when $|\gamma| = 0$, using a result in reference [12] and inspecting tabular results, we find that equation (16) yields

$$\text{maximum mean square error} = \frac{1}{\pi}. \qquad (18)$$

The appearance of a local maxima in the mean square error for n = 64 and $|\gamma| = .2$ remotely suggests that equation (18), while true for the practical range $n \leq 256$, might not hold in the limit of asymptotically large n. Similarly, an inspection of the tabulated variance clearly indicates that the peak value does not occur at $|\gamma| = 0$ as indicated by equation (12). It can be observed (see tables) that the abscissa value for which the variance, equation (11), is a maximum changes with n. This type of behavior is not predicted by equation (12).

Plots of the variance versus $|\gamma|$ are provided in Fig. 1 for the 7 values of n. It can readily be seen in this figure that the abscissa value for which the peak value of variance occurs changes with n.

A plot of the variance approximation, together with the true variance, is given in Fig. 2. The usefulness of the variance approximation, which can be determined quantitatively

from the tables, can now be seen qualitatively. In particular, one can conclude that equation (12) approximates an upper bound on equation (11) near the origin, and hence equation (13) acts as an approximate upper bound on the variance.

Plots of bias and mean square error are given in Figs. 3 and 4. They bear out the observation that bias and mean square error are maximum for $|\delta| = 0$.

AD-A101 684 SCIENTIFIC AND ENGINEERING STUDIES COMPILED 1979 3/8
COHERENCE ESTIMATION(U) NAVAL UNDERWATER SYSTEMS CENTER
NEWPORT RI G C CARTER ET AL. 1979

UNCLASSIFIED F/G 9/1 NL

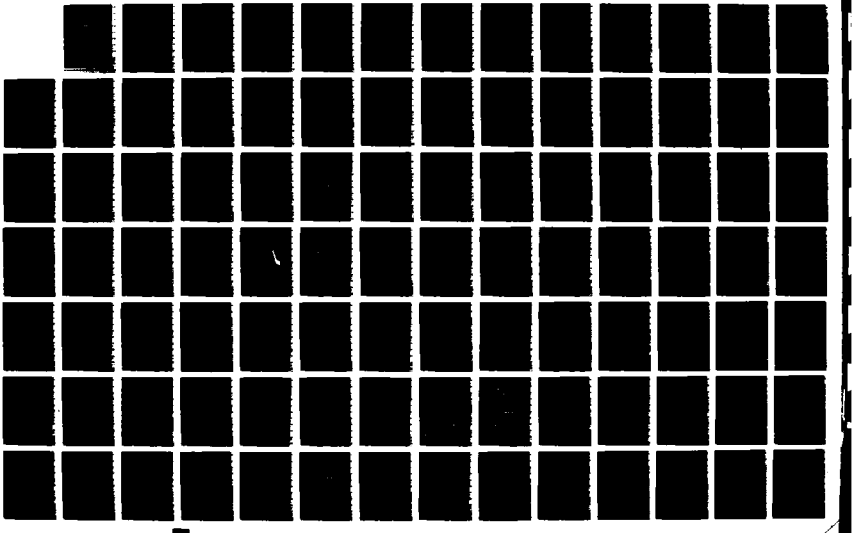

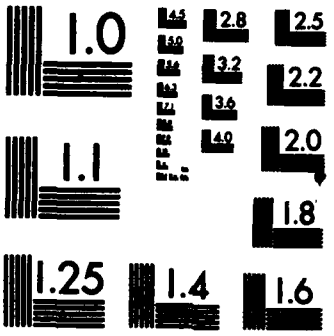

MICROCOPY RESOLUTION TEST CHART
NATIONAL BUREAU OF STANDARDS-1963-A

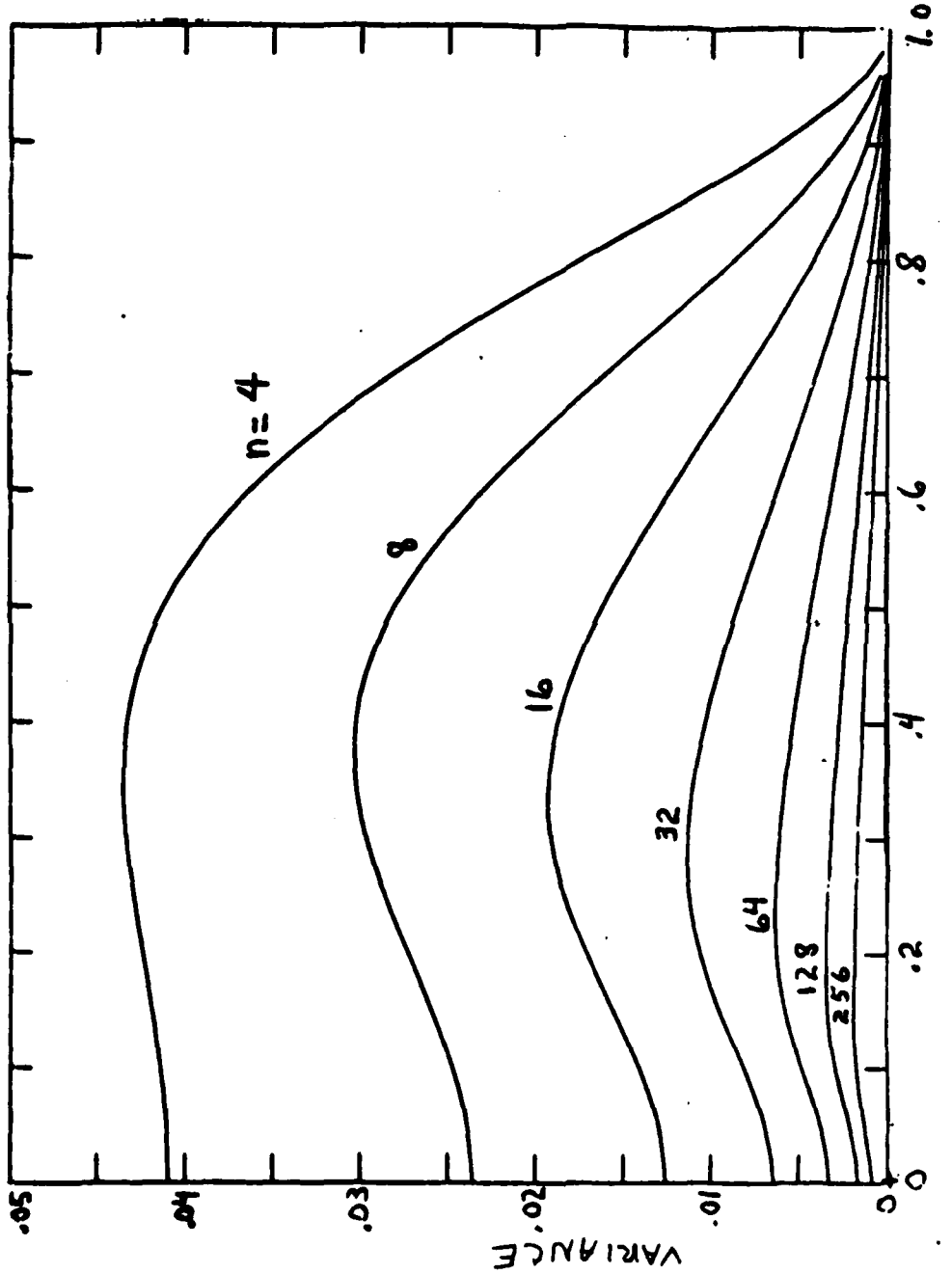

FIG 1 VARIANCE VERSUS $|x|$ (for $n=4,8,16,32,64,128$ and 256)

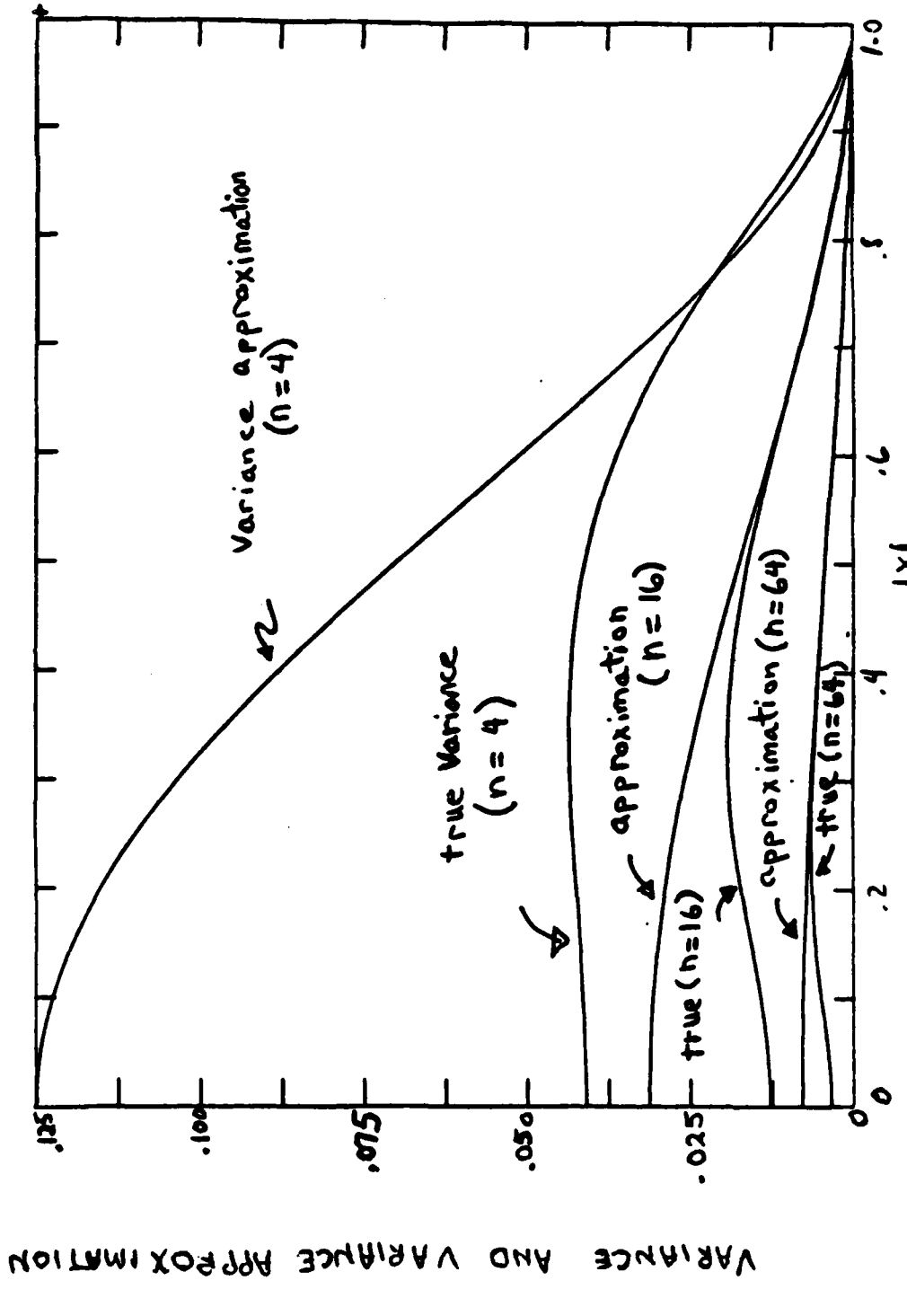

FIG 2. VARIANCE VERSUS |x| (for n= 4, 16, and 64) AND VARIANCE APPROXIMATION VERSUS |x| (for n=4, 16, and 64)

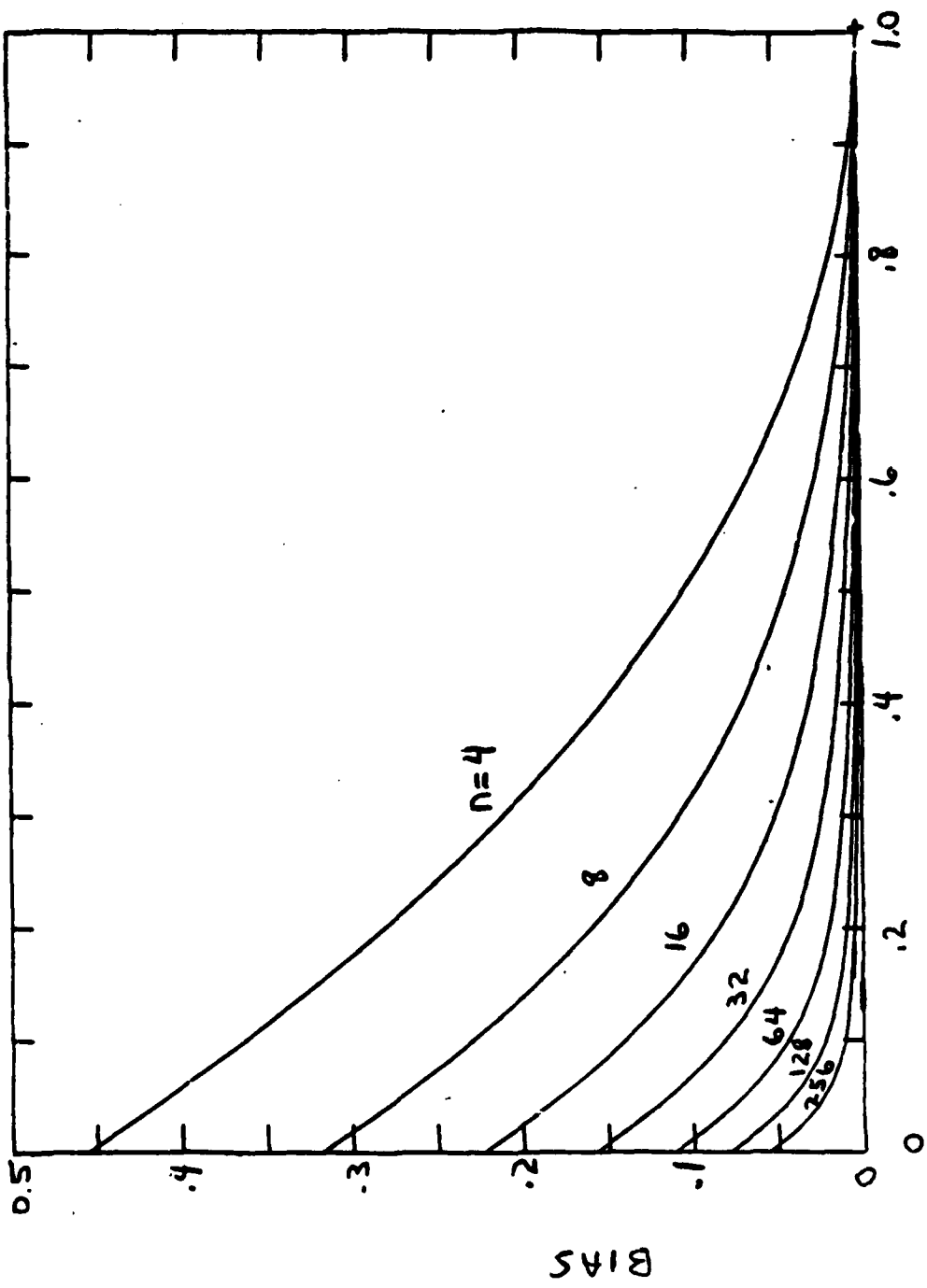

FIG 3 BIAS VERSUS |B1| (for n=4, 8, 16, 32, 64, 128, and 256)

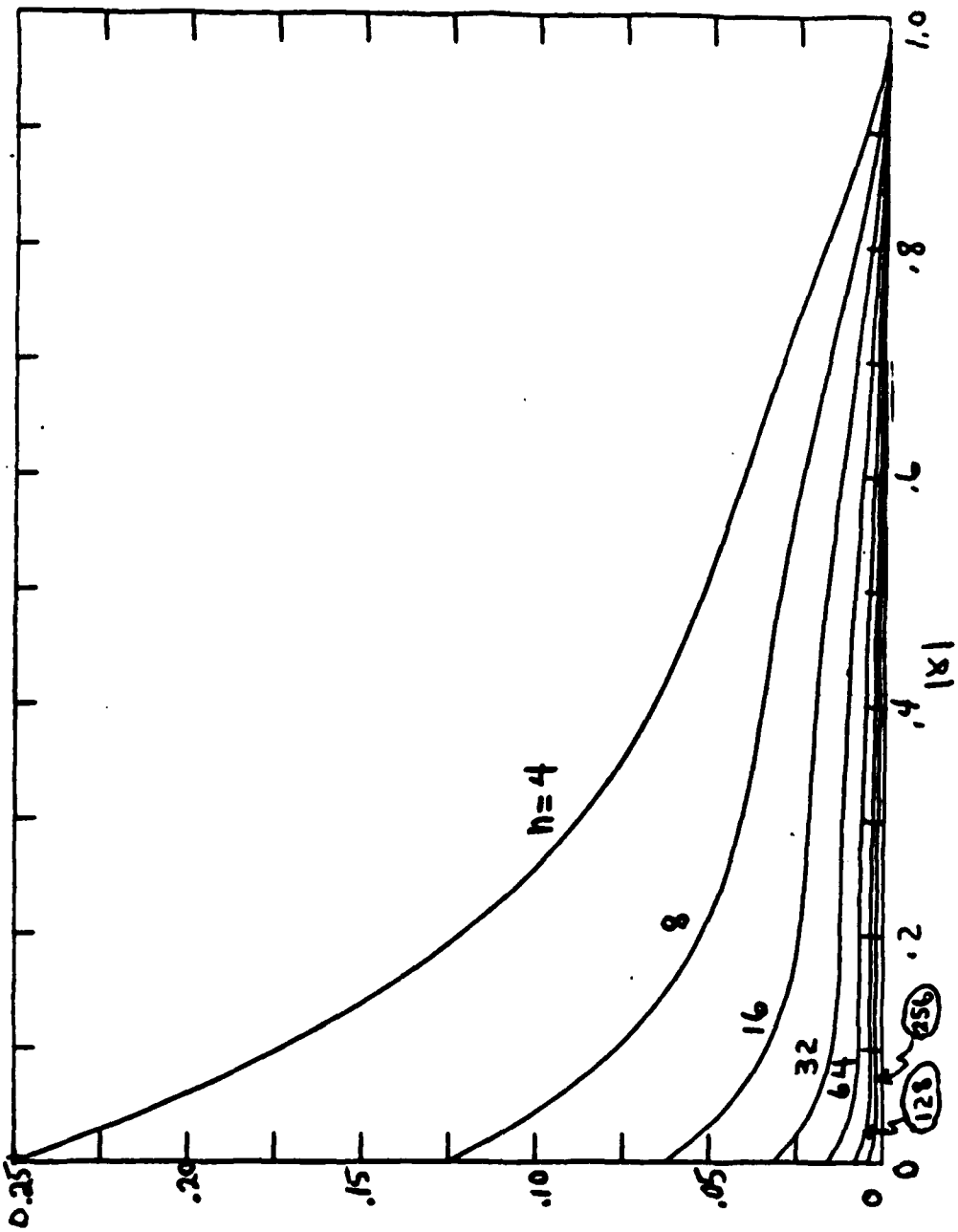

Fig 4 Mean Square Error versus |R|
(for n=4, 8, 16, 32, 64, 128, and 256)

Appendix A

FORTRAN PROGRAM FOR P32 FUNCTION

```
1*    C     THIS SUBROUTINE COMPUTES THE P32 FUNCTION * CODE BY A.H.NUTTALL
2*    C
3*          SUBROUTINE S(A1,A2,A3,B1,B2,X,F32,T,K)
4*    C
5*          DOUBLE PRECISION A1,A2,A3,B1,B2,X,F32,T,C
6*    C
7*          F32=1.D0
8*          T=1.D0
9*          DO 1 N=1,10000
10*         C=N-1
11*         T=T*(A1+C)*(A2+C)*(A3+C)*X/((B1+C)*(B2+C)*(C+1.D0))
12*         F32=F32+T
13*         IF(ABS(T).LE.1.D-7*ABS(F32)) GO TO 2
14*       1 CONTINUE
15*   C
16*       2 K=IFIX(C+1.0)
17*         IF(K.EQ.10000) WRITE(*,3) T
18*       3 FORMAT(//' ***WARNING*** AFTER 10000 TERMS IN P32 T = ',D15.6//)
19*         RETURN
20*         END

END OF UNIVAC 1108 FORTRAN V COMPILATION.      0 *DIAGNOSTIC* MESSAGE(S)
```

Appendix B

FORTRAN PROGRAM FOR EVALUATING THE STATISTICS

```
      DOUBLE PRECISION M1,S1,M2,S2,SMAR,S,S2BAR,FN,C1,C2,VAR,FNP1,E2,E1
      DOUBLE PRECISION FNP2
      DOUBLE PRECISION BIAS
      DOUBLE PRECISION COHM,G
      DOUBLE PRECISION C(2048)
      DIMENSION X(200),Z(200),YBIAS(200),YVART(200),YVARA(200),YMSE(200)
C
      CALL MODESG(2,0)

      C(1)=1.00
      DX=0.2
      INC=50
      DO 25 N=2,2048
      FN=FLOAT(N)
                  C(N)=((FN-1.00)/(FN-0.500))*C(N-1)
   25 CONTINUE
C
      DO 95 K=2,6
C
      N=2**K
C
      FN=FLOAT(N)
      SMALL=1./(2.*FN)
      SMALL=SMALL/100.0
      IF(N.EQ.1)SMALL=0.0
      FNP1=N+0.500
      FNP2=N+1.000
      WRITE(4,50)N
   50 FORMAT(/1H1,I10//)
```

Appendix B (Cont'd)

```
C
C            VARY THE TRUE VALUE OF S
C
      DO 65 I=1,INC
C
      COHMAG=FLOAT(I-1)/FLOAT(INC)
      X(I)=COHMAG
      S=COHMAG*COHMAG
C
      C1=((1.00-S)**FN)*C(N)
      C2=((1.00-S)**FN)/FN
      CALL SS(1.500,FN,FI,FIP1,1.00,S,ANS1,E1,K1)
      CALL SS(2.000,FN,FI,FIP2,1.00,S,ANS2,E2,K2)
      SUAR=C1*ANS1
      BIAS=SUAR-COHMAG
      S2UAR=C2*ANS2
      VAR=S2UAR-(SUAR*SUAR)
      THRSIG=3.00*USQRT(VAR)
      SQ=VAR+BIAS*BIAS
      APPROX=(1./(2.*FN))*(1.-S)**2
      WRITE(4, 60)N,I,COHMAG,VAR,BIAS,SQ,THRSIG,APPROX
   60 FORMAT(1X,2I5,6E9.4)
      YBIAS(I)=BIAS
      YVART(I)=VAR
      YMSE(I)=SQ
      YVARA(I)=APPROX
      IF(I.EQ.INC) GO TO 70
      IF(VAR.GE.SMALL)GO TO 80
C
C
C            PLOT SECTION
C
   70 CONTINUE
      CALL OBJCTG(2,0.,0.,2040.,1530.)
      YUMAX=0.05    MAX VAR
      DY=YUMAX/5.0
      CALL SUBJEG(2,0.,0.,1.,YUMAX)
```

```
      CALL LINESG(2,0,X(1),YVART(1))
      CALL LINESG(2,I,X(1),YVART(1))
      CALL OBJCTG(2,0.,1540.,2040.,3070.)
      YUMAX=0.25    MAX MSE
      DY=YUMAX/5.0
      CALL SUBJEG(2,0.,0.,1.,YUMAX)
      IF(K.EQ.2) CALL       LCGRID(2,0.,0.,1.,YUMAX)
      CALL LINESG(2,0,X(1),YMSE(1))
      CALL LINESG(2,I,X(1),YMSE(1))
      CALL OBJCTG(2,2050.,0.,4090.,1530.)
      YUMAX=0.5     MAX BIAS
      DY=YUMAX/5.0
      CALL SUBJEG(2,0.,0.,1.,YUMAX)
      IF(K.EQ.2) CALL       LCGRID(2,0.,0.,1.,YUMAX)
      CALL LINESG(2,0,X(1),YBIAS(1))
      CALL LINESG(2,I,X(1),YBIAS(1))
      CALL OBJCTG(2,2050.,1540.,4090.,3070.)
      YUMAX=0.125   MAX VAR APPROX
      DY=YUMAX/5.0
      CALL SUBJEG(2,0.,0.,1.,YUMAX)
      IF(K.EQ.2) CALL       LCGRID(2,0.,0.,1.,YUMAX)
      IF(N.EQ.4.OR.N.EQ.16.OR.N.EQ.64)GO TO 71
      GO TO 72
   71 CONTINUE
      CALL LINESG(2,0,X(1),YVART(1))
      CALL LINESG(2,I,X(1),YVART(1))
      CALL LINESG(2,0,X(1),YVARA(1))
      CALL LINESG(2,I,X(1),YVARA(1))
   72 CONTINUE
      WRITE(4,75)
   75 FORMAT(5X,'END OF TABLE')
      GO TO 95
   80 CONTINUE
```

Appendix B (Cont'd)

```
100*    C
101*    C            LOOP BACK TO VARY THE VALUE OF S
102*    C
103*       85 CONTINUE
104*    C
105*    C            LOOP BACK TO VARY THE VALUE OF N
106*    C
107*       95 CONTINUE
108*    C
109*          CALL PAGEG(2,0,2,1)
110*          CALL EXITG(2)
111*          STOP 6000
112*          END

END OF UNIVAC 1108 FORTRAN V COMPILATION.      0 *DIAGNOSTIC* MESSAGE(S)
```

```
1*    C     SUBROUTINE CGRID BY C.CARTER
2*    C
3*          SUBROUTINE CGRID(Z,X1,Y1,X2,Y2)
4*    C
5*          DIMENSION Z(200)
6*    C
7*          XDIFF=X2-X1
8*          YDIFF=Y2-Y1
9*          HYTICK=YDIFF/40.0
10*         HXTICK=XDIFF/40.0
11*         NTICKS=10
12*         DX=XDIFF/FLOAT(NTICKS)
13*         DY=YDIFF/FLOAT(NTICKS)
14*   C
15*   C
16*   C           DRAW BOX
17*   C
18*         CALL LINESG(Z,0,X1,Y1)
19*         CALL LINESG(Z,01,X2,Y1)
20*         CALL LINESG(Z,01,X2,Y2)
21*         CALL LINESG(Z,01,X1,Y2)
22*         CALL LINESG(Z,01,X1,Y1)
23*   C
24*   C
25*   C           DRAW TICK MARKS
26*   C
```

Appendix B (Cont'd)

```
27*           LOOP=NTICKS-1
28*     C
29*           X=X1
30*           Y=Y1+HYTICK
31*           DO 200 K=1,LOOP
32*           X=X+DX
33*           CALL LINESG(Z,0,X,Y)
34*           CALL LINESG(Z,1,X,Y1)
35*       200 CONTINUE
36*     C
37*           X=X1
38*           Y=Y2-HYTICK
39*           DO 300 K=1,LOOP
40*           X=X+DX
41*           CALL LINESG(Z,0,X,Y)
42*           CALL LINESG(Z,1,X,Y2)
43*       300 CONTINUE
44*     C
45*           Y=Y1
46*           X=X1+HXTICK
47*           DO 400 K=1,LOOP
48*           Y=Y+DY
49*           CALL LINESG(Z,0,X,Y)
50*           CALL LINESG(Z,1,X1,Y)
51*       400 CONTINUE
52*     C
53*           Y=Y1
54*           X=X2-HXTICK
55*           DO 500 K=1,LOOP
56*           Y=Y+DY
57*           CALL LINESG(Z,0,X,Y)
58*           CALL LINESG(Z,1,X2,Y)
59*       500 CONTINUE
60*     C
61*           RETURN
62*           END

END OF UNIVAC 1108 FORTRAN V COMPILATION.      0 *DIAGNOSTIC* MESSAGE(S)
```

Appendix C

TABULAR RESULTS FOR THE COMPUTER PROGRAM

n = 4

N	I	|δ|	VARIANCE	BIAS	MSE	3σ	VAR. APP.
4	1	.0000	.4102-01	.4571+00	.2500+00	.6076+00	.1250+00
4	2	.2000-01	.4104-01	.4574+00	.2503+00	.6077+00	.1249+00
4	3	.4000-01	.4109-01	.4581+00	.2509+00	.6081+00	.1246+00
4	4	.6000-01	.4117-01	.4593+00	.2518+00	.6087+00	.1241+00
4	5	.8000-01	.4129-01	.4610+00	.2532+00	.6096+00	.1234+00
4	6	.1000+00	.4145-01	.4632+00	.2550+00	.6106+00	.1225+00
4	7	.1200+00	.4169-01	.4659+00	.2572+00	.6118+00	.1214+00
4	8	.1400+00	.4198-01	.4691+00	.2601+00	.6132+00	.1201+00
4	9	.1600+00	.4234-01	.4727+00	.2636+00	.6147+00	.1187+00
4	10	.1800+00	.4280-01	.4768+00	.2678+00	.6165+00	.1170+00
4	11	.2000+00	.4342-01	.4814+00	.2729+00	.6179+00	.1152+00
4	12	.2200+00	.4424-01	.4865+00	.2789+00	.6195+00	.1132+00
4	13	.2400+00	.4535-01	.4920+00	.2860+00	.6210+00	.1110+00
4	14	.2600+00	.4685-01	.4980+00	.2943+00	.6225+00	.1087+00
4	15	.2800+00	.4882-01	.5044+00	.3040+00	.6237+00	.1062+00
4	16	.3000+00	.5137-01	.5113+00	.3153+00	.6247+00	.1035+00
4	17	.3200+00	.5447-01	.5187+00	.3282+00	.6255+00	.1007+00
4	18	.3400+00	.5853-01	.5265+00	.3427+00	.6259+00	.9777-01
4	19	.3600+00	.6353-01	.5348+00	.3587+00	.6259+00	.9470-01
4	20	.3800+00	.6946-01	.5435+00	.3763+00	.6254+00	.9151-01
4	21	.4000+00	.7633-01	.5526+00	.3953+00	.6244+00	.8820-01
4	22	.4200+00	.8411-01	.5621+00	.4159+00	.6229+00	.8479-01
4	23	.4400+00	.9280-01	.5721+00	.4380+00	.6207+00	.8129-01
4	24	.4600+00	.1024+00	.5825+00	.4615+00	.6177+00	.7770-01
4	25	.4800+00	.1129+00	.5933+00	.4865+00	.6140+00	.7404-01
4	26	.5000+00	.1243+00	.6045+00	.5129+00	.6095+00	.7031-01
4	27	.5200+00	.1365-01	.6161+00	.5407+00	.6041+00	.6654-01
4	28	.5400+00	.1496-01	.6281+00	.5699+00	.5977+00	.6273-01
4	29	.5600+00	.1636-01	.6405+00	.6005+00	.5903+00	.5889-01
4	30	.5800+00	.1784-01	.6533+00	.6324+00	.5818+00	.5505-01
4	31	.6000+00	.1941-01	.6664+00	.6658+00	.5721+00	.5120-01
4	32	.6200+00	.2106-01	.6799+00	.7004+00	.5613+00	.4737-01
4	33	.6400+00	.2280-01	.6938+00	.7363+00	.5491+00	.4357-01
4	34	.6600+00	.2463-01	.7080+00	.7736+00	.5356+00	.3982-01
4	35	.6800+00	.2654-01	.7225+00	.8121+00	.5207+00	.3613-01
4	36	.7000+00	.2853-01	.7373+00	.8520+00	.5042+00	.3251-01
4	37	.7200+00	.3061-01	.7524+00	.8931+00	.4862+00	.2899-01
4	38	.7400+00	.3277-01	.7678+00	.9355+00	.4666+00	.2558-01
4	39	.7600+00	.3502-01	.7834+00	.9792+00	.4452+00	.2230-01
4	40	.7800+00	.3736-01	.7993+00	.1024+01	.4220+00	.1917-01
4	41	.8000+00	.3978-01	.8154+00	.1069+01	.3968+00	.1620-01
4	42	.8200+00	.4229-01	.8317+00	.1116+01	.3696+00	.1342-01
4	43	.8400+00	.4488-01	.8482+00	.1164+01	.3402+00	.1083-01
4	44	.8600+00	.4756-01	.8650-02	.1214+01	.3085+00	.8476-02
4	45	.8800+00	.5032-02	.8820-02	.1265+01	.2743+00	.6362-02
4	46	.9000+00	.5316-02	.8992-02	.1318+01	.2374+00	.4512-02
4	47	.9200+00	.5609-02	.9166-02	.1372+01	.1976+00	.2949-02
4	48	.9400+00	.5910-02	.9342-02	.1427+01	.1545+00	.1694-02
4	49	.9600+00	.6220-02	.9520-02	.1484+01	.1078+00	.7683-03
4	50	.9800+00	.6538-03	.9700-03	.1541+01	.5680-01	.1960-03

Appendix C (Cont'd)

n= 8

N	I	|x|	VARIANCE	BIAS	MSE	3σ	VAR APP
8	1	.0000	.2371-01	.3183+00	.1250+00	.4620+00	.6250-01
8	2	.2000-01	.2375-01	.2987+00	.1190+00	.4624+00	.6245-01
8	3	.4000-01	.2389-01	.2799+00	.1022+00	.4637+00	.6230-01
8	4	.6000-01	.2410-01	.2620+00	.9276-01	.4657+00	.6205-01
8	5	.8000-01	.2439-01	.2449+00	.8459-01	.4686+00	.6170-01
8	6	.1000+00	.2476-01	.2287+00	.7705-01	.4720+00	.6126-01
8	7	.1200+00	.2518-01	.2132+00	.7004-01	.4761+00	.6071-01
8	8	.1400+00	.2566-01	.1985+00	.6358-01	.4806+00	.6007-01
8	9	.1600+00	.2618-01	.1847+00	.6027-01	.4854+00	.5934-01
8	10	.1800+00	.2672-01	.1715+00	.5613-01	.4903+00	.5852-01
8	11	.2000+00	.2727-01	.1591+00	.5259-01	.4954+00	.5760-01
8	12	.2200+00	.2781-01	.1474+00	.4955-01	.5003+00	.5660-01
8	13	.2400+00	.2834-01	.1365+00	.4696-01	.5051+00	.5551-01
8	14	.2600+00	.2884-01	.1261+00	.4475-01	.5094+00	.5434-01
8	15	.2800+00	.2928-01	.1165+00	.4285-01	.5134+00	.5308-01
8	16	.3000+00	.2967-01	.1074+00	.4120-01	.5168+00	.5176-01
8	17	.3200+00	.2998-01	.9892-01	.3977-01	.5195+00	.5036-01
8	18	.3400+00	.3021-01	.9100-01	.3849-01	.5214+00	.4889-01
8	19	.3600+00	.3034-01	.8362-01	.3733-01	.5226+00	.4735-01
8	20	.3800+00	.3037-01	.7674-01	.3626-01	.5228+00	.4575-01
8	21	.4000+00	.3029-01	.7033-01	.3523-01	.5221+00	.4410-01
8	22	.4200+00	.3009-01	.6437-01	.3423-01	.5204+00	.4239-01
8	23	.4400+00	.2977-01	.5883-01	.3323-01	.5176+00	.4064-01
8	24	.4600+00	.2933-01	.5368-01	.3221-01	.5138+00	.3885-01
8	25	.4800+00	.2877-01	.4890-01	.3117-01	.5089+00	.3702-01
8	26	.5000+00	.2810-01	.4447-01	.3007-01	.5029+00	.3516-01
8	27	.5200+00	.2731-01	.4035-01	.2893-01	.4957+00	.3327-01
8	28	.5400+00	.2640-01	.3655-01	.2774-01	.4875+00	.3136-01
8	29	.5600+00	.2540-01	.3299-01	.2649-01	.4781+00	.2945-01
8	30	.5800+00	.2430-01	.2970-01	.2518-01	.4676+00	.2752-01
8	31	.6000+00	.2311-01	.2666-01	.2382-01	.4560+00	.2560-01
8	32	.6200+00	.2184-01	.2383-01	.2241-01	.4434+00	.2369-01
8	33	.6400+00	.2051-01	.2121-01	.2096-01	.4296+00	.2179-01
8	34	.6600+00	.1912-01	.1879-01	.1947-01	.4148+00	.1991-01
8	35	.6800+00	.1769-01	.1655-01	.1796-01	.3990+00	.1806-01
8	36	.7000+00	.1622-01	.1447-01	.1643-01	.3821+00	.1626-01
8	37	.7200+00	.1473-01	.1256-01	.1489-01	.3641+00	.1450-01
8	38	.7400+00	.1324-01	.1080-01	.1335-01	.3452+00	.1279-01
8	39	.7600+00	.1175-01	.9189-02	.1183-01	.3252+00	.1115-01
8	40	.7800+00	.1026-01	.7716-02	.1034-01	.3042+00	.9584-02
8	41	.8000+00	.8844-02	.6378-02	.8864-02	.2821+00	.8100-02
8	42	.8200+00	.7456-02	.5171-02	.7483-02	.2590+00	.6708-02
8	43	.8400+00	.6132-02	.4094-02	.6148-02	.2349+00	.5417-02
8	44	.8600+00	.4886-02	.3142-02	.4896-02	.2097+00	.4238-02
8	45	.8800+00	.3737-02	.2316-02	.3742-02	.1834+00	.3181-02
8	46	.9000+00	.2705-02	.1615-02	.2705-02	.1560+00	.2256-02
8	47	.9200+00	.1902-02	.1038-02	.1903-02	.1273+00	.1475-02
8	48	.9400+00	.1057-02	.5867-03	.1057-02	.9753-01	.8468-03
8	49	.9600+00	.4907-03	.2614-03	.4907-03	.6645-01	.3842-03

Appendix C (Cont'd)

N= 10

N	I	|X|	VARIANCE	BIAS	MSE	3σ	VAR APP
10	1	.0000	.1264-01	.2233+00	.6290-01	.3373+00	.3125-01
10	2	.2000-01	.1270-01	.2039+00	.5430-01	.3281+00	.3123-01
10	3	.4000-01	.1269-01	.1859+00	.4744-01	.3206+00	.3115-01
10	4	.6000-01	.1319-01	.1691+00	.4178-01	.3145+00	.3103-01
10	5	.8000-01	.1359-01	.1536+00	.3718-01	.3097+00	.3085-01
10	6	.1000+00	.1408-01	.1393+00	.3347-01	.3060+00	.3063-01
10	7	.1200+00	.1463-01	.1261+00	.3054-01	.3029+00	.3036-01
10	8	.1400+00	.1523-01	.1141+00	.2826-01	.3003+00	.3004-01
10	9	.1600+00	.1586-01	.1032+00	.2650-01	.2978+00	.2967-01
10	10	.1800+00	.1648-01	.9324-01	.2517-01	.2951+00	.2926-01
10	11	.2000+00	.1706-01	.8425-01	.2417-01	.2920+00	.2880-01
10	12	.2200+00	.1763-01	.7613-01	.2343-01	.2883+00	.2830-01
10	13	.2400+00	.1812-01	.6881-01	.2286-01	.2839+00	.2775-01
10	14	.2600+00	.1854-01	.6223-01	.2241-01	.2785+00	.2717-01
10	15	.2800+00	.1887-01	.5632-01	.2204-01	.2721+00	.2654-01
10	16	.3000+00	.1910-01	.5101-01	.2171-01	.2646+00	.2588-01
10	17	.3200+00	.1924-01	.4625-01	.2137-01	.2561+00	.2518-01
10	18	.3400+00	.1926-01	.4197-01	.2103-01	.2464+00	.2444-01
10	19	.3600+00	.1919-01	.3812-01	.2084-01	.2356+00	.2367-01
10	20	.3800+00	.1902-01	.3465-01	.2062-01	.2237+00	.2288-01
10	21	.4000+00	.1875-01	.3151-01	.1974-01	.2108+00	.2205-01
10	22	.4200+00	.1839-01	.2867-01	.1922-01	.1969+00	.2120-01
10	23	.4400+00	.1796-01	.2609-01	.1864-01	.1820+00	.2032-01
10	24	.4600+00	.1745-01	.2374-01	.1801-01	.1662+00	.1942-01
10	25	.4800+00	.1687-01	.2159-01	.1733-01	.1496+00	.1851-01
10	26	.5000+00	.1623-01	.1962-01	.1662-01	.1322+00	.1758-01
10	27	.5200+00	.1555-01	.1780-01	.1587-01	.1141+00	.1663-01
10	28	.5400+00	.1482-01	.1612-01	.1508-01	.9521-01	.1568-01
10	29	.5600+00	.1406-01	.1457-01	.1427-01	.7557+00	.1472-01
10	30	.5800+00	.1327-01	.1314-01	.1344-01	.5455+00	.1376-01
10	31	.6000+00	.1245-01	.1180-01	.1259-01	.3348+00	.1280-01
10	32	.6200+00	.1162-01	.1056-01	.1173-01	.1234+00	.1184-01
10	33	.6400+00	.1078-01	.9414-02	.1086-01	.3114+00	.1089-01
10	34	.6600+00	.9927-02	.8344-02	.9936-02	.2989+00	.9955-02
10	35	.6800+00	.9077-02	.7352-02	.9131-02	.2858+00	.9032-02
10	36	.7000+00	.8232-02	.6433-02	.8273-02	.2722+00	.8128-02
10	37	.7200+00	.7397-02	.5582-02	.7428-02	.2580+00	.7248-02
10	38	.7400+00	.6576-02	.4798-02	.6599-02	.2433+00	.6396-02
10	39	.7600+00	.5776-02	.4078-02	.5793-02	.2280+00	.5576-02
10	40	.7800+00	.5003-02	.3421-02	.5014-02	.2122+00	.4792-02
10	41	.8000+00	.4260-02	.2825-02	.4268-02	.1958+00	.4050-02
10	42	.8200+00	.3555-02	.2285-02	.3560-02	.1789+00	.3354-02
10	43	.8400+00	.2894-02	.1805-02	.2897-02	.1614+00	.2708-02
10	44	.8600+00	.2282-02	.1382-02	.2284-02	.1433+00	.2119-02
10	45	.8800+00	.1727-02	.1016-02	.1728-02	.1247+00	.1590-02
10	46	.9000+00	.1235-02	.7059-03	.1235-02	.1054+00	.1128-02
10	47	.9200+00	.8141-03	.4521-03	.8143-03	.8560-01	.7373-03
10	48	.9400+00	.4721-03	.2541-03	.4722-03	.6518-01	.4234-03
10	49	.9600+00	.2173-03	.1119-03	.2173-03	.4422-01	.1921-03

Appendix C (Cont'd)

n= 32

N	I	|R|	VARIANCE	BIAS	MSE	3σ	VAR APP
32	1	.0000	.6514-02	.1575+00	.3125-01	.2421+00	.1563-01
32	2	.2000-01	.6587-02	.1382+00	.2570-01	.2435+00	.1561-01
32	3	.4000-01	.6501-02	.1211+00	.2147-01	.2474+00	.1558-01
32	4	.6000-01	.7141-02	.1056+00	.1854-01	.2535+00	.1551-01
32	5	.8000-01	.7580-02	.9229-01	.1610-01	.2612+00	.1543-01
32	6	.1000+00	.8089-02	.8044-01	.1456-01	.2698+00	.1531-01
32	7	.1200+00	.8634-02	.7013-01	.1355-01	.2788+00	.1518-01
32	8	.1400+00	.9182-02	.6122-01	.1293-01	.2875+00	.1502-01
32	9	.1600+00	.9704-02	.5357-01	.1257-01	.2955+00	.1484-01
32	10	.1800+00	.1017-01	.4703-01	.1239-01	.3026+00	.1463-01
32	11	.2000+00	.1057-01	.4145-01	.1229-01	.3085+00	.1440-01
32	12	.2200+00	.1089-01	.3669-01	.1224-01	.3131+00	.1415-01
32	13	.2400+00	.1112-01	.3263-01	.1219-01	.3164+00	.1388-01
32	14	.2600+00	.1127-01	.2916-01	.1212-01	.3185+00	.1358-01
32	15	.2800+00	.1133-01	.2617-01	.1201-01	.3193+00	.1327-01
32	16	.3000+00	.1131-01	.2359-01	.1187-01	.3191+00	.1294-01
32	17	.3200+00	.1122-01	.2134-01	.1168-01	.3178+00	.1259-01
32	18	.3400+00	.1108-01	.1936-01	.1145-01	.3157+00	.1222-01
32	19	.3600+00	.1087-01	.1761-01	.1118-01	.3128+00	.1184-01
32	20	.3800+00	.1063-01	.1604-01	.1089-01	.3093+00	.1144-01
32	21	.4000+00	.1034-01	.1464-01	.1056-01	.3051+00	.1102-01
32	22	.4200+00	.1003-01	.1336-01	.1020-01	.3004+00	.1060-01
32	23	.4400+00	.9681-02	.1220-01	.9830-02	.2952+00	.1016-01
32	24	.4600+00	.9313-02	.1113-01	.9457-02	.2895+00	.9712-02
32	25	.4800+00	.8925-02	.1015-01	.9078-02	.2834+00	.9254-02
32	26	.5000+00	.8520-02	.9245-02	.8606-02	.2769+00	.8789-02
32	27	.5200+00	.8102-02	.8405-02	.8173-02	.2700+00	.8317-02
32	28	.5400+00	.7672-02	.7620-02	.7731-02	.2628+00	.7841-02
32	29	.5600+00	.7234-02	.6901-02	.7282-02	.2552+00	.7362-02
32	30	.5800+00	.6789-02	.6227-02	.6828-02	.2472+00	.6881-02
32	31	.6000+00	.6339-02	.5596-02	.6371-02	.2389+00	.6400-02
32	32	.6200+00	.5887-02	.5013-02	.5912-02	.2302+00	.5921-02
32	33	.6400+00	.5435-02	.4467-02	.5455-02	.2212+00	.5446-02
32	34	.6600+00	.4985-02	.3960-02	.5001-02	.2118+00	.4977-02
32	35	.6800+00	.4539-02	.3488-02	.4551-02	.2021+00	.4516-02
32	36	.7000+00	.4100-02	.3051-02	.4109-02	.1921+00	.4064-02
32	37	.7200+00	.3669-02	.2647-02	.3678-02	.1817+00	.3624-02
32	38	.7400+00	.3249-02	.2274-02	.3254-02	.1710+00	.3198-02
32	39	.7600+00	.2842-02	.1931-02	.2846-02	.1599+00	.2788-02
32	40	.7800+00	.2452-02	.1616-02	.2454-02	.1485+00	.2396-02
32	41	.8000+00	.2079-02	.1335-02	.2081-02	.1368+00	.2025-02
32	42	.8200+00	.1728-02	.1079-02	.1729-02	.1247+00	.1677-02
32	43	.8400+00	.1401-02	.8514-03	.1401-02	.1123+00	.1354-02
32	44	.8600+00	.1100-02	.6511-03	.1100-02	.9950-01	.1060-02
32	45	.8800+00	.8289-03	.4779-03	.8291-03	.8837-01	.7952-03
32	46	.9000+00	.5904-03	.3315-03	.5905-03	.7490-01	.5641-03
32	47	.9200+00	.3579-03	.2117-03	.3800-03	.5509-01	.3686-03
32	48	.9400+00	.2243-03	.1184-03	.2243-03	.4493-01	.2117-03
32	49	.9600+00	.1036-03	.5115-04	.1036-03	.3053-01	.9604-04

END OF TABLE

Appendix C (Cont'd)

n = 64

N	I	|δ|	VARIANCE	BIAS	MSE	3σ	VAR APP
64	1	.0000	.3505-02	.1110+00	.1563-01	.1725+00	.7813-02
64	2	.2000-01	.3384-02	.9238-01	.1192-01	.1745+00	.7806-02
64	3	.4000-01	.3309-02	.7648-01	.9458-02	.1802+00	.7788-02
64	4	.6000-01	.3248-02	.6315-01	.7936-02	.1885+00	.7756-02
64	5	.8000-01	.4059-02	.5217-01	.7061-02	.1981+00	.7713-02
64	6	.1000+00	.4793-02	.4327-01	.6665-02	.2077+00	.7657-02
64	7	.1200+00	.5208-02	.3613-01	.6513-02	.2165+00	.7589-02
64	8	.1400+00	.5371-02	.3046-01	.6499-02	.2239+00	.7509-02
64	9	.1600+00	.5364-02	.2597-01	.6538-02	.2297+00	.7418-02
64	10	.1800+00	.6079-02	.2240-01	.6581-02	.2339+00	.7314-02
64	11	.2000+00	.6220-02	.1954-01	.6601-02	.2366+00	.7200-02
64	12	.2200+00	.6293-02	.1725-01	.6590-02	.2380+00	.7075-02
64	13	.2400+00	.6310-02	.1535-01	.6545-02	.2383+00	.6938-02
64	14	.2600+00	.6280-02	.1374-01	.6469-02	.2377+00	.6792-02
64	15	.2800+00	.6214-02	.1236-01	.6368-02	.2365+00	.6636-02
64	16	.3000+00	.6119-02	.1122-01	.6245-02	.2347+00	.6470-02
64	17	.3200+00	.6000-02	.1020-01	.6104-02	.2324+00	.6294-02
64	18	.3400+00	.5862-02	.9290-02	.5948-02	.2297+00	.6111-02
64	19	.3600+00	.5708-02	.8480-02	.5779-02	.2266+00	.5919-02
64	20	.3800+00	.5540-02	.7750-02	.5600-02	.2233+00	.5719-02
64	21	.4000+00	.5360-02	.7087-02	.5410-02	.2196+00	.5512-02
64	22	.4200+00	.5170-02	.6481-02	.5212-02	.2157+00	.5299-02
64	23	.4400+00	.4972-02	.5926-02	.5007-02	.2115+00	.5080-02
64	24	.4600+00	.4765-02	.5414-02	.4795-02	.2071+00	.4856-02
64	25	.4800+00	.4552-02	.4942-02	.4577-02	.2024+00	.4627-02
64	26	.5000+00	.4334-02	.4504-02	.4354-02	.1975+00	.4395-02
64	27	.5200+00	.4110-02	.4097-02	.4127-02	.1923+00	.4159-02
64	28	.5400+00	.3883-02	.3718-02	.3897-02	.1869+00	.3921-02
64	29	.5600+00	.3653-02	.3366-02	.3664-02	.1813+00	.3681-02
64	30	.5800+00	.3421-02	.3037-02	.3430-02	.1755+00	.3440-02
64	31	.6000+00	.3187-02	.2731-02	.3195-02	.1694+00	.3200-02
64	32	.6200+00	.2954-02	.2445-02	.2960-02	.1631+00	.2961-02
64	33	.6400+00	.2722-02	.2179-02	.2727-02	.1565+00	.2723-02
64	34	.6600+00	.2492-02	.1931-02	.2496-02	.1498+00	.2489-02
64	35	.6800+00	.2265-02	.1701-02	.2268-02	.1428+00	.2258-02
64	36	.7000+00	.2042-02	.1487-02	.2044-02	.1356+00	.2032-02
64	37	.7200+00	.1824-02	.1290-02	.1826-02	.1281+00	.1812-02
64	38	.7400+00	.1612-02	.1108-02	.1614-02	.1205+00	.1599-02
64	39	.7600+00	.1408-02	.9405-03	.1409-02	.1126+00	.1394-02
64	40	.7800+00	.1212-02	.7879-03	.1213-02	.1045+00	.1198-02
64	41	.8000+00	.1026-02	.6494-03	.1027-02	.9611-01	.1012-02
64	42	.8200+00	.8515-03	.5247-03	.8518-03	.8754-01	.8385-03
64	43	.8400+00	.6891-03	.4137-03	.6893-03	.7875-01	.6771-03
64	44	.8600+00	.5403-03	.3161-03	.5404-03	.6973-01	.5298-03
64	45	.8800+00	.4065-03	.2317-03	.4066-03	.6049-01	.3976-03
64	46	.9000+00	.2893-03	.1605-03	.2893-03	.5102-01	.2820-03
64	47	.9200+00	.1898-03	.1020-03	.1898-03	.4133-01	.1843-03
64	48	.9400+00	.1103-03	.5632-04	.1103-03	.3150-01	.1059-03
64	49	.9600+00	.5188-04	.2315-04	.5188-04	.2161-01	.4802-04

END OF TABLE

Appendix C (Cont'd)

n= 120

N	I	|X|	VARIANCE	BIAS	MSE	3σ	VAR. APP
120	1	.0000	.1065-02	.7841-01	.7813-02	.1224+00	.3906-02
120	2	.2000-01	.1745-02	.6030-01	.5391-02	.1253+00	.3903-02
120	3	.4000-01	.1960-02	.4615-01	.4096-02	.1330+00	.3894-02
120	4	.6000-01	.2270-02	.3533-01	.3518-02	.1429+00	.3878-02
120	5	.8000-01	.2592-02	.2734-01	.3339-02	.1527+00	.3856-02
120	6	.1000+00	.2878-02	.2157-01	.3343-02	.1609+00	.3829-02
120	7	.1200+00	.3099-02	.1745-01	.3404-02	.1670+00	.3795-02
120	8	.1400+00	.3250-02	.1447-01	.3459-02	.1710+00	.3755-02
120	9	.1600+00	.3338-02	.1229-01	.3469-02	.1733+00	.3709-02
120	10	.1800+00	.3379-02	.1063-01	.3492-02	.1744+00	.3657-02
120	11	.2000+00	.3385-02	.9332-02	.3472-02	.1745+00	.3600-02
120	12	.2200+00	.3366-02	.8284-02	.3435-02	.1741+00	.3537-02
120	13	.2400+00	.3330-02	.7416-02	.3385-02	.1731+00	.3469-02
120	14	.2600+00	.3281-02	.6680-02	.3326-02	.1718+00	.3396-02
120	15	.2800+00	.3222-02	.6045-02	.3258-02	.1703+00	.3318-02
120	16	.3000+00	.3154-02	.5491-02	.3184-02	.1685+00	.3235-02
120	17	.3200+00	.3078-02	.5002-02	.3103-02	.1664+00	.3147-02
120	18	.3400+00	.2997-02	.4565-02	.3017-02	.1642+00	.3055-02
120	19	.3600+00	.2909-02	.4172-02	.2927-02	.1618+00	.2959-02
120	20	.3800+00	.2817-02	.3817-02	.2831-02	.1592+00	.2860-02
120	21	.4000+00	.2720-02	.3493-02	.2732-02	.1565+00	.2756-02
120	22	.4200+00	.2619-02	.3196-02	.2629-02	.1535+00	.2650-02
120	23	.4400+00	.2514-02	.2924-02	.2523-02	.1504+00	.2540-02
120	24	.4600+00	.2406-02	.2672-02	.2413-02	.1472+00	.2428-02
120	25	.4800+00	.2296-02	.2440-02	.2302-02	.1437+00	.2314-02
120	26	.5000+00	.2183-02	.2224-02	.2188-02	.1402+00	.2197-02
120	27	.5200+00	.2068-02	.2023-02	.2072-02	.1364+00	.2079-02
120	28	.5400+00	.1951-02	.1837-02	.1955-02	.1325+00	.1960-02
120	29	.5600+00	.1834-02	.1663-02	.1837-02	.1285+00	.1840-02
120	30	.5800+00	.1716-02	.1500-02	.1718-02	.1243+00	.1720-02
120	31	.6000+00	.1597-02	.1349-02	.1599-02	.1199+00	.1600-02
120	32	.6200+00	.1479-02	.1208-02	.1481-02	.1154+00	.1480-02
120	33	.6400+00	.1362-02	.1078-02	.1363-02	.1107+00	.1362-02
120	34	.6600+00	.1245-02	.9539-03	.1246-02	.1059+00	.1244-02
120	35	.6800+00	.1131-02	.8401-03	.1132-02	.1009+00	.1129-02
120	36	.7000+00	.1019-02	.7344-03	.1019-02	.9575-01	.1016-02
120	37	.7200+00	.9093-03	.6367-03	.9097-03	.9046-01	.9060-03
120	38	.7400+00	.8030-03	.5467-03	.8033-03	.8501-01	.7995-03
120	39	.7600+00	.7007-03	.4641-03	.7009-03	.7941-01	.6970-03
120	40	.7800+00	.6029-03	.3886-03	.6031-03	.7366-01	.5990-03
120	41	.8000+00	.5100-03	.3202-03	.5101-03	.6775-01	.5062-03
120	42	.8200+00	.4229-03	.2585-03	.4230-03	.6169-01	.4192-03
120	43	.8400+00	.3419-03	.2036-03	.3420-03	.5547-01	.3386-03
120	44	.8600+00	.2680-03	.1554-03	.2680-03	.4911-01	.2649-03
120	45	.8800+00	.2017-03	.1136-03	.2018-03	.4261-01	.1988-03
120	46	.9000+00	.1436-03	.7852-04	.1436-03	.3595-01	.1410-03
120	47	.9200+00	.9477-04	.4924-04	.9477-04	.2921-01	.9216-04
120	48	.9400+00	.5564-04	.2636-04	.5564-04	.2238-01	.5293-04
120	49	.9600+00	.2781-04	.9152-05	.2781-04	.1582-01	.2401-04

END OF TABLE

Appendix C (Cont'd)

N= 250

N	I	|X|	VARIANCE	BIAS	MSE	3S	VAR. APP
250	1	.0000	.6053-03	.5542-01	.3906-02	.6670-01	.1953-02
250	2	.2000-01	.9157-03	.3820-01	.2375-02	.9978-01	.1952-02
250	3	.4000-01	.1116-02	.2610-01	.1801-02	.1002+00	.1947-02
250	4	.6000-01	.1349-02	.1829-01	.1603-02	.1102+00	.1939-02
250	5	.8000-01	.1541-02	.1336-01	.1720-02	.1178+00	.1928-02
250	6	.1000+00	.1667-02	.1028-01	.1773-02	.1225+00	.1914-02
250	7	.1200+00	.1736-02	.8294-02	.1805-02	.1250+00	.1897-02
250	8	.1400+00	.1760-02	.6934-02	.1814-02	.1261+00	.1877-02
250	9	.1600+00	.1775-02	.5942-02	.1808-02	.1263+00	.1854-02
250	10	.1800+00	.1760-02	.5181-02	.1793-02	.1261+00	.1829-02
250	11	.2000+00	.1750-02	.4574-02	.1771-02	.1255+00	.1800-02
250	12	.2200+00	.1729-02	.4076-02	.1745-02	.1247+00	.1769-02
250	13	.2400+00	.1702-02	.3658-02	.1715-02	.1238+00	.1735-02
250	14	.2600+00	.1670-02	.3301-02	.1681-02	.1226+00	.1698-02
250	15	.2800+00	.1636-02	.2991-02	.1645-02	.1213+00	.1659-02
250	16	.3000+00	.1598-02	.2720-02	.1605-02	.1199+00	.1617-02
250	17	.3200+00	.1557-02	.2479-02	.1563-02	.1184+00	.1574-02
250	18	.3400+00	.1513-02	.2264-02	.1518-02	.1167+00	.1528-02
250	19	.3600+00	.1467-02	.2070-02	.1472-02	.1149+00	.1480-02
250	20	.3800+00	.1419-02	.1895-02	.1423-02	.1130+00	.1430-02
250	21	.4000+00	.1369-02	.1734-02	.1372-02	.1110+00	.1378-02
250	22	.4200+00	.1317-02	.1587-02	.1320-02	.1089+00	.1325-02
250	23	.4400+00	.1264-02	.1452-02	.1268-02	.1066+00	.1270-02
250	24	.4600+00	.1209-02	.1328-02	.1216-02	.1043+00	.1214-02
250	25	.4800+00	.1152-02	.1214-02	.1164-02	.1018+00	.1157-02
250	26	.5000+00	.1095-02	.1105-02	.1096-02	.9928-01	.1099-02
250	27	.5200+00	.1037-02	.1006-02	.1038-02	.9660-01	.1040-02
250	28	.5400+00	.9780-03	.9126-03	.9708-03	.9382-01	.9801-03
250	29	.5600+00	.9186-03	.8264-03	.9193-03	.9093-01	.9202-03
250	30	.5800+00	.8591-03	.7457-03	.8596-03	.8793-01	.8601-03
250	31	.6000+00	.7994-03	.6705-03	.7999-03	.8482-01	.8000-03
250	32	.6200+00	.7400-03	.6002-03	.7404-03	.8161-01	.7402-03
250	33	.6400+00	.6810-03	.5348-03	.6813-03	.7829-01	.6808-03
250	34	.6600+00	.6226-03	.4739-03	.6229-03	.7486-01	.6222-03
250	35	.6800+00	.5651-03	.4173-03	.5653-03	.7132-01	.5645-03
250	36	.7000+00	.5089-03	.3648-03	.5090-03	.6768-01	.5080-03
250	37	.7200+00	.4540-03	.3162-03	.4541-03	.6392-01	.4530-03
250	38	.7400+00	.4008-03	.2714-03	.4009-03	.6006-01	.3997-03
250	39	.7600+00	.3497-03	.2303-03	.3498-03	.5610-01	.3485-03
250	40	.7800+00	.3009-03	.1927-03	.3009-03	.5204-01	.2995-03
250	41	.8000+00	.2545-03	.1586-03	.2545-03	.4786-01	.2531-03
250	42	.8200+00	.2110-03	.1280-03	.2110-03	.4357-01	.2096-03
250	43	.8400+00	.1708-03	.1009-03	.1708-03	.3921-01	.1693-03
250	44	.8600+00	.1340-03	.7647-04	.1340-03	.3473-01	.1324-03
250	45	.8800+00	.1010-03	.5504-04	.1010-03	.3014-01	.9940-04
250	46	.9000+00	.7226-04	.3787-04	.7228-04	.2551-01	.7051-04
250	47	.9200+00	.4838-04	.2307-04	.4838-04	.2087-01	.4608-04
250	48	.9400+00	.2937-04	.1123-04	.2937-04	.1626-01	.2646-04
250	49	.9600+00	.1369-04	.1554-05	.1809-04	.1226-01	.1200-04

END OF TABLE

REFERENCES

1. Fisher, R. A., Contributions to Mathematical Statistics, Wiley, New York, 1950. (Chapter 14 originally published as "The General Sampling Distribution of the Multiple Correlation Coefficient," Proceedings of the Royal Society, Series A, Vol. 121, pp. 654-673, 1928.)

2. Goodman, N. R., "On the Joint Estimation of the Spectra, CoSpectrum and Quadrature Spectrum of a Two Dimensional Stationary Process," Scientific Paper 10, NYU, New York, 1957 (AD 134 919).

3. Anderson, T. W., An Introduction to Multivariate Statistical Analysis, Wiley, New York, 1958.

4. Haubrich, Richard A., "Earth Noise 5 to 500 Millicycles per Second," Vol. 70, No. 6, Journal of Geophysical Research, March 1965, pp. 1415-1427.

5. Enochson, L. D. and Goodman, N. R., "Gaussian Approximations to the Distribution of Sample Coherence," Air Force Flight Dynamics Lab., Research and Tech. Div., AF Systems Command, Wright-Patterson AFB, Ohio, Bull. AFFDL-TR-65-67, June 1965 (AD620987).

6. Jenkins, Gwilym M. and Watts, Donald G., Spectral Analysis and its Applications, Holden Day, San Francisco, California 1968.

7. Benignus, Vernon A., "Estimation of Coherence Spectrum and Its Confidence Interval Using the Fast Fourier Transform," Vol. AU-17, No. 2, IEEE Transactions on Audio and Electroacoustics, June 1969.

8. Gradshteyn, I. S. and Ryzhik, I. M., Table of Integrals, Series, and Products, Academic Press, N. Y., 1965.

9. Cramer, Harald, Mathematical Methods of Statistics, Princeton University Press, Princeton, 1946.

10. Amos, D. E. and Koopmans, "Tables of the Distribution of the Coefficient of Coherence for Stationary Bivariate Gaussian Processes," Sandia Corp, Monograph SCR-483, 1963.

11. Carter, G. C. and Nuttall, A. H., "Evaluation of the Statistics of the Estimate of Magnitude-Squared Coherence," NUSC TM No. TC-193-71, New London, Conn., 28 September 1971. (Published in IEEE Proc. (letters) Vol. 60, No. 4, April 1972).

12. Carter, G. C., "Estimation of the Magnitude-Squared Coherence Function (Spectrum)," NUSC Report No. 4343 (to be published).

NUSC Technical Memorandum TC-159-72
8 August 1972

The Smoothed Coherence Transform (SCOT)

G. C. Carter
A. H. Nuttall
P. G. Cable

ABSTRACT

The smoothed coherence transform is defined and examples of its uses and shortcomings are given. Computation of this function shows promise for measuring time delays between weak broadband correlated noises received at two sensors.

TABLE OF CONTENTS

I. INTRODUCTION

The purpose of this memorandum is to define a new function, the smoothed coherence transform (SCOT), and to point out its utility. Also, its shortcomings and examples of its estimation are included for completeness.

II. DEFINITION

The SCOT is the smoothed Fourier transform of the complex coherence function. Consider two stationary random processes $x(t)$ and $y(t)$ with auto spectra $G_x(f)$ and $G_y(f)$, respectively, and cross spectrum $G_{xy}(f)$. The complex coherence function $\gamma(f)$ between the two processes is defined as

$$\gamma(f) = \frac{G_{xy}(f)}{\sqrt{G_x(f)\, G_y(f)}} \quad .$$

The smoothed coherence transform is defined by:

$$C(\tau) = \int_{-\infty}^{\infty} W(f)\, \gamma(f)\, \exp(j2\pi f \tau)\, df \quad .$$

where $W(f)$ is a smooth weighting function (window) such as a cosine (Hanning) bell.

Estimates of $\gamma(f)$ from n segments (or pieces) of data are frequently made according to [1]:

$$\hat{\gamma}(K) = \frac{\sum_{i=1}^{n} X_i(K)\, Y_i^*(K)}{\sqrt{\sum_{i=1}^{n} |X_i(K)|^2 \sum_{i=1}^{n} |Y_i(K)|^2}} \quad , \quad 0 \le K \le N-1$$

where $X_i(K)$ and $Y_i(K)$ are the Fourier coefficients at discrete frequency K, obtained by computing the P point discrete Fourier transform (DFT) [2] of the i-th weighted segment. Proper computation of $\hat{\gamma}(K)$ requires: (1) that a smooth weighting function be applied to each segment, (2) that each segment be of sufficient length to ensure proper frequency resolution, and (3) that the number of segments, n, be large in order to reduce the bias and variance of the estimator [3].

Estimates of the SCOT can now be obtained by computing the inverse DFT via the fast Fourier transform, FFT [4]

$$\hat{C}(P) = \sum_{K=0}^{N-1} W(K)\,\hat{\gamma}(K)\exp(j\,2\pi KP/N)$$

where W(K) are discrete samples of the smooth weighting function W(f).

III. DISCUSSION

The SCOT is an ad hoc technique discovered by the authors and believed to be new. The specific problem which prompted its computation was an attempt to determine time delays between weak broadband correlated noises received at two sensors. A related problem was discussed by Roth [5], who suggested utilization of the "impulse response" function defined by

$$h(\tau) = \int_{-\infty}^{\infty} \frac{G_{xy}(f)}{G_x(f)} \exp(j2\pi f\tau)\,df.$$

Under certain conditions (or models), $h(\tau)$ has better time resolution than the cross correlation function defined by

$$R(\tau) = \int_{-\infty}^{\infty} G_{xy}(f)\exp(j2\pi f\tau)\,df.$$

Examples of this attribute are given by Roth. The rationale for dividing the cross spectrum by the auto spectrum of the $x(t)$ process, $G_x(f)$, is that it has meaning when $x(t)$ is the input to a linear system. When there is no such physical interpretation, however, there is no justification for normalizing by $G_x(f)$ and one might be puzzled as to whether to "whiten" the cross spectrum by dividing by the auto spectrum of the $y(t)$ process, $G_y(f)$. A technique which favors neither $G_x(f)$ nor $G_y(f)$ is to divide by $\sqrt{G_x(f)G_y(f)}$. Of interest is the fact that in the special case where $G_x(f) = G_y(f)$, the Fourier transform of the coherence function is equivalent to the "impulse response" defined by Roth.

The reasons for looking at the SCOT are in part obvious. Consider a cross spectrum with certain dominant frequency components, e.g., the presence of a 60 Hz component 20 dB above the local average cross spectrum. The Fourier transform of the cross spectrum yields a cross correlation function heavily dominated in the time domain by a 60 Hz sine wave. Hence, it is difficult to measure the delays due to weak components in other bands of frequencies. One apparent method to skirt this dilemma is to compute the Fourier transform of the cross spectrum only over a limited band of frequencies. Unfortunately this requires a great deal of apriori knowledge about the data. Also the desired component may be broadband. On the other hand, the whitening process of dividing by $\sqrt{G_x(f)\,G_y(f)}$ insures a complex function which satisfies the relationship, $0 \le |\gamma(f)| \le 1$. Additionally, if the two processes are uncorrelated, the coherence is zero, and if they are linearly related, the coherence is unity [3].

Depending on the model (or actual physical situation), the SCOT can be a useful analysis tool. Two other points should be made at this time. First, both real physical data (not reported here) and the synthetic data studied in this memorandum have fortuitously borneout some of the strong assets of the SCOT. It is, however, a trivial task to synthesize sample functions of two random processes in which the SCOT would be extremely misleading. Hence the SCOT and cross correlation functions should be used together with other statistics, prior to drawing any premature conclusions. A second point to make is that other whitening functions can be useful. One of them briefly investigated is the phase transform (PHAT) defined by

$$A(\tau) = \int_{-\infty}^{\infty} \frac{G_{xy}(f)}{|G_{xy}(f)|} \exp(j2\pi f\tau)\, df \,.$$

The PHAT whitens the cross spectrum more than the SCOT. In several real data cases studied by the authors, the PHAT and SCOT gave similar results. It is possible to devise synthetic cases in which one would perform better than the other. The application of a weighting function, $W(f)$, to any frequency function prior to performing the Fourier transform, while not explicitedly called out, is useful when it has physical meaning.

Hence, one could form a smoothed PHAT or smoothed impulse response as easily as the PHAT or impulse response.

IV. COMPUTATIONAL CONSIDERATIONS

The most significant computational consideration affecting the estimation of the SCOT is the estimation of the auto and cross spectral density functions prior to estimating the coherence [3].

One computational trick which can be applied in order to reduce computer running time is described by Eby [6]. If the P point sequences x_n and y_n are both real, then the discrete Fourier transform (DFT) of x_n and the DFT of y_n can simultaneously be computed by performing one fast Fourier transform (FFT) [2 and 4] of the complex sequence $d_n = x_n + jy_n$.

If we denote D(K) as the DFT of d_n, then [7, pp 308-309]

$$X(K) = 1/2 \left[D(K) + D^*(J)\right]$$

and

$$Y(K) = 1/2j \left[D(K) - D^*(J)\right]$$

Reference to the frequency J refers to the negative frequencies which are found in the upper half of the DFT output. For example, with the Cooley-Tuckey subscripting [4] (namely, 0 to P-1), the P/2 + 1 subscripts starting with 0 and ending with P/2 denote positive frequencies from zero to the Nyquist frequency; the P/2 subscripts starting with P/2 and ending with P-1 denote negative frequencies from minus Nyquist almost to zero frequency. Hence, with the Cooley-Tukey subscripting [4], we add and subtract subscripted output from the FFT according to the following table:

Count	K	J	K + J
1	1	P-1	P
2	2	P-2	P
:	:	:	:
P/2-1	P/2-1	P/2+1	P
P/2	P/2	P/2	P

Table 1. Cooley-Tukey Subscripting

The dC component must be treated separately. Negative frequencies can be neglected since the power spectral density function of real random processes is symmetric about the origin.

Another type of subscripting is that employed by Singleton [8], where the data sequence (vector) is subscripted from 1 to P. Now the combining table becomes:

Count	K	J	K + J
1	2	P	P+2
2	3	P-1	P+2
:	:	:	:
P/2-1	P/2	P/2+2	P+2
P/2	P/2+1	P/2+1	P+2

Table 2. Singleton Subscripting

Again the dC component is handled separately. Note in Table 1 that $J = P - K$ and that in Table 2, $J = P + 2 - K$.

Let us now denote the complex vector D(K) as follows (using either Singleton or Cooley-Tukey notation)

$$D(K) = M(K) + jB(K)$$
$$D(J) = M(J) + jB(J) .$$

Consider

$$X(K)X^*(K) = 1/2 \left[D(K) + D^*(J)\right] \; 1/2 \left[D^*(K) + D(J)\right] .$$

By substitution $X(K)X^*(K)$

$$= 1/4 \left\{\left[M(K) + jB(K) + M(J) - jB(J)\right] \cdot \left[M(K) - jB(K) + M(J) + jB(J)\right]\right\}$$

$$= 1/4 \left\{ \left[M(K) + M(J) \right] + i \left[B(K) - B(J) \right] \right\}$$
$$\cdot \left\{ \left[M(K) + M(J) \right] - i \left[B(K) - B(J) \right] \right\}$$
$$= 1/4 \left\{ \left[M(K) + M(J) \right]^2 + \left[B(K) - B(J) \right]^2 \right\}$$

Similarly, it can be derived that

$$Y(K)Y^*(K) = 1/4 \left\{ \left[B(K) + B(J) \right]^2 + \left[M(K) - M(J) \right]^2 \right\}$$

and further that

$$R_e \left\{ X(K)Y^*(K) \right\} = 1/2 \left[M(K)B(J) + M(J)B(K) \right]$$

and

$$I_m \left\{ X(K)Y^*(K) \right\} = 1/4 \left[M^2(J) + B^2(J) - M^2(K) - B^2(K) \right].$$

The validity of these derivations has been verified by programming the listed equations and executing the computer algorithm with the synthetic data described in Section V of this memorandum.

V. EXAMPLE

There are many configurations (or models) which will bear out the usefulness of the SCOT. For the purposes of illustrating this usefulness it is only necessary to present one such example. From this example it can be seen which types of random processes should be studied by SCOT analysis. Consider now the following block diagram (Fig. 1).

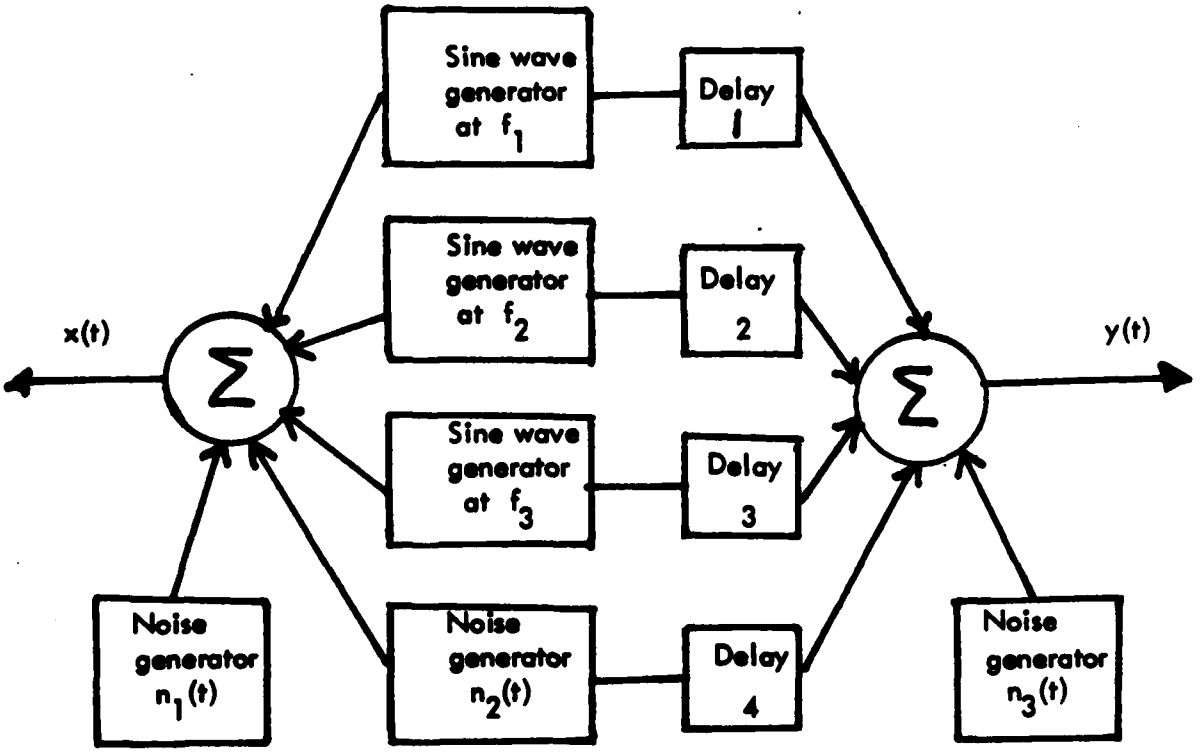

Figure 1. MODEL OF TWO RANDOM PROCESSES

The noise generators are broadband and uncorrelated. Hence, x(t) and y(t) have common (or correlated) broadband noise and sinusoids plus uncorrelated broadband noise. The cross correlation coefficient was computed and plotted in Figure 2.

The SCOT was computed and plotted in Figure 3. Notice the relative ease with which the time delay of the broadband component can be determined from the SCOT plot. This is in contrast to the difficulty encountered in the cross correlation coefficient plot. The PHAT plot, Figure 4, for this model yields results similar to the SCOT.

The power of the SCOT, which is borne out by the above example, promises to be a useful new tool for studying random processes.

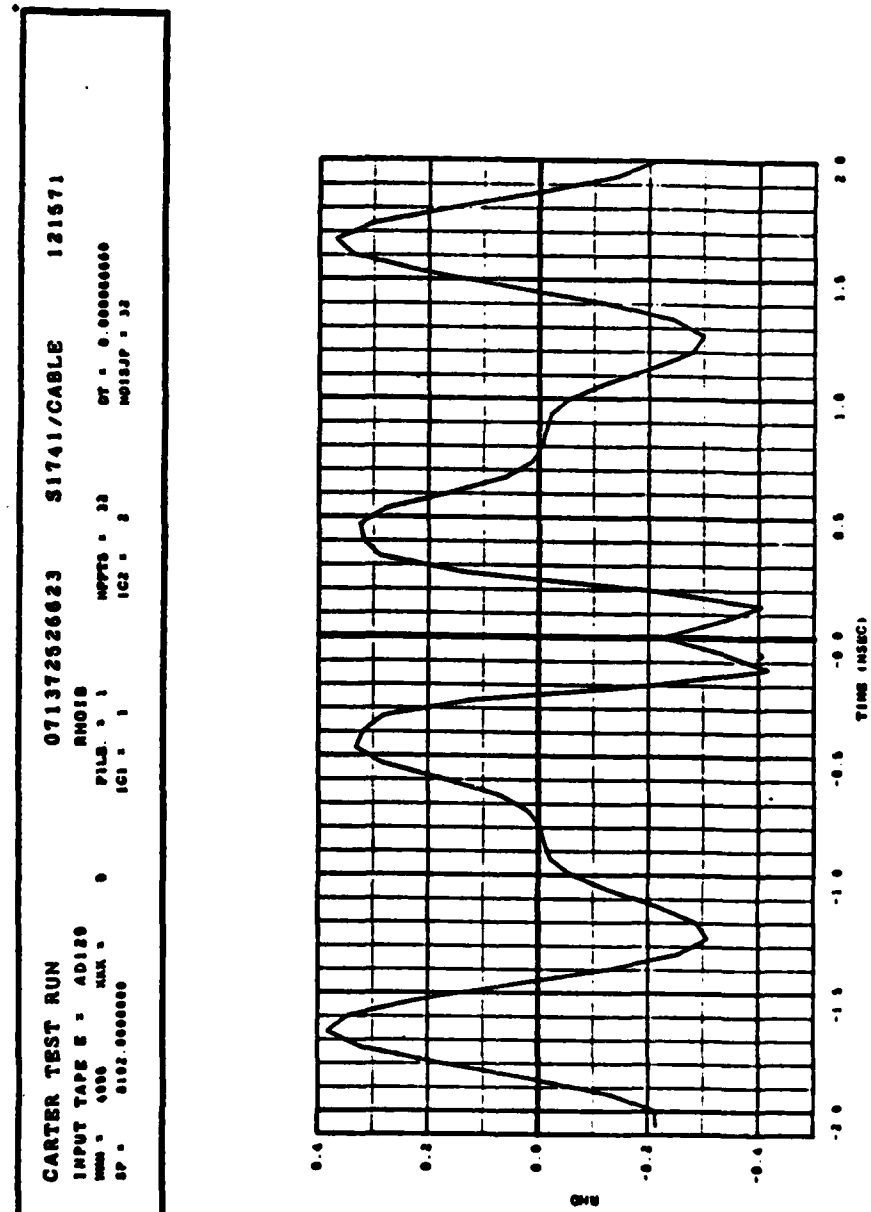

Figure 2. CROSS CORRELATION OF $x(t)$ WITH $y(t)$

CARTER TEST RUN 071372526623 S1741/CABLE 121571
SCOT1B
INPUT TAPE B = AD120
0000 = 0000 FILE = 1 NPTS = 32 DT = 0.00000000
SF = 0100.000000 IC1 = 1 IC2 = 0 NOISE = 32

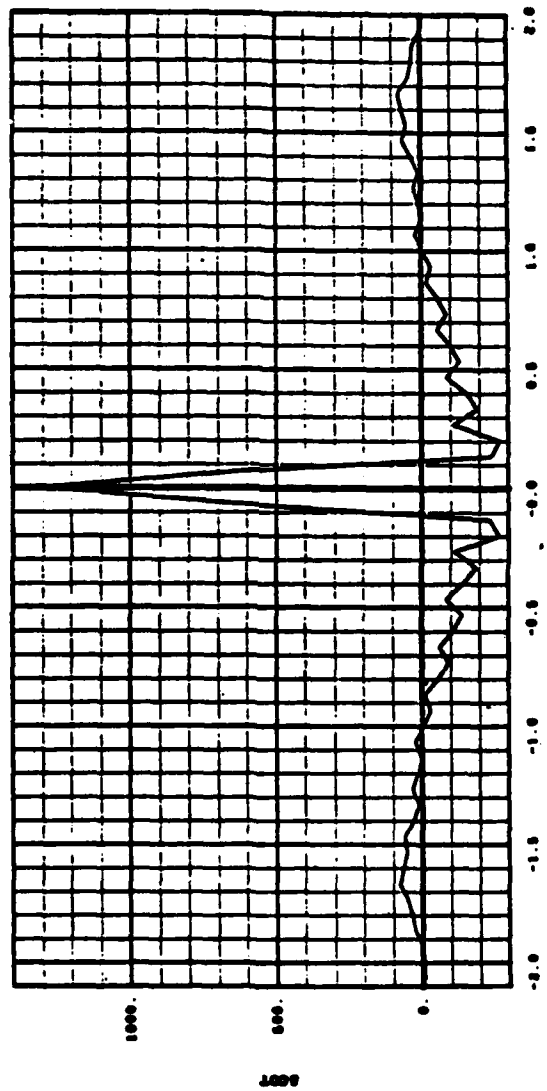

Figure 3. SCOT OF x(t) WITH y(t)

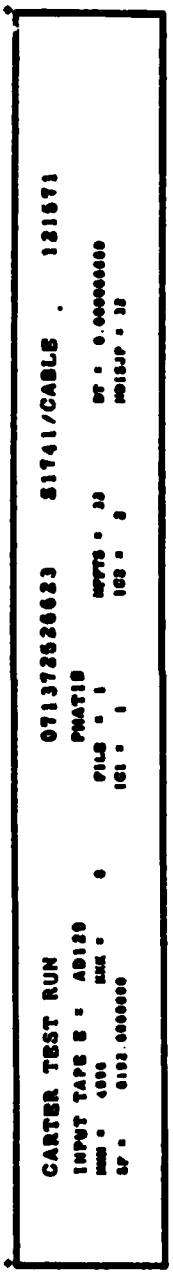

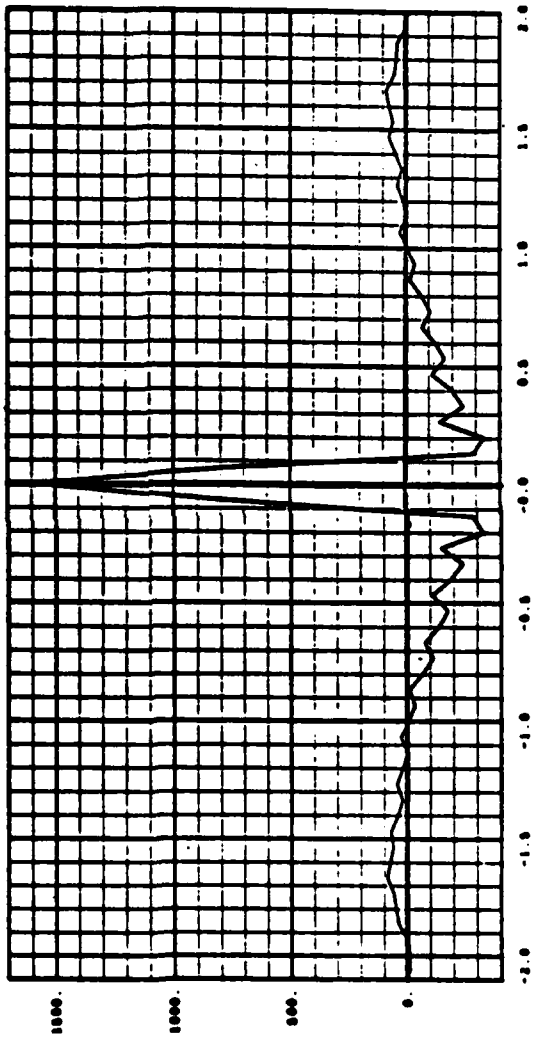

Figure4. PHAT OF x(t) WITH y(t)

VI. CONCLUSIONS

The SCOT is a useful ad hoc technique for analysis of time delay characteristics between two random processes. Examples of its power have been included together with a discussion of its applications and limitations.

VII. REFERENCES

1. G. C. Carter and A. H. Nuttall, "Statistics of the Estimate of Coherence," IEEE Proc (lett.), Vol. 60, No. 4 (April, 1972), 465-466.

2. B. Gold and C. M. Rader, Digital Processing of Signals (New York: McGraw-Hill Book Co. Inc., 1969).

3. G. C. Carter, "Estimation of the Magnitude-Squared Coherence Function (Spectrum)," University of Connecticut Masters Thesis: published as NUSC Report 4343, New London, Ct. (May, 1972).

4. J. W. Cooley and J. W. Tukey, "An Algorithm for the Machine Calculation of Complex Fourier Series," Mathematics of Computation, Vol. 19 (April, 1965), 297-301.

5. P. R. Roth, "Effective Measurements Using Digital Signal Analysis," IEEE Spectr Vol. 8, No. 4 (April, 1971), 62-70.

6. E. S. Eby, "Simultaneous Computation of the Fourier Transforms of Two Real Functions," USL Tech. Memo. 2242-262-67, New London, Ct. (18 July 1967).

7. J. S. Bendat and A. G. Piersol, Random Data Analysis and Measurement Procedures, (New York: John Wiley and Sons, Inc., 1971).

8. R. C. Singleton, "An Algorithm for Computing the Mixed Radix Fast Fourier Transform," IEEE Transactions on Audio and Electroacoustics, Vol. AU-17, No. 2 (June 1969), 93-102.

NUSC Technical Report 4423
12 October 1972

Coherence Estimation as Affected by Weighting Functions and Fast Fourier Transform Size

G. C. Carter

ABSTRACT

Given two wide-sense stationary random processes, the (complex) coherence function is the (complex) cross power spectral density function divided by the square root of the product of the two (real) auto power spectral density functions.

Estimation of the magnitude square of the complex coherence (MSC) with fast Fourier transform (FFT) processing is investigated for synthetic data. The procedure used is to partition the given finite time histories into n segments. Each segment, consisting of P data points, is multiplied by a smooth weighting function before computing the FFT. Cross and auto spectra are then averaged over a large number of segments before forming the coherence ratio.

It is demonstrated that, when the magnitude of the first derivative of either the auto spectrum or the phase of the complex coherence is large, (1) multiplication by a weighting function is absolutely necessary and (2) P must be large enough to ensure sufficient spectral resolution. While these techniques have been suggested by individuals familiar with spectral estimation, the gross bias errors encountered in the MSC estimate due to improper (rectangular) weighting functions and poor frequency resolution (small FFT size) are much more serious than might have been expected.

TABLE OF CONTENTS

REVERSE BLANK

LIST OF ILLUSTRATIONS

REVERSE BLANK

DEFINITION OF TERMS

C(f)	real part of $\Phi_{xy}(f)$
DFT	discrete Fourier transform
f	frequency
f_k	kth discrete frequency
FFT	fast Fourier transform (fast method of computing DFT)
MSC	magnitude squared coherence, $\lvert\gamma(f)\rvert^2$
n	number of segments, each of P points
P	number of data points in each FFT
Q(f)	imaginary part of $\Phi_{xy}(f)$
s	subscript denoting segment number
$\gamma(f)$	complex coherence function
$\Phi_x(f)$	auto power spectral density function of x process
$\Phi_y(f)$	auto power spectral density function of y process
$\Phi_{xy}(f)$	cross power spectral density function of x with y
$\forall$	for all
$\wedge$	estimate
*	complex conjugation

REVERSE BLANK

COHERENCE ESTIMATION AS AFFECTED BY WEIGHTING FUNCTIONS AND FAST FOURIER TRANSFORM SIZE

INTRODUCTION

Given two wide-sense stationary random processes, the (complex) coherence function is a reduced form of the (complex) cross and (real) auto power spectral density functions. The magnitude square of this complex function possesses several useful attributes. For example, it always lies between zero and one, and is zero for independent or uncorrelated processes. This report emphasizes the magnitude squared coherence (MSC) and its estimate when the true function is equal to unity.

For example, the MSC can be used to determine whether a linear relationship exists between two random processes. In particular, if the two processes are linearly related, then the MSC is identically unity.[1] Hence, when a good estimate of MSC can be obtained, it is a useful statistic in describing two wide-sense stationary random processes.

The estimation procedure is straightforward computationally; however, interpretation is more an art than a science. Several investigators have addressed the problems of MSC estimation; for example, see references 1 through 16. In this report, the effect of weighting functions and FFT size in MSC estimation is illustrated, using previously simulated signals and results of Carter and Arnold.[15]

The purpose of this study is to aid experimenters purchasing and using digital spectrum analyzers for field measurements. In particular, the inability of a (hardware or software) spectrum analyzer to estimate properly the MSC function strongly suggests that the auto and cross spectral estimates are in error.

THE COHERENCE FUNCTION

The coherence function is a normalized (complex) cross spectral density function. Specifically, given two wide sense stationary processes $x(t)$ and $y(t)$ with auto power spectral density functions $\Phi_x(f)$ and $\Phi_y(f)$, respectively, and complex cross spectral density function $\Phi_{xy}(f)$, then the complex coherence function is defined[2] by

$$\gamma(f) = \frac{\Phi_{xy}(f)}{\sqrt{\Phi_x(f)\,\Phi_y(f)}}, \tag{1}$$

and the MSC is then

$$\left|\gamma(f)\right|^2 = \frac{\left|\Phi_{xy}(f)\right|^2}{\Phi_x(f)\,\Phi_y(f)} = \frac{C^2(f) + Q^2(f)}{\Phi_x(f)\,\Phi_y(f)} . \tag{2}$$

The MSC can be used to measure system linearity, as will be proved. Consider the linear system with input, x(t), impulse response, h(t), and output, y(t). Then the output, y(t), is obtained by the convolution integral

$$y(t) = \int_{-\infty}^{\infty} h(\tau)\, x(t-\tau)\, d\tau . \tag{3}$$

The transfer function of this linear filter is obtained by means of the Fourier integral:

$$H(f) = \int_{-\infty}^{\infty} h(\tau)\, e^{-j2\pi f\tau}\, d\tau . \tag{4}$$

From reference 2 it is known that the transfer function can be expressed in terms of the (complex) cross spectrum and the input auto spectrum. In particular,

$$H(f) = \frac{\Phi_{xy}(f)}{\Phi_x(f)}, \quad \Phi_x(f) \neq 0 . \tag{5}$$

Furthermore, the auto spectrum of the output of a linear filter is given[2] by

$$\Phi_y(f) = H(f)\, H^*(f)\, \Phi_x(f) . \tag{6}$$

By using equations (5) and (6) it can be shown[15] that

$$\frac{1}{H(f)} = \frac{\Phi_{xy}^*(f)}{\Phi_y(f)} . \tag{7}$$

Substituting equations (5) and (7) into equation (2) yields

$$|\gamma(f)|^2 = H(f)\,\frac{1}{H(f)} = 1, \quad \forall f \ . \tag{8}$$

Thus, for the assumption that the system is linear, we have $|\gamma(f)|^2 = 1$, for all frequencies. If $|\gamma(f)|^2$ is not equal to unity, then either the observations of x(t) and y(t) have been corrupted by noise, or our assumption was in error and the system is nonlinear.

This could be expressed as a theorem: If a system is linear, then the MSC between the input and output is unity.

THE COHERENCE ESTIMATOR

The method used for obtaining good MSC estimates is the Welch[8]-Haubrich[5] technique. Briefly, it consists of obtaining two finite time series from the random processes being investigated and segmenting these time series into n segments.[8] The n segments may be either "overlapped" or "disjoint" from other segments. Each segment comprises P data points. A weighting (or windowing) function is then applied to each segment and the fast Fourier transform (FFT) of the weighted P-point sequence is performed. The Fourier coefficients for the sth weighted segment are then used to compute the auto and cross spectral estimates, which are then averaged over all n segments. The MSC is finally computed from a ratio of the average spectral estimates. (Note that for real data, n complex FFTs must be computed, each of size P.)

Specifically, let $\hat{\Phi}_{x_s}(f_k)$ denote the estimate of the power spectral density (PSD) function at the kth frequency, f_k, obtained from the sth weighted segment of size P of the stationary random process x(t). Similarly, let $\hat{\Phi}_{y_s}(f_k)$ be the estimate of the PSD function of the stationary random process y(t). Also, let $\hat{C}_s(f_k)$ and $\hat{Q}_s(f_k)$ denote, respectively, the real (co-) and imaginary (quad-) part of the estimate of the complex cross spectral density function of the two processes.[7] (A detailed explanation of these estimates is given in reference 1.) The estimate of the MSC function is given by references 1, 2, 15, and 16 as follows:

$$|\hat{\gamma}(f_k)|^2 = \frac{\left[\sum_{s=1}^{n} \hat{C}_s(f_k)\right]^2 + \left[\sum_{s=1}^{n} \hat{Q}_s(f_k)\right]^2}{\left[\sum_{s=1}^{n} \hat{\Phi}_{x_s}(f_k)\right]\left[\sum_{s=1}^{n} \hat{\Phi}_{y_s}(f_k)\right]}, \tag{9}$$

where n is the number of weighted segments (overlapped or disjoint) over which the individual estimates are averaged.

Because the MSC estimator is the ratio of random variables, it is imperative that good spectral estimates of C(f), Q(f), $\Phi_x(f)$, and $\Phi_y(f)$ be obtained. Random fluctuations and bias of any of the four spectral estimators become significant in the ratio used to estimate the coherence function. The theoretical results dictating that n be large are given in references 1, 12, and 16.

THE COMPUTER STUDY

A digital computer program was written to implement equation (9). (Documentation, currently in preparation, is partially contained in references 1 and 15.) Two input parameters include the FFT size P and two different weighting functions (rectangular and cosine). The FFT was coded by Singleton.[10]

During the first part of this computer study the effect of a weighting function was investigated by processing data with two different weightings. When a P-point sequence is multiplied by a rectangular weighting function (no weighting), the true spectrum is convolved with the sin x/x function. Therefore, each FFT filter centered at a specific frequency sees energy not only from the band about that frequency, but also from power which leaks from frequency bands not desired.[7] Leakage results in biased estimators $\hat{\Phi}_{x_s}(f_k)$, $\hat{\Phi}_{y_s}(f_k)$, $\hat{C}_s(f_k)$, and $\hat{Q}_s(f_k)$, which become a critical factor in MSC estimation because equation (9) is a ratio of biased estimators. This is well illustrated in the cases which follow.

An example of how this leakage problem seriously corrupts the MSC estimate is in order. Recall from the earlier derivation that the MSC between the input and output of a linear filter is unity for all frequencies. To illustrate the estimation problem when poor weighting functions are used, white Gaussian noise (flat spectrum) was filtered by the second-order linear filter specified by the recursion equation

$$Y_n = AY_{n-1} + BY_{n-2} + CX_n \quad , \tag{10}$$

where

$A = 1.97330$

$B = -0.98202$

$C = 0.00872$.

Figures 1 and 2 show estimates of the gain and phase characteristics of this sharp filter. The true MSC is unity (i.e., 100 percent). The estimate of MSC is plotted in figure 3 as a function of frequency.

The data segments were not multiplied by a weighting function. (This is equivalent to saying a rectangular weighting function was used.) The FFT side lobe "leakage" problem[7] corrupts the estimator. Note by studying figure 3 that, even though the true value of coherence is 100 percent, the MSC estimator fails to attain the true value. This result dramatically portrays the need to apply a smooth weighting function.

In other experiments, the data from this sharp filter case were reprocessed with no weighting function applied to the time series, but with higher resolving power. In particular, 16 disjoint segments of size 4096 (as opposed to 64 of 1024) were processed. Processing with higher resolving power but without a weighting function still yields poor results.[15]

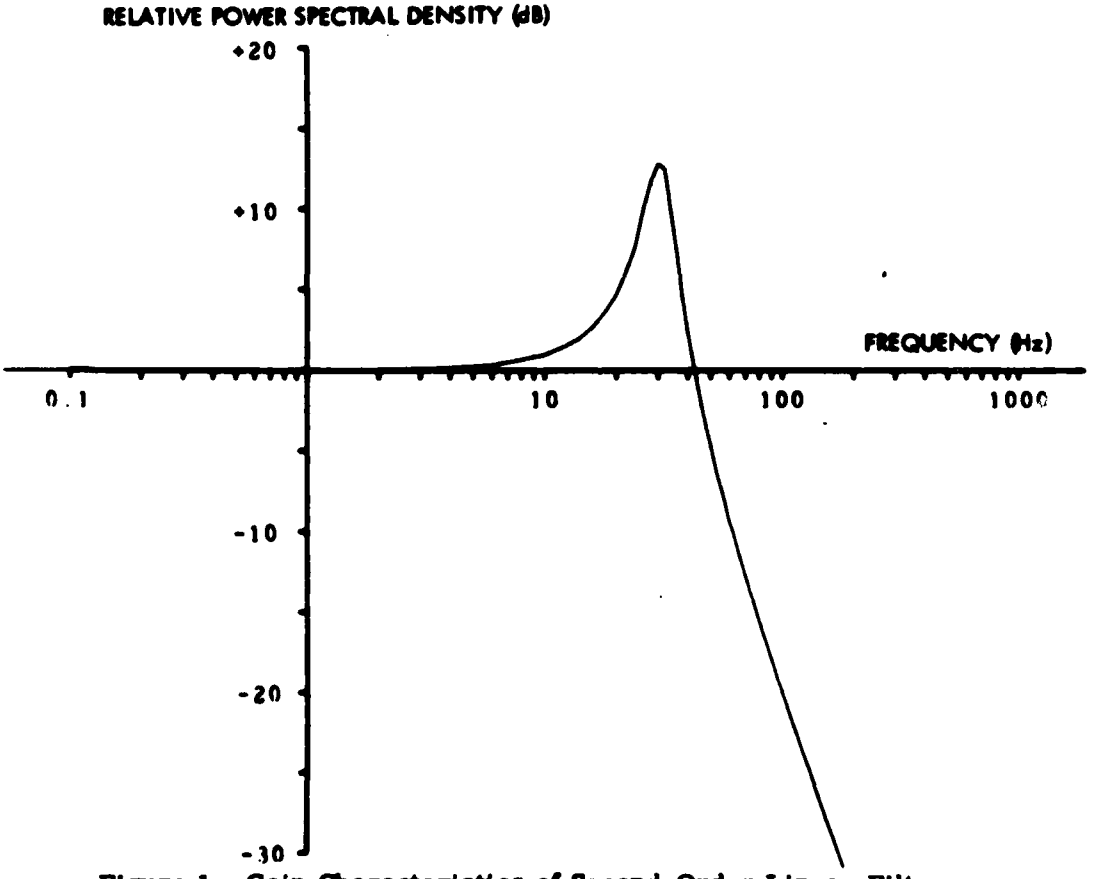

Figure 1. Gain Characteristics of Second-Order Linear Filter

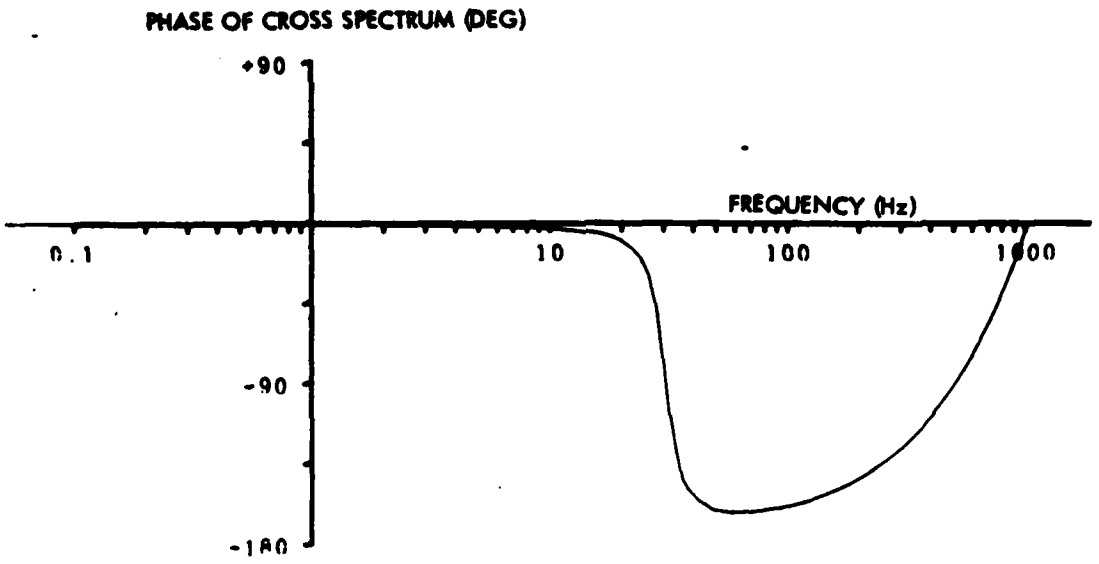

Figure 2. Phase Characteristics of Second-Order Linear Filter

The data from the sharp filter case were again reprocessed with no weighting function applied to the time series but with higher resolving power and more averaging. In particular, 64 disjoint segments of size 4096 were processed. In that case, the estimator began to stabilize but not about the correct answer.[15]

A technique for reducing the bias due to leakage is to multiply each segment of time history by a smooth weighting function. The frequency-domain equivalent of multiplying each segment by a weighting function is a convolution of the true spectrum with the Fourier transform of the weighting function. Hence, the weighting function should be judiciously selected in order that the true spectrum be least distorted. The factors affecting the selection of the segment length and window shape of the sth weighting function of length T to be applied to T_{total} seconds of data are as follows:

- $w_s(t)$ should be relatively easy to compute.
- T_{total}/T should be large in order that the amount of averaging be sufficient to reduce the bias and variance of the spectral estimates. (This problem is studied in references 1, 12, 15, and 16.)

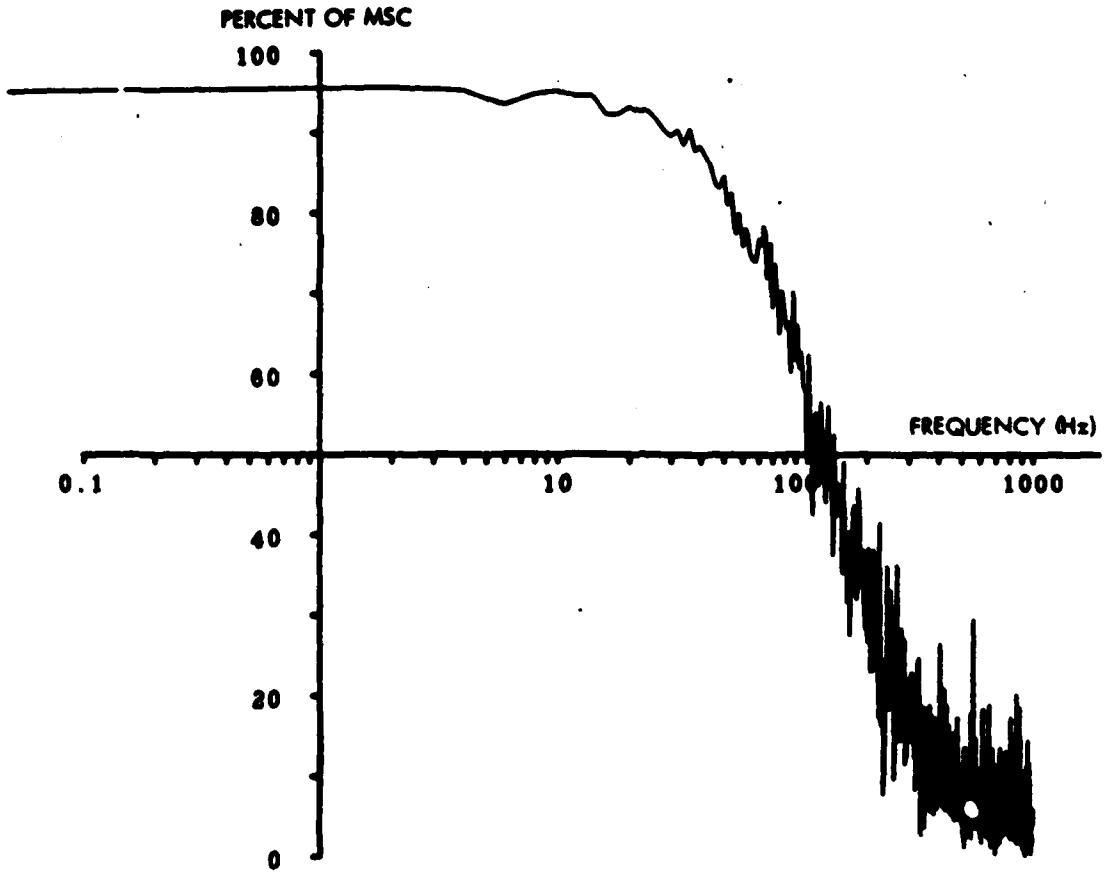

Figure 3. Estimate of MSC (Between Input and Output of Second-Order Linear Filter) Using P = 1024 and a Rectangular Weighting Function

- $d^n w_g(t)/dt^n$ should be continuous for $n = 0, 1, 2, \ldots$, up to some reasonable limit, since this ensures that the sidelobes of the Fourier transform of $w_g(t)$ die off rapidly.

- The Fourier transform of $w_g(t)$ should also be narrow in the main lobe (narrower than the finest detail of the true spectral density matrix of processes x(t) and y(t). Generally, this lobe is narrowed by increasing T.)

The specific selection of a weighting function involves a number of tradeoffs.[12] A commonly used weighting (or windowing) function is the cosine (Hanning) function defined by

$$w_s(t) = \begin{cases} 1/2\left(1 - \cos\left\{2\pi\left[\dfrac{t-(s-1)a}{T}\right]\right\}\right), & (s-1)a \le t \le T + (s-1)a, \\ 0, & \text{elsewhere,} \end{cases} \tag{11}$$

where a is a function of the overlap[1] such that for a = T there is no overlapping of segments.

As an illustration of the tremendous improvement to be derived from the use of a smooth weighting function, the data generated for the sharp filter case were reprocessed, this time with a cosine weighting function applied. The resultant estimator is plotted versus frequency in figure 4. Careful study of figures 3 and 4 dramatically portrays the necessity for applying a good weighting function. In the purchase and use of spectrum analyzers designed to estimate the true MSC function, it is incumbent that a weighting function be both available and used.

During the second part of this computer study the effect of the FFT size was studied. Cosine weighting functions (verified to be essential during the first part of this study) were used. Good frequency resolution requires large size FFTs. Other studies, for example references 1, 12, 15, and 16, point out the requirement that a large number of FFTs be computed.

The data from the sharp filter case were reprocessed with smaller size FFTs (that is, poorer frequency resolution), as an illustration of this type of bias. The resultant MSC estimates are plotted in figure 5. Note that the estimator fails in the frequency band where the estimation procedure has poor resolving power relative to the true complex coherence spectrum. As shown, the bias, due to insufficient FFT size, can be most serious when estimating coherence. This behavior of the MSC estimator was predicted by Jenkins and Watts.[4]

In other experiments the same data from the sharp filter case were reprocessed with 256 disjoint segments of size 1024. The results were the same as those given in figure 5. That is to say, the bias due to poor resolution can not be corrected by increased averaging.[15] However, by increasing the resolving power and processing the data with 16 disjoint segments each of size 4096, the

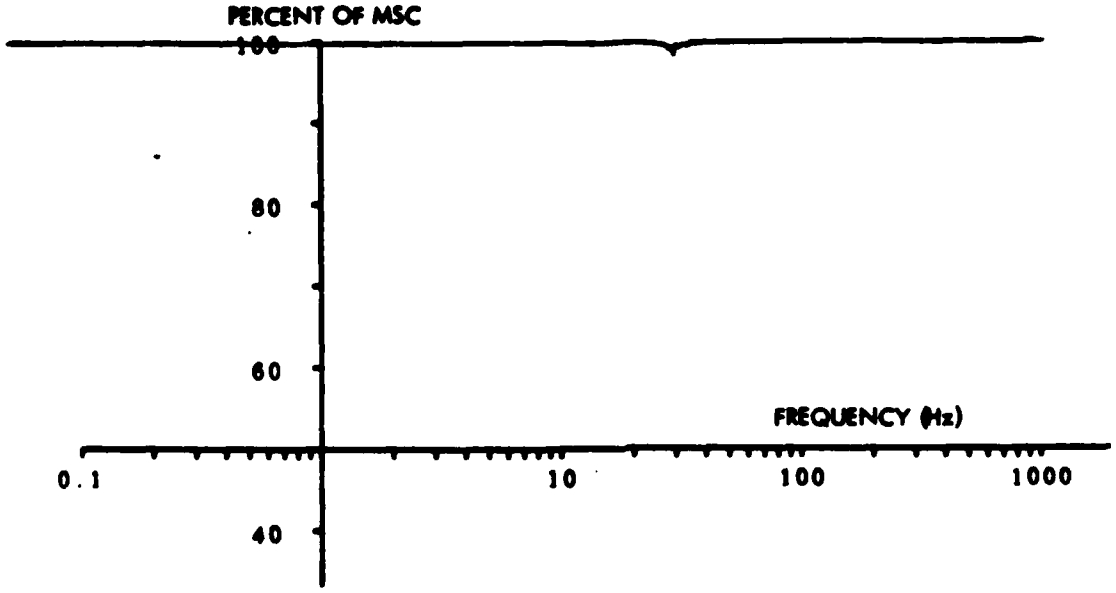

Figure 4. Estimate of MSC (Between Input and Output of Second-Order Linear Filter) Using P = 4096 and a Cosine Weighting Function

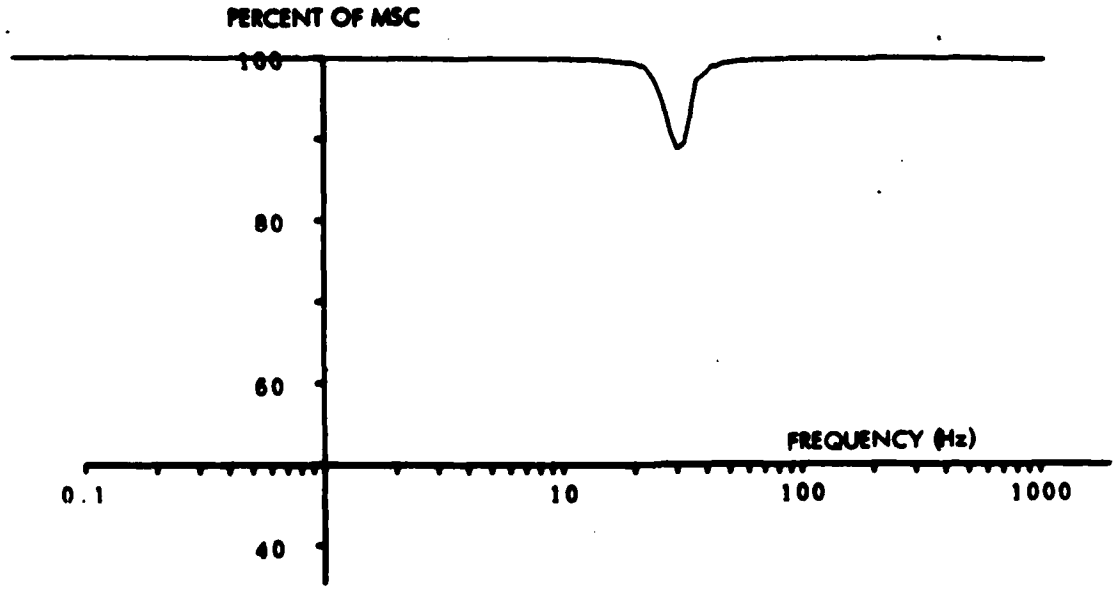

Figure 5. Estimate of MSC (Between Input and Output of Second-Order Linear Filter) Using P = 1024 and a Cosine Weighting Function

true coherence can be estimated more nearly correctly as shown earlier in figure 4. Increasing the resolving power can improve the coherence estimator, though for a finite time history, increasing resolving power means decreasing the amount of possible averaging. In this example, the improvement of the estimator at 30 Hz is due to higher resolving power of the detail of the phase of the complex coherence function.

In order to understand more fully this resolution problem, another case was studied. A stationary process consisting of the sum of white Gaussian noise and two sinusoids is filtered by the first-order linear filter specified by the recursion equation

$$Y_n = \frac{7\,Y_{n-1}}{8} + \frac{X_n}{8} \quad . \tag{12}$$

The estimate of the auto spectrum of the input to the filter is given in figure 6. Similarly, the output auto spectrum is given in figure 7. The filter specified in equation (12) is characterized by the gain and phase plots of figures 8 and 9, respectively. The estimate of MSC is given in figure 10.

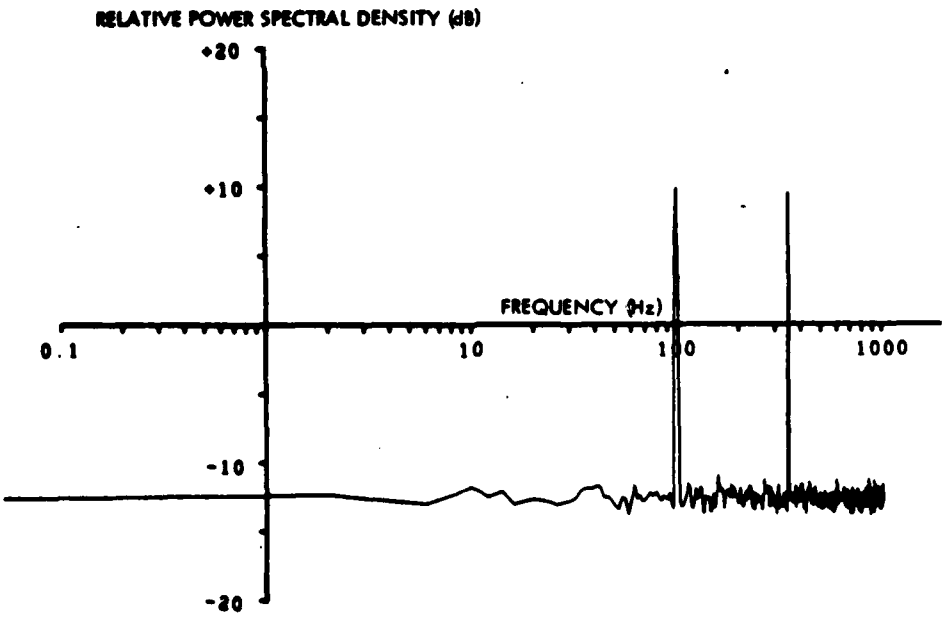

Figure 6. Estimate of Input Auto Power Spectrum to First-Order Linear Filter

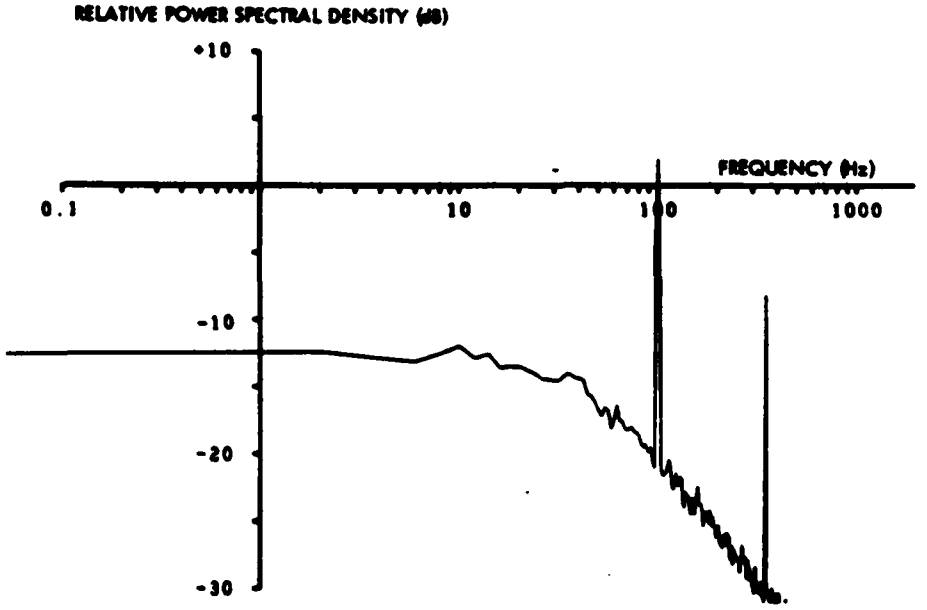

Figure 7. Estimate of Output Auto Power Spectrum from First-Order Linear Filter

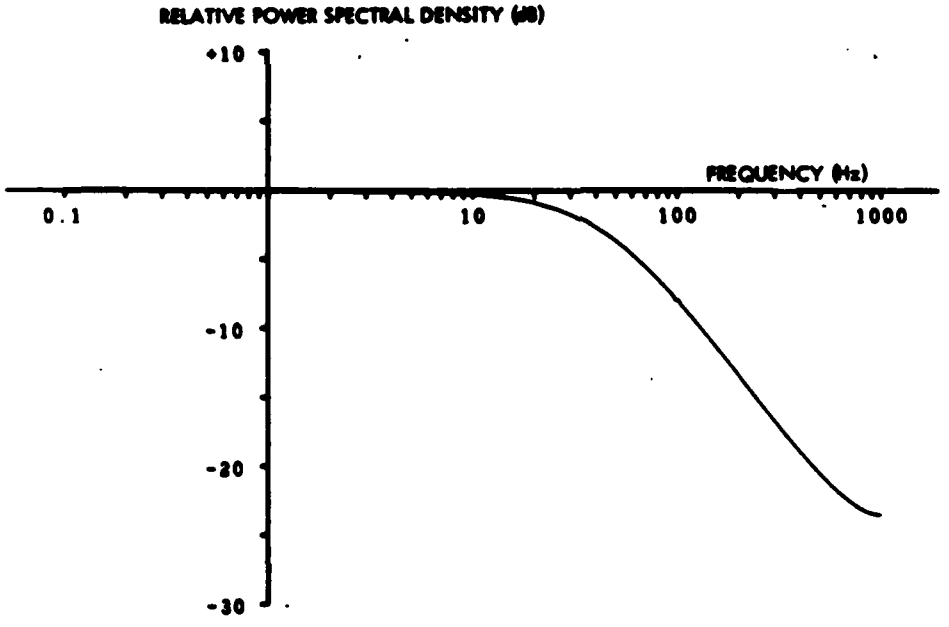

Figure 8. Gain Characteristics of First-Order Linear Filter

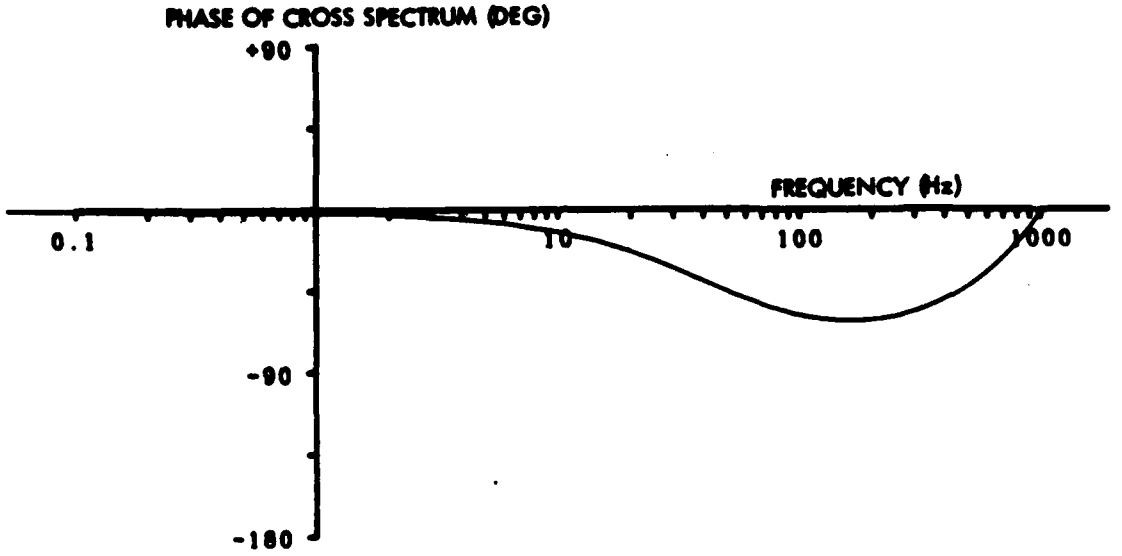

Figure 9. Phase Characteristics of First-Order Linear Filter

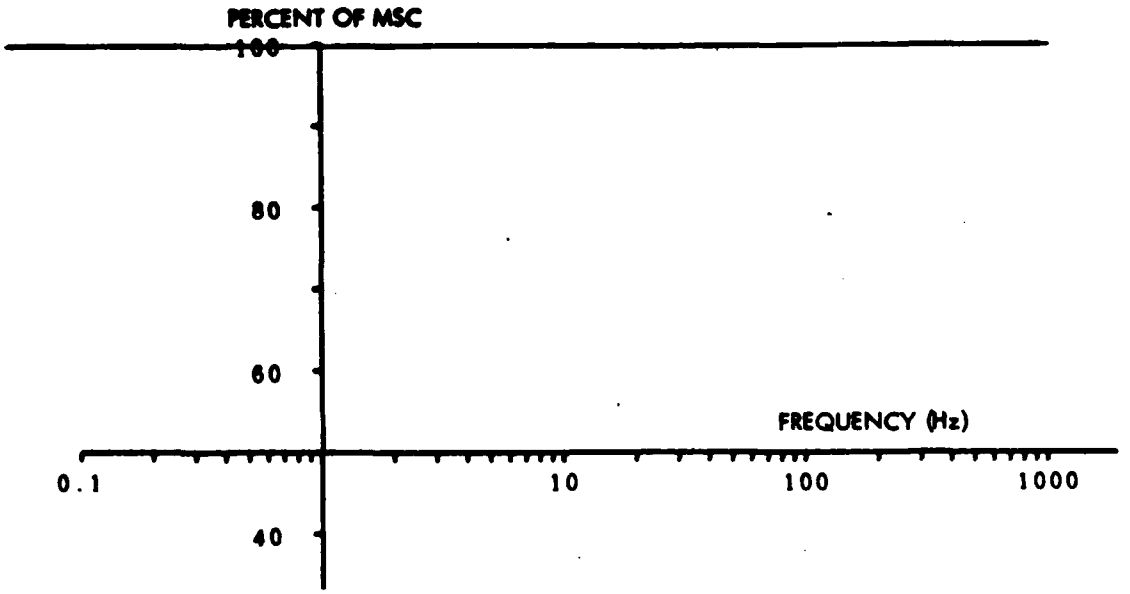

Figure 10. Estimate of MSC (Between Input and Output of First-Order Linear Filter) Using P = 1024 and a Cosine Weighting Function

The input sequence was generated by summing noise and two sine waves (one centered in an FFT frequency bin, one out). The results illustrate the ability to estimate MSC when the phase of the cross spectrum (which is the same as both the phase of the filter and the phase of the complex coherence) can be sufficiently resolved. The bias due to insufficient resolving power has been shown to be directly proportional to the first derivative of the phase.[3]

Note that the estimator, having resolved the true coherence of 100 percent, is unbiased and has zero variance. This behavior of the coherence estimator was predicted by Benignus,[6] Carter and Nuttall,[12] Carter,[1] and Carter, Knapp, and Nuttall.[16] For the special case where the spectrum of the input to the first-order filter is flat, as expected the coherence estimator is 100 percent as in figure 10.[15]

CONCLUSIONS

Some of the practical aspects of estimating the MSC function have been presented. It is difficult to analyze the results; two points which must be considered are weighting functions and resolution. First, a smooth weighting function must be applied to the data to estimate the MSC spectrum. Second, averaging of large size FFTs is required, dictating time series of long duration which are stationary over the period of observation. Spectrum analyzers purchased or used for MSC estimation must have weighting functions and large FFT sizes and should have phase displays.

Extracting from Tick,[3] "I wonder how many conclusions have been drawn over the years because of poor estimation procedures."

REFERENCES

1. G. C. Carter, Estimation of the Magnitude-Squared Coherence Function (Spectrum), NUSC Technical Report 4343, 19 May 1972.

2. J. S. Bendat and A. G. Piersol, Random Data Analysis and Measurement Procedures, John Wiley and Sons, New York, 1971.

3. L. J. Tick, "Estimation of Coherence," Spectral Analysis of Time Series, B. Harris, ed., John Wiley and Sons, New York, 1967.

4. G. M. Jenkins and D. G. Watts, Spectral Analysis and Its Application, Holden Day, San Francisco, California, 1968.

5. R. A. Haubrich, "Earth Noise 5 to 5000 Millicycles per Second," Journal of Geophysical Research, vol. 70, no. 6, March 1965, pp. 1415-1427.

6. V. A. Benignus, "Estimation of Coherence Spectrum and Its Confidence Interval Using the Fast Fourier Transform," IEEE Transactions on Audio and Electroacoustics, vol. AU-17, no. 2, June 1969, pp. 145-150.

7. C. Bingham, M. D. Godfrey, and J. W. Tukey, "Modern Techniques of Power Spectrum Estimation," IEEE Transactions on Audio and Electroacoustics, vol. AU-15, no. 2, June 1967, pp. 56-66.

8. P. D. Welch, "The Use of Fast Fourier Transform for the Estimation of Power Spectra; A Method Based on Time Averaging Over Short Modified Periodograms," IEEE Transactions on Audio and Electroacoustics, vol. AU-15, no. 2, June 1967, pp. 70-73.

9. P. R. Roth, "Effective Measurements Using Digital Signal Analysis," IEEE Spectrum, April 1971, pp. 62-70.

10. R. C. Singleton, "An Algorithm for Computing the Mixed Radix Fast Fourier Transform," IEEE Transactions on Audio and Electroacoustics, vol. AU-17, no. 2, June 1969, pp. 93-102.

11. A. H. Nuttall, Spectral Estimation by Means of Overlapped FFT Processing of Windowed Data, NUSC Technical Report 4169, 13 October 1971.

12. G. C. Carter and A. H. Nuttall, "Evaluation of the Statistics of the Estimate of Magnitude-Squared Coherence," NUSC Technical Memorandum TC-193-71, 28 September 1971.

13. A. H. Nuttall and G. C. Carter, "On Generating Processes with Specified Coherence," NUSC Technical Memorandum TC-187-71, 22 September 1971.

14. D. E. Amos and L. H. Koopmans, "Tables of the Distribution of the Coefficient of Coherence for Stationary Bivariate Gaussian Processes," Sandia Corp. Monograph SCR-483, 1963.

15. G. C. Carter and C. R. Arnold, "Some Practical Considerations of Coherence Estimation," NUSC Technical Memorandum TD113-19-71, 22 November 1971.

16. G. C. Carter, C. H. Knapp, and A. H. Nuttall, "Estimation of the Magnitude-Squared Coherence Function via Overlapped Fast Fourier Transform Processing," submitted to the IEEE Transactions on Audio and Electroacoustics.

NUSC Technical Memorandum TC -5-73
26 April 1973

A Digital Computer Algorithm for Estimation of the Power Spectral Density Matrix Using The Partitioned Modified Chirp Z Transform

G. C. Carter
J. F. Ferrie

ABSTRACT

This memorandum discusses a digital computer technique for estimation of the power spectral density matrix between two wide-sense ergodic random processes when a time-limited member function of each process is available. The digital computer algorithm, including the FORTRAN code, is given in the appendixes. The technique is based upon performing a partitioned and modified Chirp Z transform (PAM-CZT) on each channel of data, using the computationally rapid fast Fourier transform (FFT). The technique provides fine frequency resolution in a frequency band of interest despite limited computer core storage.

A complete discussion of the Chirp Z transform and the method for obtaining finer frequency resolution by partitioning is presented together with an example case.

TABLE OF CONTENTS

LIST OF FIGURES

GLOSSARY

FFT	fast Fourier transform
CZT	Chirp Z transform
MCZT	Modified CZT
PAM-CZT	Partitioned and Modified CZT
Δt	basic time increment between time samples
f	frequency
f_s	sampling frequency
Δf	frequency resolution in Hz
T	Time duration of data segment in seconds
Hz	Hertz
M	is the number of frequency points of interest
R	is the number of partitions of N data points
N	is the number of data points in T seconds
P	is the number of segments or pieces each of size N
G_{xy}	Spectral density function of x with y
H	Transfer Function
γ	Coherence function
$\|c\|$	Magnitude of c
arg [c]	Angle associated with c
MADs	Multiplications and Additions

I. INTRODUCTION

A technique for estimation of the cross-power spectral density matrix between two wide-sense ergodic processes is investigated using the partitioned modified Chirp Z transform (PAM-CZT) [1-6]. This technique has received little attention to date due to the lack of application by the originators [3, page 90]. While applications of the PAM-CZT may not be apparent when dealing with transients, there clearly is a use for the technique when dealing with stationary random data [6].

The second order probability structure of the zero-mean stationary random processes a(t) and b(t) can, in general, only be specified with knowledge of the k-th and ℓ-th joint moment

$$M_{ab}(\tau; k, \ell) = E\left[a^k(t)\, b^{\ell}(t+\tau)\right], \quad \forall \{k, \ell\} \tag{1}$$

where E denotes the mathematical expectation. For the special case of $k = \ell = 1$, we have the cross correlation function

$$R_{ab}(\tau) = E\left[a(t)\, b(t+\tau)\right] \tag{2}$$

The Fourier transform of $R_{ab}(\tau)$ is given by

$$G_{ab}(f) = \int_{-\infty}^{\infty} R_{ab}(\tau)\, e^{-j 2\pi f \tau}\, d\tau \tag{3}$$

A partial description, then, of the second order statistics of the stationary processes x(t) and y(t) is given by the power spectral density matrix,

$$M_{xy}(f) = \begin{bmatrix} G_{xx}(f) & G_{xy}(f) \\ G_{yx}(f) & G_{yy}(f) \end{bmatrix} \tag{4}$$

where

$G_{xx}(f)$ is the (real) auto power spectral density function of x(t), from eq. (3) when $a = b = x$,

$G_{yy}(f)$ is the (real) auto power spectral density function of y(t), from eq. (3) when $a = b = y$, and

$G_{xy}(f)$ is the (complex) cross power spectral density function of x(t) and y(t), (from eq. (3) when $a = x$ and $b = y$),

and consists of a real or coincidental (co) spectrum and an imaginary or quadrature (quad) spectrum [7]. ($G_{yx}(f)$ is the complex conjugate of $G_{xy}(f)$.) When these two processes are wide-sense stationary and Gaussian, knowledge of the power spectral density matrix specifies all order statistics of the processes. This is because the density function for Gaussian processes is completely known from means, variances, and correlation coefficients. It is for these reasons that study of the power spectral density matrix is of widespread interest.

In obtaining estimates of the power spectral density matrix $M_{xy}(f)$, it is incumbent upon the investigator to sufficiently resolve the true detail of the spectrum. Severe bias and variance problems can result when the true spectral matrix has not been resolved in frequency. For example, computation of the coherence from estimates of the spectral matrix can be in error by 10% or more due to insufficient resolution [8]. Fine frequency resolution,

$$\Delta f = \frac{1}{T} \tag{5}$$

where T is the length of the time segment to be transformed, can only be achieved when T is large.

The concept of obtaining fine frequency resolution, using a fast Fourier transform (FFT) was introduced by Rabiner, Schafer, and Rader [2-3]. The technique is called the Chirp Z transform (CZT). The algorithm has been studied by Schilling [4], Ahmed [5]. The CZT which will be discussed has been modified so that only frequency points on the unit circle in the Z plane are evaluated; this is called the Modified CZT (MCZT). By partitioning the input sequence to evaluate the MCZT, we can realize savings in transform size and memory. Utilization of the partitioned modifie chirp Z transform (PAM-CZT) allows computation of 1 large size FFT via several smaller size FFTs [6]. This extremely powerful technique for stationary data is available as a digital computer program to estimate the spectral matrix $M_{xy}(f)$.

II. PARTITIONED MODIFIED CHIRP Z TRANSFORM

The Z transform is given by [9]:

$$X(z) = \sum_{n=0}^{N-1} x(n) z^{-n} \tag{6}$$

where $x(n)$ is an N point sequence (of T seconds duration)

The discrete Fourier transform DFT is given by [9]:

$$X(k) = \sum_{n=0}^{N-1} x(n) e^{-j 2\pi k n / N} \tag{7}$$

The DFT can be evaluated with a fast algorithm or FFT. It can be seen that the DFT, Eq. (7), evaluates the Z-transform at N equally-spaced points around the unit circle as shown in Figure 1, thus obtaining a periodic sequence representation for $\underline{X}(z)$.

The CZT is defined by [1 - 6]:

$$\underline{X}(k) = \sum_{n=0}^{N-1} x(n) A^{-n} W^{nk} \quad , k = 0, 1, \ldots, M-1 \qquad (8)$$

where

$$W = W_0 \exp(j 2\pi \phi_0)$$

and

$$A = A_0 \exp(j 2\pi \theta_0)$$

Note that if $A_0 = 1, \theta_0 = 0, W_0 = 1$, and $\phi_0 = -\frac{1}{N}$, that Eq. (8) is the DFT, Eq. (7). By the inclusion of A_0 and W_0 in the algorithm, values other than on the unit circle are attained. That is, θ_0 defines starting frequency and A_0 defines the starting amplitude. The value ϕ_0 defines the frequency spacing and W_0 defines the spiraling rate.

We now modify Eq. (8) such that $W_0 = 1$ and $A_0 = 1$ and define the modified CZT (MCZT) [1 - 6]:

$$\underline{X}(k) = \sum_{n=0}^{N-1} x(n) A^{-n} W^{nk} \quad , k = 0, 1, \ldots, M-1 \qquad (9)$$

where

$$A = \exp(j 2\pi \phi_0)$$

$$W = \exp(j 2\pi \theta_0)$$

The Z plane interpretation of the MCZT is shown in Figure 2. A comparison of figures 1 and 2 points up the fact that the MCZT evaluates a limited band of angular frequencies.

Neither Eq. (8) nor Eq. (9) is in FFT computational form, except in the special case where $M = N$. Therefore, for the general case, we are forced to perform the DFT with NM complex multiplications and additions required. For large M this becomes prohibitive. However, by making the substitution suggested by Bluestein [10], we obtain

$$nk = \frac{n^2 + k^2 - (k-n)^2}{2} \qquad (10)$$

and substituting into Eq. (8), we obtain

$$\underline{X}(k) = \sum_{n=0}^{N-1} x(n) A^{-n} W^{(n^2/2)} W^{(k^2/2)} W^{-(k-n)^2/2} \qquad (11)$$

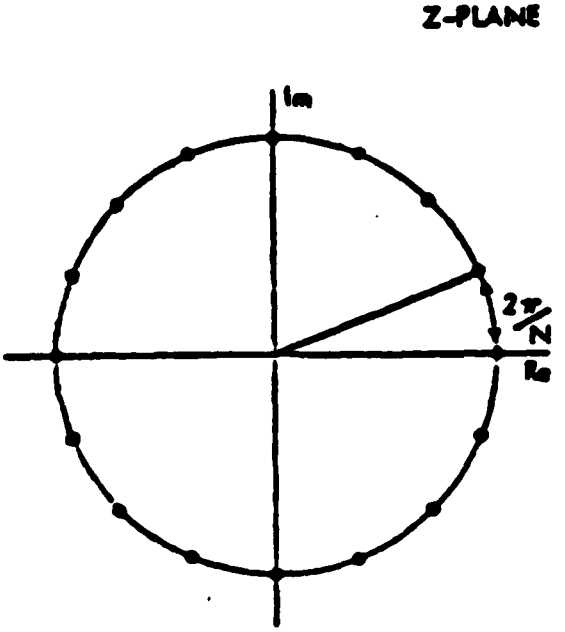

Figure 1. Evaluation of X(z) for $z = \exp(i2\pi k/N)$, $k = 0, 1, 2, \ldots N-1$; $N = 16$ [17]

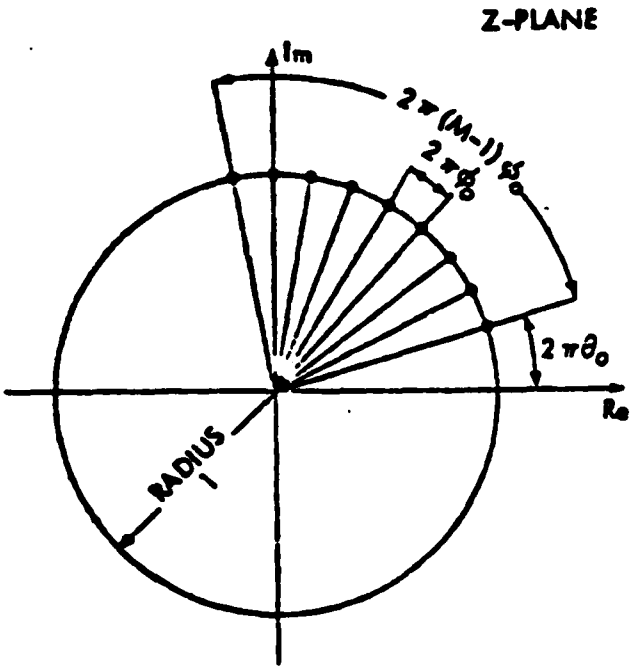

Figure 2. Z-plane interpretation of MCZT [1]

which can be simplified to

$$\underline{X}(k) = W^{(k^2/2)} \sum_{n=0}^{N-1} \left[x(n) A^{-n} W^{(n^2/2)} \right] \left[W^{-(k-n)^2/2} \right] \qquad (12)$$

$$k = 0, 1, \ldots, M-1$$

By inspection of Eq. (12), we recognize that it is in the form of a convolution sum, which can be computed via FFT techniques of Stockham [4]. Therefore, there is a way to compute Eq. (9) using an FFT.

Using the method outlined by Rabiner [2] and Shilling [4], form a new sequence defined by

$$V(n) = W^{-(n^2/2)} \qquad (13)$$

Now define

$$b(n) = x(n) A^{-n} W^{n^2/2} \qquad (14)$$

and define the convolution

$$g(k) = \sum_{n=0}^{N-1} b(n) V(k-n), \quad k = 0, 1, \ldots, M-1 \qquad (15)$$

Then weighting $g(k)$ of Eq. (15) by $W^{k^2/2}$ allows Eq. (9) to be written as

$$\underline{X}(k) = g(k) W^{k^2/2}, \quad k = 0, 1, \ldots, M-1 \qquad (16)$$

The convolution, Eq. (15), can be realized by computing an FFT on the sequences, defined by Eqs. (13) and (14), multiplying the results, and inverse transforming. In order to nullify the adverse effects of circular convolution, the FFT's performed are of size $L \geq M+N-1$ with appropriate zero filling.

Thus, as shown in Figure 3, the MCZT algorithm can be computed by performing two FFT's and the inverse FFT with appropriate weighting. Computationally the MCZT takes 3 FFTs of size greater than N. It should be noted that when many MCZT's are to be performed on different input data sequences, that the FFT of $V(n)$ should be computed once and stored. If this step is taken, then every MCZT perform would take only 2 FFTs, resulting in a substantial savings (33%) in computational time [6]. (This savings in time is done at the expense of having to store the transform of $V(n)$.)

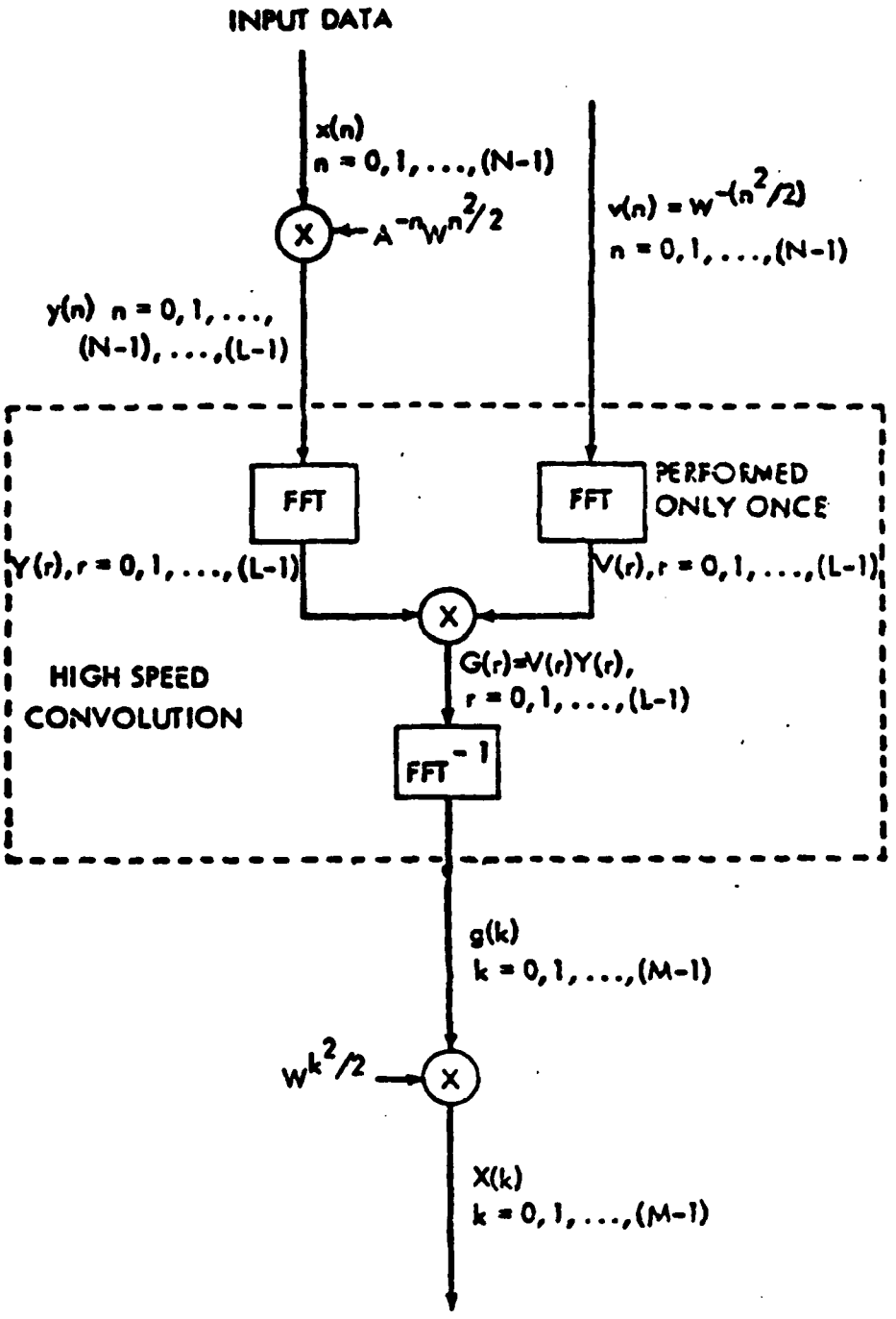

Figure 3. Block diagram of MCZT (Ref. [1])

Partitioning of the input sequences can be accomplished so as to reduce the FFT size. For example, 4 MCZT's of 512 data points can be computed in lieu of 1 MCZT of 2048 data points. This partitioned and modified CZT (PAM-CZT) technique is extremely powerful and is discussed in the next paragraphs.

The modified Chirp Z-Transform (MCZT) as defined by Eq. (9) can be evaluated by a partitioning technique. Consider the situation when the data sequence $x(n)$, $n=0,1,\ldots,N-1$ is extremely long and we desire M spectral samples where $M \ll N$. Then, three FFTs of length L have to be computed with the MCZT algorithm, where L is the smallest highly composite value greater than or equal to (M+N-1). In such cases, it is plausible that L may be so large that storage requirements prohibit computation of the MCZT. In such cases, the sum in Eq. (16) can be broken up into R sums over the N points. That is, the original data sequence is divided into R partitions, and hence Eq. (16) can be written as follows [2]:

$$X(k) = \sum_{r=0}^{R-1} A^{-r\hat{N}} W^{kr\hat{N}} \left[\sum_{n=0}^{\hat{N}-1} x(n+r\hat{N}) A^{-n} W^{nk} \right] \qquad (17)$$

$$k = 0, 1, \ldots, M-1$$

where $R\hat{N} = N$. Each of the R sums in the brackets can then be evaluated using the MCZT algorithm. Eq. (17) is referred to as the partitioned MCZT (PAM-CZT) [6].

It is possible that a saving in total time may result from this method as opposed to evaluation of an N point transform [2]. Hence, the PAM-CZT can be expected to perform in a computationally expeditious manner. Say, for example, $M = 1024 = 2^{10}$ and $N = 65,536 = 2^{16}$ and R was selected $R = 64 = 2^{6}$.

Then the brute force approach requires

$MN = 2^{10}2^{16} = 2^{26} \simeq 67 \times 10^{6}$ complex multiplications and additions (MAD's).

The FFT would take

$$N \log_2 N = 2^{16} \cdot 16 \cong 10^6 \quad MADs$$

and yield all the coefficients, provided sufficient core memory was available. The PAM-CZT would take (neglecting the FFT on $v(n)$)

$$2\left[16\,\frac{L}{16}\log_2\frac{L}{16}\right] \text{ where } L \geq 2^{10}+2^{16} = 2^{17} \qquad \text{for power of 2 algorithms}$$

$$9 \cdot 2^{18} \cong 2 \times 10^6 \quad MADs$$

so if brute force computations required 30 minutes in this case, PAM-CZT computations would require only 1 minute.

III. POWER SPECTRAL DENSITY MATRIX ESTIMATION PROCEDURE

The basic objective is to obtain estimates of the elements of the spectral density matrix,

$$M_{xy}(f) = \begin{bmatrix} G_{xx}(f) & G_{xy}(f) \\ G_{yx}(f) & G_{yy}(f) \end{bmatrix} \tag{18}$$

in order to characterize the second order statistics of the two processes being investigated. The estimation technique described is the direct method similar to the one discussed by Haubrich [11], Welch [12], Knapp [13], Bingham [14], Benignus [15], Nuttall [16 - 17], Carter [18 - 19], and Bendat [20] except that it uses the PAM-CZT in lieu of the FFT.

In this Welch-Haubrich technique, the time series are segmented into P pieces, each having N-data points. For example, from each process there may be 64 segments, each segment having 4096 points, The segments may be overlapped or disjoint, and each segment may have several partitions. Each segment must be multiplied by a smooth weighting function. Next, the PAM-CZT of the weighted N-point sequence is computed. The M Fourier coefficients for each weighted piece are then used to estimate the elements of the power spectral density matrix. The power spectral estimates thus obtained from each set of weighted sequences are then averaged over all the P segments [18]. When N is selected large enough to insure adequate spectral resolution and P is selected large enough to reduce the variance and bias of the spectral estimators, then good spectral estimates are obtained. It should be noted that the selection of large P and large N are conflicting requirements when dealing with a fixed amount of data.

The method of overlapped weighted segmentation requires that each discrete N point segment (of $x(t)$ and $y(t)$ obtained by sampling at f_s (Hz) be multiplied by a discrete weighting, $w(n)$.

The weighting function length must be selected so that its Fourier transform is narrower in the main lobe than the finest detail of the true spectral density matrix of processes x(t) and y(t). Generally, this lobe is narrowed by increasing the PAM-CZT size [19].

The specific selection of a weighting function involves a number of tradeoffs. A commonly used weighting (or windowing) function is the cosine (Hanning) function defined [14] by

$$W(n) = \frac{1}{2}\left(1 - \cos\left[\frac{2\pi n}{N}\right]\right) \qquad n = 0, 1, \ldots, N-1 \tag{19}$$

In practice, $w(n)$ can be computed once and stored in a real floating point array of size N points. Alternatively, a frequency domain convolution can be performed.

Let x (n) where n = 0, 1, 2, . . . , N-1 denote the N-point sequence obtained from the sth weighted segment of process x(t). In estimating spectra, it is necessary to evaluate a transformation of this weighted sequence. The PAM-CZT is a fast algorithm for evaluating the Z transform of the weighted sequence $x_s(n)$, n = 0, 1, . . . , N-1 where s = 1,2, . . . , P at M equi-spaced points on the unit circle with arbitrary starting frequency. The actual computation performed on each segment is

$$\underline{X}_s(k) = \sum_{r=0}^{R-1} A^{-r\hat{N}} W^{kr\hat{N}} \left[\sum_{n=0}^{\hat{N}-1} x(n+r\hat{N}) A^{-n} W^{nk}\right] \tag{20}$$

Similarly, a (complex) vector $Y_s(k)$ is formed for each piece or segment (that is, s = 1, 2, . . . , P).

The estimate of the auto power spectral density function of x(t) at the kth frequency, obtained from averaging sth weighted segment, is given by

$$\hat{G}_{xx}(k) = \frac{\Delta t}{N} \cdot \frac{1}{P} \sum_{s=1}^{P} X_s(k) X_s^*(k), \quad \Delta t = \frac{1}{f_s} \tag{21}$$

Similarly,

$$\hat{G}_{yy}(k) = \frac{\Delta t}{N} \cdot \frac{1}{P} \sum_{s=1}^{P} Y_s(k)\, Y_s^*(k) \tag{22}$$

and the estimate of the cross power spectral density function is

$$\hat{G}_{xy}(k) = \frac{\Delta t}{N} \cdot \frac{1}{P} \sum_{s=1}^{P} X_s(k) Y_s^*(k) \tag{23}$$

Equation (23) can be rewritten in terms of the real and imaginary parts,

$$\hat{C}_{xy}(k) = \mathrm{Re}\left[\hat{G}_{xy}(k)\right] \tag{24}$$

and

$$\hat{Q}_{xy}(k) = \mathrm{Im}\left[\hat{G}_{xy}(k)\right] \tag{25}$$

The averaging or integration technique utilized here reduces the variance of all four spectral estimators. Additionally, by properly averaging the real (co) and imaginary (quad) parts of the cross spectrum, we obtain unbiased estimates of this complex function. It should be noted that this type of averaging is invalid if the data is not wide-sense stationary, for in that case the correlation matrix, and hence the true power spectral matrix, varies from time segment to time segment. That is, averaging is performed to reduce random fluctuations in the estimator; it is not performed to suppress non stationarities.

A useful function immediately available from the power spectral density matrix is the (complex) coherence defined by

$$\gamma(f) = \frac{G_{xy}(f)}{\sqrt{G_{xx}(f)\,G_{yy}(f)}} = \frac{C_{xy}(f) + j\,Q_{xy}(f)}{\sqrt{G_{xx}(f)\,G_{yy}(f)}} \tag{26}$$

Further, when x is the input to a linear system and y is the output, it is useful to discuss the transfer function defined by

$$H(f) = \frac{G_{xy}(f)}{G_{xx}(f)} = \frac{C_{xy}(f) + j\,Q_{xy}(f)}{G_{xx}(f)} \tag{27}$$

Estimation of these quantities is performed by substituting the averaged estimators in place of the true quantities. Statistics of these quantities is beyond the scope of this report, but is discussed in [7] and [18 - 20].

IV. COMPUTER ALGORITHM

The fundamental building block of the PAM-CZT is the fast Fourier transform (FFT) rediscovered by Cooley and Tukey [21]. The selection of the proper FFT algorithm involves trade offs between speed, accuracy, flexibility, and storage of the nature discussed by Ferrie [22]. The mixed radix algorithm proposed (and coded) by Singleton [23] is appealing because of its speed and ability to compute FFT's when the FFT size is not a power of two. This is particularly appealing when $L \geq M+N-1$ is slightly greater than a power of two; in this case, to resort to a power of two algorithm will almost double the computation time. For example, consider $M = 1024 = 2^{10}$ and $N = 65,536 = 2^{16}$; then a power of two algorithm will require

$$\begin{aligned} L \log_2 L &= 2^{17} \log_2(2^{17}) \\ &= 17\,(131,072) \\ &\approx 2.2 \times 10^6 \quad \text{MAD's} \end{aligned}$$

whereas Singleton's routine can compute an FFT of size 75,000 and will require

$$L \log_2 L = 75{,}000 \log_2 (75000)$$
$$\approx 1.3 \times 10^6 \quad MAD's$$

Hence, Singleton's algorithm requires approximately half the MAD's, and since it is already the fastest routine available, it provides a significant savings in computational time.

Singleton's routine is not without drawbacks, however. In particular, it suffers from large errors due to round off, which grow rapidly with FFT size, unlike other algorithms [22]. A recent power of two FFT algorithm (including the FORTRAN code) is given by Markel [24]. An analysis of the error of this routine was done in reference [25]. Because Markel's FFT algorithm is the most accurate single precision technique investigated to date, it must be given serious consideration. Selection of the algorithm based on speed and flexibility dictates Singleton's FFT. On the other hand, selection of the most accurate FFT requires picking Markel's technique. The authors, while using both, have most recently been concerned with accuracy requirements and have leaned towards Markel's routine, which is currently implemented in the computer program.

V. EXAMPLE CASE

An example case is enclosed to illustrate some of the program's capabilities. White Gaussian noise is filtered by the second order low pass digital filter specified by the recursion equation [8].

$$y(n) = A\,y(n-1) + B\,y(n-2) + C\,x(n)$$

where

A = 1.97330
B = -0.98202
C = 0.00872

The block diagram for the example case is depicted in figure 4, where Z^{-1} is the standard delay element.

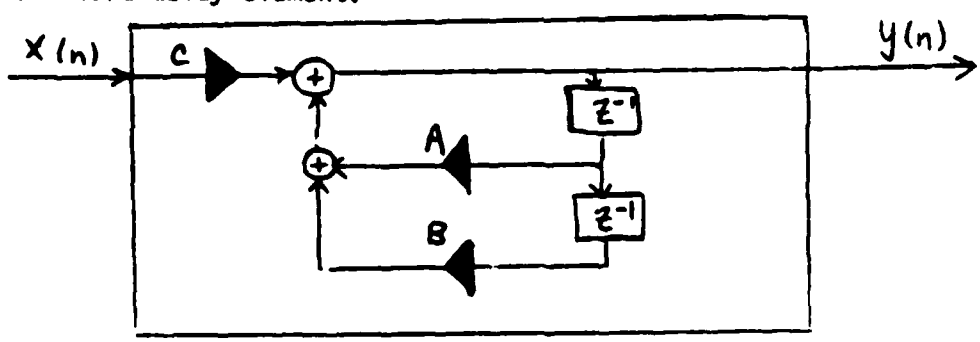

Figure 4. Second Order Digital Filter

The figures which follow are estimates of the spectral characteristics derived from the sampled time waveforms X(n) and Y(n) in the 0 - 100 Hz frequency band by utilization of computer program S2178. Figure 5 is an estimate of the auto power spectral density function of the X process (input to filter). Figure 6 is an estimate of the auto power spectral density function of the Y process obtained from the output of the filter. Figure 7 is an estimate of the phase of the transfer function between the X and Y processes. Figure 8 is an estimate of the gain characteristics of the probed system.

For the sampling frequency $f_s = 2048$, the frequency resolution

$$\Delta f = f_s / N$$

was varied from 2 Hz (when N = 1024) to 0.125 Hz (when N = 16384). The resultant two estimates of the Magnitude Squared Coherence (MSC) are given in figure 9 for N = 1024 and figure 10 for N = 16384. The true MSC between the input and output is unity at all frequencies [8]; however, when estimating the MSC, serious bias errors can result due to insufficient resolution [8]. This type of bias can be eliminated by using Program S2178, which allows N to be selected as large as desired (consistent with the amount of available data). In particular, note when N = 1024, there is insufficient resolution and the estimate of MSC is biased (i.e., not equal to the true value); however, when N is increased to 16384, sufficient resolution exists and the random variable is properly estimated.

VI. SUMMARY

A digital computer algorithm to estimate the power spectral density matrix between two wide-sense ergodic random processes when one time-limited member function from each process is available. The algorithm utilizes the Partitioned Modified Chirp Z Transform in order to obtain frequency resolution which is limited only by the available record length. This added digital processing flexibility allows easy circumvention of bias due to insufficient resolving power, as shown in the example presented. The FORTRAN implementation of the algorithm is given in the appendixes.

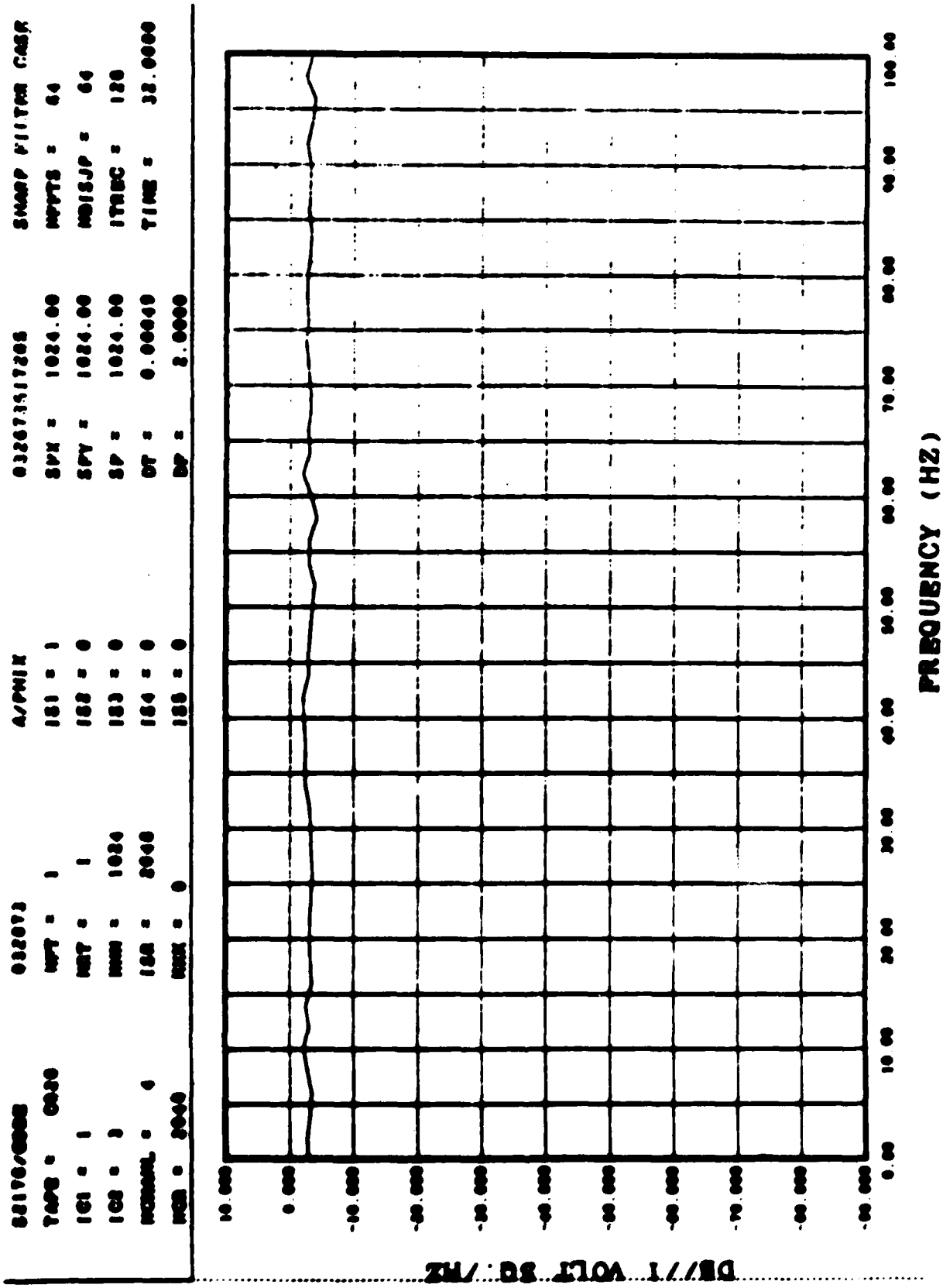

Figure 5. Estimate of $G_{xx}(f)$

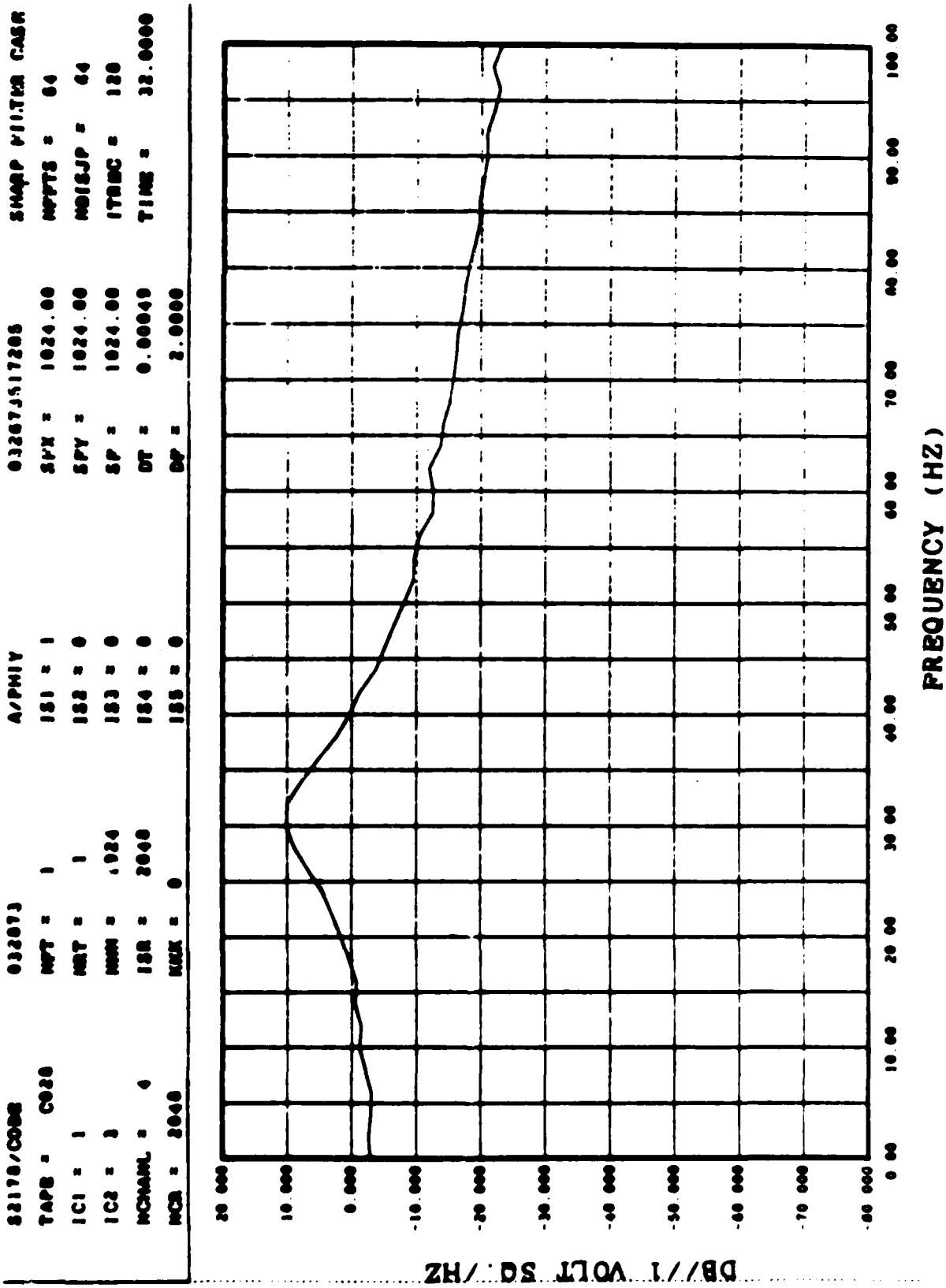

Figure 6. Estimate of G (f)

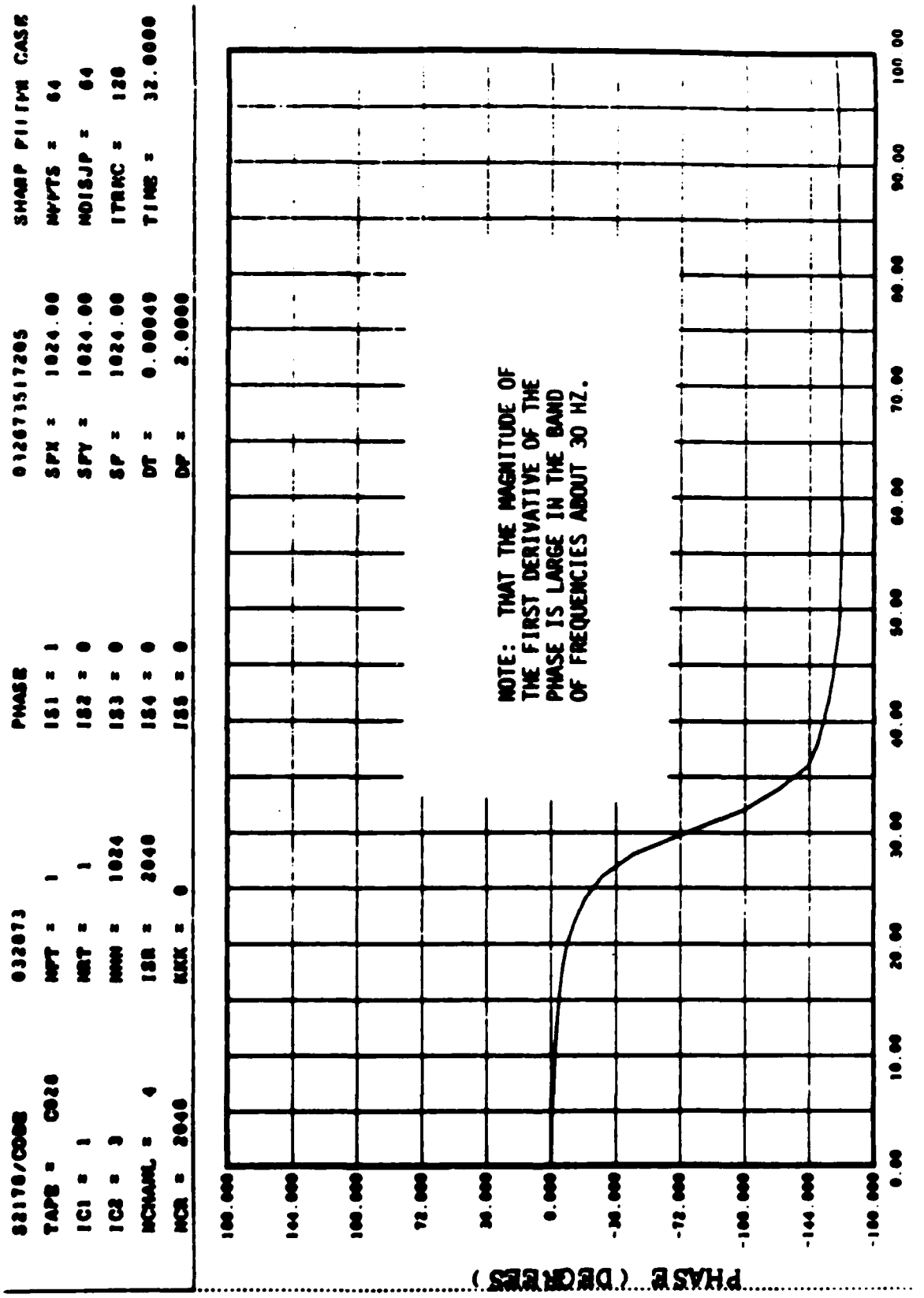

Figure 7. Estimate of arg H(f)

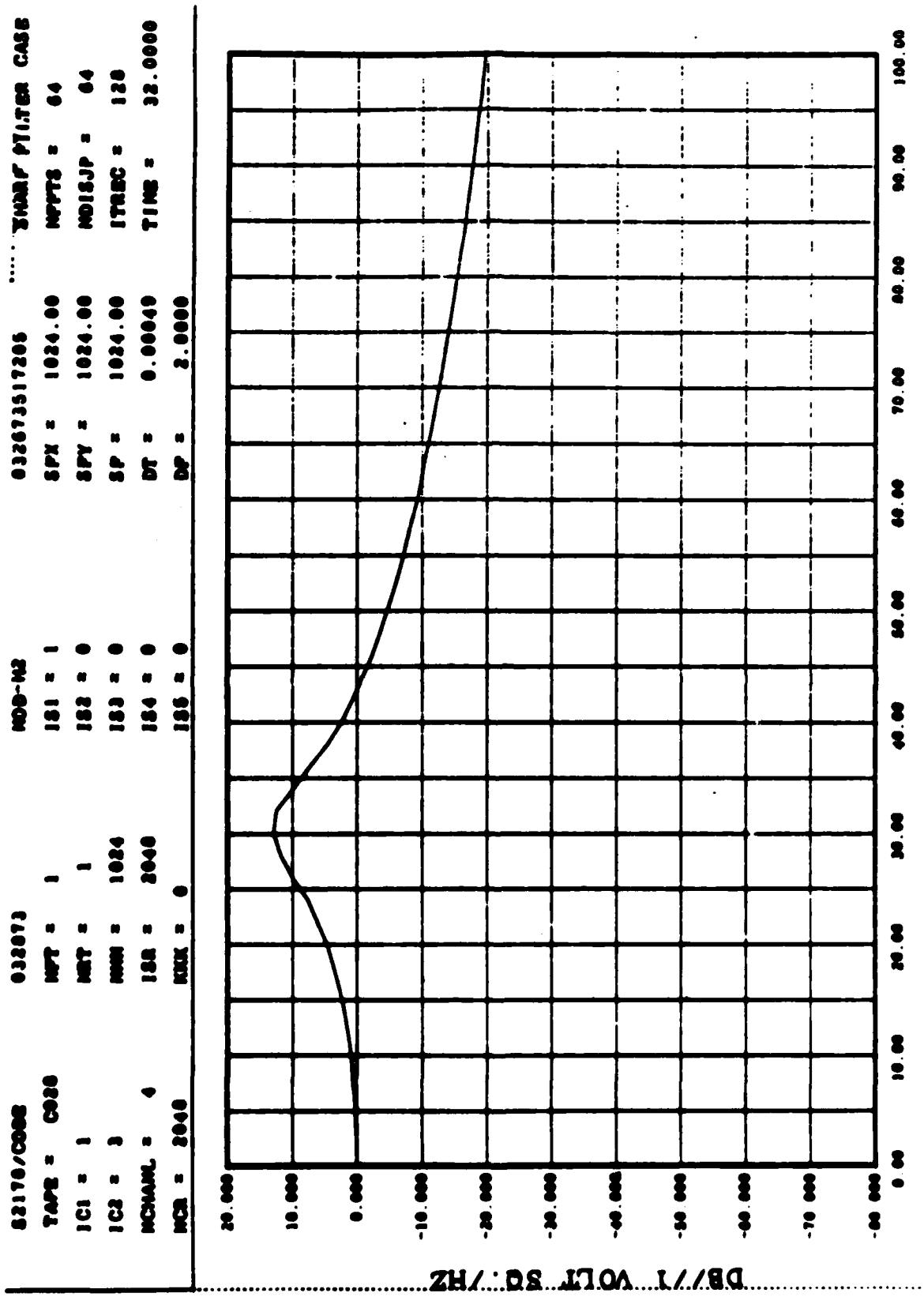

Figure 8 Estimate of $[H(f)]^2$

82178/CDDR	032673	COMPLT	032673517205	SHARP FILTER CASE
TAPE = C036	NPT = 1	IS1 = 1	SPX = 1024.00	NPFTS = 64
IC1 = 1	NRT = 1	IS2 = 0	SPY = 1024.00	NDISJP = 64
IC2 = 3	NMM = 1024	IS3 = 0	SP = 1024.00	ITREC = 128
NSKAML = 4	ISR = 2048	IS4 = 0	DT = 0.00049	TIME = 32.0000
NSR = 2048	KKK = 0	IS5 = 0	DF = 2.0000	

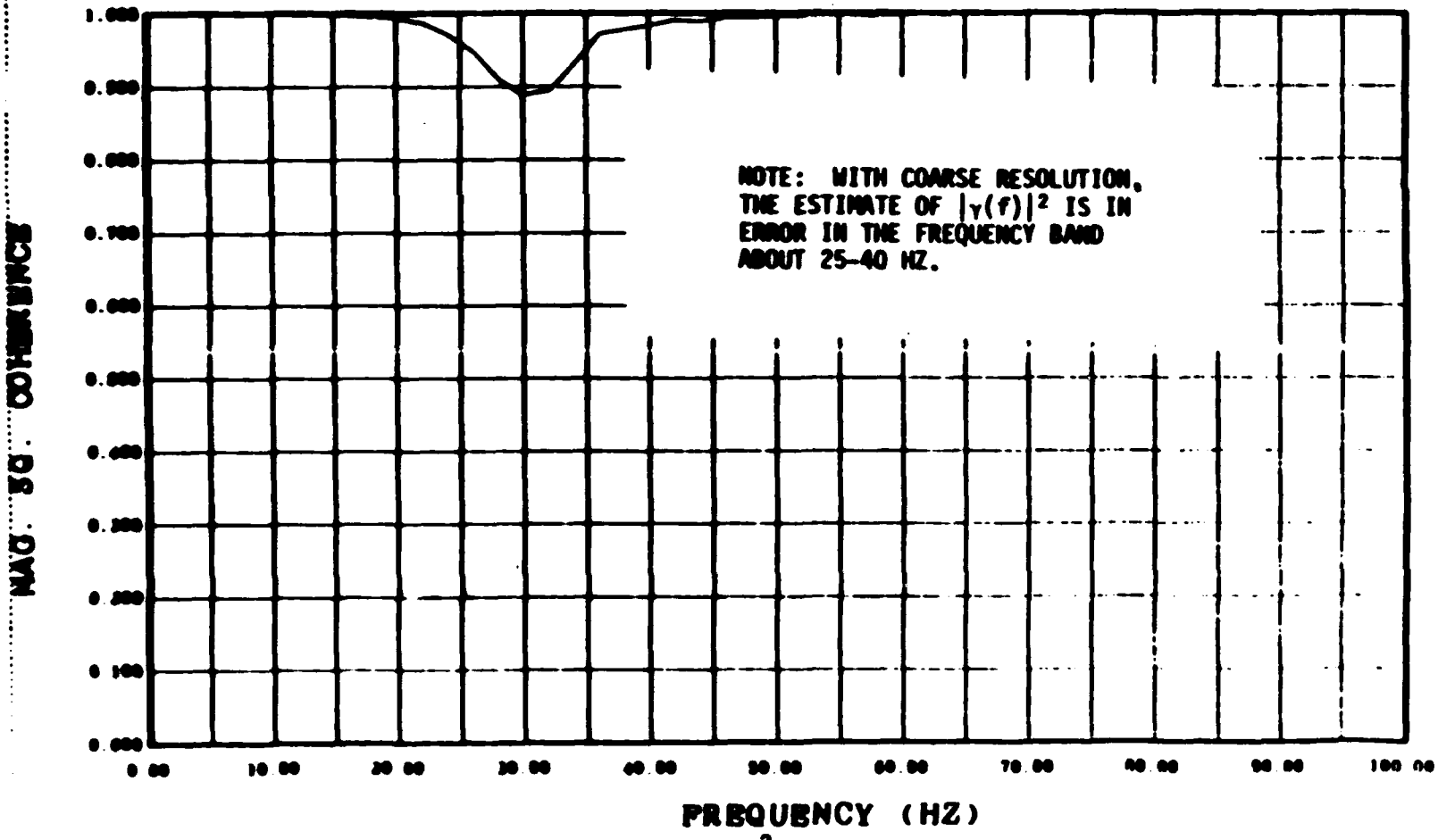

Figure 9. Biased Estimate of $|\gamma(f)|^2$ Using N = 1024 (Δf = 2 Hz)

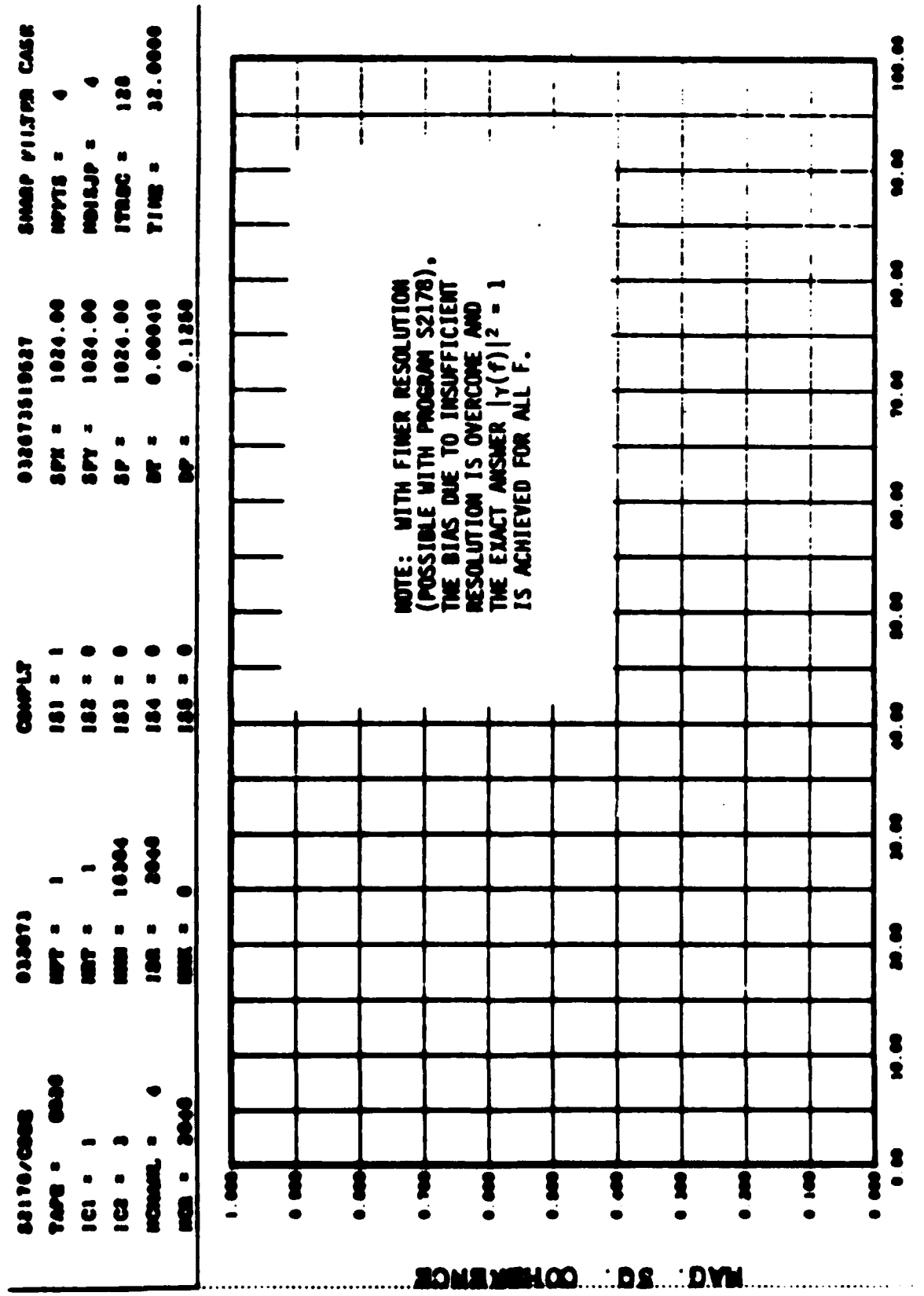

Figure 10. Unbiased Estimate of $|\gamma(f)|^2$ Using N = 16384 (Δf = 1/8 Hz)

VII. REFERENCES

1. J. F. Ferrie, C. W. Nawrocki, and G. C. Carter, "The PAM Chirp Z-Transform: a Signal Processing Technique for Simultaneous Multi-frequency Evaluation of the Surface Reradiated Spectrum in Slowly Varying Environments," paper to be presented at the IEEE Conference on Engineering in the Ocean Environment, September 25-28, 1973, Seattle, Washington.

2. L. R. Rabiner, R. W. Schafer, C. M. Rader, "The Chirp Z-Transform Algorithm and Its Application," The Bell System Technical Journal, Vol. 48, No. 5, May-June 1969, pp. 1249-1292.

3. L. R. Rabiner, R. W. Schafer, and C. M. Rader, "The Chirp Z-Transform Algorithm," IEEE Transactions on Audio and Electroacoustics, Vol. AU-17, No. 2, June 1969, pp 86-92.

4. S. A. Shilling, "A Study of the Chirp Z-Transform and Its Applications," A Master's Degree Report, Kansas State University, Manhattan, Kansas, 1972.

5. N. Ahmed, personal communication.

6. J. F. Ferrie, C. W. Nawrocki, and G. C. Carter, "Implementation and Results of the Modified Chirp Z-Transform," NUSC TM No. TC-191-72, 18 Oct 1972, New London, Conn.

7. N. R. Goodman, "On the Joint Estimation of the Spectra, Cospectrum, and Quadrature Spectrum of a Two-Dimensional Stationary Gaussian Process," Scientific Paper 10, NYU, New York (March 1957).

8. G. C. Carter, "Coherence Estimation as Affected by Weighting Functions and Fast Fourier Transform Size," NUSC Tech. Report 4423, 12 Oct 1972, New London, Ct.

9. B. Gold and C. M. Rader, Digital Processing of Signals, McGraw-Hill Co., New York, 1969.

10. L. I. Bluestein, "Several Fourier Transform Algorithms," NEREM Record, 10:218-219 (November 1968) published by Boston section of the IEEE.

11. R. A. Haubrich, "Earth Noise, 5 to 500 Millicycles per Second, 1. Spectral Stationarity, Normality, and Nonlinearity," Journal of Geophysical Research, Vol. 70, No. 6 (March 1965), 1415-1427.

12. P.D. Welch, "The Use of Fast Fourier Transform for the Estimation of Power Spectra: A Method Based on Time Averaging Over Short, Modified Periodograms," IEEE Transactions on Audio and Electroacoustics, Vol. AU-15, No. 2 (June 1967), 70-73.

13. C. H. Knapp, "An Algorithm for Estimation of the Inverse Spectral Matrix," General Dynamics Electric Boat Research Project (April 1969).

14. C. Bingham, M. D. Godfrey, and J. W. Tukey, "Modern Techniques of Power Spectrum Estimation," IEEE Transactions on Audio and Electroacoustics, Vol. AU-15, No. 2 (June 1967), 56-66.

15. V. A. Benignus, "Estimation of Coherence Spectrum and Its Confidence Interval Using the Fast Fourier Transform," IEEE Transactions of Audio and Electroacoustics, Vol. AU-17, No. 2, (June 1969), 145-150.

16. A. H. Nuttall, "Spectral Estimation by Means of Overlapped FFT Processing of Windowed Data," NUSC Report No. 4169, New London, Ct. (October 1971).

17. A. H. Nuttall, "Estimation of Cross-Spectra Via Overlapped FFT Processing," NUSC Tech. Memo. TC-83-72, New London, Ct. (18 April 1972).

18. G. C. Carter, "Estimation of the Magnitude-Squared Coherence Function (Spectrum)," NUSC Report No. 4343, New London, Ct. (19 May 1972).

19. G. C. Carter, C. H. Knapp and A. H. Nuttall, "Estimation of the Magnitude-Squared Coherence Function Via Overlapped Fast Fourier Transform Processing," accepted for publication in the IEEE Transactions on Audio and Electroacoustics.

20. J. S. Bendat and A. G. Piersol, Random Data-Analysis and Measurement Procedures, (New York: John Wiley and Sons, Inc., 1971).

21. J. W. Cooley and J. W. Tukey, "An Algorithm for the Machine Calculation of Complex Fourier Series," Mathematics of Computation, Vol. 19 (April, 1965), 297-301.

22. J. F. Ferrie and A. H. Nuttall, "Comparison of Four Fast Fourier Transform Algorithms," NUSC Report No. 4113, New London, Ct. (3 Jun 1971).

23. R. C. Singleton, "An Algorithm for Computing the Mixed Radix Fast Fourier Transform," IEEE Transactions on Audio and Electroacoustics, Vol. AU-17, No. 2, (June 1969), 93-102.

24. J. D. Markel, "FFT Pruning," IEEE Transactions on Audio and Electroacoustics, Vol. AU-19, December 1971, 305-311.

25. J. F. Ferrie, G. C. Carter, C. W. Nawrocki, "Availability of Markel's FFT Pruning Algorithm," NUSC Tech. Memo TC-1-73, 15 Jan 1973, New London, Ct.

APPENDIX A

LISTING OF COMPUTER PROGRAM S2178

```
HIGH RESOLUTION NARROW BAND SPECTRAL ANALYSIS PROGRAM VIA THE MODIFIED
PARTITIONED CHIRP Z-TRANSFORM *** ONE CHANNEL VERSION

LAST UPDATED MARCH 17,1973.

TIME DOMAIN COSINE WINDOW SPECTRAL ANALYSIS WITH 50 PERCENT OVERLAP OF
INPUT DATA

PROGRAMMED BY J.F.FERRIE + G.C.CARTER

* * * * * * * * * * * * * * * * * * * * * * * * * * * * * * * * * * * * * *

*** OPERATING INSTRUCTIONS ** PARTITIONED CHIRP Z SPECTRAL PROGRAM * S2116

CARDS 2 AND 3 MUST BE REPEATED FOR EACH DATA SAMPLE

CARD   COLUMNS   FORMAT   ARGUMENT
----   -------   ------   --------
 1      1-6       A6        MID - INPUT DATA MODE - DUMMIE, BCDFMT, CDCNCH
        7-66      10A6      FMT - VARIABLE FORMAT FOR BCD DATA, I.E. (E16.9)
       67-69     BLANK
       70-71      I2        IC1 - NUMBER OF DESIRED DATA CHANNEL STORED IN
                                  XX ARRAY
       72-73     BLANK
       74-75      I2     NCHANL - NUMBER OF DATA CHANNELS ON CDC OR BCD DATA
                                  TAPE
       76-80      I5        NCR - NUMBER OF CONVERSIONS PER RECORD ON CDC OR
                                  BCD DATA TAPE
 2      1-5       I5        NFT - NUMBER OF FILE DESIRED ON INPUT DATA TAPE
        6-10      I5        NRT - NUMBER OF RECORD DESIRED ON NFT FILE OF
                                  INPUT DATA TAPE
       11-15      I5        NNI - NUMBER OF INPUT VALUES TO BE PROCESSED
       16-21      I6        ISR - INTEGER SAMPLING RATE
       22-25      I4        KKP - NUMBER OF WEIGHTS TO THE RIGHT OF CENTER
                                  WEIGHT DURING THE USE OF SMOOTH SUBROUTINE
                                  IT IS APPLIED IN THE FREQUENCY DOMAIN
                                  (SET=0 FOR NO FREQUENCY DOMAIN SMOOTHING)
       26-26      I1        IS1 - DATA OVERLAP FLAG (SET=1 FOR NO OVERLAP)
       27-27      I1        IS2 - WINDOWING SWITCH (SET=0) FOR WINDOWING
       28-28     BLANK
       29-29      I1        IS4 - PRINT FLAG (0 FOR ZERO OUTPUT)
```

```
            30-30    BLANK
            31-40    F10.5       SFX - SCALE FACTOR FOR FIRST CHANNEL
            41-50    BLANK
            51-72    3A6,A4      LABEL - 22 CHARACTER TITLE FOR GRAPHS
            73-80      I8        ITREC - TOTAL NUMBER OF RECORDS TO BE PROCESSED
                                         ON INPUT DATA TAPE
             1-10    F10.5         DF - FREQUENCY RESOLUTION DESIRED IN HERTZ
            11-20    F10.5       FLOW - LOWER FREQUENCY OF INTEREST IN HERTZ
            21-30    F10.5      FHIGH - HIGHER FREQUENCY OF INTEREST IN HERTZ
            31-40      I10       NPAR - NUMBER OF PARTITIONS
            41-80    BLANK

      LAST  1-80     BLANK

* * * * * * * * * * * * * * * * * * * * * * * * * * * * * * * * * * * * * * * *

      SPECIFICATION AND TYPE STATEMENTS

      DIMENSION AX(4096),YY(4096)
      DIMENSION VX(4096),VY(4096),AL(4096),YL(4096)
      DIMENSION ZX(1601),ZY(1601),PHIX(1601)
      DIMENSION AC(1025)
      DIMENSION IZ(4096),LINE(100)
      DIMENSION FMT(12),LABEL(15),DUMMY(1)
      DIMENSION TITLEX(5),TITLEY(5)
      EQUIVALENCE (IZ(1),YY(1))
      COMMON ANODES(200)
      INTEGER FMT
      DATA IDATE/'031773'/

      INITIALIZE PROGRAM UNITS

      INCARD=3
      IPRINT=4
      INTAPE=7

      SET INITIAL VALUES

      CALL NTRAN(INTAPE,10)
      CALL NTRAN(INTAPE,22)
      NFILIN=1
      NRECIN=1
      LABEL(8)='52116/'
      LABEL(9)='CODE  '
      LABEL(10)=IDATE

      INITIALIZE PROGRAM

      WRITE(IPRINT,2)LABEL(8),LABEL(9),IDATE
    2 FORMAT(1H1//9X,'PROGRAM ',A6,A6,' LAST IMPUTED ',A6///)
      CALL MODESW(ANODES,0)
      CALL SETSMW(ANODES,97,1000.0)
```

```
      SET UP DB RANGE AND X,Y TITLES FOR PLOTS

      DBMAX=10.0
      DBMIN=-90.0
      TITLEX(1)='  FREQ'
      TITLEX(2)='UENCY '
      TITLEX(3)='(HZ)  '
      TITLEY(1)='DB//1 '
      TITLEY(2)='VOLT S'
      TITLEY(3)='Q./HZ '


      READ MODE OF INPUT DATA FROM DATA CARD 1

      READ(INCARD,10) MODE,(FMT(I),I=1,10),IC1,IC2,NCHANL,NCH
   10 FORMAT(11A6,3X,3I2,I5)
      I=2=0
      LABEL(11)=IC1
      LABEL(12)=IC2


      PRINT INPUT DATA INFORMATION

      WRITE(IPRNTR,12)MODE,(FMT(I),I=1,10),IC1,IC2,NCHANL,NCH
   12 FORMAT(//9X,'INPUT DATA MODE AND FORMAT',/9X,11A6,3X,3I2,I5)
      CALL NTRAN(INTAPE,<1,ITAPLE)
      CALL NTRAN(INTAPE,<2)
      ITAPEE IS THE LABEL OF TAPE F


      SET MODE = THE MODE OF INPUT DATA

      MODE=0
      IF(MID. EQ. 'DUMMIE') MODE=1
      IF(MID .EQ. 'ACCFMI') MODE=2
      IF(MID .EQ. 'CDCNCM') MODE=3
      IF(MODE .EQ. 0) STOP MODE05


      READ INPUT CONTROL PARAMETERS FROM DATA CARD 2

  100 READ(INCARD,102) NFT,NRT,NNN,ISR,KAK,IS1,IS2,IS3,IS4,IS5,SFX,(LABE
     1L(I),I=1,4),ITHEC
  102 FORMAT(3I5,I6,I4,5I1,F10.5,10X,3A6,A4,I6)


      TEST FOR END OF PROGRAM

      IF(NNN.LE.0) GO TO 900


      PRINT INPUT CONTROL PARAMETERS

      WRITE(IPRNTR,103)NFT,NRT,NNN,ISR,KAK,SFX,ITHEC,IS1,IS2,IS3,IS4,IS5
     1,(LABEL(I),I=1,4)
  103 FORMAT(/1H1//10X,'INPUT PARAMETERS'///10X,'NFT = ',I5// 23X,'NRT =
     1 ',I5// 36X,'NNN = ',I5// 49X,'ISR = ',I6// 62X,'KAK = ',I5// 75X,
```

```
     4('0FX =',F20.8//40X,'ITHEC =',I6//10X,'SWITCH SETTINGS'//10X,'IS1 =
     3',I2//23X,'IS2 =',I2//4-X,'IS3 =',I2//33X,'IS4 =',I2//38X,'IS5 =',
     4I4//19X,'LABEL = ',3A8,A4)


           READ DESIRED BANDWIDTH CONTROL PARAMETERS FROM DATA CARD 3

      DI=1.0/FLOAT(ISM)
      READ(1,CARD,114) ...,FLO,FHI,...,NPAR
  114 FORMAT(3F10.5,I10)
      ...=FLOAT(ISM)/FLOAT(...)
      IF(...LT.DTRAN) WRITE(IPRINT,115) DTRAN
  115 FORMAT(/5X,'FREQUENCY INTERPOLATION IS BEING PERFORMED.THE TRUE RE
     1SOLUTION IS ',F10.5,/)
  116 ...=(FHI-FLO)/DF+1
      IF(...LE.1OP2) GO TO 120
      FHI=FHI-DF
      GO TO 118
  120 RANGE=FLOAT
      ...=...
  122 ISPAR=...
      ...=ISPAR-1
      ...=2
  124 ...=...
      IF(LL.GE.ARMAX) GO TO 126
      ...=...+1
      GO TO 124
  126 IF(LL.LE.0096) GO TO 127
      ...=...
      GO TO 122
  127 ARG=2.*3.1415927
      ...=ISPAR
      ...=NPAR
      WRITE(IPRINT,128) DT,DF,FLO,FHI,...,LL,NPAR
  128 FORMAT(10X,'DT =',F12.6,5X,'DF =',F12.6,5X,'FLO =',F10.4,5X,'FHI=
     1H =',F10.4,5X,'M =',I6,5X,'LL =',I5,5X,'NPAR =',I3)
      CALL CIRCUM(C,LL)
      CALL EQUIL(FL,FU,C,...,ISPAR,...,LL,...,...)


           CALCULATE CONSTANTS

      IF(ITHEC.LE.0) STOP ITHEC
      CALL ...(LABEL(1),LABEL(7))
      TWOPI=PI/FLOAT(...)
      SX=20.0
      SY=SFX
      IPRINT=IS4
      IPLOT=IS5
      ...=ISPAR...CH
      IF(...LE.0) STOP ...
      ...=ITHEC/(...*NPAR)
      ...=NPAR/2
      NFTS=...-1
      ...=...
      WRITE(...,...,...,FLO,FHI,DI,ISM-1.0)
      0.92 IS FOR 99 PER CENT OVERLAP 1.001 IS FOR COSINE WINDOW
      FACTOR=.8/(3.0*DT*(ISM-1.0)
```

```
      NLOWF=10.0*(FACT+(1.0/SQRT(EDF-1.0)))
      SCOWF=10.0*(FACT-(1.0/SQRT(EDF-1.0)))
      NCUF=IFIX(EDF+0.5)
      LABEL(13)=4HDISJ
      LABEL(14)=4HNT
      IF(IBACK.EQ.0.OR.ICOL.EQ.1) NPTS=NDISJP
      CONST=TOUT/FLOAT(100)

C
C     PRINT OUT USER INFORMATION
C
      WRITE(IPRNTR,104)IPRINT,IPLOT,DT,SF
104   FORMAT(//10X,'IPRINT =',I2//23X,'IPLOT =',I2//28X,'DT = ',E13.6//33
     1X,'SF =',F6.4//)
      WRITE(IPRNTR,105)(LABEL(N),N=1,7)
105   FORMAT( 10X,'THE RUN NUMBER FOR THIS CASE IS ',7A6 )
      WRITE(IPRNTR,106) NFILE,TAPE,IU
106   FORMAT(  1HX,'THE INPUT DATA WAS READ FROM FILE',I3,' OF TAPE ',A6
     1,' IN ',A6,' UNIT.'  )
      IF(NIU.EQ.'CONSOL') WRITE(IPRNTR,107)(FMT(I),I=1,10)
107   FORMAT( 10X,'THE FORMAT OF THE BCU DATA WAS ',10A6 )
      IF(NAME.NE.1.AND.NAME.NE.2)WRITE(IPRNTR,108)NCHANL,NCR,IC1,IC2
108   FORMAT(10X,'THE TAPE HAD ',I2,' CHANNELS.'/10X
     *          ,'EACH RECORD HAD',I5,' TOTAL CONVERSIONS.' /10X,'CHANN
     1EL',I3,' WAS EQUALLY SPLEXED INTO XX AND CHANNEL',I3,' INTO YY.'  )
      IF(NPTS(5).EQ.NDISJP) WRITE(IPRNTR,109)
109   FORMAT(//10X,'THE FOLLOWING DATA WAS NOT RUN WITH 50 PERCENT OVERL
     1AP')

C
C     PLOT COVER SHEET
C
      LABEL(5)='COVER '
      CALL SUBLAB(LABEL,TAPE,ILMAX,NCH,NF1,NNN,ISR,KKK,IS1,IS2,IS3,
     1IS4,IS5,SF,SFY,DT,DF,NFF(5),ITREC)
      CALL PAGE(ANOFF,0.0,1,1)

C
C     POSITION TAPE TO CORRECT FILE AND RECORD POSITION BEFORE DATA READ
C
      CALL TAPEP(INTAPE,NFT,NRT,NFILIN,NRECIN)

C
C     PRINT EDF INFORMATION
C
      TIME=FLOAT(NDISJP)*DT/60.
      WRITE(IPRNTR,150)NDISJP,TIME,NEDF
150   FORMAT(10X,'THE',I4,' DISJOINT PIECES COMPRISE',F8.2,' SECONDS OF
     1DATA FOR ',I4,' EDF.')
      WRITE(IPRNTR,155)NCONF,SCONF
155   FORMAT(10X,'USING GAUSSIAN ASSUMPTIONS 90 PER CENT OF THE AUTO SPE
     1CTRAL'/23X,'POINTS LIE WITHIN',F6.2,' DB ABOVE AND',F7.2,' DB BELO
     2W THE PLOTTED AREA.')

C
C     CALCULATE START STOP FOR PLOTS
C
      ISTART=1
```

```
      ISTOPEN

            STORE ZEROS IN THE SUMMING ARRAYS

      DO 195 K=1,MM
      PHI4(K)=0.0
  195 CONTINUE

            COMPUTE AND ADD NFFTS NUMBER OF SPECTRAL ESTIMATES

      DO 450 KOUNT=1,NFFTS
      DO 200 I=1,MM
      ZA(I)=0.0
      ZY(I)=0.0
  200 CONTINUE
      DO 345 K=1,NPAR

            AUTOMATICALLY JUMP TO READ DATA IF PROPER MODE

      GO TO (205,210,220),MODE

            READ OR SYNTHESIZE DATA (DUMMY MODE)

  205 CONTINUE
      GO TO 280

            READ DATA FROM BCD TAPE

  210 CONTINUE
      READ(INTAPE,FMT) (AX(I),I=1,ISPAR)
      GO TO 232

            READ INPUT DATA FROM MAG TAPE IN COC FORMAT

  220 CALL COCNCH(IZ,XX,IY,ISPAR,IC1,IC2,ICHAN,NCR,INTAPE)
  232 INDICINEWREC,I=1,ISPAR,ICHAN,NCR
  280 CONTINUE

            WEIGHT THE INPUT DATA WITH COSINE WINDOW

      IF(IS2.EQ.1) GO TO 357
      ISPAR1=ISPAR*(K-1)
      DO 356 L=1,ISPAR
      XX(L)=XX(L)*(1.0-COS(TOFLOAT(ISPAR1+L-1)))*0.816496581
  356 CONTINUE
  357 CONTINUE

            COMPUTE PARTITIONED CHIRP Z-TRANSFORM

      DO 392 J=1,ISPAR
```

```
      YY(J)=0.0
 300  CONTINUE
      CALL [illegible]
      DO 380 I=1,MM
      F=[illegible]FLOAT(I-1)
      [illegible]
      ZX(I)=[illegible]
      ZY(I)=[illegible]
 380  CONTINUE
 390  CONTINUE

C          COMPUTE SPECTRA

      DO 430 K=1,MM
      PHIX(K)=PHIX(K)+ZX(K)**2+ZY(K)**2
 430  CONTINUE

C          BACKSPACE INPUT DATA TAPE [illegible] RECORDS FOR 50 PERCENT OVERLAP

      IF(IFFTS.EQ.NFFTS) GO TO 450
      CALL [illegible]
      CALL [illegible]
      [illegible]
 450  CONTINUE

C          GO BACK FOR NEXT SAMPLE

 460  CONTINUE


C          DISPLAY RESULTS

C          PRINT CONTROL PARAMETERS

      WRITE(IPRNTR,500) NFFTS
 500  FORMAT(1H1,8X,'INPUT CONTROL PARAMETERS FOR THE PROCESSING OF THIS
     1 AVERAGE OF',I5,3X,'SAMPLES',//////)
      WRITE(IPRNTR,504) NDISJP,NEDF
 504  FORMAT(/9X,'THE NUMBER OF DISJOINT PIECES IN THE AVERAGE SPECTRAL
     1ESTIMATE =',I5,//9X,'THE EQUIVALENT NUMBER OF DEGREES OF FREEDOM =
     2',I5,//)
      WRITE(IPRNTR,520) NCONF,SCONF
 520  FORMAT(/9X,'NINETY PER CENT CONFIDENCE BOUNDS ARE N*L...',2F10.2/)

C          NORMALIZE ESTIMATES

      FNSG=FLOAT(NFFTS)
      OFNSG=1.0/FNSG
      CONST=CONST*OFNSG
 601  DO 602 K=1,MM
      PHIX(K)=PHIX(K)*CONST
 602  CONTINUE
```

```
C     DISPLAY INPUT DATA
      CALL PLOT(...)
      CALL ...
      LABEL(5)='...'
      DO 600 I=1,...
      PHIX(I)=10.*ALOG10(MAX(PHI4(I),1.E-30))
600   CONTINUE
      CALL ...
      CALL ...
      CALL ...
     1...,IFA,IFY,IU,IF,...,ITHEC)
      CALL ...
     1TITLEY,3)
      CALL PAGE(ANODES,0,1,1)

C     GO BACK FOR NEXT SAMPLE

      GO TO 100

C     TERMINATE PROGRAM

900   CALL EXITC(ANNUF,5)
      CALL NTRAN(INTAPE,...)
999   STOP 999
      END
```

APPENDIX B

LISTING OF SUBROUTINE LSEQU

```
      SUBROUTINE LSEQU COMPUTES THE L POINT SEQUENCE. IT IS USED WITH SUBROUTINE
     CHIRP2 TO COMPUTE THE MODIFIED CHIRP Z-TRANSFORM. ... J.FERRIE
     MARCH 17,1973.

      BIBLIOGRAPHICAL REFERENCE

     RABIE,S.B. ... A STUDY OF THE CHIRP Z-TRANSFORM AND ITS APPLICATIONS.
     KANSAS STATE UNIVERSITY MASTER'S THESIS. MANHATTAN,KANSAS 1972.

      SUBROUTINE LSEQU(XX,YY,CC,M,N,L,RAPH,RAPH)

      DIMENSION XX(1),YY(1),CC(1)
      DATA R2PI/6.2831853071/

      DN1=R2PI/RAPH
      DN2=R2PI*RAPH*(1.0/2.0)


            FORM THE FOLLOWING L POINT SEQUENCE

      DO 120 I=1,N
      FIM1=FLOAT(I-1)
      THETA1=DN2*FIM1**2
      XX(I)=COS(THETA1)
      YY(I)=-SIN(THETA1)
  120 CONTINUE
      IF(L.EQ.M+N-1) GO TO 126
      LMNM1=L-MN+1
      M1=M+1
      DO 125 I=M1,LMNM1
      XX(I)=0.0
      YY(I)=0.0
  125 CONTINUE
  126 CONTINUE
      LMNP2=L-MN+2
      DO 130 I=LMNP2,L
      FIM1=FLOAT(L-I+1)
      THETA1=DN2*FIM1**2
      XX(I)=COS(THETA1)
      YY(I)=-SIN(THETA1)
  130 CONTINUE


            COMPUTE THE L POINT DFT

      CALL MKLFFT(XX,YY,CC,M,N,-1)

      RETURN
      END
```

APPENDIX C
LISTING OF SUBROUTINE CHIRPZ

```
      SUBROUTINE CHIRPZ COMPUTES THE MODIFIED CHIRP Z-TRANSFORM WHEN USED WITH
      SUBROUTINE LSEQU. *** J.FENRICK *** MARCH 17,1973.

      BIBLIOGRAPHICAL REFERENCE

      SHILLING,STEVE A.,"A STUDY OF THE CHIRP Z-TRANSFORM AND ITS APPLICATIONS"
      KANSAS STATE UNIVERSITY MASTER'S THESIS, MANHATTAN,KANSAS 1972.


      SUBROUTINE CHIRPZ(XX,YY,VX,VY,XL,YL,CC,MM,NN,M,L,HAPH,RHPH)

      DIMENSION XX(1),YY(1),VX(1),VY(1),XL(1),YL(1),CC(1)
      DATA R2PI/6.2831853071/

      DN1=R2PI/NN
      DN2=R2PI*NN*PH/2.0

      DO 100 I=1,NN
      FIM1=FLOAT(I-1)
      THETA1=FIM1*(DN2+DN1*(L-1))
      VX(I)=XX(I)*COS(THETA1)-YY(I)*SIN(THETA1)
      VY(I)=YY(I)*COS(THETA1)+XX(I)*SIN(THETA1)
  100 CONTINUE
      NNP1=NN+1
      DO 110 I=NNP1,L
      VX(I)=0.0
      VY(I)=0.0
  110 CONTINUE


            COMPUTE FORWARD FFT

      CALL MKLFFT(VX,VY,CC,MM,0,-1)


            MULTIPLY THE SEQUENCE WITH THE L POINT SEQUENCE FROM SUBROUTINE
            LSEQU

      DO 140 I=1,L
      XX(I)=XL(I)*VX(I)-YL(I)*VY(I)
      YY(I)=YL(I)*VX(I)+XL(I)*VY(I)
  140 CONTINUE


            COMPUTE THE IDFT

      CALL MKLFFT(XX,YY,CC,MM,0,+1)


      DN1=1.0/FLOAT(L)
      DO 150 I=1,M
      FIM1=FLOAT(I-1)
      THETA1=DN2*FIM1**2
      XSAVE=XX(I)
      XX(I)=DN1*(XX(I)*COS(THETA1)-YY(I)*SIN(THETA1))
      YY(I)=DN1*(YY(I)*COS(THETA1)+XSAVE*SIN(THETA1))
  150 CONTINUE


      RETURN
      END
```

NUSC Technical Memorandum TC1-2-74
17 January 1974

Coherence Estimation Via the Partitioned Modified Chirp-Z Transform

G. C. Carter
C. H. Knapp

ABSTRACT

This is the oral version of a paper presented (in 7 minutes) on 17 January 1974 at the 1974 IEEE Arden House Workshop on Digital Signal Processing, Harriman Campus of Columbia University, Harriman, New York. It defines the coherence, discusses uses for this function, and briefly examines issues regarding its estimation.

We shall, in this presentation, define the coherence function, discuss uses for this function, and briefly examine issues regarding its estimation. Due to the limited time available, only the major points of our work will be covered. Acknowledgements and a partial bibliography are available from the authors.

FIRST SLIDE PLEASE

(SLIDE 1)

The coherence function between two wide-sense stationary random processes x and y is equal to the cross power spectrum divided by the square root of the product of the two auto power spectra (Ref. 1). It is, in effect, a normalized cross-spectral density function which can be shown to have a magnitude that falls between zero and unity.

NEXT SLIDE PLEASE

(SLIDE 2)

The coherence function has numerous uses including system identification, measurement of signal to noise power ratio, and determination of time delay.

In the system identification problem where M maps x into y, it can be shown that if M is a linear mapping, then the magnitude coherence equals unity. On the other hand, if x and y are uncorrelated, then the magnitude coherence equals zero (Ref. 2).

NEXT SLIDE PLEASE

(SLIDE 3)

Another use of the coherence is to measure the ratio of the signal power

at the output of a linear filter H to the noise power. In particular, if the system is linear but internal disturbances independent of the input contribute an additive component, n, to the output, then it can be verified that the ratio of the power spectrum G_z to the power spectrum G_n depends on the coherence as shown. Note also that the spectral characteristics of the noise can be determined from the coherence between x and y and the power spectrum of y. Specifically, if the magnitude coherence is unity, there is no noise; whereas if the magnitude coherence is zero, then the output is all noise (Ref. 1).

NEXT SLIDE PLEASE

(SLIDE 4)

Another example of measuring signal to noise power ratio is shown in this slide. Signal, s, is received at two sensors with equal power but different relative time delay A. In addition, each signal is corrupted by additive noise and filtered. When n_1 and n_2 are uncorrelated but have the same power spectra, then the ratio of the signal to noise power is given by the magnitude coherence over one minus the magnitude coherence (Ref. 1). Estimation of the relative time delay can be accomplished using the Smoothed Coherence Transform discussed in the October issue of the Proceedings of the IEEE (Ref. 3).

NEXT SLIDE PLEASE

(SLIDE 5)

In discussing the problem of estimating the magnitude squared coherence, the bias error will be considered first; then an estimation technique which reduces this error will be presented (Ref. 4). The maximum bias error under the

assumption that sufficient frequency resolution is available is one over the number of segments (Ref. 1); hence, for 100 segments the maximum bias is only one one hundredth. When sufficient resolution is available, variance, NOT bias, is a serious problem. If on the other hand, the number of independent data points P for each segment is too small, then the resulting poor frequency resolution can cause serious bias errors in estimating coherence (Ref. 5). In fact, in some cases of insufficient resolution, the maximum bias error has been observed to be independent of the number of segments averaged (Ref. 2). Specific examples exhibited biases of one tenth; however, the trend was indicative of the fact that any bias less than one could be expected if sufficient frequency resolution wasn't available. The practical implication of this limitation is that P must be large. This apparently requires computation of a large size fast Fourier transform, or FFT (Ref. 6). An alternative computation which reduces the required FFT size is the Partitioned Modified Chirp Z Transform or PAM-CZT (Ref. 7).

NEXT SLIDE PLEASE

(SLIDE 6)

In this technique the Chirp Z transform, or CZT, is modified to evaluate a large but limited number of points on the unit circle in the z plane. A sectioning algorithm is used to partition each P point segment into several smaller pieces (Ref. 7-8). The smaller pieces, or partitions, are then processed in short, time ordered sections which are recombined with an appropriate phasing function. This technique for computing a PAM-CZT allows for computation of the coherence in a manner paralleling FFT techniques. However, now a PAM-CZT is performed

in lieu of an FFT. Current research on implementation of the CZT (Ref. 9-11) should soon lead to inexpensive PAM-CZT hardware for coherence estimation.

In summary, knowledge of the coherence function is useful for system identification, measuring signal to noise power ratios, and determining signal time delay. Current studies indicate that these powerful features of the coherence can be realized through the PAM-CZT processing technique.

The significance of providing frequency resolution limited by the physical characteristics of the problem and not of the processing technique are that while the bias error of the coherence estimate is not a problem if sufficient resolution is available, it is a very serious problem if proper resolution is not available. Analytic results presented previously fail to point out this significant shortcoming of coherence estimation and how it can be overcome.

REFERENCES

1. G. C. Carter, C. H. Knapp and A. H. Nuttall, "Estimation of the Magnitude-Squared Coherence Function Via Overlapped Fast Fourier Transform Processing", IEEE Transactions on Audio and Electroacoustics, Vol. AU-21, No. 4, August 73, pp. 337-344.

2. G. C. Carter, "Coherence Estimation as Affected by Weighting Functions and Fast Fourier Transform Size", NUSC TR 4423, 12 Oct 72, New London, Ct.

3. G. C. Carter, A. H. Nuttall and P. G. Cable, "The Smoothed Coherence Transform", Proc. IEEE, Vol. 61, No. 10, pp. 1497-1498, October 1973.

4. R. K. Otnes and L. Enochson, Digital Time Series Analysis, Wiley Interscience, New York, 1972.

5. G. M. Jenkins and D. G. Watts, Spectral Analysis and Its Applications, Holden-Day, San Francisco, 1969.

6. L. R. Rabiner and C. M. Rader (Ed.), Digital Signal Processing, IEEE Press, New York, 1972.

7. J. F. Ferrie, C. W. Nawrocki and G. C. Carter, "The PAM-Chirp Z Transform", Proc. of the 1973 IEEE Conference in the Ocean Environment, September 1973, Seattle, Washington.

8. L. R. Rabiner, R. W. Schafer and C. M. Rader, "The Chirp Z-Transform Algorithm and Its Application", The Bell System Technical Journal, Vol. 48, No. 5, pp. 1249-1292, May-June 1969 and "The Chirp Z-Transform Algorithm", IEEE Transactions on Audio and Electroacoustics, Vol. AU-17, No. 2, pp. 86-92, June 1969.

9. D. D. Buss, D. R. Collins, W. H. Bailey and C. R. Reeves, "Transversal Filtering Using Charge-Transfer Devices", IEEE Journal of Solid State Circuits, Vol. SC-8, No. 2, pp. 138-146, April 1973.

10. D. D. Buss and W. H. Bailey, "Application of Charge Coupled Devices to Signal Processing", Manuscript Draft, Texas Instrument, Inc., Dallas, Texas.

11. J. M. Alsup, R. W. Means, and H. J. Whitehouse, "Real Time Discrete Fourier Transforms Using Surface Acoustic Wave Devices", Proc. IEEE International Specialist Seminar on Component Performance and System Applications of Surface Acoustic Wave Devices, Sept. 25-27, 1973, Aviemore, Scotland, U.K.

DEFINITION

$$\gamma(f) = \frac{G_{xy}(f)}{\sqrt{G_x(f)\,G_y(f)}}$$

PROPERTY

$$0 \leq |\gamma(f)| \leq |$$

SLIDE 1

SYSTEM IDENTIFICATION

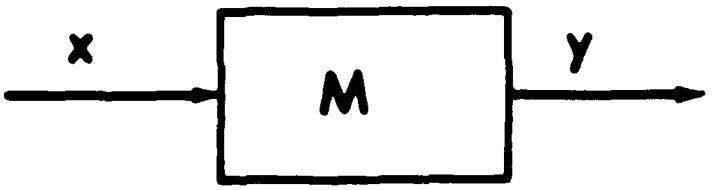

$$y = M(x)$$

CASE I: LINEAR MAPPING
CASE II: x AND y UNCORRELATED

SLIDE 2

MEASURING SIGNAL TO NOISE POWER RATIO

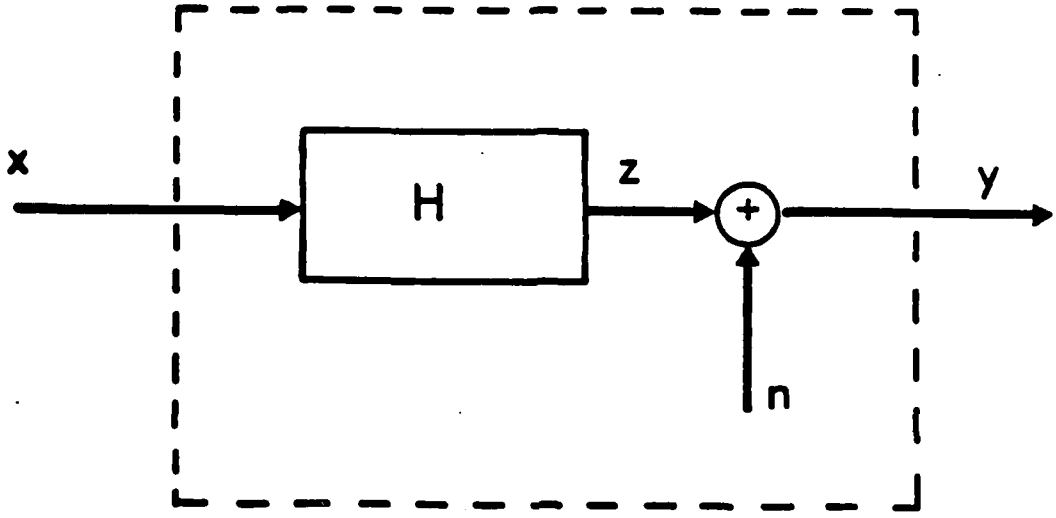

$$\frac{G_z(f)}{G_n(f)} = \frac{|\gamma_{xy}(f)|^2}{1 - |\gamma_{xy}(f)|^2}$$

$$G_n(f) = G_y(f)\left[1 - |\gamma_{xy}(f)|^2\right]$$

SLIDE 3

AD-A181 684 SCIENTIFIC AND ENGINEERING STUDIES COMPILED 1979 COHERENCE ESTIMATION(U) NAVAL UNDERWATER SYSTEMS CENTER NEWPORT RI G C CARTER ET AL. 1979 4/8

UNCLASSIFIED F/G 9/1 NL

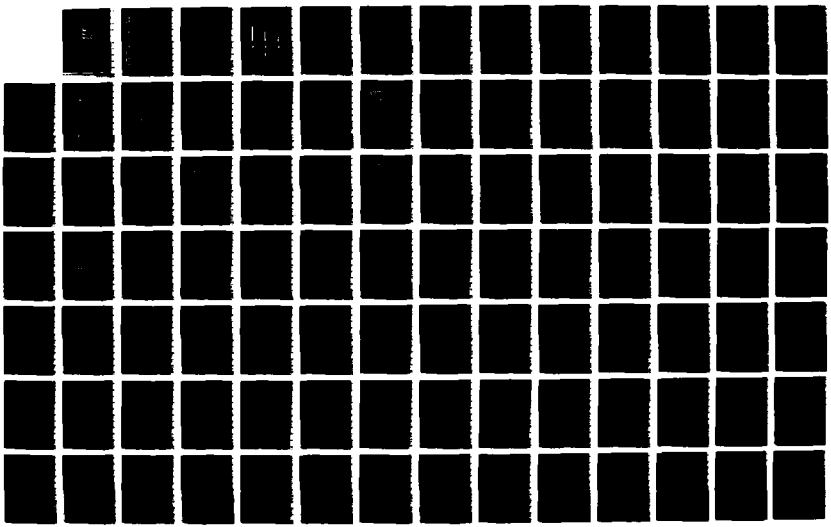

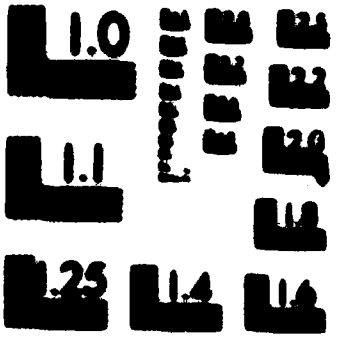

MEASURING SIGNAL TO NOISE POWER RATIO FOR DIRECTIONAL SIGNALS

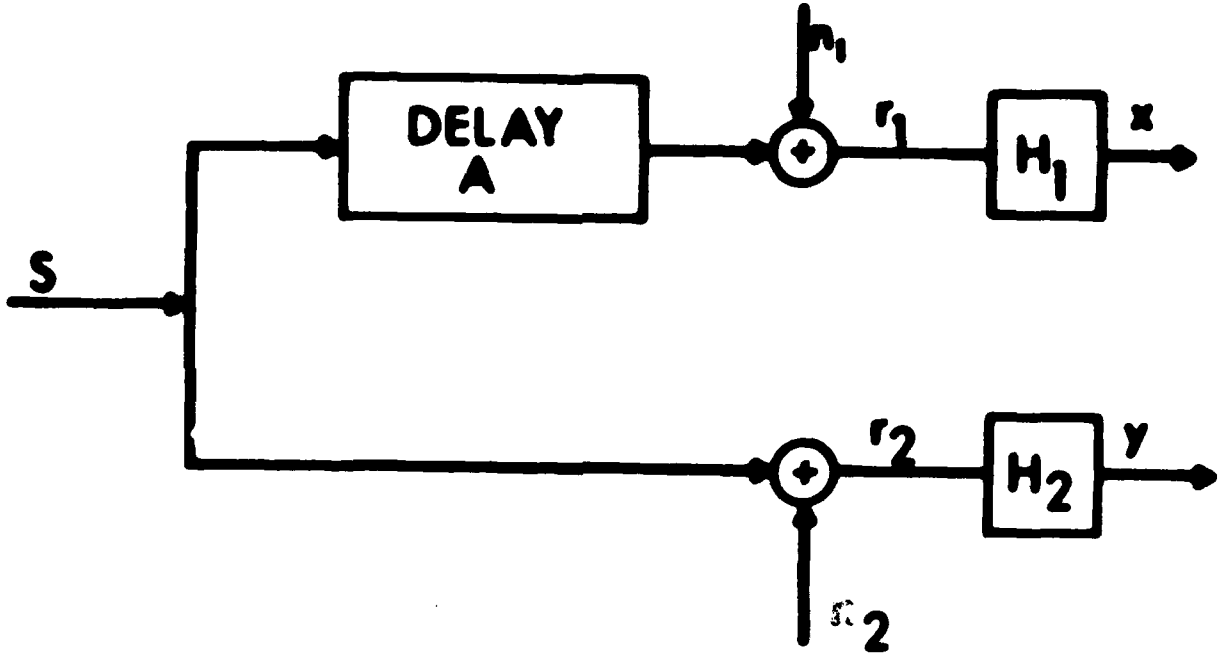

$$\frac{G_s(f)}{G_n(f)} = \frac{|\gamma_{xy}(f)|}{1-|\gamma_{xy}(f)|}$$

SLIDE 4

ESTIMATION TECHNIQUE

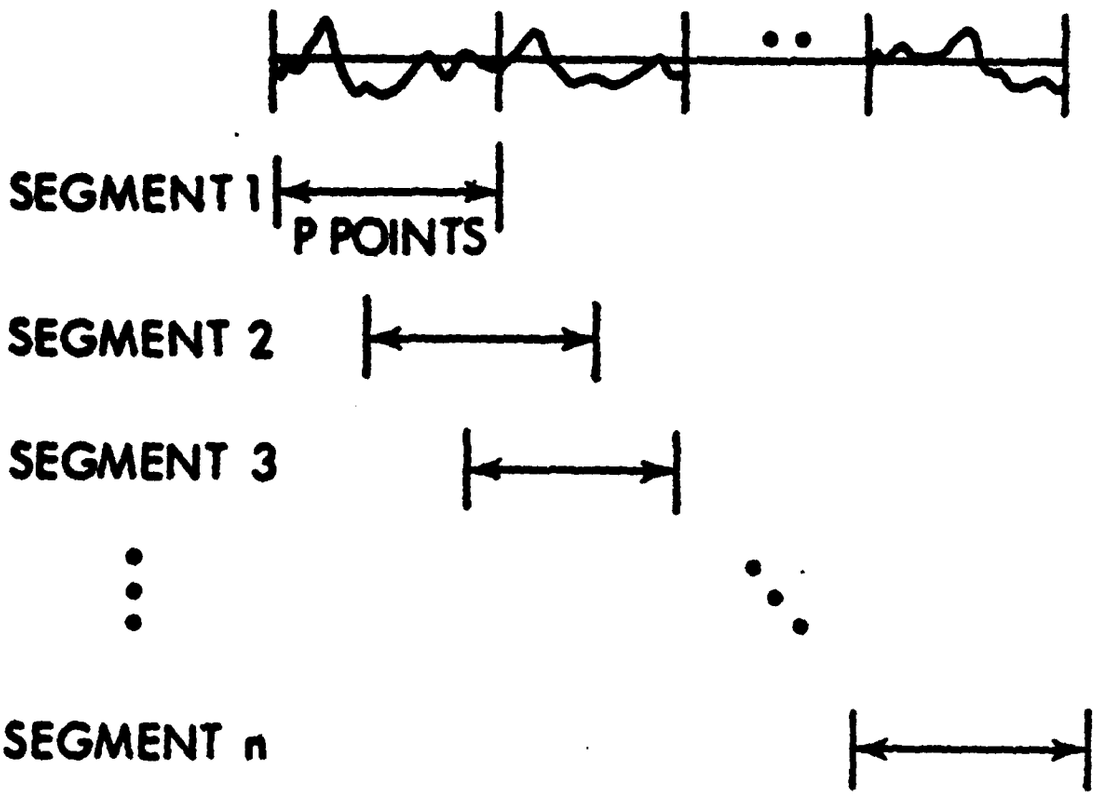

SLIDE 5

PAM CZT

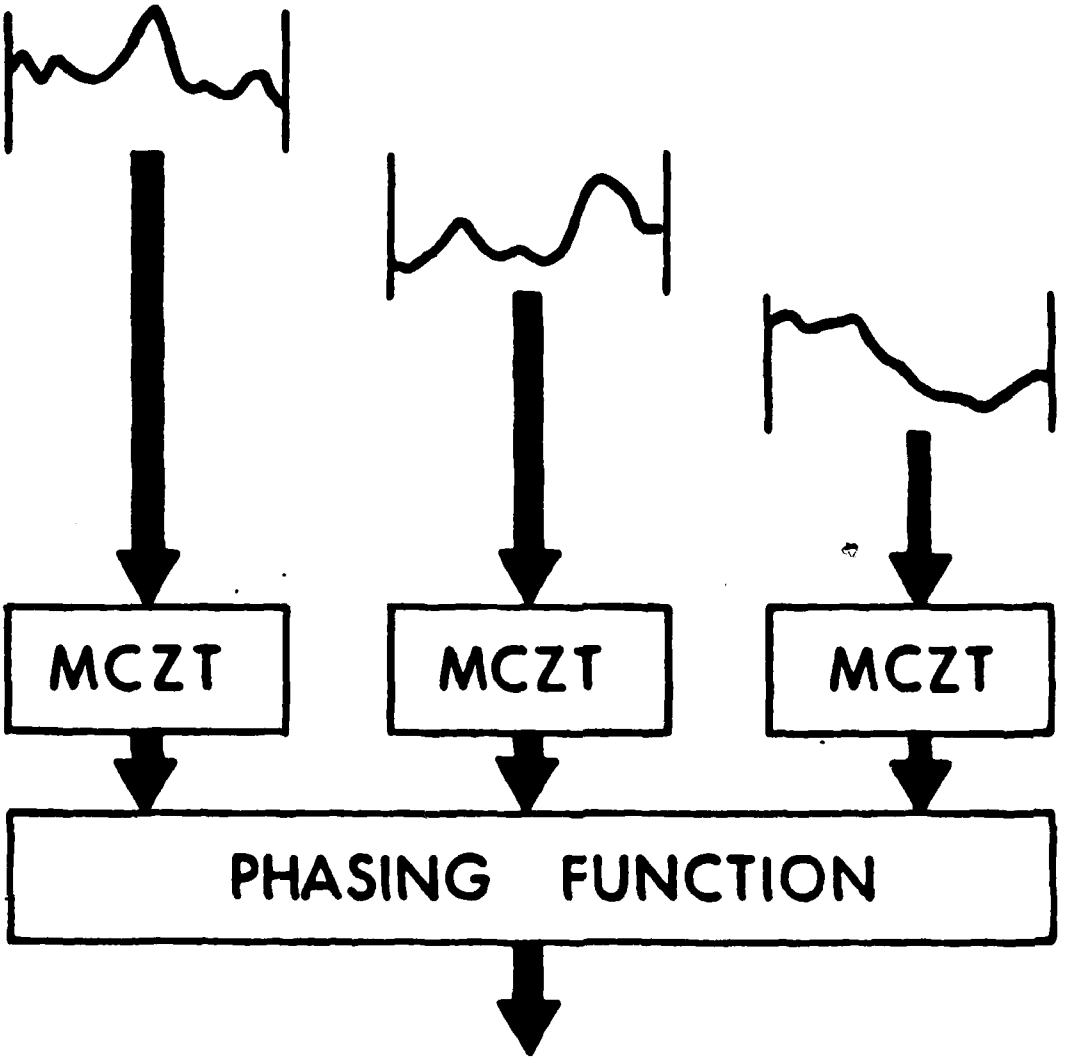

SLIDE 6

NUSC Technical Report 5291
9 March 1976

Approximations for Statistics of Coherence Estimators

A. H. Nuttall
G. C. Carter

ABSTRACT

Approximations for the bias, variance, and mean-square error of estimators of the magnitude-squared coherence and magnitude coherence are presented. The approximations are accurate for all values of true coherence and over the practically useful range of N, where N is the number of averages employed in the coherence estimators.

TABLE OF CONTENTS

LIST OF ILLUSTRATIONS

LIST OF ABBREVIATIONS AND SYMBOLS

MSC	Magnitude-Squared Coherence
MC	Magnitude Coherence
N	number of independent averages
${}_3F_2$	generalized hypergeometric function
F	Gauss hypergeometric function
x(t), y(t)	jointly stationary processes
f	frequency
$\gamma_{xy}(f)$	complex coherence
C(f), C	magnitude-squared coherence
$\hat{C}(f)$, $\hat{C}$	estimate of magnitude-squared coherence
$E\{Q\}$	ensemble average of random variable Q
μ_m	m-th moment of $\hat{C}$
Γ	gamma function
S(f), S	magnitude coherence
$\hat{S}(f)$, $\hat{S}$	estimate of magnitude coherence
$\alpha, \nu, \beta, \lambda$	constants (see (31) and (32))
σ^2_{app}	approximate variance
A, B, D	constants (see (34))
b_{app}	approximate bias
G_N	constant (see (40))

REVERSE BLANK

APPROXIMATIONS FOR STATISTICS OF COHERENCE ESTIMATORS

INTRODUCTION

Expressions for the probability density function, the cumulative distribution function, and any moment of the estimates of magnitude-squared coherence (MSC) and magnitude coherence (MC) are available in references 1-5. The expressions for the moments usually involve a generalized hypergeometric function* ${}_3F_2$ and require a time-consuming computer effort for their evaluation. Also, the fundamental dependence of statistics like the bias, variance, and mean-square error on the number of averages N and the true coherence are not obvious, because of the lack of significant results for the ${}_3F_2$ function.

This report will seek to present accurate approximations for these statistics, of as simple a nature as possible, and capable of hand calculation. Also, the dependence on N and on the true coherence will be deduced, and thereby future experiments can be designed in which the required stability can be predicted and attained with ease and certainty. As a by-product, a technique for reducing a particular type of ${}_3F_2$ function to a Gauss hypergeometric function (reference 7, chapter 15) is presented.

ESTIMATION OF MAGNITUDE-SQUARED COHERENCE

The complex coherence between two jointly stationary random processes $x(t)$ and $y(t)$ is defined as

$$\gamma_{xy}(f) = \frac{G_{xy}(f)}{\left[G_{xx}(f)\, G_{yy}(f)\right]^{1/2}}, \tag{1}$$

where $G_{xy}(f)$ is the cross-spectral density at frequency f, and $G_{xx}(f)$ and $G_{yy}(f)$ are the auto-spectral densities. The MSC is

$$C(f) = \left|\gamma_{xy}(f)\right|^2 . \tag{2}$$

*See, for example, reference 6, section 9.14.

The MSC is frequently estimated according to

$$\hat{C}(f) \equiv \frac{\left|\hat{G}_{xy}(f)\right|^2}{\hat{G}_{xx}(f)\,\hat{G}_{yy}(f)} = \frac{\left|\sum_{n=1}^{N} X_n(f)\,Y_n^*(f)\right|^2}{\sum_{n=1}^{N}\left|X_n(f)\right|^2 \sum_{n=1}^{N}\left|Y_n(f)\right|^2}, \tag{3}$$

where N is the number of data segments employed, and $X_n(f)$, $Y_n(f)$ are the (discrete) Fourier transforms of the n-th weighted data segments of $x(t)$ and $y(t)$.

GENERAL RELATIONS

The m-th moment of the random variable* $\hat{C}$ for independent data segments is given in reference 1, (4) and reference 2, (3) as

$$E\{\hat{C}^m\} \equiv \mu_m = \frac{\Gamma(N)\,\Gamma(m+1)}{\Gamma(N+m)}(1-C)^N\,{}_3F_2\,(m+1,\,N,\,N;\,N+m,\,1;\,C), \tag{4}$$

where C is the true MSC and ${}_3F_2$ is a generalized hypergeometric function. The power m need not be integer in (4).

For $m = 1$, the first moment of $\hat{C}$ can be reduced (reference 5, appendix B) to the simpler (and rapidly convergent) form

$$\mu_1 = \frac{1}{N} + \frac{N-1}{N+1} C\,F(1,\,1;\,N+2;\,C)\ , \tag{5}$$

where F is the Gauss hypergeometric function. For $m = 2$, the second moment of $\hat{C}$ can be reduced to the simpler form (see appendix A)

$$\mu_2 = -\frac{N^3 - 2N^2 + 2N - 2}{N} + \frac{N-1}{N+1}\left[N^2 - (N-2)\,C\right]\,F(1,\,1;\,N+2;\,C)\ , \tag{6}$$

which involves the F function with the same arguments as in (5). Equations (5) and (6) give exact results from which the bias, variance, and mean-square error of the MSC estimate $\hat{C}$ can be obtained.

---

*The f-dependence is suppressed for convenience.

BIAS APPROXIMATION

The bias of $\hat{C}$ is

$$\text{Bias}(\hat{C}) = E\{\hat{C}|C, N\} - C = \mu_1 - C \quad . \tag{7}$$

By expanding F in (5) in a power series in C and retaining terms to order N^{-2}, we obtain the approximation

$$\text{Bias}(\hat{C}) \cong \frac{1}{N}(1 - C)^2 \left(1 + \frac{2C}{N}\right) \quad . \tag{8}$$

Plots of (7) and (8) are given in figure 1 for $N = 8$ and 16. The discrepancy between the exact result (7) and the approximation (8) is barely discernible for $N = 8$ and is not discernible for $N = 16$. The discrepancy (between (7) and (8)) is even less for larger N. Equation (8) is a much simpler and more accurate approximation than reference 2, (5). The bias and approximation are observed to have a peak of value $1/N$ at the origin and to decrease monotonically with the value C of the true MSC.

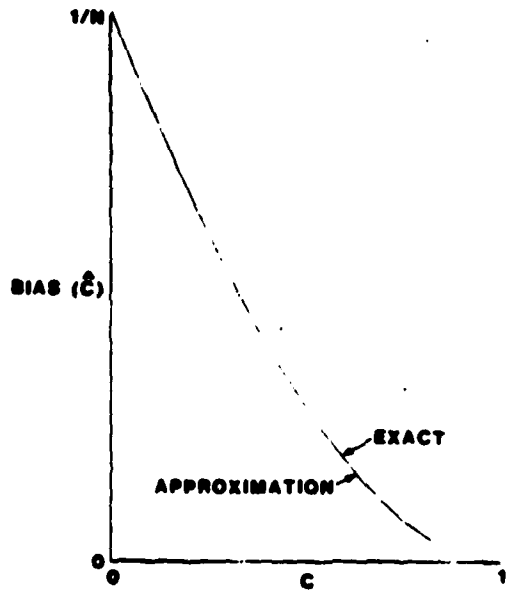

Figure 1A. $N = 8$

Figure 1. Bias of MSC Estimate

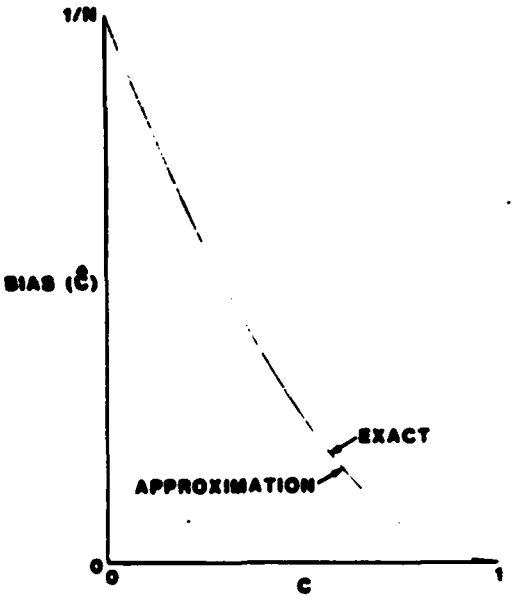

Figure 1B. N = 16

Figure 1 (Cont'd). Bias of MSC Estimate

VARIANCE APPROXIMATION

An expansion for the variance of $\hat{C}$ is given in reference 2, (6). If we expand the bracketed term to order N^{-1}, we obtain the approximation

$$\text{Variance}(\hat{C}) \cong \frac{N-1}{N(N+1)} (1-C)^2 \left[2C + \frac{1 - 6C + 13C^2}{N}\right] . \qquad (9)$$

This result can also be obtained from the exact expression

$$\text{Variance}(\hat{C}) = \mu_2 - \mu_1^2 \qquad (10)$$

combined with (5) and (6).

Plots of (9) and (10) are given in figure 2 for N = 8 and 16. The discrepancy between (9) and (10) is barely discernible for N = 16 and is not discernible for $N \geq 32$. Equation (9) is a much simpler and better approximation than reference 2, (6).

For large N, the peak of the variance occurs at $C \cong 1/3$ and is of value $8/27\ N^{-1}$. Thus, even when the true coherence is unknown, the maximum variance will be less than 0.3/N, for large N.

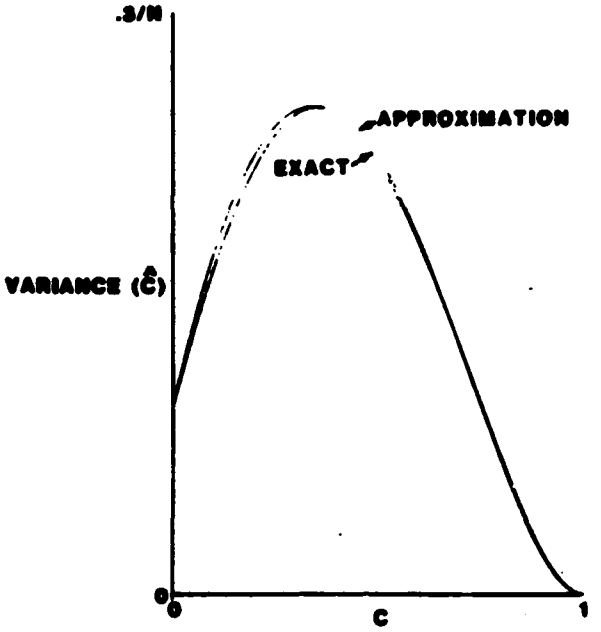

Figure 2A. N = 8

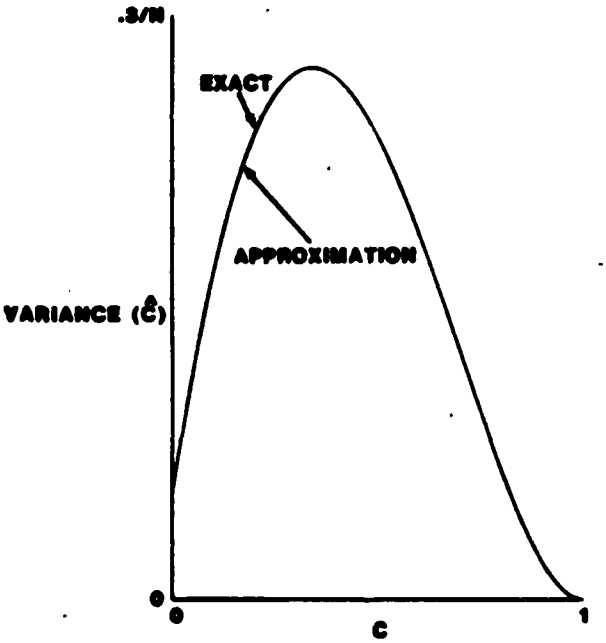

Figure 2B. N = 16

Figure 2. Variance of MSC Estimate

MEAN-SQUARE ERROR APPROXIMATION

The mean-square error of the MSC estimate $\hat{C}$ is

$$\text{Mean-Square Error}(\hat{C}) = E\left\{(\hat{C} - C)^2\right\}$$

$$= \left[\text{Bias}(\hat{C})\right]^2 + \text{Variance}(\hat{C})$$

$$= (\mu_1 - C)^2 + (\mu_2 - \mu_1^2) = \mu_2 - 2C\mu_1 + C^2 . \quad (11)$$

This exact result can be computed by means of (5) and (6). If we substitute approximations (8) and (9) in (11) and retain terms of the two highest orders in N, we obtain

$$\text{Mean-Square Error}(\hat{C}) \approx \frac{2}{N+1}(1 - C)^2\left[C + \frac{1 - 5C + 7C^2}{N}\right]. \quad (12)$$

Plots of (11) and (12) are presented in figure 3 for N = 8 and 16. The discrepancy between (11) and (12) is discernible for N = 16 but cannot be seen for $N \geq 32$.

For large N, the peak of the mean-square error occurs at C = 1/3 and is of value $8/27\ N^{-1}$.

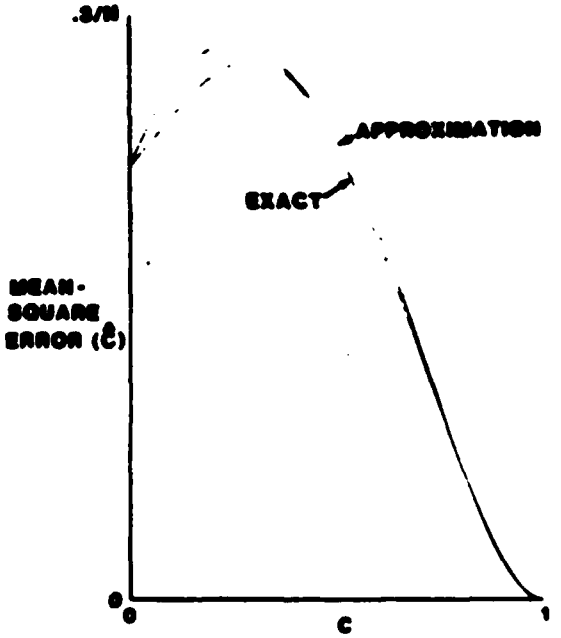

Figure 3A. N = 8

Figure 3. Mean-Square Error of MSC Estimate

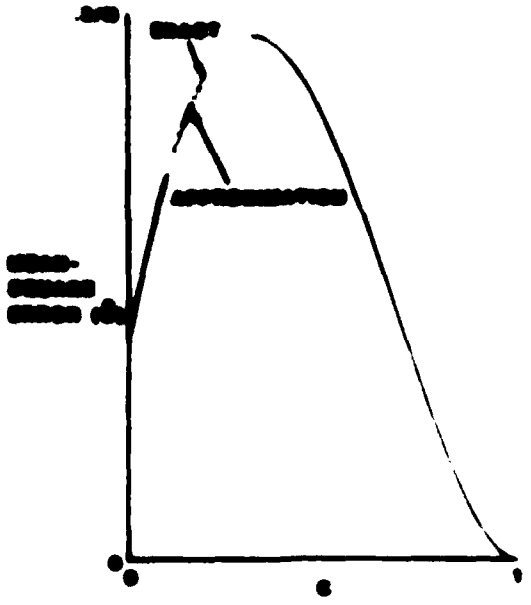

Figure 3b. M = 16

Figure 3 (Cont'd). Mean-Square Error of MSC Estimate

ESTIMATION OF MAGNITUDE COHERENCE

The magnitude coherence (MSC) is defined as

$$\gamma(f) = |\gamma_{xy}(f)| = \sqrt{C(f)} \tag{13}$$

upon use of (5). The estimate of MSC is

$$\hat{\gamma}(f) = \sqrt{\hat{C}(f)} \ , \tag{14}$$

where $\hat{C}(f)$ is defined in (9).

GENERAL RELATIONS

The first moment* of $\hat{\gamma}$ is available from (4) by setting $m = 1/2$:

$$E(\hat{\gamma}) = \frac{\Gamma(M)\Gamma(M+1/2)}{\Gamma(M)\Gamma(M+1/2)}(1-\gamma^2)^M \, {}_2F_1\left(\frac{3}{2}, M, M; M+1/2, \gamma^2\right) \ . \tag{15}$$

---

*The f-dependence is suppressed for convenience.

The second moment of $\hat{S}$ is directly available from (5):

$$E\{\hat{S}^2\} = \frac{1}{N} + \frac{N-1}{N+1} S^2 F(1, 1; N+2; S^2) \quad . \tag{16}$$

It will be noticed that (15) and (16) are even functions of S; this information will be useful in the approximate forms to be adopted later. Equations (15) and (16) give exact results from which the bias, variance, and mean-square error of the MC estimate $\hat{S}$ can be obtained.

A significant difference now exists between treatment of the MC estimate and the MMC estimate: whereas (6) could be reduced to an F function for m an integer, no such reduction has been discovered for (15). Further, (15) is not an appealing analytic result, as may be anticipated by noticing that, since (15) must equal unity at S = 1, and the leading factor contains an N-th order zero at S = 1, then ${}_3F_2(\ldots)$ must contain an N-th order pole at S = 1. No transformations or useful approximations of the ${}_3F_2$ function in (15) were discovered in references 6-11.

EXPANSIONS ABOUT S = 0

A direct series expansion of (6) yields

$$E\{\hat{S}^{2m}\} = \frac{\Gamma(N)\Gamma(m+1)}{\Gamma(N+m)} \left\{ 1 + \frac{m N(N-1)}{N+m} S^2 + \frac{m N(N-1)}{4(N+m)(N+1+m)} \left[(N^2 - N)(m-1) + 2(m+1) \right] S^4 + \ldots \right\} \quad . \tag{17}$$

Now, if m = 1, the N^2 and N terms in the S^4 term drop out, and we get a useful development in which the terms decay with N:

$$E\{\hat{S}^2\} = \frac{1}{N} + \frac{N-1}{N+1} S^2 + \frac{N-1}{(N+1)(N+2)} S^4 + \ldots \quad . \tag{18}$$

But, if m = 1/2, we obtain

$$E\{\hat{S}\} = \frac{\Gamma(N)\Gamma(3/2)}{\Gamma(N+1/2)} \left\{ 1 + \frac{N(N-1)}{2N+1} S^2 - \frac{N(N-1)(N^2-N-6)}{4(2N+1)(2N+3)} S^4 + \ldots \right\} \tag{19}$$

and the coefficients of S^2, S^4, ... increase with N, in direct contrast to results for MMC estimation. This increase is due to the two numerator terms and one denominator term in ${}_3F_2$ in (15) that depend on N.

EXPANSIONS ABOUT S = 1

If the results in (5) and (6) are expanded about $S = C = 1$ by means of reference 7, equation 15.3.11, we find the asymptotic expansions

$$E\{\hat{C}\} = C + \frac{1!}{N-2}(1-C)^2 - \frac{2!}{(N-2)(N-3)}(1-C)^3$$

$$+ \frac{3!}{(N-2)(N-3)(N-4)}(1-C)^4 + \ldots \tag{20}$$

and

$$E\{\hat{C}^2\} = 1 - 2(1-C) + \frac{N+2}{N-2}(1-C)^2$$

$$- \frac{4(N+1)}{(N-2)(N-3)}(1-C)^3 + \frac{6(3N+2)}{(N-2)(N-3)(N-4)}(1-C)^4 + \ldots \tag{21}$$

$$= C^2 + \frac{1}{N-2}(1-C^2)^2 - \frac{2}{(N-2)(N-3)}(1-C^2)^3$$

$$+ \frac{6 + \frac{N-N^2}{16}}{(N-2)(N-3)(N-4)}(1-C^2)^4 + \ldots \tag{22}$$

upon regrouping terms. Expressions (20) and (22) are useful near $C = 1$ and indicate how rapidly $E\{\hat{C}^m\} - C^m$ approach zero as C approaches one, for $m = 1$ and 2. It will be observed from (20) and (22) that the coefficients of $(1 - C^m)^2$ and $(1 - C^m)^3$ are identical, and those of $(1 - C^m)^4$ are similar.

It was thought that $E\{\hat{S}\} = E\{\hat{C}^{1/2}\}$ might possess a similar expansion in powers of $(1-C^{1/2}) = (1-S)$ and provide a useful method of evaluating (15), at least near $S = 1$. In appendix B, it is indeed shown (after considerable labor) that

$$E\{\hat{S}\} = 1 - \frac{1}{2}(1-C) - \frac{1}{8}\frac{N-4}{N-2}(1-C)^2 - \frac{1}{16}\frac{N^2-7N+16}{(N-2)(N-3)}(1-C)^3 + \ldots \tag{23}$$

$$= S + \frac{1}{N-2}(1-S)^2 - \frac{2}{(N-2)(N-3)}(1-S)^3 + \ldots \tag{24}$$

(upon regrouping terms), which has the identical coefficients as (20) and (22), up through the order computed. Equation (24) shows that the bias of the MC estimate $\hat{S}$ approaches zero as S approaches one according to $(1-S)^2/(N-2)$. Also, (24) and (20) can be combined to show that

$$\text{Variance}(\hat{S}) \cong \frac{(1-S^2)^2}{2(N-2)} \text{ as } S \to 1 \ . \tag{25}$$

This corroborates reference 4, (8).

CHOICE OF APPROXIMATION

Expansions like (20)-(25) cannot be used to evaluate the desired statistics for small S; in fact, they are divergent asymptotic expansions. When this information is combined with the earlier results about S = 0, we find that direct analytic expansions of (15) are not fruitful, in contrast with the earlier approach for MSC results. Instead, we must adopt some convenient simple approximation and try to match it to the exact results in some fashion. (The techniques in reference 12, chapter 9, are relevant in this regard.)

Before we do that, however, it is necessary to digress. We know that

$$\text{Bias}(\hat{S}) = E\{\hat{S}\} - S \ , \tag{26}$$

$$\text{Variance}(\hat{S}) = E\{\hat{S}^2\} - E^2\{\hat{S}\} \ , \tag{27}$$

$$\text{Mean-Square Error}(\hat{S}) = \left[\text{Bias}(\hat{S})\right]^2 + \text{Variance}(\hat{S}) \ , \tag{28}$$

where the exact moments are given in (15) and (16). A very good approximation to $E\{\hat{S}^2\} = E\{\hat{C}\}$ is already available from (7) and (8), namely,

$$E\{\hat{C}\} \cong C + \frac{1}{N}(1-C)^2\left(1+\frac{2C}{N}\right) \ , \tag{29}$$

or

$$E\{\hat{S}^2\} \cong S^2 + \frac{1}{N}(1-S^2)^2\left(1+\frac{2S^2}{N}\right) . \tag{30}$$

Therefore, if we can approximate $E\{\hat{S}\}$ or $\text{Bias}(\hat{S})$ or $\text{Variance}(\hat{S})$ in (26) and (27), we will have approximations for all three statistics in (26)-(28).

Initial attempts concentrated on approximating the bias (26) by the form

$$\frac{(1-S)^2}{N-2} + \alpha(1-S)^\nu, \quad \nu \geq 3 \ , \tag{31}$$

where α and ν were chosen so as to match the exact bias and its derivative at $S = 0$; these attempts were not successful for all N and S. A generalization to the form

$$\frac{(1-S)^2}{N-2} + (1-S)^\nu \left[\alpha + \beta S^2 (S-\lambda)\right], \quad \lambda = \frac{1.15}{\sqrt{N-2.85}}, \quad \nu \geq 3 \ , \tag{32}$$

was quite good for N up to 100, but deteriorated for larger N, despite also matching the exact second derivative of the bias at the origin. Numerous other forms were tried for approximating the bias but yielded poorer approximations.

VARIANCE APPROXIMATION

Succeeding attempts were aimed at approximating the variance (27). It will be recalled (from the discussion under (16)) that (27) is an even function of S. (This even property is not true of (26) or (28), because of the S term in (26).) The approximation to the variance was therefore also chosen to be even;* after much trial and error, an acceptable form was found to be

$$\text{Variance}(S) \approx \frac{(1-S^2)^2}{2(N-2)} \left[1 - \frac{3}{N}(1-S^2) + A\frac{(1-S^2)^2}{1 + BS^2 + DS^4}\right] \equiv \sigma^2_{app} \ . \tag{33}$$

The leading term in (33) is dictated by (25); the second term in the bracket was deduced from observing the numerical values of the variance near $S = 1$; and the numerator of the third term is chosen to make it decay faster than the other two terms near $S = 1$. Equation (33) already matches the value and derivative of the exact variance at $S = 1$, and the three constants were chosen so as to match the value and first four derivatives of the exact variance at $S = 0$; see appendix C. The end result of the investigation is that the constants are given by

$$A = -0.571 + \frac{1.75}{N} + \frac{0.760}{N^2}$$

$$B = 0.752\,N - 3.26$$

$$D = 0.221\,N^2 - 1.66\,N \ . \tag{34}$$

*See reference 12, pages 108 and 118.

Plots of the exact variance (27) and the approximate variance (33) are presented in figure 4 for N = 8, 16, 64, 256, and 1024. (Notice that the abscissa is S, not C.) The discrepancy does not go to zero as N increases, as it did for the MSC approximation; however, the discrepancy is small over the practical range of values of N (i.e., $N < 1000$), where N is the number of averages employed in the MC estimate.

The peak of Variance ($\hat{S}$) occurs at

$$S = \frac{4.6}{\sqrt{N}}\left(1 - \frac{9}{\sqrt{N}} + \frac{35}{N}\right) \text{ for } 64 \leq N \leq 1024 \qquad (35)$$

and is of value

$$\text{Peak Variance } (\hat{S}) = \frac{0.40}{N} - \frac{10}{N^2} + \frac{200}{N^3} \text{ for } 64 \leq N \leq 1024 \ . \qquad (36)$$

These results follow by fitting the exact numerical results in figure 4. For very large N, (36) suggests that the peak variance approaches $(2N)^{-1}$.

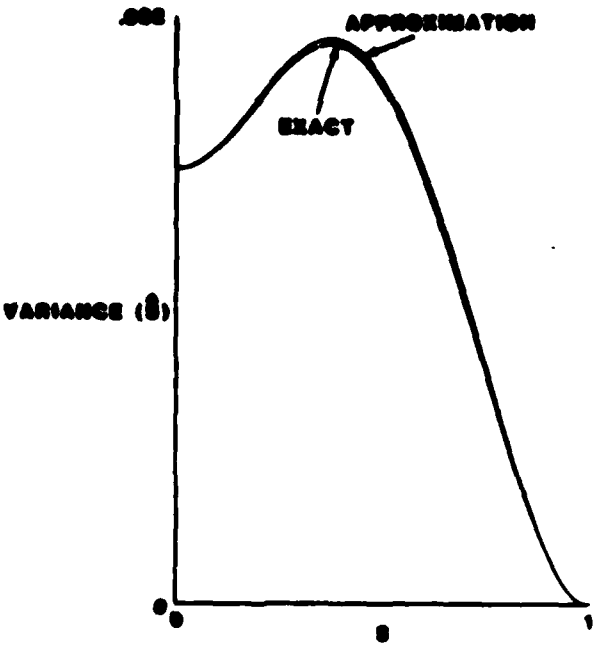

Figure 4A. N = 8

Figure 4. Variance of MC Estimate

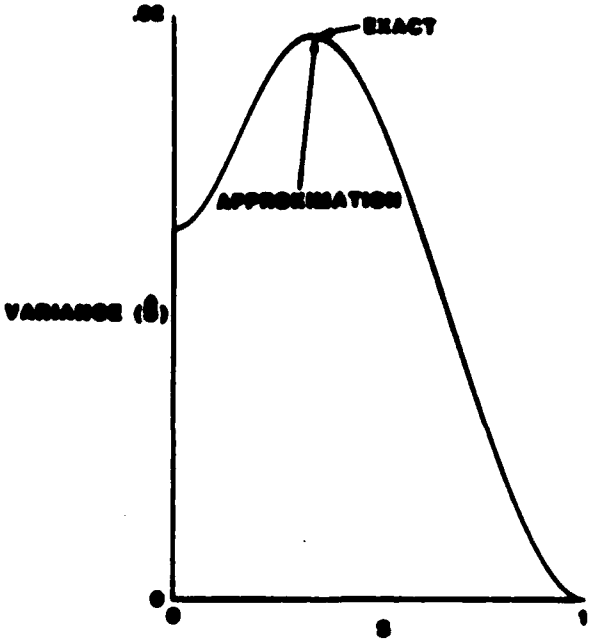

Figure 4B. N = 16

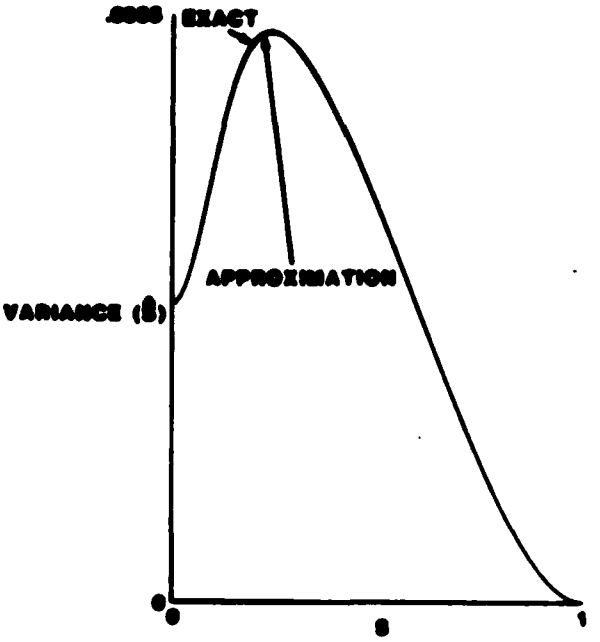

Figure 4C. N = 64

Figure 4 (Cont'd). Variance of MC Estimate

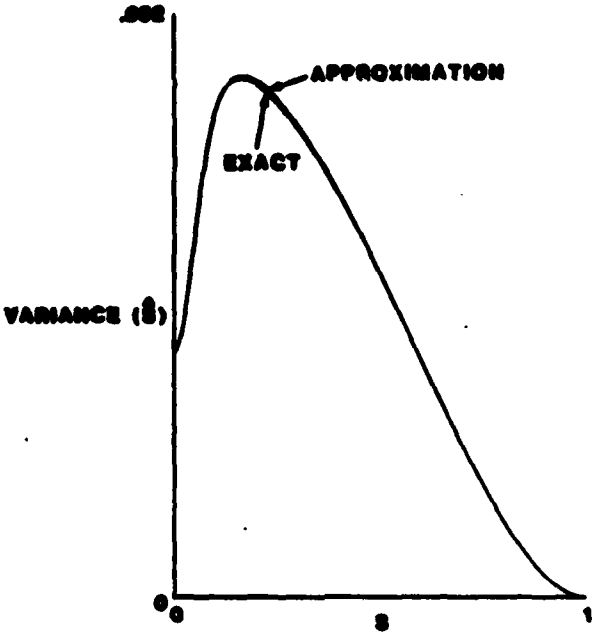

Figure 4D. N = 256

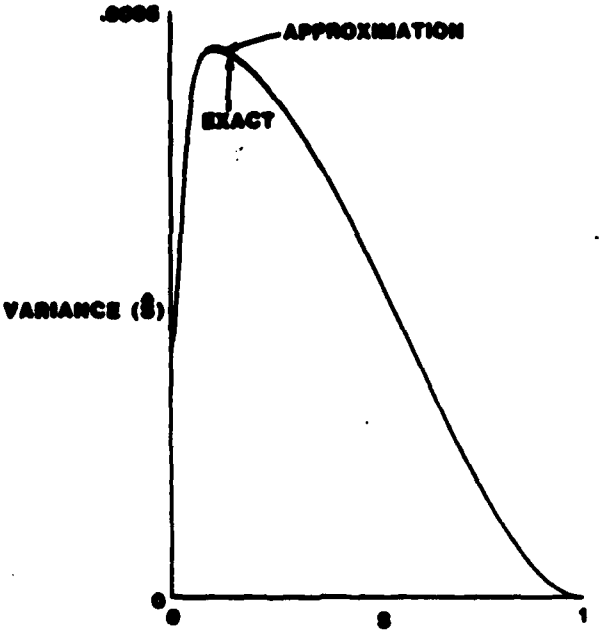

Figure 4E. N = 1024

Figure 4 (Cont'd). Variance of MC Estimate

At the origin, we have, from (15) and (16),

$$\text{Variance}\,(\hat{S}) = \frac{1}{N} - \left[\frac{\Gamma(N)\Gamma(3/2)}{\Gamma(N+1/2)}\right]^2$$

$$\cong \left(1 - \frac{\pi}{4}\right)\frac{1}{N} - \frac{\pi}{16}\frac{1}{N^2} = \frac{0.215}{N} - \frac{0.196}{N^2} \quad . \tag{37}$$

Here, we have employed the approximation (reference 7, equation 6.1.47)

$$\frac{\Gamma(N)\Gamma(3/2)}{\Gamma(N+1/2)} \cong \frac{\sqrt{\pi}/2}{\sqrt{N}}\left(1 + \frac{1}{8N}\right) \quad , \tag{38}$$

which is excellent even for N as small as 2.

BIAS APPROXIMATION

If we eliminate $E\{\hat{S}\}$ from (26) and (27), and then employ (30) and (33), we can express

$$\text{Bias}\,(\hat{S}) = \left[E\{\hat{S}^2\} - \text{Variance}\,(\hat{S})\right]^{1/2} - S$$

$$\cong \left[S^2 + \frac{1}{N}(1-S^2)^2\left(1 + \frac{2S^2}{N}\right) - \sigma_{app}^2\right]^{1/2} - S \cong b_{app} \quad . \tag{39}$$

This approach is in line with the observation made under (30). The approximate variance σ_{app}^2 in (39) is given by (33) and (34).

Plots of the exact bias (26) and the approximate bias (39) are presented in figure 5 for N = 8 and 16. The exact bias decreases monotonically with S and has an origin value of

$$\text{Bias}\,(\hat{S}\,|\,S = 0) = \frac{\Gamma(N)\Gamma(3/2)}{\Gamma(N+1/2)} \cong G_N \quad , \tag{40}$$

from (15); an excellent approximation to G_N is given in (38). The discrepancy between (26) and (39) is barely discernible for N = 8 and is not discernible for N = 16 up through N = 1024.

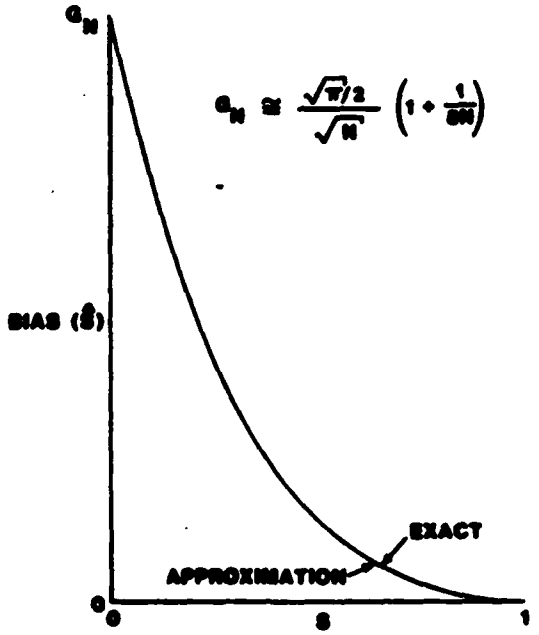

Figure 5A. N = 8

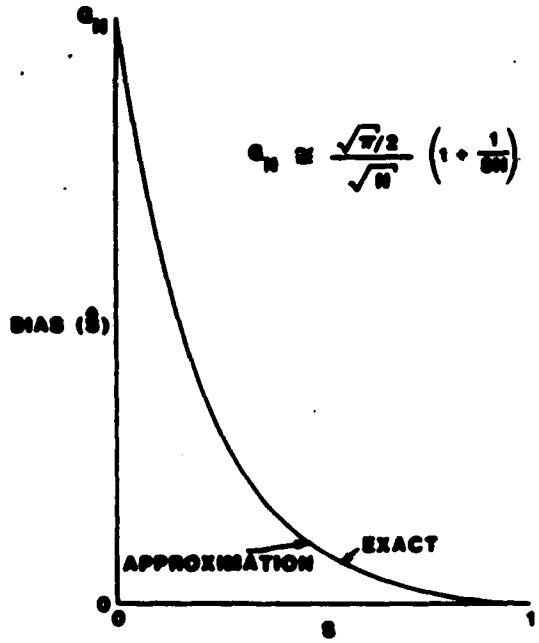

Figure 5B. N = 16

Figure 5. Bias of MC Estimate

MEAN-SQUARE ERROR APPROXIMATION

The approximation to the mean-square error is immediately available via (28):

$$\text{Mean-Square Error}\,(\hat{S}) \approx b_{app}^2 + \sigma_{app}^2 \,, \tag{41}$$

where the approximate bias and variance are given by (39) and (33), respectively. Plots of (28) and (41) are presented in figure 6 for N = 8, 16, 64, 256, and 1024. The discrepancy does not go to zero as N increases; however, it is small over the range of practically useful values of N.

The peak value of the mean-square error occurs at S = 0 and is of value 1/N, as is seen from (16). The mean-square error curve is composed of two distinct regions, one near the origin where the bias dominates, and one for larger S where the variance dominates; this explains the hump in the curves for larger N.

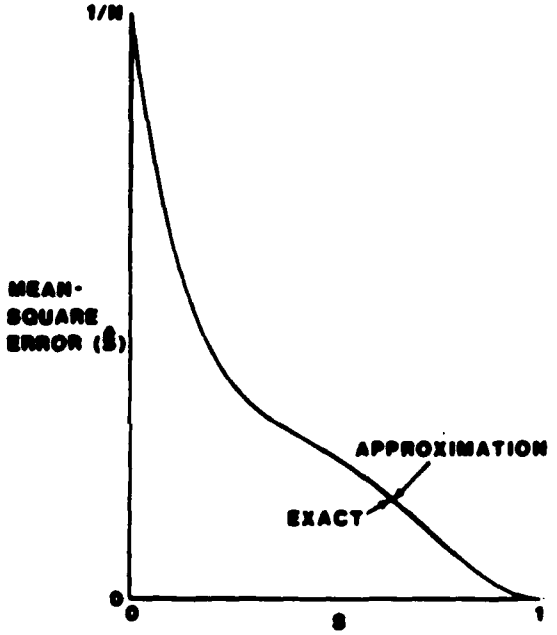

Figure 6A. N = 8

Figure 6. Mean-Square Error of MC Estimate

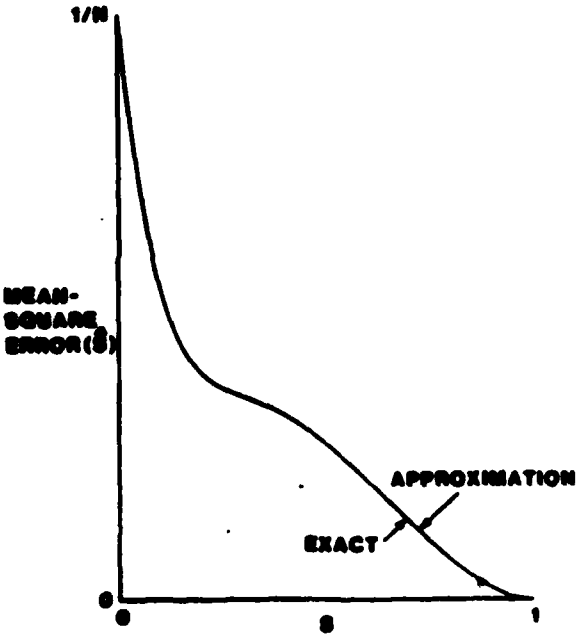

Figure 6B. N = 16

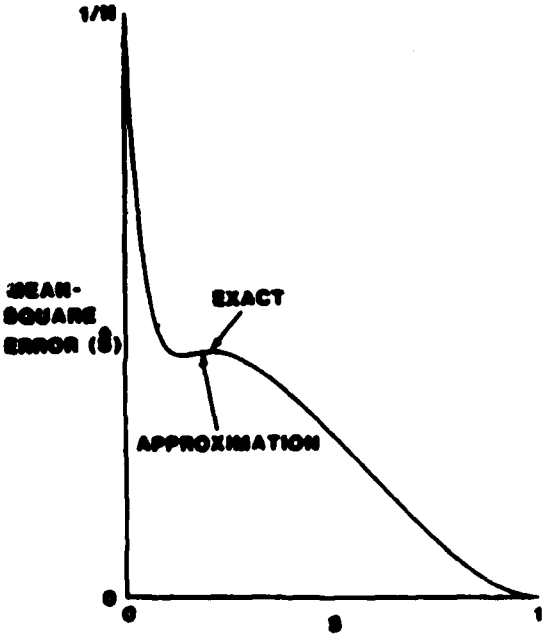

Figure 6C. N = 64
Figure 6 (Cont'd). Mean-Square Error of MC Estimate

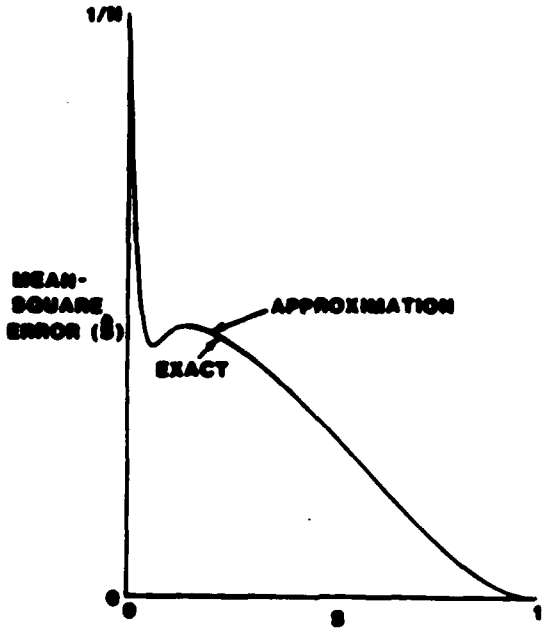

Figure 6D. N = 256

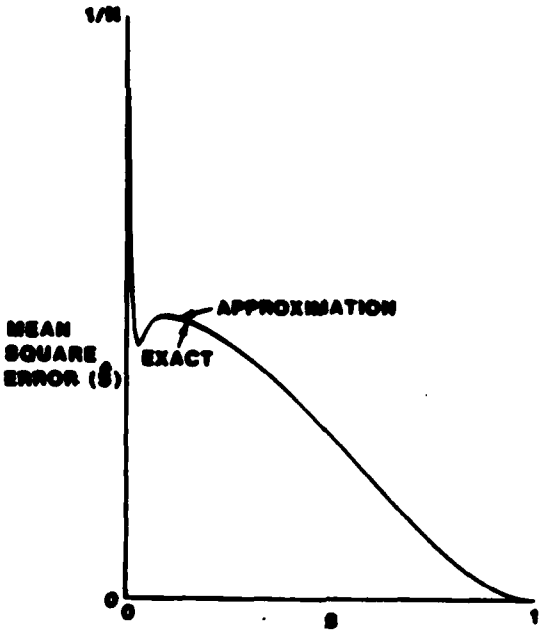

Figure 6E. N = 1024

Figure 6 (Cont'd). Mean-Square Error of MC Estimate

SUMMARY

Approximations for the MSC estimate are given by

$$\text{Bias}\,(\hat{C}) \approx \frac{1}{N}\,(1-C)^2\left(1+\frac{2C}{N}\right) \tag{8}$$

$$\text{Variance}\,(\hat{C}) \approx \frac{N-1}{N(N+1)}\,(1-C)^2\left[2C+\frac{1-6C+13C^2}{N}\right] \tag{9}$$

$$\text{Mean-Square Error}\,(\hat{C}) \approx \frac{2}{N+1}\,(1-C)^2\left[C+\frac{1-5C+7C^2}{N}\right] . \tag{12}$$

Approximations for the MC estimate are given by

$$\text{Variance}\,(\hat{S}) \approx \frac{(1-S^2)^2}{2(N-2)}\left[1-\frac{3}{N}\,(1-S^2)+A\,\frac{(1-S^2)^2}{1+BS^2+DS^4}\right] \approx \sigma^2_{app} , \tag{33}$$

where

$$A = -0.571+\frac{1.75}{N}+\frac{0.760}{N^2}$$

$$B = 0.752\,N - 3.26$$

$$C = 0.221\,N^2 - 1.66\,N . \tag{34}$$

$$\text{Bias}\,(\hat{S}) \approx \left[S^2+\frac{1}{N}\,(1-S^2)^2\left(1+\frac{2S^2}{N}\right)-\sigma^2_{app}\right]^{1/2} - S \approx b_{app} \tag{39}$$

$$\text{Mean-Square Error}\,(\hat{S}) \approx b^2_{app}+\sigma^2_{app} . \tag{41}$$

All of these are capable of hand calculation over the entire range of true coherence. The approximations for the MSC estimate are particularly simple; those for the MC estimate are somewhat more complicated, but far more tractable than the exact answers involving a ${}_3F_2$ function. The fundamental dependencies of the statistics on N and true coherence have also been deduced. Although the discrepancies between approximations and exact values do not tend to zero for the MC statistics for large N, the approximations are useful at least over the range from N = 8 to N = 1024, which is believed to encompass the region of most practical interest. How good the approximations are for larger N has not been investigated quantitatively.

REVERSE BLANK

Appendix A

REDUCTION OF THE $_3F_2$ FUNCTION

From (6) in the main text, we have

$$a_2 = \frac{2}{N(N+1)}(1-C)^N \, {}_3F_2\,(3, N, N; N+2, 1; C) \ , \qquad \text{(A-1)}$$

which is very slowly convergent for C near 1. Now, in (A-1), using reference 6, section 9.14, we have

$${}_3F_2\,(\cdots) = \sum_{k=0}^{\infty} \frac{(3)_k\,(N)_k}{(1)_k\,(N+2)_k} \, \frac{C^k}{k!} \, (N)_k \ . \qquad \text{(A-2)}$$

But

$$\frac{(3)_k}{(1)_k} = \frac{(k+1)(k+2)}{2} \qquad \text{(A-3)}$$

and

$$\frac{(N)_k}{(N+2)_k} = \frac{N(N+1)}{(N+k)(N+k+1)} \ . \qquad \text{(A-4)}$$

Substituting (A-3) and (A-4) in (A-2) and (A-1) yields

$$a_2 = (1-C)^N \sum_{k=0}^{\infty} \frac{(k+1)(k+2)}{(k+N)(k+N+1)} \, \frac{C^k}{k!} (N)_k \ . \qquad \text{(A-5)}$$

Now, a partial-fraction expansion yields

$$\frac{(k+1)(k+2)}{(k+N)(k+N+1)} = 1 + \frac{(N-1)(N-2)}{k+N} - \frac{N(N-1)}{k+N+1} \ ; \qquad \text{(A-6)}$$

and, since we can express

$$\frac{1}{k+N} = \frac{1}{N} \, \frac{(N)_k}{(N+1)_k} \ ,$$

$$\frac{1}{k+N+1} = \frac{1}{N+1} \, \frac{(N+1)_k}{(N+2)_k} \ , \qquad \text{(A-7)}$$

(A-8) takes the form

$$\mu_2 = (1-C)^N \left\{ \sum_{k=0}^{\infty} \frac{C^k}{k!} (N)_k + \frac{(N-1)(N-2)}{N} \sum_{k=0}^{\infty} \frac{(N)_k (N)_k}{(N+1)_k} \frac{C^k}{k!} \right.$$

$$\left. - \frac{N(N-1)}{N+1} \sum_{k=0}^{\infty} \frac{(N)_k (N+1)_k}{(N+2)_k} \frac{C^k}{k!} \right\} \qquad \text{(A-8)}$$

$$= (1-C)^N \left\{ F(n, b; b; C) + \frac{(N-1)(N-2)}{N} F(N, N; N+1; C) \right.$$

$$\left. - \frac{N(N-1)}{N+1} F(N, N+1; N+2; C) \right\} , \qquad \text{(A-9)}$$

upon employment of reference 7, equation 15.1.1. By use of reference 7, equation 15.3.3, this can be manipulated into the form

$$\mu_2 = 1 + \frac{(N-1)(N-2)}{N} (1-C) F(1, 1; N+1; C)$$

$$- \frac{N(N-1)}{N+1} (1-C) F(2, 1; N+2; C) , \qquad \text{(A-10)}$$

which is particularly good for developing in a series in $(1-C)$ by use of reference 7, equation 15.3.11.

At this point, a multitude of alternative forms for (A-10) are available by use of reference 7, page 558. Several rapidly convergent forms involving a single F function are now listed:

$$\mu_2 = - \frac{N^3 - 2N^2 + 2N - 2}{N} + \frac{N-1}{N+1} \left[N^2 - (N-2) C \right] F(1, 1; N+2; C) \qquad \text{(A-11)}$$

$$= \frac{2}{N(N+1)} - \frac{(N-1)(N-2)}{N+1} C$$

$$+ \frac{N-1}{(N+1)(N+2)} \left[N^2 - (N-2) C \right] C F(2, 1; N+3; C) \qquad \text{(A-12)}$$

$$= 1 + \frac{N-1}{N(N+1)} (1-C) \left\{ (N+1)(N-2) - \left[N^2 - (N-2) C \right] F(2, 1; N+2; C) \right\} . \qquad \text{(A-13)}$$

The form in (A-11) uses exactly the same F function as encountered in μ_1 in (5) and is more rapidly convergent than the latter two forms, for all values of C.

The reduction technique employed above for $m = 2$ in (4) can also be used for other integer values of m. However, it fails for m *noninteger*, because simplifications like (A-3) and (A-4) do not occur then.

Appendix B

EXPANSION ABOUT S = 1 FOR MAGNITUDE COHERENCE

The estimate of MSC is given in (3). We let

$$X_n(f) = (\xi_n + i\delta_n) \equiv \alpha_n$$

$$Y_n(f) = g(\xi_n + i\delta_n) + (\zeta_n + i\tilde{d}_n) \equiv g\alpha_n + \beta_n \quad , \tag{B-1}$$

where ξ_n, δ_n, ζ_n, $\tilde{d}_n$ are independent, zero-mean, unit-variance, real, Gaussian random variables. Then, for g real,

$$E\left\{X_n(f)\, Y_n^*(f)\right\} = E\left\{\alpha_n\, g(\alpha_n^* + \beta_n^*)\right\} = gE\left\{|\alpha_n|^2\right\} = 2g \ ;$$

$$E\left\{|X_n(f)|^2\right\} = 2; \quad E\left\{|Y_n(f)|^2\right\} = 2(1+g^2) \ . \tag{B-2}$$

Therefore, the MSC is

$$C = \frac{(2g)^2}{2 \times 2(1+g^2)} = \frac{g^2}{1+g^2}. \tag{B-3}$$

For a specified value C of the MSC, the required value of scale factor in (B-1) is

$$g = \left(\frac{C}{1-C}\right)^{1/2} \ . \tag{B-4}$$

Thus, as $S \to 1$, $C = g^2 \to 1$, $g \to \infty$, and $1/g \to 0$. Because we are interested in S near unity, we can concentrate on $1/g$ near zero.

If we define

$$A = \sum_{n=1}^{N} |\alpha_n|^2, \quad B = \sum_{n=1}^{N} |\beta_n|^2, \quad D = \sum_{n=1}^{N} \alpha_n \beta_n^* \ , \tag{B-5}$$

then substitution of (B-1) in (3) yields

$$\hat{C} = \frac{\left|\sum_{n=1}^{N} a_n (g a_n^* + \beta_n^*)\right|^2}{\sum_{n=1}^{N} |a_n|^2 \sum_{n=1}^{N} |g a_n + \beta_n|^2} = \frac{|D + gA|^2}{A(B + 2g D_r + g^2 A)}$$

$$= \frac{|D|^2 + 2gA D_r + g^2 A^2}{AB + 2gA D_r + g^2 A^2}, \qquad \text{(B-6)}$$

where D_r is the real part of D in (B-5). Rearranging (B-6), we obtain

$$\hat{C} = \frac{1 + \frac{1}{g}T + \frac{1}{g^2}U}{1 + \frac{1}{g}T + \frac{1}{g^2}V}, \qquad \text{(B-7)}$$

where

$$T = \frac{2D_r}{A}, \quad U = \frac{|D|^2}{A^2}, \quad V = \frac{B}{A}. \qquad \text{(B-8)}$$

Now a series expansion of (B-7) in powers of $1/g$ (as noted under (B-4)) yields

$$\hat{C} = 1 + \frac{a_2}{g^2} + \frac{a_3}{g^3} + \frac{a_4}{g^4} + \frac{a_5}{g^5} + \frac{a_6}{g^6} + \ldots, \qquad \text{(B-9)}$$

where

$$a_2 = U - V, \quad a_3 = -(U - V)T, \quad a_4 = (U - V)(T^2 - V),$$

$$a_5 = (U - V)(2V - T^2)T, \quad a_6 = (U - V)(T^4 + V^2 - 3T^2V). \qquad \text{(B-10)}$$

Since we are interested in the behavior of the MC estimate $\hat{S}$, we employ the expansion

$$(1 + e)^{1/2} = 1 + \frac{1}{2}e - \frac{1}{8}e^2 + \frac{1}{16}e^3 + \ldots \quad (|e| < 1) \qquad \text{(B-11)}$$

to obtain

$$\hat{S} = \sqrt{C} = 1 + \left(\frac{a_2}{2}\right)\frac{1}{\zeta^2} + \left(\frac{a_3}{2}\right)\frac{1}{\zeta^3} + \left(\frac{a_4}{2} - \frac{a_2^2}{8}\right)\frac{1}{\zeta^4}$$

$$+ \left(\frac{a_5}{2} - \frac{a_2 a_3}{4}\right)\frac{1}{\zeta^5} + \left(\frac{a_6}{2} - \frac{a_3^2}{8} - \frac{a_2 a_4}{4} + \frac{a_2^3}{16}\right)\frac{1}{\zeta^6} + \ldots . \qquad \text{(B-12)}$$

And, since we are interested in $\hat{S}$ near unity, we let

$$x = 1 - C \qquad \text{(B-13)}$$

and expand $\hat{S}$ in a power series in x. To do this, we utilize (B-4) and obtain

$$\frac{1}{\zeta} = \sqrt{\frac{x}{1-x}} = x^{1/2}\left(1 + \frac{1}{2}x + \frac{3}{8}x^2 + \ldots\right)$$

$$\frac{1}{\zeta^2} = x + x^2 + x^3 + \ldots$$

$$\frac{1}{\zeta^3} = x^{3/2}\left(1 + \frac{3}{2}x + \frac{15}{8}x^2 + \ldots\right)$$

$$\frac{1}{\zeta^4} = x^2\left(1 + 2x + 3x^2 + \ldots\right) = x^2 + 2x^3 + \ldots$$

$$\frac{1}{\zeta^5} = x^{5/2}\left(1 + \frac{5}{2}x + \ldots\right)$$

$$\frac{1}{\zeta^6} = x^3 + \ldots . \qquad \text{(B-14)}$$

Substitution of (B-14) in (B-12) yields

$$\hat{S} = 1 + x\left(\frac{1}{2}a_2\right) + x^{3/2}\left(\frac{1}{2}a_3\right) + x^2\left(\frac{1}{2}a_2 + \frac{1}{2}a_4 - \frac{1}{8}a_2^2\right)$$

$$+ x^{5/2}\left(\frac{3}{4}a_3 + \frac{1}{2}a_5 - \frac{1}{4}a_2 a_3\right)$$

$$+ x^3\left(\frac{1}{2}a_2 + a_4 - \frac{1}{4}a_2^2 + \frac{1}{2}a_6 - \frac{1}{8}a_3^2 - \frac{1}{4}a_2 a_4 + \frac{1}{16}a_2^3\right) + \ldots . \qquad \text{(B-15)}$$

Now we are ready to perform averages on the individual terms in (B-15) and obtain an expansion of $E\{\hat{S}\}$ in powers of $x = 1 - C$.

The method of obtaining $E\{a_2\}$ will be developed in full. The results for the other averages in (B-15) will merely be stated, and can easily be deduced from the method presented. From (B-10), (B-8), and (B-5),

$$a_2 = U - V = \frac{|D|^2 - BA}{A^2} = \frac{1}{A^2} \sum_{m,\, n=1}^{N} \beta_m^* \beta_n Q_{mn} \quad , \tag{B-16}$$

where we have defined

$$Q_{mn} = \alpha_m \alpha_n^* - A \delta_{mn} \quad . \tag{B-17}$$

Now, let

$$\underline{\alpha} \equiv \left[\alpha_1 \ \alpha_2 \ \ldots \ \alpha_N\right] \quad . \tag{B-18}$$

Then, since Q_{mn} depends only on $\underline{\alpha}$,

$$E\left\{U - V \middle| \underline{\alpha}\right\} = \frac{1}{A^2} \sum_{m,\, n=1}^{N} Q_{mn} E\left\{\beta_m^* \beta_n\right\}$$

$$= \frac{2}{A^2} \sum_{n=1}^{N} Q_{nn} = \frac{2}{A^2} \left[A - AN\right] = -\frac{2(N-1)}{A} \quad , \tag{B-19}$$

where we have utilized the property

$$E\left\{\beta_m^* \beta_n\right\} = 2 \delta_{mn} \quad , \tag{B-20}$$

which follows directly from the definitions (B-1). Therefore, using (B-19), we have

$$E\{U - V\} = -2(N-1) E\left\{\frac{1}{A}\right\} \quad . \tag{B-21}$$

Now, A is given by (B-5) and (B-1) as

$$A = \sum_{n=1}^{N} (\tilde{a}_n^2 + \tilde{b}_n^2) \quad . \tag{B-22}$$

Therefore, the probability density function of A is

$$p(A) = \frac{A^{N-1} \exp(-A/2)}{2^N (N-1)!}, \quad A > 0 \ . \tag{B-23}$$

There follows immediately the m-th moment of 1/A as

$$E\{1/A^m\} = \frac{1}{2^m} \frac{1}{(N-1)(N-2) \ldots (N-m)}, \quad m < N \ . \tag{B-24}$$

Employing (B-24) in (B-21), we have

$$E\{a_2\} = E\{U-V\} = -1 \ . \tag{B-25}$$

By employing the generalizations of (B-20) to the fourth and sixth orders, namely,

$$E\left\{\beta_k \beta_\ell^* \beta_m \beta_n^*\right\} = 4\left(\delta_{k\ell}\, \delta_{mn} + \delta_{kn}\, \delta_{\ell m}\right) ,$$

$$E\left\{\beta_k \beta_\ell^* \beta_m \beta_n^* \beta_p \beta_q^*\right\} = 8\left(\delta_{k\ell}\, \delta_{mn}\, \delta_{pq} + \delta_{k\ell}\, \delta_{mq}\, \delta_{np}\right.$$

$$\left. + \delta_{kn} \delta_{\ell m}\, \delta_{pq} + \delta_{kn}\, \delta_{\ell p}\, \delta_{mq} + \delta_{kq}\, \delta_{\ell m}\, \delta_{np} + \delta_{kq}\, \delta_{\ell p} \delta_{mn}\right) , \tag{B-26}$$

we find the following quantities:

$$E\left\{a_3\right\} = 0, \quad E\left\{a_4\right\} = \frac{N-1}{N-2}, \quad E\left\{a_2^2\right\} = \frac{N}{N-2} ,$$

$$E\left\{a_5\right\} = 0, \quad E\left\{a_2 a_3\right\} = 0, \quad E\left\{a_6\right\} = -\frac{N-1}{N-3},$$

$$E\left\{a_3^2\right\} = \frac{2N}{(N-2)(N-3)}, \quad E\left\{a_2 a_4\right\} = -\frac{N^2}{(N-2)(N-3)},$$

$$E\left\{a_2^3\right\} = -\frac{N(N+1)}{(N-2)(N-3)} \ . \tag{B-27}$$

When we employ (B-27) in (B-15), there follows

$$E\{\hat{S}\} = 1 - \frac{1}{2}(1-C) - \frac{1}{8}\frac{N-4}{N-2}(1-C)^2$$

$$- \frac{1}{16}\frac{N^2-7N+16}{(N-2)(N-3)}(1-C)^3 + \ldots \quad . \tag{B-28}$$

This is the end result quoted in (23) in the main text.

Appendix C

VARIANCE APPROXIMATION FOR MAGNITUDE COHERENCE

From (19) and (40) in the main text, we have

$$E\{\hat{S}\} = Q_0 + Q_1 S^2 + Q_2 S^4 + \ldots , \tag{C-1}$$

where

$$Q_0 = G_N$$

$$Q_1 = G_N \frac{N(N-1)}{2N+1}$$

$$Q_2 = G_N \frac{N(N-1)(6+N-N^2)}{4(2N+1)(2N+3)} . \tag{C-2}$$

And, from (18), we have

$$E\{\hat{S}^2\} = R_0 + R_1 S^2 + R_2 S^4 + \ldots , \tag{C-3}$$

where

$$R_0 = \frac{1}{N}$$

$$R_1 = \frac{N-1}{N+1}$$

$$R_2 = \frac{N-1}{(N+1)(N+2)} . \tag{C-4}$$

Therefore,

$$\text{Variance}(\hat{S}) = \alpha + \beta S^2 + \gamma S^4 + \ldots , \tag{C-5}$$

where

$$\alpha = R_0 - Q_0^2$$

$$\beta = R_1 - 2Q_0Q_1$$

$$\gamma = R_2 - Q_1^2 - 2Q_0Q_2 . \tag{C-6}$$

By use of (40) and reference 7, equation 6.1.47, we find

$$G_N = \frac{\sqrt{\pi}/2}{\sqrt{N}} \left[1 + \frac{1}{8N} + \frac{1}{128N^2} + \ldots \right] . \qquad \text{(C-7)}$$

Expanding the above expressions in powers of N^{-1}, we find

$$\alpha = \left(1 - \frac{\pi}{4}\right) \frac{1}{N} - \frac{\pi}{16} \frac{1}{N^2} - \frac{65\pi}{16384} \frac{1}{N^3} + \ldots$$

$$\beta = 1 - \frac{\pi}{4} - \left(2 - \frac{5\pi}{16}\right) \frac{1}{N} + \ldots$$

$$\gamma = -\frac{\pi}{32} N + \frac{7\pi}{128} + \ldots . \qquad \text{(C-8)}$$

Thus, (C-5) and (C-8) give a power series expansion of Variance ($\hat{S}$) that should be accurate for large N.

The variance approximation that we adopt is given in (33). We expand (33) in powers of S^2 and obtain

$$\sigma^2_{app} = \frac{1}{2(N-2)} \left[\left\{ 1 - \frac{3}{N} + A \right\} + S^2 \left\{ \frac{3}{N} - A(B+2) - 2\left(1 - \frac{3}{N} + A\right) \right\} \right.$$
$$\left. + S^4 \left\{ A\left((B+1)^2 - D\right) - 2\left(\frac{3}{N} - A(B+2)\right) + \left(1 - \frac{3}{N} + A\right) \right\} + \ldots \right] . \qquad \text{(C-9)}$$

We now select constants A, B, and D so that (C-5) and (C-9) match up through the power S^4. There follows

$$A = 2(N-2)\,\alpha - 1 + \frac{3}{N}$$

$$B = \frac{1}{A}\left[\frac{3}{N} - 2(N-2)(2\alpha + \beta)\right] - 2$$

$$D = (B+1)^2 - \frac{1}{A}\, 2(N-2)\,(3\alpha + 2\beta + \gamma) . \qquad \text{(C-10)}$$

We now employ the expansions for α, β, γ in (C-8) and obtain, finally,

$$A = -0.57080 + 1.7489/N + 0.76047/N^2 + \ldots$$

$$B = 0.75194N - 3.2639 + \ldots$$

$$D = 0.22142N^2 - 1.6648N + \ldots \qquad \text{(C-11)}$$

Equations (33) and (C-11) are the final results for the variance approximation. It has been found sufficient to retain only three decimals in the constants and to stop with the terms shown in (C-11).

REFERENCES

1. G. C. Carter and A. H. Nuttall, "Evaluation of the Statistics of the Estimate of Magnitude-Squared-Coherence," NUSC Technical Memorandum TC-183-71, 28 September 1971.

2. G. C. Carter and A. H. Nuttall, "Statistics of the Estimate of Coherence," Proceedings of the IEEE, vol. 60, no. 4, pp. 465-466, April 1972.

3. G. C. Carter, C. Knapp, and A. H. Nuttall, "Estimation of the Magnitude-Squared-Coherence Function Via Overlapped FFT Processing," IEEE Transactions on Audio and Electroacoustics, vol. AU-21, no. 4, pp. 377-344, August 1973.

4. G. C. Carter, C. Knapp, and A. H. Nuttall, "Statistics of the Estimate of the Magnitude-Coherence Function," IEEE Transactions on Audio and Electroacoustics, vol. AU-21, no. 4, pp. 388-389, August 1973.

5. G. C. Carter, "Estimation of the Magnitude-Squared-Coherence Function," M. S. Thesis, University of Connecticut, Storrs. Also in NUSC Technical Report 4343, 19 May 1972 (AD 743 945).

6. I. S. Gradshteyn and I. M. Ryzhik, Table of Integrals, Series and Products, Academic Press, New York, 1965.

7. Handbook of Mathematical Functions, U. S. Department of Commerce, National Bureau of Standards, Applied Mathematics Series No. 55, U. S. Government Printing Office, June 1964.

8. W. N. Bailey, Generalized Hypergeometric Series, Cambridge University Press, Great Britain, 1935.

9. Y. L. Luke, The Special Functions and Their Approximations, vols. I and II, Academic Press, New York, 1969.

10. H. Bateman, Higher Transcendental Functions, vols. I, II, and III, McGraw-Hill Book Co., Inc., New York, 1953.

11. E. D. Rainville, Special Functions, The Macmillan Company, New York, 1960.

12. C. Hastings, Jr., Approximations for Digital Computers, Princeton University Press, Princeton, New Jersey, 1955.

NUSC Technical Report 5336
9 April 1976

Time Delay Estimation

G. C. Carter

ABSTRACT

This study investigates methodologies for passive estimation of the bearing to a slowly moving acoustically radiating source. The mathematics for the solution to such a problem is analogous to estimating the time delay (or group delay) between two time series. The estimation of time delay is intimately related to the coherence between two time series. New results on using coherence to provide information about linear and nonlinear systems are presented.

The maximum likelihood (ML) estimate of time delay is derived; the explicit dependence of the estimate on coherence is evident in the realization in which the two time series are prefiltered (to accentuate frequency bands of high coherence) and subsequently crosscorrelated. The hypothesized delay at which the generalized crosscorrelation (GCC) function peaks is the time delay estimate. The variance of the time delay estimate is obtained. Other realizations are considered. The estimation formulation is extended to: multiple sources, moving sources, and multiple sensors.

Also included are statistics of the estimates of the magnitude-squared coherence (MSC), including the probability density function, the cumulative distribution function, and the m-th moment of the MSC estimate. A complete discussion of the bias and the variance of the MSC estimates is presented. The receiver operating characteristics of a linearly thresholded coherence estimation detector are also presented. A general FORTRAN IV computer program using the fast Fourier transform to estimate time delay is given.

TABLE OF CONTENTS

LIST OF TABLES

LIST OF ILLUSTRATIONS

LIST OF SYMBOLS AND ABBREVIATIONS

Symbols

B( )	bias of
$C_{x_1x_2}$( )	magnitude-squared coherence
d	distance (meters) between two sensors
d_f	deflection criterion
D	true but unknown time delay (sec)
E( )	mathematical expectation
f	frequency (Hz)
$_2F_1$	hypergeometric function
$G_{x_1x_1}$( )	auto-power spectrum of $x_1(t)$
$G_{x_1x_2}$( )	cross-power spectrum of $x_1(t)$ with $x_2(t)$
He_n( )	Hermite polynomial
H	linear time invariant filter
Im( )	imaginary part of
I_{xy}	information between x(t) and y(t)
j	$\sqrt{-1}$
J_i	cost (award) functions
n(t)	noise waveform
N	number of independent FFT's
p( )	first order probability density function
P	number of data points per FFT
Prob( )	probability

Q_x	power spectral density matrix of x
$R_{x_1x_2}(\ )$	crosscorrelation function of $x_1(t)$ with $x_2(t)$
$\underline{R}_x(\ )$	crosscorrelation matrix
Re( )	real part of
s(t)	signal waveform
t	time (sec)
T	observation time (sec)
$\underline{V}$	steering vector
$Var(\hat{v})$	variance of random variable $\hat{V}$
$Var^{R1}(\hat{v})$	variance of random variable $\hat{V}$ which has been estimated according to rule R1
$X_n(k)$	DFT of n-th weighted data segment of x(t) at k-th frequency
W( )	weighting function
α	attenuation
β	time compression
$\hat{\beta}$	β/β_a
$\gamma_{x_1x_2}(f)$	complex coherence of $x_1(t)$ with $x_2(t)$
$\Gamma(\ )$	Gamma function
$\phi_{x_1x_2}(\ )$	phase of cross-power spectrum of $x_1(t)$ with $x_2(t)$
θ	bearing angle
$\eta(\ )$	no memory nonlinearity
$\rho(\ )$	normalized crosscorrelation
σ_v^2	variance of random variable v
σ_v	standard deviation of random variable v

τ	hypothesized time delay (sec)
ω	$2\pi f$ (rad/sec)
ω_Δ	$2\pi/T$
ξ	nominal speed of sound in the nondispersive medium (water)
$\hat{}$	estimate; for example, $\hat{D}$ is the estimate of D
$\forall$	for all
$\bullet$	convolution
$(z)_k$	Pochhammer's symbol
*	complex conjugate

Abbreviations

AML	approximate maximum likelihood
CC	complex coherence
cdf	cumulative distribution function
CZT	Chirp Z-transform
DFT	discrete Fourier transform
FFT	fast Fourier transform
FIR	finite impulse response
LOP	line of position
MAD	multiplication and addition
MC	magnitude coherence
MCZT	modified Chirp Z-transform
ML	maximum likelihood
MMSE	minimum MSE
MSC	magnitude-squared coherence
MSE	mean square error
PAM-CZT	partitioned and modified CZT

pdf	probability density function
PHAT	phase transform
ROC	receiver operating characteristics
SCOT	smoothed coherence transform
SNR	signal-to-noise ratio

CHAPTER 1

INTRODUCTION

This research investigates methods for estimating the position of a moving source by the processing of an acoustically radiated signal received at two or more physically separated sensors. If the source signal is received at two geographical positions in the presence of uncorrelated noise, then, depending on the signal strength and duration, it is possible to estimate the bearing to the source relative to the sensor baseline. When the source signal is received at three sensors, range, as well as bearing to the source, can be estimated by using the intersection of two bearing lines of position (LOPs). The mathematics for the solution to the problem of finding the "best" estimate of bearing is analogous to the more general problem of estimating the time delay (or group delay) between two time series. Therefore, this dissertation derives the maximum likelihood (ML) estimate time delay.

Techniques for estimation of time delay can be applied to a variety of practical problems, in addition to those motivating this research. For example, if we consider a signal which probes a linear time invariant

system, then the problem of estimating time delay can be viewed as attempting to identify a parameter of the probed system, based on time-limited, noise-corrupted observations of the system input and output. The delay is a particularly valuable characterization of the system (and interrelationship between two processes) when the system output is an attenuated and delayed version of the input. Physical plants in which delays occur can also be visualized in terms of the bearing estimation problem.

For example, consider two geographically separated sensors that receive a signal from an acoustically radiating point source, as shown in Figure 1-1. If the properties of the medium are such that the signal from the source propagates at a constant velocity, then the travel time from the source to either sensor is directly proportional to the distance traveled. Thus, the difference between the travel time (from the source to each sensor) or time delay is given by the difference in path lengths divided by the propagation velocity. There exists a well defined locus of points (relative to the sensors) for which the time delay is constant. Hence, knowledge of the time delay is sufficient to dictate that the source is located somewhere on that locus of points. In particular, the acoustic source must be located on the locus of points that satisfies the constant time delay constraint, namely, the hyperbola in Figure 1-2. The bearing angle, θ, that the hyperbolic asymptote makes with the baseline is a good approximation

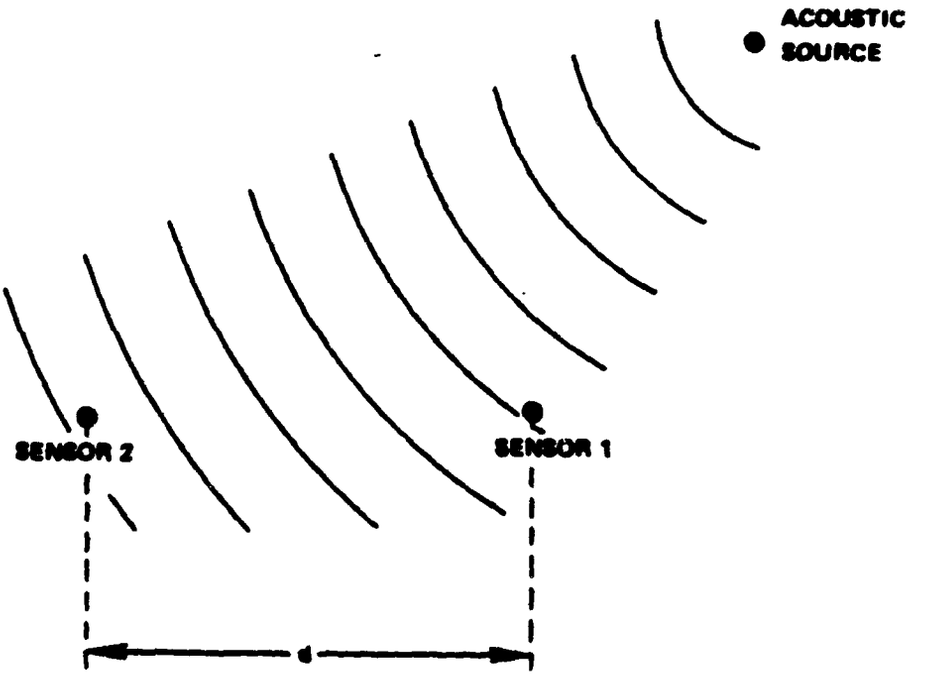

Figure 1-1 Acoustic Source and Sensors

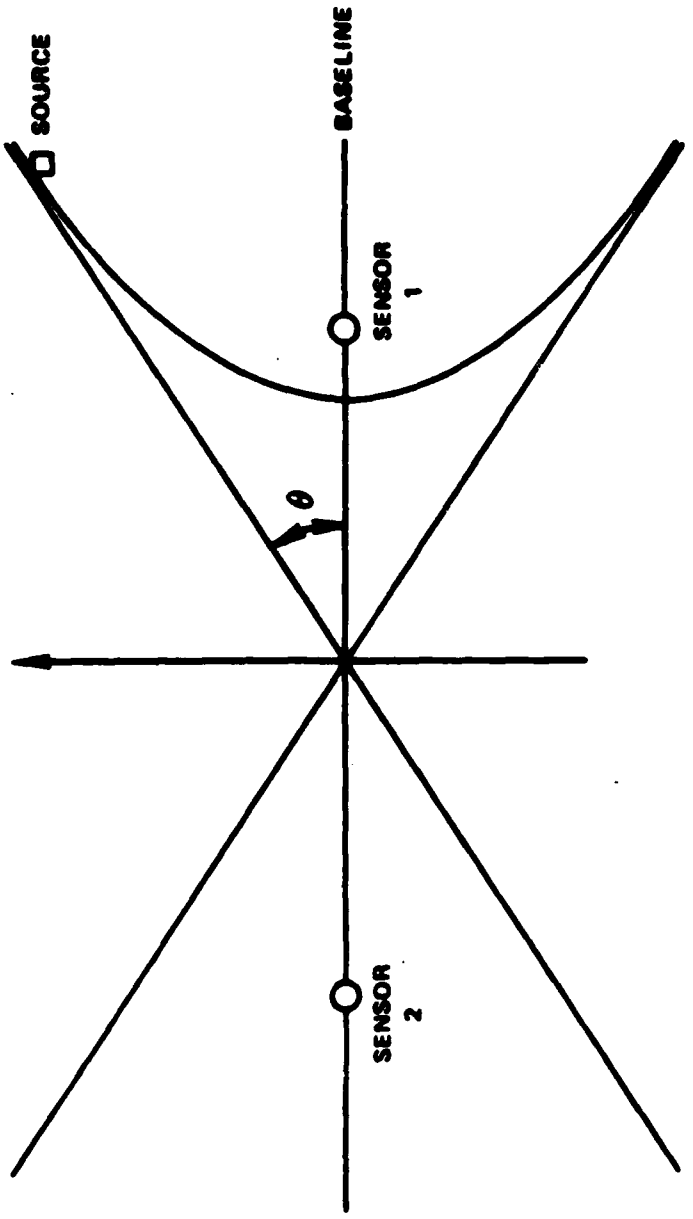

Figure 1-2 Bearing Angle Interpretation

to the true bearing to the source (relative to the midpoint of the baseline) especially for distant sources. Thus, by making a distant point source (or equivalently a plane wave) assumption and solving for the bearing angle θ, one is equivalently finding the angle that the hyperbolic asymptote (or line of position (LOP)) makes with the baseline. Familiarity with hyperbola suggests that the source need not be very distant (relative to the sensor separation d) in order for the arrival angle to be a good estimator of true source angle. In the estimation problem, the receivers are attempting to estimate bearing (or position) of a source that is radiating a signal either intentionally or unintentionally. During intentional radiation (for example, a communications system) signal statistics are selectable within certain practical and regulatory limitations. In other applications, the signal characteristics are unknown and the output of the sensors must be processed without this a priori knowledge in order to estimate time delay or equivalently source bearing. In this thesis it is assumed that the source characteristics are not under the control of the designer and at best the spectral characteristics of the signal are known or estimated.

The time delay estimation research presented in this text is arranged in six chapters and four appendices. Because the estimation of time delay and bearing is intimately related to the coherence between two received

waveforms, an extensive investigation of coherence is given (in Chapter 2). New results on using coherence to provide information about linear and nonlinear system identification are presented and proved. Among other results, Chapter 2 explicitly shows how the signal-to-noise ratio (SNR) is a function of coherence.

In Chapter 3, the ML estimate of time delay between two signals is derived under jointly stationary Gaussian assumptions. The explicit dependence of the time delay estimate on coherence is evident in the estimator realization in which the two time series are prefiltered (to accentuate frequency bands according to the strength of the coherence) and subsequently crosscorrelated. The time argument at which the generalized crosscorrelation (GCC) function peaks is the time delay estimate (Carter and Knapp (1976a)). The method of derivation is akin to the ML bearing estimate derived by MacDonald and Schultheiss (1969) with two exceptions: (1) the technique here requires no plane wave assumption but finds the ML estimate of the more general time delay parameter, from which one can estimate both the hyperbolic LOP and source bearing, and, (2) the derivation here does <u>not</u> constrain the additive noise waveforms at different sensors to have the same spectral characteristics. These conditions allow for widely spaced sensors since the spectral characteristics of the noise can be different and the

signal wavefront is not constrained to be planar.

Having derived the ML estimate of time delay, we show that it is equivalent to the GCC function with prefiltering suggested by Hannan and Thomson (1973). Although the ML estimator is the same as the method suggested by Hannan and Thomson (1973), this could not have been accurately predicted ahead of time. The Hannan Thomson (HT) processor was obtained as a GCC function with optimally determined weighting. In related work, Clay, Hinich, and Shaman (1973) arrived at a less general ML estimate for bearing, due to the assumption that the signal spectral characteristics were flat in the frequency band of interest. The results of this thesis are also more general than those of MacDonald and Schultheiss (1969) because there is no signal plane wave assumption and the noise spectral characteristics can differ from sensor to sensor.

When the received signal and noise waveforms are stationary and Gaussian with known spectral characteristics, it is shown that the ML estimate of time delay achieves the Cramér-Rao bound. Thus, the ML estimate, in this case, achieves a variance less than or equal to that attained by any other means. Two realizations of the time delay estimate are given: the first, uses the GCC function with appropriate prefilters; the second appropriately filters, sums, squares, and averages as

suggested by Carter and Knapp (1976a). Further, when the spectral characteristics are known the variance of the delay estimates is derived for all GCC processors. When the signal and noise spectral characteristics are unknown, as is often the case in the passive bearing estimation problem, it is suggested that an approximate technique be used, whereby estimates of the ML weighting are inserted in the place of the correct weighting. This heuristic procedure will converge to the ML estimate provided the weighting is properly estimated. The appendices summarize work in this area by Carter, Knapp, and Nuttall (1973a) to estimate the spectral densities including coherence. (Details of the appendices are discussed later in the introduction.)

In Chapter 4, the variances of six proposed time delay estimates, including ones suggested by Roth (1971) and Carter, Nuttall, and Cable (1973), are compared for an example case where the signal and noise have rectangular spectra with different bandwidths. The results confirm the advantages of ML time delay estimation.

The estimation formulation is extended, in Chapter 5, to three important generalizations: multiple sources, moving source, and multiple sensors. The multiple source problem introduces a new term in the award function which was maximized in Chapter 3 to obtain a single time delay estimate. This additional term is the

information between two processes. Nettheim (1966), using results of Gelfand and Yaglom (1959), has shown the Shannon (1949) definition of information to be directly related to the coherence between two processes. Thus, as with the single time delay estimation problem, coherence plays an important role. Source motion significantly complicates the bearing estimation problem as indicated in section B of Chapter 5. Indeed, unless some preprocessing is done, the received waveforms appear uncorrelated despite the presence of a common but time compressed (or less generally, Doppler shifted) signal. A method based on the ideas of Chapter 3 is suggested for preprocessing the received waveforms to remove the effect of source motion. The last section of Chapter 5 extends the filter and sum realization for time delay estimation to a multiple sensor environment. Finally, Chapter 6 is a brief discussion and summary of applications for the methods of time delay estimation and suggestions for future work.

The appendices of this dissertation are provided to implement and corroborate the theory developed in Chapter 3. Appendix A summarizes two methods of spectral estimation given in Carter, Knapp, and Nuttall (1973a) and Carter and Knapp (1975). Appendix B gives important results of the statistical behavior of the estimates of the magnitude-squared coherence (MSC), including the probability density function (pdf), the cumulative

distribution function (cdf), and the m-th moment of the MSC estimate. A complete discussion of the bias and the variance of the MSC estimates is presented, including a simulation (done by Nuttall and Carter (1976b)) that supports theoretical results of Haubrich (1965) and Carter, Knapp, and Nuttall (1973a) and refutes past simulation results of Benignus (1969a). Using a method suggested by Benignus (1969a), a reduced bias method of MSC estimation is verified; however, it is discovered that for many practical estimation situations the reduced bias MSC estimator will have increased mean square error (MSE) when compared with the MSC estimator given in Appendix A. An example is given of erroneous simulation results (in particular, unexpectedly large bias) when the assumptions of the theory have been violated.

In the process of detecting a coherent source it is desirable to establish a threshold above which a source is considered detected. Rules for establishing such a threshold are given (Carter (1976)) in order to achieve a specified probability of false alarm. Having established such a threshold, it is possible to determine the probability of detecting a coherent source; the probability of detection will depend both on the observation time and the underlying strength of the coherent source. Example receiver operating characteristics are plotted for different observation times and coherent source levels.

Appendix C gives a complete FORTRAN IV computer listing of a program to estimate time delay. The program was successfully compiled and run on both a Univac and an IBM computer. Appendix D presents an example case to validate both the theory and the computer program.

The text, then, is arranged as follows: Chapter 3 contains the derivation for the ML time delay estimator; because these results depend on the coherence between two random processes, we first demonstrate in Chapter 2 what characteristics the coherence possesses. Chapter 4 compares the ML estimator derived in Chapter 3 with other proposed methods for estimating time delay. Chapter 5 extends the results of Chapter 3 to three important generalizations: multiple sources, moving source, and multiple sensors. Applications and a general discussion are presented in Chapter 6. The four appendices are all concerned with experimental verification of approximate methods for estimating time delay presented in Chapter 3.

CHAPTER 2

THEORY AND APPLICATIONS OF COHERENCE

The solution to the physical problem of estimating source bearing is intimately tied to the coherence between spatially separated passive sensors.

This chapter presents the definition and properties of the coherence and several new results on its use. These results bear both directly and indirectly on the solution to the optimum delay estimation problem.

2A. Definition, Relationship to Crosscorrelation, and Properties

2A1. Definition

The coefficient of coherency (CC) between two wide sense stationary random processes is the normalized cross power spectral density function defined by Weiner (1930) as

$$\gamma_{x_1x_2}(f) = \frac{G_{x_1x_2}(f)}{\sqrt{G_{x_1x_1}(f)\, G_{x_2x_2}(f)}}, \qquad (2\text{-}1)$$

where f denotes the frequency (Hz), $G_{x_1x_2}(f)$ is the cross-power spectrum between $x_1(t)$ and $x_2(t)$, and $G_{x_1x_1}(f)$, $G_{x_2x_2}(f)$ denote the auto power spectra of $x_1(t)$, $x_2(t)$, respectively. Despite some confusion in the literature, Weiner intended for the CC to be complex. This is

apparent since he discusses (p. 194, Weiner (1930)) both the modulus and the argument of the CC. Moreover, in suggesting how one might compute the CC, the modulus of the complex numerator is not indicated. The CC is also referred to as the complex coherence (Carter, Knapp, and Nuttall (1973a)). Many of the results which follow depend on the magnitude-squared of the CC (MSC). The MSC is also referred to as the squared coherency (Jenkins and Watts (1968)).

In order to simplify the notation throughout the thesis, we define

$$C_{x_1x_2}(f) \equiv \left|\gamma_{x_1x_2}(f)\right|^2 . \qquad (2\text{-}2)$$

When the two processes under consideration are apparent, we further simplify the notation by letting

$C(f) \equiv C_{x_1x_2}(f) \equiv C_{12}(f)$.

The magnitude of the CC (MC) is denoted by

$$\left|\gamma_{x_1x_2}(f)\right| = \sqrt{C_{x_1x_2}(f)} . \qquad (2\text{-}3)$$

The term "coherence" can imply CC, MC or MSC. Indeed, variables that are a function of the MSC (or MC) alone are also functions of the CC alone, but not necessarily vice versa. While it seems most natural mathematically to refer to the CC as the coherence, the majority of the literature refers to the MSC as coherence.

Since $G_{x_1x_1}(f)$ and $G_{x_2x_2}(f)$ are real, the phase of the CC denoted by

$$\phi_{x_1x_2}(f) = \mathrm{Arg}\left[\gamma_{x_1x_2}(f)\right] \qquad (2\text{-}4a)$$

$$= \text{Arg}\left[G_{x_1x_2}(f)\right] \qquad (2\text{-}4b)$$

$$= \text{Arg}\left[G_{x_1x_2}(f)/G_{x_1x_1}(f)\right]; \qquad (2\text{-}4c)$$

that is, the phase of the CC is the same as the phase of the cross spectrum. Later we will interpret (2-4c) as the phase of the optimum linear filter that maps $x_1(t)$ to $x_2(t)$.

2A2. Relation to Crosscorrelation

The CC between x(t) and y(t) can be confused with the crosscorrelation coefficient or normalized cross-correlation function defined for zero mean processes by

$$\rho_{xy}(\tau) = \frac{R_{xy}(\tau)}{\left[R_{xx}(0)\ R_{yy}(0)\right]^{\frac{1}{2}}}. \qquad (2\text{-}5)$$

The normalized crosscorrelation is a function of lag and not frequency. Further note that the normalizing factor is the scalar $\left[R_{xx}(0)\ R_{yy}(0)\right]^{\frac{1}{2}}$, independent of τ. It is not a lag dependent normalization. The CC has an abscissa dependent type of normalization (2-1). However, there are two models of filtering that aid in interpreting the CC as a type of crosscorrelation.

In the first model, we are given x(t) and y(t) as depicted in Figure 2-1, and we want to find the CC between x(t) and y(t). If we prefilter x(t) by the linear filter $H_1(f)$ and y(t) by the linear $H_2(f)$, then (from p. 399, Davenport (1970)) the cross spectrum between the filter outputs is

$$G_{x_1y_1}(f) = G_{xy}(f)\ H_1(f)H_2^{*}(f) \qquad (2\text{-}6)$$

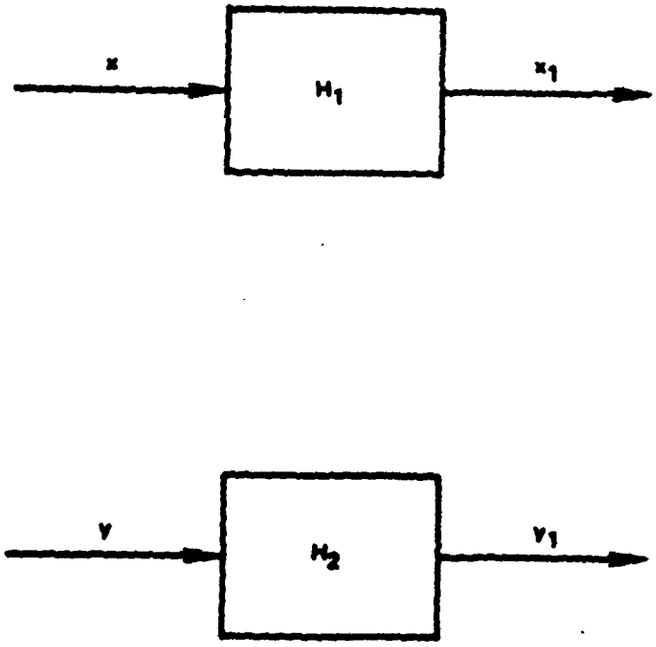

Figure 2-1 Distinct Linear Filters H_1, H_2 with Inputs x,y and Outputs x_1,y_1

Thus, if we select

$$H_1(f)H_2^*(f) = \frac{1}{\sqrt{G_{xx}(f)G_{yy}(f)}} , \qquad (2\text{-}7)$$

it follows that

$$G_{x_1y_1}(f) = \gamma_{xy}(f).$$

Thus, the CC between x(t) and y(t) can be obtained by first prefiltering x(t) by the realizable whitening filter

$$H_1(f) = \frac{1}{\sqrt{G_{xx}(f)}} e^{j\phi(f)} \qquad (2\text{-}8)$$

and prefiltering y(t) with a realizable whitening filter with the same phase as (2-8). Namely, we select

$$H_2(f) = \frac{1}{\sqrt{G_{yy}(f)}} e^{j\phi(f)} . \qquad (2\text{-}9)$$

Such filtering ensures

$$\phi_{x_1y_1}(f) = \phi_{xy}(f) . \qquad (2\text{-}10)$$

That is, the phase between input processes is invariant to equiphase filtering. Then, to compute the CC between x(t) and y(t), we compute the cross spectrum between $x_1(t)$ and $y_1(t)$. This could be accomplished by cross-correlating $x_1(t)$ and $y_1(t)$ and taking the inverse Fourier transform (or see Appendix A).

In the second model used to understand the CC we observe that for $x_1(t)$ and $y_1(t)$ (in Figure 2-1) zero mean

$$\rho_{x_1y_1}(\tau) = \frac{\int_{-\infty}^{\infty} G_{xy}(f)H_1(f)H_2^*(f)e^{j2\pi f\tau}\,df}{\left[\int_{-\infty}^{\infty} G_{xx}(f)\left|H_1(f)\right|^2 df \int_{-\infty}^{\infty} G_{yy}(f)\left|H_2(f)\right|^2 df\right]^{\frac{1}{2}}} \quad (2\text{-}11)$$

Thus if

$$H_1(f)=H_2(f) = \begin{cases} e^{j\phi(f_c)}, & f_c - \frac{\Delta f}{2} < |f| < f_c + \frac{\Delta f}{2} \\ 0, & \text{elsewhere} \end{cases}, \quad (2\text{-}12)$$

(2-11) becomes (for small Δf)

$$\rho_{x_1y_1}(\tau) \approx \frac{\left[G_{xy}(f_c)e^{j2\pi f_c\tau}+G_{xy}(-f_c)e^{-j2\pi f_c\tau}\right]\Delta f}{\left[G_{xx}(f_c)2\Delta f \cdot G_{yy}(f_c)2\Delta f\right]^{\frac{1}{2}}} \quad (2\text{-}13a)$$

$$\approx \frac{\mathrm{Re}\left[G_{xy}(f_c)e^{j2\pi f_c\tau}\right]}{G_{xx}(f_c)G_{yy}(f_c)} \quad (2\text{-}13b)$$

$$\approx \mathrm{Re}\left[\gamma_{xy}(f_c)e^{j2\pi f_c\tau}\right] \quad (2\text{-}13c)$$

$$\approx \left|\gamma_{xy}(f_c)\right|\left[\cos 2\pi f_c(\tau - D)\right] . \quad (2\text{-}13d)$$

The crosscorrelation coefficient at zero argument is given by

$$\rho_{x_1y_1}(0) = \mathrm{Re}\left[\gamma_{xy}(f_c)\right] . \quad (2\text{-}14)$$

Thus we see from (2-14)and (2-13d) how the CC is related to the crosscorrelation coefficient.

2A3. Properties

The power spectral density matrix is positive semidefinite (Jenkins and Watts (1968)). Therefore,

for two random processes, we see that

$$|Q_x(f)| = \begin{vmatrix} G_{x_1x_1}(f) & G_{x_1x_2}(f) \\ G_{x_2x_1}(f) & G_{x_2x_2}(f) \end{vmatrix} \geq 0 \quad . \qquad (2\text{-}15a)$$

For real processes, $G_{x_2x_1}(f) = G^*_{x_1x_2}(f)$ and thus

$$G_{x_1x_1}(f)G_{x_2x_2}(f) - |G_{x_1x_2}(f)|^2 \geq 0 \ , \qquad (2\text{-}15b)$$

and

$$G_{x_1x_1}(f)G_{x_2x_2}(f) \geq |G_{x_1x_2}(f)|^2 . \qquad (2\text{-}15c)$$

Further, $G_{x_1x_1}(f)$ and $G_{x_2x_2}(f)$ are nonnegative, real functions of f. When $G_{x_1x_1}(f)$, $G_{x_2x_2}(f)$ are strictly positive definite (that is, when $G_{x_1x_1}(f)G_{x_2x_2}(f)>0$), (2-15c) can be divided through by $G_{x_1x_1}(f)G_{x_2x_2}(f)$ without changing the sense of the inequality thereby yielding

$$C_{x_1x_2}(f) \leq 1, \ \forall f . \qquad (2\text{-}16a)$$

Further, the magnitude-squared of any complex number is greater than or equal to zero. Thus,

$$0 \leq C_{x_1x_2}(f) \leq 1 \quad . \qquad (2\text{-}16b)$$

The MSC always falls between zero and one. Further, as will be shown, it is zero if the processes $x_1(t)$ and $x_2(t)$ are uncorrelated; and, it is equal to unity if there exists a linear relation between $x_1(t)$ and $x_2(t)$. The cross-power spectrum is then defined by

Bendat and Thomson (1973) as

$$G_{x_1x_2}(f) = \sqrt{G_{x_1x_1}(f)G_{x_2x_2}(f)}\,\gamma_{x_1x_2}(f) \quad . \qquad (2\text{-}17)$$

This definition is interesting since it points out the importance of the coherence. It should be noted that if $\gamma_{x_1x_2}(f)$ is undefined, $G_{x_1x_2}(f)$ cannot be computed from (2-17) (as, for example, when $G_{x_1x_2}(f)$ and $G_{x_1x_1}(f)$ are zero). Here we note that the statement $C_{x_1x_2}(f) = 0$ provides more information than the statement $|G_{x_1x_2}(f)|^2 = 0$, since in the former case, both autospectra must be nonzero. However, it may be more exact to say $|G_{x_1x_2}(f)|^2$ is undefined when no measurement is made.

In order to define the MSC, it is necessary that the numerator and denominator of that ratio not be simultaneously zero. Moreover the MSC will be undefined if either autospectra is zero. For example, if $G_{x_1x_1}(f) = 0$ or $G_{x_2x_2}(f) = 0$ it must be true from (2-15c) that $|G_{x_1x_2}|^2 = 0$. Hence, it can be concluded that if either $G_{x_1x_1}(f)$ or $G_{x_2x_2}(f)$ is zero over some frequency range then the MSC is undefined over that same frequency range. Further, if this is the case, the power spectral density matrix is singular. Another property of the MSC is that the MSC is invariant under linear transformations. If x(t) is filtered by $H_1(f)$ and y(t) is filtered by $H_2(f)$ as depicted in Figure 2-1, then

$$C_{x_1y_1}(f) = \frac{|G_{xy}(f)|^2}{G_{xx}(f)G_{yy}(f)} \quad , \tag{2-18a}$$

$$= \frac{|G_{xy}(f)|^2 |H_1(f)|^2 |H_2(f)|^2}{G_{xx}(f)|H_1(f)|^2 G_{yy}(f)|H_2(f)|^2} = C_{xy}(f) \tag{2-18b}$$

Thus provided $|H_1(f)|^2|H_2(f)|^2 \neq 0$

$$C_{x_1y_1}(f) = C_{xy}(f) \quad . \tag{2-19}$$

That is, the MSC is the same between x and y as between the filtered versions x_1 and y_1.

2B. Uses of Coherence Function

The MSC function for the zero-mean, wide-sense stationary processes x(t) and y(t) is useful in several ways, which will be proved in the following sections. First, for two independent processes, the MSC function is zero. Second, the MSC measures the degree of system linearity. Third, under the assumptions to be presented, the MSC function serves as a SNR measure.

2B1. Measure of Correlation

THEOREM 2-1: If two zero-mean stationary processes x(t) and y(t) are independent, they are also uncorrelated and orthogonal;

$$R_{xy}(\tau) = E[x(t)y(t-\tau)] = E[x(t)]\,E[y(t-\tau)] = 0, \tag{2-20a}$$

$$G_{xy}(f) = \int_{-\infty}^{\infty} R_{xy}(\tau)e^{-j2\pi f\tau}d\tau = 0 \quad , \tag{2-20b}$$

and the MSC

$$C_{xy}(f) = 0 \quad , \forall f \tag{2-20c}$$

provided $G_{xx}(f)G_{yy}(f) \neq 0$.

Hence, if the two processes are independent (or uncorrelated) with zero mean, the MSC between them is zero.

DISCUSSION OF THEOREM 2-1: Note that jointly Gaussian random processes that are uncorrelated (incoherent) are also independent. However, it is possible for two processes to be highly dependent yet uncorrelated (incoherent), even if one of the two processes is Gaussian. Although one may be led by physical considerations to presume processes are independent and hence uncorrelated, in practice, it is easier to show processes are uncorrelated than independent. Note that if $C_{xy}(f) = 0$, $\forall f$, it follows that $\mathrm{Re}[\gamma_{xy}(f)] = \mathrm{Im}[\gamma_{xy}(f)] = 0 = G_{xy}(f)$, $\forall f$ and thence it follows that $R_{xy}(\tau) = 0$, $\forall \tau$. Hence, we see that if two processes are incoherent, then they are also uncorrelated. However, as stated earlier, being incoherent does <u>not</u> necessarily imply being independent. For example, suppose $y(t) = n(x)$ and $x(t)$ is a zero mean stationary random Gaussian process with variance σ^2 and first order probability density function (pdf),

$$p(x) = \frac{1}{\sqrt{2\pi\sigma^2}} e^{-x^2/2\sigma^2} \quad ; \tag{2-21}$$

then from Nuttall (1958) and Carter and Knapp (1975)

$$R_{xy}(\tau) = K\, R_{xx}(\tau), \tag{2-22}$$

where

$$K \quad \frac{1}{\sigma^2} \int_{-\infty}^{\infty} \eta(x) x \frac{1}{\sqrt{2\pi\sigma^2}} e^{-x^2/2\sigma^2} \, dx \, . \qquad (2\text{-}23)$$

Therefore, for even nonlinearities, K=0 and $R_{xy}(\tau)=0$. Hence $G_{xy}(f)=0$ and $C_{xy}(f)=0$. Thus, it is simple to derive a process y(t) which is completely dependent on x(t) but which is uncorrelated with it. Hence, the converse of theorem (2-1) does not hold and coherence does not provide information on dependence or independence but only on second order measures like correlation.

2B2. Measure of System Linearity

The MSC function can be used to measure system linearity. In Figure 2-2 consider the linear system with input x(t), impulse response h(τ), and output y(t). The output y(t) is expressed by the convolution integral

$$y(t) = \int_{-\infty}^{\infty} h(\tau)x(t-\tau) \, d\tau \, , \qquad (2\text{-}24a)$$

or

$$y(t) = h(t) \bullet x(t) \, , \qquad (2\text{-}24b)$$

where $\bullet$ denotes convolution.

In the Fourier domain the convolution is the multiplication (Oppenheim and Schafer (1975))

$$Y(f) = H(f)X(f) \, , \qquad (2\text{-}25)$$

where X, H, and Y are Fourier transforms of x, h and y, respectively.

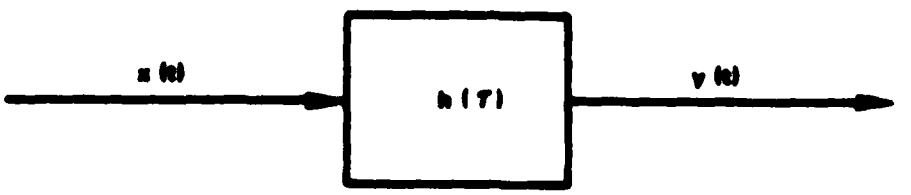

Figure 2-2 Linear System with Impulse Response $h(\tau)$

THEOREM 2-2:

If a system is linear then

$$\gamma_{xy}(f) = e^{j\phi_{xy}(f)} \quad , \ \forall f \tag{2-26}$$

and hence

$$C_{xy}(f) = 1, \ \forall f. \tag{2-27}$$

PROOF OF THEOREM 2-2:

For linear systems,

$$G_{yy}(f)=H_{xy}(f)H^*_{xy}(f)G_{xx}(f), G_{xy}(f)=H^*_{xy}(f)G_{xx}(f) \tag{2-28}$$

or when $G_{xx}(f) \neq 0$

$$G_{yy}(f) = \frac{G_{xy}(f)G^*_{xy}(f)}{G^2_{xx}(f)} \ G_{xx}(f). \tag{2-29}$$

Substituting $G_{yy}(f)$ into the basic definition of CC,

$$\gamma_{xy}(f) = \frac{G_{xy}(f)}{\sqrt{G_{xy}(f)G^*_{xy}(f)}} = \frac{|G_{xy}(f)| \ e^{j\phi_{xy}(f)}}{\sqrt{|G_{xy}(f)|^2}} \tag{2-30a}$$

$$= e^{j\phi_{xy}(f)}. \tag{2-30b}$$

Further,

$$C_{xy}(f) = |\gamma_{xy}(f)|^2 = \cos^2[\phi_{xy}(f)]+\sin^2[\phi_{xy}(f)] = 1. \tag{2-31}$$

DISCUSSION OF THEOREM 2-2: This theorem is related to work of Koopmans (1964), Jenkins and Watts (1968), Otnes and Enochson (1972), Carter, Knapp and Nuttall (1973a), Koopmans (1974), Brillinger (1975), and Halvorsen and Bendat (1975). This theorem, experience, and certain intuition lead one to believe the converse of the theorem should also be true. To date no proof has been presented for the converse. Notably, it is

the converse which would play a most important role in the applications area. This is because one is seldom given a linear system and asked to measure MSC. Rather, one is given an unidentified system and asked: "Is it linear?". In the past, if the MSC was unity, one had a "hunch" that this was true but no rigorous proof existed to assert this truth. The following theorem acts to clarify this dilemma and indeed show what can and what cannot be said about linearity when the MSC is unity.

The strongest theorem which can be proved in this regard is as follows:

THEOREM 2-3: If $C_{xy}(f)=1, \forall f$, then with probability one there exists an optimum filter with unique transfer function $H_o(f)$ that can act on the input, x(t), to an unidentified system to achieve output $y_o(t)$ exactly equal in every detail to the output y(t) of the unidentified system, (that is, $y_o(t)=y(t)$, with probability one). Moreover, the phase of the filter

$$\text{Arg } H_o(f) = \phi_{yx}(f) = \text{Arg } \gamma_{yx}(f) .$$

In order to prove theorem 2-3, it is necessary to introduce and prove a lemma.

LEMMA 2-1: If $G_{ee}(f)$ is the power spectrum of an ergodic random process with member function e(t) and if $G_{ee}(f)=0$, $\forall f$, then e(t) equals zero with probability one for all t.

PROOF OF LEMMA 2-1 From p. 150, Papoulis (1965), the Chebycheff (or Tchebycheff) inequality is

$$\text{Prob}\left\{|e(t)-E[e(t)]|<\varepsilon\right\} \geq 1-\frac{\sigma^2}{\varepsilon^2} \quad , \tag{2-32}$$

where $\varepsilon>0$ can be made arbitrarily small and σ^2 is the variance or power of $e(t)$. The autocorrelation function of $e(t)$ is

$$R_{ee}(\tau) = \int_{-\infty}^{\infty} G_{ee}(f) e^{j2\pi f\tau}\, df, \tag{2-33}$$

but $G_{ee}(f)=0$, $\forall f$ so that $R_{ee}(\tau)=0$, $\forall \tau$. In particular

$$R_{ee}(0) = E\left[e^2(t)\right]=0 = \sigma^2 + E^2[e(t)]. \tag{2-34}$$

Hence $\sigma^2=0$ and $E[e(t)]=0$. Alternatively note that the value of the tails of the autocorrelation is related to the mean value of the function. Specifically, (p. 333, Papoulis (1965))

$$\lim_{\tau\to\infty} R_{ee}(\tau) = E^2[e(t)] \quad . \tag{2-35}$$

So since $R_{ee}(\tau)=0$, $\forall \tau$

$$\lim_{\tau\to\infty} R_{ee}(\tau) = 0 \quad , \tag{2-36}$$

it follows that

$$E^2[e(t)] = 0, \tag{2-37}$$

and thus that

$$E[e(t)] = 0 \quad . \tag{2-38}$$

Therefore, the Chebycheff inequality with $\sigma^2=0$ and $E[e(t)]=0$ is

$$\text{Prob}\left[|e(t)|<\varepsilon\right] \geq 1 \quad , \tag{2-39a}$$

but $0 \leq \text{Prob}[\ ] \leq 1$ so that

$$\text{Prob}\left[|e(t)|<\epsilon\right] = 1 \ ; \qquad (2\text{-}39b)$$

that is, the probability that $|e(t)|$ is less than some arbitrarily small value is one. Statistically, we say that this event happens "with probability one" or we say that it happens "almost surely." So when the power spectrum $G_{ee}(f)$ of this random process is zero for all frequencies, then $e(t)=0$ with probability one.

DISCUSSION OF LEMMA 2-1:

The interpretation of the results can be misleading for transients (nonstationary processes). For example, consider (see, for example, p. 93 of Lee (1960)),

$$\lim_{T\to\infty} \frac{1}{2T} \int_{-T}^{T} e^2(t)dt = R_{ee}(0) = \int_{-\infty}^{\infty} G_{ee}(f)\, df. \qquad (2\text{-}40)$$

Now clearly there exists $e(t)\neq 0$ such that

$$\lim_{T\to\infty} \frac{1}{2T} \int_{-T}^{T} e^2(t)dt = 0 \ . \qquad (2\text{-}41)$$

For example, if a finite energy pulse lasts only a few seconds, then the power (or "average" energy) in such a nonrepetitive pulse is zero. This is because

$$\lim_{T\to\infty} \int_{-T}^{T} e^2(t)\, dt$$

equals some nonzero constant energy but

$$\lim_{T\to\infty} \frac{1}{2T} \int_{-T}^{T} e^2(t)dt$$

equals zero; hence, the power is zero. Transient situations of this type are disallowed by the ergodicity constraint which requires stationarity. (Ergodic processes are stationary but not necessarily vice versa.) The essence of the proof then is that for ergodic random processes almost surely $e(t)=0$ in that frequency band where $G_{ee}(f)=0$. This is a reasonable practical assumption; however, it should not be overlooked that there exists a nonstationary class of processes for which the proof of LEMMA 2-1 does not apply. We now proceed with the proof of theorem 2-3.

PROOF OF THEOREM 2-3: It is instructive to visualize the proof as attempting to select an optimum filter such that the minimum mean squared error (MMSE) is achieved, where the error $e(t)$ is defined as $e(t)=y(t)-y_o(t)$, as shown in Figure 2-3.

The solution will make no presumptions on the origin (source) of $y(t)$. It is useful, however, to envision $y(t)$ as the stationary output of an unidentified system as depicted in Figure 2-4; such a model is a special case of Figure 2-3, but is perhaps a more common system identification problem. Whether the error signal $e(t)$ is generated from Figure 2-3 or Figure 2-4, it follows that the total power is given by

$$\lim_{T\to\infty} \frac{1}{T} \int_{-T/2}^{T/2} e^2(t)dt = \int_{-\infty}^{\infty} G_{ee}(f)\, df \qquad (2\text{-}42)$$

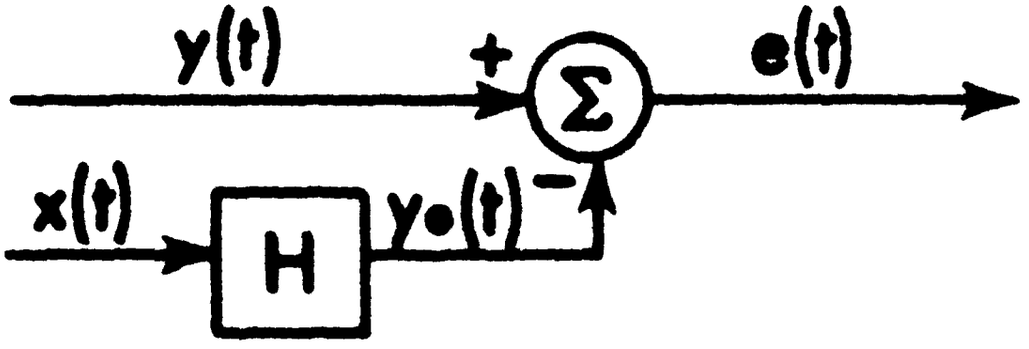

Figure 2-3 Model of Error Resulting from Linearly Filtering x(t) to Match Any Desired Signal y(t)

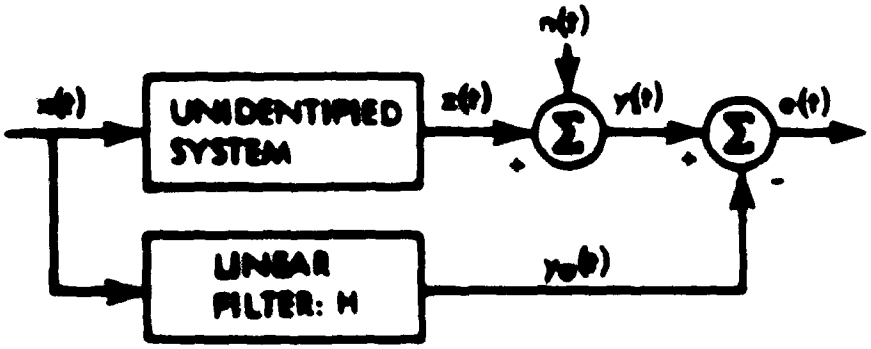

Figure 2-4 Model of Error Resulting from Linear Approximation of Nonlinearity

All power spectra have the property that they are non-negative. The implication is that in integrating over the interval $(-\infty,\infty)$, there will be no portions of $G_{ee}(f)$ that will "cancel" other portions. Solving for $G_{ee}(f)$, it can be shown that

$$G_{ee}(f)=G_{yy}(f) + G_{xx}(f)|H(f)|^2-H(f)G_{xy}(f) -H^*(f)G^*_{xy}(f), \tag{2-43}$$

which can be written, as done by Carter and Knapp (1975), as

$$G_{ee}(f)=G_{xx}(f)\left|H(f)- \frac{G_{yx}(f)}{G_{xx}(f)}\right|^2+G_{yy}(f)\left[1-C_{xy}(f)\right]. \tag{2-44}$$

Since

$$G_{xx}(f) \geq 0,\ G_{yy}(f) \geq 0,\ \text{and}\ 0 \leq C_{xy}(f) \leq 1\ ,$$

it is necessary to minimize

$$\left|H(f) - \frac{G_{yx}(f)}{G_{xx}(f)}\right|^2\ ,$$

which is done by selecting the optimum linear filter

$$H_o(f) = \frac{G_{yx}(f)}{G_{xx}(f)} = \frac{|G_{yx}(f)|}{G_{xx}(f)}e^{j\phi_{yx}(f)}\ . \tag{2-45}$$

The optimum filter is a Wiener filter and is discussed in texts by Lee (1960) and Van Trees (1968). The Fourier transform of (2-45) is the impulse response

$$h_o(\tau) = \int_{-\infty}^{\infty} H_o(f)e^{j2\pi f\tau}df\ . \tag{2-46}$$

In general, $h_o(\tau)$ will be a nonzero for $\tau<0$; hence, the system will be nonrealizable. Various methods can be applied to obtain the optimum realizable linear filter; although they are beyond the scope of this thesis, they

are discussed in standard texts such as Lee (1960) or Van Trees (1968).

From (2-45) the cross spectrum between x(t) and y(t),

$$G_{yx}(f) = H_o(f)G_{xx}(f), \tag{2-47}$$

but since x(t) excites a linear filter $H_o(f)$ to produce output $y_o(t)$, it also follows that

$$G_{y_o x}(f) = H_o(f)G_{xx}(f) \quad . \tag{2-48}$$

Substituting (2-48) into (2-47) yields

$$G_{yx}(f) = G_{y_o x}(f) \quad . \tag{2-49}$$

Since $y(t)=e(t) + y_o(t)$,

$$R_{yx}(\tau) = E\{[e(t)+y_o(t)]x(t-\tau)\} \tag{2-50a}$$

$$= R_{ex}(\tau) + R_{y_o x}(\tau) \quad . \tag{2-50b}$$

But by taking the Fourier transform of both sides of (2-49)

$$R_{yx}(\tau) = R_{y_o x}(\tau) \quad . \tag{2-51}$$

Hence, from (2-51) and (2-50)

$$R_{ex}(\tau) = 0, \; G_{ex}(f)=0; \tag{2-52}$$

that is, the error is uncorrelated with the input x(t). This is an interesting property of the error signal in it's own right. When $x_i(t)$ is linearly filtered by $H_i(f)$ to yield $y_i(t)$ for i=1,2, the cross-power spectrum of the filter outputs is given by Davenport (1970) as

$$G_{y_1y_2}(f) = H_1(f)H_2(f)G_{x_1x_2}(f) \quad . \tag{2-53}$$

Hence is the special case where $x_1(t)=x(t)$, $x_2(t)=e(t)$, $H_1(f)=H_o(f)$ and $H_2(f)=1$, it follows that

$$G_{y_oe}(f) = H_o(f)G_{xe}(f) \quad . \tag{2-54}$$

So if the error is uncorrelated with x(t) (that is, if $G_{xe}(f)=0$), then it must be true that $G_{y_oe}(f)=0$ (that is, the error is uncorrelated with the output of the optimum filter). The waveform x(t) being uncorrelated with e(t) implies that e(t) is also uncorrelated with $y_o(t)$. Further,

$$R_{ey}(\tau) = E[e(t)y(t-\tau)], \tag{2-55a}$$

but $y(t)=e(t)+y_o(t)$ so that

$$R_{ey}(\tau) = E\{e(t)\left[e(t-\tau) + y_o(t-\tau)\right]\} \tag{2-55b}$$

$$= R_{ee}(\tau) + R_{ey_o}(\tau) \quad . \tag{2-55c}$$

Recognizing that $R_{ey_o}(\tau)=0$ and taking the Fourier transform of both sides of (2-55) yields

$$G_{ey}(f) = G_{ee}(f) \quad . \tag{2-56}$$

The selection of the optimum H(f) forces (2-44) to become

$$G_{ee}(f) = G_{yy}(f)\left[1 - C_{xy}(f)\right] \quad . \tag{2-57}$$

When $C_{xy}(f)=1$, clearly (from 2-57) $G_{ee}(f)=0$, and thus (from LEMMA 2-1) e(t)=0 with probability one, but

$$y(t) = y_o(t) + e(t), \tag{2-58}$$

so that almost surely,

$$y(t) = y_o(t) \quad . \tag{2-59}$$

Thus, with probability one, the linear filter

$$H_o(f) = H_{y_o x}(f) = \frac{G_{yx}(f)}{G_{xx}(f)} e^{j\phi_{yx}(f)} \qquad (2\text{-}60)$$

will operate on x(t) to achieve $y_o(t)=y(t)$. If the optimum output $y_o(t)=x(t) \bullet h_o(t)$ then by the Fourier transform relation

$$Y_o(f) = X(f)H_o(f) \quad . \qquad (2\text{-}61)$$

The Fourier transform is a one for one reversible transformation so that a unique x(t), y(t) implies a unique X(f), Y(f), but then

$$H_o(f) = \frac{Y_o(f)}{X(f)} \qquad (2\text{-}62)$$

must be unique. This completes the proof of theorem 2-3.

DISCUSSION OF THEOREM 2-3:

Unique transfer functions do not identify unique systems. Indeed, nothing is known about the internal structure of the unidentified system. Further, the fact that the system can be modeled by a linear system $H_o(f)$ such that when both (system and model) are stimulated by an excitation x(t) they yield identical output y(t) does not prove that the system is linear over all inputs. There may indeed be unobservable nonlinearities in the unidentified system. For example, suppose the excitation x(t) is stationary but with first order pdf such that $-A \leq |x(t)| \leq A$. This implies that x(t) never excites the unidentified system for amplitudes greater than A; hence, no conclusions can be drawn about the linearity of the system over all inputs.

Many "real world" systems are linear over a certain range of amplitudes and then saturate above that amplitude as in the case of analog computers (Kochenburger (1972)). As another example, consider any stationary x(t). The stationary excitation has only one invariant power spectrum $G_{xx}(f)$. Systems which appear linear for some $G_{xx}(f)$ but which are clearly nonlinear for different input statistics are simple to envision. If a system is nonlinear but the nonlinearity is not excited (or more generally, not observed), then the system will appear linear and the measurement of the MSC will equal unity. In essence then, the class of nonlinear functions is so large that based on a single excitation (even white Gaussian noise) it is impossible to claim, without qualification, that a system is "linear" simply because the MSC is unity, for all probed frequencies. Another type of nonlinear system is one in which the MSC is observed to be unity in some frequency bands and not unity in other bands. Thus $y_o(t) \neq y(t)$, unless those frequency bands which cannot be accounted for by linear processing are removed. More precisely, if $C_{xy}(f) = 1$ in the frequency band (f_1, f_2) then with probability one there exists an optimum linear filter with unique transfer function $H_o(f)$ that can act on x(t) to achieve optimum output $y_o(t)$ where $y_o(t) = y(t) \bullet h_I(t)$ and $h_I(t)$ is the impulse response of an ideal zero phase, unity gain "box car" filter that

passes only those frequencies in the (f_1, f_2) band. The whole problem of nonlinear systems can be treated by considering what proportion of a system output can be attributed to a linear operation and what proportion is due to a residual or nonlinear operation. In general, the power spectrum of the optimum output

$$G_{y_o y_o}(f) = |H_o(f)|^2 G_{xx}(f) \tag{2-63}$$

or substituting (2-1), (2-2) and (2-45) into (2-63) yields

$$G_{y_o y_o}(f) = G_{yy}(f) C_{xy}(f) \quad . \tag{2-64}$$

This important result (Carter and Knapp (1975)) can be rewritten as

$$C_{xy}(f) = \frac{G_{y_o y_o}(f)}{G_{yy}(f)} \quad . \tag{2-65}$$

The implication is that the MSC measures the portion or amount of power ($G_{yy}(f)$) which can be obtained through optimal linear filtering (in the MMSE sense) of x(t). Moreover, it is always true (provided $C_{xy}(f)$ is defined) that

$$G_{yy}(f) = C_{xy}(f) G_{yy}(f) + \left[1 - C_{xy}(f)\right] G_{yy}(f) \quad . \tag{2-66}$$

Substituting from (2-64) and (2-57) into (2-66) yields

$$G_{yy}(f) = G_{y_o y_o}(f) + G_{ee}(f) \quad , \tag{2-67}$$

which implies the power spectrum of the output of a system is comprised only of the sum of an error spectrum and an optimum spectrum. This same result can be noticed from

$$R_{yy}(\tau) = R_{ee}(\tau) + R_{y_o e}(\tau) + R_{e y_o}(\tau) + R_{y_o y_o}(\tau) \quad , \qquad (2\text{-}68)$$

but $R_{y_o e}(\tau) = R_{e y_o}(-\tau) = 0, \forall \tau$ so that

$$R_{yy}(\tau) = R_{ee}(\tau) + R_{y_o y_o}(\tau) \quad . \qquad (2\text{-}69)$$

Computing the Fourier transform of (2-69) verifies (2-67).

Just as the MSC measured what portion of $G_{yy}(f)$ could be obtained by (optimal) linear filtering, one minus MSC is a measure of the portion of output power due to an uncorrelated error component; that is,

$$\frac{G_{ee}(f)}{G_{yy}(f)} = 1 - C_{xy}(f) \quad . \qquad (2\text{-}70)$$

Thus, it follows that the ratio of the optimum linear power to the nonlinear or error power is

$$\frac{G_{y_o y_o}(f)}{G_{ee}(f)} = \frac{C_{xy}(f)}{1 - C_{xy}(f)} \quad . \qquad (2\text{-}71)$$

(This ratio will be important in the estimation of time delay.)

For practical nonlinear systems, the identification of the optimum linear component is not always obvious. For example, in the system without noise described by $y(t)=x^3(t)+b\,x(t)$, the optimal linear part is <u>not</u> $bx(t)$. To clarify this point, it will be demonstrated that for a limited class of inputs and a limited class of non-linearities, analytic expressions for the optimal linear part can be obtained. This offers interesting insight

into both the general system identification problem and the coherence interpretation problem. First, the nonlinearity is constrained to have no memory and no noise, that is, $y=\eta(x)$. Second, the input processes are constrained to be separable in the sense defined by Nuttall (1958). A separable process with second-order pdf $p(x_1,x_2;\tau)$ and mean μ is defined as one for which the integral $\int_{-\infty}^{\infty}(x_1-\mu)p(x_1,x_2;\tau)dx_1$ separates into the product of a function of x_2 alone and a function of τ alone. For example, it can be shown that a Gaussian process possesses these properties and, hence, is a separable process.

Under the no-memory nonlinearity and separable process constraints, it has been proved by Nuttall (1958) the crosscorrelation between x(t) and y(t) at delay τ is given by

$$R_{yx}(\tau) = K \cdot R_{xx}(\tau) , \qquad (2\text{-}72a)$$

where

$$K = \frac{1}{\sigma^2} \int_{-\infty}^{\infty} \eta(x)(x-\mu)p(x)dx , \qquad (2\text{-}72b)$$

p(x) is the first-order pdf of x(t), $\eta(x)$ is a complete description of the no-memory nonlinear function, and σ^2 is the variance of x(t). Notice that the constant K does not depend on frequency or delay but only on the first-order pdf and the nonlinearity. It follows directly from (2-72a) that, for no-memory nonlinearities excited by separable processes,

$$\gamma_{yx}(f) = \gamma_{xy}(f) = K\sqrt{\frac{G_{xx}(f)}{G_{yy}(f)}} \quad . \qquad (2\text{-}73)$$

Comparison of (2-73) with (2-45) and (2-1) shows that the constant K is the optimum linear filter in the MMSE sense.

As an example, suppose x(t) has a Gaussian zero-mean, σ^2 variance pdf; then

$$K = \frac{1}{\sigma^2}\int_{-\infty}^{\infty} \eta(x)x \frac{1}{\sqrt{2\pi\sigma^2}} e^{-x^2/2\sigma^2} dx. \qquad (2\text{-}74)$$

Whenever the pdf is even and $\eta(x)$ is an even function, K=0 so that the coherence is zero. However, when $\eta(x)$ is an odd function, K does not necessarily equal zero even though the unidentified system is nonlinear. For example, when $\eta(x)=x^3(t)+b\,x(t)$, application of (2-74) yields $K=3\sigma^2+b$. Therefore, the optimal linear part of $x^3(t)+bx(t)$ is not bx(t) but rather $y_o(t)=(b+3\sigma^2)x(t)$ for a zero mean Gaussian process with variance of σ^2. For b=0, it follows that $K \neq 0$ and $C_{xy}(f) \neq 0$ provided $G_{xx}(f) \neq 0$. However, if $b=-3\sigma^2$, then K=0 and $C_{xy}(f)=0$. Thus, the MSC may still be zero even though the nonlinearity is not even. A computer simulation of the example with $\sigma^2 = 1/2$ and $b=-3/2$ was conducted, and the results verified the theory (Carter and Knapp (1975)). This result can be independently verified by calculating $R_{xy}(\tau) = E\{x(t)\left[x^3(t-\tau)+bx(t-\tau)\right]\}$, which for Gaussian processes is $3\sigma^2R_{xx}(\tau)+bR_{xx}(\tau)$. Therefore, $C_{xy}(f)=0$ if $b=-3\sigma^2$, and there is no power in the optimum linear part

of the nonlinearity $n(x) = x^3(t) - 3\sigma^2 x(t)$.

Parenthetically, we note that another approach to this problem is to expand the no-memory nonlinearity n as an infinite series of orthogonal polynomials, specifically,

$$y(t) = n[x(t)] = \sum_{n=0}^{\infty} a_n H_{e_n}[x(t)] \quad , \tag{2-75a}$$

where the $H_{e_n}(x)$ are e_n Hermite polynomials (see, for example, p. xxxv, Gradshteyn and Ryzhik (1965))

$$H_{e_0}(x)=1, \; H_{e_1}(x)=x, \; H_{e_2}(x)=x^2-1, \; H_{e_3}(x)=x^3-3x$$

and in general

$$H_{e_{n+1}}(x)=xH_{e_n}(x)-nH_{e_{n-1}}(x) \quad . \tag{2-75b}$$

Then, the crosscorrelation between x and y is given by

$$R_{xy}(\tau) = \sum_{n=0}^{\infty} a_n E\{x(t)H_{e_n}[x(t-\tau)]\} \quad . \tag{2-76}$$

The advantage to this method is that, if the family of correlations

$$R_{xH_{e_n}(x)}(\tau) = E\{x(t)H_{e_n}[x(t-\tau)]\}, \quad n=1,2,\ldots \tag{2-77}$$

had been computed once, orthogonal expansion of $n(x)$ makes $R_{xy}(\tau)$ immediately apparent by a simple weighted summation.

It is perhaps germane to clarify the significance of knowing that the MSC is unity. Just as $C_{xy}(f)=1$ for all f ensured that there was some linear filter that mapped x(t) into $y_o(t)=y(t)$ exactly, there also exists a linear filter which maps y(t) into x(t) exactly. That

is, since $|G_{xy}(f)|^2 = |G_{yx}(f)|^2$, $C_{xy}(f) = C_{yx}(f)$ and conclusions drawn with regard to x(t) and y(t) have an analogous relation between y(t) and x(t). Thus, even though one cannot make unqualified statements about the unidentified system, there certainly exists a total detailed knowledge of its output for a given input and therefore, all of its output statistics when the MSC is unity and the input remains unchanged. All this is accomplished through the utilization of a linear (though not necessarily realizable) model.

2B3. Measure of Signal-to-Noise Ratio

The coherence can be used for determining SNR as will be discussed in this section. The results of this section are of interest from two points of view. First, the SNR is a fundamental concern in the basic passive detection problem and parameter estimation problem, and second the results of this section will aid in the interpretation of optimum delay estimation and variance of the estimate of coherence phase. Hence, while these results can be derived independent of the time delay estimation problem, they will form an important role in the understanding of how to estimate time delay or source bearing.

When x(t) is linearly filtered to yield output y(t) and the output is corrupted by uncorrelated additive noise, as depicted in Figure 2-5, then the noise power spectrum is

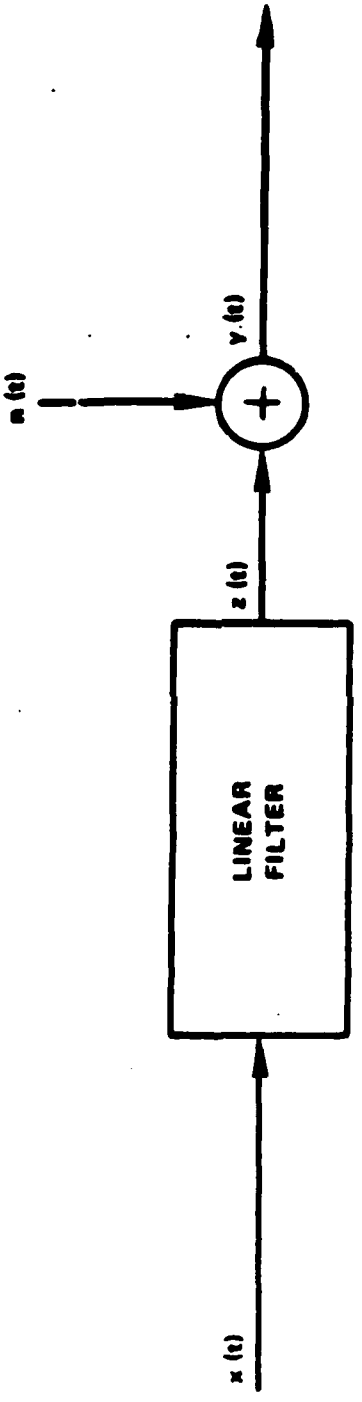

Figure 2-5 Linear Filter Whose Output is Corrupted with Additive Noise

$$G_{nn}(f) = G_{yy}(f)\left[1 - C_{xy}(f)\right] \quad . \tag{2-78}$$

This is an intuitively satisfying result since the MSC is unity if there is no noise, whereas the MSC is zero when the output is all noise. For linear systems, additive noise uncorrelated with the input reduces the MSC according to the ratio of $G_{nn}(f)$ to $G_{yy}(f)$. Measurement of $G_{nn}(f)$ is useful not only in the image processing problem discussed by Cannon (1974) but also in studying the gross effects of digital filtering when viewed as a perfect filter plus additive noise (James (1975) and Weinstein and Oppenheim (1969)). These methods can also be applied to studying special problems such as fast Fourier transform (FFT) noise (Ferrie and Nuttall (1971) and Rabiner and Rader (1972)).

The power spectrum from the output of an arbitrary system can always be viewed in terms of its two components $G_{yy}(f)C_{xy}(f)$ and $G_{yy}(f)\left[1-C_{xy}(f)\right]$ regardless of how $G_{yy}(f)$ is produced (as long as $C_{xy}(f)$ is defined). It is interesting to note that the ratio of these components

$$\frac{G_{y_o y_o}(f)}{G_{ee}(f)} = \frac{G_{zz}(f)}{G_{nn}(f)} = \frac{C_{xy}(f)}{1 - C_{xy}(f)} \tag{2-79}$$

can be considered as either the SNR or the linear-to-nonlinear ratio, depending on the application.

For situations like those shown in Figure 2-5, the coherence measures what proportion of an unidentified system output is "linear." Through the use of (2-79), the MSC provides a comparison of the proportion of system

power that is linear with the proportion that is nonlinear is exactly the same way in which the SNR was measured for the output of a linear system corrupted by additive noise. However, in other system configurations, such as that shown is Figure 2-6, where noise and signal have a different interpretation, relation (2-79) will not be useful. Figure 2-6 is of interest to the sonar community since it is analogous to the physical situation in which signal s(t) from an acoustic source is received at two geographically separated sensors. Each observed signal is corrupted by additive stationary noise and is linearly filtered. When $n_1(t)$ and $n_2(t)$ are uncorrelated but have the same power spectra $G_{nn}(f)$, the SNR, $G_{ss}(f)/G_{nn}(f)$ is readily shown to be

$$\frac{G_{ss}(f)}{G_{nn}(f)} = \frac{\sqrt{C_{xy}(f)}}{1-\sqrt{C_{xy}(f)}} \quad , \qquad (2\text{-}80)$$

which differs from (2-79). (Note from (2-19) that $C_{r_1r_2}(f)=C_{xy}(f)$.) Ironically it will turn out to be (2-79) and not (2-80) which is critical to our problem. In cases where each transmission path attenuates the source signal differently, the model must be changed to reflect an attenuation in one channel. Unless simplifying assumptions are employed, the net result is that $G_{ss}(f)/G_{nn}(f)$ cannot be determined from $C_{xy}(f)$ unless attenuation in each path is known. (See section 4 of appendix B.)

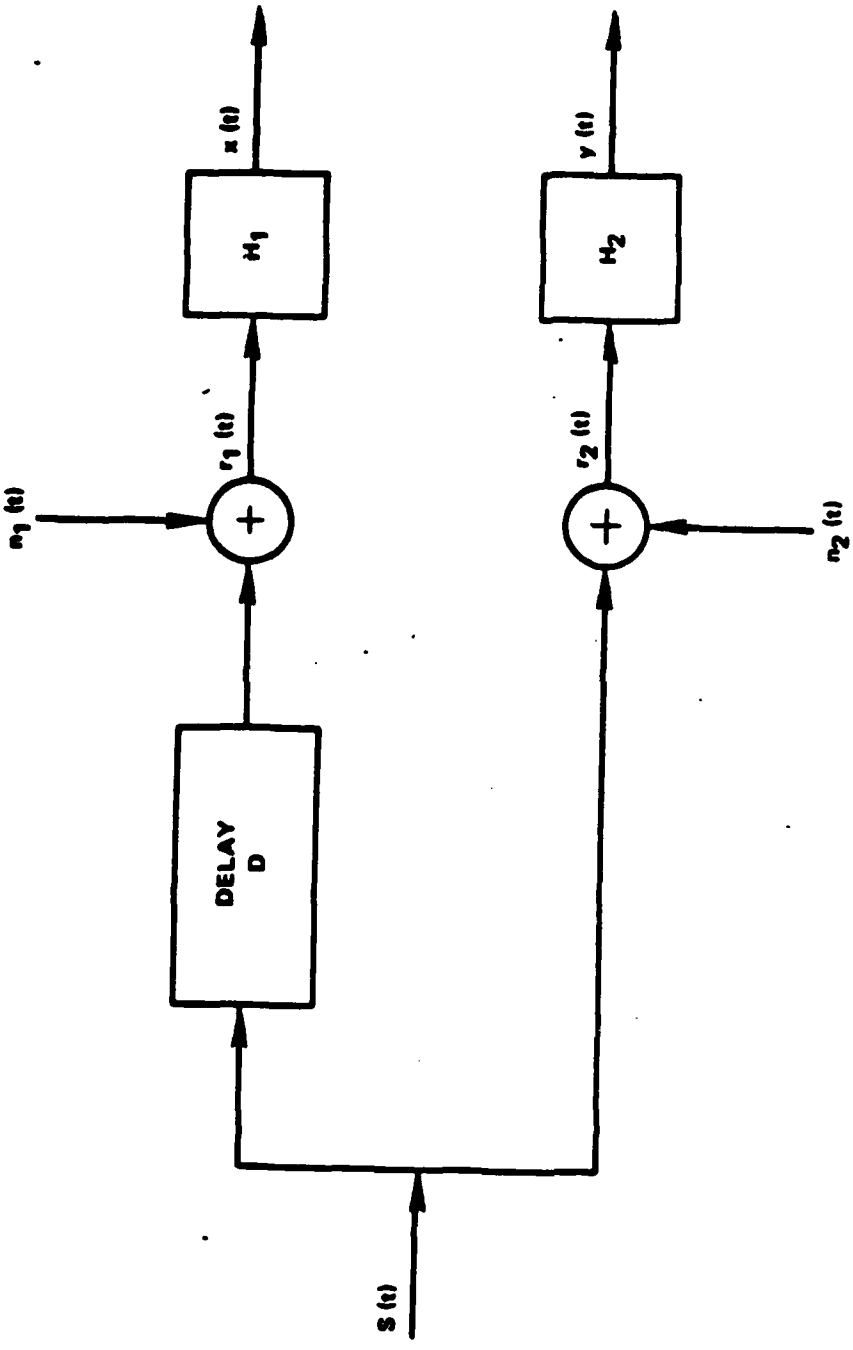

Figure 2-6 Model of Directional Signal Corrupted with Additive Noise and Processed

AD-A101 684 SCIENTIFIC AND ENGINEERING STUDIES COMPILED 1979 5/8
COHERENCE ESTIMATION(U) NAVAL UNDERWATER SYSTEMS CENTER
NEWPORT RI G C CARTER ET AL. 1979

UNCLASSIFIED F/G 9/1 NL

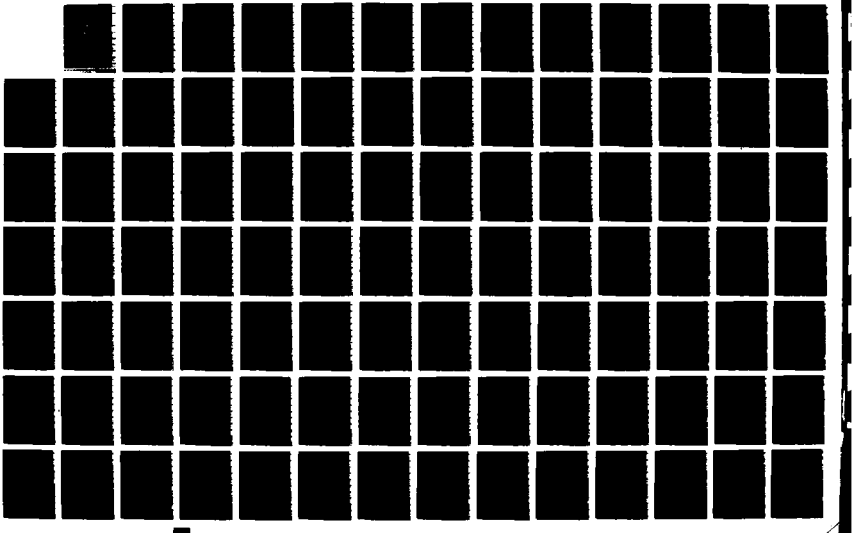

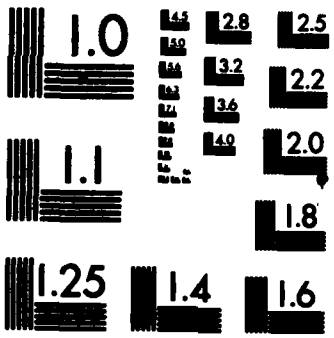

MICROCOPY RESOLUTION TEST CHART
NATIONAL BUREAU OF STANDARDS-1963-A

More generally, the source is transmitted through two ocean medium operators $H_1(f)$ and $H_2(f)$ as shown in Figure 2-7, which can attenuate the signal differently at different frequencies. For illustrative purposes, we assume that the ocean medium operators are linear time invariant filters. Thus $s_1(t)$ and $s_2(t)$ are the outputs of filters $H_1(f)$ and $H_2(f)$, respectively, which have been excited by source s(t). This model of linear filters and noise is mathematically tractable and has been proposed before, as for example, on p. 389 of Whalen (1971). (More sophisticated models are given by Kennedy (1969).) When the noise $n_i(t)$ is uncorrelated with the signal $s_i(t)$, the power spectral density at the output of the i-th sensor is given by

$$G_{x_i x_i}(f) = G_{ss}(f)|H_i(f)|^2 + G_{n_i n_i}(f), \quad i=1,2 \qquad (2\text{-}81a)$$

$$= G_{s_i s_i}(f) + G_{n_i n_i}(f), \quad i=1,2 \; . \qquad (2\text{-}81b)$$

Further, the ratio of the power at the <u>output</u> of the filter to the corruptive noise power depends on the MSC between the <u>source</u> and the <u>sensor</u>. Specifically, from equation (8) of Carter, Knapp and Nuttall (1973a) or (2-79),

$$\frac{G_{s_i s_i}(f)}{G_{n_i n_i}(f)} = \frac{C_{sx_i}(f)}{1 - C_{sx_i}(f)}, \quad i=1,2 \; . \qquad (2\text{-}82)$$

(Note that when $|H_i(f)| \neq 1$, (2-82) does <u>not</u> measure the ratio of source to noise power.) The coherence between

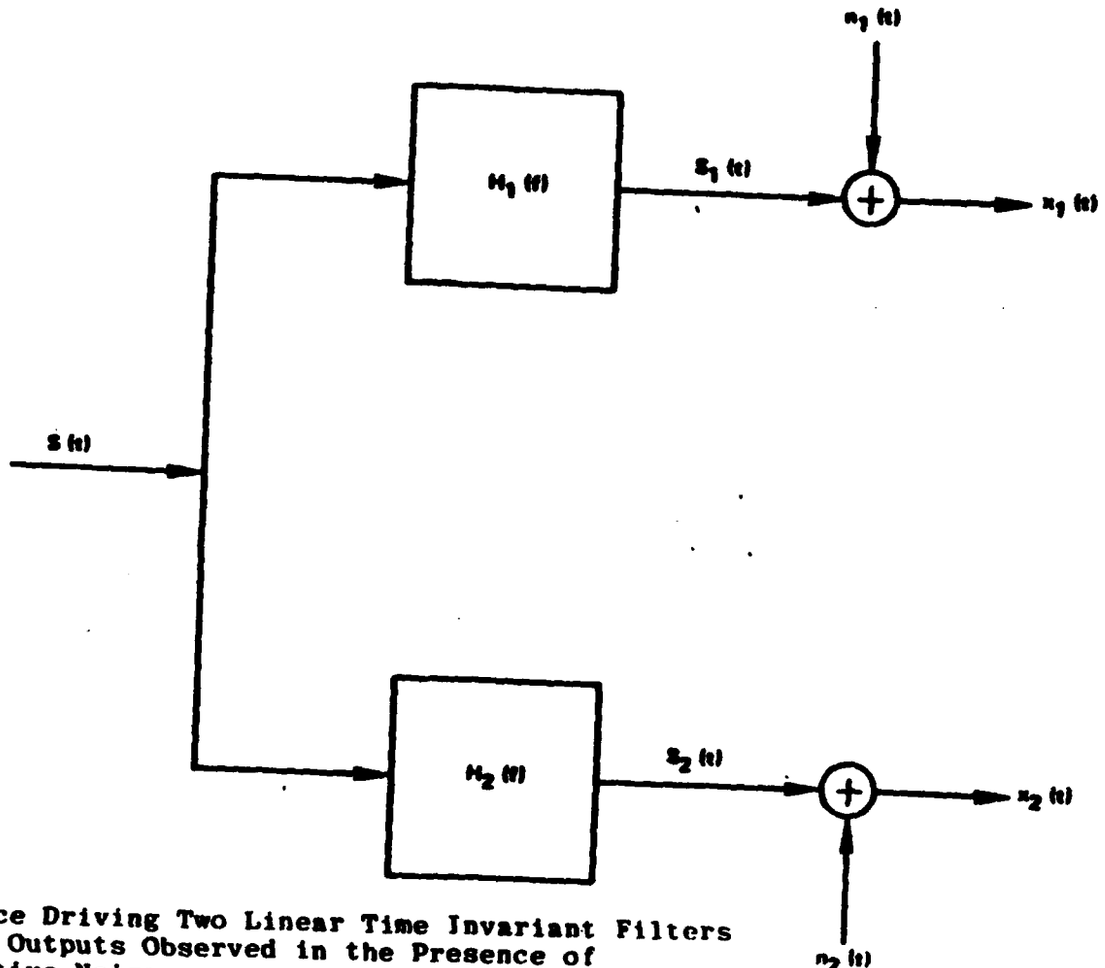

Figure 2-7 Source Driving Two Linear Time Invariant Filters with Outputs Observed in the Presence of Additive Noise

$x_1(t)$ and $x_2(t)$ in Figure 2-7 when and $n_1(t)$ and $n_2(t)$ are uncorrelated is given by

$$\gamma_{x_1x_2}(f) = \frac{G_{ss}(f)H_1(f)H_2^*(f)}{\sqrt{G_{x_1x_1}(f)G_{x_2x_2}(f)}} \quad . \tag{2-83}$$

In order to relate this result to the coherence between the source and each sensor, note that

$$\gamma_{sx_i}(f) = \frac{G_{ss}(f)H_i(f)}{\sqrt{G_{ss}(f)G_{x_ix_i}(f)}} \quad , \; i=1,2, \tag{2-84}$$

so that

$$\gamma_{x_1x_2}(f) = \gamma_{sx_1}(f)\gamma_{sx_2}^*(f) \quad . \tag{2-85}$$

Taking the magnitude-squared yields

$$C_{x_1x_2}(f) = C_{sx_1}(f)C_{sx_2}(f) \quad . \tag{2-86}$$

Thus, when a source drives two linear time invariant filters whose output is observed in the presence of uncorrelated noise, the MSC between the outputs can be no larger than the MSC between the source and any sensor. In particular, for two sensors the MSC is the product of the two source MSCs, as given in (2-86). However, it is possible to have a source transmitted through some nonlinearity such that the MSC between $s(t)$ and $x_1(t)$ is low and the MSC between $s(t)$ and $x_2(t)$ is low and the MSC between $x_1(t)$ and $x_2(t)$ is high. For example, suppose $s(t)$ is a member function of a stationary random process which is separable in the Nuttall sense. Then the MSC between $x_1(t) = s^2(t)$ and

s(t) is zero; similarly, the MSC between $x_2(t) = s^2(t)$ and s(t) is zero; however, for this example, the MSC between $x_1(t)$ and $x_2(t)$ is unity. Thus, care should be used in interpreting these results since they apply only to the case where the medium can be accurately modeled by linear time invariant filters corrupted by uncorrelated additive noise.

Using (2-86) we can compute a SNR squared quantity, namely,

$$\frac{G_{s_1s_1}(f)}{G_{n_1n_1}(f)} \cdot \frac{G_{s_2s_2}(f)}{G_{n_2n_2}(f)} = \frac{C_{x_1x_2}(f)}{\left[1-C_{sx_1}(f)\right]\left[1-C_{sx_2}(f)\right]} . \quad (2\text{-}87)$$

To be useful (2-87) requires knowledge of the source to sensor MSCs. However, if $C_{sx_1}(f) = C_{sx_2}(f) = \left[C_{x_1x_2}(f)\right]^{\frac{1}{2}}$, then it follows that

$$\left[\frac{G_{s_1s_1}(f)G_{s_2s_2}(f)}{G_{n_1n_1}(f)G_{n_2n_2}(f)}\right]^{\frac{1}{2}} = \frac{\sqrt{C_{x_1x_2}(f)}}{1-\sqrt{C_{x_1x_2}(f)}} . \quad (2\text{-}88)$$

The results on coherence from this chapter will add to the understanding of the role of coherence in ML estimation of time delay as will be seen in the next chapter.

CHAPTER 3

MAXIMUM LIKELIHOOD ESTIMATE OF TIME DELAY

In the first section of this chapter an ML estimator is derived for determining time delay between signals received at two spatially separated sensors in the presence of uncorrelated noise. This ML estimator can be realized as a pair of receiver prefilters followed by a crosscorrelator. The time argument at which the correlator achieves a maximum is the delay estimate. In the second section of this chapter, the variance of the time delay estimate is derived and compared with the Cramér-Rao lower bound, and in the final section, various realizations of the processor are considered.

3A. Derivation

For the purposes of the derivation, a signal emanating from an acoustic source and monitored in the presence of noise at two spatially separated sensors can be mathematically modeled as depicted in Figure 3-1. Mathematically,

$$x_1(t)=s_1(t)+n_1(t) \tag{3-1a}$$

$$x_2(t)=\alpha s_1(t+D)+n_2(t)\ , \tag{3-1b}$$

where $s_1(t)$, $n_1(t)$, and $n_2(t)$ are real, jointly stationary

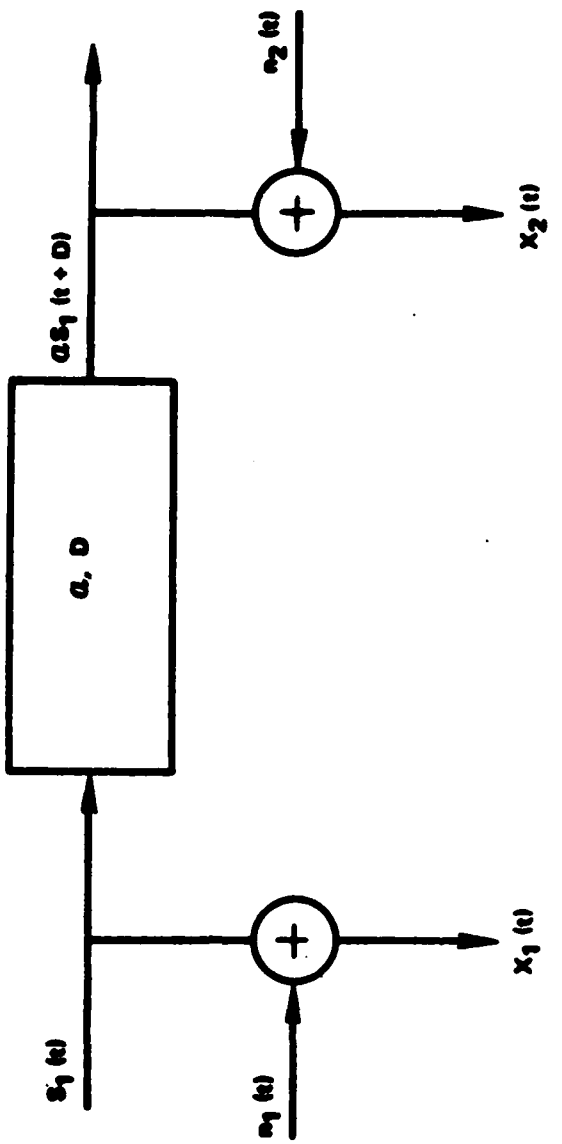

Figure 3-1 Plant with Noise Corrupted Observations of Input and Output

random processes. The delay, D, is the unknown parameter to be estimated. Signal $s_1(t)$ is assumed to be uncorrelated with noise $n_1(t)$ and $n_2(t)$. Later we also assume $n_1(t)$ and $n_2(t)$ are uncorrelated with each other.

More generally, it may be assumed that $s_2(t)$ is linearly related to $s_1(t)$ by the transfer function $H(f)=|\alpha(f)|e^{-j2\pi fD}$. Thus, unlike (3-1) where the Fourier transform of the system output is $\alpha s_1(f)e^{-j2\pi fD}$, the output transform in this case is $|\alpha(f)|s_1(f)e^{-j2\pi fD}$. The linear phase characteristic of such a system is assured when the impulse response is symmetric about $\tau=D$. For realizable systems, this implies that the duration of the impulse response must be finite. Thus, in a sense, we are estimating the midpoint of a symmetric finite impulse response (FIR) filter depicted in Figure 3-2a. Such an impulse response is not necessarily peaked at D (as for example in Figure 3-2b). In the derivation which follows, then, α can (more generally) be interpreted as a frequency dependent attenuation $|\alpha(f)|$.

There are many applications in which it is of interest to estimate the delay D. This chapter derives an ML estimator and evaluates its variance. Chapter 4 compares the estimator with other similar techniques. While the model of the physical phenomena presumes stationarity, the techniques to be developed herein may be employed in slowly varying environments where the characteristics of the signal and noise remain

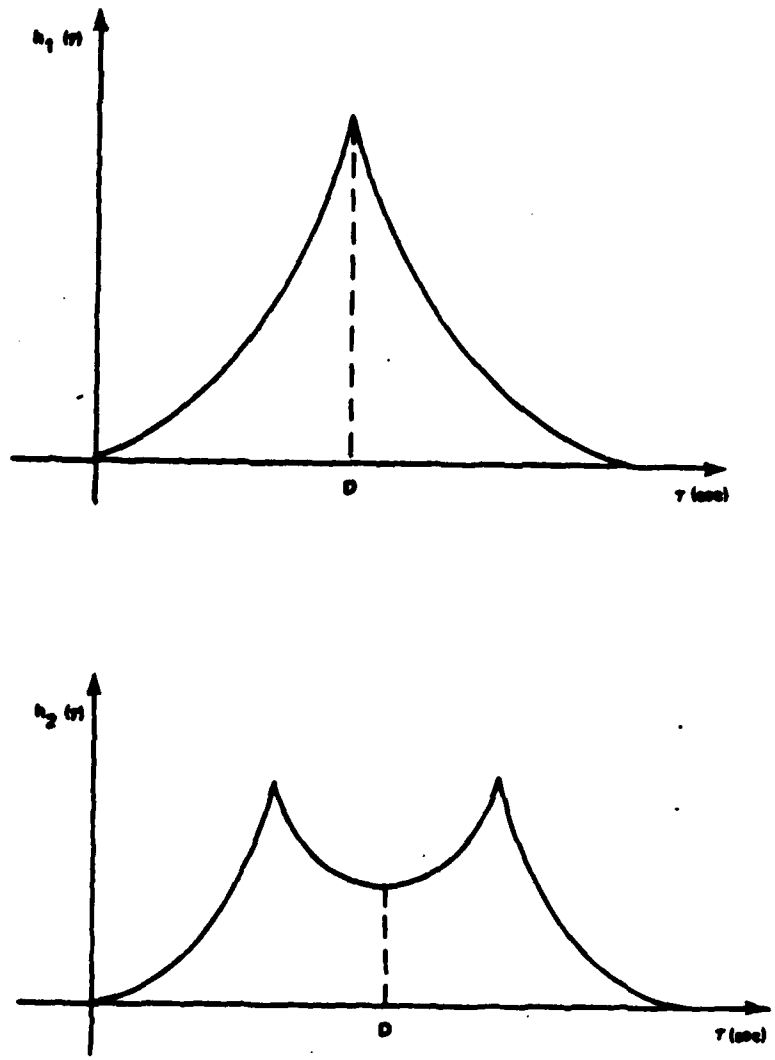

Figure 3-2 Symmetric Impulse Response for Two FIR Linear Phase Filters

stationary only for finite observation time T. Further, the delay D and attenuation α may also change slowly. The estimator is therefore constrained to operate on observations of a finite duration. Having estimated the delay, an estimate of the bearing may be obtained by mapping the delay estimate according to (Nuttall, Carter and Montavon (1974))

$$\hat{\theta} = \arccos \frac{\xi \hat{D}}{d} , \qquad (3\text{-}2)$$

where ξ is the nominal speed of sound in the non-dispersive medium and d is the sensor separation. (See pp. 93-103 of Urick (1967).) A rigorous derivation for the ML estimator of D using the mathematical model (3-1a) and (3-1b) requires that signal and noise spectra be given (that is, known). (See Hannan and Thomson (1971).) When they are unknown, a heuristic procedure of estimating these spectral characteristics is suggested. The ML estimator of delay can be realized as a pair of receiver prefilters followed by a crosscorrelator. The time argument at which the correlator achieves a maximum is the delay estimate. Qualitatively, the role of the prefilters is to weight the signal passed to the correlator according to the strength of the coherence function. This weighting turns out to be equivalent to that proposed by Hannan and Thomson (1973) and under simplifying assumptions to that proposed by MacDonald and Schultheiss (1969), but apparently differs from the results of Clay, Hinich and Shaman (1973). However, the

development presented here does not presume initially that the estimator is a GCC function. Rather, it is shown that the ML estimate may be realized by prefiltering and crosscorrelating the data $x_1(t)$ and $x_2(t)$. Indeed, other realizations of the ML processor are also possible. (See section 3C of this chapter.) For example, the data can be appropriately filtered, summed, squared and averaged in order to estimate the delay. This latter processor follows directly from the derivation presented here and is discussed fully in 3C.

To make the model (3-1) mathematically tractable, it is necessary to assume that $s_1(t)$, $n_1(t)$ and $n_2(t)$ are Gaussian. Denote the Fourier coefficients of $x_i(t)$ as

$$X_i(k) = \frac{1}{T} \int_0^T x_i(t) e^{-jkt\omega_\Delta} dt, \qquad (3\text{-}3a)$$

where

$$\omega_\Delta = \frac{2\pi}{T} \quad . \qquad (3\text{-}3b)$$

Note that the linear transformation $X_i(k)$ is Gaussian since $x_i(t)$ is Gaussian. In practice, the integral will be replaced by a discrete Fourier transform (DFT) or FFT. When the number of data points in each FFT is large (as will usually be the case) then, by a central limit theorem argument, $X_i(k)$ will tend toward being Gaussian even if the $x_i(t)$ are not Gaussian.[1] This presumption

[1]These observations were brought to the authors attention by Dr. G. Mohnkern of the Naval Undersea Center, San Diego, California.

is borne out by Benignus (1969b). Hence, the requirement that $s_1(t)$, $n_1(t)$ and $n_2(t)$ be Gaussian is <u>not</u> a strong requirement.

As the observation time $T \to \infty$,

$$T\, x_i(k) \to \tilde{X}_i(k\omega_\Delta) \quad ,$$

where $\tilde{X}_i$ is the Fourier transform of $x_i(t)$. A more complete discussion on Fourier transforms and their convergence is given in Davenport (1970), Jenkins and Watts (1968), Koopmans (1974), Otnes and Enochson (1972), Bendat and Piersol (1971) and Brillinger (1975). From MacDonald and Schultheiss (1969), it follows for T large compared with $|D|$ plus the correlation time of $R_{s_1 s_1}(\tau)$, that

$$E\left[X_1(k)X_2^*(\ell)\right] \cong \begin{cases} \frac{1}{T} G_{x_1 x_2}(k\omega_\Delta), & k=\ell \\ 0, & k\neq\ell \end{cases} \quad . \tag{3-4}$$

Note that $E[X_i(k)] = E[x_i(t)] = 0$, $i=1,2$.

Now let the vector

$$\underline{X}(k) = \left[X_1(k), X_2(k)\right]' \quad , \tag{3-5}$$

where ' denotes transpose. Then the covariance of $\underline{X}(k)$ is

$$E\left[\underline{X}(k)\underline{X}^{*'}(k)\right] = E\begin{bmatrix} X_1(k)X_1^*(k) & X_1(k)X_2^*(k) \\ X_2(k)X_1^*(k) & X_2(k)X_2^*(k) \end{bmatrix} \tag{3-6}$$

$$= \frac{1}{T} \begin{bmatrix} G_{x_1x_1}(k\omega_\Delta) & G_{x_1x_2}(k\omega_\Delta) \\ G^*_{x_1x_2}(k\omega_\Delta) & G^*_{x_2x_2}(k\omega_\Delta) \end{bmatrix} \tag{3-7}$$

$$\triangleq \frac{1}{T} \; Q_x(k\omega_\Delta) \; , \tag{3-8}$$

where $Q_x(\omega)$ is the spectral matrix of $\left[x_1(t), x_2(t)\right]'$.

The vectors $\underline{X}(k)$, $k=-N,-N+1,\ldots,N$ are, as a consequence of (3-4), uncorrelated Gaussian (hence, independent) random variables. More explicitly, the pdf for $\underline{X} \equiv \underline{X}(-N), \underline{X}(-N+1), \ldots, \underline{X}(N)$, given attenuation α and delay D is[1]

$$p(\underline{X}|\alpha,D) = h \cdot \exp - \frac{1}{2} J_1 \; , \tag{3-9}$$

where

$$J_1 = \sum_{k=-N}^{N} \underline{X}^{*'}(k) Q_x^{-1}(k\omega_\Delta) \underline{X}(k) T \tag{3-10}$$

and h is a function of $|Q_x(k\omega_\Delta)|$ (Van Trees (1968)). Replacing $TX_1(k)$ by $\tilde{X}_1(k\omega_\Delta)$, the Fourier transform of $x_1(t)$, it follows from (3-10) that

$$J_1 = \sum_{k=-N}^{N} \tilde{\underline{X}}^{*'}(k\omega_\Delta) Q_x^{-1}(k\omega_\Delta) \tilde{\underline{X}}(k\omega_\Delta) \frac{1}{T} \; . \tag{3-11}$$

The ML estimate of D (see, for example, Jenkins and Watts (1968) or Van Trees (1968)) is the value of D which maximizes $p(\underline{X}|\alpha,D)$.

---

[1]More explicitly, since the density function depends on Q_x, one could write $p(\underline{X}|\alpha,Q_x)$. This notation obscures the role of the delay but clarifies the need to know (or estimate) signal and noise spectra. Further, if $\alpha=|\alpha(f)|$ then the pdf is conditioned on knowing $|\alpha(k\omega_\Delta)|$, $k=-N, -N+1,\ldots,N$.

In general, the parameter D affects both h and J_1 in (3-9). However, for uncorrelated noise in (3-1), h is independent of the delay.

For large T, (3-11) becomes

$$J_1 \cong \int_{-\infty}^{\infty} \tilde{\underline{X}}^{*t}(f) Q_x^{-1}(f) \tilde{\underline{X}}(f) df \ . \tag{3-12}$$

From (3-6)-(3-8),

$$Q_x^{-1}(f) = \frac{\begin{bmatrix} G_{x_2x_2}(f) & -G_{x_1x_2}(f) \\ -G^*_{x_1x_2}(f) & G_{x_1x_1}(f) \end{bmatrix}}{G_{x_1x_1}(f)G_{x_2x_2}(f) - |G_{x_1x_2}(f)|^2} \tag{3-13a}$$

$$\frac{1}{[1-C_{12}(f)]} \cdot \begin{bmatrix} 1/G_{x_1x_1}(f), -G_{x_1x_2}(f) \Big/ \{G_{x_1x_1}(f) \cdot G_{x_2x_2}(f)\} \\ -G^*_{x_1x_2}(f) \Big/ \{G_{x_1x_1}(f) G_{x_2x_2}(f)\}, \ 1/G_{x_2x_2}(f) \end{bmatrix}, \tag{3-13b}$$

where $C_{12}(f) \equiv C_{x_1x_2}(f)$, which will exist provided $C_{12}(f) \neq 1$; that is, $x_1(t)$ and $x_2(t)$ cannot be obtained perfectly from one another by linear filtering (Carter and Knapp (1975)), or equivalently for the model (3-1) that observation noise is present.

When $C_{n_1n_2}(f) = G_{n_1n_2}(f) = 0$

$$G_{x_1x_1}(f) = G_{s_1s_1}(f) + G_{n_1n_1}(f) \ , \tag{3-14a}$$

$$G_{x_2x_2}(f) = \alpha^2 G_{s_1s_1}(f) + G_{n_2n_2}(f) \ , \tag{3-14b}$$

$$G_{x_1x_2}(f)=aG_{s_1s_1}(f)\,e^{-j2\pi fD} \quad . \tag{3-14c}$$

$$C_{12}(f)=a^2G_{s_1s_1}(f)\Big/G_{x_1x_1}(f)G_{x_2x_2}(f); \tag{3-14d}$$

and it follows that

$$J_1 = \int_{-\infty}^{\infty} \tilde{\underline{X}}^{*t}(f)Q_x^{-1}(f)\tilde{\underline{X}}(f)df=J_2+J_3 \quad , \tag{3-15a}$$

where

$$J_2= \int_{-\infty}^{\infty}\left[\frac{|\tilde{X}_1(f)|^2}{G_{x_1x_1}(f)}+\frac{|\tilde{X}_2(f)|^2}{G_{x_2x_2}(f)}\right]\cdot\frac{1}{1-C_{12}(f)}\,df \quad , \tag{3-15b}$$

$$-J_3= \int_{-\infty}^{\infty} A(f)+A^*(f)\,df, \tag{3-15c}$$

$$A(f)=\tilde{X}_1(f)\tilde{X}_2^*(f)\cdot\frac{G^*_{x_1x_2}(f)}{G_{x_1x_1}(f)G_{x_2x_2}(f)[1-C_{12}(f)]} \quad . \tag{3-15d}$$

In order to relate these results to Hannan and Thomson (1973) and others and interpret how to implement the ML estimation technique note that for $x_1(t)$ and $x_2(t)$ real, $A^*(f)=A(-f)$. Then (3-15c) can be rewritten as

$$-J_3= \int_{-\infty}^{\infty} A(f)df+ \int_{-\infty}^{\infty} A(-f)df=2\int_{-\infty}^{\infty} A(f)df \quad . \tag{3-16}$$

Letting $T\hat{G}_{x_1x_2}(f)\triangleq\tilde{X}_1(f)\tilde{X}_2^*(f)$, (3-16) and (3-15d) can be written as

$$-J_3=2T\int_{-\infty}^{\infty}\hat{G}_{x_1x_2}(f)\frac{1}{|G_{x_1x_2}(f)|}\,\frac{C_{12}(f)}{[1-C_{12}(f)]}\,e^{j2\pi fD}\,df. \tag{3-17}$$

Notice that the ML estimator for D will minimize $J_1=J_2+J_3$, but the selection of D has no effect on J_2.

Thus, D should maximize $-J_3$. Equivalently, when $\tilde{X}_1(f)\tilde{X}_2^*(f)$ is viewed as T times the estimated cross-power spectrum, $T\hat{G}_{x_1x_2}(f)$, the ML estimator selects as the estimate of delay the value of τ at which

$$R_{y_1y_2}^{(ML)}(\tau)=\int_{-\infty}^{\infty}\hat{G}_{x_1x_2}(f)\frac{1}{|\hat{G}_{x_1x_2}|}\frac{C_{12}(f)}{[1-C_{12}(f)]}e^{j2\pi f\tau}df, \qquad (3\text{-}18a)$$

where

$$\hat{G}_{x_1x_2}(f)=\frac{\tilde{X}_1(f)\tilde{X}_2^*(f)}{T} \qquad (3\text{-}18b)$$

achieves a peak. That is, the ML estimator selects as the estimate of delay the value of τ at which the GCC

$$\hat{R}_{x_1x_2}^{g}(\tau)=\int_{-\infty}^{\infty}\hat{G}_{x_1x_2}(f)W_g(f)e^{j2\pi f\tau}df \qquad (3\text{-}19)$$

achieves a peak, where $W_g(f)=H_1(f)H_2^*(f)$ is an appropriately selected weighting function (Knapp and Carter (1976)) The ML estimator is equivalent to one proposed by Hannan and Thomson (1973). The ML estimator can be achieved as depicted in Figure 3-3 by shaping $x_1(t)$ with filter $H_1(f)$ and $x_2(t)$ with filter $H_2(f)$ then crosscorrelating the filter outputs and observing what value of delay achieves a maximum. The estimator can also be achieved in other forms. (See section C of this Chapter.) The weighting proposed by Hannan and Thomson (1973) is

$$W_{ML}(f)=\frac{1}{|\hat{G}_{x_1x_2}(f)|}\cdot\frac{C_{12}(f)}{[1-C_{12}(f)]}, \qquad (3\text{-}20)$$

where (as required for Q_x^{-1} to exist) $C_{12}(f)\neq 1$. Such

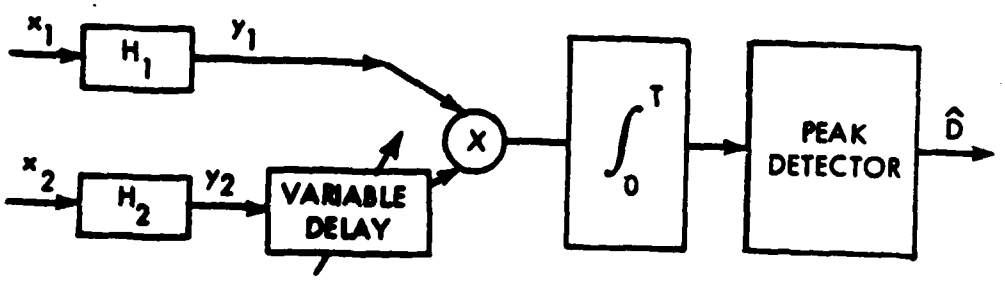

Figure 3-3 Received Waveforms Filtered, Delayed, Multiplied, and Integrated for a Variety of Delays until Peak Output is Obtained

weighting achieves the ML estimator. When $|G_{x_1x_2}(f)|$ and $C_{12}(f)$ are known, this is exactly the proper weighting. An important consideration in estimator design is the available amount of a priori knowledge of the signal and noise statistics. In many problems, this information is negligible. For example, in passive detection, unlike the usual communications problem, the source spectrum is unknown or only known approximately. When the terms in (3-20) are unknown, they can be estimated via techniques of Carter, Knapp and Nuttall (1973a), which are summarized in appendix A and programmed in appendix C. Substituting estimated weighting for true weighting is entirely a heuristic procedure whereby the ML estimator can approximately be achieved in practice. Such techniques have been referred to as approximate ML (AML) techniques by Box and Jenkins (1970) since they are not, truly speaking, ML estimation techniques.

Since the estimation of delay may, in practice, be governed by an AML rather than an ML technique, we should not expect that more complex models will yield to ML techniques without similar heuristic approximation. Rather, the estimation of D with moving sources, for example, will also require AML techniques and may be even more prone to varying interpretations.

3B. Variance of General Time Delay Estimator

The crosscorrelation form of the processor is useful in ascertaining the statistical characteristics of the delay estimate. For each of several different trials a different estimate of delay might be obtained. For example, when the true delay is about 5.0 seconds, six typical trials are sketched in Figure 3-4. One actual example case is given in appendix D. In ascending orders, values of $\hat{D}$ are 4.5, 4.9, 5.0, 5.1, 5.3 and 5.7. For trial number 5, depicted on the Figure 3-4, an estimate 4.9 is obtained. However, there appear to be many ambiguous peaks in trial 5; indeed if the noise had been slightly different, there could have been a different delay estimate, such as: 4.1, 5.7, or 6.5; such an error would increase the variation of the time delay estimate. The derivation of variance of $\hat{D}$, which follows, does not account for errors due to ambiguous peaks. It presumes that the estimated delay is in the neighborhood of the correct delay and not on a secondary peak.

A lower bound on the variance for any delay estimator (which is not necessarily attainable) is given by the Cramér-Rao bound

$$\sigma^2_{\hat{D}} \geq \frac{-1}{E\left\{\frac{\partial^2 \ln p(x \mid a, \tau)}{\partial \tau^2}\right\}}\Bigg|_{\tau=D} \qquad (3\text{-}21)$$

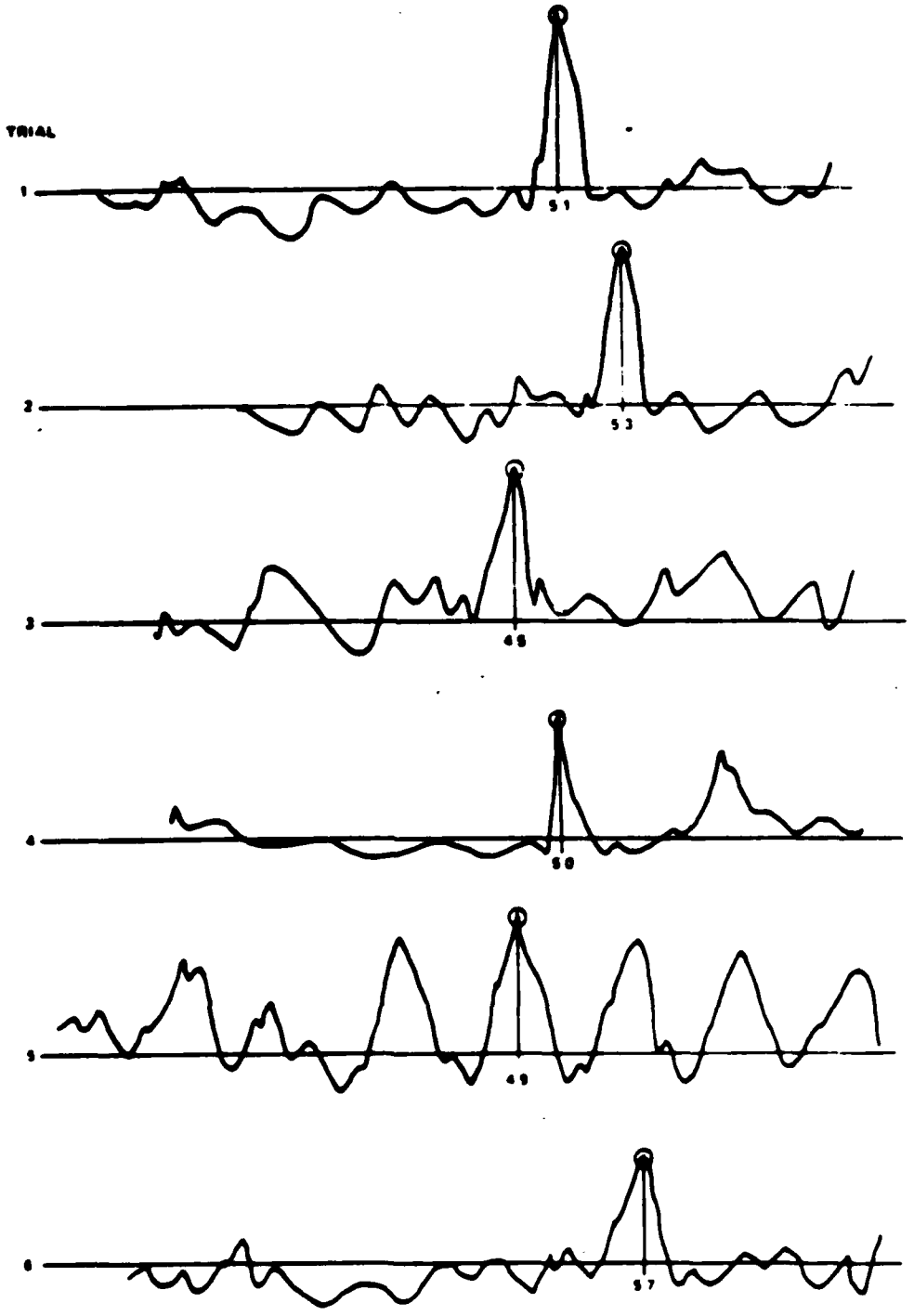

Figure 3-4 Six Hypothetical Correlator Outputs

Cramér-Rao bounds are discussed in Van Trees (1968) and Sage and Melsa (1971). The only part of the log pdf that depends on τ, the hypothesized delay, is J_3 of (3-17). That is,

$$E\left\{\frac{\partial^2}{\partial\tau^2} \ln p(\underline{x}|\alpha,\tau)\right\} = \frac{\partial^2}{\partial\tau^2} E(\tfrac{-1}{2}J_3) \quad . \tag{3-22}$$

If $G_{x_1x_2}(f)=\left|G_{x_1x_2}(f)\right|e^{-j2\pi fD}$, then since $E\left[\hat{G}_{x_1x_2}(f)\right]=G_{x_1x_2}(f)$, it follows that

$$E(\tfrac{-1}{2}J_3)=T\int_{-\infty}^{\infty} e^{j2\pi f(\tau-D)} \frac{C_{12}(f)}{[1 - C_{12}(f)]} df \quad . \tag{3-23}$$

Hence, the minimum obtainable variance for delay estimation is (Carter and Knapp (1976a))

$$\text{Minimum Var}(\hat{D})= \left[T\int_{-\infty}^{\infty} (2\pi f)^2 \frac{C_{12}(f)}{[1 - C_{12}(f)]} df\right]^{-1} \quad . \tag{3-24}$$

For the GCC processor with any weighting $W_g(f)=H_1(f)H_2^*(f)$ we will derive an expression for the local variation of the delay estimator and show that the ML weighting, (3-20), indeed achieves (3-24). The determination of the variance of delay estimates closely parallels a clever method of MacDonald and Schultheiss (1969). Equivalent to the Var $\hat{D}$ =Var $\tau\Big|_{\tau=D}$ (shown in Figure 3-5) is the left to right variation of the zero crossing of the derivative of the GCC function output

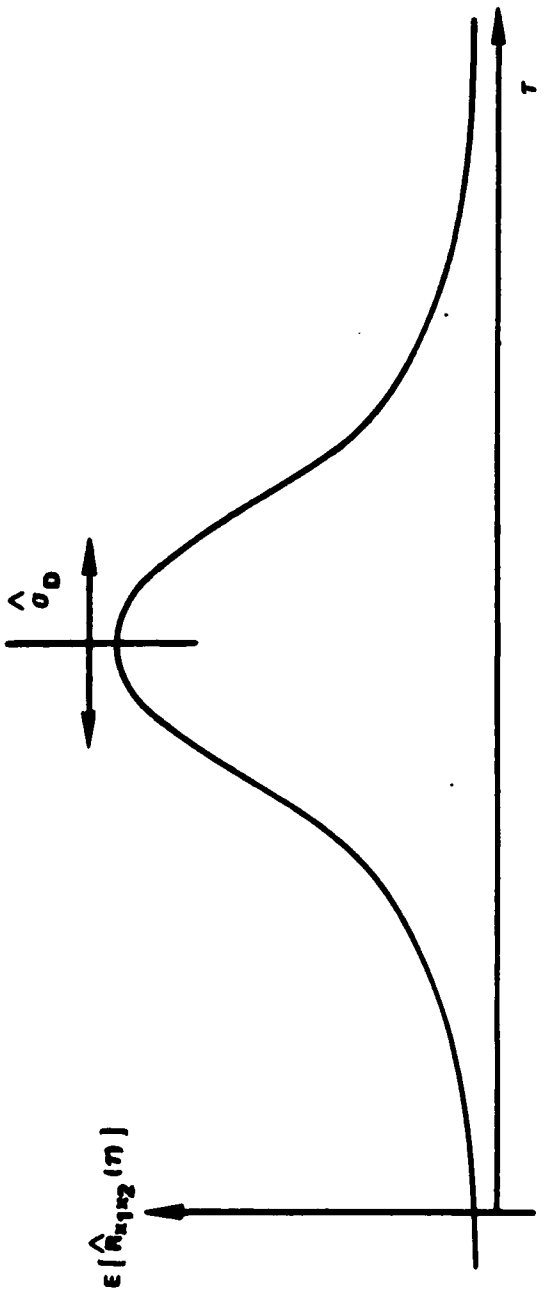

Figure 3-5 Variation of Delay Estimator

with respect to τ (shown in Figure 3-6). Typical mean output of the derivative of the correlator output, z, is plotted in Figure 3-5 together with similar curves σ_z above and below the mean. For σ_z small, so that curves are approximately linear between $D-\sigma_{\hat{D}}$ and $D+\sigma_{\hat{D}}$, the magnitude of the expected value of the slope of the output at the true value of delay is given by

$$\left|\frac{\partial}{\partial\tau}E[z]\right| = \left|\frac{\partial^2}{\partial\tau^2}\,E\;\hat{R}^{g}_{x_1x_2}(\tau)\;\right|_{\tau=D}\Bigg| = \left.\frac{\sigma_z}{\sigma_\tau}\right|_{\tau=D}, \qquad (3\text{-}25)$$

where σ denotes standard deviation. Again using $E\left[\hat{G}_{x_1x_2}(f)\right] = \frac{1}{T}\,E\left[\tilde{X}_1(f)\tilde{X}_2^*(f)\right] = G_{x_1x_2}(f)$, it follows with $G_{x_1x_2}(f) = \left|G_{x_1x_2}(f)\right|e^{-j2\pi D}$ that

$$\left|\frac{\partial^2}{\partial\tau^2}\,E\left[\hat{R}^{g}_{x_1x_2}(\tau)\right]\right|_{\tau=D}\Bigg| = T\int_{-\infty}^{\infty}(2\pi f)^2\left|G_{x_1x_2}(f)\right|W_g(f)df. \qquad (3\text{-}26)$$

In order to solve (3-25) for $\sigma_\tau \equiv \sigma_{\hat{D}}$ it is also necessary to solve for σ_z in Figure 3-6. The fundamental problem is to find the variance of the random variable z given by

$$z = \int_0^T y_1(t)y_2(t)dt\ . \qquad (3\text{-}27a)$$

(For our particular problem we will later assume that $y_1(t)$ is the output of a filter excited by $x_1(t)$ and $y_2(t)$ is the output of a filter excited by $x_2(t)$.) The variance of z is given by

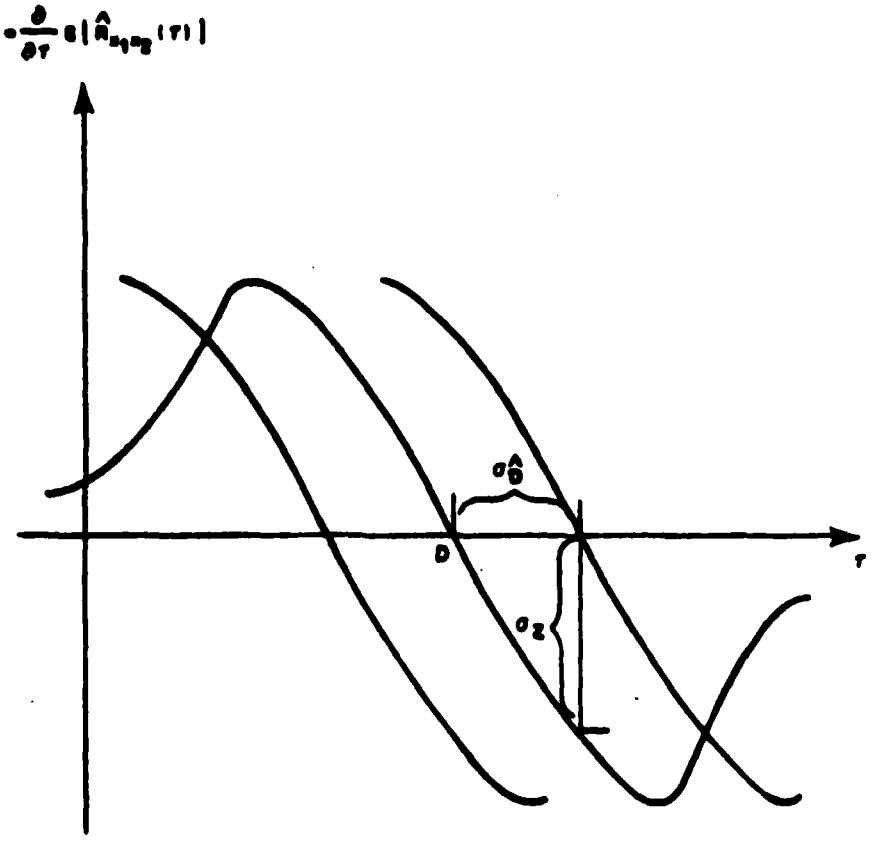

Figure 3-6 Derivative of Typical Output of Generalized Correlator

$$\sigma_z^2 = E[z^2] - E^2[z], \tag{3-27b}$$

where

$$E[z] = E\left[\int_0^T y_1(t)y_2(t)dt\right] \tag{3-27c}$$

$$= \int_0^T E[y_1(t)y_2(t)]\,dt \tag{3-27d}$$

$$= T\,R_{y_1y_2}(0) \tag{3-27e}$$

and

$$E[z^2] = \int_0^T\int_0^T E[y_1(t_1)y_2(t_1)y_1(t_2)y_2(t_2)]\,dt_1dt_2. \tag{3-27f}$$

Evaluation of the fourth moment in (3-27f) can be achieved under Gaussian assumptions. In particular, if $y_1(t)$ and $y_2(t)$ are jointly Gaussian (and stationary), then

$$E[z^2] = \int_0^T\int_0^T\Big[R^2_{y_1y_2}(0)+R^2_{y_1y_1}(t_1-t_2)R_{y_2y_2}(t_1-t_2)$$

$$+ R_{y_1y_2}(t_1-t_2)R_{y_2y_1}(t_1-t_2)\Big]dt_1dt_2 . \tag{3-27g}$$

Letting $\tau=t_1-t_2$ and using (3-27b) and (3-27e), (3-27g) becomes

$$\sigma_z^2 = \int_{-\infty}^{\infty}\int_{-\infty}^{\infty}\Big[R_{y_1y_1}(\tau)R_{y_2y_2}(\tau)+R_{y_1y_2}(\tau)R_{y_2y_1}(\tau)\Big]\cdot$$

$$\Psi(\tau+t_2)\Psi(t_2)d\tau dt_2 , \tag{3-27h}$$

where

$$\Psi(t) = \begin{cases}1 , & t\in(0,T)\\ 0 , & \text{elsewhere} .\end{cases}$$

Integrating (3-27h) with respect to t_2 and manipulating yields

$$\sigma_z^2 = T\int_{-T}^{T}\Big[R_{y_1y_1}(\tau)R_{y_2y_2}(\tau)+R_{y_1y_2}(\tau)R_{y_2y_2}(\tau)\Big]\left(1-\frac{\tau}{T}\right)d\tau . \tag{3-27i}$$

For large T (3-27i)

$$\sigma_z^2 \cong T\int_{-\infty}^{\infty}[R_{y_1y_1}(\tau)R_{y_2y_2}(\tau)+R_{y_1y_2}(\tau)R_{y_1y_2}(-\tau)]d\tau . \qquad (3\text{-}27j)$$

By Parseval's Theorem

$$\sigma_z^2 \cong T\int_{-\infty}^{\infty}[G_{y_1y_1}(f)G_{y_2y_2}(f)+G_{y_1y_2}^2(f)]df . \qquad (3\text{-}27k)$$

If $y_1(t)$ is the output of a filter $H_1(f)$ cascaded with a differentiator and $y_2(t)$ is the output of a filter $H_2(f)$ cascaded with a variable delay, then

$$G_{y_1y_1}(f) = |H_1(f)|^2 (2\pi f)^2 G_{x_1x_1}(f) \qquad (3\text{-}27l)$$

$$G_{y_2y_2}(f) = |H_2(f)|^2 G_{x_2x_2}(f) \qquad (3\text{-}27m)$$

$$G_{y_1y_2}(f) = H_1(f)H_2^*(f)e^{j2\pi f\tau}G_{x_1x_2}(f) . \qquad (3\text{-}27n)$$

For $\tau=D$ it follows, from (3-27k) - (3-27n), since $W_g(f)=H_1(f)H_2^*(f)$, that

$$\sigma_z^2\Big|_{\tau=D} = T\int_{-\infty}^{\infty}\left|W_g(f)\right|^2(2\pi f)^2G_{x_1x_1}(f)G_{x_2x_2}(f)[1-C_{12}(f)]df . \qquad (3\text{-}27o)$$

Combining (3-25) through (3-27o) yields

$$\sigma_{\hat{D}}=\sigma_\tau\Big|_{\tau=D} = \frac{\left\{\int_{-\infty}^{\infty}\left|W_g(f)\right|^2(2\pi f)^2G_{x_1x_1}(f)G_{x_2x_2}(f)[1-C_{12}(f)]\right\}^{\frac{1}{2}}}{(T)^{\frac{1}{2}}\int_{-\infty}^{\infty}(2\pi f)^2\left|G_{x_1x_2}(f)\right|W_g(f)\,df} \qquad (3\text{-}28)$$

which is valid for any $W_g(f)$. By substituting the appropriate weighting function into (3-28) the standard deviation of time delay estimates from each processor

can be analytically evaluated.

Parenthetically, we note that the results (3-28) with a particular weighting (3-20) can be related to (20) of MacDonald and Schultheiss (1969) as follows. Define the bearing to an acoustic source, similar to (3-2), as

$$\theta = \arccos\left(\frac{\xi D}{d}\right) , \tag{3-29}$$

where ξ is the (nominal) speed of sound in the nondispersive medium. Consider the case where the estimated D equals the true delay D plus a perturbation η. By a Taylor series expansion it follows that

$$\arccos\left[\frac{\xi}{d}(D+\eta)\right] \cong \arccos\left[\frac{\xi}{d}D\right] + \frac{d}{d\hat{D}} \arccos\left(\frac{\xi\hat{D}}{d}\right)\Bigg|_{\hat{D}=D} (\hat{D}-D) . \tag{3-30}$$

Thus the bearing error

$$e_b \triangleq \arccos\left[\frac{\xi}{d}(D+\eta)\right] - \arccos\left(\frac{\xi}{d}D\right) \tag{3-31a}$$

$$\cong \frac{-\xi}{d\sin\theta}(\hat{D}-D) , \tag{3-31b}$$

and

$$\left[E\left(e_b^2(t)\right)\right]^{\frac{1}{2}} \cong \frac{\xi}{d\sin\theta}\left[\mathrm{Var}\ \hat{D}\right]^{\frac{1}{2}} . \tag{3-32}$$

The term $d\sin\theta$ can be viewed as the effective array length (sensor separation) physically steered at the source. Assuming equal noise spectra, combining (3-32) with (3-28) and (3-20), and introducing a change of variables yields an expression which agrees with (20) of MacDonald and Schultheiss (1969) when θ is interpreted

as source (not wavefront) angle. Combining (3-28) and (3-32) suggests that in order to reduce to variance of the bearing estimate the observation period and the sensor separation should be made as large as possible. (In practice, there will undoubtedly be limitations on both sensor separation and observation time.) Further, since (3-32) depends on the effective array length physically steered toward the source, this suggests the desirability of sensor mobility to maximize the term $d\sin\theta$.

It has been shown that the variance of the time delay estimate in the neighborhood of the true delay, for general weighting function $W_g(f)$ is given by

$$\underset{\text{Var}}{g}\,\hat{D} = \frac{\int_{-\infty}^{\infty} |W_g(f)|^2 (2\pi f)^2 G_{x_1x_1}(f) G_{x_2x_2}(f) \left[1-C_{12}(f)\right] df}{T\left[\int_{-\infty}^{\infty} (2\pi f)^2 \left|G_{x_1x_2}(f)\right| W_g(f)\, df\right]^2} \quad (3\text{-}33a)$$

which for real processes may also be written

$$\underset{\text{Var}}{g}\,\hat{D} = \frac{\int_{o}^{\infty} |W_g(f)|^2 G_{x_1x_1}(f) G_{x_2x_2}(f) \left[1-C_{12}(f)\right] f^2 df}{8\pi^2 T \left[\int_{o}^{\infty} \left|G_{x_1x_2}(f)\right| W_g(f) f^2 df\right]^2} \quad . \quad (3\text{-}33b)$$

Notice that a scale factor change in $W_g(f)$ does <u>not</u> change the variance of the delay estimator.

The variance of the ML processor is

$$\text{Var}^{ML}\,\hat{D} = \left\{2T \int_{o}^{\infty} (2\pi f)^2 C_{12}(f) / [1-C_{12}(f)]\, df\right\}^{-1} , \quad (3\text{-}34)$$

which is the Cramér-Rao lower bound (3-24). It should be reemphasized that (3-33) and (3-34) evaluate the local variation of the time delay estimate and thus do not account for ambiguous peaks which may arise when the averaging time is not large enough for the given signal and noise characteristics. Indeed, when T is not sufficiently large, local variation may be a poor indicator of system performance and the envelope of the ambiguous peaks must be considered[1] (p. 40 of MacDonald and Schultheiss (1969) and p. 41 of Hamon and Hannan (1974)). Further, (3-33) and (3-34) predict system performance when signal and noise spectral characteristics are known. For sufficiently large T, these spectra can be estimated accurately. However, in general, (3-33) and (3-34) must be modified to account for estimation errors; alternatively, system performance can be evaluated by computer simulation. Empirical verification of expressions for variance has not been undertaken by simulation, because to do so without special purpose correlator hardware would be computationally prohibitive. For example, for a given $G_{s_1s_1}(f)$, $G_{n_1n_1}(f)$, $G_{n_2n_2}(f)$, α, and averaging time T, an estimated GCC function can be computed, from which only one number (the delay

[1]These observations were brought to the author's attention by C. Stradling and R. Trueblood of the Naval Undersea Center, San Diego, California.

estimate) can be extracted. To empirically evaluate the statistics of the delay estimate (which would be valid only for these particular signal and noise spectra) many such trials would need to be conducted. We have conducted one such trial (with T large) and verified that useful delay estimates can be obtained by inserting estimates $\left|\hat{G}_{x_1x_2}(f)\right|$ and $\hat{C}_{12}(f)$ in place of the true values in (3-20). This might have been expected since the estimated optimum weighting will converge to the true weighting as $T\to\infty$. (The statistics of the MSC estimates are given in appendix B.) In practice, T may be limited by the stationarity properties of the data, and (3-34) may be an overly optimistic prediction of system performance when signal and noise spectra are unknown.

With these qualifications in mind, consider the following example of computing the variance of the ML time delay estimate. Let

$$C_{12}(f) = \begin{cases} C, & f\in(0,B) \\ 0, & \text{otherwise} \end{cases} .$$

Then

$$\text{Var}^{ML}\,\hat{D} = \frac{1}{8\pi^2 T\,\frac{B^3}{3}\left[\frac{C}{1-C}\right]} . \qquad (3\text{-}35)$$

The strong dependence of the estimator variation to the coherence is illustrated in a plot of $\frac{1-C}{C}$ versus C in Figure 3-7. Note since

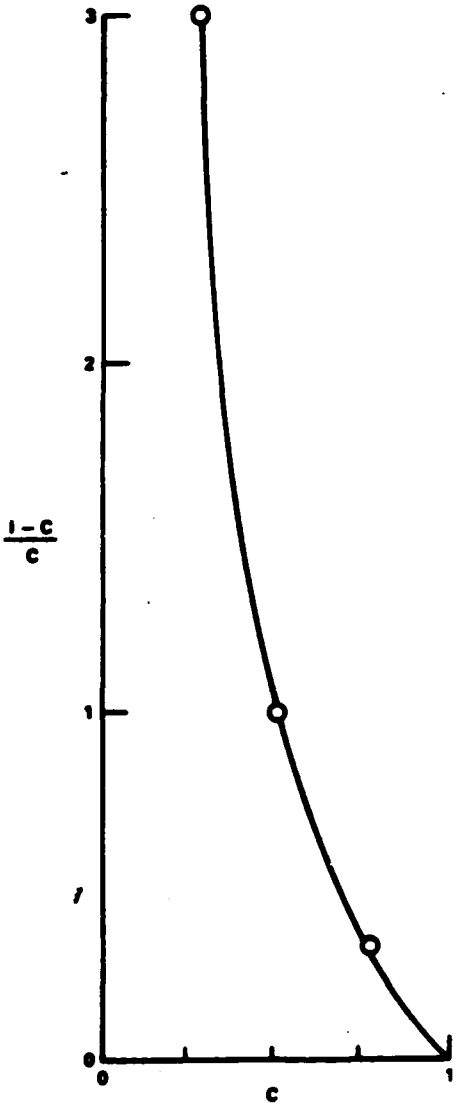

Figure 3-7 Variance of Delay Estimate as a Function of Coherence for Fixed B and T

$$\frac{C}{1-C} = C\,[1+C+C^2+\ldots]\ , \tag{3-36}$$

that for C<<1, (3-36) is

$$\frac{C}{1-C} \cong C\ . \tag{3-37}$$

But for C=1-Δ, where Δ<<1, then

$$\frac{C}{1-C} = \frac{1-\Delta}{\Delta} = \frac{1}{\Delta} - 1 \cong \frac{1}{\Delta}\ . \tag{3-38}$$

An approximate comparison of C=0.01 with C=0.99 shows the variance changed not by a factor of 100 to 1 but 10,000 to 1. The implication is that weakly coherent signals do not contribute much to reducing the variance of the delay estimate. That is not entirely so but is roughly correct. For example, high frequency, low coherent power may be important. A more complete discussion of the variance of several proposed time delay estimators is given in Chapter 4. Prior to Chapter 4, we will discuss other realizations of the ML delay estimator.

3C. Other Realizations of the ML Estimator

This section of Chapter 3 will present four methods for implementing the ML estimator for delay. One (and only) of the methods, the one considered to be most promising, has been programmed. (See appendix C.) The program presumes that signal and noise waveforms are real and that their statistics are unknown; hence the program uses appropriate estimates in lieu of known

values, when forming the weighting function.

The first realization which comes to mind is a bank of allowable delays as depicted in Figure 3-8. Each data waveform $x_1(t)$ and $x_2(t)$ is filtered by $H_1(f)$ and $H_2(f)$, respectively. The output of $H_2(f)$ is delayed for several reasonable values of delay depending on the resolution desired, a priori knowledge and processing cost allowed. Each delayed output is multiplied with the output of $H_1(f)$. After integration for T seconds, the delay that yields the maximum award is the estimate of delay.

The second method is to realize that the bank of delays in Figure 3-8 corresponds to a particular method for computing the GCC function. Indeed we need not be particular about the details of how the GCC function is estimated so long as it is estimated "accurately." The second method uses the overlapped FFT method presented by Carter, Knapp, and Nuttall (1973a) to compute the estimated cross spectrum and MSC. The estimated cross spectrum is appropriately weighted and inverse transformed via an FFT to obtain the estimated GCC function. The delay where the GCC peaks is the estimate of delay. One advantage to methods 1 and 2 is that by computing the crosscorrelation for a large range of delays the presence of more than one delay (acoustic source) can be observed. There are other advantages, too; in the GCC method uncorrelated cross

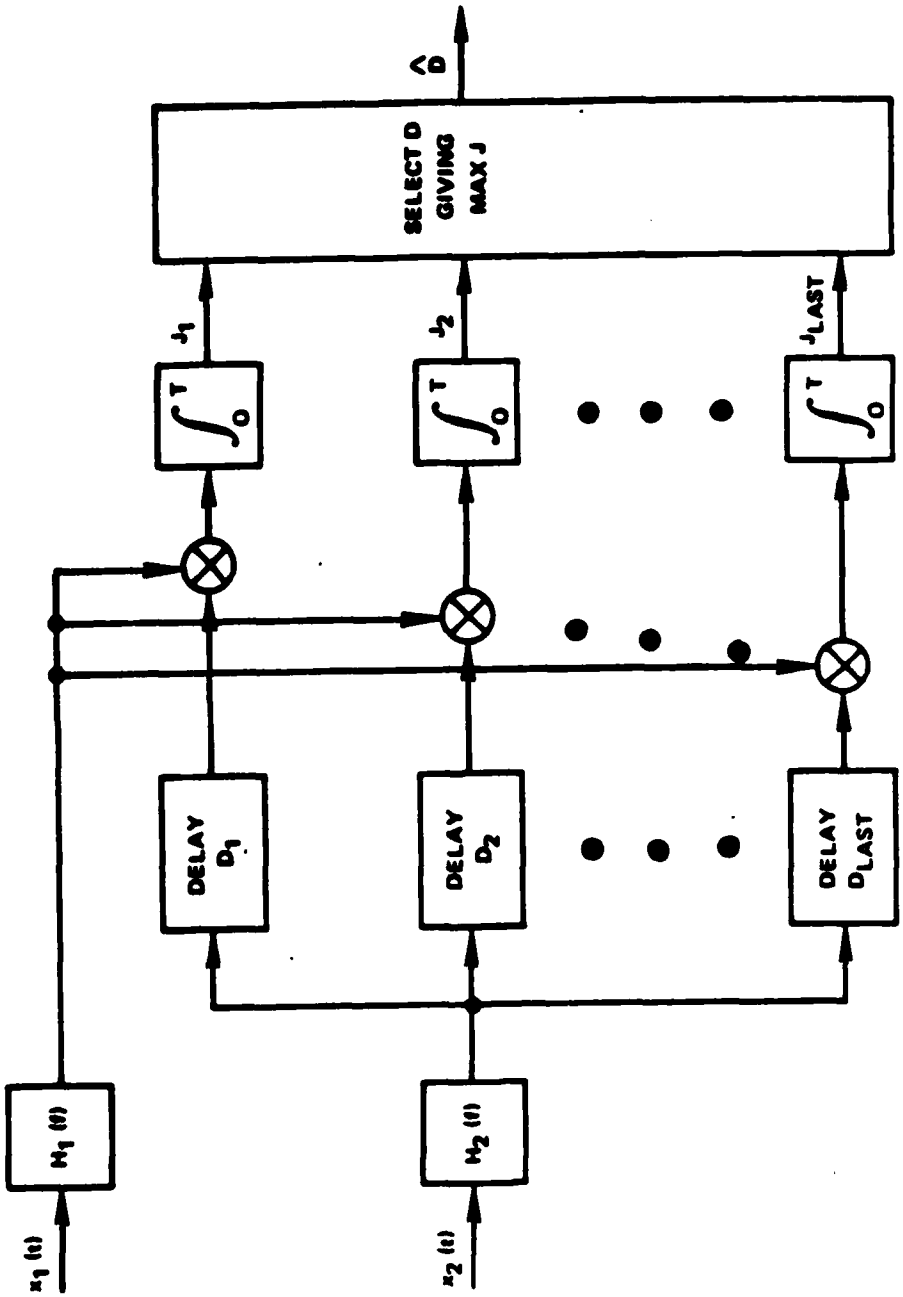

Figure 3-8 Block Diagram of Open Loop ML Time Delay Estimator Realization

terms vanish and there is no unknown residual bias to account for when establishing thresholds (other than the type discussed in appendix B).

If we desire to use a closed loop control scheme to automatically adjust the delay estimate $\hat{D}$, we can instrument the estimator with a derivative in one channel much like our discussion of the variance of the estimator.[1] When we are in the neighborhood of the correct delay, the output in Figure 3-9 should be approximately zero. Any difference from zero (that is, error) is fed back, perhaps smoothed and scaled, and used to adjust the delay estimate in order to drive the system output to zero. For estimating more than one delay (acoustic source) with this realization, more than one variable delay is required. It should be noted as pointed out by Kochenburger (1972) that differentiation is a "noisy" process which should be avoided. However, the filter $H_1(f)$ and the integrator in Figure 3-9 may reduce the adverse effect of this realization.

The final realization to be discussed is the method of Carter and Knapp (1976a). In this method we re-examine our derivation in section 3A. In

---

[1]This idea was brought to the author's attention by J. P. Ianniello of the Naval Underwater Systems Center, New London, Connecticut.

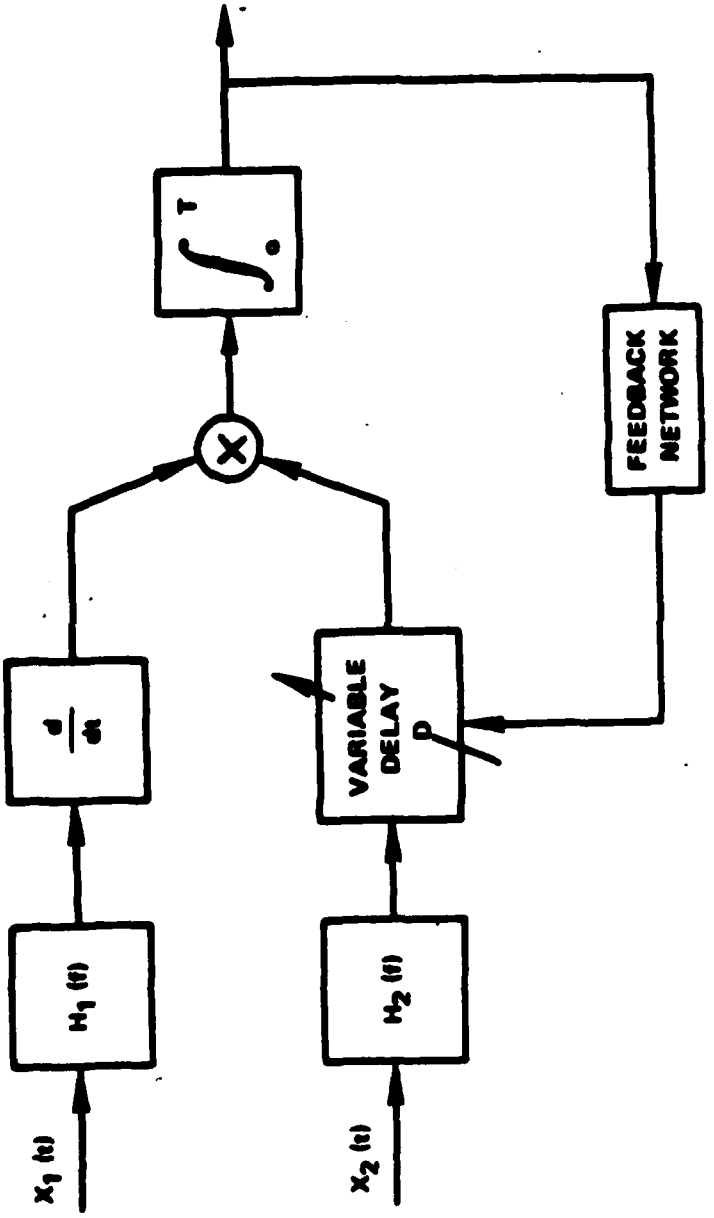

Figure 3-9 Block Diagram of ML Time Delay Estimator with Feedback

particular, the spectral density matrix (3-6), for models like (3-1) which give rise to spectral densities given by (3-14), can be expressed (suppressing the f dependence) as

$$Q_x = Q_n + G_{ss} V^* V' , \tag{3-39}$$

where the steering vector

$$V' = [1, \alpha e^{-j2\pi fD}] \tag{3-40}$$

and, for uncorrelated noises,

$$Q_n = \begin{bmatrix} G_{n_1 n_1} & 0 \\ 0 & G_{n_2 n_2} \end{bmatrix}, \tag{3-41}$$

and (for any given f) G_{ss} is a scalar. The complete award function to be maximized (3-15) requires knowledge of Q_x^{-1}. The inverse of (3-39) is given by Knapp (1966) as

$$Q_x^{-1} = Q_n^{-1} - \frac{G_{ss} Q_n^{-1} V^* V' Q_n^{-1}}{1 + G_{ss} V' Q_n^{-1} V^*} . \tag{3-42}$$

For uncorrelated noises Q_n^{-1} does not depend on D; therefore, the total award is maximized by maximizing

$$J_D = -\frac{1}{2} \int_{-\infty}^{\infty} \tilde{X}^* \tilde{H}^* \tilde{H}' \tilde{X} \, df, \tag{3-43}$$

where the 1x2 vector filter

$$\tilde{H} = [\tilde{H}_1, \tilde{H}_2]' = \frac{Q_n^{-1} V \sqrt{G_{ss}}}{\left[1 + G_{ss} V' Q_n^{-1} V^*\right]^{\frac{1}{2}}} . \tag{3-44}$$

By Parseval's Theorem, (3-43) can be implemented by filtering $x_1(t)$ with filter $\tilde{H}_1(f)$ and filtering $x_2(t)$ with filter $\tilde{H}_2(f)$, then summing, squaring, and averaging.

If we separate from $\tilde{H}_2(f)$ that portion dealing with the hypothesized delay we can realize the delay estimator as shown in Figure 3-10. Moreover, note that

$$Q_n^{-1}V\sqrt{G_{ss}} = \begin{bmatrix} \frac{1}{G_{n_1n_1}} & 0 \\ 0 & \frac{1}{G_{n_2n_2}} \end{bmatrix} \begin{bmatrix} 1 \\ \alpha e^{-j2\pi fD} \end{bmatrix} \sqrt{G_{ss}} \qquad (3\text{-}45a)$$

$$= \begin{bmatrix} \frac{\sqrt{G_{ss}}}{G_{n_1n_1}} \\ \frac{\alpha\sqrt{G_{ss}}\, e^{-j2\pi fD}}{G_{n_2n_2}} \end{bmatrix}_{2x1} \qquad (3\text{-}45b)$$

Further,

$$1+G_{ss}V'Q_n^{-1}V^* = 1+G_{ss}\,[\,1, \alpha e^{-j2\pi fD}] \begin{bmatrix} \frac{1}{G_{n_1n_1}} & 0 \\ 0 & \frac{1}{G_{n_2n_2}} \end{bmatrix} \begin{bmatrix} 1 \\ \alpha e^{j2\pi fD} \end{bmatrix} \qquad (3\text{-}46a)$$

$$= 1+G_{ss}\,[1, \alpha e^{-j2\pi fD}] \begin{bmatrix} \frac{1}{G_{n_1n_1}} \\ \frac{\alpha e^{j2\pi fD}}{G_{n_2n_2}} \end{bmatrix} \qquad (3\text{-}46b)$$

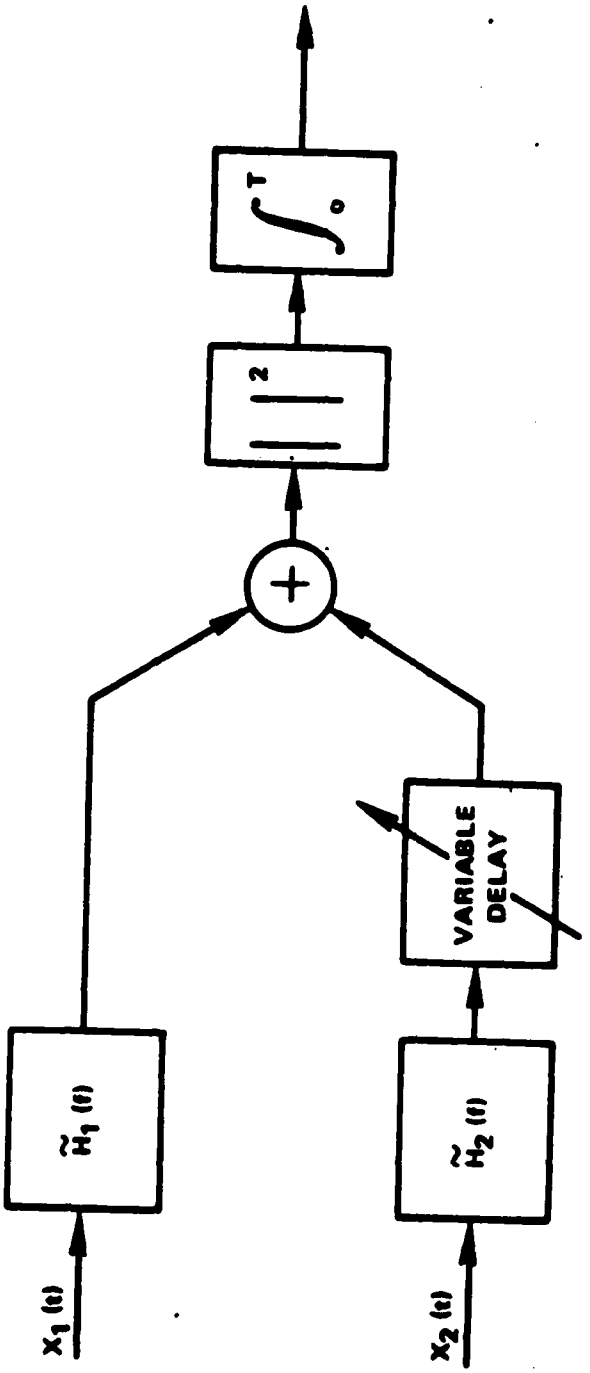

Figure 3-10 Filter and Sum Realization of ML Time Delay Estimator

$$= 1 + \frac{G_{ss}}{G_{n_1 n_1}} + \frac{a^2 G_{ss}}{G_{n_2 n_2}} \quad . \tag{3-46c}$$

Thus, the estimator can be realized as shown in Figure 3-11. For low SNR, that is, when

$$\frac{G_{ss}}{G_{n_1 n_1}(f)} \ll 1 \text{ and } \frac{a^2 G_{ss}(f)}{G_{n_2 n_2}(f)} \ll 1 \ ,$$

$$1 + G_{ss} V' Q_n^{-1} V^* \approx 1 \tag{3-47}$$

then the filter following the summation in Figure 3-11 is approximately a unity-gain zero-phase all-pass network. Note in Figure 3-11 that the form of the filters at each sensor depends on the signal and noise spectrum. In particular the estimation of D presented here requires filtering in exactly the fashion as the detection of a signal arrival presented by Knapp (1966). These low SNR filter forms are commonly referred to as Eckart filters after early work done in the detection area by Eckart (1952).

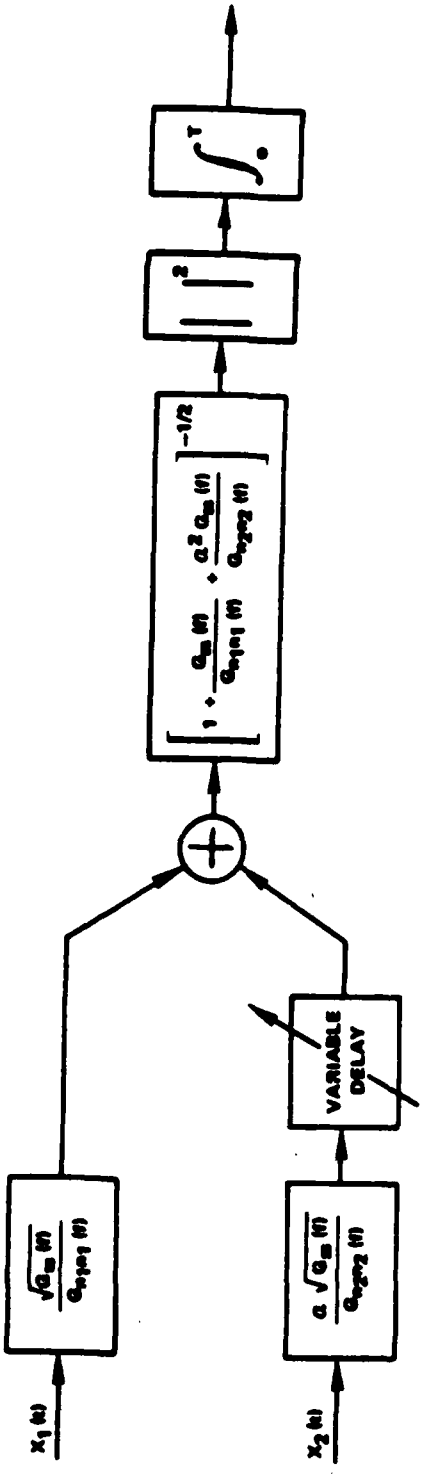

Figure 3-11 Explicit Filter and Sum Realization of ML Time Delay Estimator

CHAPTER 4

COMPARISON OF THE ML ESTIMATOR TO OTHER PROPOSED SUBOPTIMUM PROCESSORS

The objective of Chapter 4 is to compare the ML time delay estimator with several other processors that have been proposed. From Chapter 3, we know that the ML processor will have the minimum local variation. Also, the previously derived expressions for the local variation of any correlation processor can be used to analytically compare other intuitively appealing correlation processors. Additionally, the effect of erroneously identifying the signal spectrum will be investigated, since that will cause the selection of an erroneous weighting function.

The first section of this chapter presents the motivation for the use of crosscorrelation processors. The second section compares several such processors, and the third section considers the interrelationships of these various processors.

4A. Motivation for Crosscorrelation Processors

For the model

$$x_1(t) = s_1(t)+n_1(t) \tag{4-1a}$$

$$x_2(t) = \alpha s_1(t+D)+n_2(t) \tag{4-1b}$$

one common method of estimating the time delay D is to

compute the crosscorrelation function

$$R_{x_1x_2}(\tau)=E[x_1(t)x_2^*(t-\tau)] , \tag{4-2}$$

where E denotes expectation. The argument τ that maximizes (4-2) provides an estimate of delay. For models of the form of (4-1), the crosscorrelation of $x_1(t)$ and $x_2(t)$ is

$$R_{x_1x_2}(\tau)=\alpha R_{s_1s_1}(\tau-D)+R_{n_1n_2}(\tau) . \tag{4-3}$$

The Fourier transform of (4-3) gives the cross-power spectrum

$$G_{x_1x_2}(f)=\alpha G_{s_1s_1}(f)e^{-j2\pi fD}+G_{n_1n_2}(f) . \tag{4-4}$$

If $n_1(t)$ and $n_2(t)$ are uncorrelated ($G_{n_1n_2}(f)=0$), the cross-power spectrum between $x_1(t)$ and $x_2(t)$ is a scaled signal power spectrum times a complex exponential. Since multiplication in one domain corresponds to convolution in the transformed domain (see, for example, Oppenheim and Schafer (1975)), it follows for $G_{n_1n_2}(f)=0$ that

$$R_{x_1x_2}(\tau) =\alpha R_{s_1s_1}(\tau) \circledast \delta(\tau-D) . \tag{4-5}$$

One interpretation of (4-5) is that the delta function has been spread or "smeared" by the Fourier transform of the signal spectrum. If $s_1(t)$ is a white noise source, then its Fourier transform is a delta function and no spreading takes place. An important

property of autocorrelation functions is that $R_{s_1s_1}(\tau) \leq R_{s_1s_1}(0)$. Equality will hold for certain τ for periodic functions (see, for example, Davenport (1970), pp. 323-326). However, for most practical applications, equality does not hold for $\tau \neq 0$, and the true crosscorrelation (4-5) will peak at D regardless of whether or not it is spread out. The spreading simply acts to broaden the peak.

In fact, more generally, when $x_1(t)$ and $x_2(t)$ have been filtered by H_1 and H_2, respectively, then the cross-power spectrum between the filter outputs is given on p. 399 Davenport (1970) as

$$G_{y_1y_2}(f) = H_1(f)H_2^*(f)G_{x_1x_2}(f) \quad . \tag{4-6}$$

Therefore, the GCC between $x_1(t)$ and $x_2(t)$ is

$$R^g_{x_1x_2}(\tau) = \int_{-\infty}^{\infty} W_g(f)G_{x_1x_2}(f)e^{j2\pi f} \, df \quad , \tag{4-7a}$$

where

$$W_g(f) = H_1(f)H_2^*(f) \tag{4-7b}$$

denotes the general frequency weighting. The particular weighting selected is denoted by a change in the subscript g.

For all of the proposed weightings which we will investigate, $W(f) = W^*(f)$ and $W(f) = W(-f)$; that is, $W(f)$ is real and even. These properties are also held by the minimum variance ML weighting.

To distinguish which of the proposed general weightings has been applied, we denote

$$G_{y_1y_2}(f)=G^{g}_{x_1x_2}(f) \tag{4-8a}$$

and thus

$$G_{y_1y_2}(f)= W_g(f)[\alpha G_{s_1s_1}(f)e^{-j2\pi fD}+G_{n_1n_2}(f)] \ . \tag{4-8b}$$

When the noises are incoherent, taking the Fourier transform of (4-8b) yields

$$R^{g}_{x_1x_2}(\tau)=R_{ww}(\tau) \circledcirc \alpha R_{s_1s_1}(\tau) \circledcirc \delta(\tau-D) \ , \tag{4-9}$$

where $R_{ww}(\tau)$, the inverse Fourier transform of $W_g(f)$, is even. This being the case, the true GCC will also peak at D regardless of the specific weighting. Thus one might be puzzled as to why any weighting is needed. Indeed, the crosscorrelation function alone is a useful technique for estimating time delay.

Two practical reasons why prefiltering is desirable are evident. If the noise is coherent, for example, if

$$G_{n_1n_2}(f)=G_{s_2s_2}(f)e^{-j2\pi fD_2} \ , \tag{4-10}$$

then

$$R^{g}_{x_1x_2}(\tau)=R_{ww}(\tau) \circledcirc [\alpha R_{s_1s_1}(\tau) \circledcirc \delta(\tau-D) + R_{s_2s_2}(\tau) \circledcirc \delta(\tau-D_2)] \ . \tag{4-11}$$

It is clear, from (4-11), that the convolutions by $R_{s_1s_1}(\tau)$ and $R_{s_2s_2}(\tau)$ will produce two peaks which may

be spread into one another. The convolution by $R_{ww}(\tau)$ can aid to undo this smearing. For a single delay broadening of the delay peak may not be a serious problem. However, when the signal has multiple delays, the true crosscorrelation is given by

$$R_{x_1x_2}(\tau)=R_{s_1s_1}(\tau) \bullet \sum_i \alpha_i \delta(\tau-D_i) \ . \qquad (4\text{-}12)$$

In this case also, the convolution with $R_{s_1s_1}(\tau)$ can spread one delta function into another, thereby making it impossible to distinguish peaks or delay times. Under ideal conditions where $\forall f \hat{G}_{x_1x_2}(f) \cong G_{x_1x_2}(f)$, $W_g(f)$ should be chosen to ensure large sharp peaks in $R_{y_1y_2}(\tau)$ rather than a broad one (see Figure 4-1), since this will ensure good time delay resolution.

There is a second important reason why prefiltering is desirable. In practice, only an estimate $\hat{G}_{x_1x_2}(f)$ of $G_{x_1x_2}(f)$ can be obtained from finite observations of $x_1(t)$ and $x_2(t)$. Thus we can never exactly obtain the crosscorrelation from a limited amount of time data. Because of the finite observation time, then, $R_{x_1x_2}(\tau)$ can only be estimated. For example, for real ergodic processes an estimate of the crosscorrelation is given on p. 327 of Papoulis (1965), as:

$$\hat{R}_{x_1x_2}(\tau)= \frac{1}{T-\tau} \int_{\tau}^{T} x_1(t)x_2(t-\tau)dt \ , \qquad (4\text{-}13)$$

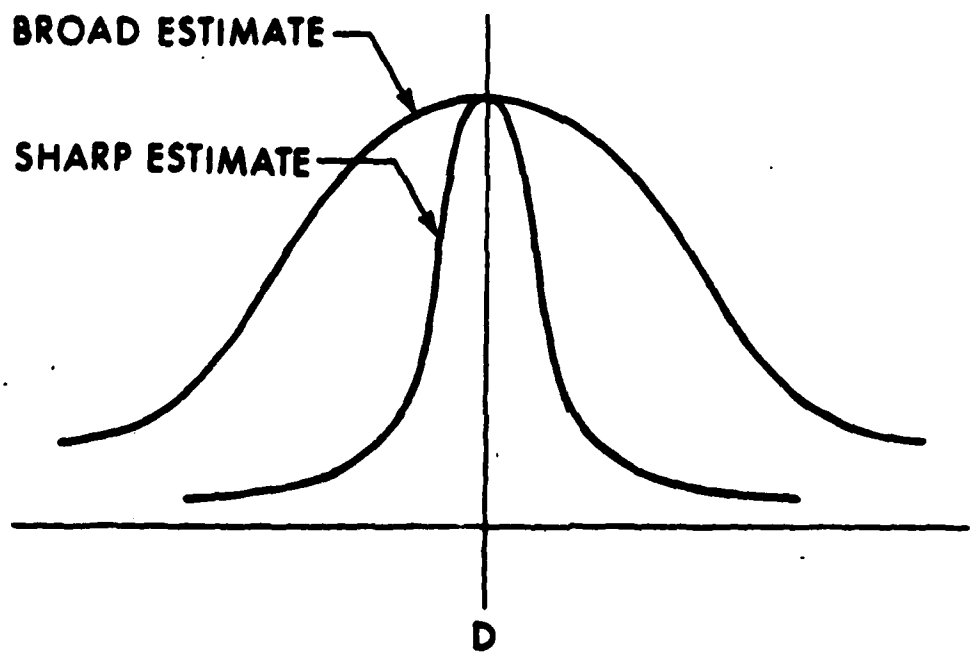

Figure 4-1 Broad and Sharp Estimates of Delay for Infinite Averaging

where T represents the observation interval. For limited duration data records, the accuracy of the delay estimate, $\hat{D}$, can be improved by prefiltering $x_1(t)$ and $x_2(t)$ prior to the integration in (4-13). In practice we can compute (4-13) by weighting the estimated cross spectrum and computing an inverse Fourier transform to obtain an estimated GCC as follows:

$$\hat{R}^{(g)}_{x_1x_2}(\tau)=\int_{-\infty}^{\infty} W_g(f)\hat{G}_{x_1x_2}(f)e^{j2\pi f\tau}df\,. \qquad (4\text{-}14)$$

$W_g(f)$ now serves to improve the estimate of $R_{x_1x_2}(\tau)$ used to estimate time delay.

In practice, depending on the particular form of $W_g(f)$ and the a priori information, it may also be necessary to estimate $W_g(f)$. For example, when the role of the prefilters is to accentuate the signal passed to the correlator at those frequencies at which the SNR is highest, then $W_g(f)$ can be expected to be a function of signal and noise spectra which must either be known a priori or estimated.

Hence, we see that the true crosscorrelation function, for the model (4-1), is sufficient to determine the correct time delay; but for practical (finite data) considerations it is desirable to prefilter $x_1(t)$ and $x_2(t)$ prior to crosscorrelation. Indeed, the problem of selecting $W_g(f)$ to optimize certain performance criteria is not new and has been studied by several investigators. (See, for example, Akaike and Yamanouchi

(1963), Bangs (1971), and Hannan and Thomson (1971).)

Our intuitive discussion of sharply peaked estimators may suggest certain types of weighting. However, sharp peaks are more sensitive to errors introduced by finite observation time, particularly in cases of low SNR. Thus, as with other spectral estimation problems, the choice of $W_g(f)$ is a compromise between good resolution and stability. In the subsequent section we compare several promising weighting functions proposed previously in the literature.

4B. Comparison of Proposed Processors

The preceding discussion provides background for the role that $W_g(f)$ is to play. Now the six versions of the generalized crosscorrelation function listed in Table 4-1 will be examined individually. In the process of comparing the processors in Table 4-1, there will be a tendency to want to look at some simple cases, for example, equal white noises and strong (or weak) white noise signals. In this regard, it can be shown for the case where $G_{n_1n_1}(f)=G_{n_2n_2}(f)=G_{nn}(f)$ is equal to a constant times $G_{s_1s_1}(f)$ (whether or not the signal is white) that five of the processors in Table 4-1 provide for the identical frequency weighting, except for a constant. (The crosscorrelation processor ($W(f)=1, \forall f$) is a delta function smeared out by the Fourier transform of the signal (noise) power spectrum.) In these cases,

Table 4-1. Proposed Processors

Processor Name	Weight $W(f)=H_1(f)H_2^*(f)$
1. Roth Impulse Response	$1/G_{x_1x_1}(f)$
2. Smoothed Coherence Transform (SCOT)	$1/\sqrt{G_{x_1x_1}(f)G_{x_2x_2}(f)}$
3. Phase Transform (PHAT)	$1/\left\|G_{x_1x_2}(f)\right\|$
4. Crosscorrelation	1
5. Eckart	$G_{s_1s_1}(f)/\left[G_{n_1n_1}(f)G_{n_2n_2}(f)\right]$
6. Maximum Likelihood (ML)	$\dfrac{C_{12}(f)}{\left\|G_{x_1x_2}(f)\right\|\left[1-C_{12}(f)\right]}$

the delay estimate from each of these five processors will have the same variance. Hence, a complete comparison can only be made when detailed signal and noise characteristics are provided. Such information is largely dependent on the particular application and a detailed comparison is therefore beyond the intent of this work. For underwater acoustic applications, characteristics of the radiated and self noise of ships, submarines, and torpedoes and the noise background of the sea are given by Urick (1967). For more fundamental signal and noise characteristics, it is useful to provide a brief example of using (3-33) and (3-34). Suppose the example corresponds to (4-1) where $\alpha=1$; $G_{ss}(f)=1$, $\forall f \epsilon (-B,B)$ otherwise $G_{ss}(f)=0$; $G_{n_1n_1}(f)=G_{n_2n_2}(f)=1, \forall f$. It follows from (2-1) and (2-2) that

$$C_{12}(f) = \frac{G_{ss}^2(f)}{[G_{ss}(f)+G_{n_1n_1}(f)][G_{ss}(f)+G_{n_2n_2}(f)]} . \quad (4\text{-}15)$$

Hence,

$$C_{12}(f) = \begin{cases} 0.25 & , \forall f \ (-B,B) \\ 0 & , \text{otherwise} . \end{cases}$$

Other values are given in Table 4-2.

4B1. Roth Processor

The weighting proposed by Roth (1971)

$$W_R(f) = \frac{1}{G_{x_1x_1}(f)} , \quad (4\text{-}16)$$

where the subscript R is to distinguish the choice of

Table 4-2. Comparison Case Data

	$f\varepsilon(0,B)$	$f\varepsilon(+B,H)$
$G_{s_1 s_1}(f)$	1	0
$G_{n_1 n_1}(f)=G_{n_2 n_2}(f)$	1	1
$G_{x_1 x_1}(f)=G_{x_2 x_2}(f)$	2	1
$\left\|G_{x_1 x_2}(f)\right\|$	1	0
$C_{12}(f)$	0.25	0

$W_g(f)$, yields[1]

$$\hat{R}^{(R)}_{x_1x_2}(\tau)=\int_{-\infty}^{\infty} \frac{\hat{G}_{x_1x_2}(f)}{G_{x_1x_1}(f)} e^{j2\pi f\tau} df \quad . \tag{4-17}$$

Equation (4-17) estimates the impulse response of the optimum linear (Wiener-Hopf) filter,

$$H_m(f)=\frac{G_{x_1x_2}(f)}{G_{x_1x_1}(f)} \quad , \tag{4-18}$$

which "best" approximates the mapping of $x_2(t)$ to $x_1(t)$ (see, for example, Van Trees (1968), Carter and Knapp (1975) and the discussion of Theorem 2-3). If $n_1(t)\neq 0$, as is generally the case for (4-1), then

$$G_{x_1x_1}(f)=G_{s_1s_1}(f)+G_{n_1n_1}(f) \quad , \tag{4-19}$$

and ideally

$$R^{(R)}_{x_1x_2}(\tau)=\delta(\tau-D) \circledast \int_{-\infty}^{\infty} \frac{\alpha G_{s_1s_1}(f)}{\left[G_{s_1s_1}(f)+G_{n_1n_1}(f)\right]} e^{j2\pi f\tau} df. \tag{4-20}$$

Therefore, except when $G_{n_1n_1}(f)$ equals any constant (including zero) times $G_{s_1s_1}(f)$, the delta function will again be spread out. The Roth processor has the desirable effect of suppressing those frequency regions

---

[1]As discussed earlier, W(f) may have to be estimated for this processor and those which follow, because of a lack of a priori information. In this case, (4-16) may require that $G_{x_1x_1}(f)$ be replaced with $\hat{G}_{x_1x_1}(f)$.

where $G_{n_1n_1}(f)$ is large and $\hat{G}_{x_1x_2}(f)$ is therefore more likely to be in error.

From (3-33),

$$\underset{\text{Var}(\hat{D})}{R} = \frac{\int_o^\infty \frac{G_{x_2x_2}}{G_{x_1x_1}}(1-C)f^2df}{8\pi^2T\left[\int_o^\infty \left|G_{x_1x_2}\right|\frac{1}{G_{x_1x_1}}f^2df\right]^2} \quad (4\text{-}21)$$

In the example of Table 4-2 this becomes

$$= \frac{\int_o^B f^2\ \frac{3}{4}\,df + \int_B^H f^2 1\,df}{8\pi^2\ T\left[\int_o^B f^2\frac{1}{2}df\right]^2} \quad (4\text{-}22a)$$

$$= \frac{B^3 + \frac{4}{3}H^3 - \frac{4}{3}B^3}{\frac{8}{9}\pi^2TB^6}\ , \quad (4\text{-}22b)$$

when B=H (4-22b) agrees with (3-35) as expected; but if H is large in comparison with B, the variance of the Roth processor will be large in comparison to the Cramér-Rao bound (3-24).

4B2. Smoothed Coherence Transform

Errors in $\hat{G}_{x_1x_2}(f)$ may be due to frequency bands where $G_{n_2n_2}(f)$ is large, as well as bands where $G_{n_1n_1}(f)$ is large. One is therefore uncertain whether to form $W_R(f)=1/G_{x_1x_1}(f)$ or $W_R(f)=1/G_{x_2x_2}(f)$; hence,

the smoothed coherence transform (SCOT) proposed by[1] Carter, Nuttall, and Cable (1973) yields

$$W_s(f) = 1/\sqrt{G_{x_1x_1}(f)G_{x_2x_2}(f)} \quad . \tag{4-23}$$

This weighting gives the SCOT

$$\hat{R}^{(s)}_{x_1x_2}(\tau) = \int_{-\infty}^{\infty} \hat{\gamma}_{x_1x_2}(f) e^{j2\pi f\tau} df \quad , \tag{4-24}$$

where the coherence estimate[2]

$$\hat{\gamma}_{x_1x_2}(f) \triangleq \frac{\hat{G}_{x_1x_2}(f)}{\sqrt{G_{x_1x_1}(f)G_{x_2x_2}(f)}} \quad . \tag{4-25}$$

For $H_1(f)=1/\sqrt{G_{x_1x_1}(f)}$ and $H_2(f)=1/\sqrt{G_{x_2x_2}(f)}$, the SCOT can be interpreted as prewhitening filters followed by a crosscorrelation. When $G_{x_1x_1}(f)=G_{x_2x_2}(f)$, the SCOT is equivalent to the Roth processor. If $n_1(t)\neq 0$ and $n_2(t)\neq 0$, the SCOT exhibits the same spreading as the Roth processor.

---

[1]The SCOT was originally proposed by G.C.Carter, A.H. Nuttall, and P.G.Cable in 1972 and successfully applied to actual data by G.C.Carter and P.G.Cable in 1972 and Brady (1973) for part of his Ph.D. work.

[2]A more standard coherence estimate is formed when the autospectra must also be estimated, as is usually the case. (See Carter, Knapp and Nuttall (1973a).)

From (3-33)

$$\overset{s}{\mathrm{Var}}(\hat{D}) = \frac{\int_0^\infty f^2\,[1-C(f)]\,df}{8\pi^2 T\left[\int_0^\infty f^2\sqrt{C(f)}\,df\right]^2} \quad . \tag{4-26}$$

Note as $C(f)\to 1$, the numerator becomes small and the denominator becomes large. For our example, since $G_{x_1x_1}(f)=G_{x_2x_2}(f)$ the SCOT has the same variance as the Roth processor.

4B3. Phase Transform

To eliminate the spreading evident above, the phase transform (PHAT) uses the weighting[1]

$$W_p(f) = \frac{1}{\left|G_{x_1x_2}(f)\right|} \quad , \tag{4-27}$$

which yields

$$\hat{R}^{(p)}_{x_1x_2}(\tau) = \int_{-\infty}^{\infty} \frac{\hat{G}_{x_1x_2}(f)}{\left|G_{x_1x_2}(f)\right|} e^{j2\pi f\tau}\,df \quad . \tag{4-28}$$

For the model (4-1) with uncorrelated noise (that is, $G_{n_1n_2}(f)=0$),

$$\left|G_{x_1x_2}(f)\right| = \alpha G_{s_1s_1}(f) \quad . \tag{4-29}$$

---

[1] The PHAT was originally suggested by G.C.Carter, A.H. Nuttall and P.G. Cable in 1972.

Ideally, when $\hat{G}_{x_1x_2}(f)=G_{x_1x_2}(f)$,

$$\frac{\hat{G}_{x_1x_2}(f)}{\left|G_{x_1x_2}(f)\right|} = e^{j\phi(f)}=e^{j2\pi fD} \tag{4-30}$$

has unit magnitude and

$$R^{(p)}_{x_1x_2}(\tau)=\delta(t-D) \ . \tag{4-31}$$

The PHAT was developed purely as an ad hoc technique. Notice that, for models of the form of (4-1) with uncorrelated noises, the PHAT (4-28), ideally, does not suffer the spreading that other processors do.

From (3-33),

$$\overset{(p)}{\text{Var}}(\hat{D}) = \frac{\int_o^\infty f^2 \frac{1}{C}(1-C)\,df}{8\pi^2T\left[\int_o^\infty f^2 df\right]^2} \ . \tag{4-32}$$

As $C\to 1$, $\frac{(1-C)}{C}\to 0$, so the processor will behave well (that is, low variance). However, as expected, as $C\to 0$ the variance grows without bound. For the example in Table 4-2, assuming the weighting is zero for $f>H$,

$$\overset{(p)}{\text{Var}}(\hat{D}) = \frac{\int_o^B f^2\cdot 4\cdot\frac{3}{4} + \lim_{C\to 0}\int_B^H f^2\frac{1-C}{C}\,df}{8\pi^2T\left[\int_o^H f^2 df\right]^2} \ . \tag{4-33}$$

Except when H=B, this processor will suffer a complete breakdown as C tends to zero. When H=B, we obtain the same variance as the Roth and SCOT processors for then

(as indicated earlier) $G_{n_1n_1}(f)=G_{n_2n_2}(f)=G_{s_1s_1}(f)$ and all processors behave equally well. For models of the form of (4-1), the poor behavior of the PHAT suggests that W(f) should not be inversely proportional to signal power. The crosscorrelator is one method of avoiding the application of weight inverse to signal characteristics. Two other processors in Table 4-1 also assign weights or filtering proportionate to SNR: the Eckart filter (Eckart (1952)) and the ML estimator or processor of Hannan and Thomson (1973). We now examine these three processors in depth.

4B4. Crosscorrelation

The variance of the delay estimate from the crosscorrelation processor is

$$\underset{\text{Var}(\hat{D})}{XC} = \frac{\int_o^\infty f^2 G_{x_1x_1} G_{x_2x_2}(1-C)df}{8\pi^2 T\left[\int_o^\infty f^2 \left|G_{x_1x_2}\right| df\right]^2} . \qquad (4\text{-}34)$$

For the example case in Table 4-2, (4-34) yields

$$\underset{\text{Var}(\hat{D})}{XC} = \frac{\int_o^\infty f^2 \cdot 4 \cdot \frac{3}{4} df + \int_B^H f^2 1 df}{8\pi^2 T\left[\int_o^B f^2 \cdot 1 df\right]^2} \qquad (4\text{-}35a)$$

$$= \frac{B^3 + \frac{H^3}{3} - \frac{B^3}{3}}{8\pi^2 T \frac{B^6}{9}} . \qquad (4\text{-}35b)$$

For H=B, (4-35b) agrees with earlier results. The crosscorrelator actually performs better than either the SCOT or the Roth processor for the particular example case in Table 4-2. In general, one can expect to find cases for particular spectra where the cross-correlator performs worse than the SCOT or Roth processors.

4B5. Eckart Filter

The Eckart filter derives its name from work in this area done by Eckart (1952). Derivations in Knapp (1966), and Nuttall and Hyde (1969), are outlined here briefly for completeness. The Eckart filter maximizes the deflection criterion, namely, the ratio of the change in mean correlator output due to signal present to the standard deviation of correlator output due to noise alone. For long averaging time T, the deflection has been shown to be

$$d_f = \frac{L\left[\int_{-\infty}^{\infty} H_1(f)H_2^*(f)G_{s_1s_2}(f)df\right]^2}{\int_{-\infty}^{\infty}\left|H_1(f)\right|^2\left|H_2(f)\right|^2 G_{n_1n_1}(f)G_{n_2n_2}(f)df}, \quad (4\text{-}36)$$

where L is a constant proportional to T, and $G_{s_1s_2}(f)$ is the cross-power spectrum between $s_1(t)$ and $s_2(t)$. For the model (4-1) $G_{s_1s_2}(f)=\alpha G_{s_1s_1}(f)\exp(j2\pi fD)$.

Application of Schwartz's inequality indicates that

$$H_1(f)H_2^*(f)=W_E(f)e^{+j2\pi fD} \quad (4\text{-}37)$$

maximizes d_f where

$$W_E(f) = \frac{\alpha G_{s_1 s_1}(f)}{G_{n_1 n_1}(f) G_{n_2 n_2}(f)} \quad . \tag{4-38}$$

Notice that the weighting (4-38), referred to as the Eckart filter, possesses some of the qualities of the SCOT. In particular, it acts to suppress frequency bands of high noise, as does the SCOT. Also note that the Eckart filter unlike the PHAT attaches zero weight to bands where $G_{s_1 s_1}(f)=0$. In practice, the Eckart filter requires knowledge or estimation of the signal and noise spectra. For (4-1), when $\alpha=1$ this can be accomplished by letting

$$W_E(f)=\left|\hat{G}_{x_1 x_2}(f)\right| \Big/ \left\{\left[\hat{G}_{x_1 x_1}(f)-\left|\hat{G}_{x_1 x_2}(f)\right|\right]\cdot\left[\hat{G}_{x_2 x_2}(f)-\left|\hat{G}_{x_1 x_2}(f)\right|\right]\right\}. \tag{4-39}$$

The variance of the time delay estimate using Eckart filtering is

$$\underset{\text{Var}(\hat{D})}{E} = \frac{\int_o^\infty f^2 \frac{G_{ss}^2}{G_{n_1 n_1}^2 G_{n_2 n_2}^2} G_{x_1 x_1} G_{x_2 x_2} (1-C)\,df}{8\pi^2 T\left[\int_o^\infty f^2 \left|G_{x_1 x_2}\right| \frac{G_{ss}}{G_{n_1 n_1} G_{n_2 n_2}}\right] df}^2 \quad . \tag{4-40}$$

For the example case in Table 4-2,

$$\underset{\text{Var}(\hat{D})}{E} = \frac{\int_o^B f^2 4\frac{3}{4}\,df}{8\pi^2 T\left[\int_o^B f^2 df\right]^2} \tag{4-41a}$$

$$= \frac{1}{\frac{8}{9}\pi^2 TB^3}; \qquad (4\text{-}41b)$$

that is, for this example the Eckart filter achieves the Cramér-Rao lower bound (3-24). In general this will not always occur. In the next section we see that (4-41b) is the variance achieved by the ML processor. This might be expected since both the Eckart and ML processors pass nothing in the signal frequency band (B,H) and both have constant weighting over the band (0,B). Actually, the ML estimator is closely related to the Eckart filter, as will be seen in section 4C of this chapter.

4B6. Maximum Likelihood Processor

As shown in Chapter 3 the ML processor always has minimum variance. For the Table 4-2 example, the correct weighting from (3-20) is $W(f)=1/3$ for $f\varepsilon(-B,B)$ and zero otherwise. Now from (3-34)

$$\mathrm{Var}^{ML}(\hat{D}) = \left[\frac{8}{9}\, T\pi^2 B^3\right]^{-1}. \qquad (4\text{-}42)$$

Thus, the minimum variance depends on a time bandwidth product, TB multiplied by the bandwidth squared, B^2. Suppose an error had been made identifying the frequency band of the signal. Then if we presumed that the weighting was $W(f)=1/3$ for, say, $f\varepsilon(-aB,aB)$, in lieu of $f\ (-B,B)$, we would obtain from (3-33)

when $a \geq 1$

$$\mathrm{Var}(\hat{D}) = \frac{(2+a^3)}{3}\left[\frac{8}{9}\,T\pi^2B^3\right]^{-1} , \qquad (4\text{-}43)$$

which reduces to (4-42) when a=1. For example, in this case, a 10 percent error (that is, a=1.1) leads to more than an 11 percent increase in variance. If $a \leq 1$ then (3-33) becomes

$$\mathrm{Var}(\hat{D}) = \frac{1}{a^3}\left[\frac{8}{9}\,T\pi^2B^3\right]^{-1} , \qquad (4\text{-}44)$$

which agrees with (4-42) when a=1. Thus a 10 percent error (a=0.9) leads to an increase in variances of 37 percent. Thus our example suggests it may be more desirable to let in extra noise than to omit signal power. Finally, if our error led to processing the band $f_c(aB,B)$ and $f_c(-B,-aB)$, we would obtain

$$\mathrm{Var}(\hat{D}) = \frac{1}{1-a^3}\left[\frac{8}{9}\,T\pi^2B^3\right]^{-1} , \qquad (4\text{-}45)$$

which agrees with (4-42) when a=0.

The ratio of variances (4-45) to (4-42) for $a \ll 1$ is

$$\frac{1}{1-a^3} \approx 1+a^3 . \qquad (4\text{-}46)$$

If we again err by 10 percent (i.e., a=0.1), then (4-46) yields 1.001 or little change in the variance. (This error is at lower frequencies in the signal band and as (3-33) suggests, proper weighting is most critical at higher frequencies.) Thus, for this example,

depending on how we make a 10 percent error in frequency band selection, we can have anywhere from 0.1 percent to a 37.0 percent increase in variance of the time delay estimate.

4C. Interpretation of Relationship Between Correlation Processors

For the case where $\alpha=1$

$$W_{ML}(f)=\frac{1}{G_{s_1s_1}(f)}\left\{\left[G_{s_1s_1}(f)+G_{n_1n_1}(f)\right]\left[G_{s_1s_1}(f)+G_{n_2n_2}(f)\right]-G^2_{s_1s_1}(f)\right\}^{-1} \tag{4-47a}$$

$$= \frac{\frac{G_{s_1s_1}(f)}{G_{n_1n_1}(f)G_{n_2n_2}(f)}}{1+\frac{G_{s_1s_1}(f)}{G_{n_2n_2}(f)}+\frac{G_{s_1s_1}(f)}{G_{n_1n_1}(f)}} , \tag{4-47b}$$

which agrees with equation (28) of MacDonald and Schultheiss (1969) if in (4-47b) $G_{n_1n_1}(f)=G_{n_2n_2}(f)$.[1] For low SNR,

$$\frac{G_{s_1s_1}(f)}{G_{n_1n_1}(f)} \ll 1 \text{ and } \frac{G_{s_1s_1}(f)}{G_{n_2n_2}(f)} \ll 1 ,$$

it follows that

$$W_{ML}(f)\approx \frac{G_{s_1s_1}(f)}{G_{n_1n_1}(f)G_{n_2n_2}(f)} = W_E(f) ; \tag{4-48}$$

[1] Notice that agreement requires $\alpha=1$.

that is, for $\alpha=1$ and low SNR, the ML processor is identical to the Eckart filter. Similarly, for low SNR,

$$W_s(f) \approx 1/\sqrt{G_{n_1n_1}(f)G_{n_2n_2}(f)} \quad . \tag{4-49}$$

Therefore, if $\alpha=1$,

$$W_{ML}(f) \approx \frac{G_{s_1s_1}(f)}{\sqrt{G_{n_1n_1}(f)G_{n_2n_2}(f)}} \; W_s(f) \quad . \tag{4-50a}$$

Furthermore, for $G_{n_1n_1}(f)=G_{n_2n_2}(f)=G_{nn}(f)$,

$$W_{ML}(f) \approx \frac{G_{s_1s_1}(f)}{G_{nn}(f)} \; W_s(f) = \left[\frac{G_{s_1s_1}(f)}{G_{nn}(f)}\right]^2 W_p(f). \tag{4-50b}$$

Thus, under low SNR approximations with $\alpha=1$, both the Eckart and ML prefilters can be interpreted either as SCOT prewhitening filters with additional SNR weighting or PHAT prewhitening filters with additional SNR squared weighting.

We can rewrite (4-47) as

$$W_{ML}(f) = \frac{\dfrac{1}{\sqrt{G_{n_1n_1}G_{n_2n_2}}}}{\sqrt{\dfrac{G_{n_1n_1}G_{n_2n_2}}{G_{s_1s_1}}} + \sqrt{\dfrac{G_{n_1n_1}G_{n_2n_2}}{G_{n_1n_1}}} + \sqrt{\dfrac{G_{n_1n_1}G_{n_2n_2}}{G_{n_2n_2}}}} \tag{4-51}$$

for uniformly high SNR,

$$\lim_{\sqrt{\frac{G_{n_1n_1}G_{n_2n_2}}{G_{s_1s_1}}}\to 0} W_{ML}(f) = \frac{1}{G_{n_2n_2}+G_{n_1n_1}} \quad ; \tag{4-52}$$

that is, giving the weighting characteristics similar to the SCOT at low SNR. Note that, like the ML processor, the PHAT computes a type of transformation on

$$\left|\frac{\hat{G}_{x_1x_2}(f)}{G_{x_1x_2}(f)}\right|^{\alpha} \exp\ j\hat{\phi}(f) \quad . \tag{4-53}$$

However, the ML processor, like the SCOT, weights the phase according to the strength of the coherence. From p. 379 of Jenkins and Watts (1968), comparing (B-22) with equation (9.2.19) and (9.2.20) of Jenkins and Watts (1968) the variance of the phase estimates is given by

$$\text{Var}\ \hat{\phi}(f) \approx \frac{(1-C)}{C}\cdot\frac{1}{(2N)} \quad , \tag{4-54}$$

where N is the number of independent FFTs used to estimate phase. Notice as C→1, Var $\hat{\phi}$ →0. Thus,

$$R^{(ML)}_{x_1x_2}(\tau) = \frac{1}{N}\int_{-\infty}^{\infty} e^{j\hat{\phi}(f)} \cdot \frac{1}{\text{Var}\ \hat{\phi}(f)} e^{j2\pi f\tau} df \quad . \tag{4-55}$$

Comparison of (4-55) with (4-53) reveals that the ML estimator is the PHAT inversely weighted according to the variability of the phase estimates.

The ML processor has been compared with five other candidate processors to demonstrate the interrelation of all six estimation techniques. The derivation of the ML delay estimator (in Chapter 3),

together with its relation to various ad hoc techniques of intuitive appeal (in this chapter), suggests the practical significance of ML processing for estimation of time delay and, thence, bearing. The remainder of this thesis deals with extensions of the ML processor to more complex models and a discussion of the results and suggestions for future work.

CHAPTER 5

MORE COMPLEX MODELS

Chapter 3 answered, for a simple model, the fundamental question of this thesis: What is the "best" method of estimating time delay" Chapter 4 compared this method with several other candidate processors. Chapter 5 considers three conceptually straightforward extensions of the problem considered in Chapter 3: (1) multiple source models, (2) moving source models, and (3) multiple sensor models. The "solution" to these problems is more difficult than the problem of estimating a single time delay for a stationary source. For example, in the multiple source and multiple sensor models, there is more than one delay to be estimated. Indeed, if we treated multiple sources and multiple sensors together, we would need to estimate a parameter vector for each source, corresponding to the (relative) delays between that source and each sensor; thus, a (nonsquare) matrix of delays (comprised of a parameter vector for each source) would need to be estimated. Finally, it is necessary, in effect, to estimate the motion of each source so as to be able to Doppler correct the received signals prior to crosscorrelation. Failure to apply some sort

of Doppler correction will cause the received signals to be essentially uncorrelated even if a common (but frequency shifted) signal is present.

Both notationally and analytically, the methods applied to estimate the unknown parameters become more complex than the methods in Chapter 3. Yet even in Chapter 3 where a "solution" for the ML estimate of time delay was possible, we noted that, in practice, it would be necessary to resort to an AML estimation technique; for more complex models there is no reason to expect that the solution will become simpler; indeed, in this chapter (especially with regard to moving sources), we appeal more to approximate and ad hoc techniques based on the ideas of Chapter 3 than to rigorous methodologies. The reasons for this approach are apparent in section B and have to do with the nonstationarities introduced by the source motion.

5A. Multiple Source Models

The simplest multiple source model is a two source case where receiving sensors are physically steered at one source and the second source acts as an interference. Such a model is depicted in Figure 5-1 (Carter and Knapp (1975)). Mathematically,

$$x_1(t) = s_1(t)+s_2(t)+n_1(t) \tag{5-1a}$$

and

$$x_2(t) = s_1(t)+s_2(t-D)+n_2(t) \; . \tag{5-1b}$$

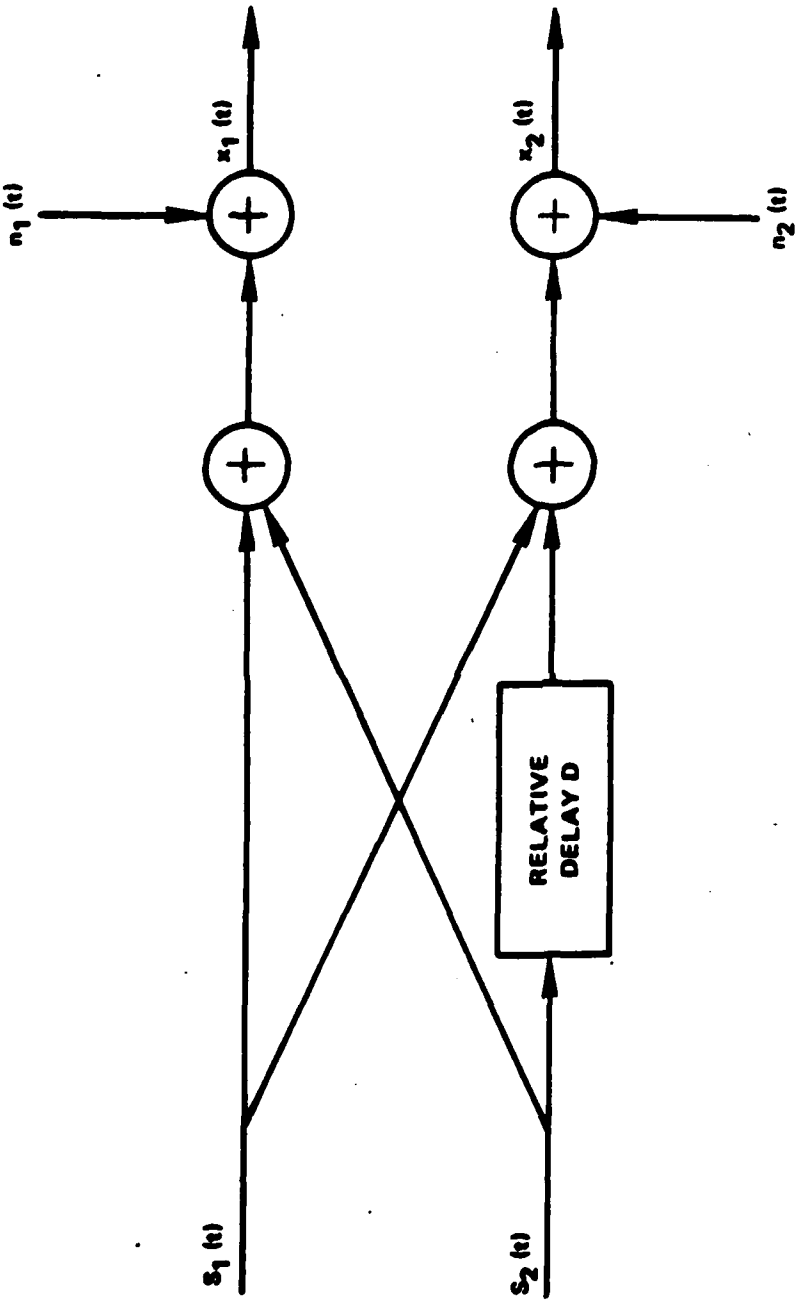

Figure 5-1 Two Directional Source Signals Received with Noise

(The effect of an interfering source on detection is considered by Schultheiss (1968).) The problem is to estimate the parameter D. In effect $s_1(t)$ accounts for correlated noise insofar as estimation of D is concerned.

When $s_1(t)$ and $s_2(t)$ are stationary uncorrelated signals with power spectra $G_{s_1s_1}(f)$ and $G_{s_2s_2}(f)$ and when $n_1(t)$ and $n_2(t)$ are stationary uncorrelated noises with the same power spectrum $G_{nn}(f)$, it has been shown by Carter and Knapp (1975) that

$$\gamma_{x_1x_2}(f)=\left[1+\frac{G_{s_2s_2}(f)}{G_{s_1s_1}(f)}e^{-j2\pi fD}\right]\frac{G_{s_1s_1}(f)}{G_{s_1s_1}(f)+G_{s_2s_2}(f)+G_{nn}(f)} \tag{5-2}$$

In the special case when $G_{nn}(f)=0$ and $G_{s_1s_1}(f)=G_{s_2s_2}(f)$

$$\gamma_{x_1x_2}(f)=\tfrac{1}{2}(1+e^{-j2\pi fD})=e^{-j\pi fD}\cos\pi fD \tag{5-3}$$

and

$$C_{x_1x_2}(f)=\cos^2\pi fD=\tfrac{1}{2}(1+\cos 2\pi fD). \tag{5-4}$$

Because of the sinusoidal oscillation between 0 and 1 of $C_{x_1x_2}(f)$, the Fourier transform of (5-3) will exhibit a peak at the value of time delay. This suggests the usefulness of computing the Fourier transform of the coherence or SCOT (Carter, Nuttall and Cable (1973)).

A more general, multiple source, two sensor model is

$$x_1(t)=\sum_i s_i(t)+n_1(t) \tag{5-5a}$$

$$x_2(t)=\sum_i \alpha_i s_i(t+D_i)+n_2(t)\ . \tag{5-5b}$$

The limit on the sum depends on the number of sources. Since each source will be presumed to be independent of the others, the sources will be mutually uncorrelated. For the general two source case depicted as a multiinput, multioutput system in Figure 5-2, it follows that

$$x_1(t) = s_1(t)+s_2(t)+n_1(t) \tag{5-6a}$$

$$x_2(t) = a_1 s_1(t+D_1)+a_2 s_2(t+D_2)+n_2(t) \tag{5-6b}$$

and therefore

$$G_{x_1x_1}(f) = G_{s_1s_1}(f)+G_{s_2s_2}(f)+G_{n_1n_1}(f) \tag{5-7a}$$

$$G_{x_2x_2}(f) = a_1^2 G_{s_1s_1}(f)+a_2^2 G_{s_2s_2}(f)+G_{n_2n_2}(f) \tag{5-7b}$$

and

$$G_{x_1x_2}(f) = a_1 G_{s_1s_1}(f)e^{-j2\pi fD_1} + a_2 G_{s_2s_2}(f)e^{-j2\pi fD_2} + G_{n_1n_2}(f) \quad . \tag{5-7c}$$

However, we can accommodate coherent noise through the inclusion of additional sources so that without loss of generality $G_{n_1n_2}(f)=0$ for all frequencies. From the two-source model with incoherent noise, we generalize that

$$G_{x_1x_1}(f) = G_{n_1n_1}(f)+\sum_i G_{s_is_i}(f) \tag{5-8a}$$

$$G_{x_2x_2}(f) = G_{n_2n_2}(f)+\sum_i a_i^2 G_{s_is_i}(f) \tag{5-8b}$$

and

$$G_{x_1x_2}(f) = \sum_i a_i G_{s_is_i}(f)e^{-j2\pi fD_i} \quad . \tag{5-8c}$$

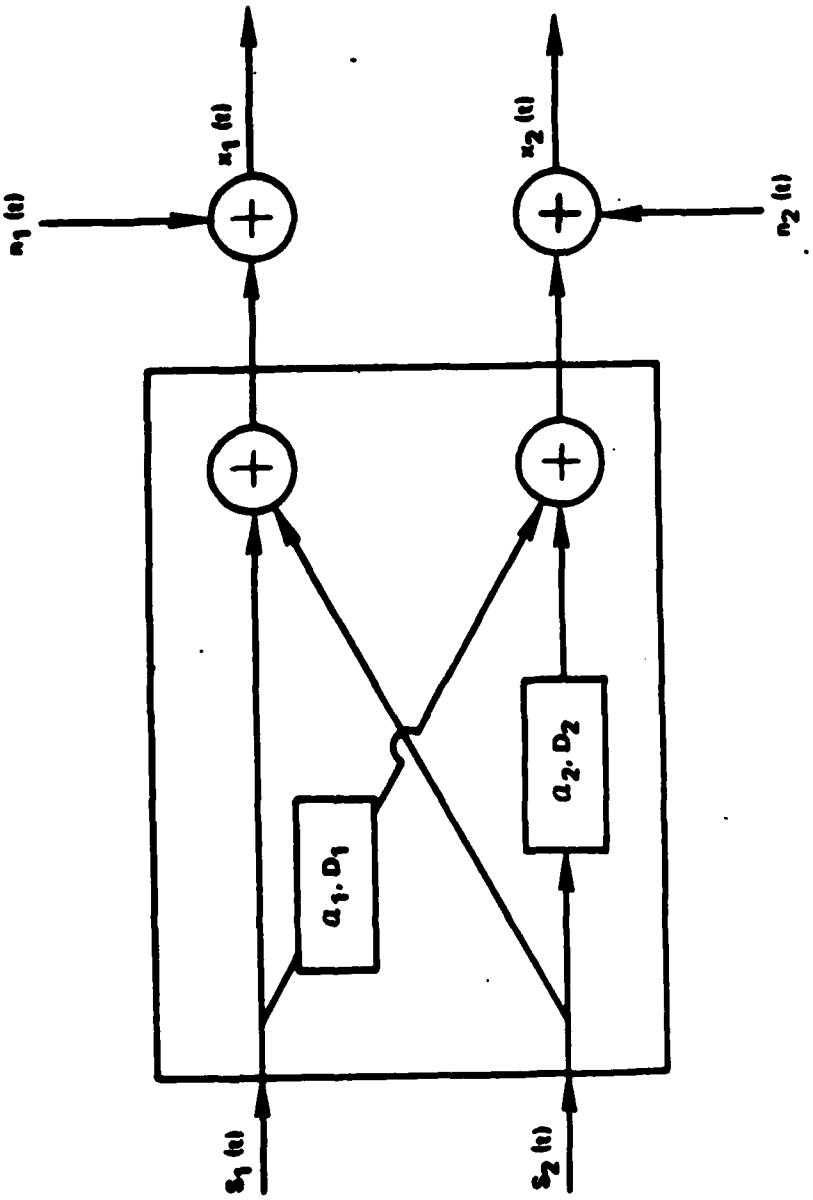

Figure 5-2 General Two Source, Two Sensor Model

In the ML estimation procedure earlier the determinant of Q_x could be ignored since it did not depend on D. Now, however, for the two-source model, we see (suppressing f) that

$$|Q| = \begin{vmatrix} G_{s_1s_1}+G_{s_2s_2}+G_{n_1n_1}, & \alpha_1 G_{s_1s_1} e^{-j2\pi fD_1}+\alpha_2 G_{s_2s_2} e^{-j2\pi fD_2} \\ \alpha_1 G_{s_1s_1} e^{+j2\pi fD_1}+\alpha_2 G_{s_2s_2} e^{+j2\pi fD_2}, & G_{x_2x_2} \end{vmatrix} \quad (5\text{-}9a)$$

does depend on (D_1D_2). For example, even when $G_{n_1n_1}=G_{n_2n_2}=G_{nn}$, $\alpha_1=\alpha_2=1$ and $G_{s_1s_1}=G_{s_2s_2}=G_{ss}$,

$$|Q| = (2G_{ss}+G_{nn})^2 - G_{ss}^2 (e^{-j2\pi fD_1}+e^{-j2\pi fD_2})(e^{+j2\pi fD_1}+e^{+j2\pi fD_2}) \quad (5\text{-}9b)$$

$$|Q| = 4G_{ss}^2+2G_{ss}G_{nn}+G_{nn}^2-G_{ss}^2\left[2+e^{-j2\pi f(D_2-D_1)}+e^{+j2\pi f(D_2-D_1)}\right]. \quad (5\text{-}9c)$$

In general, $|Q|$ depends on the parameter vector (D_1D_2). Thus, we must be concerned by the $|Q|$ as well as the exponent in (3-9), for the multiple source model. Specifically, we want to maximize the sum of both (3-17) and the $\log_c|Q|$ term. The latter is given by

$$h = \sum_{k=-N}^{N} \log_e |Q|^{-\frac{1}{2}}, \quad (5\text{-}10)$$

but

$$|Q| = \begin{vmatrix} G_{x_1x_1} & G_{x_1x_2} \\ G_{x_1x_2}^* & G_{x_2x_2} \end{vmatrix} = G_{x_1x_1} G_{x_2x_2} [1-C_{x_1x_2}] . \quad (5\text{-}11)$$

Thus,

$$\log_e |Q|^{-\frac{1}{2}} = -\tfrac{1}{2}[\log_e G_{x_1x_1} G_{x_2x_2} + \log_e (1-C_{x_1x_2})]. \qquad (5\text{-}12)$$

But $\log_e G_{x_1x_2} G_{x_2x_2}$ does not depend on $(D_1, D_2, \ldots)$ so that the critical parameters in the $|Q|$ term are approximately given by

$$-\tfrac{1}{2}T \int_{-\infty}^{\infty} \log_e [1-C_{x_1x_2}(f)]\,df. \qquad (5\text{-}13)$$

In practice, x_1 and x_2 will have finite bandwidth; therefore the limits of the integral (5-13) will also be finite. It is noteworthy that the second term is related to the definition by Shannon (1949) for the amount of information about $x_2(t)$ contained in $x_1(t)$. More specifically, Gelfand and Yaglom (1959) and Nettheim (1966) have shown that the amount of information about x contained in y (or <u>vice versa</u>) is given by[1]

$$I_{xy} = -\tfrac{1}{2} \int \log_e [1-C_{xy}(f)]\,df, \qquad (5\text{-}14)$$

where the limits of integration are over the nonzero range of the integrand. Hence, for $C_{xy}(f)=0$, there is no information (in the linear sense)[2] contained in one

---

[1] These results can be combined with (2-79) for models like Figure 2-5 to show that I_{xy} is the integral of the logarithm of 1 plus received signal to noise ratio.

[2] See Carter and Knapp (1975) or Chapter 2 for a discussion of nonlinear relations which can yield $C_{xy}(f)=0$ and yet y(t) can be entirely due to x(t). as for example, when $y(t)=x^2(t)$.

time series with regard to the other. Alternatively, if $C_{xy}(f)=1$, for some particular f_p, then there is an infinite amount of information about x(t) knowing y(t) at the particular frequency f_p. More generally, for nonzero $C_{xy}(f)<1$, the amount of information depends on the bandwidth (limits of integration in (5-14)) and the MSC in that band.

Thus, following (3-15) and (5-10) through (5-14), we see that it is desired to maximize

$$J=T\left[I_{x_1x_2}+2\int_{-\infty}^{\infty}\frac{\hat{G}_{x_1x_2}G_{x_1x_2}^{*}}{G_{x_1x_1}G_{x_2x_2}(1-C_{x_1x_2})}df\right] . \qquad (5\text{-}15)$$

For the two source model,

$$J=T\left[I_{x_1x_2}+2\int_{-\infty}^{\infty}\frac{\hat{G}_{x_1x_2}a_1G_{s_1s_1}e^{+j2\pi fD_1}}{|Q|}df + 2\int_{-\infty}^{\infty}\frac{\hat{G}_{x_1x_2}a_2G_{s_2s_2}e^{+j2\pi fD_2}}{|Q|}df\right] , \qquad (5\text{-}16)$$

or for two-sensor, multiple source model we maximize

$$J=T\left[I_{x_1x_2}+2\int_{-\infty}^{\infty}\frac{\hat{G}_{x_1x_2}(f)\Sigma_i a_iG_{s_is_i}(f)e^{+j2\pi fD_i}}{|Q(f)|}df\right] . \qquad (5\text{-}17)$$

Thus, the important regions of the estimated cross spectrum for determining D_i are these frequency bands where $G_{s_is_i}(f)$ is large. However, even when the signal spectrum is strong, if the intersource interference is such that the intersensor coherence $C_{x_1x_2}(f)$ is low, the

weight attached to the estimated cross spectrum is degraded, as shown above.

While we can estimate auto spectra and coherence between sensors, more sophisticated methods must be applied in order to estimate the source signal spectrum. The mathematics shows how to process for known signal spectrum. In the communications problem, signal spectrum will generally be known, although α, which more generally could be a function of frequency, will probably not be known. In other problems, methods involving classification and data bank retrieval need to be studied. In the absence of a priori knowledge, we might assume that every frequency band where the coherence was high was a different source. Tracking (that is, estimating bearing continuously) for each frequency band then becomes a classification problem where the number of sources is ascertained by noting the number of clustered sources. The fewer the sources for a given total source power the easier tracking will be. However, repeated clustering analysis will be desirable to ascertain whether two or more sources are being classified as one.

In "real world" problems, there may well be more than one source; hence, the application of Chapter 3 results must include the concepts of multiple sources. There are other concerns, too, in the practical application of our Chapter 3 results. The next generalization which we will discuss is the moving source

problem.

5B. Moving Source Models

The model we shall consider is a simplified one characterized by the observed waveforms (Carter and Knapp (1976b))

$$x_1(t)=s(t)+n_1(t) \tag{5-18a}$$

$$y_2(t)=\alpha s(\beta t+D)+n_2(t)\,, \tag{5-18b}$$

where $s(t)$, $n_1(t)$ and $n_2(t)$ are zero mean jointly stationary Gaussian random processes which are mutually uncorrelated. The problem addressed here is ML estimation of the time compression and delay parameters β and D, respectively; the problem is related to the Doppler shift work by Van Trees (1971). The characteristics of the signal and noise are such that $x_1(t)$ is a member function of a zero mean stationary Gaussian random process. Further, despite the attenuation, delay and time compression, $y_2(t)$ is also stationary and Gaussian. That is, both autocorrelation functions given by

$$R_{x_1x_1}(\tau) = R_{n_1n_1}(\tau)+R_{ss}(\tau) \tag{5-19a}$$

and

$$R_{y_2y_2}(t_1,t_2)=R_{n_2n_2}(t_2-t_1)+\alpha R_{ss}(\beta(t_2-t_1)) \tag{5-19b}$$

depend only on the time difference t_2-t_1.

However, the crosscorrelation for model (5-18) depends on β as follows:

$$R_{x_1y_2}(t_1,t_2)=\alpha E[s(t_1)s(\beta t_2+D)]=\alpha R_{ss}(t_1-\beta t_2-D) \qquad (5\text{-}19c)$$

$$R_{y_2x_1}(t_1,t_2)=\alpha E[s(\beta t_1+D)s(t_2)]=\alpha R_{ss}(\beta t_1+D-t_2) \; . \qquad (5\text{-}19d)$$

As required,

$$R_{x_1y_2}(t_1,t_2) = R_{y_2x_1}(t_2,t_1) \; . \qquad (5\text{-}20)$$

Notice the crosscorrelation depends on β as well at t_1 and t_2, and not simply the difference between t_1 and t_2. Hence the processes $x_1(t)$ and $y_2(t)$ are <u>not</u> jointly second order stationary, but depend on the absolute time origin. Thus, the introduction of time compression β in our model thereby complicates the theory through the imposition of a second order nonstationarity. [For a variety of practical reasons, we desire to operate on $y_2(t)$ in order to ensure complete stationarity.]

An ad hoc technique for estimating D is to operate on $y_2(t)$ to remove (or adjust) the time scale change β. The result, referred to as $x_2(t)$, may then be used with $x_1(t)$ in the usual ML estimator of Chapter 3. This indeed turns out to be the ML estimator for this problem (as is subsequently shown). A major problem, of course, is that β as well as delay D must be estimated to undo the time scaling introduced by motion of the source. Suppose β_a, for example, is one estimate (or hypothesis) of β (like τ was a hypothesized delay in Chapter 3) and let

$$x_2(t) \triangleq y_2(t/\beta_a) \qquad (5\text{-}21a)$$

$$= \alpha s(\beta t/\beta_a + D) + n_2(t/\beta_a) \quad . \tag{5-21b}$$

Now the crosscorrelation of $x_1(t)$ with $x_2(t)$ is given by

$$R_{x_1x_2}(t_1,t_2) = E[x_1(t_1)x_2(t_2)] \tag{5-22a}$$

$$= \alpha R_{ss}(t_1 - \frac{\beta}{\beta_a}t_2 - D) \quad . \tag{5-22b}$$

Thus, for $\beta_a=\beta$, we see that $x_1(t)$ and $x_2(t)$ are second order jointly stationary, for then $R_{x_1x_2}(t_1,t_2)$ depends only on the time difference $\tau=t_1-t_2$. For $\beta_a=\beta$, it is possible to compute a single Fourier transformation on τ to achieve

$$G_{x_1x_2}(f) = \int_{-\infty}^{\infty} R_{x_1x_2}(\tau)e^{-j2\pi f\tau}d\tau \tag{5-23a}$$

$$= \alpha G_{ss}(f)e^{-j2\pi fD} \quad . \tag{5-23b}$$

Similar results can be obtained using the concept of locally stationary random processes (Silverman (1957)). However, in general, when $\beta\neq\beta_a$, a two-dimensional Fourier transformation must be performed. For convenience let $\tilde{\beta}=\beta/\beta_a$ (where we ultimately hope to make $\tilde{\beta}\approx 1$ by proper choice of β_a)[1]; then it follows that

$$E\left[X_1(k)X_2^*(l)\right] = \frac{\alpha}{T^2}\int_0^T dt_1 \int_0^T dt_2 R_{ss}(t_1 - \tilde{\beta}t_2 - D) \quad . \tag{5-24a}$$
$$e^{-j\omega_o(kt_1 - lt_2)}$$

---

[1] In the following it may be assumed that $\beta_a=1$ and $\tilde{\beta}=\beta$; that is, that $y_2(t)$ has not been preprocessed. Results can then be applied with $\beta\approx 1$ (rather than $\tilde{\beta}\approx 1$); for many problems $\beta\approx 1$.

However,

$$R_{ss}(t_1-\tilde{\beta}t_2-D) = \frac{\alpha}{2\pi}\int_{-\infty}^{\infty} G_{ss}(\omega)e^{j\omega(t_1-\tilde{\beta}t_2-D)}d\omega \qquad (5\text{-}24b)$$

so that

$$E\left[X_1(k)X_2^*(\Omega)\right] = \frac{1}{2\pi}\int_{-\infty}^{\infty} G_{ss}(\omega)e^{-j\omega D}d\omega \cdot \frac{1}{T}\int_0^T e^{j(\omega-k\omega_\Delta)t_1}dt_1 \;\; \frac{1}{T}\int_0^T e^{-j(\tilde{\beta}\omega-l\omega_\Delta)t_2}\,dt_2 \qquad (5\text{-}24c)$$

$$= \frac{1}{2\pi}\int_{-\infty}^{\infty} G_{ss}(\omega)e^{-j\omega D}\left[\frac{e^{j(\omega-k\omega_\Delta)T}-1}{j(\omega-k\omega_\Delta)T}\right]\left[\frac{1-e^{-j(\tilde{\beta}\omega-l\omega_\Delta)T}}{j(\tilde{\beta}\omega-l\omega_\Delta)T}\right]d\omega \qquad (5\text{-}24d)$$

$$= \frac{1}{2\pi}\int_{-\infty}^{\infty} G_{ss}(\omega)e^{-j\omega D}e^{j(\omega-k\omega_\Delta)T/2}e^{-j(\tilde{\beta}\omega-l\omega_\Delta)T/2}\left[\frac{\sin(\omega-k\omega_\Delta)T/2}{(\omega-k\omega_\Delta)T/2}\cdot\frac{\sin\tilde{\beta}T/2(\omega-\frac{l\omega_\Delta}{\tilde{\beta}})}{\tilde{\beta}T/2(\omega-\frac{l\omega_\Delta}{\tilde{\beta}})}\right]d\omega \qquad (5\text{-}24e)$$

$$= \frac{1}{2\pi}\int_{-\infty}^{\infty} G_{ss}(\omega)e^{-j\omega D}e^{j\omega T/2(1-\tilde{\beta})}e^{j(1-k)T}\,\frac{\sin(\omega-k\omega_\Delta)T/2}{(\omega-k\omega_\Delta)T/2}\cdot\frac{\sin\tilde{\beta}T/2(\omega-l\omega_\Delta/\tilde{\beta})}{\tilde{\beta}T/2(\omega-l\omega_\Delta/\tilde{\beta})}\;d\omega\,. \qquad (5\text{-}24f)$$

Equation (5-24) offers a more rigorous interpretation of (5-23). For large T and $\tilde{\beta}$ near unity, it follows from (5-24f) (since the discrepancy between the sinc functions is minor) that

$$G_{x_1x_2}(f) = T\,E[X_1(k)X_2^*(1)] \tag{5-25a}$$

$$= \begin{cases} \alpha G_{ss}(k\omega_\Delta)e^{-jk\omega_\Delta D}, & 1=k\tilde{\beta} \\ 0, & 1\neq k\tilde{\beta}\ . \end{cases} \tag{5-25b}$$

Also,

$$T\,E[X_1(k)X_1^*(1)] = \begin{cases} G_{n_1n_1}(k\omega_\Delta)+G_{ss}(k\omega_\Delta), & 1=k \\ 0, & 1\neq k \end{cases} \tag{5-25c}$$

and

$$T\,E[X_2(k)X_2^*(1)] = \begin{cases} \beta_a G_{n_2n_2}(\beta_a k\omega_\Delta)+\frac{\alpha}{\tilde{\beta}}G_{ss}(\frac{k\omega_\Delta}{\tilde{\beta}}), & 1=k \\ 0, & 1\neq k \end{cases}\ . \tag{5-25d}$$

Note in (5-25d) $G_{n_2n_2}$ is evaluated at $\beta_a k\omega_\Delta$ not $k\omega_\Delta$. Similarly, it can be shown for $\tilde{\beta}\simeq 1$ and large T, that

$$E[X_2(k)X_1^*(1)] = \begin{cases} \alpha G_{ss}(k\omega_\Delta)e^{jk\omega_\Delta D} & 1=k/\tilde{\beta} \\ 0 & 1\neq k/\tilde{\beta}\ . \end{cases} \tag{5-26}$$

We now proceed as in Chapter 3, Section A. In particular, we desire to maximize a total award function J_A, as depicted in Figure 5-3, through the adjustment of hypothesized compression β_a and hypothesized delay τ; when J_A is maximized, the ML estimates $\hat{\beta}$ and $\hat{D}$ depicted in Figure 5-3 are achieved.

It is important to the discussion that follows to note that if β_a is incorrectly selected such that $\tilde{\beta}$ is

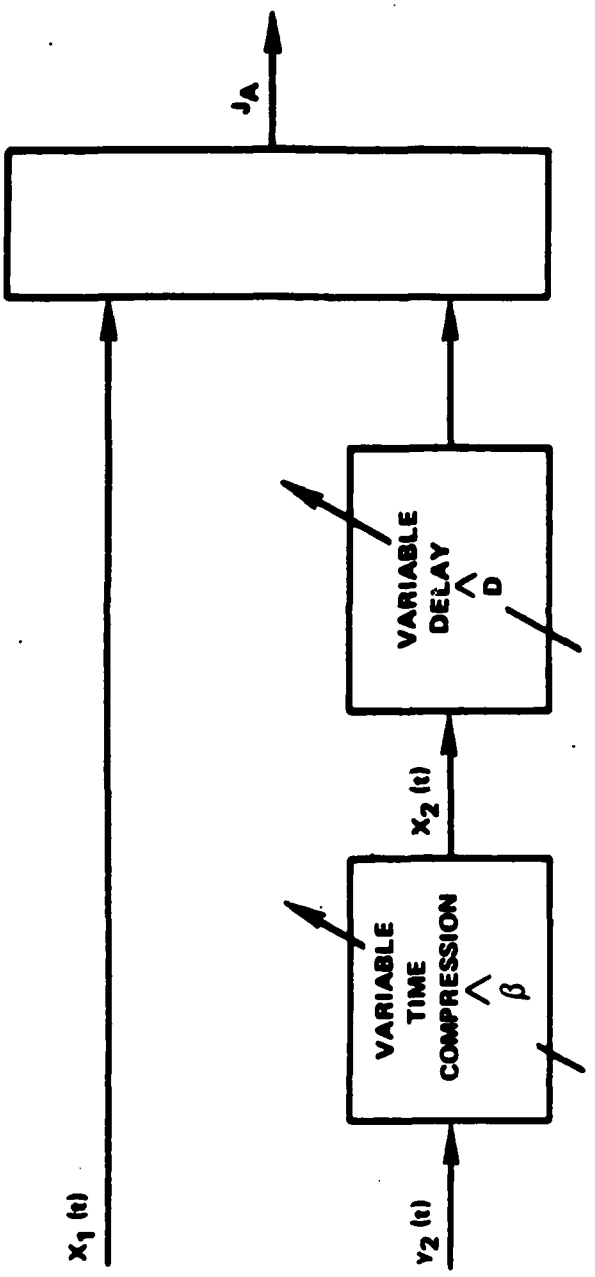

Figure 5-3 Processing to Estimate β and D

much different from unity, the processes $x_1(t)$ and $x_2(t)$ are second order jointly nonstationary and the estimators are not ML estimators. However, once we have begun to estimate delay and compression correctly, the processor is an ML estimator; that is, in the sequential estimation problem where several observation intervals are available, then ML or at least AML estimation is possible in the last intervals. Before proceeding, we also note that if $\tilde{\beta} \neq 1$ any crosscorrelation (coherence) terms in the award J_A will be zero. More specifically, if β is much different from unity, then time delay cannot be estimated without some type of Doppler or time compression preprocessing. The importance of this statement is that Chapter 3 cannot be applied to estimate bearing to moving sources which are nearfield (relative to the sensor separation) unless time compression preprocessing is done. Denote the Fourier coefficients of $x_1(t)$ and $x_2(t)$ as in Chapter 3. The 2N+1 vectors $\underline{X}(k) \tilde{=} [X_1(k), X_2(\tilde{\beta}k)]'$, $k = -N, -N+1, \ldots, N$ for $\tilde{\beta} \tilde{=} 1$, are uncorrelated Gaussian (hence, independent) random variables. More explicitly, because of the independence, the pdf for

$$\underline{X} \equiv \{X_1(-N), X_2(-N\tilde{\beta})\}', \{X_1(-N+1), X_2[(-N+1)\tilde{\beta}]\}', \ldots \{X_1(N), X_2(N\tilde{\beta})\}'$$

given the true values of attenuation α, delay D and time compression β (actually we also are given β_a; hence are "given" $\tilde{\beta} = \beta/\beta_a$) is the product of the individual densities.

Specifically when $\beta_a=1$ and $\beta=1$ the pdf of $\underline{X}$ is

$$p(\underline{X}|\alpha,\beta,D) = \prod_{k=-N}^{N} [h_k \exp(-\tfrac{1}{2}J_k)] \tag{5-27a}$$

where

$$J_k = T[x_1^*(k)x_2^*(k)]Q_x^{-1}(k\omega_\Delta)\begin{bmatrix} x_1(k) \\ x_2(k) \end{bmatrix}, \tag{5-27b}$$

and

$$h_k = [(2\pi)|Q_x(k\omega_\Delta)|^{\frac{1}{2}}]^{-1}, \tag{5-27c}$$

and $Q_x(f)$ is the power spectral density matrix between the random processes $x_1(t)$ and $x_2(t)$.

For ML estimation, it is desired to simultaneously choose as $\hat{D}$ and $\hat{\beta}$ those values which maximize the pdf evaluated for hypothesized compression β_a and hypothesized delay τ. Equivalently, $\hat{\beta}$ and $\hat{D}$ are selected to maximize any monotonically increasing transformation of the pdf. Hence, $\hat{\beta}$ and $\hat{D}$ are selected to maximize the log pdf, namely,

$$J_A = \ln p(\underline{X}|\alpha,\beta,D) \sum_{k=-N}^{N} \ln h_k - \frac{1}{2} \sum_{k=-N}^{N} J_k \quad . \tag{5-28}$$

While the derivation provides sufficient information on estimating the parameters β and D, it is valuable to interpret (5-28) in order to understand both its meaning and its implementation. The award to be maximized (5-28) can be written (assuming large T) as three terms substituting (5-14) and (3-15)

$$J_A = I_{x_1x_2} - \int_{-\infty}^{\infty} \frac{1}{2}\left[\frac{\hat{G}_{x_1x_1}}{G_{x_1x_1}} + \frac{\hat{G}_{x_2x_2}}{G_{x_2x_2}}\right]\left[\frac{1}{1-C_{12}}\right] df + \int_{-\infty}^{\infty} \frac{-\hat{G}_{x_1x_2}}{|G_{x_1x_2}|}\left[\frac{C_{12}}{1-C_{12}}\right] e^{+j2\pi f\tau} df \quad . \quad (5\text{-}29)$$

Unlike Chapter 3, C_{12} depends on β. Equation (5-29) is difficult to interpret; it is comprised of three terms. For ML estimation (versus AML estimation), only the last two terms of (5-29) depend on the data. However, the parameters β and D appear in all three terms of (5-29); hence, all three terms must be considered. The first term of (5-29) is small with respect to the second term (because, from (5-14), the information has a logarithm in it); also, the first term of (5-29) is small with respect to the third term. Hence, we might expect that the first term can be ignored. However, under some common degenerate cases (specifically, τ=D and T very large) the sum of the second and third terms does <u>not</u> depend on the parameters β and D. For example, for τ=D and very large T, $\hat{G}_{x_ix_i} = G_{x_ix_i}$, i=1,2 and $\hat{G}_{x_1x_2} = |G_{x_1x_2}|e^{-j2\pi fD}$ and the sum of the last two terms of (5-29) becomes $-\int_{-\infty}^{\infty} \frac{1-C}{1-C} df$, which is a constant. This situation is perplexing since the remaining term in (5-29) (namely, the information (5-14)) does <u>not</u> depend on the data, but only on the (assumed known) statistics of the data. It is interesting that when this is the case and when we apply AML techniques (that is, we use estimated data statistics for assumed known statistics), the data do

appear in the expression for the information.

Finally, we notice if as a suboptimum technique, we were to take the first or last term in (5-29) and simply maximize it, that to do so would require adjusting the parameter estimates so as to attempt to increase the coherence across the entire frequency band; the second term of (5-29) does just the opposite. Notice when the time compression is estimated incorrectly, $C_{12}=0$ and only the information I_{12} (or $\hat{I}_{12}$) is needed to estimate compression. Having estimated compression correctly, only the last term of (5-29) is needed to estimate delay. This suggests a suboptimum ad hoc technique for estimating β and D, namely, maximize the information to estimate β then use that $\hat{\beta}$ to estimate D with the award function of Chapter 3. In practice, this suboptimum technique should compare favorably with maximizing (5-29), since there are a number of assumptions and approximations leading to the award function (5-29); most notably, (5-29) presumes $\tilde{\beta}\approx 1$ so that joint second order stationarity holds. When this is not the case, maximizing (5-29) becomes simply an advisable but ad hoc estimation procedure.

There are some degenerate cases of the model (5-18) that are easier to work with analytically (namely, D known and equal to zero, $n_2(t)=0$ and $\alpha=1$). Such models have rather predictable results (namely, the cross-correlation terms are important except as $G_{n_1 n_1}(f)\to\infty$,

that is, as one of the observation channels becomes noise dominated; in the later case, the hypothesized time compression attempts to align the estimated auto spectrum with the (known) signal spectrum). Thus, the degenerate cases do not add insight into the fundamental issue of stationarity. We are thus led to state that maximizing (5-29) (or first (5-14) and then the last term of (5-29)) by choice of $\hat{\beta}$ and $\hat{D}$ (respectively) is merely an intuitively appealing ad hoc technique.

5C. Multiple Sensor Models

The problem we address here is estimation of a parameter vector $\underline{D}$ from a set of sensors with received voltages

$$x_i(t) = \alpha_i s(t+D_i)+n_i(t) \quad i=1,2\ldots \quad . \tag{5-30}$$

Although the notation for D_i is the same as Section A, this model should <u>not</u> be confused with a multiple source model, since this model is only one source but many sensors. To extend the problem to many moving sources received at many sensors requires that

$$x_i(t) = \left\{\sum_k \alpha_{i,k} s\left[\beta_{i,k} t+D_{i,k}\right]\right\}+n_i(t) \tag{5-31}$$

In the model (5-30), we assume (without loss of generality) that $\alpha_1=1$ and $D_1=0$; thus

$$x_1(t) = s(t)+n_1(t) \tag{5-32}$$

$$x_2(t) = \alpha_2 s(t+D_2)+n_2(t)$$

$$\vdots \qquad\qquad \vdots$$

$$x_M(t) = \alpha_M s(t+D_M)+n_M(t)$$

and we desire to estimate the M-1 dimension relative delay vector $(D_2-D_1,\ D_3-D_1,\ldots,D_M-D_1)$.

The general solution to this problem is simply an extension of the alternate realization in Chapter 3, Section 3C. In particular, the steering vector is now

$$V' = [1,\ a_2 e^{-j2\pi f D_2},\ldots a_M e^{-j2\pi f D_M}] \quad . \tag{5-33}$$

For uncorrelated noises

$$Q_n = \text{diag}[G_{n_i n_i}] \quad . \tag{5-34}$$

The 1xM vector filter is given by

$$\tilde{H} = [\tilde{H}_1, \tilde{H}_2, \ldots, \tilde{H}_M] = \frac{Q_n^{-1} V \sqrt{G_{ss}}}{[1+G_{ss} V' Q_n^{-1} V^*]^{\frac{1}{2}}} \quad . \tag{5-35}$$

Hence, the generalization is realized by extending Figure 3-10 to M prefilters with one at each sensor location as shown in Figure 5-4. A more explicit realization is given in Figure 5-5, which is the extension of Figure 3-11.

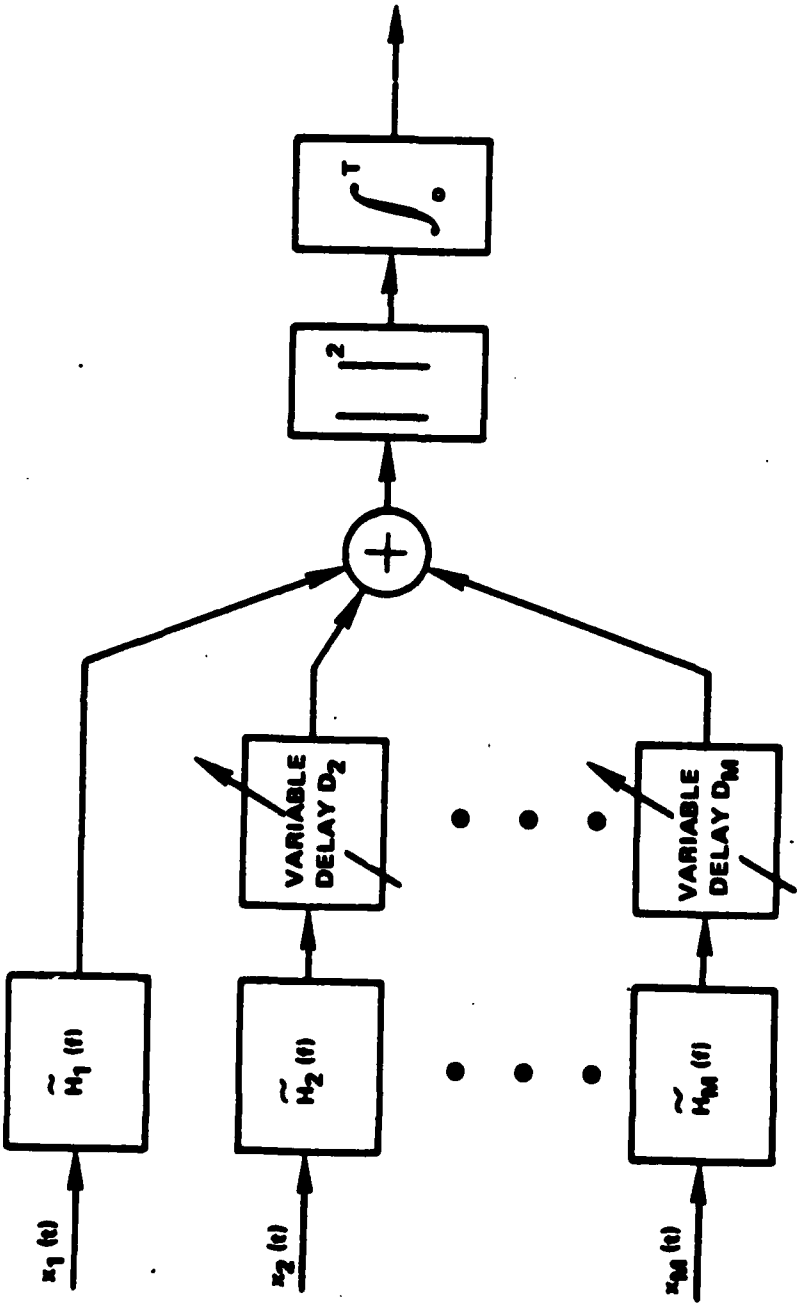

Figure 5-4 Multiple Sensor Estimation of Delay Vector

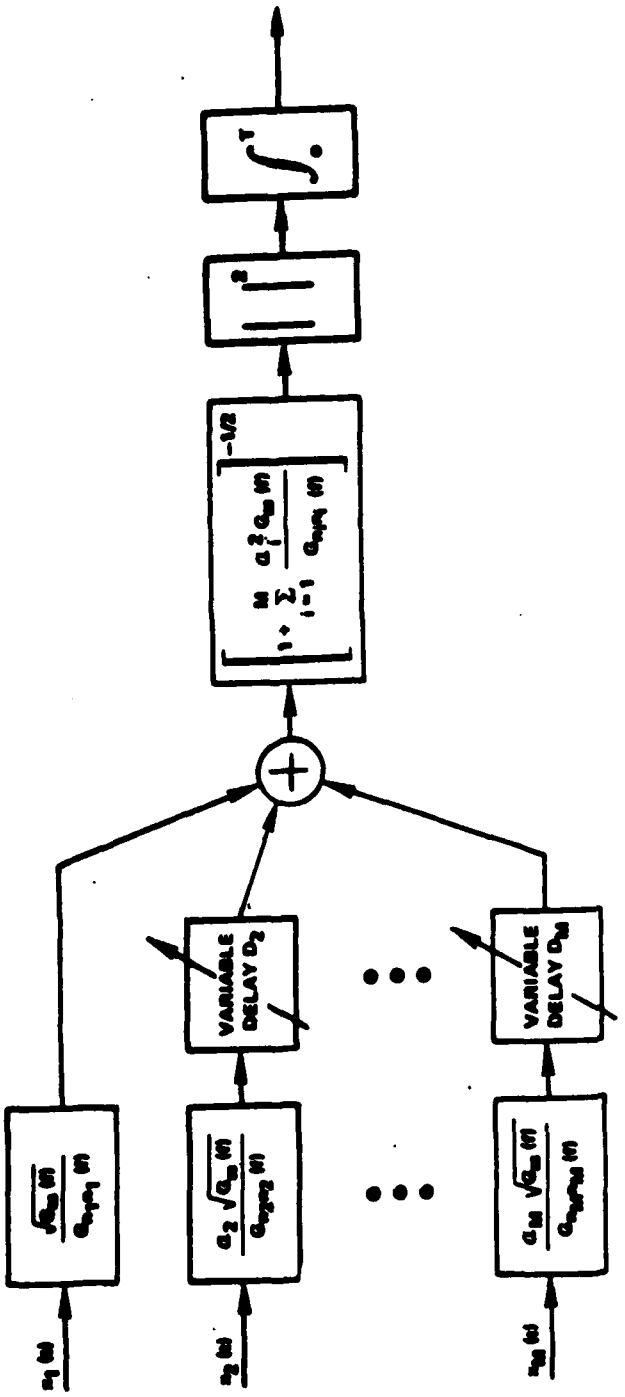

Figure 5-5 Explicit Multiple Sensor Processor for Estimating Delay Vector

CHAPTER 6

DISCUSSION

6A. Applications and Summary

The purpose of this section is to briefly summarize and discuss the applications of this work. Most of the applications are intimately tied to the theoretical results already presented which are summarized in the subsequent paragraphs. The primary purpose of this section is to highlight applications of the theory with a minimum of reliance on mathematical notation. There are three main applications for the theory of time delay estimation discussed in the following three subsections. First, it is a useful vehicle for parameter identification. Second, we can use it to obtain bearing estimates. Finally, under certain conditions we can estimate source position. These applications rely on the theory developed in the preceding text, which is summarized in the following two paragraphs.

This dissertation has investigated methodologies for passive estimation of the bearing to a slowly moving acoustically radiating source. As demonstrated, the mathematics for the solution to this problem is analogous to estimating the time delay between two time series. Because the estimation of time delay is

closely related to the coherence between two time series an extensive investigation of coherence has been presented. New results on using coherence to provide information about linear and nonlinear systems have been presented and proved.

The ML estimate of time delay (under jointly stationary Gaussian assumptions) has been derived. The explicit dependence of the time delay estimate on coherence is evident in the estimator realization in which the two time series are prefiltered (to accentuate frequency bands according to the strength of the coherence) and subsequently crosscorrelated. The hypothesized delay at which the GCC function peaks is the time delay estimate. From the GCC realization the variance of the time delay estimate has been obtained. By use of a different interpretation of the ML estimator derivation, other realizations have been obtained. The GCC realization with ML weighting is compared to several other proposed weightings. The estimation formulation has been extended to three important generalizations: multiple sources, moving source and multiple sensors. Nonstationarities introduced as a result of source motion are studied. These results can now be applied to three problem areas of interest.

6A1. Parameter Identification

In the system identification problem we are given a system with unknown description. We design a probe

to excite the system and ensure that the probe is sufficiently rich in frequency content ($G_{xx}(f)>0$, $f\epsilon(-B,B)$). Then we simultaneously observe (perhaps record) the probe (input) and response (output) of the system. The objective of these observations is to characterize the system. In Chapter 2 it has been shown that there exists a linear filter which will characterize the system if the MSC is unity at all frequencies. (Appendix C provides a computer program for estimating MSC between two waveforms (input and output).) When the MSC is not unity, the characterization is considerably more complex. We have looked at certain no memory nonlinearities and shown how they can be characterized by orthogonal polynomial expansions.

The main thrust of the dissertation, however, has been to estimate one parameter (delay) when the system is linear, but the observations are corrupted by noise. Proper estimation of just this one parameter requires knowledge of the magnitude transfer function α (or more generally $|\alpha(f)|$), and finally knowledge of the noise spectral densities. When this a priori knowledge is not available, we have proposed estimating the unknown quantities and substituting them in place of the known quantities. There is no rigorous derivation to support this procedure other than to note that as the observation time becomes large the estimated quantities converge to the true ones. Thus, the

methodologies applied to the time delay estimations can be expected to be even more complex if, for example, the filter output were $x_2(t)=a_1S(t+D_1)+a_2S(t+D_2)+n_2(t)$. More generally, if $x_2(t)$ was the output of an FIR digital filter of unknown order then the problem of estimating the order, the delays and the attenuations (see Hannan and Thomson (1971), Hannan and Robinson (1973) and Carter and Knapp (1976a)) is a more general problem than the one addressed here. However, to solve the bearing estimation problem motivating this research, the added generality is not required. Thus, the problem considered here is only a subset of the parameter identification problem. Further, note that the solution to the time delay estimation problem does not involve the Fourier transform of the optimum Wiener-Hopf filter (Roth processor), which maps $x_1(t)$ closest to $x_2(t)$; that is, the technique does not look at the peaks or midpoint of the impulse response of the filter that in the MMSE sense filters $x_1(t)$ to obtain an optimum $x_2^o(t)$. With these comments in mind, we have generalized our model to an important class of nonstationarities in order to estimate bearing.

6A2. Bearing Estimation

The bearing estimate follows directly from the delay estimate according to the simple arccos transformation (3-2). The range does not need to be too great relative to the sensor separation in order for the

angle that the hyperbola asymptote makes with the baseline to accurately represent the source bearing. For stationary sources or closely spaced sensors, the relative Doppler (or more generally, the time compression) can be ignored. However, to apply these techniques to widely separated sensors and moving sources, it is necessary to process the data in order to perform Doppler correction (that is, a time scale correction or time scale expansion). To ignore this processing would result in an apparent uncorrelated behavior between the two received waveforms. One contribution of this work has been to specify an ML estimate of time compression. However, because of the nonstationarity of the processes involved, the results tend to be more heuristic and more difficult to interpret (and implement) than those for the time delay estimation problem. In fact, the implementation is hindered by practical computational issues of achieving the time compression. Nevertheless, in the future as computational methods allow for broadband time compression, the methods hypothesized here could actually be tested in practical environments. This should not be interpreted to mean that time compression cannot currently be accomplished. Exact time compression can be achieved, as for example, with variable speed tape recorders or with exact DFT's. Approximate time compression can also be achieved through complex inter-

polation of FFT points or nearest FFT bin approaches. In practice, all of these techniques are expensive to implement; hence, any production application of the theory will benefit from advances in methodologies and mechanizations for achieving time compression. Having techniques for estimating the bearing to moving acoustic sources, we can extend the applications of our theory to estimating range.

6A3. Passive Ranging

In the two sensor models, we are able to estimate delay from which we can estimate bearing. In the multiple sensor situation more information is available. Indeed, with three sensors we can also estimate source location. For example, in Figure 6-1 three equispaced collinear sensors are depicted. As indicated in section 5C, the estimate of θ_1, θ_2 requires simultaneously processing data <u>from all three sensors</u> (one suboptimum processor would be to estimate each bearing from generalized crosscorrelations between only <u>two</u> sensors). When the sensor-pair midpoints are separated by distance d (meters), the range (meters) to the source is given by

$$R = \frac{d\sin\theta_2}{\sin(\theta_1-\theta_2)} \quad . \tag{6-1}$$

An estimated range is obtained by inserting estimated

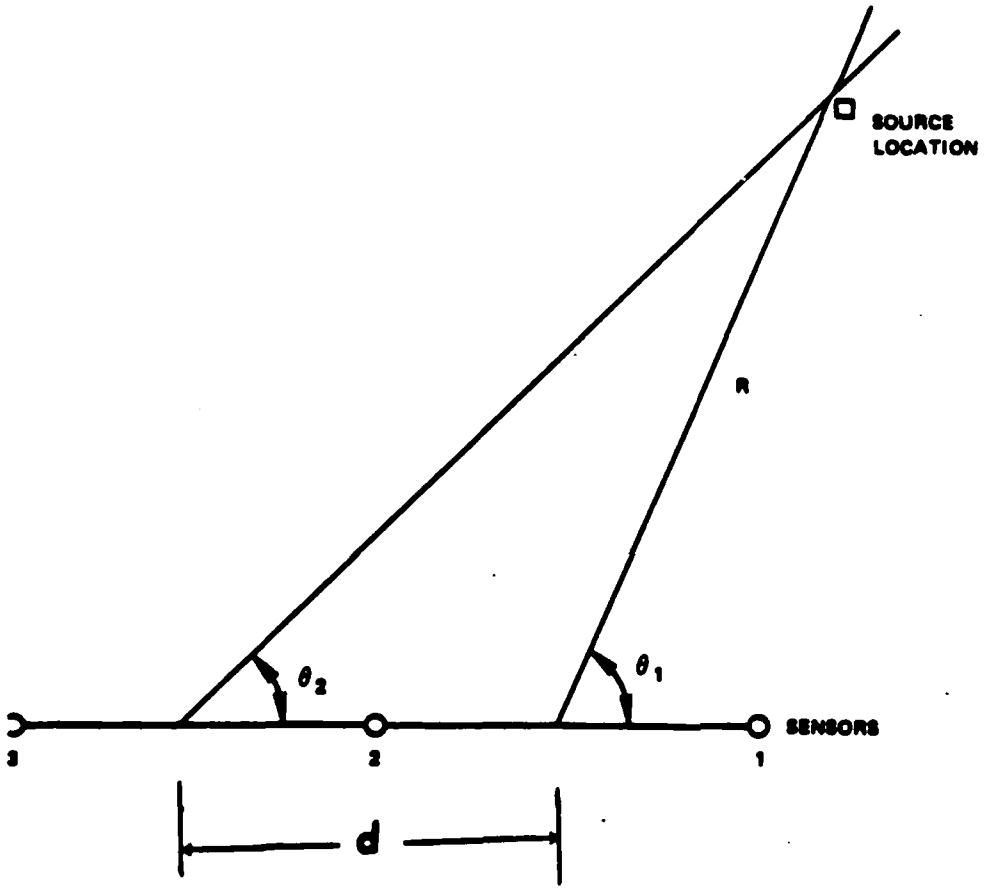

Figure 6-1 Three Collinear Sensors, Single Source Passive Ranging Geometry

AD-A101 684 SCIENTIFIC AND ENGINEERING STUDIES COMPILED 1979 6/8
COHERENCE ESTIMATION(U) NAVAL UNDERWATER SYSTEMS CENTER
NEWPORT RI G C CARTER ET AL. 1979

UNCLASSIFIED F/G 9/1 NL

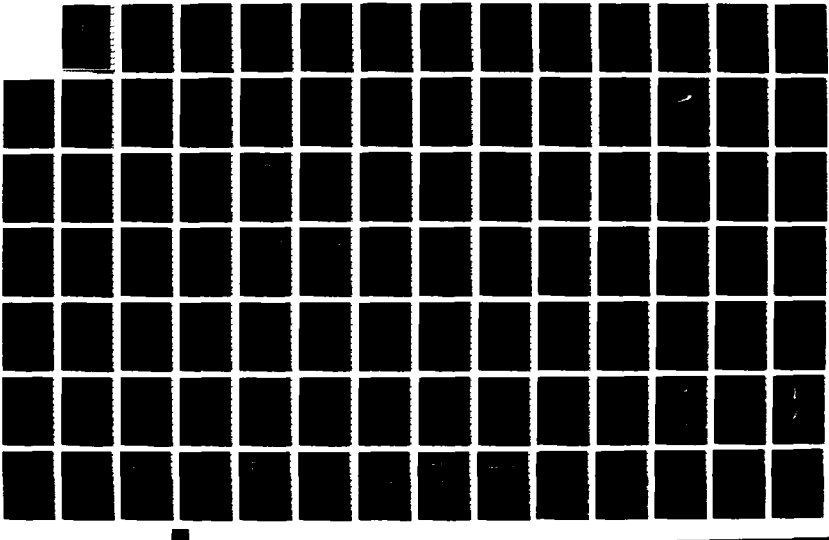

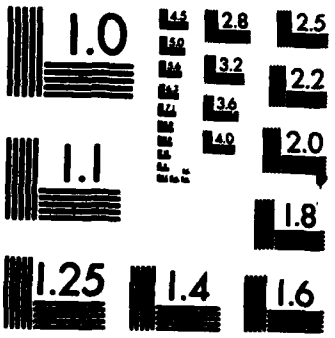

bearings in (6-1).[1] The asymptotes depicted in Figure 6-1 are upper bounds (biased estimates of hyperbolic LOP's); hence, the actual source location will be slightly "below" the intersection depicted. For R>>d, the bias will not be a practical concern.

For more complicated sensor geometries (see Figure 6-2), the bearings θ_1 and θ_2 are used to obtain effective bearings θ_1^e and θ_2^e. When the sensor geometry is known, the effective bearings are easily obtained by the addition of a correction term to the observed bearing. Similarly, the effective separation d_e is simply the shortest distance between the midpoints of the sensor pairs (1,2) and (2,3). The range estimate is then obtained by substituting effective measurements into (6-1). When four or more sensors are used to estimate three or more LOP's, source position may be ambiguously specified, as shown by points A, B, C in Figure 6-3. In such a case, it is reasonable to presume that the source is the least squares distance from existing LOP's; although it is possible for two or three sources to be present.

---

[1] The estimated position (range and bearing, in polar coordinates) obtained by substituting ML estimates of the bearings into (6-1) is <u>not</u> necessarily the ML estimate of position.

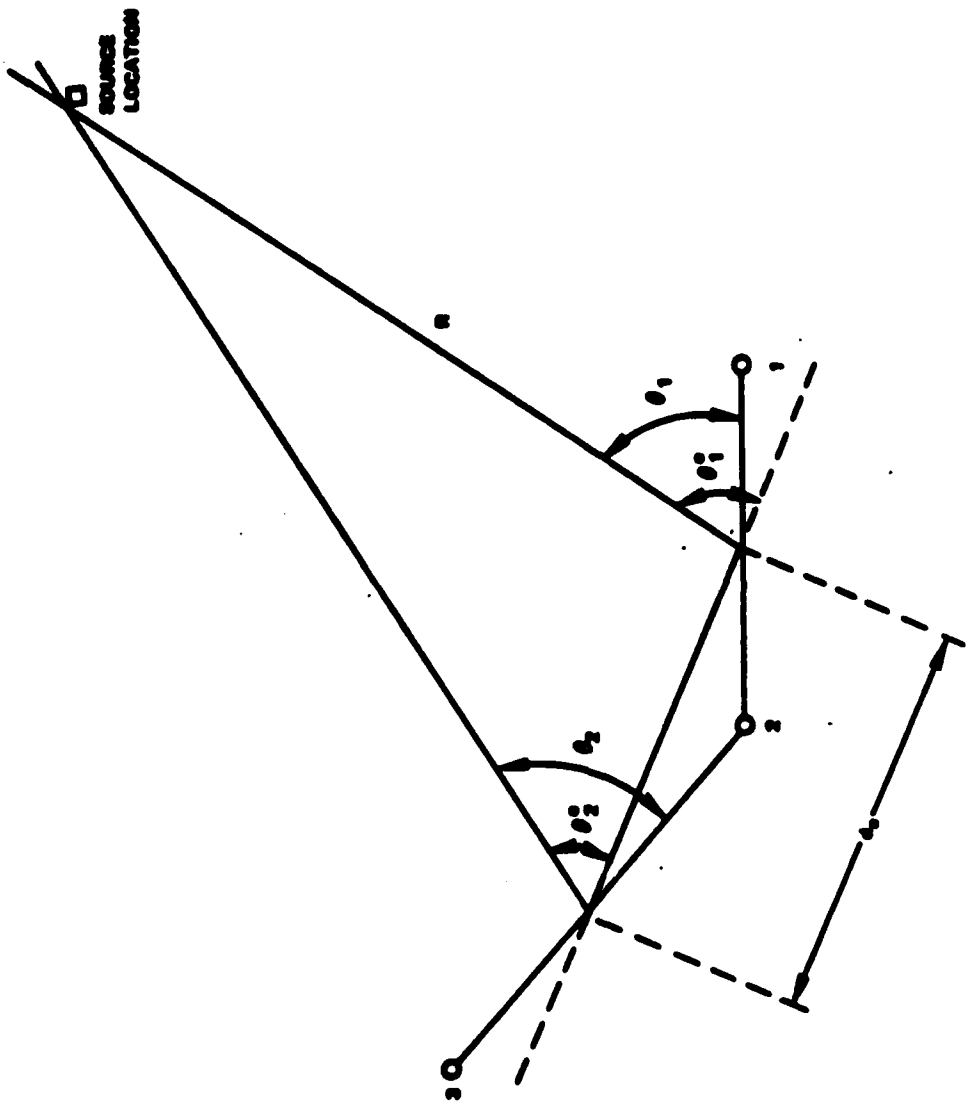

Figure 6-2 Three Noncollinear Sensors, Single Source Passive Ranging Geometry

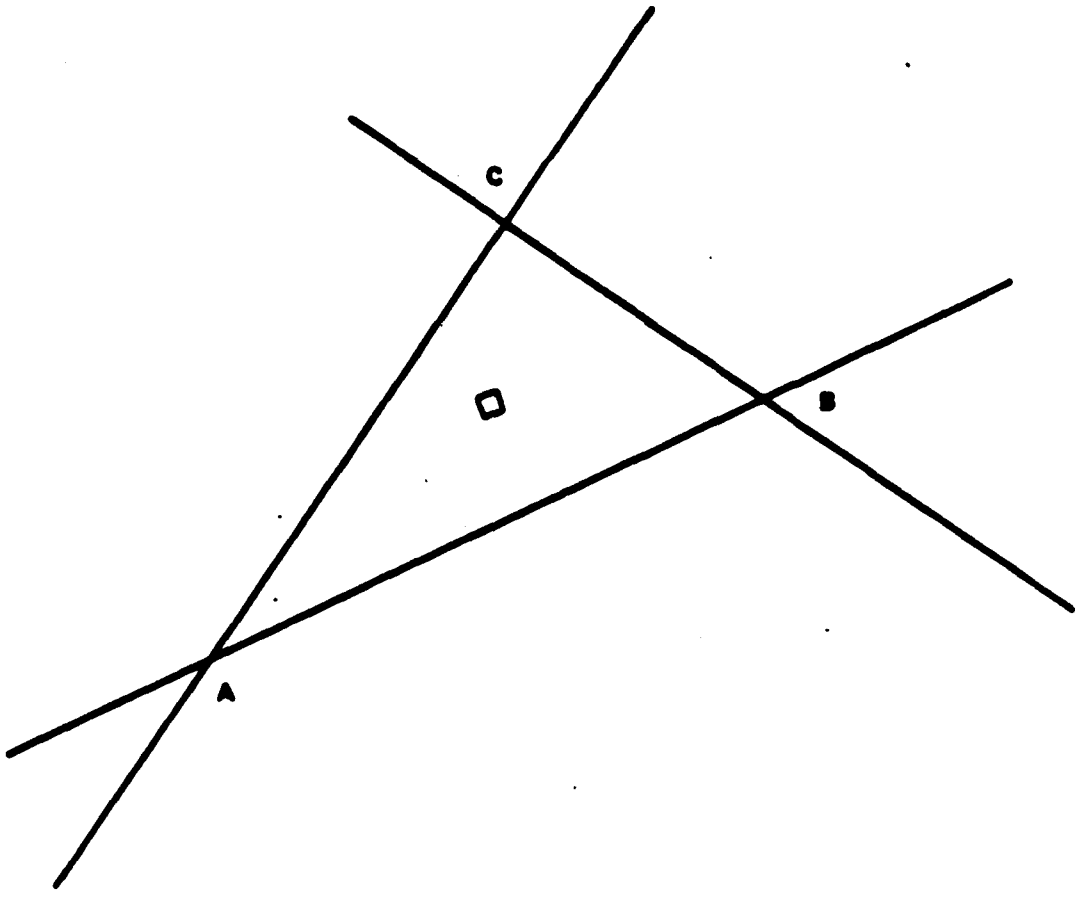

Figure 6-3 Three Estimated LOPs to One Source

6B. Suggestions for Future Work

This section suggests four areas for future work. In a sense, it provides an insight into what we still do not know about the problem at hand. Or stated differently, having solved the problem we set out to solve, we now understand how to pose new problems which we have uncovered. First, in the parameter identification area there appear to be several fruitful research questions: How to identify parameters for (1) general (or particular) nonlinear systems, (2) multi-input, multi-output linear systems, (3) general linear systems, and finally (4) "real world" socio-economic systems. The complexity of estimating time delay suggests that the solution to these problems will be more complex.

The second area is verification of the theory by simulation. We have already conducted one costly computer experiment (Appendix D) which substantiates our belief that insertion of estimated spectra for true spectra enhances the estimation of time delay. However, without running many such experiments, we have no statistical argument to substantiate the theory. Because the cost of running this analysis is prohibitive on a large scale, digital computer, special purpose FFT hardware should be used to empirically validate the theory. The cost of such a system will be significant.

The third area of investigation is an extension of the theory to sequential estimation. In practice, our observation interval will not be just T seconds; rather there will be several consecutive periods of T seconds. Knowing that the source is constrained in its rate of speed, we should be able to rule out certain ambiguous estimates of delay (bearing). More generally, we could model the ship's track and use Kalman filter techniques to extrapolate best projected position (bearing) based on the filter outputs.

Finally, the theory presumes a great deal about (1) ocean acting as a linear time invariant filter over the observation period T, (2) the characteristics of the noise, and (3) the source motion. Thus, the true engineering test is to make controlled measurements with actual acoustic sources in the ocean in order to test the hypothesis. Based on what we currently know, there is every reason to believe such an endeavor will be successful.

APPENDIX A

TECHNIQUES FOR SPECTRAL ESTIMATION

The basic objective of this appendix is to briefly describe two (similar) techniques used to estimate the elements of the power spectral density matrix. The estimates obtained are then used to form an AML estimate of time delay. The two techniques are the overlapped FFT technique (discussed by Carter, Knapp, and Nuttall (1973a)) and the Chirp-Z transform (CZT) technique (discussed by Carter and Knapp (1975)). The methods discussed are sometimes referred to as direct methods (as opposed to indirect correlation methods) and have been discussed in part by Knapp (1966), Welch (1967), Bingham, Godfrey and Tukey (1967), Benignus (1969a), Nuttall (1971), Williams (1971), and Rabiner and Rader (1972).

Both methods begin with two (one from each process) digital waveforms (or with analog waveforms that have been lowpass filtered and digitized). Briefly, there are four steps in the estimation procedure: First, each time series is segmented into N segments, each having P-data points. Second, each segment is multiplied by a smooth weighting function. Third, the Z transform of the weighted P-point sequence is evaluated on the unit

circle in the Z-plane. Finally, the Fourier coefficients thus obtained are used to estimate the elements of the power spectral density matrix by averaging "raw" power spectral estimates over all the N segments. The two methods of spectral estimation differ in how the Z transform is evaluated. One method uses the FFT; the other uses the Partitioned and Modified CZT (PAM-CZT).

More explicitly, two random processes that are jointly stationary over N data segments are processed as follows (Carter and Knapp (1975)):

1. Each of the two time series is segmented into N segments of P points. The segments may either be disjoint or overlapped. Then one segment of P data points with the same time origin is selected from each of two time records. Even if each of the N data segments is large (for example, greater than 4096), P should be selected to ensure that the sampling frequency divided by P will afford adequate spectral resolution.

2. Each of the two P point segments is multiplied by a smooth weighting function. Here smooth means that the ℓ-th order derivative is continuous over the full interval of data points, for ℓ=0, 1, 2, ... up to some reasonable limit. The smoother the weighting function, the more rapidly the side lobes of its Fourier transform, or window function, will decay. The more impulse-like the window, the less leakage there will be of extraneous power, which corrupts spectral measurements.

Hence, good weighting functions result in better spectral estimates. The price paid for impulse-like window functions with rapidly decaying side lobes is a wider main lobe, that is, poorer frequency resolution when P is held fixed. If better resolution is desired, more data points per segment will be required. This in turn requires both that the data be available and that they can be efficiently processed. Moreover, from a stability point of view, increasing P decreases the available number of independent data segments when the data duration is finite.

The specific selection of a weighting function involves a number of tradeoffs. A commonly used weighting (or windowing) function is the cosine (Hanning) function defined at the p-th instant in the interval (0,P) as

$$\frac{1}{2}\left(1 - \cos\frac{2\pi p}{P}\right);$$

such a function starts out at zero for p=0 smoothly rises to unity by p=P/2 and smoothly decays to zero at p=P.

The application of a cosine-weighting function, which is <u>necessary</u> to reduce errors due to side lobe leakage, has the disadvantage of apparently wasting the available data. This apparent wastage can be overcome through overlapped processing. In particular, Nuttall (1971) has shown that the same stability (as measured by the number of equivalent degrees of freedom) can be obtained from a fixed amount of data via overlapped

processing as with Blackman and Tukey (1958) correlation processing for both auto and cross spectral density estimation. (Results on cross spectra processing followed in a supplemental report.)

Quite naturally, there is an increase in computational cost associated with overlapped processing. Specifically, the number of FFTs to be performed (a measure of the computational cost) increases with the percent overlap specified. For example, the number of FFTs required for 50-percent overlap is approximately twice the number for 0-percent overlap. Increasing the overlap from 50-percent to 62.5 percent requires 32-percent more FFTs. For Hanning weighting, the improvement to be derived from using 62.5-percent overlap, as opposed to 50-percent overlap, will not usually warrant the increased computational costs (Carter, Knapp, and Nuttall (1973a)).

Note that if there is no overlap, each segment would be virtually independent of the previous one (except for correlated edge effects). Independent data segments facilitate certain analytic computations. Hence, all theoretical results here are concerned with the case of independent segments; that is, no overlap. This is true even though overlapped processing is recommended for actual data processing. The amount of overlap desirable can be predicted by picturing the apparent wastage for a specific weighting.

3. The transform of the weighted P-point sequence is evaluated on the unit circle in the z plane. The two sided Z-transform of an infinite sequence is defined by Gold and Rader (1969) and Oppenheim and Schafer (1975) as

$$X_n(z) = \sum_{p=-\infty}^{\infty} x_n(p)z^{-p}, \quad n=1,2,\ldots,N \ , \qquad \text{(A-1)}$$

where z equals any complex variable.

Similarly, $Y_n(z)$ is defined as the Z-transform of $y_n(p)$. When $x_n(p)$, $y_n(p)$ are finite in duration, the infinite series (A-1) becomes finite. Evaluation of the Z-transform at P equally spaced points around the circle yields the DFT:

$$X_n(k) = \sum_{p=0}^{P-1} x_n(p)e^{-j2\pi pk/P} \ . \qquad \text{(A-2)}$$

Similarly, $Y_n(k)$ is the DFT of the n-th weighted data segment $y_n(p)$, p=0,1,...,P-1. The DFT can <u>rapidly</u> be evaluated by two methods: the Cooley-Tukey (1965) or the PAM-CZT (see, for example, Rabiner, Schafer, and Rader (1969), Schilling (1972), Ferrie, Nawrocki, and Carter (1973), and Carter and Knapp (1975)). The FFT is a fast algorithm for evaluating the DFT. If the DFT, (A-2), is evaluated for P frequencies (k=0,1,...,P-1) it requires P^2 (complex) multiplications and additions (MADs). The FFT uses an ingenious computation method to evaluate (A-2) in just $P\log_2 P$ MADs. Thus, for P=4096, the number of MADs is reduced by a factor of more than 340. Thus,

computations requiring more than 5 hours can be done in less than 1 minute using FFTs in lieu of DFTs. Specific details of the FFT are beyond the scope of this dissertation.

The DFT, (A-2), is a special case of the CZT, which was introduced by Rabiner, Schafer, and Rader (1969) and amplified, including software implementation, by Schilling (1972)[1] and hardware development by Alsup, Means, and Whitehouse (1973), and Buss, Collins, Bailey and Reeves (1973). Given sufficient data, it is a fast and efficient technique for computing the Z-transform of a sequence on any Z-plane spiral. The modified CZT (MCZT) evaluates equispaced frequency points on the unit circle in the Z-plane. With proper spacing and starting points, it is equivalent to the DFT. Computationally, the MCZT requires three FFTs each of size greater than N (for example, 2N) to compute the DFT, (A-2). However, the tradeoffs are really more complex than this. (For example, if many MCZTs are to be performed one of the three required FFTs does not need to be repeated after its first computation since it is a transformed cosine data table.) The major advantage of the MCZT occurs when the number of data points P (in each of the N data segments) is large.

---

[1]This work was brought to the author's attention by Dr. N. Ahmed, Kansas State University, Manhattan, Kansas.

In such cases, the original P point data segment can be again segmented into R partitions each disjoint with size P/R data points. The R partitions are processed with R MCZTs; the outputs are summed together with appropriate phasing to achieve a PAM-CZT that is equivalent to the DFT, (A-2). The mathematical details of this technique are covered in length by Ferrie, Nawrocki, and Carter (1975); their inclusion here does not appreciably add to the discussion but does considerably complicate the notation due to conflicts with assigned symbols. For most broad band cases of interest (and certainly the example case in Appendix D), the FFT will be preferable to the PAM-CZT. A complete discussion of the tradeoffs is given by Carter and Knapp (1975).

Having computed the DFT, (A-2), either by an FFT or PAM-CZT, we are ready to proceed with the fourth step in the spectral estimation algorithm.

4. The spectral estimates are

$$\hat{G}_{xx}(k) = c_g \sum_{n=1}^{N} |X_n(k)|^2, \qquad \text{(A-3a)}$$

$$\hat{G}_{yy}(k) = c_g \sum_{n=1}^{N} |Y_n(k)|^2, \qquad \text{(A-3b)}$$

$$\hat{G}_{xy}(k) = c_g \sum_{n=1}^{N} X_n(k) Y_n^*(k), \qquad \text{(A-3c)}$$

where the constant

$$c_g = \frac{1}{N \cdot f_s \cdot P} \quad , \tag{A-3d}$$

and $f_s \equiv$ sampling frequency. (The estimated cross spectrum (A-3c) is complex.) The estimate of MSC

$$\hat{C}_{xy}(k) = \frac{|\hat{G}_{xy}(k)|^2}{\hat{G}_{xx}(k)\hat{G}_{yy}(k)} \quad . \tag{A-4}$$

The AML estimation of time delay requires substituting the estimates $\hat{C}_{xy}$ in place of the true (but unknown) value of MSC. Therefore, we are concerned about the statistical variability of the MSC. Further, the statistical characteristics of $\hat{C}$ are of interest in their own right, since $\hat{C}$ is useful not only in time estimation (Chapter 3) but also for other applications (Chapter 2). Appendix B discusses the statistics of the MSC estimate.

APPENDIX B

STATISTICS OF THE MSC ESTIMATE

The MSC estimate, from (A-3) through (A-4), is

$$\hat{C}_{xy}(k) = \frac{\left| \sum_{n=1}^{N} X_n(k) Y_n^*(k) \right|^2}{\sum_{n=1}^{N} \left| X_n(k) \right|^2 \sum_{n=1}^{N} \left| Y_n(k) \right|^2} , \qquad \text{(B-1)}$$

where N is the number of data segments employed and $X_n(k)$, $Y_n(k)$ are the DFTs of the n-th weighted data segments of x(t), y(t), respectively. Under certain assumptions the statistical characteristics of $\hat{C}$ can be evaluated. This appendix is divided into four sections. The first section gives the pdf, cumulative distribution function (cdf) and m-th moment of $\hat{C}$, given C and N. The second section gives the bias of the estimate $\hat{C}$ including a discussion of when the analytic results fail and simulations to support the theory. The third section gives the variance of $\hat{C}$. The fourth section gives a computer program for evaluating receiver operating characteristics (ROC) of a linearly thresholded coherence estimation processor. The results in all four sections are based on the derivation by Goodman (1957) of an analytical expression for the pdf of the MC estimate and the subsequent extensions to

MSC by Carter, Knapp, and Nuttall (1973a). These results are based on two zero-mean stochastic processes that were jointly stationary, Gaussian, and had been segmented into N independent segments.[1] Each segment was assumed large enough to ensure adequate spectral resolution. Further, each segment was assumed perfectly weighted (windowed), in the sense that the Fourier coefficient at some k-th frequency was to have "leaked" no power from other bins. The statistics do not hold at the zero-th or folding frequencies (Hannan (1970)). Extensions to Goodman's work are given by Alexander and Vok (1963), Amos and Koopmans (1963), Enochson and Goodman (1965), Nettheim (1966), Wahba (1966), Tick (1967), Carter and Nuttall (1972), Carter, Knapp and Nuttall (1973b), Halvorsen and Bendat (1975), and Nuttall and Carter (1976a).

B1. Probability Density, Cumulative Distribution and m-th Moment of $\hat{C}$

The first-order pdf, cdf and m-th moment of the estimate of MSC, given the true value of MSC and the number, N, of independent segments processed, are presented in this section in closed form.

---

[1] Despite the fact that it is only mathematically tractable to obtain analytic expressions when the segments are independent, we would in practice use some overlapped processing to regain the apparent data wastage incurred by the necessity of data weighting. Carter, Knapp, and Nuttall (1973a) report the results of an empirical study that demonstrates how bias and variance decrease as a function of increased data segment overlap. Fifty percent overlap is recommended with cosine weighting.

The conditional pdf for $\hat{C}$, between two processes, given C and N, is (Carter, Knapp, and Nuttall (1973a))

$$p(\hat{C}|N,C) = (N-1)(1-C)^N(1-\hat{C})^{N-2}\ (1-C\hat{C})^{1-2N}\ {}_2F_1(1-N,1-N;1;C\hat{C}). \tag{B-2}$$

The ${}_2F_1$ is a hypergeometric function with two numerator terms and one denominator term. (It is a special case of (B-7) and is discussed more fully in Section B4.) For present, we note equation (B-2) is desirable because ${}_2F_1(1-N,1-N;1;C\hat{C})$ can be expressed as an (N-1)st order polynomial (Abramowitz and Stegun (1964), Equation (15.5.1)).

A special case of the density function occurs when C=0. In that event,

$$p(\hat{C}|N,C=0) = (N-1)(1-\hat{C})^{N-2}\ . \tag{B-3}$$

Using a result of Fisher (1950), Carter, Knapp, and Nuttall (1973a) have determined (in closed form) the cumulative distribution of the estimate of MSC, namely,

$$P(\hat{C}|N,C)=\hat{C}\left(\frac{1-C}{1-C\hat{C}}\right)^N \sum_{k=0}^{N-2}\left(\frac{1-\hat{C}}{1-C\hat{C}}\right)^k \cdot\ {}_2F_1\left(-k,1-N;1;C\hat{C}\right). \tag{B-4}$$

A digital computer program to evaluate equation (B-4) is given in Section B4. In the special case when C=0, the cdf can be simplified to give

$$P(\hat{C}|N,C=0) = 1-(1-\hat{C})^{N-1}\ . \tag{B-5}$$

Equation (B-5), when differentiated, yields the pdf equation (B-2).

The m-th moment of the MSC estimate can be found by application of Equation 7.512(12) by Gradshteyn (1965) to

a different form of (B-1) to yield (Carter, Knapp, and Nuttall (1973a))

$$E[(\hat{C}^m|N,C)] = (1-C)^N \frac{\Gamma(N)\,\Gamma(m+1)}{\Gamma(N+m)}$$

$$\cdot\, {}_3F_2(m+1,\ N,\ N;\ m+N,\ 1;C) \quad . \qquad \text{(B-6)}$$

These results can be confirmed using Carter (1972a) and Anderson (1958).

The ${}_3F_2$ hypergeometric functions (with three numerator terms and two denominator terms) are given by

$${}_3F_2(a,b,c;\ d,e;\ z) = \sum_{k=0}^{\infty} \frac{(a)_k (b)_k (c)_k}{(d)_k (e)_k} \frac{z^k}{k!} \quad , \qquad \text{(B-7a)}$$

where the $(a)_k$ notation is Pochhammer's symbol (Abramowitz and Stegun (1964)) defined by

$$(a)_k \triangleq \frac{\Gamma(a+k)}{\Gamma(a)} \quad , \qquad \text{(B-7b)}$$

where $\Gamma(\ )$ is the Gamma function. Similarly, the F two-one function has two numerator and one denominator terms.

B2. Bias of $\hat{C}$

This section deals with the bias of the MSC estimate. Exact and approximate expressions are presented. In addition, computer evaluation of the exact expressions is presented to lend meaning to these results, and two computer simulations are presented. The first simulation demonstrates the need to have adequate spectral resolution. The second simulation verifies the theoretical results for bias (and also variance, which is discussed in the next section, B3).

Consider now the first moment of the estimate of MSC which can be written as

$$E[\hat{C}|N,C] = \frac{(1-C)^N}{N} \, {}_3F_2(2,N,N;N+1,1;C) \quad , \tag{B-8}$$

which can be manipulated into the form (Carter (1972a))

$$E(\hat{C}|N,C) = \frac{1}{N} + \frac{N-1}{N+1} C \, {}_2F_1(1,1;N+2;C) \quad . \tag{B-9}$$

The bias or expected estimation error is defined as

$$\text{Bias} = B(\hat{C}|N,C) = E(\hat{C}|N,C) - C \quad . \tag{B-10}$$

An exact expression for the bias is

$$B(\hat{C}|N,C) = \frac{1}{N} + \frac{N-1}{N+1} C \, {}_2F_1(1,1;N+2;C) - C \quad . \tag{B-11}$$

The maximum bias is 1/N (regardless of N and C). The bias is plotted in Figure B-1. It should be noted that

$$\lim_{N \to \infty} (\text{Bias}) = 0 \quad ; \tag{B-12}$$

therefore, the estimator may be referred to as asymptotically unbiased. By expanding ${}_2F_1$ in (B-11) in a power series in C and retaining terms to order N^{-2}, the following approximation is obtained (Nuttall and Carter (1976b)):

$$B_1(C,N) = \frac{1}{N}(1 - C)^2\left(1 + \frac{2C}{N}\right) \quad . \tag{B-13}$$

Plots of N B(C,N) and N B_1(C,N) are presented in Figure B-2 for N=4 (they cross near C=0.4). Approximation (B-13) is seen to be excellent over the entire range of C. Furthermore, the discrepancy between the approximation (B-13) and the true bias (B-11) is even less for larger

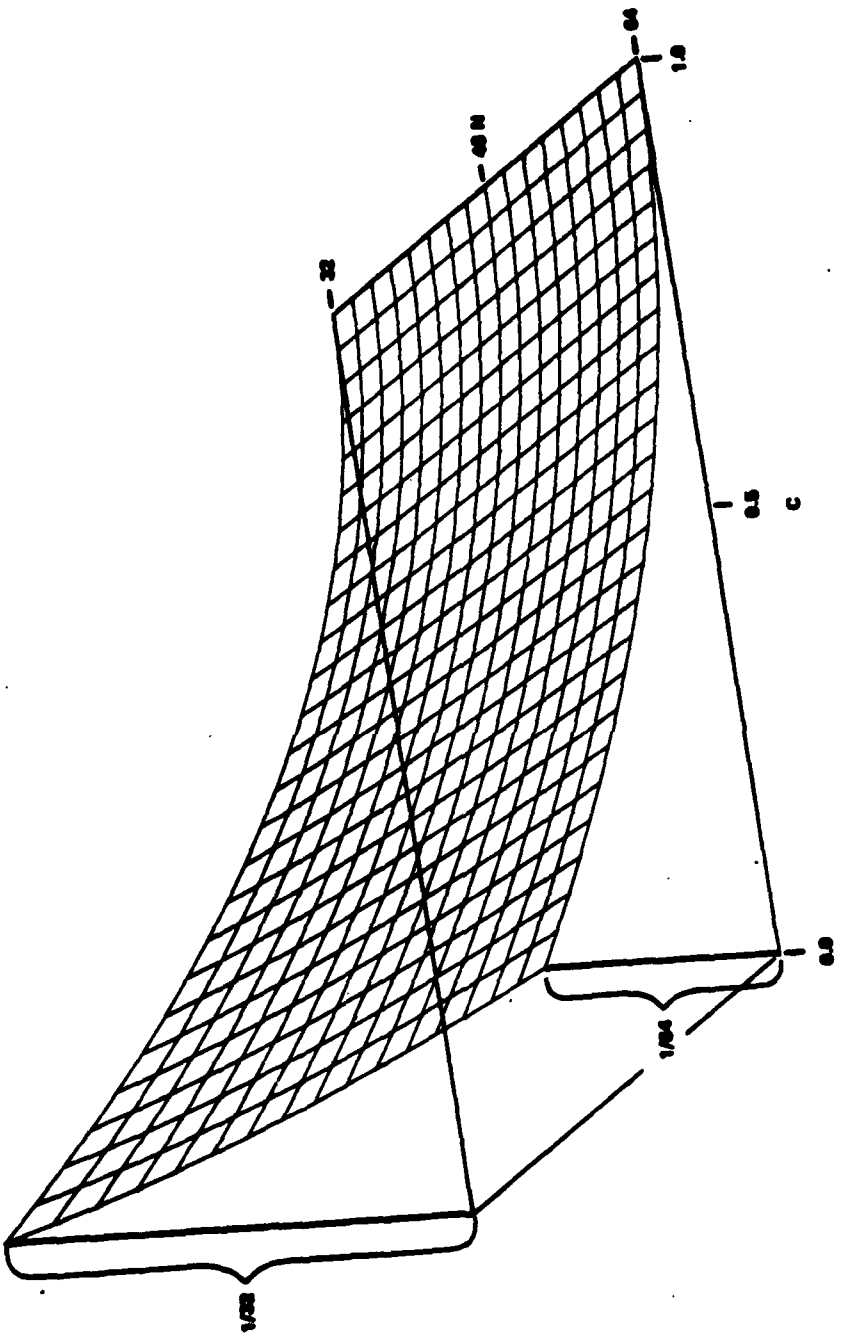

Figure B-1 Bias of $\hat{C}$ versus C and N

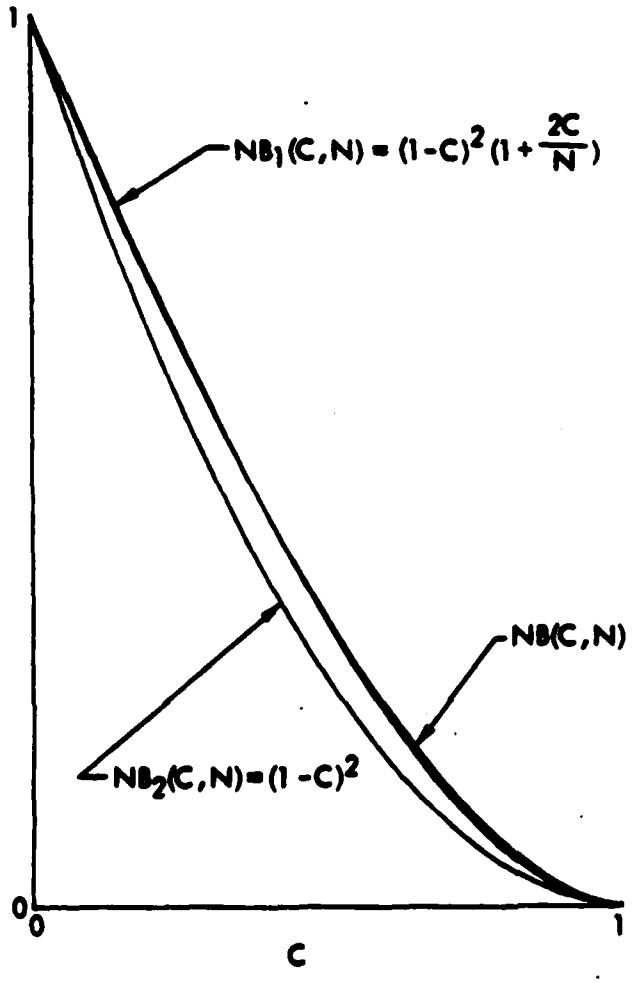

Figure B-2 Bias of $\hat{C}$ and Approximations for N=4

values of N.

For large N, (B-13) is further reduced to the approximation given by Carter, Knapp, and Nuttall (1973a):

$$B_2(C,N) = \frac{1}{N}(1-C)^2; \text{ good for large } N \; . \qquad (B\text{-}14)$$

Therefore, as N leads to infinity, N B(C,N) tends to $(1-C)^2$, which is also plotted in Figure B-2; furthermore, the approach is monotonic.

In Benignus (1969a), (2), an approximate expression for the bias, based upon a simulation approach, is presented as

$$B_3(C,N) = \frac{1}{N}(1-C) \; . \qquad (B\text{-}15)$$

Whereas the results in Haubrich (1965) and (B-14) dictate a quadratic behavior for bias, the approximation by (B-15) indicates a linear behavior. Since (B-11) through (B-14) is based upon theory and (B-15) is based upon simulation, it was decided to verify (or invalidate) (B-11) through (B-14) by a simulation approach. Two computer simulations were conducted.

In order to verify the theory, the simulation must preserve those assumptions present in the derivation of the theoretical expression (B-11) for bias. Specifically, as pointed out by Carter and Knapp (1975), (B-11) holds under the following assumptions:

1. jointly Gaussian stationary processes
2. N independent (non overlapped) data segments

3. smooth weighting function to reduce side lobe leakage

4. adequate frequency resolution

When any of the specified assumptions are violated, analytic results derived for bias (and variance) of the estimator can be grossly misleading. (The Gaussian part of the first assumption is weak; see the discussion after (3-3).) As an empirical verification of this statement, consider the study reported by Carter and Knapp (1975), where $C_{xy}(f) = 1, \forall f$. Specifically, consider a simple linear second-order digital filter of the form

$$Y_n = 1.97300Y_{n-1} - 0.98202Y_{n-2} + 0.00872X_n. \quad \text{(B-16)}$$

The system behavior was studied by probing the filter with a white pseudorandom noise source. The sampling rate was set equal to 2048 Hz; hence, the Nyquist rate of π radians is depicted as 1024 Hz in the figures that follow.

The filter phase characteristics were estimated, Figure B-3, with P=1024, cosine weighting, and 64 independent segments. Despite the fact that the MSC between input and output should equal unity (hence, the bias of the estimator would normally be zero), the estimate of MSC is grossly biased when a rectangular weighting function is used. Specific MSC estimates are depicted in Figure B-4 for the rectangular weighting case. The bias attributable to improper windowing, while

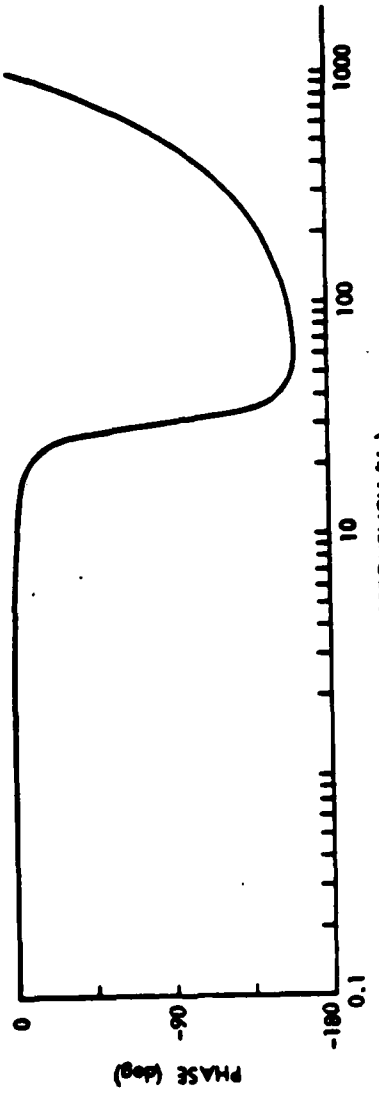

Figure B-3 Phase Characteristics of Second Order Linear Filter

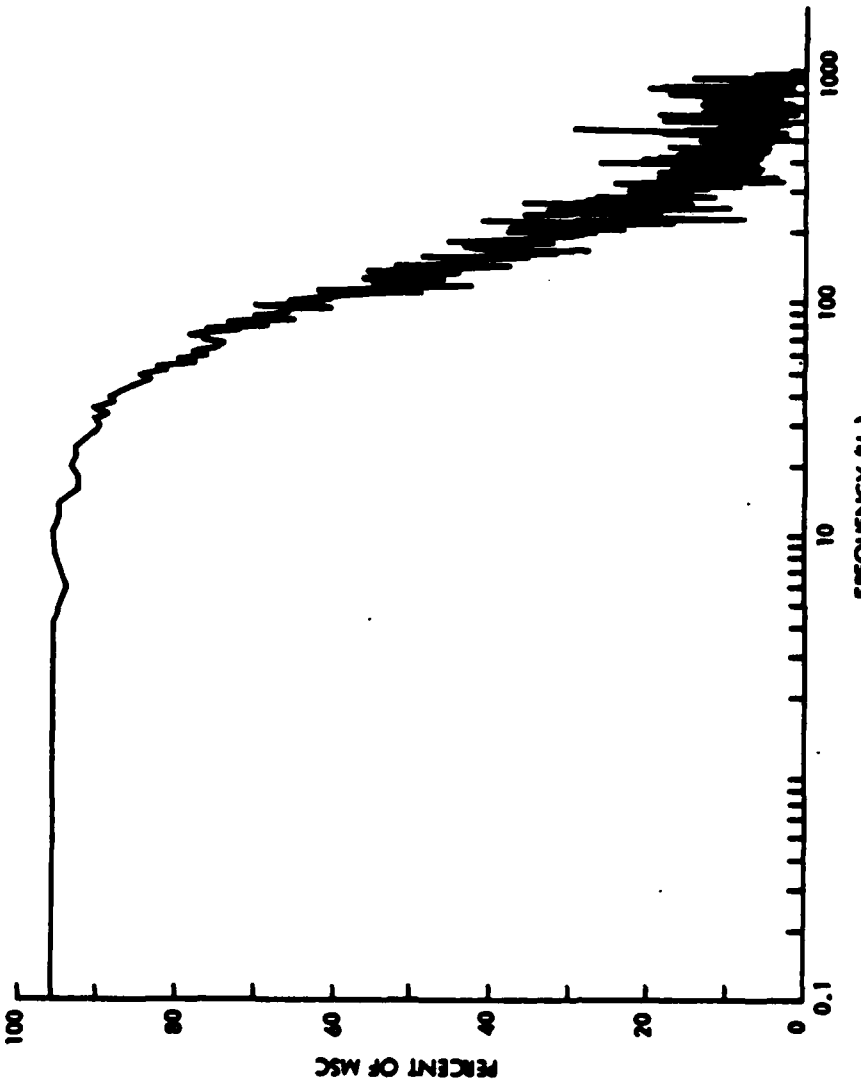

Figure B-4 Biased Estimates of C (True Value of C is Unity) Due to Rectangular Weighting Function

severe, can be substantially eliminated through selection of a leakage-suppressing window. When a cosine or Hanning window is utilized and the data are reprocessed, estimates depicted in Figure B-5 are obtained. Notice now that the bias, though greatly improved, still exists in the vicinity of 30 Hz. Referring to Figure B-3, notice that 30 Hz is the center of a frequency band in which the first derivative of the phase is large. The dependence of the bias of the MSC estimate on this characteristic of phase is predicted in Jenkins and Watts (1968), Hannan (1970), and Koopmans (1974).

Once sufficient resolution has been achieved, this bias no longer exists. To determine whether the bias in Figure B-5 could be reduced by more averaging, as analytically predicted by the approximation in Jenkins and Watts (1968), additional independent data segments were processed in the simulation (that is, N was made larger without changing P). In this case of insufficient resolution, the maximum bias error was observed to be independent of the number of segments averaged; that is, the estimator is biased as $N \to \infty$ when the number of data points per segment is small.

When large amounts of data are used, as in the case of a computer simulation, better resolution can be obtained without loss of averaging (variance reduction) capability. However, when the data are of limited

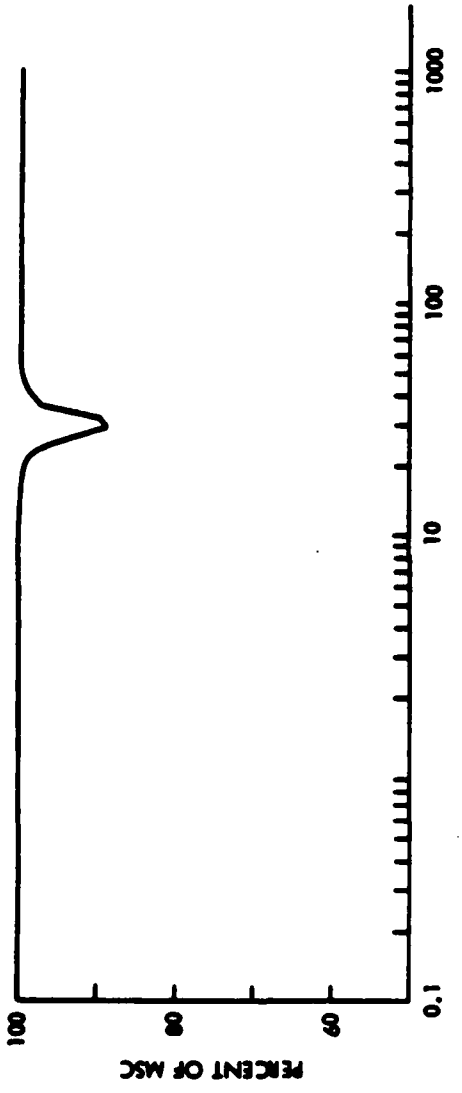

Figure B-5 Example of Biased Estimates of C Due to Inadequate Frequency Resolution

duration then--dependent on the length of actual data cuts and the stationarity of events over that duration--another method can be employed to improve MSC estimation in the face of rapidly changing phase angles. These methods are referred to as alignment, or translation methods, and are used to remove the time delay or group delay of a filter. Translation (that is, prefiltering by a single time delay) of one time series with respect to another permits the rate of change of the phase in a particular frequency band to be controlled and reduced to yield better MSC estimates in that frequency band. The implication is that MSC estimates are valid in frequency bands where the phase has little or no slope. Various methods for estimating the time delays are discussed in Chapter 4.

Translation was applied to align the time series for the example presented here. After alignment, unbiased estimates were obtained in a 20 Hz band about 30 Hz; however, as expected, outside that band, biases were severe, making interpretation meaningless. In general, translation must be applied for "all" time delays and the results combined into one result (graph); hence, when sufficient data are available, the author's preference is for finer frequency resolution rather than for the piecemeal approach which may be dictated for reasons of limited data or limited stationarity. In the latter case (of P sufficiently large), $\hat{C}$ will not depend on D.

The example used here exhibited biases of one tenth (see Figure B-5); furthermore the trend was clearly indicative of the fact that any bias (less than one) could be expected with insufficient frequency resolution even when as many as 64 independent data segments have been processed (Carter (1972b)). The practical implication of this limitation is that it is highly desirable that the actual number of data points per segment, P, be large. For a finite duration data set, this will mean increased instability in the estimator (that is, smaller N and hence larger variance). It should be noted that one cannot simply increase P by adding zeros or by increasing the sampling rate of the original data, for then no additional information content is added. Quite the contrary, the minimum data sampling rate should be selected, for this ensures the maximum amount of actual time per data segment for a given value of P. Good resolution, that is, large P, apparently requires computation of a large size FFT. An alternative computation that reduces the required FFT size is the PAM-CZT (Appendix A).

The results of the first simulation show two critical things: first, when estimating MSC (or any spectral quantities) it is important to use both smooth weighting functions and adequate frequency resolution. Second, simulation experiments to validate expressions for bias of $\hat{C}$ can give misleading results due to the sensitivity

of the four fundamental assumptions upon which the theory rests. Another difficulty in experimentally estimating bias is that when the assumptions do hold, the bias is a small quantity to measure. For example, for C=0.3, N=32, we find B(C,N)=0.0156. However, the standard deviation of $\hat{C}$ is approximately 0.3. (See Section 3 of Appendix B.) Thus a large number of independent trials, in each of which C is computed, must be used in order to obtain a sample mean that has statistical significance. We use 10,000 different independent trials at each value of C=0 (.1).9; the results of Benignus (1969a) employed less than 1,000 trials.

Lastly, the smallness of the bias dictates that the desired value of C be accurately realized in the simulation. As an example of the danger of not doing so, consider the following: suppose we believe we have generated processes with a desired coherence of 0.300, and subsequently observe a sample mean of 0.315; in such a situation, the estimated bias is 0.015. But if the generated coherence is not precisely under the experimenter's control and is off by only 1 percent (giving rise to a true coherence in this example of 0.303), then the bias should have been reported as 0.315-0.303=0.012. Thus, a 1 percent error in true coherence gives rise to a 25 percent error in estimated bias in this example. We generate our correlated

processes according to

$$x(t) = a(t) , \qquad \text{(B-17a)}$$

$$y(t) = b(t) + g\,a(t), \qquad \text{(B-17b)}$$

where a(t) and b(t) are uncorrelated complex Gaussian processes, and

$$g = \sqrt{\frac{C}{1-C}} \quad . \qquad \text{(B-18)}$$

The statistical characteristics of $\hat{C}$ in (B-1) are derived on the fact that X(k) and Y(k) are Gaussian. This will be the case if x(t) and y(t) are Gaussian; however, the essence of the theory does not require X(k) and Y(k) to be DFT outputs but merely complex Gaussian random variables. Thus, we can simply avoid the issues of weighting and frequency resolution by simulating the DFT outputs directly; this technique reduces the cost of the experiment (and indeed will verify the theory). The essential features of the simulation are given in Figure B-6.

The results of the simulation for N=4 are superposed in Figure B-7 on the exact bias curve.

In particular, the sample mean of 10,000 independent trials at each value of C=0(.1).9 is plotted, along with a vertical bar between the $\pm\sigma$ points of the random variable. In seven out of the ten cases of selected MSC, the $\pm\sigma$ points bracket the theoretical curve, and the remaining three out of ten are included within the $\pm 2\sigma$ points. The possibility of (B-15) falling within

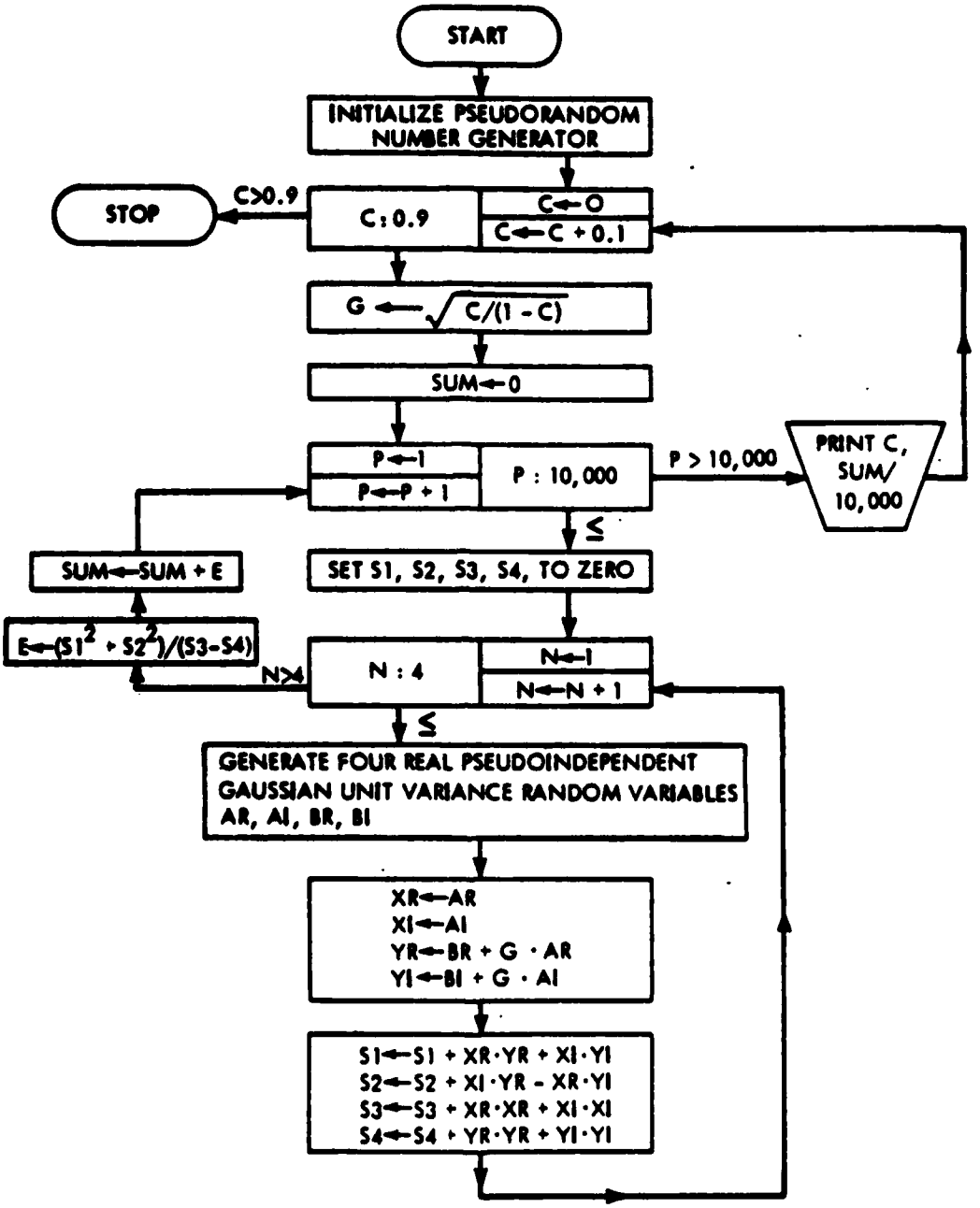

Figure B-6 Flow Diagram for Empirical Determination of Bias of $\hat{C}$; N=4; 10,000 Trials

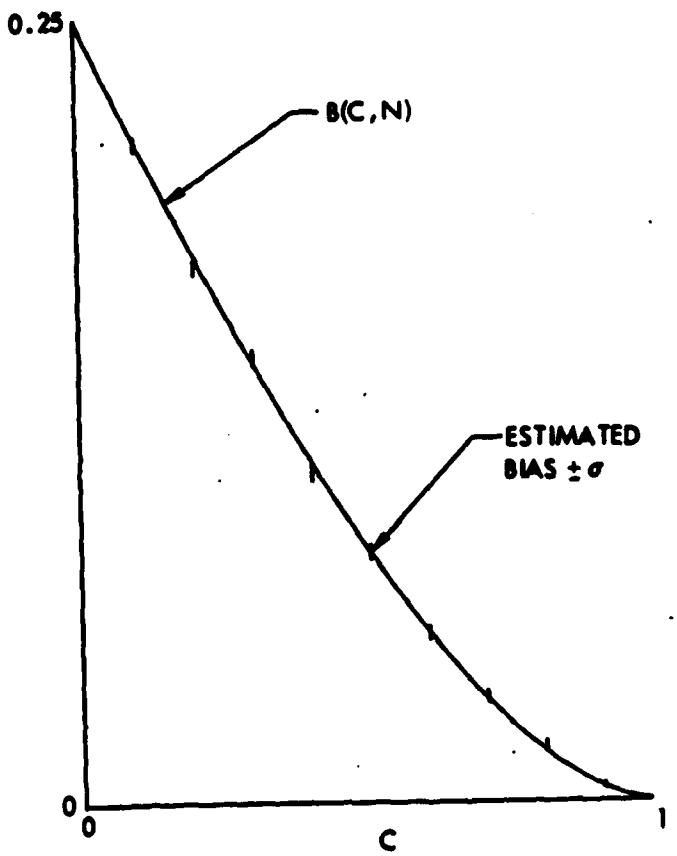

Figure B-7 Theoretical and Simulation Results for Bias of $\hat{C}$; N=4; 10,000 Trials

these tolerances is completely ruled out. Thus, the simulation confirms the theoretical result in (B-11) and rules out the approximation in (B-15).

Since we have a simulation technique which corroborates the theory so well, it is possible to employ it to investigate other more complicated functions of $\hat{C}$ which are very difficult (if not impossible) analytically. In particular, we use a bootstrap idea based upon that of Benignus (1969a) in an attempt to reduce the bias of the coherence estimate. Namely, we consider a modified estimate of MSC as

$$\hat{\hat{C}} = \max\left[0, \hat{C} - \frac{1}{N}(1-\hat{C})^2\left(1+\frac{2\hat{C}}{N}\right)\right], \qquad \text{(B-19)}$$

where we have estimated the bias by means of (B-13) and the initial estimate $\hat{C}$ of MSC. The reason for the 0 in (B-19) is that we are unwilling to accept negative estimates of coherence. (Without the 0 in (B-19) we can reduce the bias further at the expense of added variance.) The estimated bias and variance of $\hat{C}$ and $\hat{\hat{C}}$ are presented in Table B-1. It is observed that the bias of $\hat{C}$ is significantly reduced. However, the variance is increased. In fact, the estimated mean square error (MSE) (which equals the variance plus the square of the bias) is presented in Table B-1 and is greater for $\hat{\hat{C}}$ than for $\hat{C}$ when C is greater than 0.3; the opposite behavior holds when C is less than 0.3. (For N=4, C=0.3 is the crossover.) Thus, the choice

Table B-1

Estimated Bias, Variance and MSE of $\hat{C}$ and $\hat{\hat{C}}$ for N=4; 10,000 Trials

C	Bias ($\hat{C}$)	Bias ($\hat{\hat{C}}$)	Var ($\hat{C}$)	Var ($\hat{\hat{C}}$)	MSE ($\hat{C}$)	MSE ($\hat{\hat{C}}$)
0	.249	.146	.037	.040	.099	.062
.1	.210	.111	.045	.054	.090	.066
.2	.171	.076	.050	.064	.079	.070
.3	.142	.057	.053	.072	.073	.075
.4	.105	.030	.052	.073	.063	.074
.5	.080	.019	.048	.068	.054	.069
.6	.054	.008	.041	.059	.044	.059
.7	.033	.003	.030	.042	.031	.042
.8	.018	.0014	.018	.024	.019	.024
.9	.005	-.0006	.006	.008	.006	.008
1	0	0	0	0	0	0

between the two estimators, $\hat{C}$ and $\hat{\hat{C}}$, depends on whether one is bothered more by bias or MSE.

For larger N, the crossover value of C, at which $\hat{C}$ or $\hat{\hat{C}}$ has less MSE, decreases. For example, at N=8, it was observed to occur at C=0.2. Thus, for practical useful values of N (which are usually much larger than 1), the estimator $\hat{C}$ will have less MSE than $\hat{\hat{C}}$ over almost the whole range of C and will probably be preferred. Also, the bias is quite small for large N. The variance of $\hat{C}$ is discussed in the next section. Under the assumptions of smooth weighting functions and adequate frequency resolution, we will see variance is a more significant problem than bias. However, as seen in this section, when the assumptions are violated, the bias can be a significant source of estimation error.

B3. Variance of $\hat{C}$

An exact expression for the variance of C is Carter (1972a):

$$V = \frac{2(1-C)^N}{N(N+1)}\ {}_3F_2\left(3,\ N,\ N;N+2,\ 1;\ C\right) - \left[\frac{(1-C)^N}{N}\ {}_3F_2\left(2,N,N;N+1,\ 1;\ C\right)\right]^2 \quad \text{(B-20)}$$

(B-20) is plotted in Figure B-8. For the special case of C=0,

$$V = \frac{2}{N(N+1)} - \left(\frac{1}{N}\right)^2 = \frac{N-1}{N^2(N+1)}, \quad C=0, \quad \text{(B-21a)}$$

and

$$\cong \frac{1}{N^2}, \text{ for large N and C=0.} \quad \text{(B-21b)}$$

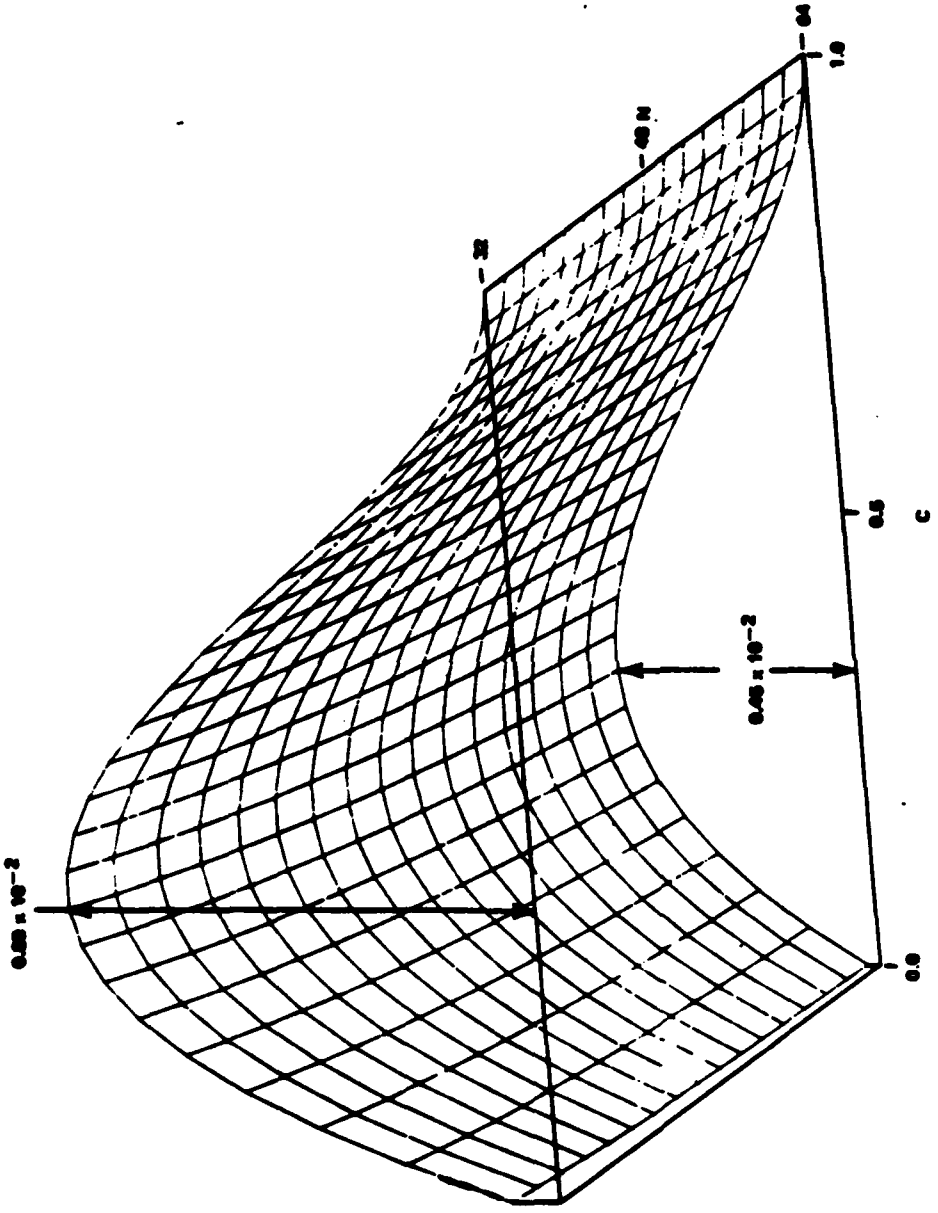

Figure B-8 Variance of $\hat{C}$ versus C and N

For large N and C≠0,

$$V \approx \frac{2}{N} C\left(1-C\right)^2 \quad , \qquad \text{(B-22)}$$

which has a maximum value of $8/27N \approx 0.30/N$ at C=1/3. Thus the maximum variance is always less than 0.30/N regardless of the value of C. Hence, the variance of the estimator in the case where C is unknown (but nonzero) decreases inversely proportional to N. We note, by inspecting (B-20), that for larger and larger N, (B-22) becomes a better and better approximation.

Since, in general, we do not know the true value of MSC, we select N based on a worst case (maximum variance) analysis.

Provided we have used good weighting functions and good frequency resolution, the variance has a more serious effect than bias. For example, if C=1/3 and N=100, then the bias of $\hat{C}$ is less than 0.01, while the standard deviation (square root of the variance) is approximately equal to .05. Hence, even when 100 independent segments are processed, the MSC estimate still has significant variability.

B4. Receiver Operating Characteristics for a Linearly Thresholded Coherence Estimation Detector

An algorithm for computing the ROC, or the probability of detection, P_D, versus the probability of false alarm, P_F, for a linearly thresholded MSC estimation detector is presented together with an

example of a ROC table[1] (Carter (1976). A recent article (Gevins, Yeager, Diamond, Spire, Zeitlin, and Gevins (1975)) presents new results on using linearly thresholded MSC estimates to detect biomedical phenomena. The desire to establish a threshold below which MSC estimates are not presented to a human decision maker is an important issue in certain areas, such as brain wave analysis and sonar, where the volume of sensor data is large. For a fixed amount of averaging and a fixed threshold value, E, in the absence of a coherent source, there is still a certain probability, P_F, that an MSC estimate will exceed the threshold. Moreover, although the false alarm rate can be reduced by increasing E, to do so decreases P_D, when a coherent source is present. How much it decreases P_D will depend on the strength of the coherent source, that is, the true or underlying coherence that is being estimated. This section presents an algorithm for computing P_D versus P_F for a specified amount of averaging and underlying coherence. The pdf of $\hat{C}$, when C=0, is (from (B-3)):

$$p(\hat{C}|N, C=0) = (N-1)(1-\hat{C})^{(N-2)} . \qquad \text{(B-23)}$$

---

[1]The idea for computing ROC curves was suggested to the author by R. Trueblood, Naval Undersea Center, San Diego, California.

Hence, the probability of false alarm is

$$P_F = 1 - \int_0^E (N-1)(1-\hat{C})^{(N-2)} d\hat{C} \qquad (B\text{-}24)$$

or

$$E = 1 - \exp[\log(P_F)/(N-1)]; \qquad (B\text{-}25)$$

that is, for a specified P_F we establish a threshold according to (B-25). Now the computationally more complex question is: What probability of detection is achieved for this threshold value E? The answer, for a given value of C, is

$$P_D = \int_E^1 p(\hat{C}|N,C)\, d\hat{C} = 1 - P(\hat{C} \leq E|N,C) , \qquad (B\text{-}26)$$

where $P(\hat{C} \leq E|N,C)$ is the cdf. The cdf is given by (B-4), namely,

$$P(\hat{C} \leq E|N,C) = R \sum_{\ell=0}^{N-2} \left[\frac{1-E}{1-Z}\right]^{\ell} {}_2F_1(-\ell,\ 1-N;1;Z) , \qquad (B\text{-}27a)$$

where

$$Z = EC \qquad (B\text{-}27b)$$

$$R = E\left[\frac{(1-C)}{(1-Z)}\right]^N \qquad (B\text{-}27c)$$

${}_2F_1$ is the hypergeometric function.

The hypergeometric function is, in general, an infinite series; however, for negative integers, it is given by equation (15.4.1) of Abramowitz and Stegun (1964) as

$${}_2F_1(-\ell,1-N;1;Z) = \sum_{k=0}^{\ell} T_k , \qquad (B\text{-}28a)$$

where

$$T_k = \frac{(-\ell)_k (1-N)_k z^k}{(1)_k k!} \quad . \qquad \text{(B-28b)}$$

Pochhammer's Symbol $(z)_k$ (p. 256 of Abramowitz and Stegun (1964))

$$(z)_k = \frac{\Gamma(z+k)}{\Gamma(z)} \quad , \qquad \text{(B-28c)}$$

and where the Gamma function is given by Hankel's Contour integral (p. 255 of Abramowitz and Stegun (1964)) as

$$\Gamma(z) = \left[\frac{j}{2\pi}\oint(-t)^{-z}e^{-t}dt\right]^{-1}, \quad |z|<\infty \; . \qquad \text{(B-28d)}$$

The path of integration starts at $+\infty$ on the real axis, circles the origin in the counterclockwise direction, and returns to the starting point. However, (B-27) can be computed without resort to complex integration methods (even when the real part of z=0) by noting for k an integer that Pochhammer's Symbol,

$$(z)_k = \begin{cases} z(z+1)(z+2)\ldots(z+k-1) \; , & k>0 \\ 1 & k=0 \; , \end{cases} \qquad \text{(B-29)}$$

is the product of k incrementally increasing terms. Now in (B-28b) when $Z=EC\neq 0$, the first term $T_0=1$ and the ratio of the k-th to the (k-1)-st term is

$$\frac{T_k}{T_{k-1}} = \frac{(k-1-\ell)(k-1+1-N)z}{k^2} \quad . \qquad \text{(B-30)}$$

Now each term in the sum can be computed from the previous term in a simple fashion. Indeed, the actual

computations can be implemented in BASIC on the Hewlett-Packard 9830A desk top calculator in less than 30 lines of code, Figure B-9. For models of the form

$$x(t) = s(t)+n_1(t) \qquad \text{(B-31a)}$$

$$y(t) = s(t+D)+n_2(t) \ , \qquad \text{(B-31b)}$$

where $s(t)$, $n_1(t)$, and $n_2(t)$ are mutually uncorrelated, and when $G_{n_1n_1}(f)=G_{n_2n_2}(f)=G_{nn}(f)$, the SNR is

$$\frac{G_{ss}(f)}{G_{nn}(f)} = \frac{\sqrt{C_{xy}(f)}}{1-\sqrt{C_{xy}(f)}} \ . \qquad \text{(B-32)}$$

More generally, if

$$x(t) = z_1(t)+n_1(t) \qquad \text{(B-33a)}$$

$$y(t) = z_2(t)+n_2(t) \ , \qquad \text{(B-33b)}$$

where $z_i(t)$ is the output of a linear filter $H_i(f)$ excited by $s(t)$, $i=1, 2$ and the noises are mutually uncorrelated and uncorrelated with the signal, then it can be shown that (2-86)

$$C_{xy}(f)=C_{sx}(f)C_{sy}(f) \ ; \qquad \text{(B-34)}$$

that is, the coherence between two receivers is the product of the coherence between the source and each of the individual receivers for the model (B-33). Substituting for the model in (B-33) results in

$$\frac{G_{z_1z_1}(f)}{G_{n_1n_1}(f)} \cdot \frac{G_{z_2z_2}(f)}{G_{n_2n_2}(f)} = \frac{C_{xy}(f)}{\left[1-C_{sx}(f)\right]\left[1-C_{sy}(f)\right]} \qquad \text{(B-35)}$$

Now <u>if</u> $C_{sx}(f)=C_{sy}(f)=\left[C_{xy}(f)\right]^{1/2}$, then it follows

```
10   N=8
20   N1=N-1
30   N2=N-2
40   A=1-N
50   C=0.25
60   PRINT "THIS RUN IS FOR N="N" AND MSC="C
70   FOR F1=0.04 TO 1 STEP 0.04
80   E=1-EXP(LOG(F1)/N1)
90   Z=E*C
100  C4=(1-E)/(1-Z)
110  C2=E*((1-C)/(1-Z))↑N
120  S=0
130  FOR L=0 TO N2
140  C3=C4↑L
150  T=1
160  F=1
170  IF (L=0) THEN 230
180  FOR K=1 TO L
190  K1=K-1
200  T=T*(A+K1)*(K1-L)*Z/(K*K)
210  F=F+T
220  NEXT K
230  S=S+C3*F
240  NEXT L
250  P=C2*S
260  FIXED 3
270  PRINT E;F1;P,1-P
280  NEXT F1
290  END
```

Figure B-9 Computer Program to Compute ROC Tables

that SNR is

$$\left[\frac{G_{z_1z_1}(f)G_{z_2z_2}(f)}{G_{n_1n_1}(f)G_{n_2n_2}(f)}\right]^{1/2} = \frac{\sqrt{C_{xy}(f)}}{1-\sqrt{C_{xy}(f)}} \quad . \qquad \text{(B-36)}$$

Hence, for models of the form of (B-31) or (B-33) if we want to look at the 0 dB (or equal SNR case), we must select

$$10 \log_{10}\left[\frac{\sqrt{C}}{1-\sqrt{C}}\right] = 0 \quad , \qquad \text{(B-37)}$$

which implies C=0.25. Now suppose we average for only N=8 independent data segments. Then for P_F=0.04(0.04)1.00, the thresholds, P_F, cdf and P_D are given in Table B-2. If a sufficient amount of stationary data exists, effective performance can be improved by increasing N; if not, N can only be increased at the expense of degrading the frequency resolution with its inherent difficulties. For many problems, N=8 will be too small and P_F=0.04 will be too large or the performance will be desired for a different value (or family of values) of C. Example plots are given in Figures B-10 and B-11; more extensive results can be obtained by modifying the program, Figure B-9.

Table B-2. Threshold, P_F, cdf, and P_D for N=8 and C=0.25

THIS RUN IS FOR N=8 AND MSC=0.25

0.369	0.040	0.606	0.394
0.393	0.080	0.473	0.527
0.261	0.120	0.389	0.611
0.230	0.160	0.327	0.673
0.205	0.200	0.279	0.721
0.184	0.240	0.240	0.760
0.166	0.280	0.208	0.792
0.150	0.320	0.181	0.819
0.136	0.360	0.157	0.843
0.123	0.400	0.137	0.863
0.111	0.440	0.119	0.881
0.100	0.480	0.104	0.896
0.089	0.520	0.090	0.910
0.079	0.560	0.078	0.922
0.070	0.600	0.066	0.934
0.062	0.640	0.057	0.943
0.054	0.680	0.048	0.952
0.046	0.720	0.039	0.961
0.038	0.760	0.032	0.968
0.031	0.800	0.025	0.975
0.025	0.840	0.019	0.981
0.018	0.880	0.014	0.986
0.012	0.920	0.009	0.991
0.006	0.960	0.004	0.996
0.000	1.000	0.000	1.000

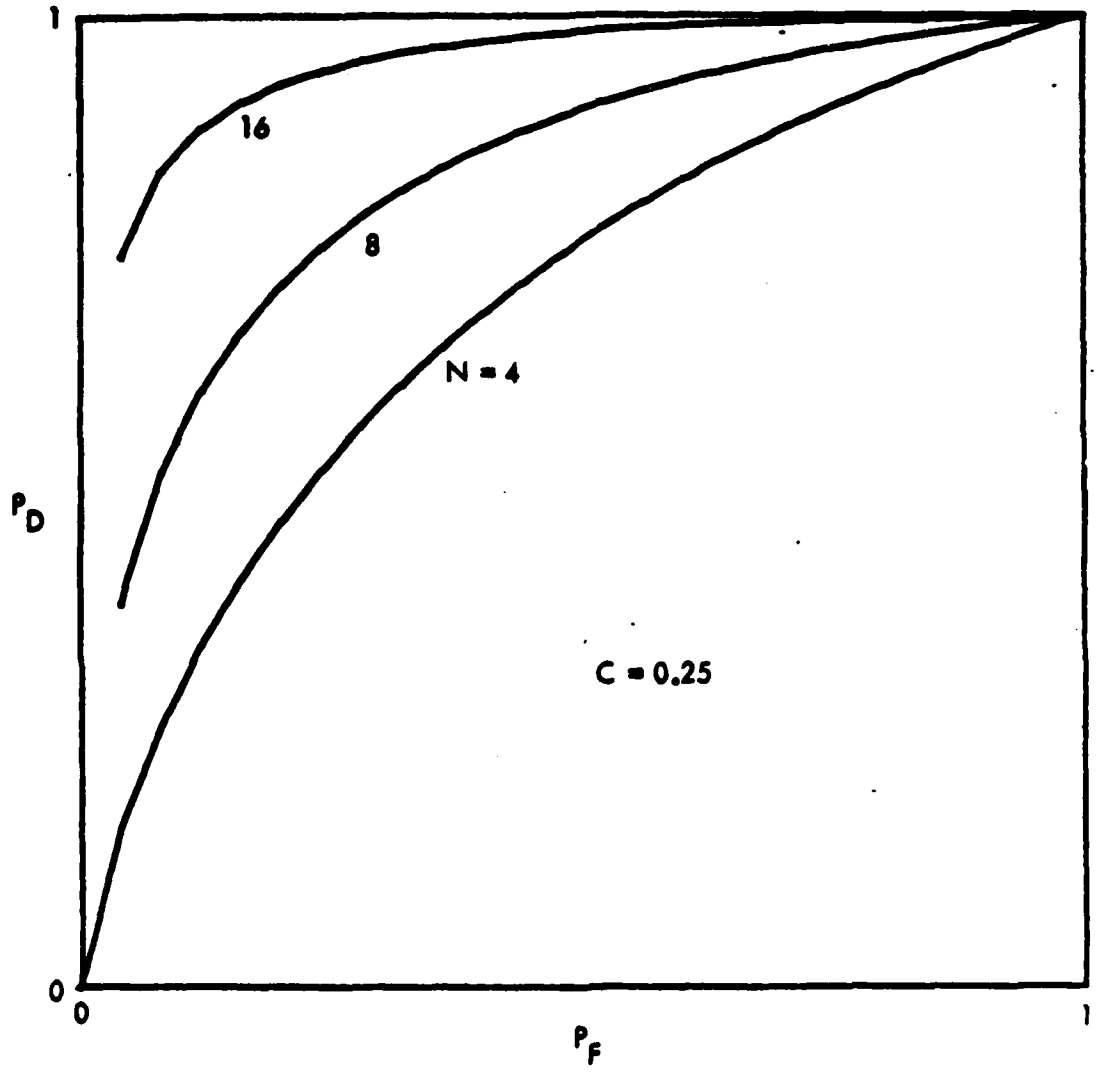

Figure B-10 ROC Curves for C=0.25; N=4. 8. 16

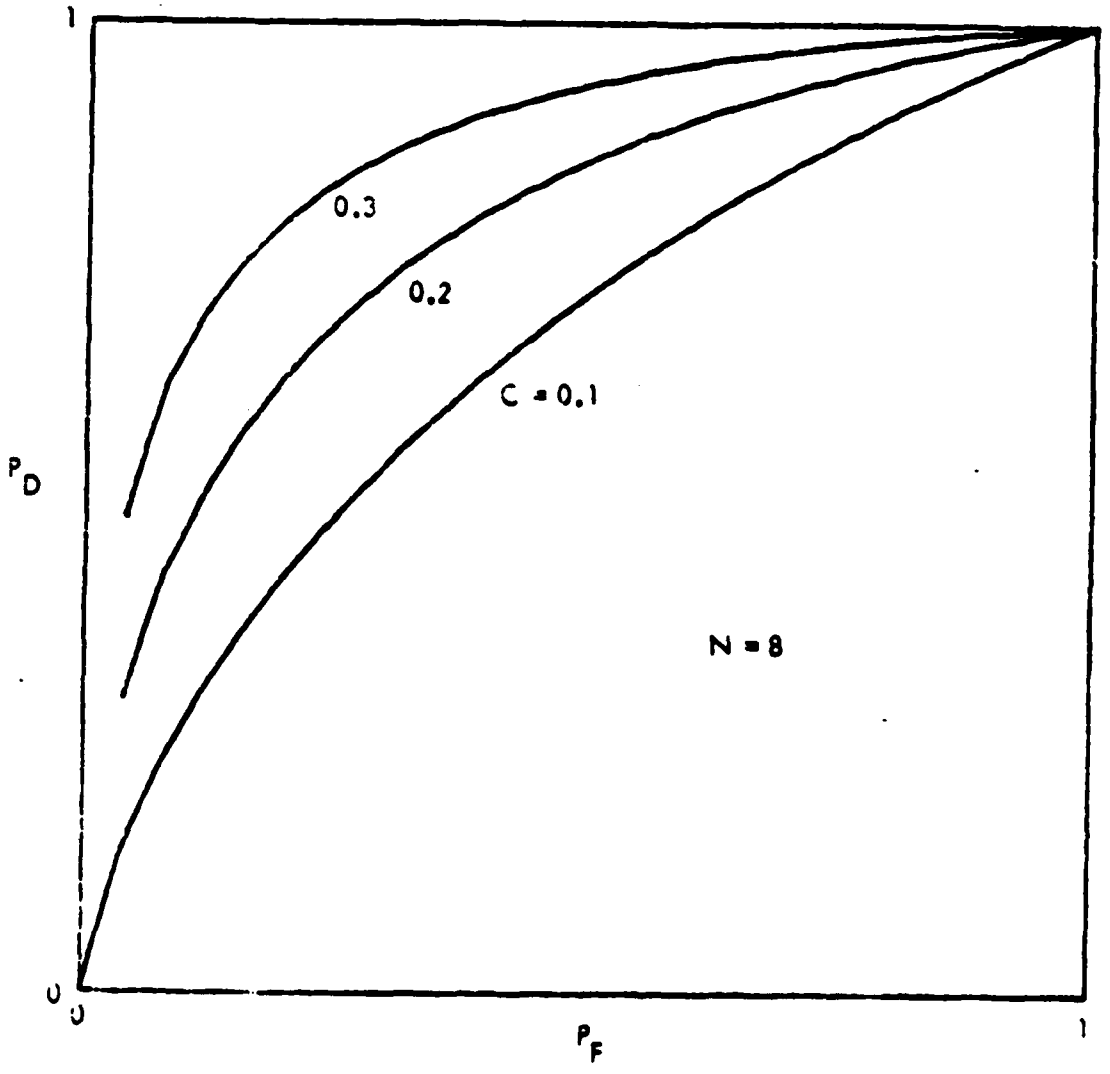

Figure B-11 ROC Curves for N=8; C=0.1, 0.2, 0.3

APPENDIX C

COMPUTER PROGRAM FOR SPECTRAL AND TIME DELAY ESTIMATION

This appendix is divided into two sections. The first section is a brief program description. The second section is a complete listing of the main program and subroutines necessary for program execution.

C1. Program Description

The main program estimates the auto and cross spectral density functions. These spectral estimates are used by the subroutine PRCES to estimate six different AML estimates for time delay (See Table 4-1 of the main text.) Facilities with spectral estimation programs can simply augment their computations with a call to PRCES. Facilities without spectral estimation algorithms will be able to use the programs listed in Section 2 of this appendix. The programs listed are intended to be general FORTRAN IV programs; they have been compiled and executed on the Univac 1108, the Control Data Corporation (CDC) 6600 and International Business Machine (IBM) 360. The spectral estimation programs have been used for research projects by: Williams (1971), Carter (1972a) and (1972b), Brady (1973), Carter, Knapp, and Nuttall (1973a), Carter, Nuttall, and Cable (1973), Santopietro (1973), Carter and Knapp (1975), and Appendix D

of this dissertation. These research projects were conducted entirely on the Univac 1108 and a significant program rewrite was undertaken to make the programs more transferable from one computer system to another.[1] The programs as a complete data processing system consist of input, computations and display. We have concentrated our rewrite efforts on the computations; both the input and display programs are expected to contain peculiarities of the particular computer being used. The input and display subroutines are modular so that only a minimum rewrite is required to transfer the program to another installation. The function of the input subroutine LOAD is to load the XX and YY arrays with NNN data points. If the data were stored on logical magnetic tape number 6 in binary format the call to LOAD could be replaced by the FORTRAN statement

"READ 6, XX(I), YY(I), I=1, NNN".

The subroutine LOAD listed in Section 2 is used to generate synthetic data for a suitable test case (though not the example for Appendix D). The display subroutine DPLOT is called either: (1) to initialize the plotter, (2) to plot the specified array, or (3) to terminate plotting. The subroutine listed in Section 2 is written for the Stromberg Carlson 4060 plot system. It must be rewritten for other systems. If a facility

---

[1]The programs originally written and documented by C.R.Arnold, G.C.Carter, and J.F.Ferrie, have been rewritten and tested by J.C.Sikorski,G.C.Carter and Dr. R.G.Williams.

has no plotting system, the subroutine should simply be a subroutine which returns; alternatively, the subroutine could print the XX array for I=ISTRT to ISTOP. Thus, for use at a new site, two subroutines (LOAD and DPLOT) need to be rewritten.

The main program also calls (in addition to DPLOT and LOAD): HICMP, FFT, LIST, LIST2, PRCES, and LREMV. The subroutine LREMV computes (and optionally removes) the linear trend and dc for the input time waveforms. These computations are performed for every time segment and are printed out by the main program as an aid to detecting nonstationarities or digitizing errors. The subroutines LIST and LIST2 are used to print out (list) results. The subroutine FFT computes the FFT (see, for example, Cooley-Tukey (1965)); coded and listed by Singleton (1969). Singleton's mixed radix algorithm has been shown by Ferrie and Nuttall (1971) to be significantly faster (though less accurate) than other proposed FFTs. Singleton's 600 line FORTRAN subroutine can be replaced with shorter programs (see, for example, p. 332 of Oppenheim and Schafer (1975)). Because of the availability of Singleton's listing in the literature, the FFT is not listed here. Note that the subroutine PRCES and the main program presume that the FFT output array is subscribed from 1 to NPFFT and <u>not</u> from 0 to (NPFFT-1). The subroutine PRCES implements the six AML processors given in Table 4-1. The subroutine PRCES calls on the

subroutines FFT and DPLOT (already discussed). Singleton's subroutine performs a mixed radix FFT; that is, the number of data points do not need to be integer powers of 2 such as 512, 1024, 2048 and 4096 but can have factors of 2's, 3's, and 5's, such as 1000, 1500, 2000 and 3000. Numbers which can be factored into 2's, 3's, and 5's only are called highly composite. Given the FORTRAN variable NNN, the subroutine HICMP finds the highly composite number closest to (but greater than or equal to) NNN. The output of HICMP is NEWNNN. For some applications, the program user will want NEWNNN to be twice as large as NNN; this is because the main program fills the data arrays with zero from NNN + 1 to NEWNNN. Such zero filling is (theoretically) required to inhibit the effect of circular convolution; in practice, though, (with stochastic data) zero filling does not warrant the added (doubled) computational cost. If it is desired, zero filling can simply be achieved by adding one line to HICMP: "NEWNNN = 2*NEWNNN".

In addition to calling several critical subroutines, the main program performs computations necessary to estimate the spectral characteristics of the two waveforms under investigation. The computations performed are briefly outlined in four major steps in appendix A. When the two input waveforms are complex, one FFT of each waveform segment is required as specified in

Appendix A. However, in most (though not all) practical data collection facilities, the input waveforms are real (not complex). When x(t) and y(t) are real, one FFT of the complex waveform x(t) + jy(t) can be computed and quickly be manipulated to form the FFT of x(t) and the FFT of y(t). (See p. 333-334 of Oppenheim and Schafer (1975); see also p. 271-293 of Rabiner and Rader (1972).) These observations, combined with (A-3) give rise to the FORTRAN statements used to estimate the spectral characteristics of x(t) and y(t). The application of this theory reduces the computation time for two real waveforms by a factor of two. The final comment necessary before presenting the computer listings is to describe the input FORTRAN variables. NNN is the number of data points per segment. ISR is the integer sampling rate (Hz). NDSJP is the number of disjoint segments in the total time waveform. SFX and SFY are scale factors used to adjust the (voltage) level of the input waveform to correct for frequency independent attenuations in the data collection and digitizing process. (When no correction is desired, the user sets SFX=SFY=1.0.) When the user desires the spectral estimates to appear 3 dB higher, he sets SFX=SFY=2.0.) With these five sample inputs, the input time data are processed. The next section gives a complete program and subroutine listing.

C2. Program and Subprogram Listings

```
      C     FFT SPECTRUM ANALYSIS PROGRAM
      C
      C           SPECIFICATION AND TYPE STATEMENTS
      C
            DIMENSION XX(4098), YY(4098)
            DIMENSION GXX(2051), GYY(2051), GXYRE(2051), GXYIM(2051)
            DIMENSION WEGHT(4099), SCRCH(4099)
            EQUIVALENCE (WEGHT(1),SCRCH(1))
            DIMENSION PHI(4097)
      C
      C           SET INITIAL VALUES
      C
            IPRTR=4
            CALL DPLOT (XX,0,0,1)
      C
      C           READ INPUT CONTROL PARAMETERS FROM COMPUTER DATA CARD
      C
            READ 100, NNN,ISR,NDSJP,SFX,SFY
      C     NNN IS THE NUMBER OF DATA POINTS PER SEGMENT
      C     ISR IS THE SAMPLING RATE
      C     NDSJP IS THE NUMBER OF DISJOINT SEGMENTS
      C     SFX AND SFY ARE SCALE FACTORS FOR THE INPUT DATA
        100 FORMAT (3I5,2F10.5)
            NFFTS=NDSJP
      C
      C           PRINT INPUT CONTROL PARAMETERS
      C
            WRITE (IPRTR,105) NNN,ISR,NDSJP,SFX,SFY
        105 FORMAT (/1X,3I10,2E20.8/)
```

```
      C
      C            CALCULATE CONSTANTS
      C
           IF (NNN.GT.0.AND.NNN.LE.4096) GO TO 115
           WRITE (IPRTR,110)
  110 FORMAT (10X,'NNN ERROR')
           STOP
  115 CONTINUE
           VARX=0.0
           VARY=0.0
           DT=1.0/FLOAT(ISR)
           SF=SQRT(ABS(SFX*SFY))
      C
      C            PRINT OUT USER INFORMATION
      C
           IF (NFFTS.EQ.NOSUP) WRITE (IPRTR,120)
  120 FORMAT (//10X,'THE FOLLOWING DATA WAS NOT RUN WITH 50 PERCENT OVER
     1LAP')
           TIME=FLOAT(NOSUP*NNN)*DT
           WRITE (IPRTR,125) NOSUP,TIME
  125 FORMAT (18X,'THE',I4,' DISJOINT PIECES COMPRISE',F8.2,' SECONDS OF
     1 DATA')
      C
      C            COMPUTE NEW COMPOSITE NUMBER NNN AND INCREASE ARRAYS
      C
           CALL HICMP (NNN,NPFFT)
           IF (NPFFT.GT.4096) STOP
           WRITE (IPRTR,130) NPFFT
  130 FORMAT (18X,'NUMBER OF POINT FFT =',I5/)
```

```
      C
      C            CALCULATE CONSTANTS
      C
            NP2=NPFFT+2
            ND2=NPFFT/2
            ND2P1=ND2+1
            ND2M1=ND2-1
            DF=1.0/(DT*FLOAT(NPFFT))
            FNYQ=FLOAT(ISR)/2.0
            CONST=0.25*DT/FLOAT(NNN)
            FLOW=0.0
            FHIGH=FNYQ
            ISTRT=IFIX(FLOW/DF)+1
            ISTOP=IFIX(FHIGH/DF)+1
      C
      C            COMPUTE AND SAVE WEIGHTING FUNCTION
      C
            TPI=8.0*ATAN(1.0)
            TEMP=TPI/FLOAT(NNN)
            DO 135 I=1,NNN
            WEGHT(I)=0.81649658*(1.0-COS(TEMP*FLOAT(I-1)))
        135 CONTINUE
      C
      C            STORE ZEROS IN THE SUMMING ARRAYS
      C
            DO 140 K=1,ND2P1
            GXX(K)=0.0
            GYY(K)=0.0
            GXYRE(K)=0.0
            GXYIM(K)=0.0
        140 CONTINUE
```

```
      C
      C        COMPUTE AND SUM N FFT ESTIMATES
      C
           DO 145 KOUNT=1,NFFTS
      C
           DO 145 I=1,NPFFT
           XX(I)=0.0
  145      YY(I)=0.0
      C
      C             LOAD XX AND YY ARRAYS WITH NNN DATA POINTS
      C
           CALL LOAD (XX,YY,PHI,NNN,KOUNT,ISR)
      C
      C             PRINT OF FIRST 150 INPUT VALUES
      C
           IF (KOUNT.NE.1) GO TO 170
           WRITE (IPRTR,150)
  150      FORMAT (1H1,9X,'PRINTOUT OF FIRST 150 VALUES OF INPUT DATA',///)
           DO 160 I=1,50
           J=I+50
           K=I+100
           PRINT 155, (I,XX(I),YY(I),J,XX(J),YY(J),K,XX(K),YY(K))
  155      FORMAT (3(I7,1X,2F15.8,5X))
  160      CONTINUE
           WRITE (IPRTR,165)
  165      FORMAT (/1H1)
  170      CONTINUE
```

```
      C
      C           REMOVE THE LINEAR TREND AND COMPUTE THE VARIANCE
      C
            IS3=0
            CALL LREMV (XX,NNN,IS3,DX,SX)
            CALL LREMV (YY,NNN,IS3,DY,SY)
            VARXI=0.0
            VARYI=0.0
            DO 175 I=1,NNN
            VARXI=VARXI+XX(I)*XX(I)
        175 VARYI=VARYI+YY(I)*YY(I)
            VARXI=VARXI/FLOAT(NNN-1)
            VARYI=VARYI/FLOAT(NNN-1)
            WRITE (IPRTR,180) KOUNT,DX,DY,SX,SY,VARXI,VARYI,IS3
        180 FORMAT (5X,I5,' DX=',E12.6,' DY=',E12.6,' SX=',E12.6,' SY=',E12.6,'
           1 VX=',E12.6,' VY=',E12.6,I5)
            VARX=VARX+VARXI
            VARY=VARY+VARYI
      C
      C           WEIGHT THE INPUT DATA WITH COSINE WINDOW
      C
            DO 185 I=1,NNN
            XX(I)=XX(I)*WEGHT(I)
            YY(I)=YY(I)*WEGHT(I)
        185 CONTINUE
      C
      C           COMPUTE FAST FOURIER TRANSFORM
      C
            CALL FFT (XX,YY,NPFFT,MPFFT,MPFFT,-1)
```

```
      C
      C            COMPUTE SPECTRA
      C
           GXX(1)=GXX(1)+4.0*XX(1)**2
           DO 190 K=2,NU2P1
           J=NP2-K
           GXX(K)=GXX(K)+(XX(K)+XX(J))**2+(YY(K)-YY(J))**2
           GYY(K)=GYY(K)+(YY(K)+YY(J))**2+(XX(J)-XX(K))**2
           GXYRE(K)=GXYRE(K)+XX(K)*YY(J)+XX(J)*YY(K)
           GXYIM(K)=GXYIM(K)+XX(J)**2+YY(J)**2-XX(K)**2-YY(K)**2
     190 CONTINUE
           GYY(1)=GYY(1)+4.0*YY(1)**2
           GXYRE(1)=GXYRE(1)+2.0*(XX(1)*YY(1))
           GXYIM(1)=0.0
      C
      C        GO BACK FOR NEXT SEGMENT
      C
     195 CONTINUE
      C
      C            NORMALIZE ESTIMATES
      C
           FNSG=FLOAT(NFFTS)
           OFNSG=1.0/FNSG
           VARX=VARX*OFNSG
           CONST=CONST*OFNSG
           CNSTC=2.0*CONST
           DO 200 K=1,NU2P1
           GXX(K)=GXX(K)*CONST*SFX
           GYY(K)=GYY(K)*CONST*SFY
           GXYRE(K)=GXYRE(K)*CNSTC*SF
           GXYIM(K)=GXYIM(K)*CONST*SF
           SCRCH(K)=DF*FLOAT(K-1)
     200 CONTINUE
           VARY=VARY*OFNSG
```

```
C
C            PRINT OUT VARIANCES
C
      WRITE (IPRTR,205) VARX,VARY
  205 FORMAT (/10X,'AVERAGE VARIANCES ARE, VX=',E12.6,' VY=',E12.6//)
      VARX=0.0
      VARY=0.0
      DO 210 K=1,ND2P1
      VARX=VARX+GXX(K)
      VARY=VARY+GYY(K)
  210 CONTINUE
      VARX=VARX*DF*2.0/SFX
      VARY=VARY*DF*2.0/SFY
      WRITE (IPRTR,215) VARX,VARY
  215 FORMAT (/10X,'INTEGRATED VARIANCES ARE, VX=',E12.6,' VY=',E12.6//)
C
C            CONVERT GXX  TO DB AND PLOT
C
      DO 220 I=1,ND2P1
      XX(I)=GXX(I)
      PHI(I)=10.0*ALOG10(MAX(GXX(I),1.0E-30))
  220 CONTINUE
      CALL DPLOT (PHI,ISTRT,ISTOP,2)
      WRITE (IPRTR,225)
  225 FORMAT (1H1,/10X,'DUMP OF XX PSD')
      CALL LIST (PHI,SCRCH,ISTRT,ISTOP,IPRTR)
```

```
C
C            COMPUTE AND DISPLAY AUTOCORRELATION FUNCTION OF INPUT SIGNAL
C
      DO 230 I=1,NPFFT
      YY(I)=0.0
  230 CONTINUE
      DO 235 K=2,NU2P1
      J=NP2-K
      XX(J)=XX(K)
  235 CONTINUE
      CALL FFT (XX,YY,NPFFT,NPFFT,NPFFT,+1)
      RO=XX(1)*DF
      WRITE (IPRTR,240) RO
  240 FORMAT (//9X,'RO FOR INPUT SIGNAL XX =',E15.8,//)
      ONERO=1.0/XX(1)
      DO 245 I=1,NU2P1
      XX(I)=XX(I)*ONERO
  245 CONTINUE
      XMIN=0.0
      CALL DPLOT (XX,1,NU2P1,2)
      WRITE (IPRTR,250)
  250 FORMAT (1H1,10X,'DUMP OF X DATA AUTO CORRELATION')
      CALL LIS12 (XX,XMIN,1,NU2P1,IPRTR,DT)
C
C            CONVERT GYY  TO DB AND PLOT
C
      DO 255 I=1,NU2P1
      XX(I)=GYY(I)
      PHI(I)=10.0*ALOG10(MAX(GYY(I),1.0E-30))
  255 CONTINUE
      CALL DPLOT (PHI,ISTRT,ISTOP,2)
      WRITE (IPRTR,260)
  260 FORMAT (1H1,/10X,'DUMP OF YY PSD')
      CALL LIS1 (PHI,SCRCH,ISTRT,ISTOP,IPRTR)
```

```
240       C
241       C          COMPUTE AND DISPLAY AUTOCORRELATION FUNCTION OF INPUT SIGNAL
242       C
243             DO 265 I=1,NPFFT
244             YY(I)=0.0
245         265 CONTINUE
246             DO 270 K=2,ND2P1
247             J=NP2-K
248             XX(J)=XX(K)
249         270 CONTINUE
250             CALL FFT (XX,YY,NPFFT,NPFFT,NPFFT,+1)
251             RO=XX(1)*DF
252             WRITE (IPRTR,275) RO
253         275 FORMAT (//9X,'RO FOR INPUT SIGNAL YY =',E15.8,//)
254             ONURO=1.0/XX(1)
255             DO 280 I=1,ND2P1
256             XX(I)=XX(I)*ONURO
257         280 CONTINUE
258             CALL OPLOT (XX,1,ND2P1,2)
259             WRITE (IPRTR,285)
260         285 FORMAT (1H1,10X,'DUMP OF Y DATA AUTO CORRELATION')
261             CALL LIST2 (XX,XMIN,1,ND2P1,IPRTR,DT)
262       C
263       C          COMPUTE AND DISPLAY PHASE FROM AVERAGED GAYME AND GAYIM SPEC
264       C
265             DO 305 K=1,ND2P1
266             AXK=GXYRE(K)
267             IF (AXK) 300,290,300
268         290 IF (GXYIM(K)) 300,295,300
269         295 AXK=1.0
270         300 PHI(K)=57.29577951*ATAN2(GXYIM(K),AXK)
271         305 CONTINUE
```

```
C
C           PLOT PHASE FROM -PHLIM TO PHLIM
C
      PHLIM=1800.0
      XX(1)=0.0
      DO 310 K=2,ND2P1
      XX(K)=UF*FLOAT(K-1)
      X=PHI(K)-PHI(K-1)
      PHI(K)=PHI(K)-SIGN(360.,X)*AINT(0.5+ABS(X)/360.0)
      IF (PHI(K).GT.PHLIM) PHI(K)=PHI(K)-PHLIM
      IF (PHI(K).LT.-PHLIM) PHI(K)=PHI(K)+PHLIM
  310 CONTINUE
      CALL DPLOT (PHI,ISTRT,ISTOP,2)
      WRITE (IPRTR,315)
  315 FORMAT (1H1,10X,'DUMP OF CONTINUOUS PHASE VALUES')
      CALL LIST (PHI,SCRCH,ISTRT,ISTOP,IPRTR)
C
C           COMPUTE CROSS SPECTRUM AND SQUARED COHERENCY
C
      DO 320 K=1,ND2P1
      PHI(K)=GXYRE(K)**2+GXYIM(K)**2
      XX(K)=PHI(K)/(GXX(K)*GYY(K))
  320 CONTINUE
      CALL DPLOT (XX,1,ND2P1,2)
      WRITE (IPRTR,325)
  325 FORMAT (1H1,10X,'DUMP OF THE SQUARED COHERENCE')
      CALL LIST (XX,SCRCH,ISTRT,ISTOP,IPRTR)
```

```
C
C            CONVERT GXY TO DB AND PLOT
C
      DO 330 I=1,ND2P1
      PHI(I)=5.0*ALOG10(MAX(PHI(I),1.0E-30))
  330 CONTINUE
      CALL DPLOT (PHI,ISTRT,ISTOP,2)
      WRITE (IPRTR,335)
  335 FORMAT (1HI,10X,'DUMP OF THE CROSS SPECTRUM')
      CALL LIST (PHI,SCRCH,ISTRT,ISTOP,IPRTR)
C
C            COMPUTE SIX TIME FUNCTIONS
C
      CALL PRCES (GXX,GYY,GXYRE,GXYIM,NPFFT,XX,YY,IPRTR,DT)
C
C            COMPUTE MODULUS OF TRANSFER FUNCTION IN DB AND PLOT
C
      DO 340 K=1,ND2P1
      TEMP=(GXYRE(K)**2+GXYIM(K)**2)/GXX(K)**2
      PHI(K)=10.0*ALOG10(MAX(TEMP,1.0E-30))
  340 CONTINUE
      WRITE (IPRTR,345)
  345 FORMAT (1HI,10X,'DUMP OF THE TRANSFER FUNCTION')
      CALL LIST (PHI,SCRCH,ISTRT,ISTOP,IPRTR)
      CALL DPLOT (PHI,ISTRT,ISTOP,2)
C
C            TERMINATE PROGRAM
C
      CALL DPLOT (XX,0.0,3)
      STOP
C
      END
```

```
      SUBROUTINE GPLOT (XX,ISTART,ISTOP,INTSW)
C
C********** INTSW=1-INITIALIZE PLOTTER
C                 2-PLOT DATA
C                 3-CLOSE OUT PLOTTER
C
      DIMENSION Z(200), XX(1)
C
      IF (INTSW.EQ.2) GO TO 100
      IF (INTSW.EQ.3) GO TO 115
C
C        INITIALIZE PLOTTER
C
      CALL MODES6 (Z,0)
      GO TO 120
C
  100 CALL SETSM6 (Z,14,11,0)
      CALL SETSM6 (Z,20,8,25)
C
C        DRAW GRIDS
C
      CALL OBJCT6 (Z,0.5,0.5,10.5,7.5)
      CALL SUBJE6 (Z,0.0,0.0,10.0,7.0)
      DX=7.0/7.0
      DY=10.0/10.0
      CALL GRID6 (Z,DX,DY,0.,0.)
C
C        SEARCH FOR MAXIMUM DATA VALUE
C
      TEMP=1.0E-20
      DO 105 I=ISTART,ISTOP
      TEMP=AMAX(ABS(XX(I)),TEMP)
  105 CONTINUE
```

```
34      C
35      C          WRITE MAXIMUM VALUE ON THE PLOTTER
36      C
37            CALL OBJCTG (Z,0.0,0.0,11.0,8.25)
38            CALL SUBJEG (Z,0.0,0.0,11.0,8.25)
39            CALL LEGNDG (Z,1.0,7.75,15,'MAXIMUM VALUE =')
40            CALL NUMBRG (Z,2.5,7.75,-12.5,TEMP)
41      C
42      C          PLOT NORMALIZED DATA
43      C
44            CALL OBJCTG (Z,0.5,0.5,10.5,7.5)
45            CALL SUBJEG (Z,0.0,-1.0,10.0,1.0)
46      C
47            NXIVLS=ISTOP-ISTART
48            DLTAX=10.0/FLOAT(NXIVLS)
49            XCORD=0.0
50            IBEGIN=ISTART+1
51            TEMP2=XX(ISTART)/TEMP
52            CALL LINESG (Z,0,XCORD,TEMP2)
53            DO 110 I=IBEGIN,ISTOP
54            XCORD=XCORD+DLTAX
55            TEMP2=XX(I)/TEMP
56            CALL LINESG (Z,1,XCORD,TEMP2)
57        110 CONTINUE
58            CALL PAUSG (Z,0,1,1)
59      C
60      C          CLOSE OUT PLOTTER
61      C
62        115 IF (INTSW.EQ.3) CALL EXITG (Z)
63        120 CONTINUE
64            RETURN
65      C
66            END
```

```
      SUBROUTINE MICMP (NNN,NEWNN)
C
      DIMENSION NFACT(7)
C
      DATA (NFACT(I),I=1,7) /512,500,128,100,5,3,2/
      NUMBR=7
      NUP=NNN
      IF (NUP.LE.1) NUP=2
C
  100 CONTINUE
      NEWNN=NUP
C
      DO 115 L=1,NUMBR
C
  105 M=MOD(NEWNN,NFACT(L))
      IF (M.NE.0) GO TO 110
      NEWNN=NEWNN/NFACT(L)
      GO TO 105
  110 IF (NEWNN.EQ.1) GO TO 120
C
  115 CONTINUE
C
      NUP=NUP+1
      GO TO 100
C
  120 NEWNN=NUP
      RETURN
C
      END
```

```
      SUBROUTINE LIST (DATA,FREQ,ISTRT,ISTOP,IPRNT)
      DIMENSION DATA(1), FREQ(1)
C
      WRITE (IPRNT,100)
  100 FORMAT (3X,'FREQUENCY')
C
      DO 110 I=ISTRT,ISTOP,10
      J=I+9
      IF (J.GT.ISTOP) J=ISTOP
      WRITE (IPRNT,105) FREQ(I),(DATA(K),K=I,J)
  105 FORMAT (2X,F8.3,10(2X,F10.4))
  110 CONTINUE
C
      RETURN
C
      END
```

```
      SUBROUTINE LIST2 (DATA,XMIN,ISTRT,ISTOP,IPRNT,DT)
C
      DIMENSION DATA(1)
C
      WRITE (IPRNT,100)
  100 FORMAT (5X,'TIME')
C
      TIME=XMIN
C
      DO 110 I=ISTRT,ISTOP,10
      J=I+9
      IF (J.GT.ISTOP) J=ISTOP
      WRITE (IPRNT,105) TIME,(DATA(K),K=I,J)
  105 FORMAT (2X,F8.4,10(2X,F10.4))
      TIME=TIME+(10.0*DT)
  110 CONTINUE
C
      RETURN
C
      END
```

```
      SUBROUTINE LOAD (XA,YY,PHI,NNN,KOUNT,ISR)
C
      DIMENSION XX(1), YY(1), PHI(1)
      DIMENSION PHASE(5), FREQ(5)
C
      DT=1.0/FLOAT(ISR)
      TPI=8.0*ATAN(1.00)
      FREQ(1)=10.0
      FREQ(2)=27.0
      FREQ(3)=43.9
      FREQ(4)=71.8
      FREQ(5)=108.31
      TPID=TPI/10.0
      DO 100 K=1,5
      PHASE(K)=K*TPI/5.0
  100 FREQ(K)=TPI*FREQ(K)
C
      DO 110 I=1,NNN
      TIME=((KOUNT-1)*NNN+I)*DT
      SUM=0.0
      DO 105 K=1,5
  105 SUM=SUM+SIN(FREQ(K)*TIME+PHASE(K))
      XX(I)=SUM
      IF (XX(I).GT.1.0) XX(I)=1.0
      IF (XX(I).LT.-1.0) XX(I)=-1.0
      YY(I)=XA(I)+3.0*XX(I)**2
  110 CONTINUE
C
      RETURN
C
      END
```

```
      SUBROUTINE LREAV (XX,NNN,ISWCH,DC,SLOPE)
C
C           DIMENSION ARRAY AND ESTABLISH CONSTANTS
C
      DIMENSION XX(1)
C
      FLN=FLOAT(NNN)
      DC=0.0
      SLOPE=0.0
C
      DO 100 I=1,NNN
      DC=DC+XX(I)
      SLOPE=SLOPE+XX(I)*FLOAT(I)
  100 CONTINUE
C
C           COMPUTE STATISTICS
C
      DC=DC/FLN
      SLOPE=12.0*SLOPE/(FLN*(FLN*FLN-1.0))-6.0*DC/(FLN-1.0)
```

```
      C
      C           PRINT OUT CHECK OUT INFORMATION
      C
          IF (ISWCH-1) 125,115,105
      C
      C           REMOVE TREND (MEAN AND SLOPE) AND REPOINT REMOVAL
      C
  105 CONTINUE
          FLN=DC-0.5*(FLN+1.0)*SLOPE
          DO 110 I=1,NNN
          XX(I)=XX(I)-FLOAT(I)*SLOPE-FLN
  110 CONTINUE
          GO TO 125
      C
      C           REMOVE THE DC COMPONENT
      C
  115 CONTINUE
          DO 120 I=1,NNN
          XX(I)=XX(I)-DC
  120 CONTINUE
      C
  125 RETURN
      C
          END
```

```
      SUBROUTINE PRCES (GXX,GYY,GXYRE,GXYIM,NPFFT,XX,YY,IFRTN,LT)
C
      DIMENSION GXX(1), GYY(1), GXYRE(1), GXYIM(1), XX(1), YY(1)
      DO 100 NTIME=1,6
C
      NP2=NPFFT+2
      ND2P1=(NPFFT/2)+1
      ND2=NPFFT/2
      ND2M1=ND2-1
      DO 100 K=1,ND2P1
C
      IF (NTIME.EQ.1) TEMP=1.0/SQRT(GXX(K)*GYY(K))
      IF (NTIME.EQ.2) TEMP=1.0/SQRT(GXYRE(K)**2+GXYIM(K)**2)
      IF (NTIME.EQ.3) TEMP=1.0
      IF (NTIME.EQ.4) TEMP=1.0/GXX(K)
      GXYMG=SQRT(GXYRE(K)**2+GXYIM(K)**2)
      COHR2=GXYMG**2/(GXX(K)*GYY(K))
      COHR2=MIN(COHR2,.9999999)
      IF (NTIME.EQ.5) TEMP=COHR2/((1.-COHR2)*GXYMG)
      TEMP1=GXX(K)-GXYMG
      M=1.0
      IF (ABS(TEMP1).LT.0.000C001) TEMP1=0.000001*SIGN(M,TEMP1)
      IF (NTIME.EQ.6) TEMP=GXYMG/(TEMP1**2)
      IF (NTIME.EQ.7) TEMP=1./(TEMP1**2)
      IF (NTIME.EQ.8) TEMP=1./TEMP1
C
      XX(K)=GXYRE(K)*TEMP
      YY(K)=GXYIM(K)*TEMP
C
  100 CONTINUE
C
```

```
      DO 105 K=2,ND2P1
      J=NP2-K
      XX(J)=XX(K)
      YY(J)=-YY(K)
  105 CONTINUE
      YY(ND2P1)=0.0
C
      CALL FFT (XX,YY,NPFFT,NPFFT,NPFFT,1)
C
      TEMP=0.0
      DO 110 K=1,NPFFT
      IF (TEMP.GE.ABS(XX(K))) GO TO 110
      KOFMX=K
      TEMP=ABS(XX(K))
  110 CONTINUE
C
      WRITE (IPRTR,115) NTIME
  115 FORMAT ('1','  RESULTS OF PROCESSOR',I5//)
      WRITE (IPRTR,120) TEMP,KOFMX
  120 FORMAT (' MAX OF',E20.8,' AT DELAY',I5/)
      TEMP=1.0/TEMP
      DO 125 K=1,NPFFT
      XX(K)=XX(K)*TEMP
  125 CONTINUE
      DO 135 K=1,40
      J=NP2-K
      TEMP1=XX(K)*100.0
      TEMP2=XX(J)*100.0
      WRITE (IPRTR,130) NTIME,K,TEMP1,TEMP2
  130 FORMAT (5X,2I10,2F10.4)
  135 CONTINUE
C
```

```
64              DO 140 I=1,ND2P1
65              YY(I+ND2M1)=XX(I)
66          140 CONTINUE
67              DO 145 I=1,ND2M1
68              YY(I)=XX(ND2P1+I)
69          145 CONTINUE
70              NLAG=100
71              ITMP1=ND2-NLAG
72              ITMP2=ND2+NLAG
73              XMIN=-DT*FLOAT(1-NLAG)
74              XMAX=DT*FLOAT(1+NLAG)
75        C
76              IF (NTIME.EQ.1) WRITE (IPRTR,150)
77          150 FORMAT (1H1,10X,'DUMP OF SCOT FUNCTION')
78              IF (NTIME.EQ.2) WRITE (IPRTR,155)
79          155 FORMAT (1H1,10X,'DUMP OF PHAT FUNCTION')
80              IF (NTIME.EQ.3) WRITE (IPRTR,160)
81          160 FORMAT (1H1,10X,'DUMP OF CROSS CORRELATION')
82              IF (NTIME.EQ.4) WRITE (IPRTR,165)
83          165 FORMAT (1H1,10X,'DUMP OF IMPULSE RESPONSE')
84              IF (NTIME.EQ.5) WRITE (IPRTR,170)
85          170 FORMAT (1H1,10X,'DUMP OF H-T(I) FUNCTION')
86              IF (NTIME.EQ.6) WRITE (IPRTR,175)
87          175 FORMAT (1H1,10X,'DUMP OF ECKART FUNCTION')
88              CALL LIST2 (YY,XMIN,ITMP1,ITMP2,IPRTR,DT)
89        C
90              CALL OPLOT (YY,ITMP1,ITMP2,2)
91          180 CONTINUE
92              RETURN
93        C
94              END
```

APPENDIX D

EXAMPLE COMPUTER RUN FOR SPECTRAL AND TIME DELAY ESTIMATION

Theoretical equations have been derived in Chapter 3 for ML estimation of time delay. A computer program to achieve an AML estimate of delay is given in Appendix C. The purpose of this chapter is to describe four example cases which were run to substantiate the theory and validate the computer program. One computer run was made for each of the cases. Only one of the runs will be explicitly reported here. In all of the four cases studied, the true delay was set equal to zero (without loss of generality). Further, the signal attenuation was set equal to unity so that (3-1) becomes

$$x_1(t) = s(t)+n_1(t) \qquad \text{(D-1a)}$$

$$x_2(t) = s(t+D)+n_2(t) \qquad \text{(D-1b)}$$

$$D = 0 \; . \qquad \text{(D-1c)}$$

Our desire is to see whether (and "how well") we can estimate the (assumed unknown) parameter D, given a T second observation of $x_1(t)$ and $x_2(t)$. The variance of the ML processor (as discussed after (3-34)) depends on the particular signal and noise spectral characteristics (in particular, $C_{12}(f)$). Moreover, the variance of the

delay estimate can only be empirically determined by resort to numerous (expensive) computer runs. We have not done that here (but have suggested further work in this area (Chapter 6)). We have, however, made four computer runs for the data cases synthesized by Figure D-1. As shown in the figure, the signal spectrum has two nonzero frequency bands. The bands are 10 Hz wide centered at 5 and 50 Hz. Each of the five filters represented in Figure D-1 is the cascade of two sections, each with a 48 dB/octave roll off. The noise generators generate white noise. Details of the hardware are the same as described on pages 71-72 of Carter (1972a). The actual data generation required less hardware than shown in Figure D-1, but the simulation is easier to visualize by studying Figure D-1 and is closer to what would be done in a real time simulation of the type suggested in Chapter 6. In our experiment, we adjust the SNR by adjusting the gain in Figure D-1.

The digital outputs of the data synthesized are stored on magnetic tape for use by the computer program (Appendix C). Longer observation time is achieved by reading more data from the magnetic tape. In the four example cases, the ML processor output was examined for two different signal levels and two different averaging times T. Expect for absolute SNR level all four example cases had the same signal and the same noise spectral densities. As expected, when the SNR

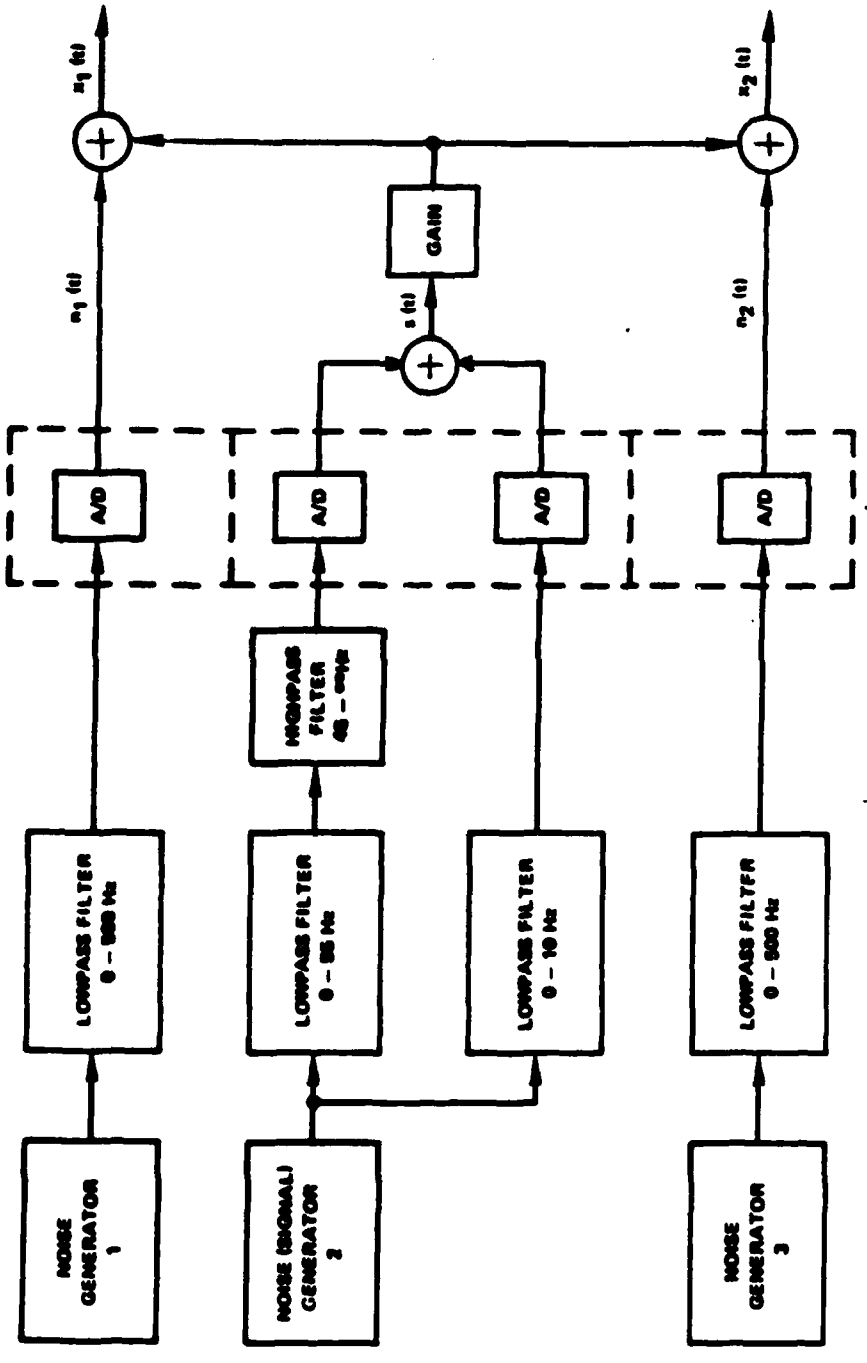

Figure D-1 Data Synthesis for Example Case

was low, more averaging time was required to extract a "good" delay estimate; this behavior is predicted by (3-34). In particular, of our four cases, the low SNR and short averaging case resulted in unusable delay estimates. The reason for this was apparent upon inspecting the coherence estimates used to approximate the true coherence. As predicted in appendix B with short averaging times (that is, small N), we were unable to detect a low coherent source.

This happened to our one trial at low SNR and short averaging; however, by increasing the averaging time, an acceptable time delay estimate was obtained. We were able to increase the averaging time (essentially without bound) since the example cases were using laboratory data.

The case which we will report in detail is the high-coherence, short-averaging case. In particular, the gain in Figure D-1 is adjusted so that $C \cong 0.6$ in the frequency bands with signal power and $C \cong 0$ in the other bands. The characteristics of $x_1(t)$ and $x_2(t)$ were estimated from 8 seconds of data with 16 independent segments (each of 1/2 second duration, that is, 2 Hz resolution). FFTs of 600 samples (1/2 sec times 1200 samples/sec) can be performed using the fast mixed radix FFT of Singleton (1969).

The characteristics of the noise generators in Figure D-1 were essentially identical. Thus, for the

model (D-1), $G_{x_1x_1}(f)=G_{x_2x_2}(f), \forall f$. The estimates of $G_{x_1x_1}(f)$ are depicted in Figure D-2. The estimates of $G_{x_2x_2}(f)$ were extremely similar and are not repeated. The extent to which $x_1(t)$ and $x_2(t)$ are similar is measured by the MSC estimate in Figure D-3. Since the CC and delay D depend upon the phase, the phase estimates are depicted in Figure D-4. The slope of the phase estimates is an important indicator of delay[1] in those frequency bands where the MSC is strong (namely, 0-10 Hz and 45-55 Hz). Using the algorithm discussed in Chapter 3 and the estimation techniques of appendix A implemented in appendix C, we have obtained the delay estimate given in Figure D-5. From Figure D-5 we see that the GCC with ML weighting peaks very close to the true value of delay, namely, D=0. A blowup of Figure D-5 given in Figure D-6 shows that the peak is within 10 msec of the true value. Clearly, the estimation technique proposed is a viable method for estimating time delay.

---

[1]Dimensionally the slope is the phase angle in radians divided by the frequency in radians per sec. Thus the slope of the phase is measured in seconds.

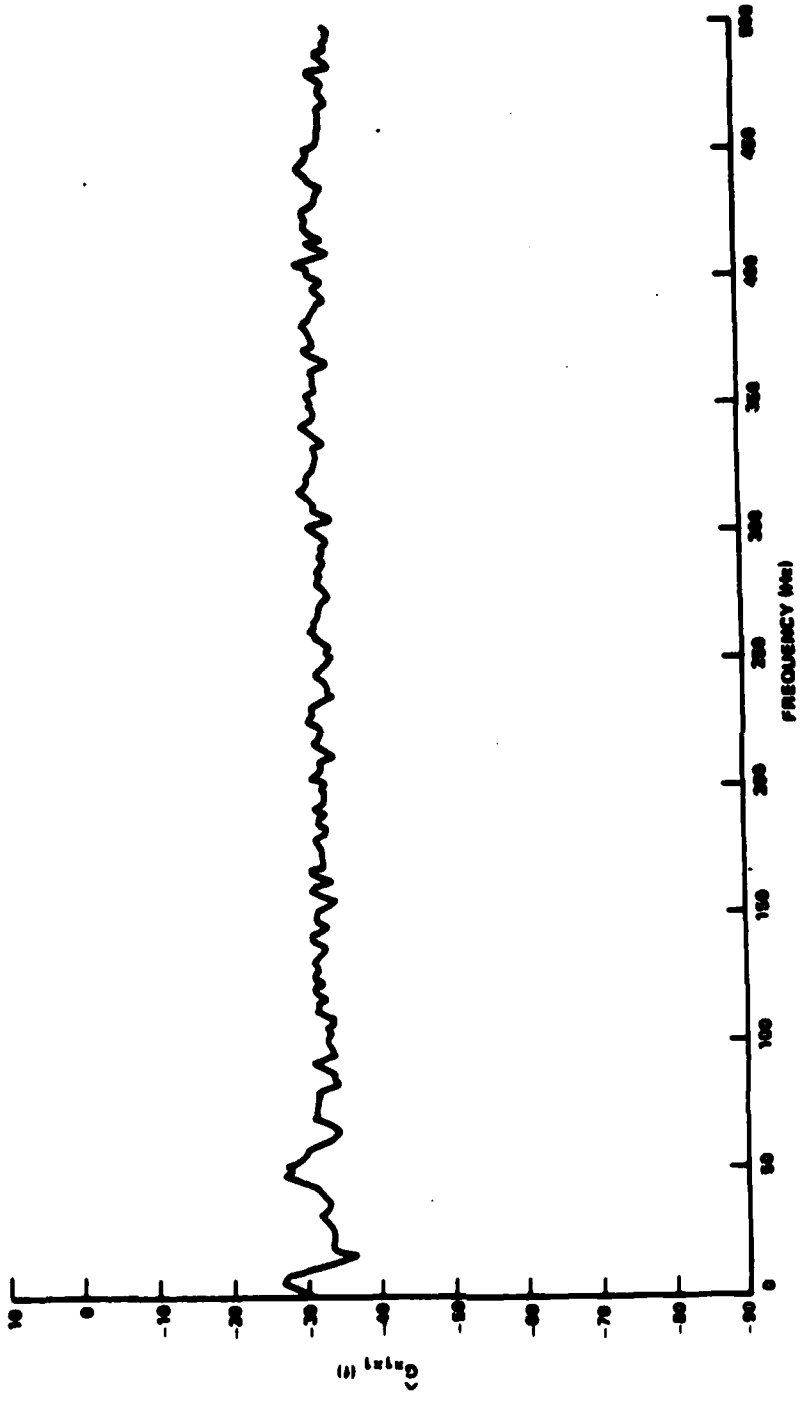

Figure D-2 Estimates of $G_{x_1x_1}(f)$ for Example Case

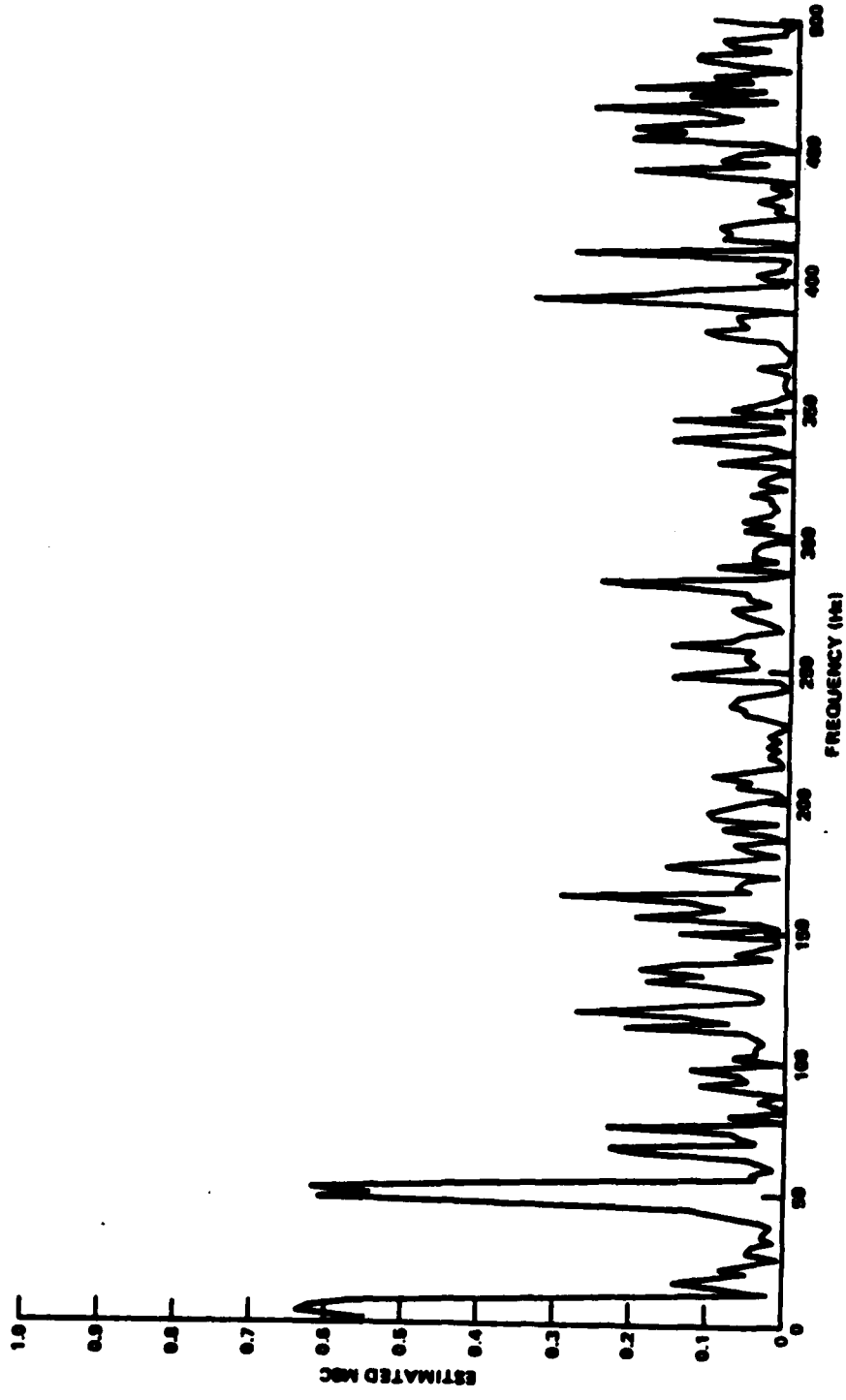

Figure D-3 Estimates of $C_{x_1x_2}(f)$ for Example Case

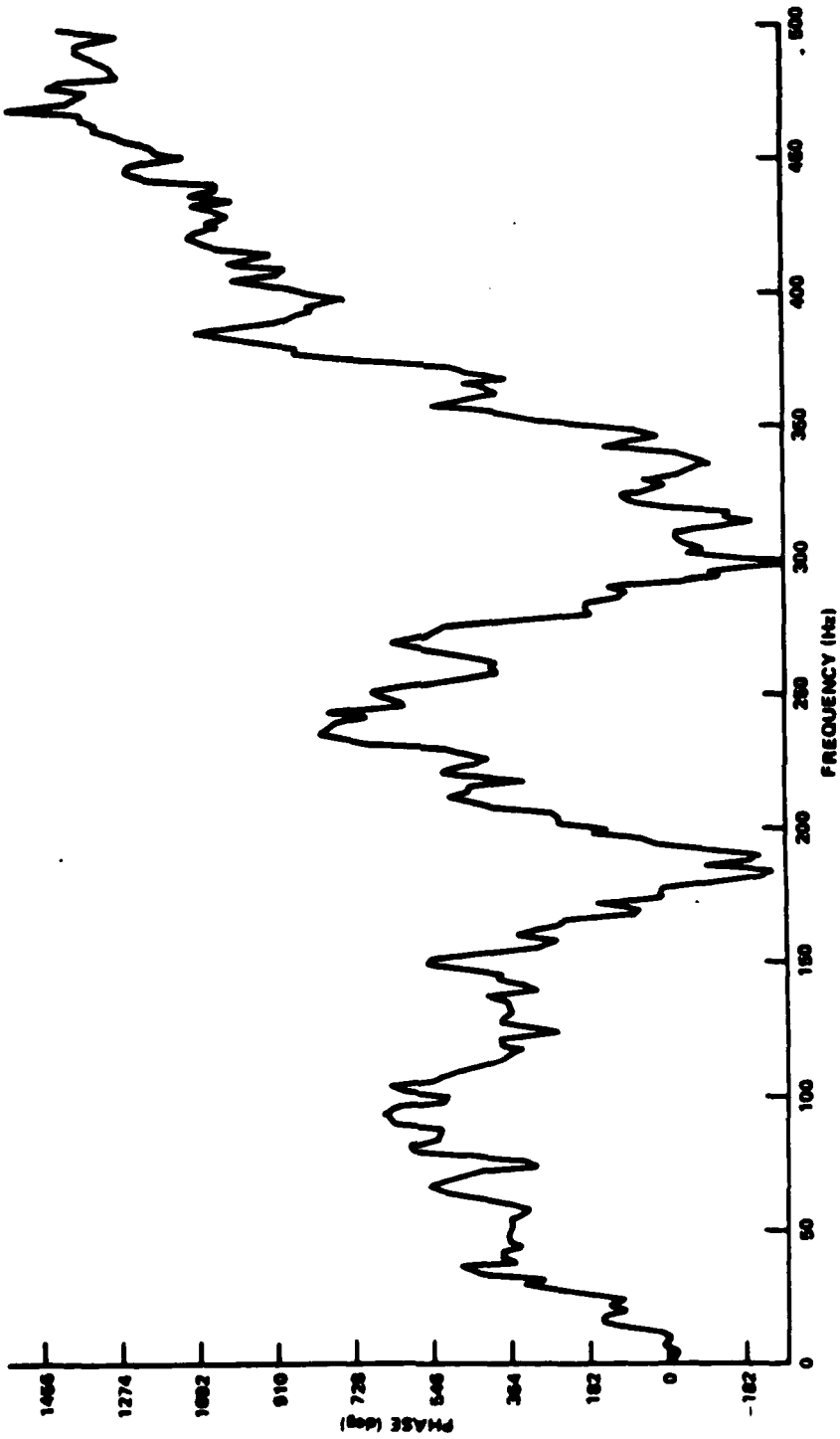

Figure D-4 Estimates of $\phi_{x_1x_2}(f)$ for Example Case

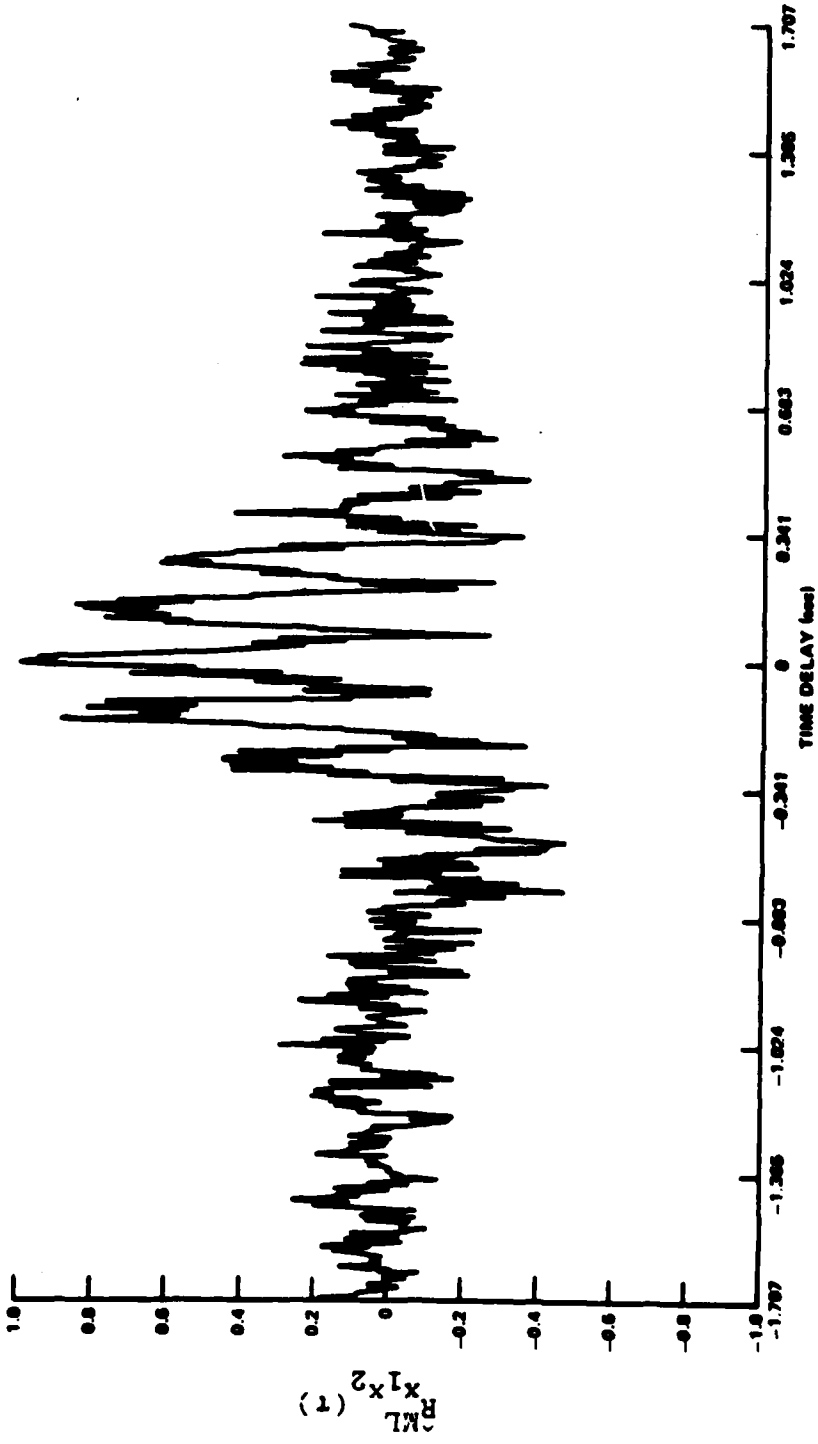

Figure D-5 Estimates of Time Delay Using ML Weighting with GCC Processing

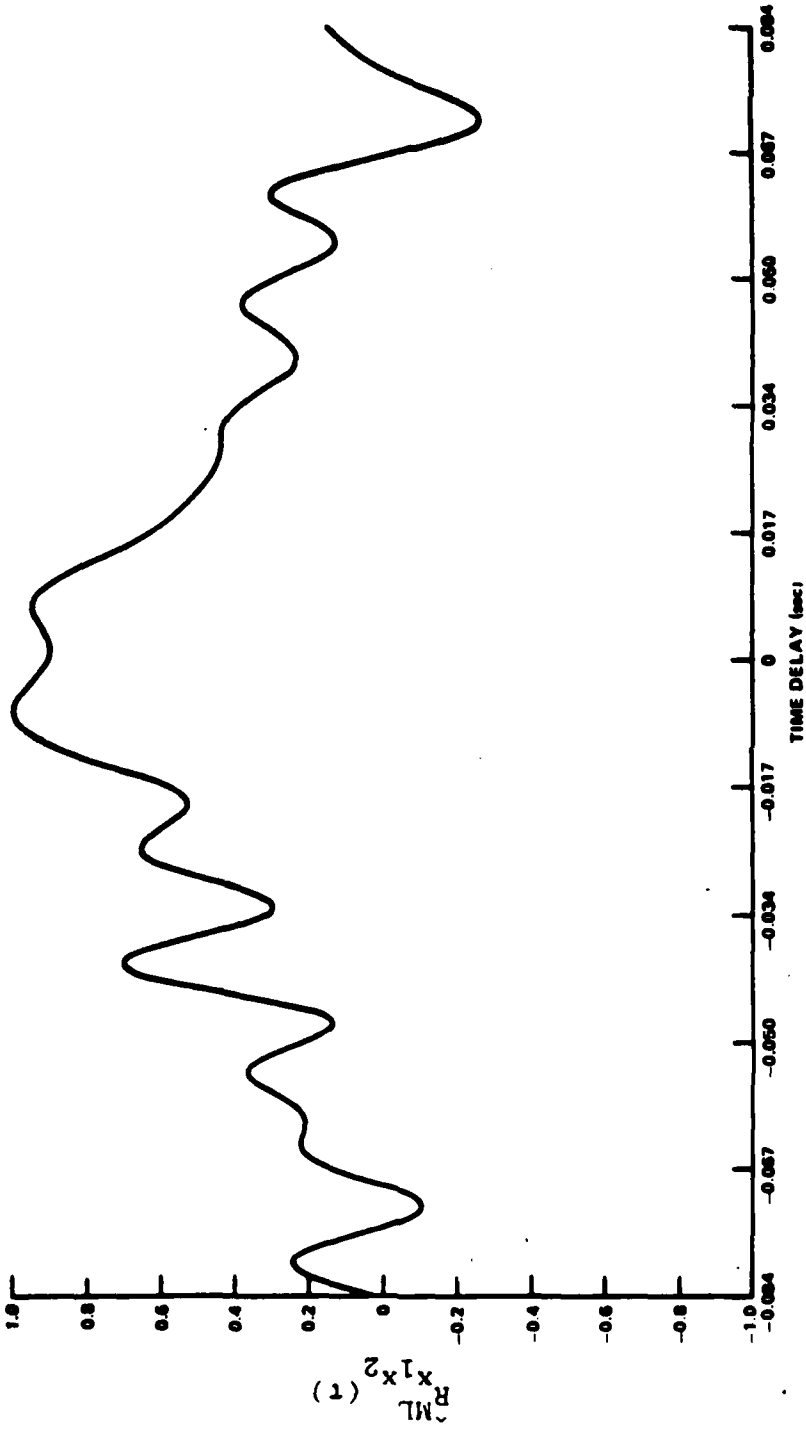

Figure D-6 Expanded Figure D-5 Time Delay Estimates

BIBLIOGRAPHY

Abramowitz and Stegun, I.A., (ed.), (1964), Handbook of Mathematical Functions with Formulas, Graphs, and Mathematical Tables, U. S. Government Printing Office, Washington, D.C.

Akaike, H. and Yamanouchi, Y., (1963), "On the statistical estimation of frequency response function," Ann. of Inst. Statist. Math., 14, 23-56.

Alexander, M. J. and Vok, C. A., (1963), Tables of the Cumulative Distribution of Sample Multiple Coherence, Rocketdyne Division, North American Aviation, Inc., Research Report 63-67.

Alsup, J. M., Means, R. W., and Whitehouse, H. J., (1973), "Real Time Discrete Fourier Transforms Using Surface Acoustic Wave Devices," Proc. IEEE International Specialist Seminar on Component Performance and System Applications of Surface Acoustic Wave Devices, Aviemore, Scotland, U.K.

Amos, D. E. and Koopmans, L. H., (1963), Tables of the Distribution of the Coefficient of Coherence for Stationary Bivariate Gaussian Processes, Sandia Corp. Monograph SCR-483.

Anderson, T. W., (1958), An Introduction to Multivariate Statistical Analysis, New York, John Wiley and Sons, Inc.

Bangs, W. J., III, (1971), Array Processing with Generalized Beam-Formers, Yale Ph.D. Thesis, New Haven, CT.

Bendat, J. S. and Piersol, A. G., (1971), Random Data: Analysis and Measurement Procedures, New York, John Wiley and Sons, Inc.

Benignus, V. A., (1969a), "Estimation of the Coherence Spectrum and its Confidence Interval Using the Fast Fourier Transform," IEEE Trans. Audio Electroacoustics, AU-17, No. 2, 145-150.

Benignus, V. A., (1969b), "Estimation of Coherence Spectrum of Non Gaussian Time Series Populations," IEEE Trans. Audio Electroacoustics, AU-17, No. 3, 198-201.

Bingham, C., Godfrey, M. D., and Tukey, J. W., (1967), "Modern Techniques of Power Spectrum Estimation," IEEE Trans. Audio Electroacoustics, AU-15, No. 2, 56-66.

Blackman, R. B. and Tukey, J. W., (1958), The Measurement of Power Spectra, New York, Dover Publications, Inc.

Box, G. E. and Jenkins, G. M., (1970), Time Series Analysis: Forecasting and Control, San Francisco, CA, Holden-Day, Inc.

Brady, J. F., (1973), An Experimental Study of Vibration Noise, and Drag of a Cylinder Rotating in Water and Certain Polymer Solutions, University of Rhode Island Ph.D. Thesis, Kingston, R.I.

Brillinger, D. R., (1975), Time Series, Data Analysis and Theory, New York, Holt, Rinehart and Winston.

Buss, D. D., Collins, D. R., Bailey, W. H. and Reeves, C.R., (1973), "Transversal Filtering Using Charge-Transfer Devices," IEEE Journal of Solid State Circuits, SC-8, No. 2, 138-146.

Cannon, M., (1974), "Blind Image Deblurring with Phase Reversals," presented at IEEE Arden House Workshop, Harriman, N.Y. (See also Stockham, T. G., Jr., Cannon, T. M., and Ingeretsen, R. B.,(1965),"Blind Deconvolution Through Digital Signal Processing," Proc. IEEE, Vol. 63, No. 4 , 678-692.)

Carter, G. C., (1972a), Estimation of the Magnitude-Squared Coherence Function (Spectrum), University of Connecticut MSEE Thesis, Storrs, CT. (See also Naval Underwater Systems Center, TR 4343, New London, CT.)

Carter, G. C., (1972b), Coherence Estimation as Affected by Weighting Functions and Fast Fourier Transform Size, Naval Underwater Systems Center TR 4423, New London, CT.

Carter, G. C., (1976), "Receiver Operating Characteristics for a Linearly Threshold Coherence Estimator Detector," submitted to IEEE Trans. Acoust. Speech, Signal Processing.

Carter, G. C. and Knapp, C. H., (1975), "Coherence and Its Estimation via the Partitioned Modified Chirp-Z Transform," IEEE Trans. Acoust., Speech, Signal Processing, ASSP-23, No. 3, 257-264.

Carter, G. C. and Knapp, C. H., (1976a), "Time Delay Estimation," accepted for publication in Proc. of the First International Conference on Acoustic, Speech, and Signal Processing, Philadelphia, PA.

Carter, G. C. and Knapp, C. H., (1976b), "Time Compression Estimation," Manuscript Draft.

Carter, G. C., Knapp, C. H. and Nuttall, A. H., (1973a), "Estimation of the Magnitude-Squared Coherence Function via Overlapped Fast Fourier Transform Processing," IEEE Trans. on Audio Electroacoustics, AU-21, 337-344.

Carter, G. C., Knapp, C. H. and Nuttall, A. H., (1973b), "Statistics of the Estimate of the Magnitude-Coherence Function," IEEE Trans. on Audio Electro-acoustics, AU-21, 388-389.

Carter, G. C. and Nuttall, A. H., (1972), "Statistics of the Estimate of Coherence," Proc. IEEE, 60, No. 4, 465-466.

Carter, G. C., Nuttall, A. H. and Cable, P. G., (1973), "The Smoothed Coherence Transform," Proc. IEEE, 61, 1497-1498.

Clay, C. S., Hinich, M. J. and Shaman, P., (1973), "Error Analysis of Velocity and Direction Measurements of Plane Waves Using Thick Large-Aperture Arrays," J. Acoustic Soc. Am., 53, No. 4, 1161-1166.

Cooley, J. W. and Tukey, J. W., (1965), "An Algorithm for the Machine Calculation of Complex Fourier Series," Mathematics of Computation, 19, 297-301.

Davenport, W. B., Jr., (1970), Probability and Random Processes, New York, McGraw-Hill Book Company.

Dubes, R. C., (1968), The Theory of Applied Probability, Englewood Cliffs, New Jersey, Prentice-Hall, Inc.

Eckart, C., (1952), Optimal Rectifier Systems for the Detection of Steady Signals, University of California, Scripps Institution of Oceanography, Marine Physical Laboratory Rep. SIO 12692, SIO Ref. 52-11.

Enochson, L. D. and Goodman, N. R., (1965), Gaussian Approximations to the Distribution of Sample Coherence, Air Force Flight Dynamics Laboratory, Research and Tech. Division, AF Systems Command, Wright-Patterson AFB, OH, Bull. AFFDL-TR-65-67.

Ferrie, J. F., Nawrocki, C. W. and Carter, G. C., (1973), "The PAM-Chirp-Z Transform," Proc. of the 1973 IEEE International Conference on the Ocean Environment, Seattle, WA.

Ferrie, J. F., Nawrocki, C. W. and Carter, G. C., (1975), "Applications of the Partitioned and Modified Chirp-Z Transform to Oceanographic Measurements," IEEE Trans. on Acoustic, Speech, Signal Processing, 243-244.

Ferrie, J. F. and Nuttall, A. H., (1971), Comparison of Four Fast Fourier Transform Algorithms, Naval Underwater Systems Center, TR 4113, New London, CT.

Fisher, R. A., (1950), Contributions to Mathematical Statistics, New York, John Wiley and Sons, Inc., (Chapter 14 originally published as "The General Sampling Distribution of the Multiple Correlation Coefficient," Proc. of the Royal Society, Series A, 121, (1928), 654-673.)

Gelfand, I. M. and Yaglom, A. M., (1959), "Calculation of the Amount of Information about a Random Function Contained in Another Such Function," Amer. Math. Soc. Transl., 12 Series 2, 199-246.

Gevins, A. S., Yeager, C. L., Diamond, S. L., Spire, J. P., Zeitlin, G. M. and Gevins, A. H., (1975), "Automated Analysis of the Electrical Activity of the Human Brain (EEG): A Progress Report," Proc. IEEE, 63, No. 10, 1382-1399.

Gold, B. and Rader, C. M., (1969), Digital Processing of Signals, New York, McGraw-Hill Book Company.

Goodman, N. R., (1957), On the Joint Estimation of the Spectra, Cospectrum, and Quadrature Spectrum of a Two-Dimensional Stationary Gaussian Process, Scientific Paper 10, New York University, New York.

Gradshteyn, I. S. and Ryzhik, I. M., (1965), Table of Integrals, Series, and Products, New York, Academic Press.

Halvorsen, W. G. and Bendat, J. S., (1975), "Noise Source Identification Using Coherent Output Power Spectra," Sound and Vibration, 15-24.

Hamon, B. V. and Hannan, E. G., (1974), "Spectral Estimation of Time Delay for Dispersive and Non-Dispersive Systems," J. Royal Sta. Soc. Ser. C. (Appl. Statist.), 23, 134-142.

Hannan, E. J., (1970), Multiple Time Series, New York, John Wiley and Sons, Inc.

Hannan, E. J. and Robinson, P. M., (1973), "Lagged Regression with Unknown Lags," J. Royal Statist. Soc., Ser. B, 35, No. 2, 252-267.

Hannan, E. J. and Thomson, P. J., (1971), "The Estimation of Coherence and Group Delay," Biometrika, 58, 469-481.

Hannan, E. J. and Thomson, P. J., (1973), "Estimating Group Delay," Biometrika, 60, 241-253.

Haubrich, R. A., (1965), "Earth Noise, 5 to 500 Millicycles per Second, 1. Spectral Stationarity, Normality, and Non Linearity," J. Geophysical, Res., 70, No. 6, 1415-1427.

James, D. V., (1974), "Quantization Errors in the Fast Fourier Transform," presented at IEEE Arden House Workshop, Harriman, N.Y. (See also, James, D. V., (1975), "Quantization Errors in the Fast Fourier Transform", IEEE Trans. on Acoustic, Speech, Signal Processing, ASSP-23, No. 3, 277-282.)

Jenkins, G. M. and Watts, D. G., (1968), Spectral Analysis and Its Applications, San Francisco, Holden-Day, Inc.

Jury, E. I., (1964), Theory and Application of the Z Transform Method, New York, John Wiley and Sons, Inc.

Kennedy, R. S., (1969), Fading Dispersive Communications Channels, New York, Wiley-Interscience.

Knapp, C. H., (1966), Optimum Linear Filtering for Multi-Element Arrays, General Dynamics/Electric Boat Division, Rep. U417-66-031, Groton, CT.

Knapp, C. H. and Carter, G. C., (1976), "The Generalized Correlation Method for Estimation of Time Delay," accepted for publication in IEEE Trans. on Acoustic, Speech, Signal Processing.

Kochenburger, R. J. (1972), Computer Simulation of Dynamic Systems, Englewood Cliffs, N. J., Prentice-Hall, Inc.

Koopmans, L. H., (1964), "On the Coefficient of Coherence for Weakly Stationary Stochastic Processes," Ann. Math. Statist., 35, 532-549.

Koopmans, L. H. (1974), The Spectral Analysis of Time Series, New York, Academic Press.

Lee, Y. W., (1960), Statistical Theory of Communications, New York, John Wiley and Sons, Inc.

Lindorff, D. P., (1965), Theory of Sampled Data Control Systems, New York, John Wiley and Sons, Inc.

MacDonald, V. H. and Schultheiss, P. M., (1969), "Optimum Passive Bearing Estimation," J. Acoust. Soc. Am., 46, 37-43.

Nettheim, N., (1966), The Estimation of Coherence, Stanford University Department of Stat. TR No. 5, Stanford, CA.

Nuttall, A. H., (1958), Theory and Application of the Separable Class of Random Processes, MIT Ph.D. Thesis. (Also published as Research Laboratory of Electronics Report 343, Cambridge, MA.)

Nuttall, A. H., (1971), Spectral Estimation by Means of Overlapped FFT Processing of Windowed Data, Naval Underwater Systems Center Report No. 4169, New London, CT. (and supplement NUSC TR-4169S).

Nuttall, A. H. and Carter, G. C., (1976a), Approximations for Statistics of Coherence Estimators, Naval Underwater Systems Center TR 5291, New London, CT.

Nuttall, A. H. and Carter, G. C., (1976b), "Bias of the Estimate of Magnitude-Squared Coherence," submitted to IEEE Trans. on Acoustic, Speech, Signal Processing.

Nuttall, A. H. and Carter, G. C. and Montavon, E. M., (1974), "Estimation of the Two-Dimensional Spectrum of the Space-Time Noise Field for a Sparse Line Array," J. Acoust. Soc. Am., 55, 1034-1041.

Nuttall, A. H. and Hyde, D. W., (1969), A Unified Approach to Optimum and Sub-Optimum Processing for Arrays, Naval Underwater Systems Center, TR 992, New London, CT.

Oppenheim, A. V. and Schafer, R. W., (1975), Digital Signal Processing, Englewood Cliffs, N.J., Prentice-Hall, Inc.

Otnes, R. K. and Enochson, L., (1972), Digital Time Series Analysis, New York, Wiley-Interscience.

Papoulis, A., (1965), Probability, Random Variables and Stochastic Processes, New York, McGraw-Hill Book Company.

Rabiner, L. R. and Rader, C. M. (ed.), (1972), Digital Signal Processing, New York, IEEE Press.

Rabiner, L. R., Schafer, R. W. and Rader, C. M., (1969), "The Chirp-Z Transform Algorithm and Its Application," The Bell System Technical Journal, 48, No. 5, 1249-1292, and (1969), "The Chirp-Z Transform Algorithm," IEEE Transactions Audio Electroacoustics, AU-17, No. 2, 86-92.

Roth, P. R., (1971), "Effective Measurements Using Digital Signal Analysis," IEEE Spectrum, 8, 62-70.

Sage, A. P. and Melsa, J. L., (1971), Estimation Theory with Applications to Communications and Control, New York, McGraw-Hill Book Company.

Santopietro, R. F., (1973), Measurement, Analysis and Reduction of Noise in the High Frequency, University of Pennsylvania, Ph.D. Thesis, Philadelphia, PA.

Schilling, S. A., (1972), A Study of the Chirp-Z Transform and Its Applications, MSEE Thesis, University of Kansas, Manhattan, KS.

Schultheiss, P. M., (1968), "Passive Sonar Detection in the Presence of Interference," J. Acoust. Soc. Am., 43, No. 3, 418-425.

Shannon, C. E. and Weaver, W., (1949), The Mathematical Theory of Communication, Urbana, IL., University of Illinois Press.

Singleton, R. C., (1969), "An Algorithm for Computing the Mixed Radix Fast Fourier Transform," IEEE Transactions on Audio Electroacoustics, AU-17, No. 2., 93-102.

Silverman, R. A., (1957), "Locally Stationary Random Processes," IRE Trans. on Info. Th., 182-187.

Tick, L. J., (1967), Spectral Analysis of Time Series, ed. by B. Harris, New York, John Wiley and Sons, Inc., 133-152.

Urick, R. J., (1967), Principles of Underwater Sound for Engineers, New York, McGraw-Hill Book Company. (Also second edition, 1975, Principles of Underwater Sound, same publisher.)

Van Trees, H. L., (1968), Detection, Estimation and Modulation Theory, Part I., Detection Estimation and Linear Modulation Theory, New York, John Wiley and Sons, Inc.

Van Trees, H. L., (1971), Detection, Estimation and Modulation Theory, Part III, Radar/Sonar Signal Processing and Gaussian Signals in Noise, New York, John Wiley and Sons, Inc.

Wahba, G., (1966), Cross Spectral Distribution Theory for Mixed Spectra and Estimation of Prediction Filter Coefficients, Stanford University Department of Stat. TR No. 15, Stanford, CA.

Weiner, N., (1930), "Generalized Harmonic Analysis," Acta. Math., 55, 117-258.

Weinstein, C. and Oppenheim, A., (1969), "A Comparison of Round-Off Noise in Floating Point and Fixed Digital Filter Realizations," Proc. IEEE, 57, 1181-1183, (see also 429-431 of Rabiner and Rader (1972)).

Welch, P. D., (1967), "The Use of Fast Fourier Transform for the Estimation of Power Spectra: A Method Based on Time Averaging Over Short, Modified Periodograms," IEEE Transactions on Audio Electroacoustics, AU-15, No. 2, 70-73.

Whalen, A. D., (1971), Detection of Signals in Noise, New York, Academic Press.

Williams, R. G., (1971), Estimating Ocean Wind Wave Spectra by Means of Underwater Sound, Ph.D. Dissertation, New York University, N.Y., (Also published as Naval Underwater Systems Center TR 4097, New London, CT., and in a condensed form in J. Acoust. Soc. Am., 53, No. 3, 910-920, (1973).)

Wozencraft, J. M. and Jacobs, I. M., (1967), Principles of Communication Engineering, New York, John Wiley and Sons, Inc.

NUSC Technical Document 5507
27 August 1976

The Role of Coherence in Time Delay Estimation

A Paper Presented at the

NATO Advanced Study Institute,

LaSpezia, Italy

30 August-11 September 1976

G. C. Carter

ABSTRACT

This paper investigated methods for passive estimation of the bearing to a slowly moving acoustically radiating source. The mathematics for the solution to such a problem is analogous to estimating the time delay (or group delay) between two time series. Since the estimation of time delay is intimately related to the coherence between two time series, a summary of the properties of coherence is presented.

The Role of Coherence in Time Delay Estimation

$$C_{ab}(f) = \frac{|G_{ab}(f)|^2}{G_{aa}(f)\,G_{bb}(f)}$$

$$0 \leq C_{ab}(f) \leq 1, \forall f$$

SLIDE 1

(SLIDE 1)

THE TERM COHERENCE HAS SEVERAL DIFFERENT MEANINGS AND INDEED DEFINITIONS. THE ONE WE USE HERE IS THE MAGNITUDE SQUARED OF THE COEFFICIENT OF COHERENCY DEFINED BY WEINER IN 1930. IN PARTICULAR, FOR OUR PURPOSES HERE, WE DEFINE THE COHERENCE BETWEEN TWO STATIONARY RANDOM PROCESSES A AND B AS THE MAGNITUDE SQUARED OF THE CROSS POWER SPECTRUM DIVIDED BY THE PRODUCT OF THE TWO AUTO POWER SPECTRA. THE COHERENCE IS A FUNCTION OF FREQUENCY AND HAS THE USEFUL PROPERTY THAT IT LIES BETWEEN ZERO AND UNITY. IT IS, IN EFFECT, A NORMALIZED CROSS SPECTRAL DENSITY THAT, IN SOME SENSE, MEASURES THE EXTENT TO WHICH TWO RANDOM PROCESSES ARE SIMILAR. FOR EXAMPLE, TWO UNCORRELATED RANDOM PROCESSES ARE ALSO INCOHERENT; THAT IS, THE COHERENCE IS ZERO BETWEEN UNCORRELATED PROCESSES. FURTHER, THE COHERENCE BETWEEN TWO LINEARLY RELATED PROCESSES IS UNITY.

-NEXT SLIDE PLEASE-

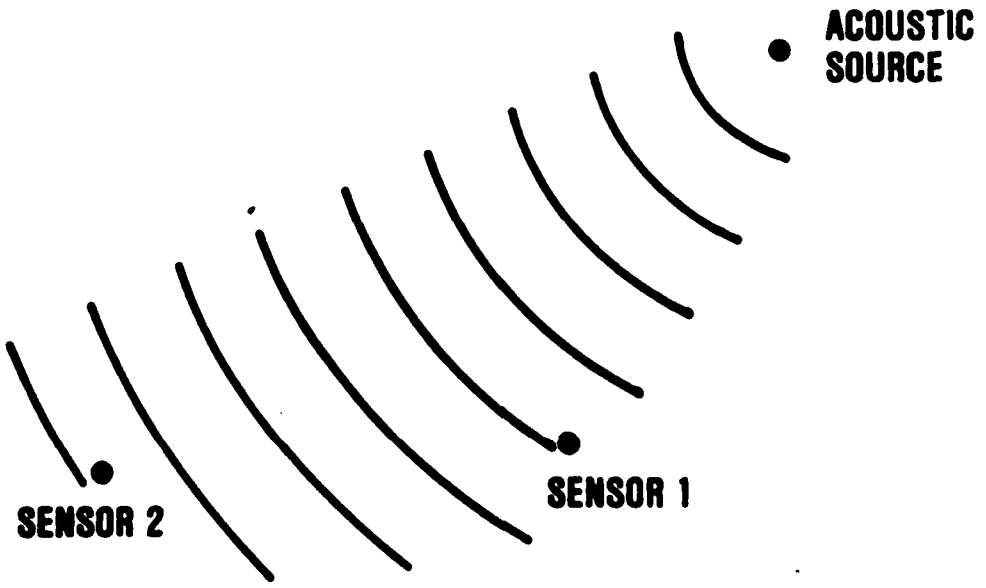

SLIDE 2

AD-A101 684 SCIENTIFIC AND ENGINEERING STUDIES COMPILED 1979 7/8
COHERENCE ESTIMATION(U) NAVAL UNDERWATER SYSTEMS CENTER
NEWPORT RI G C CARTER ET AL. 1979

UNCLASSIFIED F/G 9/1 NL

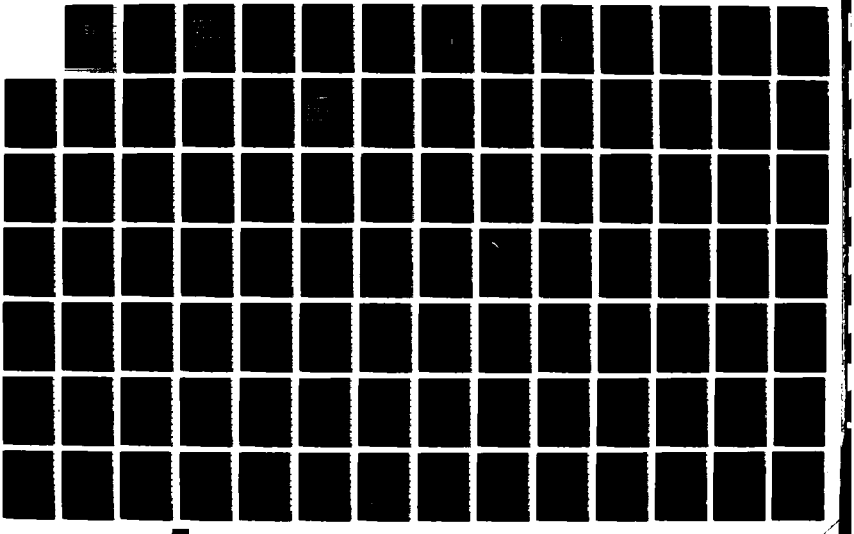

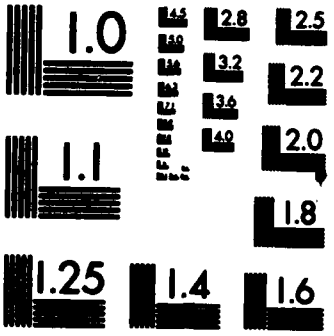

(SLIDE 2)

THE PHYSICAL PROBLEM THAT MOTIVATES THIS RESEARCH IS A DESIRE TO PASSIVELY ESTIMATE GEOGRAPHICAL INFORMATION ABOUT THE STATE OF AN ACOUSTIC SOURCE. IN THE DEVELOPMENT HERE AN ACOUSTIC POINT SOURCE RADIATES SPHERICAL WAVES, RECEIVED, FIRST, AT ONE SENSOR AND SOME DELAYED TIME LATER, AT A SECOND SENSOR. THE SOURCE IS ASSUMED STATIONARY FOR THE OBSERVATION PERIOD AND THE SENSOR SEPARATION IS ASSUMED KNOWN. EACH RECEIVED WAVEFORM IS OBSERVED IN THE PRESENCE OF UNCORRELATED NOISE. THE PROBLEM WE ADDRESS IS HOW TO ESTIMATE THE TRAVEL TIME OF THE WAVEFRONT OR TIME DELAY FROM ONE SENSOR TO THE NEXT.

THE IMPORTANCE OF OBTAINING A GOOD TIME DELAY ESTIMATE IS THAT IT CAN BE USED TO FIX THE SOURCE LOCATION ON A HYPERBOLIC LOCUS OF POINTS. OF COURSE, IF WE HAVE THREE SENSORS WE CAN ESTIMATE TWO TIME DELAYS AND THE INTERSECTING HYPERBOLIC CURVES CAN BE USED TO ESTIMATE SOURCE POSITION.

-NEXT SLIDE PLEASE-

GENERAL CASE

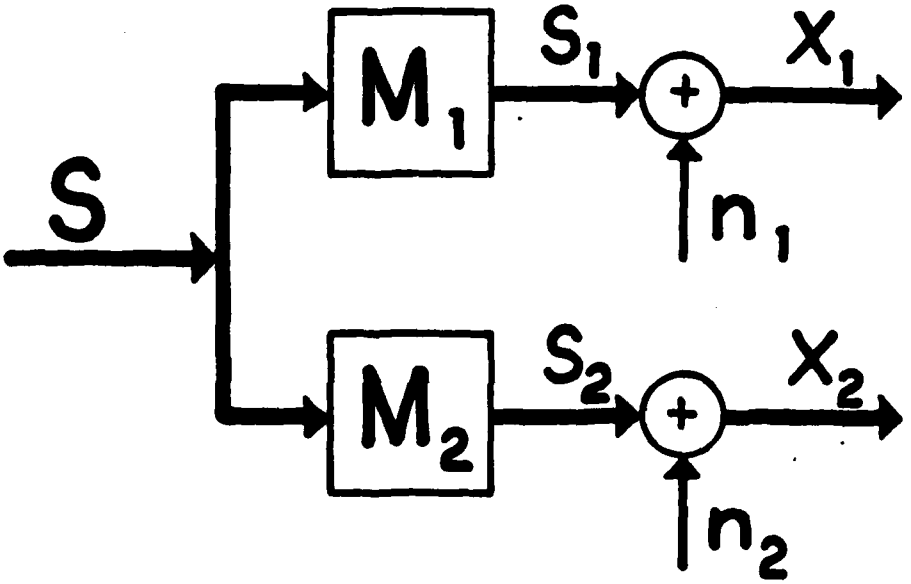

SPECIFIC CASE

$$X_1(t) = S(t) + n_1(t)$$

$$X_2(t) = \alpha S(t+D) + n_2(t)$$

SLIDE 3

(SLIDE 3)

IN THE GENERAL CASE WE CAN MODEL THE ACOUSTIC SOURCE PROPAGATION AND NOISE CORRUPTED RECEPTION AS SHOWN HERE. IN PARTICULAR, WE TREAT THE PATH FROM THE SOURCE TO EACH RECEIVER AS A LINEAR TIME INVARIANT FILTER. THE RECEIVED SIGNALS X ONE AND X TWO CONSIST OF THE FILTER OUTPUTS PLUS NOISE.

A SPECIAL CASE OF THIS MODEL IS SHOWN ON THE BOTTOM OF THE SLIDE. THE FIRST RECEIVED WAVEFORM CONSISTS OF SIGNAL PLUS NOISE. THE SECOND RECEIVED WAVEFORM CONSISTS OF AN ATTENUATED AND DELAYED SIGNAL IN THE PRESENCE OF NOISE. THE MATHEMATICAL PROBLEM WE ADDRESS IS: HOW TO BEST ESTIMATE THE TIME DELAY OR EQUIVALENTLY SOURCE BEARING. FURTHER WE ARE CONCERNED WITH THE ROLE OF COHERENCE IN THIS PROCESS.

FOR ANALYTIC PURPOSES WE TREAT THE NOISE AS STATIONARY AND UNCORRELATED. LATER WE MAKE AN IMPLICIT ASSUMPTION THAT THE NOISE IS NORMAL (GAUSSIAN).

-NEXT SLIDE PLEASE-

$$\frac{G_{s_i s_i}(f)}{G_{n_i n_i}(f)} = \frac{C_{sx_i}(f)}{1 - C_{sx_i}(f)},$$

$$i = 1, 2;$$

$$C_{12}(f) \equiv C_{x_1 x_2}(f) = C_{sx_1}(f)\, C_{sx_2}(f)$$

SLIDE 4

(SLIDE 4)

FOR THE GENERAL MODEL WE CAN SHOW THAT THE RECEIVED SIGNAL-TO-NOISE RATIO IS A FUNCTION OF ONLY THE COHERENCE BETWEEN THE SOURCE AND THE RECEIVER. INDEED, RELATIVE TO THE SENSOR NOISE POWER, THE AMOUNT OF POWER RECEIVED FROM THE SOURCE AFTER IT HAS BEEN ATTENUATED BY ACOUSTIC TRANSMISSION THROUGH THE OCEAN MEDIUM IS DESCRIBED BY THE SOURCE-TO-SENSOR COHERENCE DIVIDED BY ONE MINUS SOURCE-TO-SENSOR COHERENCE. MOREOVER, THE COHERENCE BETWEEN THE TWO RECEIVED WAVEFORMS CANNOT EXCEED THE COHERENCE BETWEEN THE SOURCE AND ANY SENSOR; THIS IS TRUE WHEN THE OCEAN MEDIUM IS MODELED AS A LINEAR TIME INVARIANT FILTER.

MORE SPECIFICALLY, THE COHERENCE BETWEEN THE TWO RECEIVED WAVEFORMS IS EQUAL TO THE PRODUCT OF THE COHERENCES BETWEEN THE SOURCE AND EACH OF THE RECEIVED WAVEFORMS.

-NEXT SLIDE PLEASE-

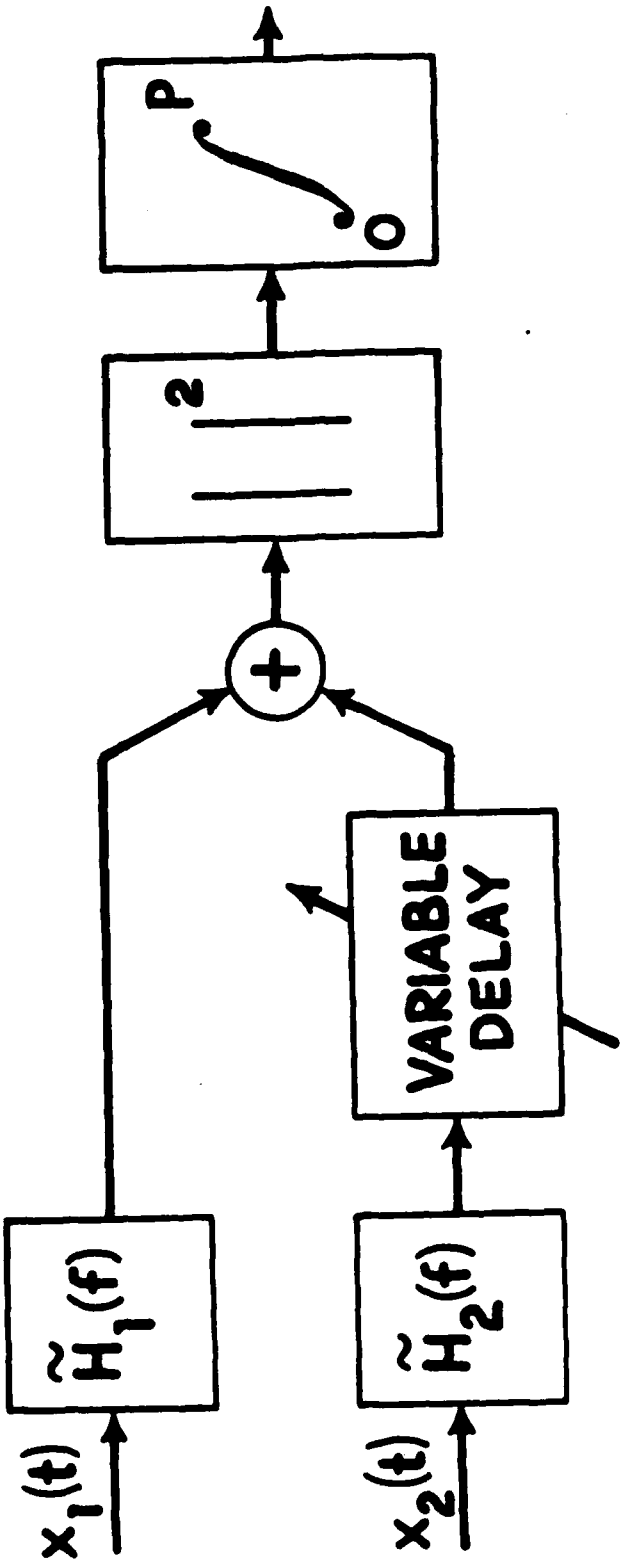

SLIDE 5

(SLIDE 5)

UNDER STANDARD ASSUMPTIONS, NAMELY, THAT THE TWO RECEIVED WAVEFORMS, X ONE AND X TWO, ARE JOINTLY STATIONARY, NORMAL (GAUSSIAN) RANDOM PROCESSES AND THAT THE OBSERVATION TIME P IS LARGE, THE MAXIMUM LIKELIHOOD ESTIMATE OF TIME DELAY CAN BE DERIVED. THE MAXIMUM LIKELIHOOD, OR ML, ESTIMATE OF TIME DELAY CAN BE INSTRUMENTED INONE OF TWO WAYS. SHOWN HERE IS ONE REALIZATION. THE FIRST RECEIVED WAVEFORM IS FILTERED BY H ONE TILDE, AND THE SECOND RECEIVED WAVEFORM IS FILTERED BY H TWO TILDE AND DELAYED. THE FILTERS MUST HAVE IDENTICAL PHASE RESPONSES. THE FILTER OUTPUTS ARE SUMMED, SQUARED, AND INTEGRATED AS SHOWN. THE HYPOTHESIZED VARIABLE DELAY THAT MAXIMIZES THIS SYSTEM OUTPUT IS THE MAXIMUM LIKELIHOOD ESTIMATE OF TIME DELAY. THE SPECIFIC FILTER CHARACTERISTICS DEPEND ON THE SIGNAL AND NOISE SPECTRA, WHICH MUST BE KNOWN OR ESTIMATED.

-NEXT SLIDE PLEASE-

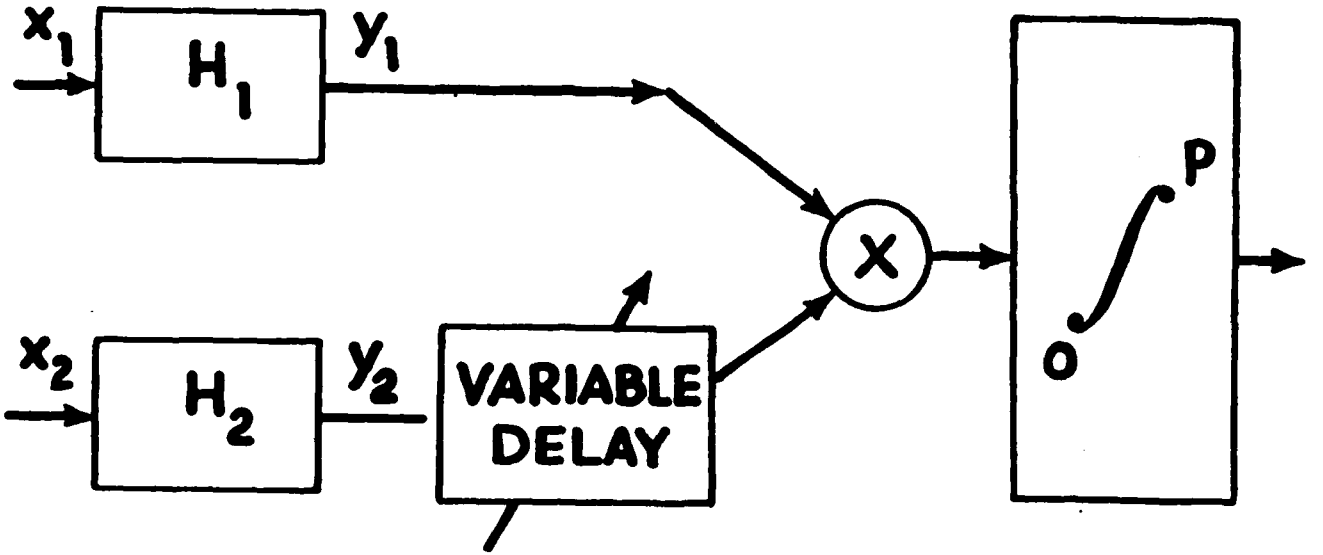

$$W_g(f) \triangleq H_1(f)\, H_2^*(f)$$

$$R^g_{x_1 x_2}(\tau) = \int_{-\infty}^{\infty} W_g(f)\, G_{x_1 x_2}(f)\, e^{j2\pi f\tau}\, df$$

SLIDE 6

(SLIDE 6)

ANOTHER REALIZATION FOR THE MAXIMUM LIKELIHOOD ESTIMATE OF TIME DELAY IS A SPECIAL CASE OF THE GENERALIZED CROSSCORRELATION PROCESSOR. IN THIS PROCESSOR THE FIRST RECEIVED WAVEFORM IS FILTERED BY H ONE AND THE SECOND RECEIVED WAVEFORM IS FILTERED BY H TWO, DELAYED, MULTIPLIED, AND INTEGRATED AS SHOWN ON THE DIAGRAM AT THE TOP OF THE SLIDE. BY PROPER CHOICE OF THE GENERAL WEIGHTING FUNCTION, W, WHICH IS THE PRODUCT OF H ONE AND H TWO CONJUGATE, WE CAN ACHIEVE THE MAXIMUM LIKELIHOOD ESTIMATE FOR TIME DELAY. HOWEVER, WE CAN ALSO ACHIEVE A GENERALIZED CROSSCORRELATION FUNCTION, R OF TAU, BY MULTIPLYING THE CROSS SPECTRUM, G, BETWEEN THE TWO RECEIVED WAVEFORMS, BY THE GENERAL WEIGHTING, W, AND COMPUTING THE FOURIER TRANSFORM AS INDICATED ON THE BOTTOM OF THE SLIDE.

-NEXT SLIDE PLEASE-

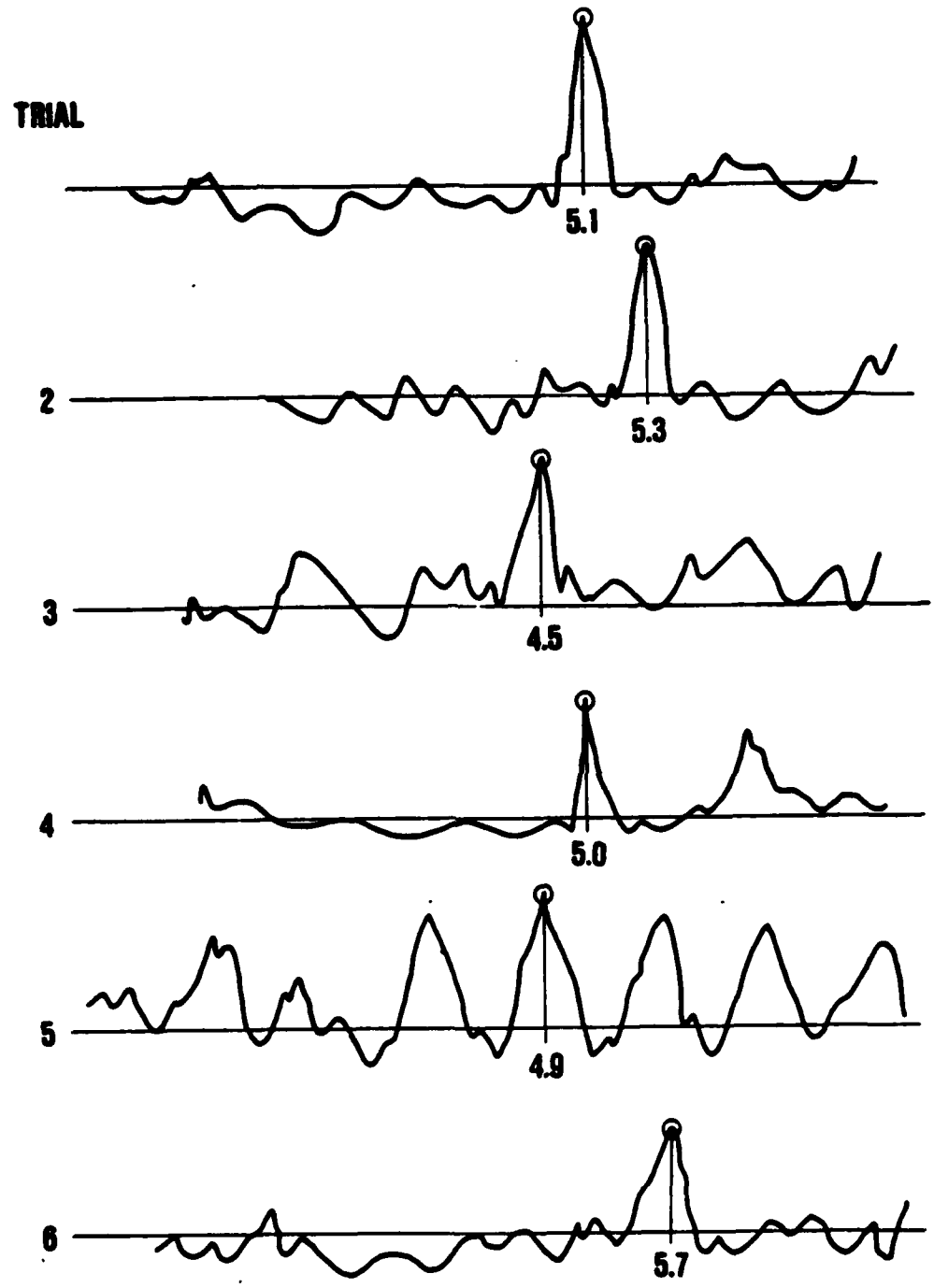

SLIDE 7

(SLIDE 7)

IF WE ESTIMATED THE GENERALIZED CROSSCORRELATION FUNCTION FOR SIX DIFFERENT TRIALS, THE PEAK OF THE FUNCTION MIGHT VARY AS A FUNCTION OF TRIAL. WE HAVE ACTUALLY IMPLEMENTED THE TECHNIQUE FOR SEVERAL EXAMPLE CASES ON THE UNIVAC 1108. BASED ON OUR EXPERIMENTAL RESULTS, WE SPECULATE THAT A TYPICAL GENERALIZED CROSSCORRELATION FUNCTION MIGHT PEAK, AS INDICATED IN THE HYPOTHETICAL TRIALS SKETCHED HERE. IN PARTICULAR, THE ABSCISSA VALUE OF THE PEAK LOCATION, THAT IS, THE ESTIMATE OF TIME DELAY, HAS A CERTAIN AMOUNT OF VARIATION. NOTICE ALSO IN TRIAL NUMBER 5, NEXT TO THE BOTTOM PLOT, THAT A NUMBER OF AMBIGUOUS PEAKS CAN ARISE IN ADDITION TO THE LOCAL VARIATION OF THE TIME DELAY ESTIMATE. THE AMBIGUITY PROBLEM IS NOT TREATED IN THIS WORK. THE PROBLEM OF COMPUTING THE VARIANCE OF THE TIME DELAY ESTIMATE IS A DIFFICULT ONE IN WHICH ONE IS PUZZLED HOW TO PROCEED. HOWEVER, IF WE COULD COUNT THE NUMBER OF PEAKS THAT OCCURRED AT EACH OF SEVERAL ABSCISSA VALUES, THEN WE COULD PLOT A FREQUENCY DISTRIBUTION OF THE PEAK LOCATION. FROM THIS DISTRIBUTION WE CAN OBTAIN THE VARIANCE OF THE TIME DELAY ESTIMATE.

-NEXT SLIDE PLEASE-

VARIANCE OF DELAY ESTIMATE

$$\frac{\int_{-\infty}^{\infty} df \left|W_g(f)\right|^2 (2\pi f)^2 G_{11}(f) G_{22}(f) \left[1 - C_{12}(f)\right]}{P\left[\int_{-\infty}^{\infty} df (2\pi f)^2 \left|G_{12}(f)\right| \cdot \left|W_g(f)\right|\right]^2}$$

SLIDE 8

(SLIDE 8)

THE VARIANCE OF THE TIME DELAY ESTIMATE IS A COMPLICATED FUNCTION OF SEVERAL PARAMETERS. IT DEPENDS ON THE LENGTH OF THE OBSERVATION TIME, P, THE GENERAL WEIGHTING FUNCTION, W, THE AUTO-SPECTRAL DENSITIES OF THE TWO RECEIVED WAVEFORMS, AND THE MAGNITUDE CROSS SPECTRUM BETWEEN THE TWO RECEIVED WAVEFORMS. IT ALSO DEPENDS ON THE COHERENCE, C, DEFINED EARLIER AS THE MAGNITUDE SQUARED CROSS SPECTRUM DIVIDED BY THE PRODUCT OF THE TWO AUTO-SPECTRAL DENSITIES. RECALL THE COHERENCE IS GREATER THAN OR EQUAL TO ZERO AND IS LESS THAN OR EQUAL TO UNITY. WHEN THE OBSERVATION TIME IS LARGE OR THE COHERENCE IS NEAR UNITY, THE VARIANCE IS GENERALLY QUITE LOW AND YOU CAN DO WELL IN SPITE OF THE WEIGHTING SELECTED. OF COURSE, AN IMPORTANT ROLE TO BE PLAYED BY THE EXPRESSION HERE IS TO EVALUATE HOW DIFFERENT PROCESSORS COMPARE WITH ONE ANOTHER. ANOTHER IMPORTANT USE OF THIS EXPRESSION IS IF ONE KNOWS THEORETICALLY THE BEST WEIGHTING FUNCTION TO APPLY, BUT APPLIES AN INCORRECT OR SUBOPTIMUM WEIGHTING, THEN THE VARIANCE OF THE SUBOPTIMUM DELAY ESTIMATOR CAN BE EVALUATED.

-NEXT SLIDE PLEASE-

MINIMUM VARIANCE

$$\left[2P \int_0^\infty df\, (2\pi f)^2 \frac{C_{12}(f)}{1 - C_{12}(f)} \right]^{-1}$$

FOR

$$W_{ML}(f) = \frac{C_{12}(f)}{\left|G_{12}(f)\right| \left[1 - C_{12}(f)\right]}$$

SLIDE 9

(SLIDE 9)

THE MINIMUM VARIANCE FOR ANY TIME DELAY ESTIMATION SCHEME CAN BE OBTAINED FROM THE CRAMÉR RAO LOWER BOUND. AS SHOWN HERE, IT IS A FUNCTION OF ONLY TWO PARAMETERS: THE OBSERVATION TIME P AND THE COHERENCE BETWEEN THE TWO RECEIVED WAVEFORMS. AS P IS INCREASED THE VARIANCE DROPS; FURTHER, AS THE COHERENCE C TENDS TOWARD UNITY THE TERM C OVER ONE MINUS C SQUARED TENDS TOWARDS INFINITY. THUS, AS THE COHERENCE OR C TENDS TOWARDS UNITY, THE VARIANCE TENDS TOWARDS ZERO. HOWEVER, THE COHERENCE IS NOT UNDER OUR CONTROL. THE FACTORS WHICH WE CAN CONTROL ARE THE OBSERVATION TIME P AND THE WEIGHTING. THE MINIMUM VARIANCE IS ACHIEVED FOR THE MAXIMUM LIKELIHOOD WEIGHTING FUNCTION GIVEN BY C OVER ONE MINUS C TIMES THE MAGNITUDE CROSS SPECTRUM.

-NEXT SLIDE PLEASE-

$$\frac{\hat{G}_{12}(f)}{\left|\hat{G}_{12}(f)\right|} \cdot \frac{\hat{C}_{12}(f)}{\left[1-\hat{C}_{12}(f)\right]}$$

$$e^{j\hat{\theta}(f)} \cdot \frac{\hat{C}_{12}(f)}{\left[1-\hat{C}_{12}(f)\right]}$$

SLIDE 10

(SLIDE 10)

THE MAXIMUM LIKELIHOOD WEIGHTING MULTIPLIES THE ESTIMATED CROSS SPECTRUM TO YIELD A SINGLE FUNCTION TO BE FOURIER TRANSFORMED. IN GENERAL, WHEN THE TRUE VALUES OF COHERENCE AND MAGNITUDE CROSS SPECTRUM ARE UNKNOWN, THEY MUST BE ESTIMATED. ESTIMATES ARE INDICATED BY HATS. WHEN SPECTRAL ANALYSIS IS USED TO YIELD ESTIMATES IN PLACE OF THE TRUE QUANTITIES, THE FUNCTION TO BE FOURIER TRANSFORMED IS INDICATED ON THIS SLIDE. THE CROSS SPECTRUM OVER THE MAGNITUDE CROSS SPECTRUM CAN BE THOUGHT OF AS E TO THE MINUS J PHASE. IN PARTICULAR, NOTE THAT THE WEIGHTING EMPHASIZES THE PHASE OF THE ESTIMATED CROSS SPECTRUM IN THOSE FREQUENCY BANDS WHERE THE COHERENCE IS HIGH. ONE WOULD EXPECT THE ESTIMATED PHASE OF THE CROSS SPECTRUM TO PLAY AN IMPORTANT ROLE IN TIME DELAY ESTIMATION, SINCE THE SLOPE OF THE PHASE IS A MEASURE OF THE TIME DELAY. WE CAN SEE THIS BY NOTING THAT THE PHASE SLOPE IS MEASURED IN RADIANS, DIVIDED BY RADIANS PER SECOND, OR SECONDS. OF COURSE, THE PHASE ESTIMATES WILL BE NOISY IN THOSE FREQUENCY BANDS WHERE THE COHERENCE IS LOW SO WE WILL EMPHASIZE THE PHASE IN THOSE BANDS WHERE THE COHERENCE IS HIGH.

-NEXT SLIDE PLEASE-

SUMMARY

- ACOUSTIC SOURCE
- TIME DELAY MODEL
- DERIVED ML TIME DELAY ESTIMATE
- DERIVED CRAMÉR RAO LOWER ROUND
- DERIVED THE VARIANCE FOR ANY GCC
- SHOWN ML ESTIMATE IS MINIMUM VAR
- IMPLEMENTED RESULTS
- APPLICATIONS TO ESTIMATING SOURCE POSITION

SLIDE 11

(SLIDE 11)

IN SUMMARY, THE PHYSICAL PROBLEM MOTIVATING THIS RESEARCH IS A DESIRE TO ESTIMATE POSITIONAL INFORMATION ABOUT AN ACOUSTIC SOURCE. WE HAVE PROPOSED A TIME DELAY MODEL AND DERIVED THE MAXIMUM LIKELIHOOD ESTIMATE FOR TIME DELAY. ADDITIONALLY WE HAVE DERIVED THE CRAMÉR RAO LOWER BOUND ON THE VARIANCE OF THE TIME DELAY ESTIMATE. SUBSEQUENTLY WE HAVE DERIVED AN EXPRESSION FOR THE VARIANCE OF THE TIME DELAY ESTIMATE FOR ANY GENERALIZED CROSS-CORRELATION PROCESSOR. WE HAVE SHOWN THAT THE MAXIMUM LIKELIHOOD ESTIMATE OF TIME DELAY ACHIEVES THE CRAMÉR RAO LOWER BOUND AND IS THEREFORE MINIMUM VARIANCE; AS SUCH THE PROPOSED TECHNIQUE IS THE BEST PROCESSING THAT CAN BE DONE TO ESTIMATE TIME DELAY OR, EQUIVALENTLY, TO ESTIMATE THE HYPERBOLIC LOCUS OF POINTS ON WHICH THE ACOUSTIC SOURCE IS LOCATED. THERE IS NO BETTER TECHNIQUE. WE HAVE IMPLEMENTED THE RESULTS IN AN APPROXIMATE METHOD BY SUBSTITUTING ESTIMATED MAXIMUM LIKELIHOOD WEIGHTING IN PLACE OF TRUE WEIGHTING AND FOUND THAT THE TECHNIQUE WORKS ON A LARGE SCALE DIGITAL COMPUTER. OF COURSE, THE ABILITY TO LOCATE A SOURCE ON A HYPERBOLIC LOCUS OF POINTS SUGGESTS THAT, WITH THREE SENSORS, INTERSECTING HYPERBOLIC CURVES CAN BE USED TO ESTIMATE SOURCE POSITION.

ADDITIONAL REFERENCES NOT GIVEN IN THE CONFERENCE PROCEEDINGS INCLUDE MY RECENTLY COMPETED PH.D. THESIS AND AN ARTICLE ON GENERALIZED CORRELATION PROCESSING THAT HAS JUST APPEARED IN THE AUGUST IEEE TRANSACTIONS ON ACOUSTICS SPEECH AND SIGNAL PROCESSING.

Proceedings Reprint

THE ROLE OF COHERENCE IN TIME DELAY ESTIMATION

G. Clifford Carter

Naval Underwater Systems Center
New London, Connecticut 06320 U.S.A.

ABSTRACT. This paper investigates methods for passive estimation of the bearing to a slowly moving acoustically radiating source. The mathematics for the solution to such a problem is analogous to estimating the time delay (or group delay) between two time series. Since the estimation of time delay is intimately related to the coherence between two time series, a summary of the properties of coherence is presented.

The maximum likelihood (ML) estimate of time delay (under jointly stationary Gaussian assumptions) is presented. The explicit dependence of time delay estimates on coherence is evident in the estimator realization in which the two time series are prefiltered (to accentuate frequency bands according to the strength of the coherence) and subsequently crosscorrelated. The hypothesized delay at which the generalized crosscorrelation (GCC) function peaks is the time delay estimate. The variance of the time delay estimate is presented and discussed.

INTRODUCTION. An acoustic source whose signal, $s(t)$, is transmitted through the ocean medium and received in the presence of additive noise can be characterized by

$$x_i(t) = s_i(t) + n_i(t) \quad , i = 1,2 \tag{1}$$

For the main purposes of this paper $s_1(t)=s(t)$, $s_2(t)=\alpha s(t+D)$, and we desire to present an ML estimator [1] for the time delay D. The delay parameter can be used, in a nondispersive medium with known speed of transmission, to estimate the bearing to an acoustic source (relative to the sensor baseline) or, more generally, to

estimate a hyperbolic "line" of position. Since the final result depends heavily on the coherence between x_1 and x_2, we precede the development with a concise review of the properties of the coherence function and of results that bear directly on the estimation of time delay.

THEORY OF COHERENCE. For any two jointly stationary random processes x_1 and x_2, the coefficient of coherency or the complex coherence has been defined by Weiner (1930) as the ratio

$$\frac{G_{x_1x_2}(f)}{\sqrt{G_{x_1x_1}(f)\ G_{x_2x_2}(f)}}$$

where $G_{x_1x_2}(f)$ is the cross power spectral density function between x_1 and x_2, and $G_{x_ix_i}(f)$, i=1,2 are the auto power spectral density functions at frequency, f.

The magnitude-squared coherence (MSC) or simply the coherence is defined by (see, for example, Carter, Knapp and Nuttall (1973))

$$C_{x_1x_2}(f) = \frac{\left|G_{x_1x_2}(f)\right|^2}{G_{x_1x_1}(f)\ G_{x_2x_2}(f)} \qquad (2)$$

A useful property of the MSC is

$$0 \leq C_{x_1x_2}(f) \leq 1$$

provided the autospectra are positive (in particular non zero).

In order to attach some physical significance to what the coherence measures, consider that the ocean medium operators M_1 and M_2 are linear time-invariant filters. Thus $s_1(t)$ and $s_2(t)$ in equation (1) are the respective outputs of filters $M_1(f)$ and $M_2(f)$ when excited by source $s(t)$. When the noise, $n_i(t)$, is uncorrelated with the signal, $s(t)$, at the i-th sensor, the ratio of the received signal power at the output of the ocean channel to the corruptive noise power depends on the coherence between the source and the sensor. Specifically, from Carter, Knapp, and Nuttall (1973)

$$\frac{G_{s_i s_i}(f)}{G_{n_i n_i}(f)} = \frac{C_{sx_i}(f)}{1-C_{sx_i}(f)}, \quad i = 1,2 \tag{3}$$

That is, the received signal-to-noise ratio (SNR) at the i-th sensor depends on the coherence between the source and the received waveform. This result has been expressed by Carter and Knapp (1976) more compactly as

$$C_{x_1x_2}(f) = C_{sx_1}(f)\, C_{sx_2}(f) \tag{4}$$

These results apply only to the case where the medium can be accurately modeled by linear time-invariant filters corrupted by uncorrelated additive noise.

RESULTS. For the purpose of obtaining an ML estimate of delay, certain assumptions are required. In particular, for a signal emanating from a nearfield source and monitored in the presence of noise at two spatially separated sensors we require in equation (1) that $s_1(t) = s(t)$ and $s_2(t) = \alpha s(t+D)$. Further, we require that α is real and $s(t)$, $n_1(t)$, and $n_2(t)$ are real, jointly stationary, Gaussian random processes. Source $s(t)$ and noises, $n_1(t)$ and $n_2(t)$ are assumed to be mutually uncorrelated.

An estimated value of D is the hypothesized value τ that maximizes the generalized crosscorrelation (GCC) function defined by

$$\hat{R}(\tau) = \int_{-\infty}^{\infty} \hat{G}_{x_1x_2}(f) W(f) e^{j2\pi f\tau}\, df. \tag{5}$$

For $x_1(t)$ and $x_2(t)$ real, the ML estimator requires a particular weighting,

$$W(f) = H_1(f)H_2^*(f) = \frac{C_{x_1x_2}(f)}{\left|G_{x_1x_2}(f)\right| \left[1 - C_{x_1x_2}(f)\right]} \tag{6}$$

A complete derivation is given by Carter (1976).

Note from equation (6) that for the ML estimate of delay that $W(f)$ is real. The ML estimator is virtually equivalent to one proposed by Hannan and Thomson (1973). The ML estimator can be achieved by shaping $x_1(t)$ with filter $H_1(f)$ and $x_2(t)$ with filter $H_2(f)$ crosscorrelating the filter outputs, and observing what hypo-

thesized value of delay achieves a maximum.

The estimator can also be achieved by other methods. For example, Hahn (1975), Carter and Knapp (1976) and Carter (1976) present a method of filtering and summing the outputs, squaring and averaging in order to estimate the delay D. The processor could also be realized as a number of "best" estimates of D for a variety of frequencies. The ML estimate is then achieved by performing a weighted average across frequency. For example, Clay, Hinich and Shaman (1973) develop ML estimates of bearing (analogous to delay) for each of a number of different frequencies. To obtain a single estimate of source bearing, these individual estimates should then be combined with weighting dependent upon the particular underlying signal and noise characteristics.

The role of coherence in the weighting used for ML estimation of D is specified in equation (6). Note that those values of coherence near unity are most important; conversely, in those frequency bands where there is no source signal power (hence, where the received waveforms are incoherent), the delay estimate, as would be expected, receives no weight. The ML estimator is actually a function of more fundamental spectral measurements than those specified in equation (6). However, expressing the processor in more fundamental but unnormalized quantities can make interpretation more difficult, though equally correct.

The ML weighting agrees with MacDonald and Schultheiss (1969), and Hahn (1975) under specific conditions (including when there are two sensors and no attenuation).

VARIANCE OF GENERAL TIME DELAY ESTIMATORS. The variance of the time delay estimate in the neighborhood of the true delay for general weighting function W(f) is given by

$$\mathrm{Var}\left[\hat{D}-D\right] = \frac{\int_{-\infty}^{\infty} |W(f)|^2 (2\pi f)^2 G_{x_1x_1}(f) G_{x_2x_2}(f) \left[1 - C_{12}(f)\right] df}{P\left[\int_{-\infty}^{\infty} (2\pi f)^2 \left|G_{x_1x_2}(f)\right| W(f) df\right]^2} \qquad (7)$$

where P is the observation period (in seconds). From equations (6) and (7), the variance of the ML processor is

$$\mathrm{Var}^{ML}\left[\hat{D}-D\right] = \left[2P \int_0^{\infty} \frac{(2\pi f)^2 C_{12}(f)}{1 - C_{12}(f)} df\right]^{-1} \qquad (8)$$

The ML processor achieves the Cramér-Rao lower bound (see Carter (1976)). Therefore, the ML processor achieves a variance less than or equal to that provided by other correlation processors.

These results for variance can be related to MacDonald and Schultheiss (1969) as follows. Define the bearing to an acoustic source, as in Nuttall, Carter and Montavon (1974)

$$\phi = \arccos \frac{\xi D}{d} \tag{9}$$

where ξ is the speed of sound in the nondispersive medium and d is the sensor separation. Consider the case where the estimated D equals the true delay plus a perturbation. By a Taylor series expansion, it follows for the bearing error defined by the difference between the true bearing and the estimated bearing that the standard deviation of the bearing error is given by (Carter (1976)):

$$\left[\mathrm{Var}\,(\hat{\phi} - \phi)\right]^{\frac{1}{2}} = \frac{\xi}{d \sin \phi} \left[\mathrm{Var}\,(\hat{D} - D)\right]^{\frac{1}{2}} \tag{10}$$

The term $d \sin \phi$ can be viewed as the effective array length (sensor separation) physically steered at the source. The combining of equations (8) and (10) suggests that, in order to reduce the variance of the bearing estimate, the observation period and the sensor separation should be made as large as possible. This agrees with one's intuition and the results of MacDonald and Schultheiss (1969). Further, the fact that equation (10) depends on the effective array length physically steered toward the source suggests the desirability of sensor mobility to maximize $\sin \phi$ when d is limited.

REFERENCES.

1. G.C. Carter (1976), Time Delay Estimation, University of Connecticut, PH.D. Dissertation, Storrs, Connecticut (also NUSC Report 5335).

2. G.C. Carter and C.H. Knapp (1976), "Time Delay Estimation," Proc. IEEE 1976 International Conference on Acoustics, Speech and Signal Processing, pp. 357-360.

3. G.C. Carter, C.H. Knapp and A.H. Nuttall (1973), "Estimation of the Magnitude-Squared Coherence Function via Overlapped

Fast Fourier Transform Processing," IEEE Trans. on Audio Electroacoustics, Vol. AU-21, p. 337-344.

4. C.S. Clay, M.J. Hinich and P. Shaman (1973), "Error Analysis of Velocity and Direction Measurements of Plane Waves Using Thick Large-Aperture Arrays," J. Acoust. Soc. Amer., Vol. 53, No. 4, pp. 1161-1166.

5. W.R. Hahn (1975), "Optimum Signal Processing for Passive Sonar Range and Bearing Estimation," J. Acoust. Soc. Amer., Vol. 58, No. 1, pp. 201-207.

6. E.H. Hannan and P.J. Thomson (1973), "Estimating Group Delay," Biometrika, Vol. 60, pp. 241-253.

7. V.H. MacDonald and P.M. Schultheiss (1969), "Optimum Passive Bearing Estimation," J. Acoust. Soc. Amer., Vol. 46, pp. 37-43.

8. A.H. Nuttall, G.C. Carter, and E.M. Montavon (1974), "Estimation of the Two-Dimensional Spectrum of the Space-Time Noise Field for a Sparse Line Array," J. Acoust. Soc. Amer., Vol. 55, pp. 1034-1041.

9. N. Weiner (1930), "Generalized Harmonic Analysis," Acta Math, Vol. 55, pp. 117-258.

NUSC Technical Memorandum 771112
10 June 1977

On the Variance of the Phase Estimate of the Cross Spectrum and Coherence

A. H. Nuttall

ABSTRACT

The variance of the phase estimate of the cross spectrum and coherence is numerically evaluated for values of the true magnitude-squared coherence, S, equal to 0(.1).9 and .99, and for the number of independent averages, n, equal to 1(1)500. It is found that the approximation $(1 - S)/(SK)$, where $K = 2n$ for independent averages, is a good one for all S and for $K > 10$, although the approximation is generally optimistic. A useful recursion formula for the probability density function of the phase estimate is also derived. The danger of employing a Gaussian approximation is demonstrated dramatically in a numerical example. An extension of the equivalent degrees of freedom to complex averages is made and suggested for use in cross spectral estimation.

TABLE OF CONTENTS

REVERSE BLANK

INTRODUCTION

Approximate expressions for the variance of the phase estimate of the cross spectrum and coherence are given in Ref. 1, pp. 378-9, and Ref. 2, eq. (25B). However, both of these results are limited in applicability to the region where the variance is small in comparison with unity. Here we will use the results of Ref. 3 and evaluate numerically the exact variance of the phase estimate for the complete range of possibilities. As a by-product, we will be able to tell exactly when the approximation is accurate.

The method of processing used to obtain the estimates is given in Refs. 1-3, and will not be elaborated on here, for the sake of brevity. The reader is referred to these references for additional details and assumptions.

RECURSION EQUATION FOR PROBABILITY DENSITY FUNCTION

We let γ denote the true magnitude coherence, and ϕ_0 denote the true argument (phase) of the cross spectrum or coherence, of two stationary random processes. Then if ϕ is the estimate of the phase, the probability density function of ϕ, based on an average of n statistically independent pairs of samples, is given in Ref. 3, eqs. 4.100 and 4.102 by the form

$$p_n(\phi) = \frac{\delta^n}{2\pi}\left[1 - \frac{2nz}{(1-z^2)^{n+\frac{1}{2}}}\int_{\arcsin z}^{\pi/2} dv \cos^{2n} v\right], \tag{1}$$

where we have added sub-n to the probability density function for distinction, and where

$$\delta = 1 - \gamma^2 \qquad (\text{eq. } 4.26), \tag{2}$$

$$z = -\gamma\cos(\phi - \phi_0) \qquad (\text{eq. } 4.98). \tag{3}$$

In order to develop a useful recursion for (1), let

$$I_n(b) = \int_b^{\pi/2} dv \cos^{2n} v. \tag{4}$$

Then for $n \geq 1$ (Ref. 4, eq. 2.510, line 5),

$$I_n(b) = \frac{1}{2n}\left[(2n-1) I_{n-1}(b) - \sin b \cos^{2n-1} b\right]. \tag{5}$$

Therefore

$$I_n(\arcsin z) = \frac{1}{2n}\left[(2n-1) I_{n-1}(\arcsin z) - z(1-z^2)^{n-\frac{1}{2}}\right], \tag{6}$$

and (1) becomes

$$p_n(\phi) = \frac{\delta^n}{2\pi}\left[1 - \frac{2nz}{(1-z^2)^{n+\frac{1}{2}}} I_n(\arcsin z)\right]$$

$$= \frac{\delta^n}{2\pi}\left[\frac{1}{1-z^2} - \frac{(2n-1)z}{(1-z^2)^{n+\frac{1}{2}}} I_{n-1}(\arcsin z)\right]. \qquad (7)$$

But since (for $n \geq 2$)

$$p_{n-1}(\phi) = \frac{\delta^{n-1}}{2\pi}\left[1 - \frac{2(n-1)z}{(1-z^2)^{n-\frac{1}{2}}} I_{n-1}(\arcsin z)\right], \qquad (8)$$

we can solve for $I_{n-1}()$ and substitute it in $p_n(\phi)$ to obtain the recursion:

$$p_n(\phi) = \frac{\delta}{2(n-1)(1-z^2)}\left[-\frac{1}{2\pi}\delta^{n-1} + (2n-1)p_{n-1}(\phi)\right], \; n \geq 2. \qquad (9)$$

To start this recursion, we need:

$$p_1(\phi) = \frac{\delta}{2\pi}\left[1 - \frac{2z}{(1-z^2)^{3/2}} \int_{\arcsin z}^{\pi/2} dv \cos^2 v\right], \qquad (10)$$

which is given by

$$p_1(\phi) = \frac{\delta}{2\pi(1-z^2)}\left[1 - \frac{z}{\sqrt{1-z^2}}\left(\frac{\pi}{2} - \arcsin z\right)\right]. \qquad (11)$$

Equations (9) and (11) constitute a useful recursion procedure for evaluating high-order probability density functions of the phase estimate.

VARIANCE OF THE PHASE ESTIMATE

For $\phi_0 = 0$ (or for a redefined origin of phase relative to ϕ_0), the mean of ϕ is zero, since probability density function $p_n(\phi)$ in (1) is obviously even about zero. Therefore the variance of ϕ is

$$\overline{\phi^2} = \int_{-\pi}^{\pi} d\phi\, \phi^2 p_n(\phi) = 2\int_0^{\pi} d\phi\, \phi^2 p_n(\phi). \tag{12}$$

A closed form expression for (12) does not appear possible. Hence, we use numerical integration to evaluate (12). Let $\Delta = \pi/J$ be the increment in approximating (12). Then

$$\overline{\phi^2} \cong 2\Delta \sum_{k=0}^{J} (k\Delta)^2 p_n(k\Delta) w_k \tag{13}$$

$$= \frac{2\Delta^3}{3}\left[J^2 p_n(\pi) + \sum_{k=1}^{J-1} k^2 \{3-(-1)^k\} p_n(k\Delta)\right], \tag{14}$$

where $\{w_k\}$ is a general set of integration weights in (13), and where (14) applies for Simpson weights. A program for the evaluation and plotting of (14) is presented in Appendix A. The results are given in Figure 1, where we have defined

$$S = \gamma^2 = \text{magnitude-squared coherence}, \tag{15}$$

$$K = 2n = \text{equivalent degrees of freedom}. \tag{16}$$

Straight lines have been drawn between the integer values of n ($K = 2, 4, 6, \ldots$) for ease of interpretation. The reason for definition (16) is considered in the next section.

An approximation for the variance, $\overline{\phi^2}$, is given by

$$\overline{\phi^2} \cong \frac{1-S}{SK}, \tag{17}$$

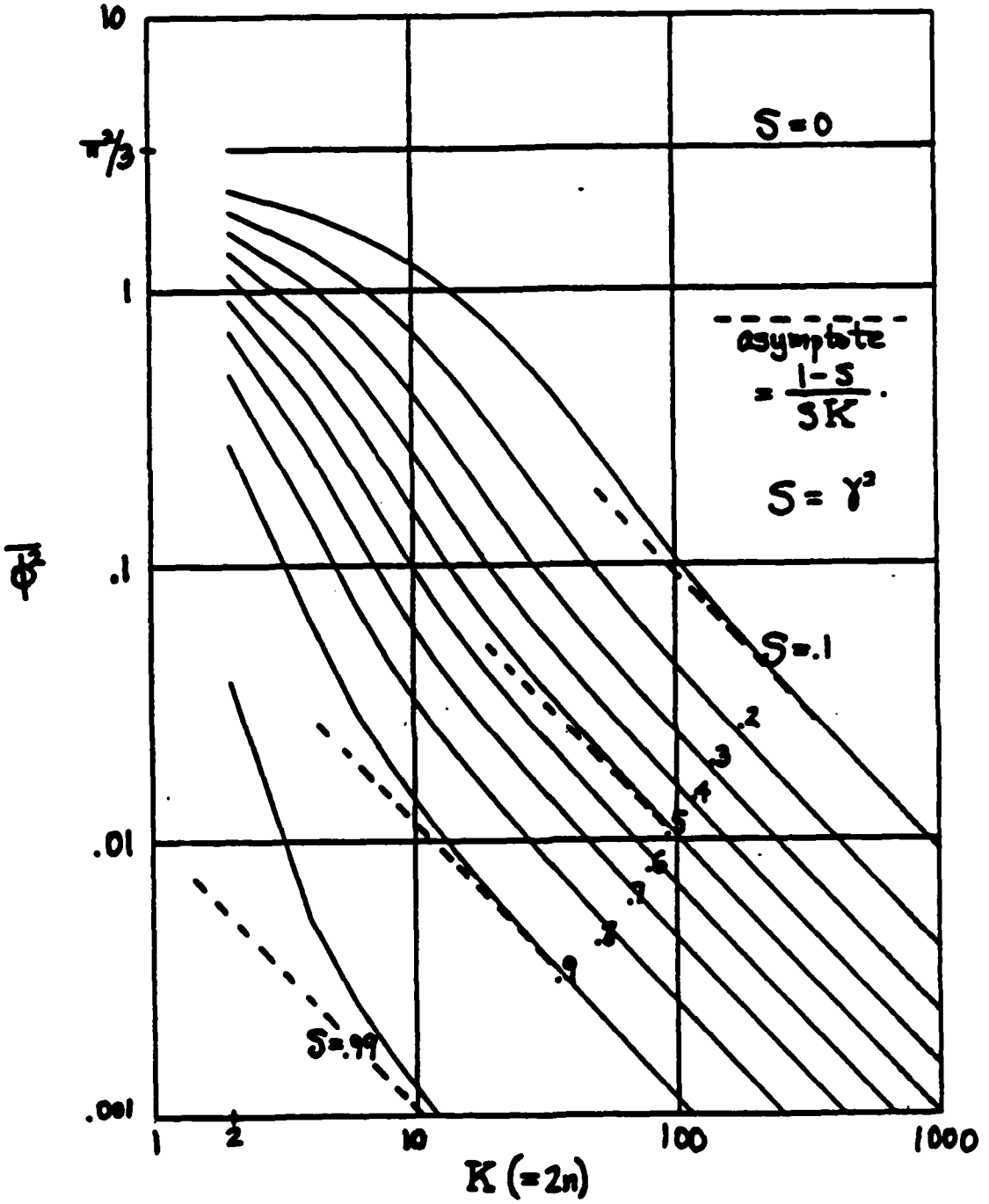

Figure 1. Variance of Phase Estimate

as mentioned in the Introduction; this result is claimed accurate if $SK \gg 1$. The asymptote (17) for large K is shown as dashed lines in Figure 1 for $S = .1, .5, .9$, and .99, and shows quantitatively when (17) can be used. In particular, if $SK > 20$, the error in using (17) appears to be only a few per cent.

USE OF RESULTS FOR OVERLAPPED PROCESSING

In References 2 and 5, spectral estimation via overlapped FFT processing of windowed data was considered, and an equivalent degrees of freedom was defined as:

$$K = \frac{2n}{\sum_{k=-w+1}^{n-1} \left(1 - \frac{|k|}{n}\right) \left| \frac{\phi_w(ks)}{\phi_w(0)} \right|^2}, \qquad (18)$$

where n is the total number of (overlapped) pieces entering the spectral estimate, $w(t)$ is the data window, $\phi_w(\tau)$ is the autocorrelation of window w, and s is the shift between adjacent overlapping windows. An informative interpretation of (18) for complex averages is presented in Appendix B.

When shift s is greater than the length of window w, the autocorrelation $\phi_w(ks)$ is zero except for $k=0$, in which case (18) yields $K = 2n$; this is the case treated in Ref. 1 and plotted above in Figure 1. When shift s is less than the length of window w, K decreases below the value $2n$, and in fact as $s \to 0$, $K \to 2$. Thus K is bounded by 2 and $2n$, depending on the amount of overlap of the individual windows.

The exact derivation of the variance of the phase estimate of the cross spectrum and coherence for overlapped processing appears to be very difficult. However, an approximation is available via use of Figure 1, if K is computed via (18), for the particular window and overlap of interest; the justification for this approach is presented in Appendix B. The accuracy of this approximation is unknown.

COMMENT

An alternative technique for approximating the variance of the phase estimate, which utilizes a Gaussian assumption, is presented in Appendix C. It is found to grossly overestimate the variance in some cases, and points out the danger of using the Gaussian assumption without care.

APPENDIX A

PROGRAM FOR EVALUATION AND PLOT OF (14)

```
      PARAMETER NT=500        @ N=1(1)NT
      DOUBLE PRECISION Q(NT),P(NT),K2,P1,P2,O2PI,
     $DEL,TDEL3,GAMSQ,DELTA,D2PI,DELTA2,GAMMA,PHI,KSQ
      DIMENSION X(NT),S(NT),Z(200)
      JCAP=512
      K1=JCAP-1
      K2=JCAP**2
      PI=3.14159265358979324D0
      P2=.5*PI
      O2PI=.5/PI
      DEL=PI/JCAP
      TDEL3=2.*DEL**3/3.D0
      CALL MODESG(Z,0)
      CALL SUBJEG(Z,0.,-3.,3.,1.)
      CALL OBJCTG(Z,1200.,335.,2900.,2735.)
      CALL SETSMG(Z,30,2.)
      DO 11 I=0,3
      CALL LINESG(Z,0,FLOAT(I),-3.)
11    CALL LINESG(Z,1,FLOAT(I),1.)
      DO 12 I=-3,1
      CALL LINESG(Z,0,0.,FLOAT(I))
12    CALL LINESG(Z,1,3.,FLOAT(I))
      DO 6 N=1,NT
6     X(N)=LOG10(2.*N)
      DO 1 IGAMSQ=0,10
      GAMSQ=.1D0*IGAMSQ
      IF(IGAMSQ.EQ.10) GAMSQ=.9900
      DELTA=1.-GAMSQ
      D2PI=DELTA*O2PI
      DELTA2=.5*DELTA
      GAMMA=SQRT(GAMSQ)
      PHI=PI
      CALL PRECUR
      DO 2 N=1,NT
2     Q(N)=K2*P(N)
      DO 3 K=1,K1
      KSQ=K**2*(3.-(-1.)**K)
      PHI=K*DEL
      CALL PRECUR
      DO 4 N=1,NT
4     Q(N)=Q(N)+P(N)*KSQ
3     CONTINUE
```

```
      DO 5 N=1,NT
5     S(N)=Q(N)*TDEL3
      PRINT 88, GAMSQ
88    FORMAT(/D20.2)
      NT9=NT-9
      DO 7 I=1,NT9,10
7     PRINT 8, S(I),S(I+1),S(I+2),S(I+3),S(I+4),
     $S(I+5),S(I+6),S(I+7),S(I+8),S(I+9)
8     FORMAT(2X,10E13.8)
      DO 9 I=1,NT
9     S(I)=LOG10(S(I))
      CALL LINESG(Z,NT,X,S)
1     CONTINUE
      CALL PAGEG(Z,0,1,1)
      CALL EXITG(Z)
      SUBROUTINE PRECUR
      DOUBLE PRECISION ZI,Z2,DZ,DELTAN
      ZI=-GAMMA*COS(PHI)
      Z2=1./(1.-ZI**2)
      P(1)=D2PI*Z2*(1.-ZI*SQRT(Z2)*(P2-ASIN(ZI)))
      DZ=DELTA2*Z2
      DELTAN=1.
      DO 1 N=2,NT
      DELTAN=DELTAN*DELTA
1     P(N)=DZ/(N-1.)*(-D2PI*DELTAN+(2.*N-1.)*P(N-1))
      RETURN
      END
```

APPENDIX B

EQUIVALENT DEGREES OF FREEDOM FOR COMPLEX AVERAGES

General Definition of Effective Number of Independent Samples

Suppose samples $\{z_k\}_1^n$ are n complex, statistically independent, identically distributed, random variables. Define complex sum (average)

$$w = \sum_{k=1}^{n} z_k . \tag{B-1}$$

Then its mean is

$$\bar{w} = n\bar{z}, \tag{B-2}$$

and its variance is

$$\sigma_w^2 \equiv \overline{|w-\bar{w}|^2} = \overline{|w|^2} - |\bar{w}|^2 = n\sigma_z^2, \tag{B-3}$$

where we have defined

$$\sigma_z^2 \equiv \overline{|z-\bar{z}|^2} = \overline{|z|^2} - |\bar{z}|^2 . \tag{B-4}$$

Therefore the relative stability of w is (defined as)

$$\frac{|\bar{w}|^2}{\sigma_w^2} = n\frac{|\bar{z}|^2}{\sigma_z^2} . \tag{B-5}$$

Now when $\{z_k\}$ are correlated, this equation can be taken as a definition of the effective number of statistically independent terms in the sum (B-1) ; that is, define (for identically distributed variables)

$$n_e \equiv \frac{|\bar{w}|^2/\sigma_w^2}{|\bar{z}|^2/\sigma_z^2} . \tag{B-6}$$

Equation (B-6) is a satisfactory definition provided that $n_e \leq n$; if not, some other approach is necessary, because n_e should never be larger than n.

Effective Number for Correlated Samples

Let us express each random variable in terms of its mean and a zero-mean component according to

$$z_k = \bar{z} + a_k , \tag{B-7}$$

where

$$\overline{a_k} = 0 , \quad \overline{a_k^2} = \sigma_z^2 . \tag{B-8}$$

Also let the zero-mean component of z_k satisfy

$$\overline{a_k a_\ell^*} = \sigma_z^2 \rho_{k-\ell} \qquad (\rho_0 = 1), \tag{B-9}$$

where $\{\rho_n\}$ can be complex. Then from (B-1) and (B-7),

$$w = n\bar{z} + \sum_{k=1}^{n} a_k , \tag{B-10}$$

and

$$\bar{w} = n\bar{z},$$

$$\sigma_w^2 = \sum_{k=1}^{n}\sum_{\ell=1}^{n} \overline{a_k a_\ell^*} = \sigma_z^2 \, n \sum_{k=-n+1}^{n-1} \left(1 - \frac{|k|}{n}\right)\rho_k . \tag{B-11}$$

Substituting these results in (B-6), we obtain, for correlated random variables,

$$n_e = \frac{n}{\sum_{k=-n+1}^{n-1} \left(1 - \frac{|k|}{n}\right) \rho_k} \,. \qquad (B-12)$$

This is satisfactory if the denominator of (B-12) is greater than (or equal to) 1. For example, if $n = 2$, then $n_e = 2/(1 + \mathrm{Re}\,\rho_1)$, which dictates that $\mathrm{Re}\,\rho_1 \geq 0$ for a meaningful definition.

As particular examples of (B-12), we have:

$$\begin{aligned} &(a)\quad \rho_k = \delta_{k0}\,, \quad n_e = n \\ &(b)\quad \rho_k = 1\,, \quad n_e = 1 \\ &(c)\quad n = 1\,, \quad n_e = 1 \end{aligned} \qquad (B-13)$$

These correspond to (a) uncorrelated, (b) completely correlated, and (c) one sample; the values of n_e agree with physical interpretation.

Application to Product of Gaussian Random Variables

Suppose random variables $\{z_k\}$ are given by

$$z_k = x_k y_k^*\,, \quad 1 \leq k \leq n, \qquad (B-14)$$

where $\{x_k\}_1^n$ and $\{y_k\}_1^n$ are zero-mean complex Gaussian random variables. Then

$$w = \sum_{k=1}^{n} x_k y_k^*\,, \qquad (B-15)$$

and

$$\bar{z} = \bar{z}_k = \overline{x_k y_k^*} \equiv \overline{x y^*}\,. \qquad (B-16)$$

Also

$$a_k = z_k - \bar{z} = x_k y_k^* - \overline{xy^*}, \tag{B-17}$$

with

$$\overline{a_k a_\ell^*} = \overline{(z_k - \bar{z})(z_\ell^* - \bar{z}^*)} = \overline{z_k z_\ell^*} - |\bar{z}|^2 = \overline{z_k z_\ell^*} - |\overline{xy^*}|^2. \tag{B-18}$$

In order to evaluate $\overline{z_k z_\ell^*}$, we need the property that

$$\overline{c_1 c_2 c_3 c_4} = \overline{c_1 c_2}\,\overline{c_3 c_4} + \overline{c_1 c_3}\,\overline{c_2 c_4} + \overline{c_1 c_4}\,\overline{c_2 c_3} \tag{B-19}$$

for zero-mean complex Gaussian random variables $\{c_j\}$; this property is derived in the next subsection. Then we have

$$\overline{z_k z_\ell^*} = \overline{x_k y_k^* x_\ell^* y_\ell} = |\overline{xy^*}|^2 + \overline{x_k x_\ell^*}\;\overline{y_k^* y_\ell} + \overline{x_k y_\ell}\;\overline{y_k^* x_\ell^*}, \tag{B-20}$$

from which there follows

$$\overline{a_k a_\ell^*} = \overline{x_k x_\ell^*}\;\overline{y_k^* y_\ell} + \overline{x_k y_\ell}\;\overline{y_k^* x_\ell^*}. \tag{B-21}$$

Proof of Fourth-Order Average Property (B-19)

Let

$$c_j = r_{j0} + i\, r_{j1} = \sum_{k=0}^{1} i^k r_{jk}, \tag{B-22}$$

where $\{r_{jk}\}$ are zero-mean real Gaussian random variables. Then

$$\overline{c_1 c_2 c_3 c_4} = \sum_{k\ell mn=0}^{1} i^{k+\ell+m+n} \overline{r_{1k} r_{2\ell} r_{3m} r_{4n}}$$

$$= \sum_{k\ell mn=0}^{1} i^{k+\ell+m+n} \left[\overline{r_{1k} r_{2\ell}}\ \overline{r_{3m} r_{4n}} + \overline{r_{1k} r_{3m}}\ \overline{r_{2\ell} r_{4n}} + \overline{r_{1k} r_{4n}}\ \overline{r_{2\ell} r_{3m}} \right]$$

$$= \left[\sum_{k\ell=0}^{1} i^{k+\ell} \overline{r_{1k} r_{2\ell}} \right] \left[\sum_{mn=0}^{1} i^{m+n} \overline{r_{3m} r_{4n}} \right] + \left[\sum_{km=0}^{1} i^{k+m} \overline{r_{1k} r_{3m}} \right] \left[\sum_{\ell n=0}^{1} i^{\ell+n} \overline{r_{2\ell} r_{4n}} \right]$$

$$+ \left[\sum_{kn=0}^{1} i^{k+n} \overline{r_{1k} r_{4n}} \right] \left[\sum_{\ell m=0}^{1} i^{\ell+m} \overline{r_{2\ell} r_{3m}} \right]$$

$$= \overline{c_1 c_2}\ \overline{c_3 c_4} + \overline{c_1 c_3}\ \overline{c_2 c_4} + \overline{c_1 c_4}\ \overline{c_2 c_3} . \qquad (B-23)$$

No special properties for $\overline{c_j c_k}$ or $\overline{c_j c_k^*}$ need be assumed for this property to hold.

Specialization to Cross-Spectral Estimation

In order to utilize (B-12), we need to evaluate (B-21) and substitute it in (B-9), so as to determine $\{\rho_k\}$. Now for cross-spectral estimation, x_k and y_k are given in Ref. 2, eq. (3) as (suppressing f-dependence)

$$x_k = \int dt\ \exp(-i2\pi ft)\, w_k(t)\, x(t),$$
$$y_k = \int dt\ \exp(-i2\pi ft)\, w_k(t)\, y(t), \qquad (B-24)$$

Then

$$\overline{X_k X_\ell^*} = \iint dt_1\, dt_2\, \exp\left(-i 2\pi f (t_1 - t_2)\right) w_k(t_1)\, y_\ell(t_2)^*\, R_{xx}(t_1 - t_2)$$

$$= \int du\, G_{xx}(f-u)\, W_k(u)\, W_\ell(u)^* \qquad (B-25)$$

$$= \int du\, G_{xx}(f-u)\, |W(u)|^2 \exp\left(-i 2\pi u (k-\ell) s\right),$$

where s is the shift of adjacent data windows. Now if f is greater than the width of window $|W|^2$, and if the window width is narrower than the finest detail in spectrum G_{xx} at frequency f, we have

$$\overline{X_k Y_\ell^*} \cong G_{xx}(f)\, \phi_w\left((k-\ell)s\right)^*, \qquad (B-26)$$

where ϕ_w is the autocorrelation of data window w. In a similar fashion, there follows

$$\overline{Y_k Y_\ell^*} \cong G_{yy}(f)\, \phi_w\left((k-\ell)s\right)^*. \qquad (B-27)$$

And if f is larger than the width of window $|W|^2$, it may be shown that

$$\overline{X_k Y_\ell} \cong 0; \qquad (B-28)$$

see Ref. 2, eq. (A14) et seq. Substituting (B-26)-(B-28) in (B-21), we obtain

$$\overline{a_k a_\ell^*} = G_{xx}(f)\, G_{yy}(f) \left| \phi_w\left((k-\ell)s\right) \right|^2, \qquad (B-29)$$

and therefore, by (B-9),

$$\rho_k = \left| \frac{\phi_w(ks)}{\phi_w(0)} \right|^2 . \qquad (B-30)$$

Then finally, (B-12) yields

$$n_e = \frac{n}{\sum_{k=-n+1}^{n-1} \left(1 - \frac{|k|}{n}\right) \left| \frac{\phi_w(ks)}{\phi_w(0)} \right|^2} . \qquad (B-31)$$

As noted under (B-12), the denominator of (B-31) certainly satisfies the requirement of being greater than or equal to 1, for any window w.

Equivalent Degrees of Freedom for Cross-Spectral Estimation

Equation (B-31) gives the effective number of independent terms in the sum (B-15), when x_k and y_k are given by (B-24). However, to determine the equivalent degrees of freedom, we expand (B-15) in terms of its real and imaginary parts as

$$\begin{aligned} w &= \sum_{k=1}^{n} x_k y_k^* = \sum_{k=1}^{n} (x_{kr} + i x_{ki})(y_{kr} - i y_{ki}) \\ &= \sum_{k=1}^{n} \left[(x_{kr} y_{kr} + x_{ki} y_{ki}) + i (x_{ki} y_{kr} - x_{kr} y_{ki}) \right] . \end{aligned} \qquad (B-32)$$

Since the real and imaginary components of w each have 2n terms in their averages, it is appropriate to define the equivalent degrees of freedom of random variable w as

$$K \equiv 2n_e = \frac{2n}{\sum_{k=-n+1}^{n-1} \left(1 - \frac{|k|}{n}\right) \left| \frac{\phi_w(ks)}{\phi_w(0)} \right|^2} . \qquad (B-33)$$

As a special case, for non-overlapping windows, $K = 2n$, which is the result used in the main text. And if $y_n = x_n$, $w = \sum_{n=1}^{N} |x_n|^2 = \sum_{n=1}^{N} (x_{nr}^2 + x_{ni}^2)$, which is the standard quantity for real variables, such as encountered in auto-spectral estimation. The result (B-33) is the one presented in Ref. 2, eq. (12). (Equation (9) in Ref. 2 should be defined as a measure of stability, and not as the equivalent degrees of freedom.)

APPENDIX C

APPROXIMATION TO VARIANCE OF PHASE ESTIMATE

From Ref. 2, eq. 22 (suppressing f dependence), the cross spectrum estimate $\hat{G}_{xy}$ can be expressed as

$$\hat{G}_{xy}\exp(-i\hat{P}_{xy}) = |G_{xy}| + \hat{a} + i\hat{b} = u + iv = r\exp(i\phi), \tag{C-1}$$

where P_{xy} is the true phase, and $|G_{xy}|$ is the true magnitude of the cross spectrum. We make the simplifying assumption (of unknown validity) that $\hat{a}$ and $\hat{b}$ are Gaussian; for small K, this could yield misleading conclusions. Then from Ref. 2, eqs. (15) and (19),

$$\begin{aligned}
&\overline{\hat{a}} = \overline{\hat{b}} = 0, \\
&\overline{\hat{a}^2} = \sigma_a^2 = \frac{G_{xx}G_{yy}}{K}(1+S), \\
&\overline{\hat{b}^2} = \sigma_b^2 = \frac{G_{xx}G_{yy}}{K}(1-S), \\
&\overline{\hat{a}\hat{b}} = 0,
\end{aligned} \tag{C-2}$$

where

$$S = |\gamma_{xy}|^2. \tag{C-3}$$

Then the Gaussian assumption allows us to express the probability density function of u and v in (C-1) as

$$p(u,v) = \frac{1}{2\pi\sigma_a\sigma_b}\exp\left[-\frac{(u-M)^2}{2\sigma_a^2} - \frac{v^2}{2\sigma_b^2}\right], \tag{C-4}$$

where

$$M \equiv |G_{xy}|. \tag{C-5}$$

The probability density function of r and ϕ defined in (C-1) is then

$$p(r,\phi) = \frac{r}{2\pi\sigma_a\sigma_b}\exp\left[-\frac{(r\cos\phi - M)^2}{2\sigma_a^2} - \frac{(r\sin\phi)^2}{2\sigma_b^2}\right], 0 < r, \quad |\phi| < \pi. \tag{C-6}$$

The first-order probability density function of ϕ itself is available from (C-6) by integrating on r over the range $(0,\infty)$. By use of the result

$$\int_0^\infty dx\, x \exp\left(-\tfrac{1}{2}\alpha^2 x^2 + \beta x\right) = \frac{1}{\alpha^2}\left[1 + \sqrt{2\pi}\frac{\beta}{\alpha}\exp\left(\frac{\beta^2}{2\alpha^2}\right)\Phi\left(\frac{\beta}{\alpha}\right)\right], \tag{C-7}$$

where

$$\Phi(t) \equiv \int_{-\infty}^{t} dx\,(2\pi)^{-1/2}\exp(-x^2/2), \tag{C-8}$$

we find, after simplification and use of (C-2),

$$p(\phi) = \frac{1}{2\pi}\frac{\sqrt{1-S^2}}{1 - S\cos 2\phi}\exp\left[-\frac{K}{2}\frac{S}{1+S}\right]\left[1 + \sqrt{2\pi}\, r \exp(r^2/2)\Phi(r)\right], |\phi| < \pi, \tag{C-9}$$

where

$$r = \left[K\frac{S(1-S)}{(1+S)(1-S\cos 2\phi)}\right]^{1/2}\cos\phi. \tag{C-10}$$

The two fundamental parameters of $p(\phi)$ are K and S.

Since $p(\phi)$ is even in ϕ, $\bar{\phi}=0$. The variance $\overline{\phi^2}$ is numerically computed via

$$\overline{\phi^2} = 2\int_0^{\pi} d\phi\, \phi^2 p(\phi), \qquad (C\text{-}11)$$

and is presented in Figure C.1, for $S=0(.1).9$. The range of K given is (1, 1000); however, physical significance should be attached only to $K \geq 2$ (see (18)).

Comparison of Figure C.1 with Figure 1 immediately reveals that gross overestimates of the variance can result from use of (C-9) - (C-11). For example, at $K=10$, $S=.9$, the result in Figure C.1 is ten times greater than that in Figure 1. The results are in better agreement for small S, like 0.1. On the other hand, for $S=.99$, the discrepancy would be greater than an order of magnitude for a wide range of K. For large K, the asymptote (17) is once again approached in Figure C.1, as indicated by the dashed lines.

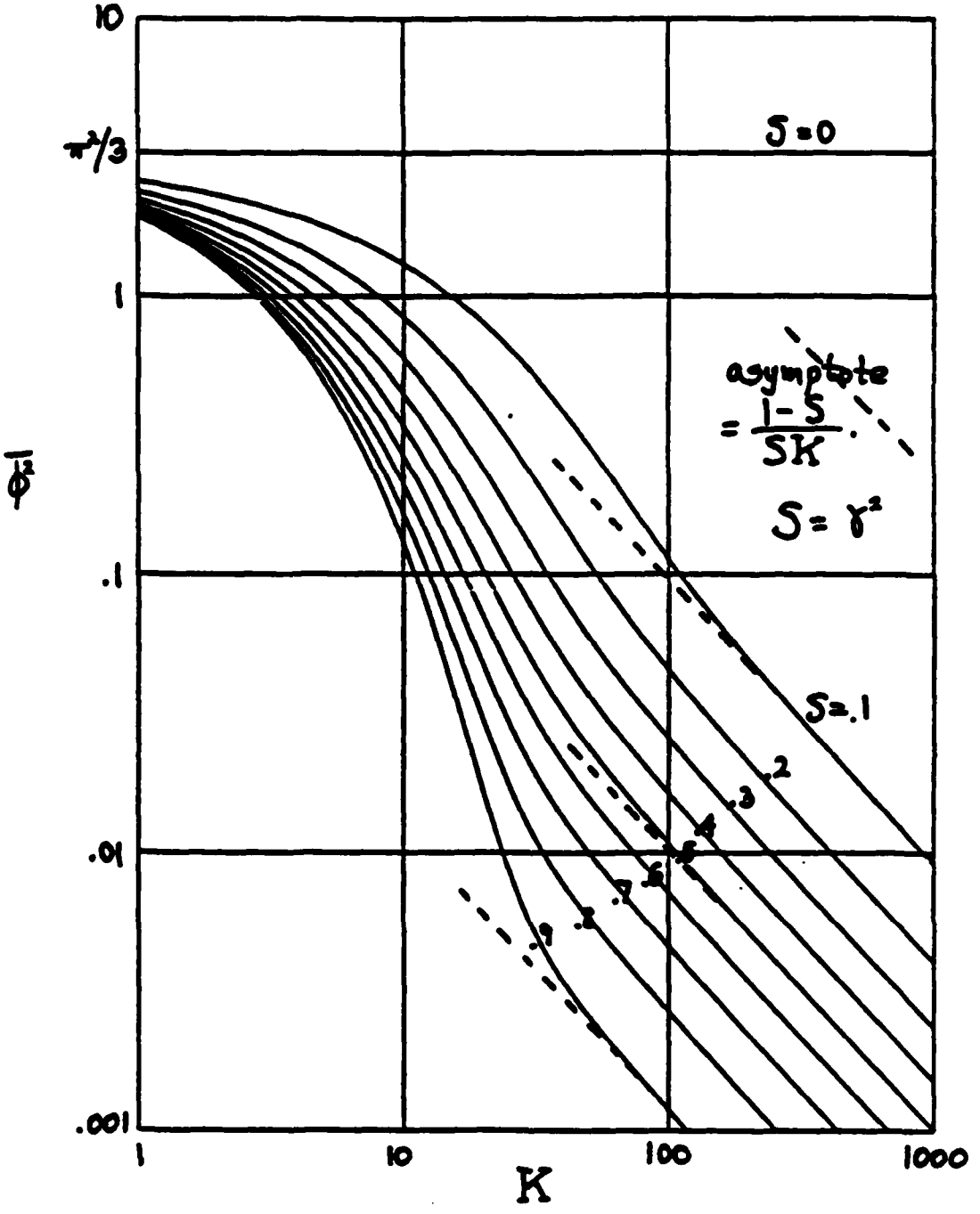

Figure C.1 Approximation to Variance of Phase Estimate

REFERENCES

1. G. M. Jenkins and D. G. Watts, Spectral Analysis and its Applications, Holden-Day, San Francisco, 1969.

2. A. H. Nuttall, "Estimation of Cross-Spectra via Overlapped FFT Processing", NUSC Technical Report 4169-S, 11 July 1975.

3. N. R. Goodman, "On the Joint Estimation of the Spectra, Cospectrum, and Quadrature Spectrum of a Two-Dimensional Stationary Gaussian Process", Technical Report No. 8, David Taylor Model Basin, and Science Paper No. 10, Engineering Statistics Lab, College of Engineering, New York University, March 1957.

4. I. S. Gradshteyn and I. W. Ryzhik, Table of Integrals, Series, and Products, Academic Press, N.Y., 1965.

5. A. H. Nuttall, "Spectral Estimation by Means of Overlapped FFT Processing of Windowed Data", NUSC Technical Report 4169, 13 October 1971.

NUSC Technical Report 5729
14 November 1977

Positive Definite Spectral Estimate and Stable Correlation Recursion for Multivariate Linear Predictive Spectral Analysis

A. H. Nuttall

ABSTRACT

The questions regarding a positive definite spectral estimate and a stable correlation recursion (raised in NUSC Technical Report 5501) are answered in the affirmative for the particular choice of weighting recommended in the above reference. A modified and updated FORTRAN program for multivariate spectral analysis, which incorporates calculation of the correlation matrices via recursion, and the aliased correlation matrices via a fast Fourier transform (FFT), are included.

TABLE OF CONTENTS

LIST OF SYMBOLS*

M_{p-1}	Auxiliary matrix
$R_m^{(p)}$	m-th order correlation matrix
$\mathcal{R}_m^{(p)}$	Block Toeplitz matrix
$Q_m^{(p)}$	Auxiliary block matrix
w_k, $\tilde{w}_k$	Trapezoidal weights
$\hat{R}_m$	Aliased correlation matrix
G_k	$G\left(\frac{k}{N_F\Delta}\right)$
$G_k^{(\ell j)}$	Element ℓ,j of G_k
u_k	Auxiliary scalar sequence
FFT	Fast Fourier transform

*This list of symbols is supplementary to that in an earlier report,[1] to which this report is a sequel.

POSITIVE DEFINITE SPECTRAL ESTIMATE AND STABLE CORRELATION RECURSION FOR MULTIVARIATE LINEAR PREDICTIVE SPECTRAL ANALYSIS

INTRODUCTION

A generalization of Burg's algorithm for spectral analysis to the multivariate case was the subject of an earlier report.[1] All the desirable properties of the univariate case were shown to hold true, except that it was not proven that the residual matrix was positive definite, nor that the correlation recursion was stable. Both of these assumptions can be affirmed by drawing on the results in Strand[2] and Burg.[3]

In addition to affirming these two assumptions, this report contains a modified and updated FORTRAN program that supersedes the program previously reported.[1] The modified program incorporates some more-explanatory format statements, the calculation of the (normalized) correlation matrices via recursion, and the aliased (normalized) correlation matrices by means of a Fast Fourier Transform (FFT).

This report is a sequel to an earlier report.[1] In order to eliminate duplication, that report is referenced for background information, a list of symbols used, and processing technique. We shall draw freely on that report; for example, equation (5) of the earlier report will be denoted by (5).[1]

POSITIVE DEFINITE RESIDUAL MATRIX

The (p-1)-th order forward residual matrix, U_{p-1}, was defined in equation (95).[1] We wish to show that U_p is positive definite; the following proof is based on reference 2, equations (3.25-3.32).

From equation (H-5),[1] we have, using the Hermitian property of U_p and V_p,

$$U_p = U_{p-1} - A_p^{(p)} V_{p-1} A_p^{(p)H} ; \qquad (1)$$

and from equation (137),[1] eliminating $B_p^{(p)H}$,

$$A_p^{(p)} V_{p-1} = U_{p-1} S_{p-1}^{(ya)-1} \left(2 S_{p-1}^{(ya)} - A_p^{(p)} S_{p-1}^{(b*a)} \right). \qquad (2)$$

Notice that we have made specific use of the inverse weighting in equation (136).[1] Substituting equation (2) into equation (1), we find

$$U_p = U_{p-1} - U_{p-1} S_{p-1}^{(yy)^{-1}} \left(2S_{p-1}^{(ya)} - A_p^{(p)} S_{p-1}^{(aa)}\right) A_p^{(p)H} \quad ; \tag{3}$$

therefore,

$$S_{p-1}^{(yy)} U_{p-1}^{-1} U_p = S_{p-1}^{(yy)} - 2S_{p-1}^{(ya)} A_p^{(p)H} + A_p^{(p)} S_{p-1}^{(aa)} A_p^{(p)H} . \tag{4}$$

Taking the conjugate transpose of both sides of equation (4) and using equations (106)[1] and (114)[1] yields

$$U_p U_{p-1}^{-1} S_{p-1}^{(yy)} = S_{p-1}^{(yy)} - 2A_p^{(p)} S_{p-1}^{(ya)^H} + A_p^{(p)} S_{p-1}^{(aa)} A_p^{(p)H} . \tag{5}$$

Adding equations (4) and (5) together and multiplying by -1, there follows

$$\begin{aligned} &\left(-S_{p-1}^{(yy)} U_{p-1}^{-1}\right) U_p + U_p \left(-U_{p-1}^{-1} S_{p-1}^{(yy)}\right) \\ &= -2\left[S_{p-1}^{(yy)} - A_p^{(p)} S_{p-1}^{(ya)^H} - S_{p-1}^{(ya)} A_p^{(p)H} + A_p^{(p)} S_{p-1}^{(aa)} A_p^{(p)H}\right] = -2E_p ; \end{aligned} \tag{6}$$

the last identity was derived from equation (113).[1]

Define

$$M_{p-1} = -U_{p-1}^{-1} S_{p-1}^{(yy)} . \tag{7}$$

Then equation (6) becomes simply

$$M_{p-1}^H U_p + U_p M_{p-1} = -2E_p . \tag{8}$$

Now, E_p is Hermitian and positive definite* (see equation (112)[1]); also, $S_{p-1}^{(yy)}$ is Hermitian and positive definite (see equation (114A)[1]). We assume that U_{p-1} is positive definite. Then, U_{p-1}^{-1} is positive definite, and so $U_{p-1}^{-1} S_{p-1}^{(yy)}$ must have all its eigenvalues positive

*All of the positive definite statements should be qualified with the proviso "with probability 1."

(see appendix A). As a result, M_{p-1} has all its eigenvalues negative, making it a stable matrix (reference 4, page 270). Therefore, the solution of equation (8) exists and is unique (reference 5, equation 3).

According to reference 4, page 278, problem 3, there exists a positive definite solution of equation (8) for U_p. Therefore, there is a unique positive definite solution of equation (8) for U_p. Since

$$U_0 = R_0 = \frac{1}{N} \sum_{k=1}^{N} X_k X_k^H \tag{9}$$

(from equations (95)[1] and (82)[1]) is positive definite, the assumption above, that U_{p-1} is positive definite, can be justified by induction.

In summary, the residual matrix U_p, calculated by means of equation (105)[1] or (181),[1] is positive definite. The quantity V_p is also positive definite; the equation analogous to equation (6) is

$$\left(-S_{p-1}^{(ba)} V_{p-1}^{-1}\right) V_p + V_p \left(-V_{p-1}^{-1} S_{p-1}^{(ba)}\right) = -2F_p , \tag{10}$$

and all the comments above apply directly. It is worth repeating that the positive definite conclusion on U_p and V_p holds for the specific inverse weighting indicated in equation (136)[1]; whether it also holds for other weightings is unknown.

STABLE CORRELATION RECURSION

The correlation recursion is given in equation (164)[1] according to

$$\begin{aligned} R_m^{(p)} &= \sum_{n=1}^{p} A_n^{(p)} R_{m-n}^{(p)} , \quad p+1 \le m, \\ R_m^{(p)} &= R_{-m}^{(p)H} , \quad m < 0, \end{aligned} \tag{11}$$

where superscript p has been added to the correlation matrices to indicate specifically their dependence on the p-th order predictive filter; and starting values have been defined, as in equation (D-3),[1] namely,

$$R_{m}^{(p)} = R_{m} \quad , |m| \leq p. \tag{12}$$

The latter quantities in equation (12) are, according to equation (78A),[1] solutions of

$$R_{m} = \sum_{n=1}^{p} A_{n}^{(p)} R_{m-n} \quad , 1 \leq m \leq p. \tag{13}$$

Combining equations (11) through (13), we have

$$R_{m}^{(p)} = \sum_{n=1}^{p} A_{n}^{(p)} R_{m-n}^{(p)} \quad , 1 \leq m. \tag{14}$$

We will show that recursion (11) is stable; that is, we will show that (the elements of) matrix $R_{m}^{(p)}$ does not tend to infinity as m tends to infinity, with p fixed. The proof is an extension of reference 3, section III.C.2 (which was for known correlation), to fit the unknown correlation case.

We have, from equations (82)[1] and (80A),[1] respectively,

$$\begin{aligned} R_{0} &= \frac{1}{N} \sum_{k=1}^{N} X_{k} X_{k}^{H} \quad , \\ R_{p} &= \sum_{n=1}^{p} A_{n}^{(p)} R_{p-n} \quad \text{for} \quad p = 1, 2, \ldots . \end{aligned} \tag{15}$$

For a given value of p, define the $(m + 1) \times (m + 1)$ block Toeplitz matrix

$$R_{m}^{(p)} \equiv \begin{bmatrix} R_{0}^{(p)} & R_{1}^{(p)} & \cdots & R_{m}^{(p)} \\ R_{-1}^{(p)} & R_{0}^{(p)} & & \\ \vdots & & \ddots & \\ R_{-m}^{(p)} & & & R_{0}^{(p)} \end{bmatrix} \tag{16}$$

If $m \leq p$, the entries in equation (16) are according to equation (12), whereas if $m > p$, the entries are those generated by equation (11). It follows immediately, from equations (16) and (12), that

$$Q_m^{(p)} = R_m^{(m)} \quad \text{if } m \leq p. \tag{17}$$

The s,t-th block of $R_m^{(p)}$ in equation (16) is

$$\left\{R_m^{(p)}\right\}_{st} = R_{t-s}^{(p)} \quad \text{for } 0 \leq s,t \leq m. \tag{18}$$

Also, define a $(m+1) \times (m+1)$ block matrix,

$$Q_m^{(p)} = \begin{bmatrix} I & 0 & 0 & \cdots & & 0 \\ -A_1^{(p)H} & I & 0 & \cdots & & \\ -A_2^{(p)H} & 0 & I & \ddots & & \\ \vdots & 0 & 0 & & & \\ \vdots & \vdots & \vdots & & & \\ -A_p^{(p)H} & & & & & \\ 0 & & & & & \\ 0 & & & & \ddots & \vdots \\ \vdots & & & & I & 0 \\ & & & \cdots & 0 & I \end{bmatrix} \tag{19}$$

where we require $m \geq p \geq 1$ for this definition. Then, using the notation established in equation (18),

$$\left\{Q_m^{(p)}\right\}_{tu} = \delta_{tu} I - \delta_{u0} A_t^{(p)H} \quad \text{for } 0 \leq t,u \leq m, \tag{20}$$

where

$$\bar{A}_t^{(p)} \equiv \left\{ \begin{array}{l} A_t^{(p)}, \; 1 \le t \le p \\ 0, \; \text{otherwise} \end{array} \right\}. \tag{21}$$

Also,

$$\left\{ Q_m^{(p)H} \right\}_{rs} = \delta_{rs} I - \delta_{r0} \bar{A}_s^{(p)} \quad \text{for} \quad 0 \le r, s \le m. \tag{22}$$

Then, the r,u-th block of the product $Q_m^{(p)H} R_m^{(p)} Q_m^{(p)}$ is

$$\left\{ Q_m^{(p)H} R_m^{(p)} Q_m^{(p)} \right\}_{ru} = \sum_{s,t=0}^{m} \left\{ Q_m^{(p)H} \right\}_{rs} \left\{ R_m^{(p)} \right\}_{st} \left\{ Q_m^{(p)} \right\}_{tu}$$

$$= \sum_{s,t=0}^{m} \left[\delta_{rs} I - \delta_{r0} \bar{A}_s^{(p)} \right] R_{t-s}^{(p)} \left[\delta_{tu} I - \delta_{u0} \bar{A}_t^{(p)H} \right]$$

$$= \sum_{s,t=0}^{m} \left[\delta_{rs} \delta_{tu} R_{t-s}^{(p)} - \delta_{r0} \delta_{tu} \bar{A}_s^{(p)} R_{t-s}^{(p)} - \delta_{rs} \delta_{u0} R_{t-s}^{(p)} \bar{A}_t^{(p)H} \right.$$

$$\left. + \delta_{r0} \delta_{u0} \bar{A}_s^{(p)} R_{t-s}^{(p)} \bar{A}_t^{(p)H} \right] \tag{23}$$

$$= R_{u-r}^{(p)} - \delta_{r0} \sum_{s=0}^{m} \bar{A}_s^{(p)} R_{u-s}^{(p)} - \delta_{u0} \sum_{t=0}^{m} R_{t-r}^{(p)} \bar{A}_t^{(p)H} + \delta_{r0} \delta_{u0} \sum_{s,t=0}^{m} \bar{A}_s^{(p)} R_{t-s}^{(p)} \bar{A}_t^{(p)H}$$

$$= R_{u-r}^{(p)} - \delta_{r0} \sum_{s=1}^{p} A_s^{(p)} R_{u-s}^{(p)} - \delta_{u0} \sum_{t=1}^{p} R_{t-r}^{(p)} A_t^{(p)H} + \delta_{r0} \delta_{u0} \sum_{s,t=1}^{p} A_s^{(p)} R_{t-s}^{(p)} A_t^{(p)H}.$$

In the last line, above, we have used equation (21) to simplify equation (23).

At this point, we consider four subcases:

(a) for $1 \le r, u \le m$, equation (23) reduces to $R_{u-r}^{(p)}$;

(b) for $r = 0$, $u = 0$, equation (23) becomes

$$R_0^{(p)} - \sum_{s=1}^{p} A_s^{(p)} R_{-s}^{(p)} - \sum_{t=1}^{p} R_t^{(p)} A_t^{(p)H} + \sum_{s,t=1}^{p} A_s^{(p)} R_{t-s}^{(p)} A_t^{(p)H} \; ; \tag{24}$$

but, by use of equation (14), the sum on s in the last term of equation (24) is $R_t^{(p)}$, in which case the last two terms of equation (24) cancel. We are left with

$$R_0^{(p)} - \sum_{s=1}^{p} A_s^{(p)} R_{-s}^{(p)} = - \sum_{s=0}^{p} A_s^{(p)} R_{-s} = U_p \, , \tag{25}$$

using equations (12) and (95)[1];

(c) for $r = 0$, $1 \le u \le m$, equation (23) yields

$$R_u^{(p)} - \sum_{s=1}^{p} A_s^{(p)} R_{u-s}^{(p)} = 0, \tag{26}$$

using equation (14); and

(d) for $u = 0$, $1 \le r \le m$, equation (23) yields

$$R_{-r}^{(p)} - \sum_{t=1}^{p} R_{t-r}^{(p)} A_t^{(p)H} = 0, \tag{27}$$

since this is the conjugate transpose of equation (26). Therefore, we have

$$Q_m^{(p)H} R_m^{(p)} Q_m^{(p)} = \begin{bmatrix} U_p & 0 & 0 & \cdots & 0 \\ 0 & R_0^{(p)} & R_1^{(p)} & & R_{m-1}^{(p)} \\ 0 & R_{-1}^{(p)} & R_0^{(p)} & \ddots & \\ \vdots & & & & \\ & & & & \\ 0 & R_{1-m}^{(p)} & & & R_0^{(p)} \end{bmatrix} = \left[\begin{array}{c|ccc} U_p & 0 & \cdots & 0 \\ \hline 0 & & & \\ \vdots & & R_{m-1}^{(p)} & \\ 0 & & & \end{array}\right] . \tag{28}$$

This relation holds for $m \geq p \geq 1$, as noted under equation (19) (some relations for determinants are noted in appendix B).

Now, let $\{V_k\}$ be arbitrary nonzero complex M × 1 column matrices. Then, using equation (28),

$$\left[V_0^H \cdots V_{m-1}^H\right] Q_m^{(p)H} R_m^{(p)} Q_m^{(p)} \begin{bmatrix} V_0 \\ \vdots \\ V_{m-1} \end{bmatrix} = V_0^H U_p V_0 + \left[V_1^H \cdots V_m^H\right] R_{m-1}^{(p)} \begin{bmatrix} V_1 \\ \vdots \\ V_m \end{bmatrix} . \tag{29}$$

We recall that U_p is positive definite, by the previous section. Therefore, if $R_{m-1}^{(p)}$ is positive definite, then $Q_m^{(p)H} R_m^{(p)} Q_m^{(p)}$ is positive definite, which, in turn, implies that $R_m^{(p)}$ is positive definite. That is, for $m \geq p \geq 1$,

$$\text{if } R_{m-1}^{(p)} \text{ is positive definite, then } R_m^{(p)} \text{ is positive definite.} \tag{30}$$

In particular, letting $m = p$, we see that if $R_{p-1}^{(p)}$ is positive definite, then $R_p^{(p)}$ is positive definite. But $R_{p-1}^{(p)} = R_{p-1}^{(p-1)}$, by equation (17). Hence, if $R_{p-1}^{(p-1)}$ is positive definite, then $R_p^{(p)}$ is positive definite. But $R_0^{(0)} = R_0$ is positive definite (see equation (15)). Therefore, we conclude by induction that

$$R_p^{(p)} \text{ is positive definite for all } p. \tag{31}$$

This statement is used as a priori information in Burg's derivation in the known correlation case (see reference 3, page 85).

Now, we return to equation (30) with this information and can draw the conclusion that $R_m^{(p)}$ is positive definite for all $m \geq p$. Finally, using equation (17), we can state

$$R_m^{(p)} \text{ is positive definite for all } m \text{ and } p. \tag{32}$$

For fixed p, since $R_m^{(p)}$ is positive definite for all m, (the elements of) $R_m^{(p)}$ cannot tend to infinity as m tends to infinity, since $R_0^{(p)} = R_0$ is fixed. Therefore, recursion (11) is stable. This implies (using equation (23)[1]) that

$$\det\left(I - \sum_{n=1}^{p} z^{-n} A_n^{(p)}\right) = \det \mathcal{A}_A^{(p)}(z) \tag{33}$$

possesses all its zeros inside the unit circle in the z-plane; that is, predictive error filter $\mathcal{A}_A^{(p)}(z)$ is minimum phase.

The proof above hinges critically on the positive definiteness of U_p, which was demonstrated in the previous section. In particular, this condition is employed in equation (29) to guarantee that the right-hand side be positive.

A word of caution about an apparent alternative proof is worth mentioning here. Having shown that U_p is positive definite, one might be tempted to <u>define</u> $\tilde{R}_m^{(p)}$ by the inverse of equation (165),[1]

$$G^{(p)}(f) = \Delta\, H_A^{(p)}(f)^{-1}\, U_p\, H_A^{(p)}(f)^{-H}, \quad |f| < \frac{1}{2\Delta}, \tag{34}$$

according to

$$\tilde{R}_m^{(p)} = \int_{-\frac{1}{2\Delta}}^{\frac{1}{2\Delta}} df\, \exp(i2\pi f m\Delta)\, G^{(p)}(f), \quad \text{all } m. \tag{35}$$

It is obvious that $G^{(p)}(f)$ in equation (34) is positive definite for any f; and it is now easy to demonstrate that $\tilde{R}_m^{(p)}$ is positive definite:

$$\begin{aligned}
\left[q_0^H \cdots q_m^H\right] \tilde{R}_m^{(p)} \begin{bmatrix} q_0 \\ \vdots \\ q_m \end{bmatrix} &= \sum_{s,t=0}^{m} q_s^H \tilde{R}_{t-s}^{(p)} q_t \\
&= \sum_{s,t=0}^{m} q_s^H \int_{-\frac{1}{2\Delta}}^{\frac{1}{2\Delta}} df\, \exp(i2\pi f(t-s)\Delta)\, G^{(p)}(f)\, q_t \\
&= \int_{-\frac{1}{2\Delta}}^{\frac{1}{2\Delta}} df \left[\sum_{s=0}^{m} \exp(i2\pi f s\Delta) q_s\right]^H G^{(p)}(f) \left[\sum_{t=0}^{m} \exp(i2\pi f t\Delta) q_t\right] > 0,
\end{aligned} \tag{36}$$

since $G^{(p)}(f)$ is positive definite for any f.

However, the problem is that we now would have to show that $\tilde{R}_m^{(p)}$, as generated by equation (35), satisfies the recurrence (11). An example in appendix C shows that for an unstable sequence, the values returned by equation (35) are not the same sequence; thus, equation (35) should not be used until <u>after</u> the stability of $\{R_m^{(p)}\}$ has been ascertained.

ALIASED CORRELATIONS VIA FFT

Based upon the previous results, we know that we can express

$$G(f) = \Delta \sum_{m=-\infty}^{\infty} \exp(-i 2\pi f m \Delta) R_m \ , \ |f| < \frac{1}{2\Delta} \ , \tag{37}$$

and

$$R_m = \int_{-\frac{1}{2\Delta}}^{\frac{1}{2\Delta}} df \ \exp(i 2\pi f m \Delta) G(f), \ \text{all} \ \ m. \tag{38}$$

We have dropped the superscript p above, since the results to follow will hold for any correlation-spectrum pair satisfying equations (37) and (38).

If spectrum G(f) is calculated only at a discrete set of $N_F + 1$ points on $\left(-\frac{1}{2\Delta}, \frac{1}{2\Delta}\right)$ (which is a typical practical situation for plotting purposes, for example), a discrete approximation is afforded to the integral in equation (38). It is, for trapezoidal weights $\{w_k\}$,

$$\frac{1}{N_F \Delta} \sum_{k=-N_F/2}^{N_F/2} w_k \exp\left(i 2\pi \frac{k}{N_F \Delta} m \Delta\right) G\left(\frac{k}{N_F \Delta}\right) = \sum_{k=-\infty}^{\infty} R_{m+kN_F} \equiv \hat{R}_m \ . \tag{39}$$

That is, the discrete approximation to integral (38) yields aliased samples of correlation sequence $\{R_m\}$ at separations of N_F; this is easily proven by substituting equation (37) into the left-hand side of equation (39) and interchanging summations.

The aliased sequence $\{\hat{R}_m\}$ has period N_F. Therefore, $\hat{R}_m$ is a good approximation to R_m for $|m| < N_F/2$ if $|R_m|$ is sufficiently small for

$|m| > N_F/2$. (Generally, $N_F >> p_{BEST}$ in the linear predictive approach, and this is true.) The reason for considering this approach to the approximate evaluation of correlation sequence $\{R_m\}$ follows.

The left-hand side of equation (39) can be accomplished by means of an N_F-point FFT (one FFT for each element of the M × M matrices involved). For trapezoidal weights, using the fact that $G\left(-\frac{1}{2\Delta}\right) = G\left(\frac{1}{2\Delta}\right)$, equation (39) is expressible as

$$\hat{R}_m = \frac{1}{N_F \Delta} \sum_{k=-N_F/2}^{\frac{N_F}{2}-1} \exp\left(i 2\pi k m / N_F\right) G_k$$

$$= \frac{1}{N_F \Delta}\left[\sum_{k=-N_F/2}^{-1} \exp\left(i 2\pi k m / N_F\right) G_k + \sum_{k=0}^{\frac{N_F}{2}-1} \exp\left(i 2\pi k m / N_F\right) G_k\right], \tag{40}$$

where we have defined

$$G_k = G\left(\frac{k}{N_F \Delta}\right), \; |k| \le \frac{N_F}{2}. \tag{41}$$

Letting $n = N_F + m$ in the first sum of equation (40), and $n = m$ in the second sum, we obtain

$$\hat{R}_m = \sum_{n=0}^{N_F-1} \exp\left(i 2\pi n m / N_F\right) \gamma_n, \tag{42}$$

where M × M matrix

$$\gamma_n = \frac{1}{N_F \Delta}\left\{\begin{array}{l} G_n, \; 0 \le n \le \frac{N_F}{2} - 1 \\ G_{n-N_F}, \; \frac{N_F}{2} \le n \le N_F - 1 \end{array}\right\}. \tag{43}$$

But equation (42) is recognized as an N_F-point FFT of the matrices

$$G_0, G_1, \ldots, G_{\frac{N_F}{2}-1}, G_{-\frac{N_F}{2}}, \ldots, G_{-1}; \tag{44}$$

thus, we obtain $\hat{R}_0, \hat{R}_1, \ldots, \hat{R}_{N_F-1}$ by means of this N_F-point FFT, one FFT for each element of the M × M matrices. (The quantities $\{\hat{R}_m\}$ for $|m| < N_F/2$ are available by use of the periodic nature of sequence $\{\hat{R}_m\}$.) This use of an N_F-point FFT to obtain (good) estimates of correlation sequence $\{R_m\}$ circumvents the use of recursion (11), which would yield the exact correlation sequence $\{R_m\}$. It can save time in some cases and uses already available quantities $\{G_k\}$, if they have been computed previously for plotting or observation purposes.

REAL PROCESSES

The preceding results for complex multivariate processes can be specialized to real processes. We have, from equations (171)[1] and (39),

$$G_{-k} = G_k^* \quad , \quad \hat{R}_m \text{ real.} \tag{45}$$

Therefore, equation (39) becomes

$$\hat{R}_m = \frac{2}{N_F \Delta} \mathrm{Re} \sum_{k=0}^{N_F/2} \tilde{w}_k \exp\left(i 2\pi k m / N_F\right) G_k, \tag{46}$$

where

$$\tilde{w}_k = \begin{cases} \frac{1}{2}, & k = 0 \text{ or } N_F/2 \\ 1, & 0 < k < N_F/2 \end{cases}. \tag{47}$$

Now, let the elements of matrices G_k and $\hat{R}_m$ be expressed as

$$G_k = \left[G_k^{(\ell j)}\right] \quad , \quad \hat{R}_m = \left[\hat{R}_m^{(\ell j)}\right], \quad 1 \le \ell, j \le M. \tag{48}$$

Then, $G_k^{(\ell\ell)}$ is real for all ℓ; and from equation (46),

$$\hat{R}_m^{(\ell\ell)} = \frac{2}{N_F \Delta} \sum_{k=0}^{N_F/2} \tilde{w}_k \cos\left(2\pi k m / N_F\right) G_k^{(\ell\ell)}. \tag{49}$$

In addition, since

$$\hat{R}_{-m}^{(\ell\ell)} = \hat{R}_{m}^{(\ell\ell)} \quad , \quad \hat{R}_{\frac{N_F}{2}-m}^{(\ell\ell)} = \hat{R}_{\frac{N_F}{2}+m}^{(\ell\ell)} \quad , \tag{50}$$

the fundamental range of m is $[0, N_F/2]$ for sequence $\{\hat{R}_m^{(\ell\ell)}\}$.

REAL BIVARIATE PROCESSES

We can specialize further to the bivariate case, M = 2, and make use of some of the properties previously discussed. (The goal of these manipulations will not be clear until the final result.) Define the complex scalar sequence $\{u_k\}$ such that

$$u_k = \frac{1}{N_F \Delta} \left\{ \begin{array}{l} G_k^{(11)} + i\, G_k^{(22)} \quad , \quad 0 \le k \le \frac{N_F}{2} - 1 \\ G_{N_F-k}^{(11)} + i\, G_{N_F-k}^{(22)} \quad , \quad \frac{N_F}{2} \le k \le N_F - 1 \end{array} \right\} . \tag{51}$$

Then,

$$\begin{aligned} &\sum_{k=0}^{N_F-1} u_k \exp\left(\pm i 2\pi k m / N_F\right) \\ &= \frac{1}{N_F \Delta} \sum_{k=0}^{\frac{N_F}{2}-1} \left[G_k^{(11)} + i\, G_k^{(22)}\right] \exp\left(\pm i 2\pi k m / N_F\right) \\ &+ \frac{1}{N_F \Delta} \sum_{k=\frac{N_F}{2}}^{N_F-1} \left[G_{N_F-k}^{(11)} + i\, G_{N_F-k}^{(22)}\right] \exp\left(\pm i 2\pi k m / N_F\right). \end{aligned} \tag{52}$$

If, on the right-hand side of equation (52), we let n = k in the first sum, and n = N_F - k in the second sum, we get

$$
\begin{aligned}
&\frac{1}{N_F\Delta}\sum_{n=0}^{\frac{N_F}{2}-1}\left[G_n^{(11)}+iG_n^{(22)}\right]\exp\left(\pm i2\pi nm/N_F\right)\\
&+\frac{1}{N_F\Delta}\sum_{n=1}^{N_F/2}\left[G_n^{(11)}+iG_n^{(22)}\right]\exp\left(\mp i2\pi nm/N_F\right)\\
&=\frac{1}{N_F\Delta}\left\{\left[G_0^{(11)}+iG_0^{(22)}\right]+\sum_{n=1}^{\frac{N_F}{2}-1}\left[G_n^{(11)}+iG_n^{(22)}\right]2\cos\left(2\pi nm/N_F\right)\right.\\
&\qquad\left.+\left[G_{\frac{N_F}{2}}^{(11)}+iG_{\frac{N_F}{2}}^{(22)}\right](-1)^m\right\}\\
&=\frac{2}{N_F\Delta}\sum_{n=0}^{N_F/2}\hat{w}_n\left[G_n^{(11)}+iG_n^{(22)}\right]\cos\left(2\pi nm/N_F\right) \qquad (53)\\
&=\hat{R}_m^{(11)}+i\hat{R}_m^{(22)},
\end{aligned}
$$

the last step by equation (49); that is, using equation (52) again,

$$
\left\{\hat{R}_m^{(11)}+i\hat{R}_m^{(22)}\right\}_0^{N_F-1}=FFT_{N_F}\left\{u_k\right\}_0^{N_F-1}. \qquad (54)
$$

Thus, one N_F-point FFT of scalar sequence $\{u_k\}$, defined in equation (51), will give both (aliased) real scalar autocorrelations $\{\hat{R}_m^{(11)}\}$ and $\{\hat{R}_m^{(22)}\}$; and by the statement under equation (50), $\{\hat{R}_m^{(\ell\ell)}\}$ need be printed out only for $0 \le m \le N_F/2$.

For the crosscorrelation, equation (46) yields

$$\hat{R}_m^{(12)} = \frac{2}{N_F \Delta} \mathrm{Re} \sum_{k=0}^{N_F/2} \tilde{w}_k \exp(i 2\pi k m / N_F) G_k^{(12)}$$

$$= \frac{2}{N_F \Delta} \mathrm{Re} \sum_{k=0}^{N_F/2} \tilde{w}_k \exp(-i 2\pi k m / N_F) G_k^{(12)*} \qquad (55)$$

$$= \mathrm{Re}\ \mathrm{FFT}_{N_F} \left\{ \tilde{w}_k \frac{2}{N_F \Delta} G_k^{(12)*} \right\}_0^{N_F/2} .$$

This N_F-point FFT of $\frac{N_F}{2} + 1$ nonzero numbers would yield $\left\{\hat{R}_m^{(12)}\right\}_0^{N_F-1}$; and from equation (39), since

$$\hat{R}_{-m} = \hat{R}_m^H \text{ (for general complex M × M matrices)}, \qquad (56)$$

it follows (using the periodicity of $\{\hat{R}_m\}$) that for the present case

$$\hat{R}_m^{(21)} = \hat{R}_{-m}^{(12)} = \hat{R}_{N_F-m}^{(12)} . \qquad (57)$$

Thus, print out of $\hat{R}_m^{(12)}$ and $\hat{R}_m^{(21)}$ for $0 \le m \le \frac{N_F}{2}$ suffices to give complete information about the aliased crosscorrelation. Furthermore, all this information is available from the single N_F-point FFT of equation (55).

In summary, only the two FFT's indicated in equations (54) and (55) need be conducted to obtain complete information about the aliased correlation sequence $\{\hat{R}_m\}$, for M = 2. These relations, in addition to the exact correlation recursion (11), have been incorporated in the FORTRAN program listed in appendix D. The comments in appendix K of the earlier report[1] are relevant here also.

SUMMARY

It has been shown above that, for the weighting introduced in equation (136),[1]

$$\Lambda_{p-1} = U_{p-1}^{-1} \quad , \quad \Gamma_{p-1} = V_{p-1}^{-1} \quad , \quad \text{choice 2,} \tag{58}$$

U_p and V_p are guaranteed positive definite, and the correlation recursion (11) is stable. Therefore, equation (58) is a sufficient condition for the desired properties to hold true. It is not known whether this is a necessary condition, that is, whether equation (58) is the only choice that results in the desired properties of positive definiteness and stability.

However, for M = 1, since, by equation (129),[1] $U_{p-1} = V_{p-1}$, it is possible to show that

$$\Lambda_{p-1} = \Gamma_{p-1} \qquad (M = 1) \tag{59}$$

is the only choice that guarantees the desired properties (see reference 1, page 32). Namely, equations (124),[1] (130),[1] and (114)[1] yield scalar

$$A_p^{(p)} = \frac{\left(\Gamma_{p-1}^{-1} + \Lambda_{p-1}^{-1}\right) Y_N^{(p-1)} Z_{N-1}^{(p-1)*}}{\Gamma_{p-1}^{-1} \left|Z_{N-1}^{(p-1)}\right|^2 + \Lambda_{p-1}^{-1} \left|Y_N^{(p-1)}\right|^2} \quad \text{for } N = p+1, M = 1. \tag{60}$$

In addition, if the data samples happen to take on values such that*

$$\left| \frac{Y_N^{(p-1)}}{Z_{N-1}^{(p-1)}} \right| = \left(\frac{\Lambda_{p-1}}{\Gamma_{p-1}} \right)^{1/2} , \tag{61}$$

then

$$\left|A_p^{(p)}\right| = \frac{1}{2}\left[\left(\frac{\Lambda_{p-1}}{\Gamma_{p-1}} \right)^{1/2} + \left(\frac{\Gamma_{p-1}}{\Lambda_{p-1}} \right)^{1/2} \right], \quad (M = 1) \ . \tag{62}$$

*If the sample mean of the original data is (made) zero, this choice is not possible for p = 1. For p > 1, the sample means of $\{Y_n^{(p-1)}\}$ and $\{Z_n^{(p-1)}\}$ are not necessarily zero.

which is always larger than 1 (unless $A_{p-1} = \Gamma_{p-1}$); then, U_p is negative and an unstable correlation recursion results. Thus, equation (59) is the only choice that guarantees positive U_p and a stable correlation recursion, regardless of the data set, for $M = 1$.

It should be noticed that the absolute level of the weights is not specified by equation (59). Thus, for $M > 2$, freedom in equation (58), at least to the extent of a common scale factor, must be allowed. Whether this is the only degree of freedom allowed to the choice of A_{p-1} and Γ_{p-1} is unknown for $M \geq 2$.

Appendix A

SOME PROPERTIES OF COMPLEX MATRICES

An arbitrary complex square matrix A is called real definite if

$$q^H A q = r \text{ (real) for any } q, \tag{A-1}$$

where q is a complex column matrix.

It then follows that

$$A \text{ real definite} \Rightarrow A^H = A, \{\lambda_k\} \text{ real}, \tag{A-2}$$

where $\{\lambda_k\}$ are the eigenvalues of A.

For proof, first take the conjugate transpose of equation (A-1),

$$q^H A^H q = r \text{ for any } q. \tag{A-3}$$

Subtracting equations (A-1) and (A-3) gives

$$q^H (A^H - A) q = 0 \text{ for any } q. \tag{A-4}$$

Therefore,

$$A^H - A = 0, \quad \text{or} \quad A^H = A. \tag{A-5}$$

Also, if $\{V_k\}$ are the eigenvectors of A, then

$$\begin{aligned} A V_k &= \lambda_k V_k, \\ V_k^H A V_k &= \lambda_k V_k^H V_k. \end{aligned} \tag{A-6}$$

Since the left-hand side and $V_k^H V_k$ are real, λ_k is real.

If r in equation (A-1) is positive for any q, then A is said to be positive definite. It follows that

$$A \text{ positive definite} \Rightarrow A^H = A, \{\lambda_k\} > 0. \tag{A-7}$$

The proof is the same as the proof above, except that now $V_k^H A V_k > 0$ in equation (A-6).

Now, we are in position to prove that

$$\left.\begin{array}{l}\text{A positive definite}\\ \text{B positive definite}\end{array}\right\} \Rightarrow \text{Eigenvalues of AB are all positive.} \tag{A-8}$$

For proof, let $\{\lambda_k\}$ and $\{V_k\}$ be the eigenvalues and eigenvectors of AB; then, we have

$$\begin{aligned}(AB)V_k &= \lambda_k V_k \\ BV_k &= \lambda_k A^{-1} V_k \\ V_k^H B V_k &= \lambda_k V_k^H A^{-1} V_k = \lambda_k (A^{-1}V_k)^H A (A^{-1}V_k),\end{aligned} \tag{A-9}$$

where we have used $A^H = A$ (equation (A-7)). Since A and B are positive definite, the left-hand side and the factor multiplying λ_k are positive. Therefore, λ_k is positive.

It should be noted that AB need not be Hermitian or positive definite. For example, if

$$\begin{aligned}A &= \begin{bmatrix}\alpha & \beta^* \\ \beta & \alpha\end{bmatrix} \quad \alpha \text{ real}, \alpha > 0, \alpha^2 > |\beta|^2, \\ B &= \begin{bmatrix}\mu & \nu^* \\ \nu & \mu\end{bmatrix} \quad \mu \text{ real}, \mu > 0, \mu^2 > |\nu|^2,\end{aligned} \tag{A-10}$$

then,

$$AB = \begin{bmatrix}\alpha\mu + \beta^*\nu & \alpha\nu^* + \mu\beta^* \\ \mu\beta + \alpha\nu & \alpha\mu + \beta\nu^*\end{bmatrix}. \tag{A-11}$$

Since the main diagonal terms of AB need not be real, AB is not necessarily Hermitian. Also, if we assume that AB is positive definite, equation (A-7) says that AB is Hermitian, which is contradictory.

A numerical example follows:

$$A = \begin{bmatrix} 2 & 1-i \\ 1+i & 2 \end{bmatrix}, \quad B = \begin{bmatrix} 2 & 1+i \\ 1-i & 2 \end{bmatrix}. \tag{A-12}$$

A and B are positive definite and Hermitian. The eigenvalues of both are $\{\lambda_k\} = 2 \pm \sqrt{2} > 0$. Their product is

$$AB = \begin{bmatrix} 4-i2 & 4 \\ 4 & 4+i2 \end{bmatrix}, \tag{A-13}$$

with eigenvalues $4 \pm 2\sqrt{3} > 0$, as predicted. But AB is not Hermitian nor positive definite because, for instance,

$$\begin{bmatrix} 1 & 0 \end{bmatrix} AB \begin{bmatrix} 1 \\ 0 \end{bmatrix} = 4 - i2. \tag{A-14}$$

The matrix AB in equation (A-13) points out that specifying a matrix to have positive eigenvalues does not make that matrix positive definite. However, if the matrix is also Hermitian, we have the generalization of equation (A-7) to

$$A \text{ positive definite} \Leftrightarrow A^H = A, \{\lambda_k\} > 0. \tag{A-15}$$

Appendix B

RELATIONS OF DETERMINANTS

Since $\det Q_m^{(p)} = 1$ (see equation (19)), equation (28) yields

$$\det \mathcal{R}_m^{(p)} = \det U_p \ \det \mathcal{R}_{m-1}^{(p)} , \quad m \geq p. \tag{B-1}$$

Setting $m = p$ in equation (B-1) and employing equation (17), there follows

$$\det \mathcal{R}_p^{(p)} = \det U_p \ \det \mathcal{R}_{p-1}^{(p-1)} . \tag{B-2}$$

Since $\mathcal{R}_0^{(0)} = R_0 = U_0$ (see equation (95)[1]), this recursion may be written in closed form as

$$\det \mathcal{R}_p^{(p)} = \prod_{k=0}^{p} \det U_k . \tag{B-3}$$

This relation is given in Burg,[3] page 86.

By letting $m = p + 1, p + 2, \ldots$, in equation (B-1), it follows immediately that

$$\det \mathcal{R}_m^{(p)} = (\det U_p)^{m-p} \prod_{k=0}^{p} \det U_k , \quad m \geq p. \tag{B-4}$$

In addition, for $m < p$, using equations (17) and (B-3),

$$\det \mathcal{R}_m^{(p)} = \det \mathcal{R}_m^{(m)} = \prod_{k=0}^{m} \det U_k , \quad m < p. \tag{B-5}$$

Combining equations (B-4) and (B-5), we have

$$\det \mathcal{R}_m^{(p)} = \begin{cases} \prod_{k=0}^{m} \det U_k , & m \leq p \\ (\det U_p)^{m-p} \prod_{k=0}^{p} \det U_k , & m \geq p \end{cases} . \tag{B-6}$$

Appendix C

EXAMPLE OF UNSTABLE CORRELATION RECURSION

Consider the univariate (M = 1) correlation values,

$$R_m = r^{|m|}, \text{ all } m, \text{ r real and positive.} \tag{C-1}$$

The value of r can be greater or less than unity. The z-transform of equation (C-1) is

$$\sum_m z^{-m} R_m = 1 + \sum_{m=1}^{\infty} z^{-m} r^m + \sum_{m=-1}^{-\infty} z^{-m} r^{-m} = 1 + S_1 + S_2 . \tag{C-2}$$

Now,

$$S_1 = \frac{r}{z-r} \quad \text{if } |z| > r,$$

$$S_2 = \frac{-z}{z-\frac{1}{r}} \quad \text{if } |z| < \frac{1}{r} . \tag{C-3}$$

But, if $r \geq 1$, there is no common region of convergence; also, sequence $\{R_m\}$ is unstable if $r > 1$. Nevertheless, if we blithely add terms in equation (C-2), we get

$$\sum_m z^{-m} R_m = \frac{\left(r-\frac{1}{r}\right) z}{(z-r)\left(z-\frac{1}{r}\right)} . \tag{C-4}$$

Then, continuing on, setting $z = \exp(i2\pi f\Delta)$ and multiplying by Δ,

$$G(f) = \frac{\Delta\left(r-\frac{1}{r}\right)\exp(i2\pi f\Delta)}{\left[\exp(i2\pi f\Delta)-r\right]\left[\exp(i2\pi f\Delta)-\frac{1}{r}\right]} , \tag{C-5}$$

which is real, and

$$\tilde{R}_m = \int_{-\frac{1}{2\Delta}}^{\frac{1}{2\Delta}} df \exp(i2\pi f m\Delta)\, G(f) = \frac{1}{i2\pi\Delta} \oint_{\text{unit circle}} \frac{dz}{z} z^m \frac{\Delta\left(r-\frac{1}{r}\right)z}{(z-r)\left(z-\frac{1}{r}\right)} \qquad \text{(C-6)}$$

In the following, let $r \neq 1$, $\alpha = \min(r, \frac{1}{r})$, and $\beta = \max(r, \frac{1}{r})$. Then,

$$\tilde{R}_m = \left(r-\frac{1}{r}\right)\frac{\alpha^{|m|}}{\alpha-\beta} \quad \text{for all } m. \qquad \text{(C-7)}$$

This is a stable sequence for any r. But, notice that if

$$r<1,\ \alpha = r,\ \beta = \frac{1}{r},\ \tilde{R}_m = r^{|m|} \text{ for all } m; \qquad \text{(C-8)}$$

whereas, if

$$r>1,\ \alpha = \frac{1}{r},\ \beta = r,\ \tilde{R}_m = -\left(\frac{1}{r}\right)^{|m|} \text{ for all } m. \qquad \text{(C-9)}$$

The former sequence is correct; the latter is not. Yet both are stable. So, although equation (C-6) always generates a stable sequence, it is not necessarily the original sequence.

Appendix D

FORTRAN PROGRAM FOR SPECTRAL ANALYSIS

A FORTRAN listing of the spectral analysis technique is given in this appendix, in addition to a sample printout of an application. The notation and scaling adopted is identical to that given in reference 1, appendix K. The equation numbers referenced are those in the earlier report,[1] except in Subroutine ACM, where they correspond to the equations in this report.

```
C  MULTIVARIATE LINEAR PREDICTIVE SPECTRAL ANALYSIS,
C  EMPLOYING WEIGHTED FORWARD AND BACKWARD AVERAGING.
C  THIS PROGRAM IS WRITTEN FOR REAL PROCESSES AND GENERAL M, WITH THE
C  EXCEPTION OF FUNCTION DETERM AND SUBROUTINES SDM, INVERT, AND SOLVE,
C  AND THE PRINT OUT OF THE SPECTRAL DENSITY MATRIX.
C  USER: CHANGE LINES 24 AND 41, AND REPLACE SUBROUTINE DATA.
C  M = DIMENSIONALITY OF MULTIVARIATE PROCESS; INTEGER INPUT
C  N = NUMBER OF DATA POINTS IN EACH PROCESS; INTEGER INPUT
C  X(1,1)...X(N,1),...,X(1,M)...X(N,M) = INPUT DATA; ALTERED ON OUTPUT
C  PMAX = MAXIMUM ORDER OF FILTER; INTEGER INPUT
C  NF = SIZE OF FFT (MUST BE A POWER OF 2 TO USE MKLFFT); INTEGER INPUT
C  AVE = MEANS OF INPUT DATA; OUTPUT
C  R = COVARIANCE MATRIX OF INPUT DATA; OUTPUT
C  AIC = AKAIKE'S INFORMATION CRITERION; OUTPUT
C  PBEST = BEST ORDER OF FILTER; INTEGER OUTPUT
C  UBEST = MATRIX OF COEFFICIENTS IN SPECTRAL ESTIMATE; OUTPUT
C  AP = MATRIX OF FORWARD PARTIAL CORRELATION COEFFICIENTS; THEN =
C  MATRIX OF FORWARD PREDICTIVE FILTER COEFFICIENTS FOR PBEST; OUTPUT
C  BP = MATRIX OF BACKWARD PARTIAL CORRELATION COEFFICIENTS; OUTPUT
C  RN = MATRIX OF NORMALIZED CORRELATIONS OF INPUT DATA; OUTPUT
C  XX,YY = SPECTRAL MATRICES OF INPUT DATA; OUTPUT
C  XX = ALIASED NORMALIZED CORRELATION MATRIX OF INPUT DATA; OUTPUT
      PARAMETER M=2     MULTIVARIATE PROCESS
      PARAMETER N= 100 , PMAX= 10, NF=1024, NF41=NF/4+1
      INTEGER PBEST,P,LOG2NF,IA
      REAL T,TA,TB
      DOUBLE PRECISION D
      DIMENSION X(N,M),Y(N,M),Z(N,M),UBEST(M,M),AP(M,M,PMAX),
     $BP(M,M,PMAX),AVE(M),XX(NF,M,M),YY(NF,M,M),COSI(NF41),
     $U(M,M),V(M,M),UI(M,M),VI(M,M),A(M,M),B(M,M),R(M,M),RN(M,M,PMAX),
     $WA(M,M),WB(M,M),WC(M,M),WD(M,M),WE(M,M),AIC(PMAX),AIC0(2),S(M)
      EQUIVALENCE (X,Y),(AIC(1),AIC0(2))
```

```
C  PRINT OUT VALUES OF PARAMETERS
      I=N
      J=PMAX
      K=M
      L=NF
      PRINT 1, I,J,K,L
1     FORMAT(1H1,' N =',I6,10X,'PMAX =',I4,10X,'M =',I2,10X,'NF =',I5)
C  INPUT DATA IN X(1,1)...X(N,1),...,X(1,M)...X(N,M)
      CALL DATA
      PRINT 2
2     FORMAT(/' INPUT DATA:')
      J=N-99
      L=N-200
      DO 3 I=1,M
      PRINT 4, I
      IF(N.LE.200) GO TO 5
      PRINT 6, (X(K,I),K=1,100)
      PRINT 7, L
7     FORMAT(I6,' INPUT DATA POINTS NOT PRINTED HERE')
      PRINT 6, (X(K,I),K=J,N)
      GO TO 3
5     PRINT 6, (X(K,I),K=1,N)
3     CONTINUE
4     FORMAT('   PROCESS NUMBER',I2)
6     FORMAT(5E20.8)
C  EVALUATE PARTIAL CORRELATION COEFFICIENTS
      CALL PCC
      PRINT 8
8     FORMAT(/' MEANS OF INPUT DATA:')
      PRINT 6, (AVE(I),I=1,M)
      PRINT 9
9     FORMAT(/' COVARIANCE MATRIX OF INPUT DATA:')
      PRINT 6, ((R(I,J),I=1,M),J=1,M)
      PRINT 10
10    FORMAT(/' AKAIKE INFORMATION CRITERION:'/
     $9X,'P',11X,'AIC(P)')
      PRINT 11, (P,AIC(P),P=0,PMAX)
```

```
11    FORMAT(I10,E20.8)
      PRINT 12, PBEST
12    FORMAT(/' PBEST =',I3)
      PRINT 13
13    FORMAT(/' UBEST:')
      PRINT 6, ((UBEST(I,J),I=1,M),J=1,M)
      PRINT 14
14    FORMAT(/' FORWARD PARTIAL CORRELATION COEFFICIENTS:'/9X,'P',
     $10X,'A(P,P)11',12X,'A(P,P)21',12X,'A(P,P)12',12X,'A(P,P)22')
      PRINT 15, (P,((AP(I,J,P),I=1,M),J=1,M),P=1,PMAX)
15    FORMAT(I10,4E20.8)
      PRINT 16
16    FORMAT(/' BACKWARD PARTIAL CORRELATION COEFFICIENTS:'/9X,'P',
     $10X,'B(P,P)11',12X,'B(P,P)21',12X,'B(P,P)12',12X,'B(P,P)22')
      PRINT 15, (P,((BP(I,J,P),I=1,M),J=1,M),P=1,PMAX)
      IF(PBEST.EQ.0) GO TO 17
C  EVALUATE PREDICTIVE FILTER COEFFICIENTS
C  AND NORMALIZED CORRELATION MATRICES
      CALL PFC
      PRINT 18
18    FORMAT(/' FORWARD PREDICTIVE FILTER COEFFICIENTS FOR PBEST:'/
     $9X,'K',8X,'A(PBEST,K)11',8X,'A(PBEST,K)21',
     $8X,'A(PBEST,K)12',8X,'A(PBEST,K)22')
      PRINT 15, (P,((AP(I,J,P),I=1,M),J=1,M),P=1,PBEST)
      PRINT 19
19    FORMAT(/' NORMALIZED CORRELATION MATRICES FOR M=2, UP TO PMAX:'/
     $7X,'DELAY',9X,'AUTO11',13X,'CROSS21',13X,'CROSS12',14X,'AUTO22')
      P=0
      PRINT 15, P,((R(I,J),I=1,M),J=1,M)
      PRINT 15, (P,((RN(I,J,P),I=1,M),J=1,M),P=1,PMAX)
C  EVALUATE PREDICTIVE-ERROR FILTER TRANSFER FUNCTION
17    CALL PEFTF
C  EVALUATE SPECTRAL DENSITY MATRIX AND COHERENCE
      CALL SDM
      PRINT 20
```

```
20    FORMAT(/' SPECTRAL DENSITY MATRIX AND COHERENCE FOR M=2:'/
     $8X,'BIN',10X,'AUTO11',14X,'AUTO22',10X,'REAL(CROSS12)',7X,
     $'IMAG(CROSS12)',9X,'MAG SQ COH',11X,'ARGUMENT')
      PRINT 21, (L,XX(L,1,1),XX(L,2,2),XX(L,1,2),
     $YY(L,1,2),YY(L,1,1),YY(L,2,2), L=1,NFD2P1)
21    FORMAT(I10,6E20.8)
C  EVALUATE ALIASED NORMALIZED CORRELATION MATRICES VIA FFT
      CALL ACM
      PRINT 22
22    FORMAT(/' ALIASED NORMALIZED CORRELATION MATRICES FOR M=2:'/
     $7X,'DELAY',9X,'AUTO11',13X,'CROSS21',13X,'CROSS12',14X,'AUTO22')
      L=0
      PRINT 15, L,XX(NFD2P2,1,1),XX(1,2,1),XX(1,2,1),XX(NFD2P2,2,2)
      PRINT 15, (L,XX(NFD2P2+L,1,1),XX(NFP1-L,2,1),
     $XX(1+L,2,1),XX(NFD2P2+L,2,2), L=1,NFD2M2)
      PRINT 15, NFD2M1,XX11M1,XX(NFD2P2,2,1),XX(NFD2,2,1),XX22M1
      PRINT 15, NFD2,XX11M0,XX(NFD2P1,2,1),XX(NFD2P1,2,1),XX22M0
C
      SUBROUTINE DATA
C  THIS SUBROUTINE GENERATES DATA FOR M=2, BIVARIATE PROCESS
      DEFINE IRAND=I*5**15+((1-SIGN(1,I*5**15))/2)*34359738367
      DEFINE RAND=FLOAT(I)/34359738367.
      I=5281
      TA=0.
      TB=0.
      DO 1 K=1,100   0 WILL DISCARD THESE INITIAL POINTS
      I=IRAND
      T=.85*TA-.75*TB+RANC-.5
      I=IRAND
      TB=.65*TA+.55*TB+RAND-.5
```

TR 5729

```
      1     TA=T
            X(1,1)=TA
            X(1,2)=TB
            DO 2 K=2,N
            I=IRAND
            T=.85*TA-.75*TB+RAN -.5
            I=IRAND
            TB=.65*TA+.55*TB+RA 0-.5
            TA=T
            X(K,1)=TA
      2     X(K,2)=TB
            RETURN
      C
            SUBROUTINE PCC
      C  THIS SUBROUTINE COMPUTES PBEST, UBEST, AND THE PARTIAL
      C  CORRELATION COEFFICIENTS FOR P = 1 TO PMAX; ANY M
            I=N
            J=PMAX
            IA=3.*SQRT(N)/M
            IF(PMAX.GT.IA) PRINT 1, J,I,IA
      1     FORMAT(/' PMAX =',I4,' IS TOO LARGE FOR NUMBER OF DATA POINTS N ='
           $,I5,';  SEARCH LIMITED TO P =',I4)
            IA=MIN(IA,PMAX)       @ UPPER BOUND ON PMAX; EQ 183
            FAC=2.*M*M/N          @ FAC=0.  WOULD FORCE PBEST EQUAL TO PMAX
      C  SUBTRACT MEANS; FILL IN DATA ARRAYS; EQ 11
            DO 2 I=1,M
            TA=0.
            DO 3 K=1,N
      3     TA=TA+Y(K,I)
            TA=TA/N
            AVE(I)=TA
            DO 2 K=1,N
            Y(K,I)=Y(K,I)-TA
      2     Z(K,I)=Y(K,I)
```

```
C  INITIALIZE CORRELATION MATRICES; EQS 82, 114, AND 105
      CALL AUTO(2,N-1,Y,WC)
      DO 4 I=1,M
      DO 4 J=I,M
      TA=Y(1,I)*Y(1,J)
      TB=Y(N,I)*Y(N,J)
      R(I,J)=(WC(I,J)+TA+TB)/N
      WA(I,J)=WC(I,J)+TB
      WB(I,J)=WC(I,J)+TA
      R(J,I)=R(I,J)
      WA(J,I)=WA(I,J)
4     WB(J,I)=WB(I,J)
      CALL EQUAL(R,U)
      CALL EQUAL(R,V)
      CALL CROSS(2,N,Y,Y,WC)
C  BEGIN RECURSION
      AIC(0)=LOG(DETERM(U))
      AICMIN=AIC(0)
      PBEST=0
      CALL EQUAL(U,UBEST)
      DO 5 P=1,IA
C  EVALUATE MATRICES REQUIRED IN BILINEAR MATRIX EQUATION; EQ 126
      CALL INVERT(V,VI)
      CALL MULT(VI,WB,WD)
      CALL EQUAL(WD,WB)
      CALL INVERT(U,UI)
      CALL EQUAL(WA,WD)
      CALL MULT(WD,UI,WA)
      CALL ADD(WC,WC,WC)
C  SOLVE BILINEAR MATRIX EQUATION; EQS 157-161
      CALL SOLVE
C  EVALUATE PARTIAL CORRELATION COEFFICIENTS; EQ 124
      CALL MULT(WC,VI,A)
      CALL TRANS(WC,WD)
      CALL MULT(WD,UI,B)
      CALL EQUAL(A,AP(1,1,P))
      CALL EQUAL(B,BP(1,1,P))
```

```
C  UPDATE MATRICES U AND V: EQ 101
       CALL MULT(A,WU,WE)
       CALL SUB(U,WE,U)
       CALL MULT(B,WC,WE)
       CALL SUB(V,WE,V)
C  CALCULATE AKAIKE'S INFORMATION CRITERION: EQ 100
       AIC(P)=LOG(DETERM(U))+FAC*P
       IF(AIC(P).GE.AICMIN) GO TO 6
       AICMIN=AIC(P)
       PBEST=P
       CALL EQUAL(U,UBEST)
6      IF(P.EQ.IA) GO TO 5
C  UPDATE DATA SEQUENCES Y AND Z: EQ 111
       L=P+1
       DO 7 K=N,L,-1
       DO 8 I=1,M
       TA=Z(K-1,I)
       DO 9 J=1,M
9      TA=TA-B(I,J)*Y(K,J)
8      Z(K,I)=TA
       DO 10 I=1,M
       TA=Y(K,I)
       DO 11 J=1,M
11     TA=TA-A(I,J)*Z(K-1,J)
10     Y(K,I)=TA
7      CONTINUE
C  CALCULATE NEW CORRELATION MATRICES: EQ 114
       CALL AUTO(P+2,N,Y,WA)
       CALL AUTO(P+1,N-1,Z,WB)
       CALL CROSS(P+2,N,Y,Z,WC)
5      CONTINUE
       IF(M.EQ.1) RETURN
       K=M-1
       DO 12 I=1,K
       L=I+1
       DO 12 J=L,M
       UBEST(I,J)=.5*(UBEST(I,J)+UBEST(J,I))
```

```
12      UBEST(J,I)=UBEST(I,J)
        RETURN
C
        SUBROUTINE PFC
C   THIS SUBROUTINE COMPUTES THE PREDICTIVE
C   FILTER COEFFICIENTS; ANY M; EQ 79
C   IT ALSO COMPUTES THE NORMALIZED CORRELATION
C   MATRICES, UP TO PMAX; EQS 80A, 26, AND 164
        CALL MULT(AP,R,RN)
        IF(PBEST.EQ.1) GO TO 3
        DO 1 P=2,PBEST
        CALL MULT(AP(1,1,P),R,WC)
        IA=P-1
        DO 2 L=1,IA
        IB=P-L
        CALL MULT(AP(1,1,P),BP(1,1,IB),WA)
        CALL SUB(AP(1,1,L),WA,WA)
        CALL MULT(BP(1,1,P),AP(1,1,L),WB)
        CALL SUB(BP(1,1,IB),WB,BP(1,1,IB))
        CALL EQUAL(WA,AP(1,1,L))
        CALL MULT(WA,RN(1,1,IB),WD)
2       CALL ADD(WC,WD,WC)
1       CALL EQUAL(WC,RN(1,1,P))
3       CONTINUE
        IF(PBEST.EQ.PMAX) GO TO 6
        IA=PBEST+1
        DO 7 P=IA,PMAX
        CALL SUB(WA,WA,WA)
        DO 8 L=1,PBEST
        CALL MULT(AP(1,1,L),RN(1,1,P-L),WB)
8       CALL ADD(WA,WB,WA)
7       CALL EQUAL(WA,RN(1,1,P))
6       DO 4 IA=1,M
```

```
    4     S(IA)=1./SQRT(R(IA,IA))
          DO 5 IA=1,M
          DO 5 IB=1,M
          T=S(IA)*S(IB)
          R(IA,IB)=R(IA,IB)*T
          IF(IA.EQ.IB) R(IA,IB)=1.
          DO 5 P=1,PMAX
    5     RN(IA,IB,P)=RN(IA,IB,P)*T
          RETURN
C
          SUBROUTINE PEFTF
C   THIS SUBROUTINE COMPUTES THE PREDICTIVE-ERROR
C   FILTER TRANSFER FUNCTION; ANY NF EQS 64 AND (J-3)-(J-6)
          LOG2NF=1.4427*LOG(NF)+.5
          CALL QTRCOS(COSI,NF)
          DO 1 I=1,M
          DO 1 J=1,M
          XX(1,I,J)=0.
          IF(I.EQ.J) XX(1,I,J)=1.
          YY(1,I,J)=0.
          IF(PBEST.EQ.0) GO TO 2
          IA=PBEST+1
          DO 3 L=2,IA
          XX(L,I,J)=-AP(I,J,L-1)
    3     YY(L,I,J)=0.
    2     IA=PBEST+2
          DO 4 L=IA,NF
          XX(L,I,J)=0.
    4     YY(L,I,J)=0.
    1     CALL MKLFFT(XX(1,I,J),YY(1,I,J),COSI,LOG2NF,-1)
          RETURN
C
```

```
      SUBROUTINE SDM
C  THIS SUBROUTINE COMPUTES THE SPECTRAL DENSITY
C  MATRIX AND COHERENCE FOR M=21 EQS 178 AND K=5
      T=2./NF
      NFD2P1=NF/2+1
      DO 1 L=1,NFD2P1
      WA(1,1)=XX(L,2,2)
      WA(1,2)=-XX(L,1,2)
      WA(2,1)=-XX(L,2,1)
      WA(2,2)=XX(L,1,1)
      WB(1,1)=YY(L,2,2)
      WB(1,2)=-YY(L,1,2)
      WB(2,1)=-YY(L,2,1)
      WB(2,2)=YY(L,1,1)
      TA=DETERM(WA)-DETERM(WB)
      TB=WA(1,1)*WB(2,2)+WA(2,2)*WB(1,1)-WA(1,2)*WB(2,1)-WA(2,1)*WB(1,2)
      TA=T/(TA**2+TB**2)
      CALL TRANS(WA,WC)
      CALL MULT(UBEST,WC,WD)
      CALL MULT(WB,WD,WC)
      TB=WC(1,2)-WC(2,1)
      CALL MULT(WA,WD,WC)
      CALL TRANS(WB,WD)
      CALL MULT(UBEST,WD,WE)
      CALL MULT(WB,WE,WD)
      CALL ADD(WC,WD,WC)
      YY(L,1,1)=(WC(1,2)**2+TB**2)/(WC(1,1)*WC(2,2))    @ MAG SQ COH
      YY(L,2,2)=ATAN2(TB,WC(1,2))                       @ ARGUMENT
      XX(L,1,1)=TA*WC(1,1)                              @ AUTO11
      XX(L,2,2)=TA*WC(2,2)                              @ AUTO22
      XX(L,1,2)=TA*WC(1,2)                              @ REAL(CROSS12)
      YY(L,1,2)=TA*TB                                   @ IMAG(CROSS12)
      XX(L,2,1)=0.
      YY(L,2,1)=0.
    1 CONTINUE
      RETURN
C
```

```
      SUBROUTINE ACM
C  THIS SUBROUTINE COMPUTES THE ALIASED NORMALIZED CORRELATION
C  MATRICES VIA TWO FFTS, FOR M=2; TECH RPT 5729, ECS 54-57
      NFP1=NF+1
      NFD2=NF/2
      NFD2P1=NFD2+1
      NFD2P2=NFD2+2
      NFD2M1=NFD2-1
      NFD2M2=NFD2-2
C  COMPUTE AUTO CORRELATIONS
      DO 1 L=1,NFD2
      XX(L,2,1)=.5*XX(L,1,1)
      YY(L,2,1)=.5*XX(L,2,2)
      XX(NFD2+L,2,1)=.5*XX(NFD2P2-L,1,1)
1     YY(NFD2+L,2,1)=.5*XX(NFD2P2-L,2,2)
      CALL MKLFFT(XX(1,2,1),YY(1,2,1),COSI,LOG2NF,-1)
C  NORMALIZE AND STORE IN SECOND HALF OF AUTO ARRAYS
      TA=1./XX(1,2,1)
      TB=1./YY(1,2,1)
      T=SQRT(TA*TB)
      XX(NFD2P2,1,1)=1.
      XX(NFD2P2,2,2)=1.
      DO 2 L=2,NFD2M1
      XX(NFD2P1+L,1,1)=XX(L,2,1)*TA
2     XX(NFD2P1+L,2,2)=YY(L,2,1)*TB
      XX11M1=XX(NFD2,2,1)*TA
      XX22M1=YY(NFD2,2,1)*TB
      XX11M0=XX(NFD2P1,2,1)*TA
      XX22M0=YY(NFD2P1,2,1)*TB
C  COMPUTE NORMALIZED CROSS CORRELATIONS
      XX(1,2,1)= .5*XX(1,1,2)*T
      YY(1,2,1)=-.5*YY(1,1,2)*T
      DO 3 L=2,NFD2
      XX(L,2,1)= XX(L,1,2)*T
      YY(L,2,1)=-YY(L,1,2)*T
      XX(NFD2+L,2,1)=0.
```

```
3       YY(NFD2+L,2,1)=0.
        XX(NFD2P1,2,1)= .5*XX(NFD2P1,1,2)*T
        YY(NFD2P1,2,1)=-.5*YY(NFD2P1,1,2)*T
        CALL MKLFFT(XX(1,2,1),YY(1,2,1),COSI,LOGNF,-1)
        RETURN
C
        SUBROUTINE CROSS(N1,N2,A,B,C)     @ A,B,A NB
C   THIS SUBROUTINE COMPUTES A CROSS CORRELATION MATRIX; ANY N! EQ 1190
        DIMENSION A(N,M),B(N,M),C(M,M)
        DO 1 I=1,M
        DO 1 J=1,M
        D=0.D0
        DO 2 K=N1,N2
2       D=D+A(K,I)*B(K-1,J)
1       C(I,J)=D
        RETURN
C
        SUBROUTINE AUTO(N1,N2,A,B)    @  A,A NB
C   THIS SUBROUTINE COMPUTES AN AUTO CORRELATION MATRIX; ANY N! EQ 1194
        DIMENSION A(N,M),B(M,M)
        DO 1 I=1,M
        DO 1 J=I,M
        D=0.D0
        DO 2 K=N1,N2
2       D=D+A(K,I)*A(K,J)
        B(I,J)=D
1       B(J,I)=B(I,J)
        RETURN
C
        SUBROUTINE EQUAL(A,B)
C   THIS SUBROUTINE SETS TWO MXM MATRICES EQUAL
        DIMENSION A(M,M),B(M,M)
        DO 1 I=1,M
        DO 1 J=1,M
1       B(I,J)=A(I,J)
        RETURN
```

```
C
      SUBROUTINE TRANS(A,P)      B  A,A OK
C  THIS SUBROUTINE TRANSPOSES AN NXN MATRIX
      DIMENSION A(N,N),B(N,N)
      DO 1 I=1,N
      DO 1 J=1,N
1     B(I,J)=A(J,I)
      RETURN
C
      SUBROUTINE ADD(A,B,C)      B  A,B,A OK
C  THIS SUBROUTINE ADDS TWO NXN MATRICES
      DIMENSION A(N,N),B(N,N),C(N,N)
      DO 1 I=1,N
      DO 1 J=1,N
1     C(I,J)=A(I,J)+B(I,J)
      RETURN
C
      SUBROUTINE SUB(A,B,C)      B  A,B,A OK
C  THIS SUBROUTINE SUBTRACTS TWO NXN MATRICES
      DIMENSION A(N,N),B(N,N),C(N,N)
      DO 1 I=1,N
      DO 1 J=1,N
1     C(I,J)=A(I,J)-B(I,J)
      RETURN
C
      SUBROUTINE MULT(A,B,C)     B  A,B,A OK
C  THIS SUBROUTINE MULTIPLIES TWO NXN MATRICES
      DIMENSION A(N,N),B(N,N),C(N,N)
      REAL T
      DO 1 I=1,N
      DO 1 J=1,N
      T=0.
      DO 2 K=1,N
2     T=T+A(I,K)*B(K,J)
1     C(I,J)=T
      RETURN
```

```
C
      SUBROUTINE INVERT(A,B)     B  A,A MB
C  THIS SUBROUTINE INVERTS A 2X2 MATRIX
      DIMENSION A(2,2),B(2,2)
      REAL T
      T=1./DETERM(A)
      B(1,1)=A(2,2)*T
      B(2,2)=A(1,1)*T
      B(1,2)=-A(1,2)*T
      B(2,1)=-A(2,1)*T
      RETURN
C
      SUBROUTINE SOLVE
C  THIS SUBROUTINE SOLVES BILINEAR MATRIX EQUATION
C  FOR M=2, BIVARIATE PROCESS; EQS 157, 158, AND 162
      TA=WA(1,1)+WA(2,2)+WB(1,1)+WB(2,2)
      TB=DETERM(WA)-DETERM(WB)
      CALL MULT(WC,WB,WD)
      WE(1,1)=WA(2,2)
      WE(1,2)=-WA(1,2)
      WE(2,1)=-WA(2,1)
      WE(2,2)=WA(1,1)
      CALL MULT(WE,WC,WA)
      CALL ADD(WD,WA,WD)
      WB(1,1)=TA*WB(1,1)+TB
      WB(2,2)=TA*WB(2,2)+TB
      WB(1,2)=TA*WB(1,2)
      WB(2,1)=TA*WB(2,1)
      CALL INVERT(WB,WE)
      CALL MULT(WD,WE,WC)
      RETURN
C
```

```
      FUNCTION DETERM(A)
C  THIS FUNCTION COMPUTES THE DETERMINANT OF A 2X2 MATRIX
      DIMENSION A(2,2)
      DETERM=A(1,1)*A(2,2)-A(1,2)*A(2,1)
      RETURN
      END

      SUBROUTINE MKLFFT(X,Y,CC,M,ISN)
      DIMENSION X(1),Y(1),CC(1),L(12)
      EQUIVALENCE (L12,L(1)),(L11,L(2)),(L10,L(3)),(L9,L(4)),(L8,L(5)),
     1(L7,L(6)),(L6,L(7)),(L5,L(8)),(L4,L(9)),(L3,L(10)),(L2,L(11)),
     2(L1,L(12))
      N=2**M
      ND4=N/4
      ND4P1=ND4+1
      ND4P2=ND4P1+1
      ND2P2=ND4+ND4P2
      DO 8 LO=1,M
      LMX=2**(M-LO)
      LIX=2*LMX
      ISCL=N/LIX
      DO 8 LM=1,LMX
      IARG=(LM-1)*ISCL+1
      IF(IARG.LE.ND4P1) GO TO 4
      C=-CC(ND2P2-IARG)
      S=ISN*CC(IARG-ND4)
      GO TO 6
    4 C=CC(IARG)
      S=ISN*CC(ND4P2-IARG)
    6 DO 8 LI=LIX,N,LIX
      J1=LI-LIX+LM
      J2=J1+LMX
      T1=X(J1)-X(J2)
      T2=Y(J1)-Y(J2)
      X(J1)=X(J1)+X(J2)
```

```
      Y(J1)=Y(J1)+Y(J2)
      X(J2)=C*T1-S*T2
      Y(J2)=C*T2+S*T1
    8 CONTINUE
      DO 40 J=1,12
      L(J)=1
      IF(J-M) 31,31,40
   31 L(J)=2**(M+1-J)
   40 CONTINUE
      JN=1
      DO 60 J1=1,L1
      DO 60 J2=J1,L2,L1
      DO 60 J3=J2,L3,L2
      DO 60 J4=J3,L4,L3
      DO 60 J5=J4,L5,L4
      DO 60 J6=J5,L6,L5
      DO 60 J7=J6,L7,L6
      DO 60 J8=J7,L8,L7
      DO 60 J9=J8,L9,L8
      DO 60 J10=J9,L10,L9
      DO 60 J11=J10,L11,L10
      DO 60 JR=J11,L12,L11
      IF(JN-JR) 51,51,52
   51 R=X(JN)
      X(JN)=X(JR)
      X(JR)=R
      FI=Y(JN)
      Y(JN)=Y(JR)
      Y(JR)=FI
   52 JN=JN+1
   60 CONTINUE
      RETURN
      END
```

```
      SUBROUTINE QTRCOS(C,N)
      DIMENSION C(1)
      N41=N/4+1
      SCL=6.283185307/N
      DO 1 I=1,N41
    1 C(I)=COS((I-1)*SCL)
      RETURN
      END
```

N = 100 MMAX = 10 M = 2 NF = 1224

INPUT DATA:

PROCESS NUMBER 1

.5349[illegible]	.2457[illegible]	-.4[illegible]	-.9923[illegible]	-.6[illegible]
.5[illegible]	.7457[illegible]	.9[illegible]	.1517[illegible]	-.7[illegible]
-.1[illegible]	.2[illegible]	.7[illegible]	.7[illegible]	.8[illegible]
.4[illegible]	-.[illegible]	-.7[illegible]	-.1[illegible]	-.9[illegible]
-.3[illegible]	.5[illegible]	.1[illegible]	.1[illegible]	.5[illegible]
-.1[illegible]	-.2[illegible]	-.1[illegible]	-.1[illegible]	-.1[illegible]
.1[illegible]	.3[illegible]	.2[illegible]	-.[illegible]	-.2[illegible]
-.3[illegible]	-.2[illegible]	-.2[illegible]	.1[illegible]	.3[illegible]
.2[illegible]	.5[illegible]	-.2[illegible]	-.3[illegible]	-.2[illegible]
-.4[illegible]	.2[illegible]	.3[illegible]	.2[illegible]	-.2[illegible]
-.2[illegible]	-.3[illegible]	-.2[illegible]	-.[illegible]	.2[illegible]
.4[illegible]	.3[illegible]	.9[illegible]	-.1[illegible]	-.2[illegible]
-.2[illegible]	-.1[illegible]	.9[illegible]	.3[illegible]	.3[illegible]
.1[illegible]	-.8[illegible]	-.2[illegible]	-.2[illegible]	-.1[illegible]
.6[illegible]	.3[illegible]	.3[illegible]	.2[illegible]	-.[illegible]
-.3[illegible]	-.4[illegible]	-.3[illegible]	-.6[illegible]	.2[illegible]
.4[illegible]	.3[illegible]	.5[illegible]	-.1[illegible]	-.3[illegible]
-.2[illegible]	-.1[illegible]	.1[illegible]	.2[illegible]	-.[illegible]
.1[illegible]	-.1[illegible]	-.3[illegible]	-.3[illegible]	-.1[illegible]
.1[illegible]	.2[illegible]	.2[illegible]	.1[illegible]	-.1[illegible]

PROCESS NUMBER 2

.6[illegible]	.8[illegible]	.1[illegible]	.1[illegible]	-.8[illegible]
-.5[illegible]	-.6[illegible]	.7[illegible]	.5[illegible]	-.3[illegible]
-.6[illegible]	-.3[illegible]	.1[illegible]	.3[illegible]	.8[illegible]
.5[illegible]	.3[illegible]	.1[illegible]	.[illegible]	-.1[illegible]
-.1[illegible]	-.8[illegible]	.1[illegible]	.6[illegible]	.1[illegible]
.1[illegible]	.5[illegible]	.1[illegible]	-.6[illegible]	.1[illegible]
-.1[illegible]	-.1[illegible]	-.2[illegible]	.6[illegible]	.1[illegible]
.1[illegible]	.8[illegible]	-.2[illegible]	-.1[illegible]	-.2[illegible]
-.1[illegible]	-.2[illegible]	.2[illegible]	.2[illegible]	.2[illegible]
.1[illegible]	.3[illegible]	-.2[illegible]	-.2[illegible]	-.1[illegible]
-.1[illegible]	-.2[illegible]	-.2[illegible]	-.1[illegible]	.5[illegible]

.2540[illegible]78+01	.30[illegible]5762+01	.18[illegible]49+01	-.84529681+00	-.28813978+01
-.31391280+01	-.17331168+01	.92467979+00	.25[illegible]586+01	.30833978+01
.19451272+01	-.49972268+00	-.29130998+01	-.33993366+01	-.25382963+01
.43e25807+0[illegible]	.2792e130+01	.31383639+01	.25105703+01	.87298217+00
-.12635761+01	-.25076506+01	-.25708112+01	-.99739413+00	.13897388+01
.20e30553+01	.23373065+01	.82068657+00	-.11139540+01	-.21637063+01
-.25236639+01	-.10761964+01	.98666745+00	.30014957+01	.30864179+01
.2352e349+01	-.81600191+00	-.32755376+01	-.45758461+01	-.25778198+01
-.21e9[illegible]36+00	.29419152+01	.36481336+01	.28266277+01	-.60319698-01
-.19425681+01	-.27615544+01	-.28589668+01	-.64737991+00	.17339168+01
.31e29709+01	.26245975+01	.30358645+00	-.19868774+01	-.27638567+01
-.24165864+01	-.10180275+01	.11536821+01	.19672282+01	.16684788+01

MEANS OF INPUT DATA:

.12068478-01 .29368686-01

COVARIANCE MATRIX OF INPUT DATA:

.46210387+01	.91577268+00	.91577268+00	.37986981+01

AKAIKE INFORMATION CRITERION:

P	AIC(P)
0	.28156752+01
1	-.47116187+01
2	-.46664973+01
3	-.46229553+01
4	-.46316842+01
5	-.45650773+01
6	-.45422159+01
7	-.45357835+01
8	-.44974548+01
9	-.44907188+01
10	-.44369324+01

PBEST = 1

UBEST:

.89904132-01	-.79014897-03	-.79014897-03	.93252867-01

FORWARD PARTIAL CORRELATION COEFFICIENTS:

P	A(P,P)11	A(P,P)21	A(P,P)12	A(P,P)22
1	.87150893+00	.63431677+00	-.77[illegible]333+00	.[illegible]+00
2	-.24060[illegible]+01	.15[illegible]790+00	-.[illegible]8-01	-.13[illegible]+00
3	.12915[illegible]+00	.10[illegible]343+00	-.6912[illegible]-01	-.12937[illegible]+00
4	-.11394597+00	.22871864+00	.18[illegible]+00	.72[illegible]-02
5	.39750190-01	.27[illegible]169-01	-.10[illegible]8+00	.10[illegible]-01

6	.247327d6+00	-.1110[illegible]661-01	-.134948[illegible]6-01	-.36488686-02
7	.1821b120+00	.1007[illegible]856+00	.96155[illegible]4-01	-.10703941+00
8	.1912164e+00	.9358[illegible]546-01	-.251440[illegible]0-01	.10188047-01
9	.822197bb-01	.1273[illegible]163+00	-.104756[illegible]6+00	-.22288333+00
10	-.534220[illegible]38-01	.167b[illegible]631+00	-.420759[illegible]6-01	-.26114821-01

BACKWARD PARTIAL CORRELATION COEFFICIENTS:

P	R(P,P)11	R(P,P)21	R(P,P)12	R(P,P)22
1	.5661249[illegible]+00	-.63141833+00	.77[illegible]98[illegible]3+00	.86872675+00
2	-.38369942-01	-.66131392-01	.95437[illegible]32-01	-.11108892+00
3	.97749d89-01	-.3861[illegible]501-01	.515550[illegible]1-01	-.11780613+00
4	-.33532630-01	.1809[illegible]538+00	.21567[illegible]73+00	.90908506-01
5	-.220977b9-02	-.1138[illegible]029+00	.319942[illegible]6-01	.28316177-01
6	.22[illegible]4d01+00	.7762[illegible]009-01	-.750399[illegible]0-02	-.71869090-02
7	.20997133+00	.1925[illegible]909+00	.536765[illegible]2-01	-.89760510-01
8	.17425943+00	.3845[illegible]344-01	.858705[illegible]8-01	.43625234-01
9	.3991473e-01	-.1197[illegible]495+00	.339875[illegible]6-01	-.22667234+00
10	-.586b3233-01	-.7421[illegible]017-01	.132840[illegible]3+00	.24026474-01

FORWARD PREDICTIVE FILTER COEFFICIENTS FOR PBEST:

K	A(PBEST,K)11	A(PBEST,K)21	A(PBEST,K)12	A(PBEST,K)22
1	.[illegible]715[illegible]893+00	.63431677+00	-.77[illegible]24[illegible]3+00	.56034775+00

NORMALIZED CORRELATION MATRICES FOR M=2, UP TO PMAX:

DELAY	AUTO11	CROSS21	CROSS12	AUTO22
0	.1[illegible]000000+01	.2186[illegible]251+00	.218642[illegible]1+00	.10000000+01
1	.714[illegible]2e3+00	.[illegible]224[illegible]727+00	-.507468[illegible]1+00	.7133[illegible]686+00
2	.5242+931-01	.9640[illegible]763+00	-.940219[illegible]6+00	.44541466-01
3	-.627249[illegible]5+00	.[illegible]769[illegible]243+00	-.[illegible]5[illegible]3+00	-.63314941+00
4	-.9493[illegible]32e+00	-.1157[illegible]169+00	-.299269[illegible]3+00	-.95009293+00
5	-.746[illegible]417e+00	-.7293[illegible]963+00	.402365[illegible]8+00	-.74185658+00
6	-.1415[illegible]21e+00	-.[illegible]312[illegible]804+00	.868493[illegible]9+00	-.13406150+00
7	.5[illegible]b[illegible]119+00	-.6206[illegible]877+00	.850477[illegible]5+00	.53278237+00
8	.[illegible]923[illegible]32[illegible]+00	.2075[illegible]851-01	.369307[illegible]8+00	.89383619+00
9	.76324[illegible]72+00	.[illegible]362[illegible]244+00	-.302958[illegible]7+00	.75935619+00
10	.[illegible]2[illegible]+00	.[illegible]907 968+00	-.793290[illegible]2+00	.21407713+00

SPECTRAL DENSITY MATRIX AND COHERENCE FOR M=2:

BIN	AUTO11	AUTO22	REAL(CROSS12)	IMAG(CROSS12)	MAG SQ COH	ARGUMENT
1	.[illegible]0031e16-03	.24469287-03	.10474293-03	.00000000	.93347806-01	.00000000
2	.[illegible]039190-03	.24479571-03	.10475898-03	.51851717-05	.93569521-01	.49485843-01
3	.[illegible]0662528-03	.24490670-03	.10480719-03	.10374396-04	.94234384-01	.98664136-01
4	.[illegible]0101653-03	.24517527-03	.10488758-03	.15571732-04	.95341385-01	.14738464+00
5	.[illegible]0150422-03	.24555178-03	.10500028-03	.20781259-04	.96888931-01	.19839113+00
6	.[illegible]0220298-03	.24603673-03	.10514542-03	.26007074-04	.98876767-01	.24967721+00
7	.[illegible]0312344-03	.24663077-03	.10532316-03	.31253307-04	.10129598+00	.28846080+00
8	.[illegible]0414399-03	.24733472-03	.10553375-03	.36524137-04	.10414911+00	.33318695+00
9	.[illegible]0528230-03	.24814953-03	.10577746-03	.41823766-04	.10743000+00	.37852935+00
10	.[illegible]0654450-03	.24907630-03	.10605455-03	.47156497-04	.11113392+00	.41839078+00

AD-A101 684 SCIENTIFIC AND ENGINEERING STUDIES COMPILED 1979 COHERENCE ESTIMATION(U) NAVAL UNDERWATER SYSTEMS CENTER NEWPORT RI G C CARTER ET AL. 1979 8/8

UNCLASSIFIED F/G 9/1 NL

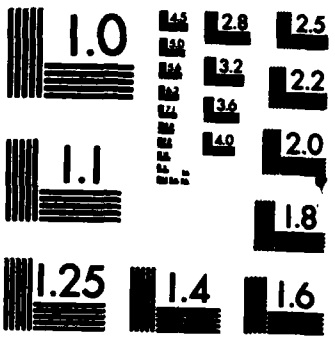

11	.98817101-03	.28811633-03	.10636541-03	.88864463-04	.11828884+00	.98870180+00
12	.98984208-03	.28127188-03	.10671948-03	.87888488-04	.11978988+00	.99781831+00
13	.99168078-03	.28284198-03	.10709971-03	.63287883-04	.12472788+00	.99881878+00
14	.99368039-03	.28383693-03	.10750948-03	.89964378-04	.13066583+00	.99990811+00
15	.99587871-03	.28543986-03	.10798498-03	.79471342-04	.13579387+00	.99387272+00
.						
.						
.						
.						
500	.98817091-04	.61373986-04	.74083339-05	.17278185-05	.21125130-01	.28868398+00
501	.98888945-04	.61383487-04	.74823757-05	.19942888-05	.20965389-01	.28998277+00
502	.98488271-04	.61334818-04	.74798548-05	.14669883-05	.20818384-01	.19888888+00
503	.98478968-04	.61317868-04	.74771719-05	.12876617-05	.20688288-01	.17873898+00
504	.98488832-04	.61381668-04	.74798873-05	.11948419-05	.20862888-01	.19884688+00
505	.98448662-04	.61287715-04	.74728191-05	.10613383-05	.20858233-01	.19118678+00
506	.98438858-04	.61279418-04	.74711478-05	.98662868-06	.20388428-01	.12388669+00
507	.98427814-04	.61284706-04	.74698138-05	.77888378-06	.20275391-01	.18813884+00
508	.98419934-04	.61255728-04	.74683158-05	.68388687-06	.20285148-01	.88888377-01
509	.98413816-04	.61248388-04	.74678533-05	.63837828-06	.20147667-01	.78987875-01
510	.98409858-04	.61242612-04	.74664271-05	.59773487-06	.20182963-01	.83219391-01
511	.98405661-04	.61235134-04	.74658378-05	.56813838-06	.20071836-01	.38498218-01
512	.98403621-04	.61234856-04	.74654839-05	.13884886-06	.20051881-01	.17784433-01
513	.98402941-04	.61232236-04	.74653662-05	.89138259-21	.20043497-01	.39888842-16

ALIASED NORMALIZED CORRELATION MATRICES FOR M=2:

DELAY	AUTO11	CROSS21	CROSS12	AUTO22
0	.10000000+01	.2186[illegible]252+00	.[illegible]2[illegible]642.2+00	.10000000+01
1	.71889274+00	.8224[illegible]738+00	-.507468[illegible]1+00	.71338704+00
2	.52424690-01	.9640[illegible]794+00	-.94[illegible]	.44541551-01
3	-.62724051+00	.5789 270+00	-.85[illegible]9+00	-.63314964+00
4	-.94933394+00	-.11577175+00	-.29926977+00	-.95009356+00
5	-.74654241+00	-.72934019+00	.[illegible]9+00	-.74185784+00
6	-.14151228+00	-.93123896+00	.[illegible]9+00	-.13406173+00
7	.52669183+00	-.62084952+00	.[illegible]8+00	.53278291+00
8	.89239447+00	.2075[illegible]831-01	.36930775+00	.89383740+00
9	.76324192+00	.6362[illegible]337+00	-.30205[illegible]8+00	.75935744+00
10	.22104927+00	.8907[illegible]124+00	-.79329[illegible]9+00	.21407763+00
11	-.42912048+00	.6538[illegible]996+00	-.84079[illegible]7+00	-.43530803+00
12	-.83034806+00	.6602[illegible]523-01	-.42894[illegible]3+00	-.83243695+00
13	-.76977769+00	-.54423415+00	.20726[illegible]7+00	-.76666664+00
14	-.29096326+00	-.84376757+00	.71577[illegible]7+00	-.28452705+00
15	.33536998+00	-.67647757+00	.82241[illegible]4+00	.34157506+00
.				
.				
.				
500	-.49372766-02	-.24867039-02	.34[illegible]92646-03	-.49081369-02
501	-.25524314-02	-.48767743-02	.37631[illegible]5-02	-.25471501-02

502	.1295y344-02	-.4573.349-02	.5193?6 3-02	.12112272-02
503	.4280925?7-02	-.1746' 129-02	.362?6?' 2-02	.42914713-02
504	.4995?4497-02	.2036' 386-02	.1475?6: 7-03	.49972947-02
505	.2946?97?-02	.4667 941-02	-.339938?0-02	.2945?784-02
506	-.7247390?-03	.4747' 435-02	-.5064?9. 1-02	-.72796869-03
507	-.3969?956-02	.2167. 377-02	-.3931?0? 3-02	-.39933533-02
508	-.5043175?-02	-.1576 553-02	-.63?7?? 7-03	-.50506222-02
509	-.3316?23?-02	-.4465 66?-02	.3?1479' ?-02	-.33192618-02
510	.24177?43-03	-.4887' 877-02	.4993?9; 3-02	.24286025-03
511	.3666?247-02	-.?610 ?03-02	.4213?4.7-02	.36689682-02
512	.5?657272-02	.1107 301-02	.11?743 1-02	.50683549-02

REFERENCES

1. A. H. Nuttall, Multivariate Linear Predictive Spectral Analysis Employing Weighted Forward and Backward Averaging: A Generalization of Burg's Algorithm, NUSC Technical Report 5501, 13 October 1976.

2. O. N. Strand, "Multichannel Complex Maximum Entropy (Autoregressive) Spectral Analysis," IEEE Transactions on Automatic Control, vol. AC-22, no. 4, August 1977, pp. 634-640.

3. J. P. Burg, "Maximum Entropy Spectral Analysis," Ph. D. Dissertation, Dept. of Geophysics, Stanford University, May 1975.

4. J. N. Franklin, Matrix Theory, Prentice-Hall, Inc., Englewood Cliffs, NJ, 1968.

5. A. Jameson, "Solution of the Equation AX + XB = C by Inversion of an M × M or N × N Matrix," SIAM Journal of Applied Mathematics, vol. 16, no. 5, September 1968, pp. 1020-1023.

NUSC Technical Document 5881
13 July 1978

Confidence Bounds for Magnitude-Squared Coherence Estimates

A Paper Presented at the

1978 IEE International

Conference on Acoustics,

Speech, and Signal Processing

G. C. Carter
E. H. Scannell, Jr.

ABSTRACT

This document presents both the oral and written versions of a paper presented (in 15 minutes) on 12 April 1978 at the 1978 IEEE International Conference on Acoustics, Speech, and Signal Processing, in Tulsa, Oklahoma.

The main emphasis of the talk was on explaining coherence and its usefulness. The paper given in the coherence record emphasizes how to estimate coherence and how accurately this can be done. In underwater acoustics where signals are digitally processed at the outputs of two or more receiving sensors, it is desirable to estimate the coherence spectrum, both for detection and position estimation.

A processing technique for computing arbitrary confidence bounds for stationary Gaussian signals is presented. New computationally difficult examples are given for 80-95 percent confidence with independent averages of 8, 16, 32, 64, and 128. A discussion of the computational difficulties together with algorithmic details (including the FORTRAN program) are presented.

CONFIDENCE BOUNDS FOR MAGNITUDE-SQUARED COHERENCE ESTIMATES

- *What is coherence?*
- *How and how accurately do you estimate it?*

THE PURPOSE OF THIS TALK IS TO ANSWER TWO FUNDAMENTAL QUESTIONS: FIRST, WHAT IS COHERENCE; SECOND, HOW DO YOU ESTIMATE COHERENCE AND HOW ACCURATE CAN THIS ESTIMATION BE.

THE MAIN EMPHASIS OF THIS TALK IS THE EXPLANATION OF COHERENCE AND ITS USEFULNESS. THE PAPER GIVEN IN THE CONFERENCE RECORD EMPHASIZES HOW TO ESTIMATE COHERENCE AND HOW ACCURATELY THIS CAN BE DONE. THE IMPORTANCE OF DETERMINING CONFIDENCE BOUNDS FOR ESTIMATES OF COHERENCE WILL ONLY BE APPARENT TO SOMEONE WHO WANTS TO ESTIMATE COHERENCE. THUS, THE TALK THIS MORNING WILL SHOW HOW USEFUL THE COHERENCE IS AND HOW TO USE THE RESULTS IN THE COHERENCE RECORD TO DETERMINE THE ACCURACY WITH WHICH THE COHERENCE CAN BE ESTIMATED.

-NEXT SLIDE PLEASE-

$$\gamma_{ab}(f) = \frac{G_{ab}(f)}{\left[G_a(f)\, G_b(f)\right]^{1/2}}$$

$$0 \le \left|\gamma_{ab}(f)\right|^2 \le 1, \quad \forall f$$

a,b either source, receiver pair or receiver, receiver pair

THE TERM COHERENCE HAS SEVERAL DIFFERENT MEANINGS AND DEFINITIONS. THE ONE WE USE HERE IS THE COMPLEX COHERENCE OR COEFFICIENT OF COHERENCY DEFINED BY WEINER IN 1930. FOR OUR PURPOSES, WE DEFINE THE COHERENCE BETWEEN TWO STATIONARY RANDOM PROCESSES, A AND B, AS THE CROSS POWER SPECTRUM DIVIDED BY THE SQUARE ROOT OF THE PRODUCT OF THE AUTO POWER SPECTRA. THE COHERENCE IS A FUNCTION OF FREQUENCY AND HAS THE USEFUL PROPERTY THAT ITS MAGNITUDE SQUARED IS BOUNDED BETWEEN ZERO AND UNITY. IT IS A NORMALIZED CROSS SPECTRAL DENSITY THAT, IN SOME SENSE, MEASURES THE EXTENT TO WHICH TWO RANDOM PROCESSES ARE SIMILAR. FOR EXAMPLE, TWO UNCORRELATED RANDOM PROCESSES ARE INCOHERENT; THAT IS, THE COHERENCE IS ZERO BETWEEN UNCORRELATED PROCESSES. FURTHER, THE COHERENCE BETWEEN TWO LINEARLY RELATED PROCESSES IS UNITY. THE TWO PROCESSES UNDER CONSIDERATION CAN BE AN UNDERWATER ACOUSTIC SOURCE AND RECEIVER PAIR OR TWO RECEIVER PAIRS.

-NEXT SLIDE PLEASE-

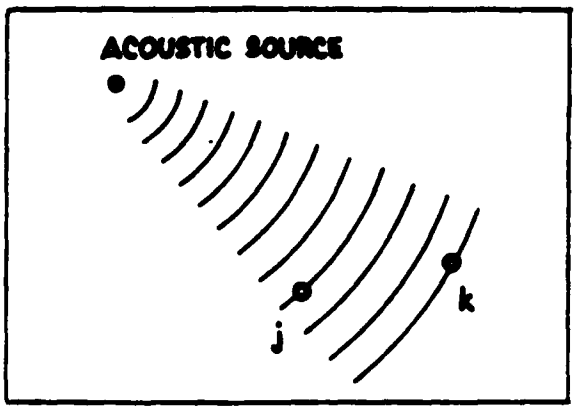

ONE PHYSICAL PROBLEM THAT MOTIVATES THIS RESEARCH IS THE DESIRE TO PASSIVELY ESTIMATE GEOGRAPHICAL INFORMATION ABOUT THE STATE OF AN ACOUSTIC SOURCE. IN THE DEVELOPMENT HERE, AN ACOUSTIC POINT SOURCE RADIATES SPHERICAL WAVES THAT ARE RECEIVED FIRST AT ONE SENSOR AND SOME DELAYED TIME LATER AT A SECOND SENSOR. THE SOURCE IS ASSUMED STATIONARY FOR THE OBSERVATION PERIOD AND THE SENSOR SEPARATION IS ASSUMED KNOWN. EACH RECEIVED WAVEFORM IS OBSERVED IN THE PRESENCE OF UNCORRELATED NOISE. THE PROBLEM WE ADDRESS HERE IS THE PHYSICAL INTERPRETATION OF THE COHERENCE FOR THIS MODEL.

-NEXT SLIDE PLEASE-

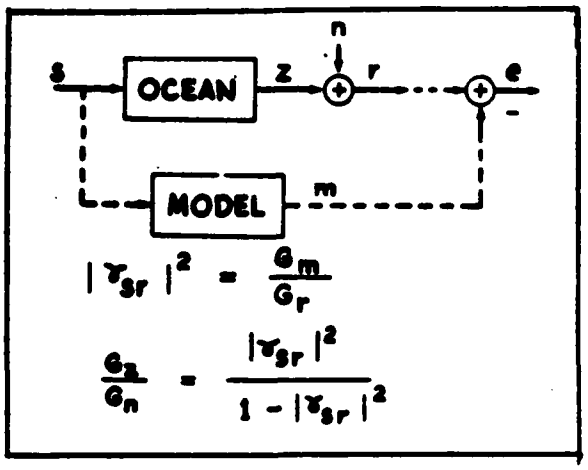

$$|\gamma_{sr}|^2 = \frac{G_m}{G_r}$$

$$\frac{G_s}{G_n} = \frac{|\gamma_{sr}|^2}{1 - |\gamma_{sr}|^2}$$

A SOURCE SIGNAL S EXCITES THE MEDIUM TO YIELD AN OUTPUT Z. THIS OUTPUT Z IS CORRUPTED BY ADDITIVE NOISE N AND RECEIVED AS R. WE CONSTRUCT A LINEAR MODEL OF THE MEDIUM THAT GENERATES AN OUTPUT M. BY PROPER CHOICE OF THE MODEL WE CAN MINIMIZE THE MEAN SQUARE ERROR E, OR DIFFERENCE BETWEEN THE RECEIVED SIGNAL R AND MODEL OUTPUT M. THE MAGNITUDE SQUARED COHERENCE BETWEEN SOURCE AND RECEIVER IS GIVEN BY THE RATIO OF THE MODEL OUTPUT POWER TO THE RECEIVER OUTPUT POWER. SINCE GAMMA SQUARED IS BOUNDED BY UNITY, IT PROVIDES AN INDICATION OF WHAT PORTION OF THE RECEIVED POWER CAN BE ATTRIBUTED TO A MINIMUM MEAN SQUARE ERROR LINEAR MODEL OF THE OCEAN MEDIUM. THE POWER RATIO OF THE OCEAN OUTPUT DUE TO THE SOURCE VERSUS AMBIENT IS ALSO DIRECTLY RELATED TO THE SOURCE-TO-RECEIVER COHERENCE. IN PARTICULAR, THIS SIGNAL-TO-NOISE RATIO IS GIVEN BY GAMMA SQUARED OVER ONE MINUS GAMMA SQUARED.

-NEXT SLIDE PLEASE-

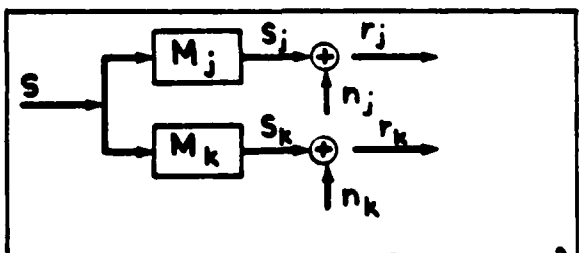

$$|\gamma_{r_j r_k}|^2 = |\gamma_{sr_j}|^2 \, |\gamma_{sr_k}|^2$$

$$\frac{G_s}{G_n} = \frac{|\gamma_{r_j r_k}|}{1 - |\gamma_{r_j r_k}|}$$

IN THE GENERAL CASE, WE CAN MODEL THE ACOUSTIC PROPAGATION OF A SINGLE ACOUSTIC SOURCE AND NOISE CORRUPTED RECEPTION AT TWO RECEIVERS AS SHOWN HERE. IN PARTICULAR, WE TREAT THE PATH FROM THE SOURCE TO EACH RECEIVER AS A LINEAR TIME INVARIANT FILTER. THE RECEIVER SIGNALS R SUB J AND R SUB K CONSIST OF THE FILTER OUTPUTS PLUS NOISE.

A SPECIAL CASE OF THIS MODEL IS WHEN THE FIRST RECEIVER WAVEFORM CONSISTS OF SIGNAL PLUS NOISE, AND THE SECOND RECEIVED WAVEFORM CONSISTS OF AN ATTENUATED AND DELAYED SIGNAL IN THE PRESENCE OF UNCORRELATED NOISE. THE MATHEMATICAL PROBLEM OF ESTIMATING THE TIME DELAY OR EQUIVALENT SOURCE BEARING AND, THUS, SOURCE RANGE, IS CLOSELY RELATED TO COHERENCE.

UNDER CERTAIN ASSUMPTIONS WE CAN SHOW THAT THE MAGNITUDE SQUARED COHERENCE BETWEEN TWO RECEIVER PAIRS IS THE PRODUCT OF THE INDIVIDUAL SOURCE-TO-RECEIVER COMBINATIONS. THUS, THE RECEIVED SIGNAL-TO-NOISE RATIO IS THE RECEIVER-TO-RECEIVER MAGNITUDE COHERENCE OVER ONE MINUS THE RECEIVER-TO-RECEIVER MAGNITUDE COHERENCE.

-NEXT SLIDE PLEASE-

$$\hat{\gamma}_{ab} = \frac{\sum_{n=1}^{N} A_n B_n^*}{\left[\sum_{n=1}^{N} |A_n|^2 \sum_{n=1}^{N} |B_n|^2\right]^{1/2}}$$

NOW THAT COHERENCE HAS BEEN DEFINED, IT IS APPROPRIATE TO DISCUSS ITS ESTIMATION. FROM EACH OF TWO FINITE DURATION MEMBER FUNCTIONS OF CAPITAL N SEGMENTS, WE WEIGHT EACH SEGMENT BY A SMOOTH WEIGHTING FUNCTION, COMPUTE ITS DISCRETE FOURIER TRANSFORM VIA AN FFT, AND DENOTE THEM A SUB N AND B SUB N. AT ANY PARTICULAR FREQUENCY, THE COMPLEX COHERENCE IS ESTIMATED BY COMPUTING THE THREE SUMMATIONS SHOWN OVER THE AVAILABLE CAPITAL N SEGMENTS. THE LOWER CASE N DENOTES THE N-TH DATA SEGMENT AND THE FREQUENCY INDICATOR IS NOT SHOWN. IN THE NUMERATOR, WE MULTIPLY THE FFT OF THE A PROCESS BY THE COMPLEX CONJUGATE OF THE FFT OF THE B PROCESS AND SUM OVER N SEGMENTS TO OBTAIN AN ESTIMATE OF THE COMPLEX CROSS SPECTRUM. IN THE DENOMINATOR WE SUM THE MAGNITUDE SQUARED FFTS OVER THE N TIME SEGMENTS. UNDER CERTAIN SIMPLIFYING ASSUMPTIONS GIVEN IN THE CONFERENCE RECORD WE CAN DETERMINE THE STATISTICS OF THIS ESTIMATOR.

-NEXT SLIDE PLEASE-

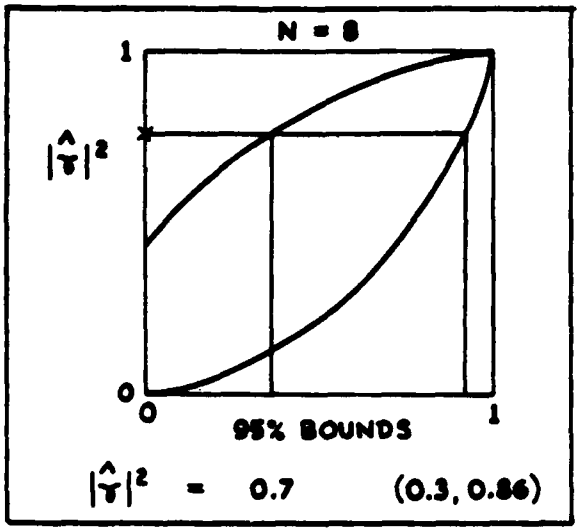

CONCLUSIONS

- COHERENCE
  - NORMALIZED CROSS SPECTRUM
  - SIGNAL TO NOISE MEASURE
  - LINEARITY MEASURE
- ESTIMATION
  - DIFFICULT
  - BOUNDS LARGE

IN THE CONFERENCE RECORD WE DISCUSS HOW TO DETERMINE THE CONFIDENCE BOUNDS. FOR A PARTICULAR NUMBER OF FFT AVERAGES (N = 8) AND A PRESPECIFIED CONFIDENCE BOUND (95%), WE OBTAIN THE TWO CURVES SKETCHED HERE. WHEN WE OBTAIN AN ESTIMATE OF GAMMA SQUARED FROM THE SAME NUMBER OF FFTs AS USED TO DRAW THE CURVES, WE USE THESE CURVES TO DETERMINE CONFIDENCE BOUNDS. IN PARTICULAR, IF WE HAVE AN ESTIMATE DENOTED BY AN X ON THE ORDINATE, WE DRAW A HORIZONTAL LINE FROM THE X UNTIL IT INTERSECTS BOTH CURVES. THEN WE DROP TWO VERTICAL LINES TO THE ABSCISSA AND THESE ARE THE CONFIDENCE BOUNDS. WE CAN THEN STATE THAT THE TRUE VALUE OF GAMMA SQUARED LIES IN THE REGION BOUNDED BY THE TWO ABSCISSA VALUES WITH THE PRESPECIFIED CONFIDENCE. FOR EXAMPLE, WITH EIGHT FFTs AND AN ESTIMATE OF 0.7, THE 95% CONFIDENCE BOUNDS ARE 0.3 AND 0.86. WITH 128 FFTs AND AN ESTIMATE OF 0.3, THE BOUNDS ARE 0.2 AND 0.38. THUS, THE BOUNDS ARE LARGE EVEN WHEN THE NUMBER OF FFTs IS LARGE.

-NEXT SLIDE PLEASE-

IN CONCLUSION, WE HAVE LOOKED AT WHAT THE COHERENCE IS. WE HAVE SEEN THAT IT IS A NORMALIZED CROSS SPECTRUM THAT CAN PROVIDE A MEASURE OF SIGNAL-TO-NOISE RATIO AND THE EXTENT TO WHICH THE OCEAN MEDIUM CAN BE MODELED BY A LINEAR FILTER. IN TERMS OF MEASURING COHERENCE, WE HAVE PRESENTED ESTIMATION EQUATIONS THAT DEPEND ON THE APPLICATION OF SMOOTH WEIGHTING FUNCTIONS AND LARGE NUMBERS OF. OF FFTs. THESE COMPUTATIONAL DIFFICULTIES RESULT IN LARGE BOUNDS ON THE COHERENCE ESTIMATES.

IN SUMMARY, THE COHERENCE IS AN EXTREMELY USEFUL DESCRIPTOR IN UNDERWATER ACOUSTICS THAT CAN BE ESTIMATED WITH CAREFUL ATTENTION TO DETAIL AND LARGE NUMBERS OF FFTs.

-SLIDE OFF-

ARE THERE ANY QUESTIONS?

TD 5881

PREPRINT: Proceedings of the 1978 IEEE International Conference on Acoustics, Speech, and Signal Processing p 670-673

CONFIDENCE BOUNDS FOR MAGNITUDE-SQUARED COHERENCE ESTIMATES

by

E. M. Scannell, Jr. and G. Clifford Carter

Naval Underwater Systems Center
New London, CT 06320

ABSTRACT

In underwater acoustics where signals are digitally processed at the outputs of two or more receiving sensors, it is desirable to estimate the coherence spectrum, both for detection and position estimation. A processing technique for computing arbitrary confidence bounds for stationary Gaussian signals is presented. Few computationally difficult examples are given for 80 to 95% confidence with independent averages of 8, 16, 32, 64 and 128. A discussion of the computational difficulties together with algorithmic details are presented.

INTRODUCTION

The magnitude-squared coherence (MSC) between two jointly stationary random processes x(t) and y(t) is defined as

$$C_{xy}(f) = \frac{|G_{xy}(f)|^2}{G_{xx}(f)G_{yy}(f)}, \qquad (1)$$

where $G_{xy}(f)$ is the cross-spectral density at frequency f and $G_{xx}(f)$ and $G_{yy}(f)$ are the autospectral densities. The MSC can be estimated as in [1] by

$$\hat{C}_{xy}(f) = \frac{\left|\sum_{n=1}^{N} X_n(f)Y_n^*(f)\right|^2}{\sum_{n=1}^{N}|X_n(f)|^2 \sum_{n=1}^{N}|Y_n(f)|^2} \qquad (2)$$

where * denotes complex conjugate, N is the number of data segments employed, and $X_n(f)$ and $Y_n(f)$ are the Fast Fourier Transform (FFT) outputs of the nth data segments of x(t) and y(t). Both the MSC and its estimates are bounded by zero and unity. The cumulative distribution functions (CDF) for the MSC estimate in (2) have been determined in [1] under the assumptions that 1) the data are jointly stationary Gaussian random processes; 2) the N data segments are independent; 3) the data segments have been multiplied by a smooth weighting function to reduce sidelobe leakage; and 4) each data segment is sufficiently long to ensure adequate spectral resolution.

The MSC is useful in detection, see for example [2] and [3] , but is also of value in estimating the amount of coherent power common between two received signals. Therefore it would be desirable having estimated a particular value of MSC to state with certain confidence that the true coherence falls in a specified interval. Early attempts to do this for 95% confidence were accomplished by Haubrich [4] who apparently used precomputed CDF curves and used a different method of presentation than the one used here. Related confidence work for the magnitude coherence (MC) or squareroot of (2) is presented by Koopmans [5]. Empirical results for 95% confidence are given by Benignus [6].

DETERMINING CONFIDENCE BOUNDS

Let C be the true but unknown parameter and $\hat{C}$ be its estimate. Then there exists a family of CDFs such as the two sketched in Fig. (1) for all values of C and N. For a fixed value of N, a number of

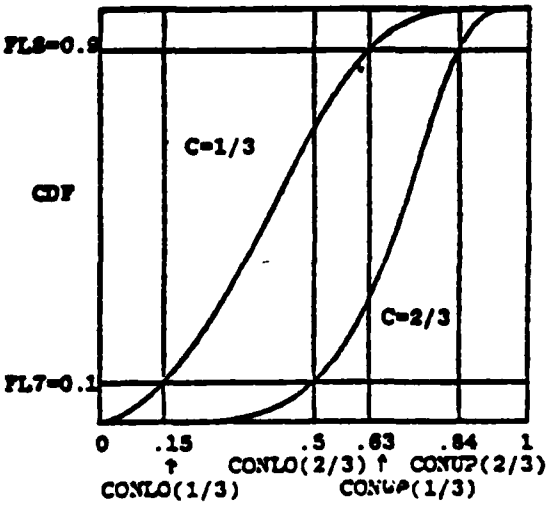

FIG. (1). PLOT OF CDF CURVES FOR N=8, C=1/3, AND N=8, C=2/3

CDF curves, such as plotted in Fig. (1), are generated, for various values of C. For each of the numerous CDF curves, we select, as closely as possible, the abscissa values such that the ordinate values FL8 minus FL7 yield the desired confidence. The confidence intervals are not unique, since there is no constraint such as FL8 equal FL7. We have selected FL8 equal FL7 but could have selected FL8 and FL7 such that the difference in abscissa values in Fig. (1) CONUP(C) minus CONLO(C) was minimum. However, as long as FL8 minus FL7 equals the desired confidence the method presented here is correct. Now we plot CONUP(C) and CONLO(C) versus C for this particular value of N. A result is sketched in Fig. (2).

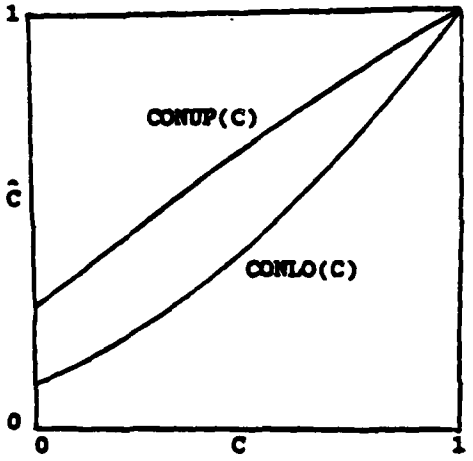

FIG. (2). HANDSKETCH OF CONFIDENCE BOUNDS FOR A PARTICULAR VALUE OF N

MAKING CONFIDENCE STATEMENTS ABOUT MSC ESTIMATES

A computer program has been written to evaluate the CDF and confidence limits. The mathematical details of the CDF as a finite sum of F21 hypergeometric functions, each one a polynomial, are given in [2]. For large values of N and C, a brute force approach to computing the CDF results in numeric overflows, attempts to avoid this problem can result in underflows or other inaccuracies. The program listed in the Appendix avoids these difficulties, it also incorporates CDF values when C equals zero or unity, since these can be computed in closed form.

Figures (3a) and (3b) are computer generated 80% and 95% confidence limits, respectively. The five pairs of curves in each figure are for N = 8, 16, 32, 64, and 128 from outer to inner, respectively. Having made an estimate with a particular value of N, only one pair of curves applies. An excellent discussion of the types of statements that can be made with confidence bounds is given by Cramér [7]. Suppose we obtain an estimated MSC of 0.7 from N = 8 disjoint FFTs, then we draw a horizontal line from 0.7 on Fig. (3b) for 95% confidence limits and see where it intersects the pair of N = 8 (outer) curves. This occurs at (approximate abscissa values) 0.3 and 0.86. Thus we state with 95% confidence that the true but unknown parameter C falls in the interval (0.3, 0.86). No matter what the true value of C, we have a 5% probability of giving an incorrect statement. That is, if we make many estimates of MSC and keep applying the rule described (whether or not C is random or constant) we will correctly include the true value of C in the interval that we specify 95% of the time. Sometimes the method of applying the rule is in doubt as for example in Fig. (3b) if the estimate comes out to be 0.3 and N = 8 then a horizontal line does not intersect the upper confidence limit curve unless we extrapolate it backwards. Doing this means making statements like: with 95% confidence the true MSC is in the region (-0.1, 0.62). Since we know apriori that the true value of C is non-negative, we could just as easily say (but with no more confidence) that with 95% confidence (for N = 8 and Ĉ = 0.3) the true MSC falls in the region (0.0, 0.62). Moreover, if both intersections result in negative regions (as for example when Ĉ = 0.001 and N = 8) we may have to make statements like with 80% confidence the true MSC lies in (0.0, 0.0). However, if we continue to apply the rule and run the experimental trials we will make correction statements "80%" of the time. It is interesting to note that due to the properties of the estimate and our selection of FL7 and FL8 that larger values of N do not always result in the upper confidence bound being lower. This also occurs in MC estimate confidence limits [5]. It is also interesting to note that while increasing N is desirable, the confidence bounds for N = 128 are still very large. For example, even when N = 128 if Ĉ = 0.3 the 95% confidence intervals are still (0.2, 0.38) and the 80% confidence intervals (0.24, 0.36) are not much better.

REFERENCES

1. G. C. Carter, C. H. Knapp, and A. H. Nuttall, "Estimation of the Magnitude-Squared Coherence Function via Overlapped Fast Fourier Transform Processing", IEEE Trans. Audio Electroacoust., Vol. AU-21, pp. 337-344, Aug 1973
2. G. C. Carter, "Receiver Operating Characteristics for a Linearly Thresh-

holded Coherence Estimation Detector", IEEE Trans. Acoust., Speech, Signal Processing, vol. ASSP-25, pp. 90-92, Feb 1977

3. J. J. Gosselin, "Comparative Study of Two-Sensor (Magnitude-Squared Coherence) and Single-Sensor (Square-Law) Receiver Operating Characteristics", Proc. IEEE ICASSP-77, pp. 311-314, 1977
4. E. A. Haubrich, "Earth Noise 5 to 500 Millicycles per Second, 1. Spectral Stationarity, Normality and Nonlinearity", J. Geophysical Res., vol. 70, No. 6, pp. 1415-1427, 1965
5. L. H. Koopmans, The Spectral Analysis of Time Series, Academic Press, New York, 1974
6. V. A. Benignus, "Estimation of Coherence Spectrum of Non Gaussian Time Series Populations", IEEE Trans. Audio Electroacoustic., vol. AU-17, pp. 198-201, Sept 1969 (and Sept 70 correction)
7. H. Cramer, Mathematical Methods of Statistics, Princeton University Press 1946

SAMPLE OUTPUT FROM PROGRAM LISTED IN APPENDIX

8	.000	.015	.200	.004	.410
8	.167	.055	.467	.015	.611
8	.333	.154	.626	.061	.747
8	.500	.305	.741	.175	.815
8	.667	.500	.838	.365	.866
8	.833	.732	.924	.637	.947
8	1.000	1.000	1.000	1.000	1.000
16	.000	.007	.142	.002	.218
16	.167	.065	.372	.023	.486
16	.333	.190	.533	.111	.614
16	.500	.354	.669	.259	.732
16	.667	.546	.769	.458	.832
16	.833	.762	.899	.705	.921
16	1.000	1.000	1.000	1.000	1.000
32	.000	.003	.072	.001	.112
32	.167	.064	.307	.044	.369
32	.333	.225	.470	.164	.532
32	.500	.393	.618	.327	.668
32	.667	.586	.754	.523	.769
32	.833	.783	.882	.747	.869
32	1.000	1.000	1.000	1.000	1.000
64	.000	.002	.036	.000	.057
64	.167	.102	.258	.071	.308
64	.333	.253	.426	.239	.478
64	.500	.423	.586	.377	.645
64	.667	.605	.729	.567	.752
64	.833	.793	.869	.775	.869
64	1.000	1.000	1.000	1.000	1.000
128	.000	.001	.018	.000	.029
128	.167	.119	.230	.094	.269
128	.333	.275	.407	.243	.447
128	.500	.445	.585	.413	.549
128	.667	.623	.715	.597	.740
128	.833	.802	.860	.793	.879
128	1.000	1.000	1.000	1.000	1.000

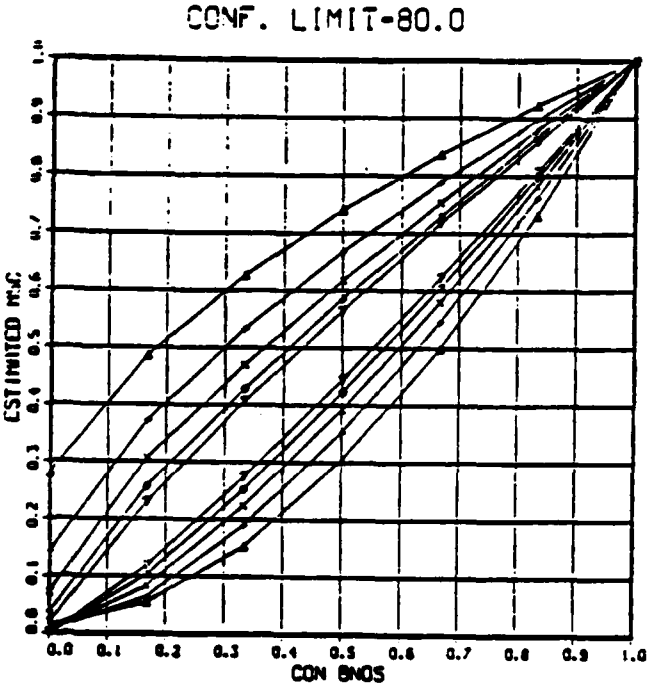

FIG. (3a). 80% CONFIDENCE LIMITS FOR N = 8, 16, 32, 64, AND 128

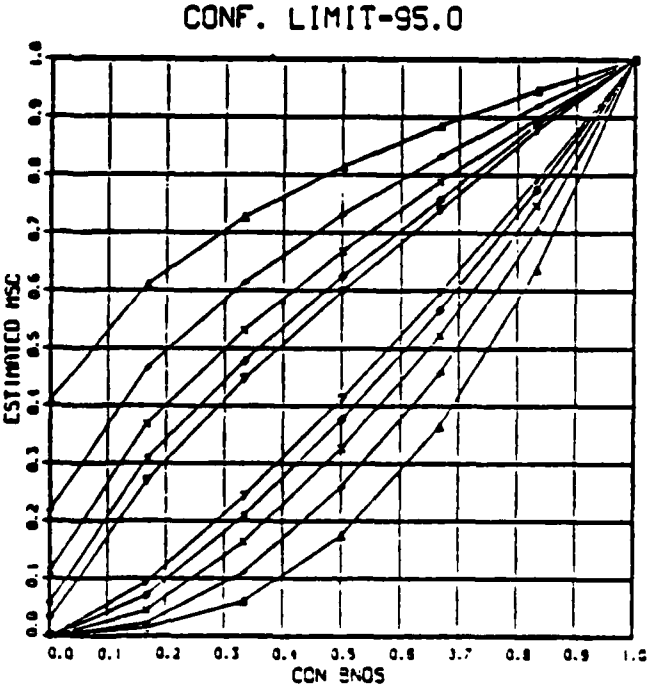

FIG. (3b). 95% CONFIDENCE LIMITS FOR N = 8, 16, 32, 64, AND 128

APPENDIX. PROGRAM FOR CONFIDENCE BOUNDS

```
      PARAMETER (IC=7,IN=7
      DIMENSION B(101),LAB(5),FIL(2)
      DOUBLE PRECISION C2,C3,C4,T,E,T2,F
      DIMENSION CONUP(2,IN,NC),CONLO(2,IN,NC)
      DIMENSION X(NC),Y1(NC),Y2(NC)
      DO 50 IL=1,2
      DO 50 IJ=1,IN
      DO 50 IC=1,NC
      CONUP(IL,IJ,IC)=1.0
      CONLO(IL,IJ,IC)=0.0
   50 CONTINUE
      LOOP=NC-2
  100 DO 600 IC=1,LOOP
      C=FLOAT(IC)/FLOAT(NC-1)
  200 DO 590 IL=1,2
      FL6=.65+(IL-1)*.15
  300 DO 580 IJ=3,IN
      N=2*IJ
  400 DO 410 I=1,101
      B(I)=1.0
  410 CONTINUE
      A=1.0-FLOAT(N)
      FL7=(100.0-FL6)/200.0
      FL8=1.0-FL7
      TEMP=1.0/FLOAT(N-1)
      CONLO(IL,IJ,1)=1.0-(FL6+TEMP)
      CONUP(IL,IJ,1)=1.0-(FL7*TEMP)
      CONUP(IL,IJ,NC)=1.0
      CONLO(IL,IJ,NC)=1.0
      DO 510 K=1,100
      E= FLOAT(K-1)/100.0
      Z=E*C
      P=0
      IF (Z .EQ. 0) GO TO 480
      C4=(1-E)/(1-Z)
      T2=(1-C)/(1-Z)
      C2=E*T2**N
      IF(E .EQ. 0)  GO TO 480
      IR=N-2
      DO 470 L=0,IR
      C3=C4**L
      T=C3
      F=T
      IF(L.EQ.0)GO TO 455
      DO 450 K2=1,L
      K1=K2-1
      FK=FLOAT(K2)
      T=T*Z*(FLOAT(A+K1)/FK)*(FLOAT(K1-L)/FK)
      IF(T.LT.0.0001*F*L)GO TO 455
      F=F+T
  450 CONTINUE
  455 CONTINUE
      P=P+C2*F
      IF(P.GT.FL8)GO TO 480
  470 CONTINUE
  480 B(K)=P
      IF(P.GT.FL8)GO TO 515
  510 CONTINUE
  515 CONTINUE
      DO 570 I=1,100
      IF (B(I).GE.FL7) GO TO 520
      IF (B(I+1).LT.FL7) GO TO 520
      D2=B(I+1)-B(I)
      E=((I-1)/100.0) + ((FL7-B(I))/(100*D2))
      CONLO(IL,IJ,IC+1)=E
  520 IF (B(I).GE.FL8) GO TO 570
      IF (B(I+1).LT.FL8) GO TO 570
      D3 =B(I+1) -B(I)
      E=((I-1)/100.0) + ((FL8-B(I))/(100*D3))
      CONUP(IL,IJ,IC+1)=E
  570 CONTINUE
  580 CONTINUE
  590 CONTINUE
  600 CONTINUE
      DO 640 IL=1,2
      DO 640 IJ=3,IN
      N=2*IJ
      DO 640 IC=1,NC
      CON=(IC-1)/FLOAT(NC-1)
      F1=CONLO(1,IJ,IC)
      F2=CONUP(1,IJ,IC)
      F3=CONLO(2,IJ,IC)
      F4=CONUP(2,IJ,IC)
      PRINT 630,N,CON,F1,F2,F3,F4
  630 FORMAT(1X,I5,5F6.3)
  640 CONTINUE
      CALL COMPRS
      DO 750 IL=1,2
      FIL=.65+(IL-1)*.15
      ENCODE(30,651,LAB)FIL
  651 FORMAT('CON.F. LIMIT=',F4.1,' IS')
      CALL TITLAB(100,'CON BNDS',100,
     'ESTIMATED NSCS',100,6,6,)
      CALL FRAME
      CALL GRAF(0.0,1.0,1.0,0.0,0.0,0.1,1.0)
      CALL GRID(1,1)
      DO 740 IJ=3,IN
      DO 700 IC=1,NC
      X(IC)=FLOAT(IC-1)/FLOAT(NC-1)
      Y1(IC)=CONUP(IL,IJ,IC)
      Y2(IC)=CONLO(IL,IJ,IC)
  700 CONTINUE
      ITEMP=IJ-1
      CALL MARKER(ITEMP)
      CALL CURVE(X,Y1,NC,1)
      CALL CURVE(X,Y2,NC,1)
  740 CONTINUE
      CALL ENDPL(IL)
  750 CONTINUE
      CALL DONEPL
      END
```

SUBJECT MATTER INDEX

END

7-87

DTIC